

NATIONAL AERONAUTICS AND SPACE ADMINISTRATION

Technical Memorandum 33-585

Volume I

Mariner Mars 1971 Television Picture Catalog

Experiment Design and Picture Data

James A. Cutts

(NASA-CR-141966) MARINER MARS 1971
TELEVISION PICTURE CATALOG. VOLUME 1:
EXPERIMENT DESIGN AND PICTURE DATA (Jet
Propulsion Lab.) 430 p HC \$11.25 CSCL 03B
G3/91 06583 N75-15564
Unclassified

JET PROPULSION LABORATORY
CALIFORNIA INSTITUTE OF TECHNOLOGY
PASADENA, CALIFORNIA

June 30, 1974



NATIONAL AERONAUTICS AND SPACE ADMINISTRATION

Technical Memorandum 33-585

Volume I

Mariner Mars 1971 Television Picture Catalog

Experiment Design and Picture Data

James A. Cutts

JET PROPULSION LABORATORY
CALIFORNIA INSTITUTE OF TECHNOLOGY
PASADENA, CALIFORNIA

June 30, 1974

Prepared Under Contract No. NAS 7-100
National Aeronautics and Space Administration

Preface

The work described in this Technical Memorandum was performed under the cognizance of the Mariner Mars 1971 Project.

PRECEDING PAGE BLANK NOT FILMED

Acknowledgments

To list all of the many persons who have contributed in some way to the publication of this document would be a monumental task. However, I acknowledge particularly the support of R. H. Steinbacher, S. Z. Gunter, and T. E. Thorpe of the Mariner Mars 1971 Project. Among my colleagues on the television team, R. M. Batson, G. A. Briggs, M. E. Davies, and J. Neverka provided information which was included in the text and reviewed selected portions of the manuscript. W. Cameron and V. Pritts of the National Space Science Data Center also reviewed early drafts of the material.

I am grateful to D. J. Crosby for preparing footprint charts, L. N. Seeley for generating limb plots, T. C. Duxbury for providing information on satellite pictures, and M. D. Martin for production of almost all tables of computer-generated information.

I acknowledge with much appreciation the tireless efforts of J. D. Patterson for assembly and layout of the tables and of the almost 3000 narrow-angle frames.

Finally, my very special thanks to Ermine van der Wyk for her specialized knowledge, writing and editorial talents, enthusiasm, and dedication and who deserves most of the credit for successful completion of this document.

Contents

I. Project Background and Catalog Organization	1
A. Mission Summary	6
1. Mission Redesign	6
2. Mariner 9 Mission Description	6
B. Catalog Organization	12
References	14
II. The Television Experiment: Camera Description and Data Processing Summary	15
A. Camera Design	16
1. Mechanical Design	16
2. Electronic Design	16
3. Automatic Exposure Control	16
4. Camera Performance	20
B. Television Experiment Summary	22
1. Mariner 9 Adaptive Capability	22
2. The Science Cycles	27
3. Pre-orbital Science	29
4. Reconnaissance Coverage	29
5. Mapping Coverage	31
6. Extended Mission	34
References	35
III. Television Camera Calibration and Data Products	37
A. Television Camera Calibration	37
1. Preflight Calibration	37
2. Inflight Camera Performance Verification	38
B. Camera Performance	38
1. Geometric Characteristics	38
2. Photometric Characteristics	41
3. Resolution and Focus	45
4. Noise Level	46
C. Television Experiment Data Processing	49
1. Video Data Products	51

Contents (contd)

2. Picture Summaries and Navigation Data	51
3. Graphical Data, Photomosaics, and Maps	58
References	61
IV. Real-Time Pictures	63
A. Mission Test Computer and Mission Test Video System	63
B. Picture Supporting Information	66
1. Picture Identification	66
2. Picture Geometry Predicts	66
3. Telemetry Errors	66
4. Electronic Gray Scale	67
C. Image Processing	67
1. Digital Processing	67
2. Enhancement Details	67
3. Experiment Data Record	74
D. Image Display and Film Processing	75
1. Negatives and Film Transparencies	75
2. Contact Prints and Enlargements	75
3. Optimal Display of Film Copies	75
References	77
V. Reduced Data Record	79
Reference	81
VI. Rectified and Scaled Picture Data	83
A. Processing Details	84
References	89
VII. Photographic Mapping, Geology, and Cartography	91
A. Photographic Mapping (Wide-Angle Pictures)	91
1. The Dust Storm	91
2. Mapping Sequence Design	92
3. Mapping the North Polar Collar	93
4. Quality of the Mapping Pictures	96

Contents (contd)

B. Geology (Narrow-Angle Pictures)	97
1. Systematic Sampling	97
2. Special Targets and Stereo Coverage	97
3. Viking Landing Sites	97
C. Cartography	97
References	234
 VIII. Polar Studies	 235
A. Fixed Feature Observations	235
1. Wide-Angle Pictures	235
2. Narrow-Angle Pictures	240
B. Frost Studies	243
1. Mare Australe Quadrangle: Wide- and Narrow-Angle Frames	243
2. North Polar Cap and Haze Cover	245
References	300
 IX. Geodesy	 301
A. Mariner 9 Geodesy Data	302
B. Control Net	305
C. Central Meridian	312
References	312
 X. Variable Surface Features	 313
A. Observational Strategy	313
B. Data Reduction	314
References	328
 XI. Atmospheric Photography	 329
A. Global Pictures	330
B. Targeted Pictures	336
C. Limb Pictures	339
D. Terminator Pictures	340
References	388
 XII. Satellites	 389
References	402

Contents (contd)

Appendix A. Martian Nomenclature	403
References	414
Appendix B. Mars Data	415
Appendix C. Technical Terms and Acronyms	417

Abstract

This document is a compilation of Mariner 9 television data which have been arranged and edited to help the serious scientific user in the study of the planet Mars and of its two satellites, Phobos and Deimos. Although only a part of the entire data base can be reproduced in a document of this size, an attempt has been made to indicate its size and availability. The concept of the basic mission, camera characteristics, and various processing techniques of the raw television data recovered from the spacecraft are discussed. In later sections, data are arranged into disciplines: mapping and geology, polar studies, geodesy, variable surface features, atmospheric phenomena, and satellites. Reproduction and arrangements of approximately 3000 individual pictures and photomosaics are presented.

I. Project Background and Catalog Organization

In 1968, the National Aeronautics and Space Administration authorized the Mariner Mars 1971 Project—a dual-spacecraft mission to Mars. The objectives of this mission were to map the surface of the planet and to observe the dynamic characteristics of the surface and atmosphere from orbit for a minimum period of 90 days.

The spacecraft that were to achieve these objectives were similar in design to the successful Mariners 6 and 7, launched in 1969, with modifications as necessary to convert from a flyby to an orbiter mission (Ref. I-1). Mariners 8 and 9 (Fig. I-1) were to be three-axis inertially stabilized with the solar panels always facing the Sun and with the roll position about the Sun controlled by a star tracker pointed nominally at the star Canopus. Six experiments were carried as part of the science payload: television, ultraviolet spectroscopy, infrared spectroscopy, infrared radiometry, S-band occultation, and celestial mechanics (see Table I-1). Two experiments (S-band occultation and celestial mechanics) utilized the radio telemetry subsystem to derive data; the others required specially developed instruments. These science instruments (infrared radiometer, infrared and ultraviolet spectrometers, and wide- and narrow-angle television cameras) were mounted, boresighted on a special two-degree-of-freedom turret called the scan platform (Fig. I-2). This arti-

culating mount provided a pointing selection capability of 215° in azimuth and 69° in elevation. The fields of view, relative coverages, and boresight relationships of each instrument are shown in Fig. I-3; Fig. I-4 shows their spectral ranges.

Designed into the two identical spacecraft were the capabilities of either temporarily storing science data with a digital tape recorder or transmitting it immediately (in real time) back to Earth. The real-time capability was available only for non-television data. The capacity for more than 30 pictures, each comprising more than 5 million digital bits of information, was available on the tape recorder. The spacecraft's telecommunications subsystem, in conjunction with the 64-m (210-ft) antenna at the Goldstone tracking station, was capable of transmitting these images in association with other science data at rates ranging from 1012 to 16,200 bits per second.

Each spacecraft also could execute a complex data-acquisition plan that had been programmed on the ground and then telemetered to the spacecraft for storage in the memory of the central computer and sequencer (CC&S). A similar CC&S had been carried on the previous Mariner mission to Mars and had enabled the spacecraft to perform data-taking

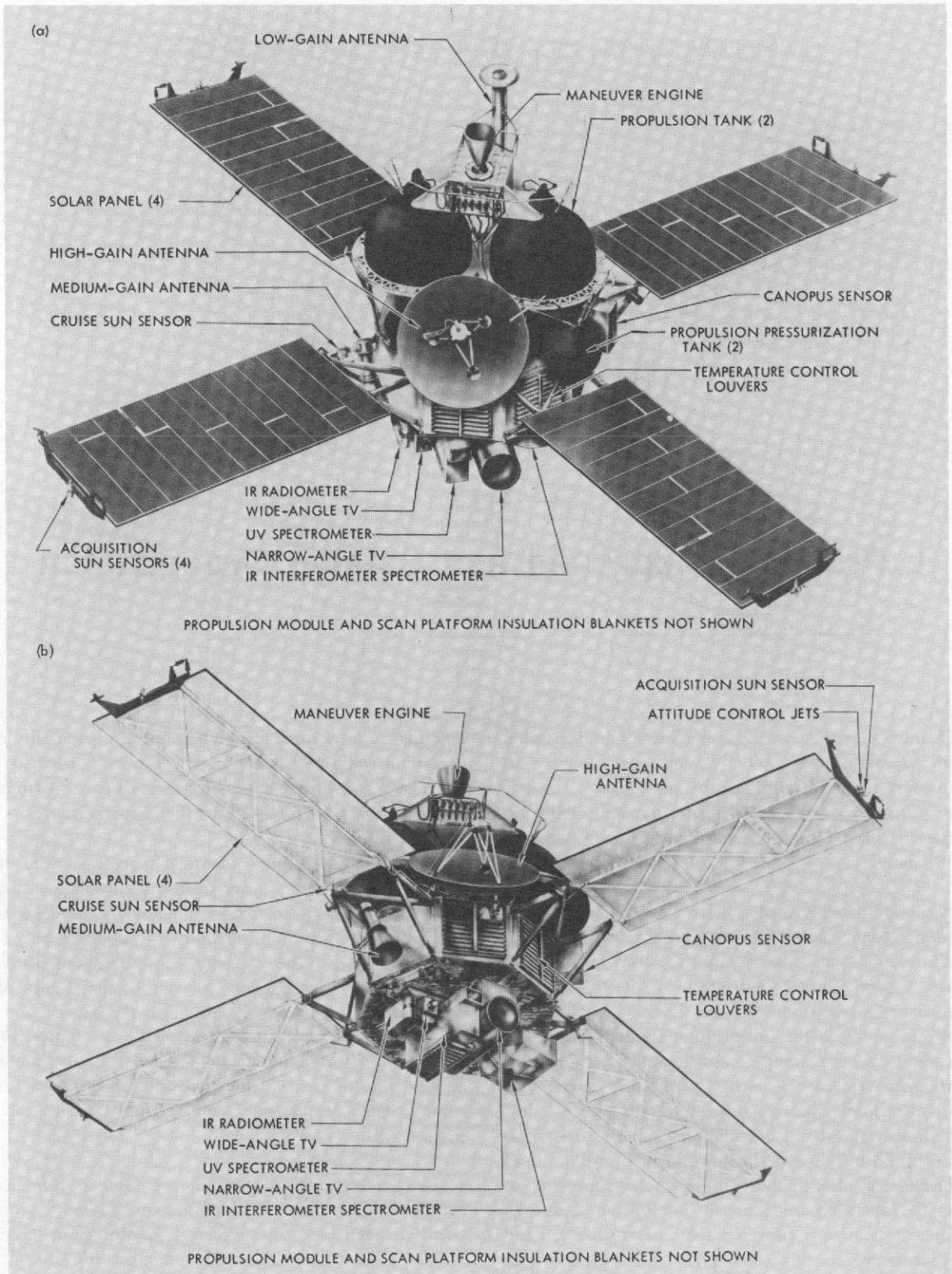


Fig. I-1. Mariner 9 spacecraft configuration. (a) Top view. (b) Bottom view.

Table I-1. Mariner 9 science experiments and Principal Investigators

Experiment	Instrument	Instrument weight, kg	Principal Investigator
Television	Television cameras	26.3	Mr. H. Masursky, ^a U. S. Geological Survey, Flagstaff Dr. G. Briggs, JPL Dr. G. de Vaucouleurs, University of Texas Dr. J. Lederberg, Stanford University Dr. B. Smith, New Mexico State University
Ultraviolet spectrometer	Ultraviolet spectrometer	15.6	Dr. C. Barth, University of Colorado
Infrared spectroscopy	Infrared interferometer spectrometer	24.1	Dr. R. Hanel, Goddard Space Flight Center
Infrared radiometry	Infrared radiometer	3.6	Dr. G. Neugebauer, California Institute of Technology
S-band occultation	None	—	Dr. A. Kliore, JPL
Celestial mechanics	None	—	Mr. J. Lorell, ^a JPL Dr. I. Shapiro, Massachusetts Institute of Technology
Total 69.6			

^aTeam Leader.

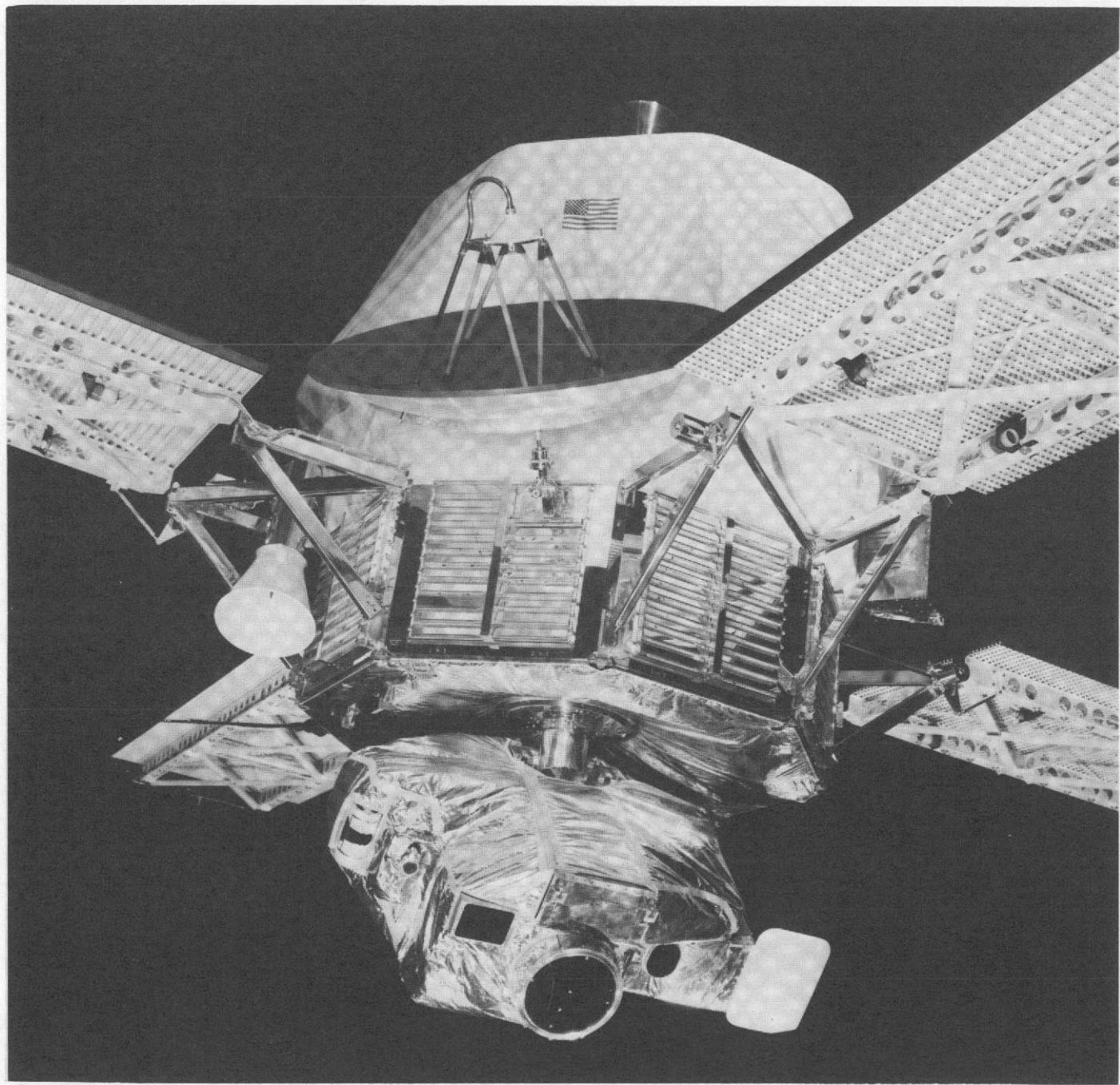


Fig. I-2. Science instruments mounted on scan platform.

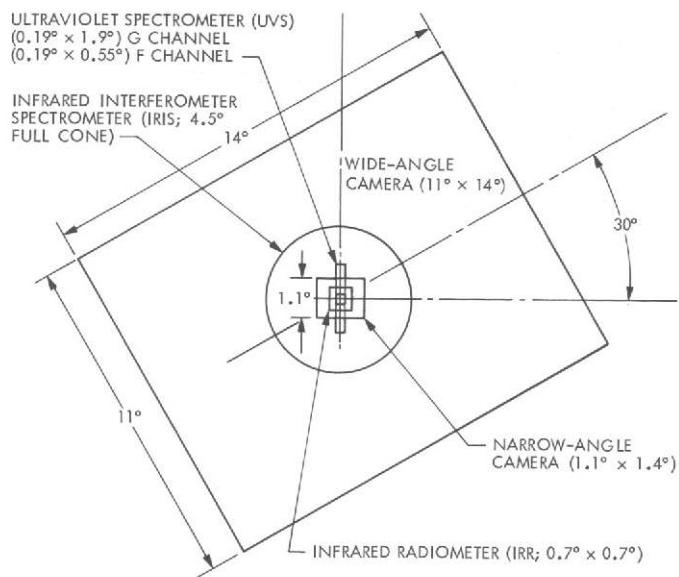


Fig. I-3. Nesting field-of-view configuration of the boresighted scan platform instruments.

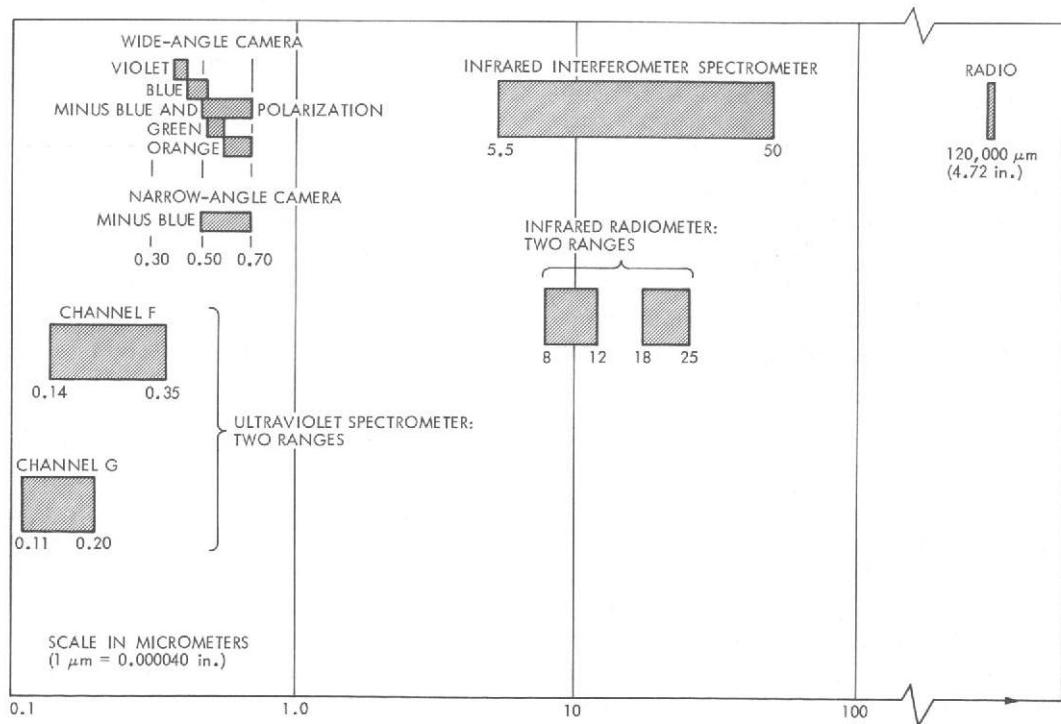


Fig. I-4. Spectral ranges of instruments.

sequences loaded before or soon after launch. For Mariners 8 and 9, the intention was to update the CC&S periodically while in orbit. This avoided the necessity for carefully timed and sequenced commands from the ground stations during the data-acquisition sequences, and therefore permitted sequences of greater complexity.

The stored sequence capability of the Mariner spacecraft was an advantage to the concept of the 1971 Mars orbiter, but design flexibility also was required so that the mission could be restructured as new and unexpected phenomena were observed. This "adaptive mode" capability was a major new feature of the Mariner Mars 1971 Project.

A. Mission Summary

Prelaunch planning encompassed two separate, but complementary, missions. The orbit of each spacecraft was optimized to match the corresponding objective (Ref. I-2).

The first spacecraft to be launched was scheduled for insertion into a 12-h, near-polar (80° inclination) orbit with a perapsis altitude of 1250 km. The primary objectives of this first mission were to map systematically at least 70% of the planet's surface, to study in detail the polar regions, to take pictures allowing a detailed geodetic network to be constructed, and to conduct various experiments with the non-visual instruments.

The second spacecraft was to be inserted into a 20.5-h, 500° inclination orbit with a periapsis altitude of 850 km. The 20.5-h orbital period was chosen because it is a 5/6 multiple of the Martian sidereal rotation period, allowing the spacecraft ground track to cover six sectors of the planet separated by 60° of longitude in 5 days with the ground tracks repeated each 5 days. The primary objectives of this mission were to study the time-variable features of the Martian surface and the dynamics of the atmosphere. In addition, the 850-km periapsis altitude allowed the acquisition of the data with the highest resolution of the two missions.

1. Mission Redesign

The failure of Mariner 8 at launch required the first of several mission redesigns. With only a single spacecraft remaining, it was decided to try to accomplish in the remaining flight some of the objectives of both of the original missions. During the few weeks that remained in the 1971 launch window opportunity, a compromise mission was developed that retained the major objectives of each of the original missions, although in somewhat degraded form. The orbit selected had a 12-h period, 65° inclination, and periapsis altitude of 1350 km (Fig. I-5). The 1350-km nominal periapsis altitude was selected

to enhance the possibility that only one orbit trim maneuver would be needed after insertion to correct the orbital period. It was selected slightly larger than the optimal value of 1250 km for television mapping. The 12-h period was selected because it yielded the maximum data return from the planet, as it was possible to play back two tapeloads of data each day. The 65° inclination represented a compromise between the 80° orbit, which would have given excellent polar coverage, and the 50° inclination orbit, which would have allowed better observations in the mid-latitudes near high noon for study of the variable surface features. The ellipse orientation angle (Fig. I-6) selected for this compromise orbit was 140° . This was about 20° larger than the value that corresponded to the minimum rocket engine impulse required for the orbit insertion maneuver, but provided improved long-range (global) viewing of the illuminated disk of the planet early in the mission.

2. Mariner 9 Mission Description

Mariner 9 was successfully launched from Cape Kennedy, Florida, on May 30, 1971, and 6 days later, on June 5, a planned trajectory correction was made. This maneuver was so precise and Martian ephemeris data and spacecraft tracking calculations were determined with such accuracy that no other midcourse corrections were necessary for the entire 167-day flight to Mars. Details of the orbital operation sequences (Ref. I-3) were designed and studied during the Earth-to-Mars transfer trajectory flight (see Fig. I-7).

The insertion into planetary orbit, on November 14, 1971, gave Mariner 9 the distinction of being the first man-made object to orbit another planet. The 1398-km periapsis altitude of the insertion orbit was accurate to within 50 km from the aiming point (Fig. I-8), and the initial period of 12 h and 34 min was within seconds of the time desired for the insertion orbit. The non-synchronization with Earth provided the timing slip until coincidence of the Goldstone 64-m antenna zenith position and periapsis was obtained and a trim maneuver "locked" the two into synchronization. From that time on, data could be transmitted to the Goldstone antenna only during the even revolutions of Mariner 9, which became known as the zenith passes. Data acquired on odd, or nadir, revolutions (see Fig. I-5) had to be stored on the tape recorder for about 7 h before they could be played back to Goldstone on the subsequent zenith pass.

It had been planned that, upon arrival at Mars, Mariner would almost immediately begin the systematic medium-resolution television mapping and simultaneously acquire and record boresighted spectral and radiometric data. However, the Martian dust storm, first observed through Earth-based telescopes in late September, was still in full development,

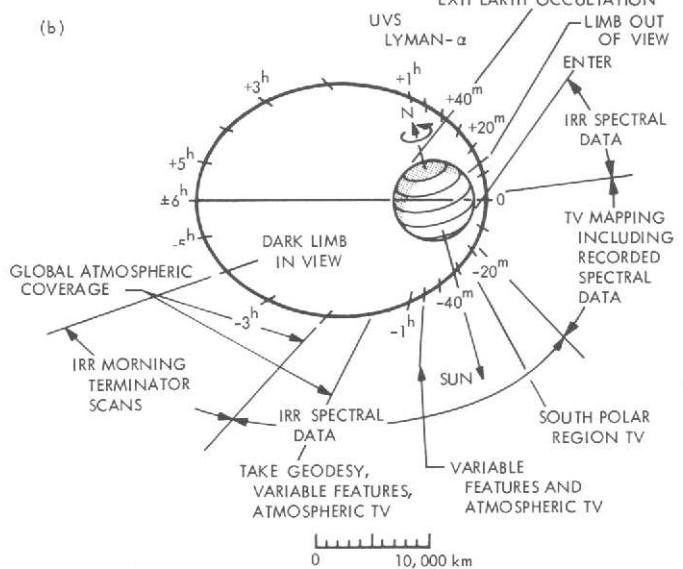
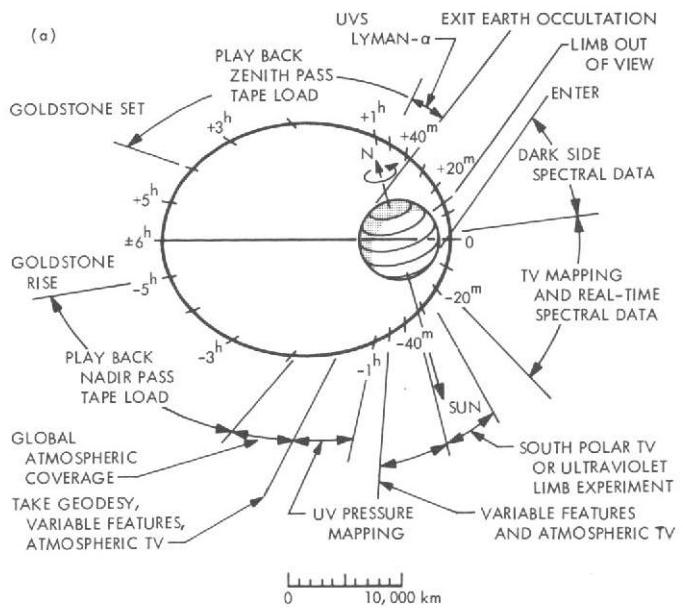


Fig. I-5. Single spacecraft orbital plan. (a) Goldstone zenith pass (even revolutions). (b) Goldstone nadir pass (odd revolutions).

obscuring the entire surface of the planet with the exception of the bright south polar cap and four dark spots in the equatorial regions. The well laid plans had to be abandoned. The hope of some science investigators to glimpse a Martian dust storm were fully realized.

On November 16, during Rev 4, the spacecraft's orbital period was reduced by more than 30 min by a 6-s firing of the rocket engines (see Table I-2). This maneuver was intended to

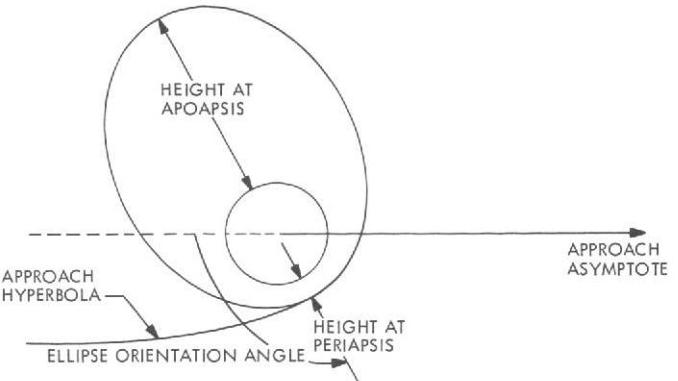


Fig. I-6. Definition of ellipse orientation angle.

preserve for many months the relationship of the Goldstone 64-m-antenna zenith position with spacecraft periapsis that was reached on Rev 4. An orbital period of 11 h, 58 min, 52 s was desired for synchronization, but because of the previously unknown gravity-field variation of Mars, the actual average orbital period achieved was slightly shorter (Fig. I-9). The resulting small drift out of synchronization was tolerable for several weeks, but in time would have curtailed the duration of tape playback of data from the nadir pass (see Figs. I-10 and I-5a).

During the next 38 days in orbit, new science data-acquisition sequences were designed and implemented (Fig. I-11). The Martian satellites Phobos and Deimos received unexpected attention and were frequent targets of the scan platform instruments. While the continued probing of the dust storm on Mars itself had scientific significance, most investigators anxiously awaited some sign that the dust storm was subsiding. Mission parameters such as orbital period, orbital height, and communications performance were analyzed thoroughly by the mission design team so that, when the atmosphere was cleared of the obscuring dust, the optimal plan for observing fixed and variable features on Mars would be immediately available.

On December 30 (Rev 94), a second trim maneuver adjusted the orbital period, correcting periapsis-passage timing with the view period of the 64-m antenna (Fig. I-9). This new orbit also established a higher periapsis altitude, which provided a broader area coverage for each television picture, thus requiring fewer pictures to complete the original objective of mapping 70% of the surface of Mars. The broader area coverage for each picture resulted in a corresponding loss of surface resolution. The fewer pictures required allowed the mapping to be conducted before communications capability deteriorated, but still required stretching the standard mission 20 days beyond the planned 90 days.

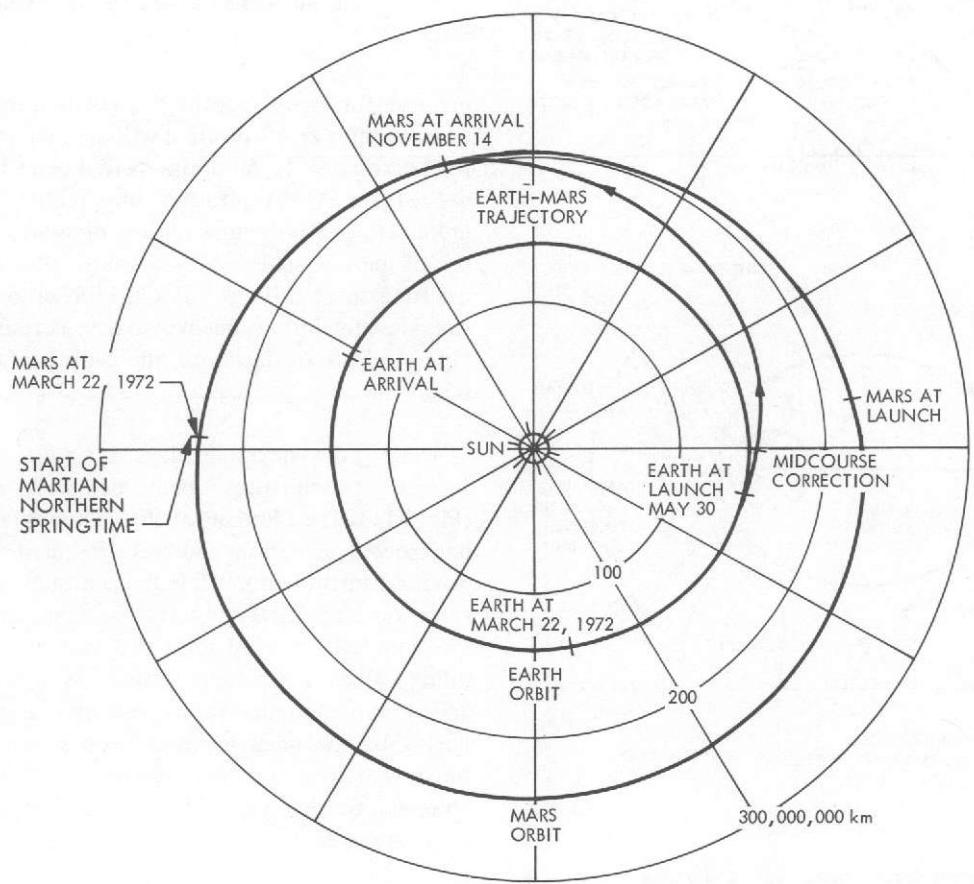


Fig. I-7. Earth-Mars heliocentric view with spacecraft trajectory.

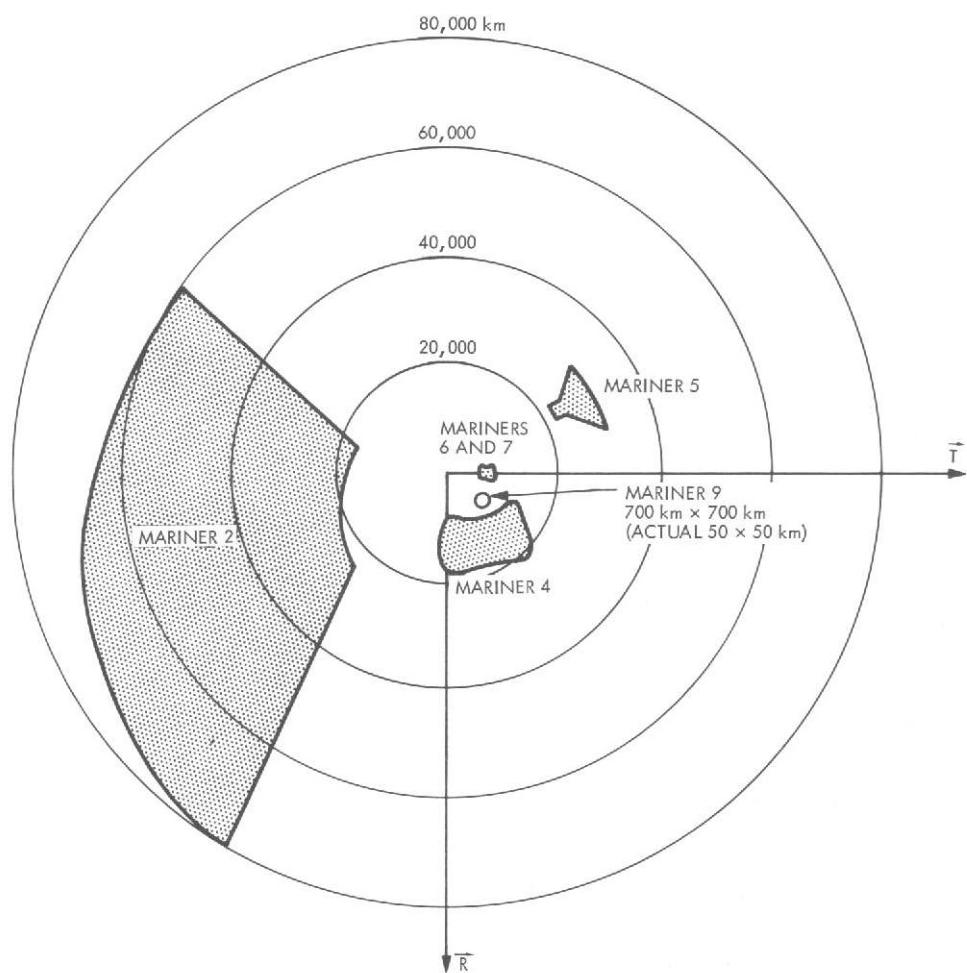


Fig. I-8. Relative size of interplanetary mission aiming zones.

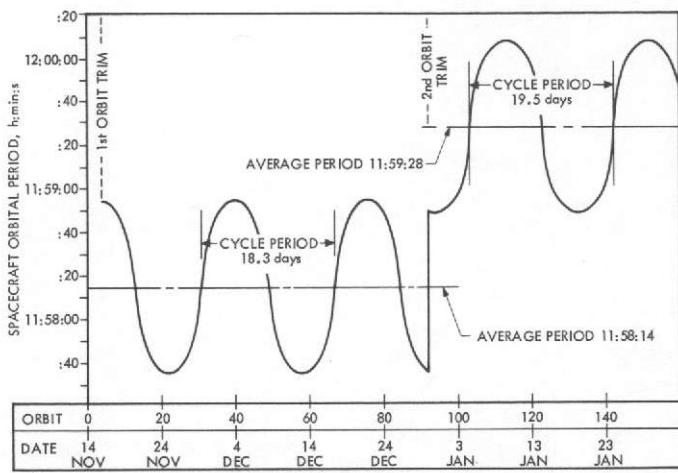


Fig. I-9. Orbital period variation.

In three 20-day cycles between Revs 100 and 217, the surface between 65°S and 45°N latitude was systematically covered by the television cameras and by the other scan platform instruments. The south polar regions, including the area of the small summertime polar frost cap, were also frequent targets. The northern hemisphere from about 45° to the pole was obscured by a seasonal haze cover, or polar "hood." Television pictures of this region showed little surface detail at that time. The successful acquisition of haze-free medium-resolution television pictures of the rest of the planetary surface on Rev 217 signalled the end of the Mariner 9 standard mission. However, the acquisition of science data continued through an extended mission that lasted for another 8 months.

During the extended mission period, various problems were encountered as a result of the fact that the Mariner 9 mission was optimized around the original concept of the 90-day standard mission. The first of these problems involved the communication of science data at high rates from the spacecraft to Earth. The apparent direction of Earth from Mariner 9 changed continuously during the mission because the orientation of the spacecraft in space nominally was fixed with respect to the directions of the Sun and Canopus. The high-gain antenna was not steerable, however, but had a fixed pointing direction optimized for best communication during the first 90 days in orbit. Beyond that period, high-rate data communications rapidly deteriorated; in order to continue the recovery of data, a high-gain antenna maneuver (HGAM) was necessary to point the antenna at Earth for the duration of each data transmission. These nonpropulsive maneuvers caused the spacecraft to be reoriented in space, away from the Sun and Canopus, utilizing gyros to maintain stability. Upon their completion the spacecraft was reoriented with solar panels facing the Sun, and the guide star, usually Canopus, was reacquired.

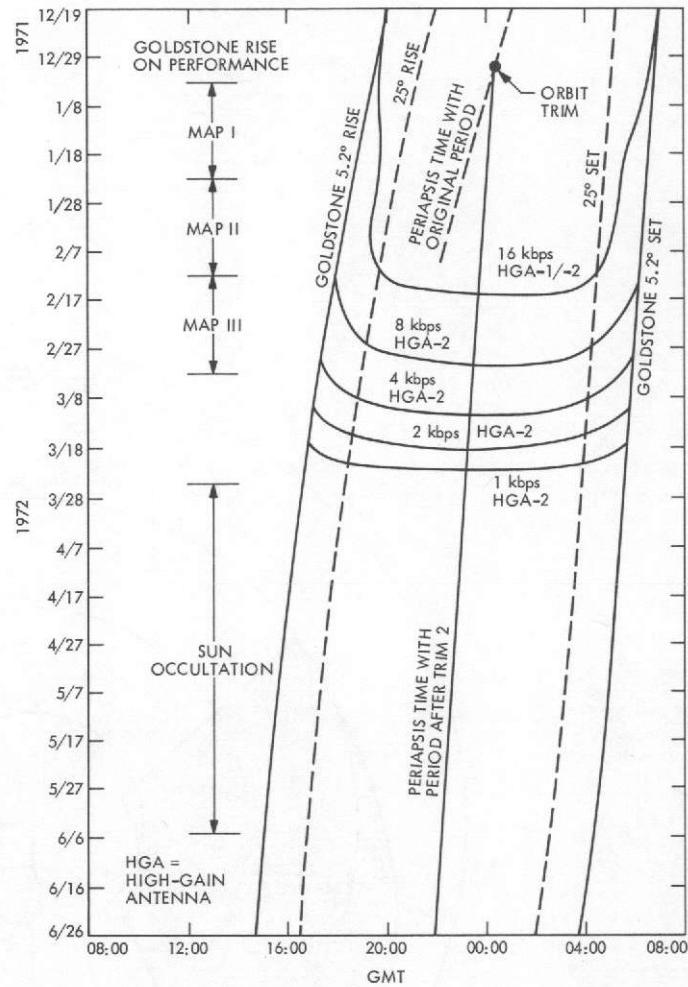


Fig. I-10. Goldstone rise and set times on performance for various data rates vs days.

The first test of a HGAM was made on March 23, 1972, for relay to Earth of the last scan platform science data recording before the spacecraft began a series of solar occultations (Fig. I-11). After this successful test, the spacecraft's trajectory cut through the shadow of the planet on each revolution requiring the use of the battery to maintain vital systems functions. A battery-recharging sequence then was required in readiness for the next occultation. For a period of 60 days there was insufficient remaining solar panel power to conduct scan platform science activities, although significant S-band occultation data were obtained during this time (Figs. I-11 and I-12).

Reconnaissance of the planet with the scan platform instruments began again on June 9 with Rev 416. A considerable change in the seasonal state of Mars had transpired during the solar occultation period. Most of the haze had disappeared from the north polar region, permitting television coverage of

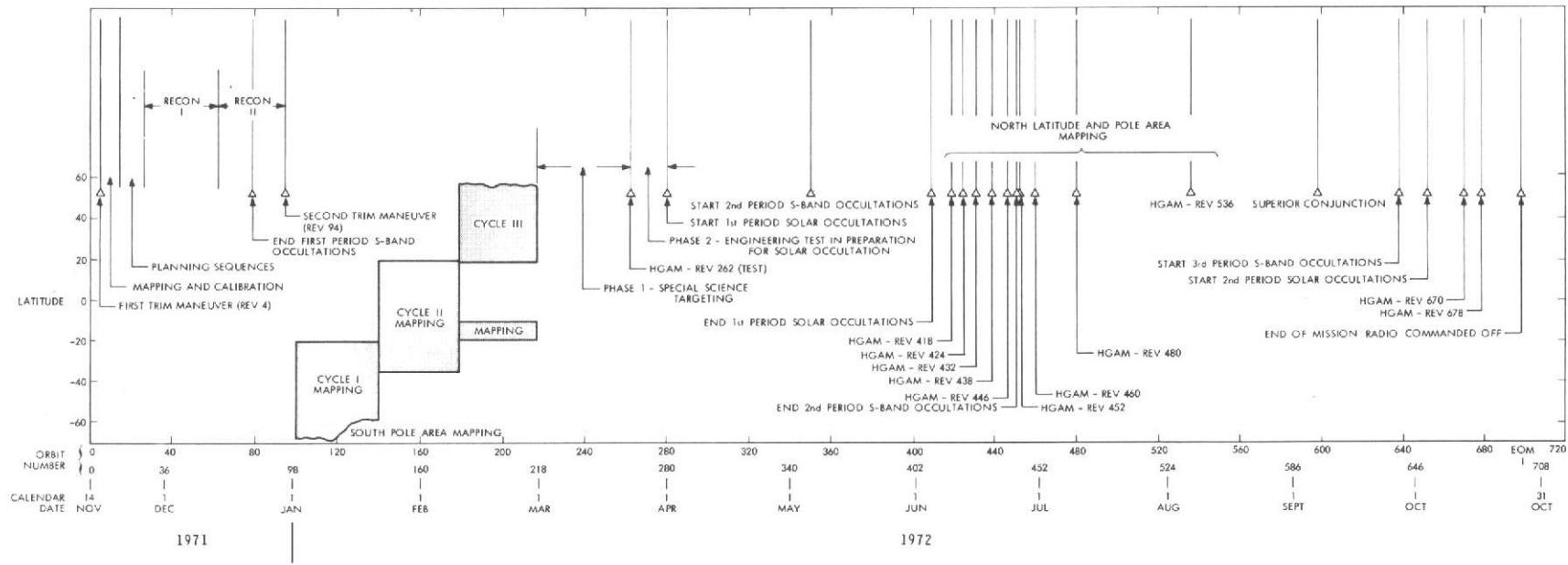


Fig. I-11. Mission sequences and planetary coverage as a function of time in orbit.

Table I-2. Mariner 9 orbit parameters

Event	Period of orbit, h:min:s	Periapsis, km	Inclination, deg
After orbit insertion	12:34:01	1398	64.4
After first orbit trim (Rev 4)	11:58:14 (mean period)	1387	64.4
After second orbit trim (Rev 94)	11:59:28 (mean period)	1650	64.4

the surface in that part of the planet, including the seasonal retreat of the frost caps. Each week during June, July, and August 1972, the spring season in the northern hemisphere, a tapeload of data was recorded on one or two revolutions, and the HGAM was executed for science data playback. These playbacks occurred only once each week as the HGAM sequences were particularly extravagant in the use of the limited supply of the compressed gas that was expelled from jets located on the ends of the solar panels (see Fig. I-1b) to provide spacecraft attitude control.

One reason for extending the life of the spacecraft by reducing the frequency of data-acquisition sequences was to continue observations as far as possible into the Martian northern summer season. The other reason was the opportunity to test one of the predictions of Einstein's theory of general relativity. The opportunity for the relativity test arose when the changing Earth-Mars-Sun relationship brought Earth and Mars to diametrically opposite sides of the Sun (superior conjunction), causing the path of the radio signals to and from Mariner 9 to approach closely the surface of the Sun. The Einstein theory predicted that the gravitational field of the Sun would cause a 200- μ s increase in the time for a radio signal to travel from Earth to Mariner 9 and back again. Careful measurements of the round-trip time were made by the Mariner 9 celestial mechanics experiment team for several weeks near solar conjunction (Ref I-4). During this period, there was a deterioration in the quality of the radio signal because of its passage through the solar corona. This affected the precision of the general relativity test and also increased the noise level in the telemetered scan platform science data. Acquisition of more of the science instrument data was postponed until the line of sight to the spacecraft had moved sufficiently away from the Sun for clear telemetry signal reception.

High-gain antenna maneuvers for science data playbacks were performed next on October 13 and 17, and data from Revs 667, 668 and 675, 676 were successfully transmitted. However, by that time the supply of compressed gas for the attitude control subsystem was so low that it seemed unlikely that another HGAM could be completed successfully. On October 27, 1972, telemetry data indicated that the space-

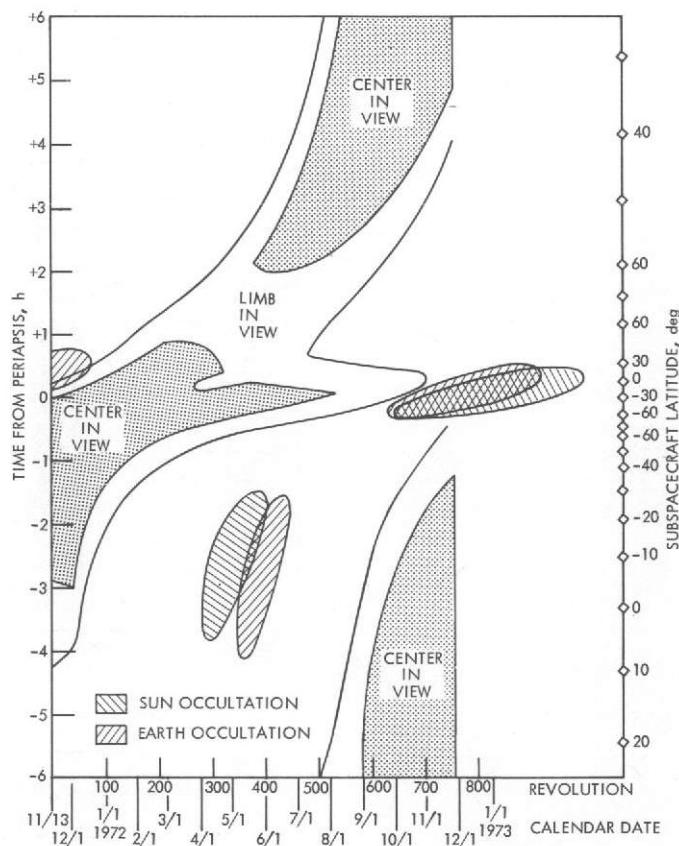


Fig. I-12. Mars limb and center viewing times and solar and Earth occultation times: Revs 0-760.

craft was no longer capable of holding a fixed attitude, and a final command was sent from Earth to turn off the spacecraft's radio transmitter. The slowly tumbling Mariner 9 will remain in orbit for a minimum of 50 yr before it enters the atmosphere of Mars and disintegrates.

B. Catalog Organization

The purpose of this Mariner Mars 1971 Television Picture Catalog, Volume I, is to provide a comprehensive guide to the

Mariner 9 television experiment and the imaging data that resulted from observations during almost 1 yr of spacecraft operation in orbit around Mars.

This Catalog describes the detailed objectives of the television experiment and the way in which these objectives were realized. The design of the cameras, their inflight performance, and the processing of the pictures is discussed. A detailed description is given of the evolution of the television experiment as new problems emerged and new information was acquired about the planet and its two satellites. The intention is to indicate to the serious scientific user not only what was done, but why and how it was done. As an additional aid to the user of the television imagery, the data have been organized into six separate areas of scientific interest which correspond closely to the discipline groups (see Section II) that were organized to plan details of the mission. Reproductions and arrangements of more than 3000 individual pictures and mosaics are presented according to discipline area or subject matter. Information concerning the size, quality, and availability of the entire Mariner 9 television data base is also included.

A more detailed chronological summary of each event during the Mariner 9 mission pertinent to the mission analysis aspects of the television experiment and other information which complements that presented in this document appear in Volume II and Addendum I of the Mariner Mars 1971 Television Picture

Catalog. These two companion volumes include orthographic and Mercator plots of all pictures and pertinent numerical information for picture center points. Other comprehensive information on the technical aspects of the mission and the results of scientific analyses derived from Mariner 9 appear in Refs. I-5 through I-9.

Although some readers may object to the use of jargon in a document intended for general scientific use, many of these terms used during the Mariner 9 mission have become firmly established in the scientific community, and it would be difficult to reach agreement on palatable alternatives. A glossary of standard technical terms and acronyms is included as Appendix C.

The systematic coverage of Mars obtained by Mariner 9 has resulted in detailed new maps of the planet which display the many topographic features discovered in television pictures. The International Astronomical Union has assigned to these features new names that complement the classical names of the light and dark markings given by astronomers. Both systems of nomenclature are described in Appendix A. In addition to the formal or official names, various informal names have been used in publications utilizing the Mariner 9 television pictures. In this document both of the formal naming schemes are used as well as some of the informal names originated by the Mariner 9 experimenters.

References

- I-1. Steinbacher, R. H., and Gunter, S. Z., "The Mariner Mars 1971 Experiments: Introduction," *Icarus*, Vol. 12, p. 3, 1970.
- I-2. Steinbacher, R. H., and Haynes, N. R., "Mariner 9 Mission Profile and History," *Icarus*, Vol. 18, p. 64, 1973.
- I-3. Haynes, N. R., Bollman, W. E., Neilson, R. A., Nock, K. T., and Travers, E. S., *Mariner Mars 1971 Adaptive Mission Planning*, AIAA Paper 72-944 presented at the AIAA/AAS Astrodynamics Conference, Palo Alto, Calif., Sept. 11-12, 1972.
- I-4. Lorell, J., Anderson, J. D., Jordan, J. F., Reasenberg, R. D., and Shapiro, I. I., "Celestial Mechanics Experiment," *Mariner Mars 1971 Project Final Report. Volume V: Science Experiment Reports*, Technical Report 32-1550, p. 13, Jet Propulsion Laboratory, Pasadena, Calif., 1973.
- I-5. *Mariner Mars 1971 Project Final Report. Volume I: Project Development Through Launch and Trajectory Correction Maneuver*, Technical Report 32-1550, Jet Propulsion Laboratory, Pasadena, Calif., 1973.
- I-6. Mariner Mars 1971 Science Experimenter Teams, *Mariner Mars 1971 Project Final Report. Volume II: Preliminary Science Results*, Technical Report 32-1550, Jet Propulsion Laboratory, Pasadena, Calif., 1972.
- I-7. *Mariner Mars 1971 Project Final Report. Volume III: Mission Operations System Implementation and Standard Mission Flight Operations*, Technical Report 32-1550, Jet Propulsion Laboratory, Pasadena, Calif., 1973.
- I-8. Mariner Mars 1971 Science Experimenter Teams, *Mariner Mars 1971 Project Final Report. Volume IV: Science Results*. Technical Report 32-1550, Jet Propulsion Laboratory, Pasadena, Calif., 1973.
- I-9. Mariner Mars 1971 Science Experimenter Teams and Science Evaluation Team Working Groups, *Mariner Mars 1971 Project Final Report. Volume V: Science Experiment Reports*, Technical Report 32-1550, Jet Propulsion Laboratory, Pasadena, Calif., 1973.
- I-10. *J. Geophys. Res.* (The Mariner 9 Mission), Vol. 78, No. 20, pp. 4007-4440, July 10, 1973.
- I-11. *Globe Supplement to The Many Faces of Mars*, Technical Memorandum 33-654, Jet Propulsion Laboratory, Pasadena, Calif., 1973.

II. The Television Experiment: Camera Description and Data Processing Summary

The overall objective of the television experiment was to provide imaging data that would vastly extend man's scientific knowledge of Mars, and thus provide additional insights into the nature and origin of the entire solar system. To achieve this goal, the Mariner 9 television studies consisted of two types of investigations: fixed-feature and variable-feature. The objectives of each investigation, as originally stated, were (see Ref. II-1):

Fixed-feature investigation

- (1) To obtain a broad range of image information to be used for regional stratigraphic studies of tectonic features, crater configuration and distribution, and local surface environment.
- (2) To measure, by photometric and photogrammetric analysis, surface slopes and elevations; to determine surface brightness and albedo; and to perform analyses related to improving the accuracy of the photometric function for various regions on Mars.
- (3) To obtain an improved value for the shape of the planet, and thereby investigate possible departures from hydrostatic equilibrium.

- (4) To study the surface characteristics of Phobos and Deimos.

Variable-feature investigation

- (1) To obtain information on atmospheric structure and circulation.
- (2) To obtain details of diurnal and seasonal changes.
- (3) To obtain clues regarding the possibility of life on Mars.
- (4) To study the following specific phenomena:
 - (a) Wave of darkening.
 - (b) Polar caps and adjacent areas.
 - (c) Nightside atmosphere and surface fluorescence.
 - (d) Haze in the atmosphere.
 - (e) White "clouds" in nonpolar regions.

- (f) Dust clouds and dust storms.
- (g) Phenomena of possible exobiological significance.

At the inception of the Mariner Mars 1971 Project in 1968, the experiment's Principal Investigators and Co-Investigators, selected by the National Aeronautics and Space Administration, were organized into a collectively functioning television team. Scientific disciplines and technical task groups were formed to provide plans for instrument development and requirements for mission planning (see Ref. II-1). The organization of this television team at the arrival of Mariner 9 at Mars is shown in Fig. II-1.

A. Camera Design

The Mariner 9 television subsystem (TVS) consisted of two television cameras: one wide-angle (camera A; see Fig. II-2) and one narrow-angle (camera B; see Fig. II-3), mounted on the spacecraft's planetary scan platform. Supporting electronics for the cameras were located in the bus portion of the spacecraft. The wide- and narrow-angle optics and some parts of the electronics were identical to the equipment developed for the Mariner 6 and 7 television subsystem. Several modifications were made to create greater flexibility in camera operation and increased instrument reliability required for an extended orbital mission. An all-digital data storage subsystem was the major new feature in the electronic design. A simplified block diagram of one of the cameras is shown in Fig. II-4; a block diagram showing the camera signal processing is shown in Fig. II-5.

1. Mechanical Design

The wide-angle camera (nominal 50-mm focal length), which had a field of view of approximately 11° by 14° , utilized a six-element lens and was equipped with a filter wheel that could be commanded to place any one of eight spectral and/or polarizing filters in the optical path (see Table II-1, Figs. II-2 and II-6). The wheel could be advanced zero, one, or two steps between consecutive wide-angle pictures by ground command or could take two steps between each picture, cycling continuously through a four-filter sequence when in the automatic mode (see Section II-B).

The narrow-angle camera (nominal 500-mm focal length), which had a field of view of approximately 1.1° by 1.4° , utilized a 216-mm-diameter Schmidt Cassegrain telescope and the same type of video design as the wide-angle camera; it had a single fixed filter that passed all colors except blue

(Fig. II-3). Both cameras had focal plane shutters, similar to the type used on Surveyor and on Mariners 6 and 7 (Ref. II-2).

2. Electronic Design

After passing through the filter and the shutter, the optical image was focused onto a slow-scan vidicon, which was operated with a cathode-modulated electron beam. Vidicon electron beam focus, alignment, and vertical and horizontal deflections were performed magnetically. (Some of the significant instrument parameters are given in Table II-1.)

The video signal was processed by a video amplifier. The modulated baseband video from the vidicon photocathode was current-amplified by a preamplifier (maximum photocathode current was about 5 namp), then bandpass-filtered, amplified, and refiltered. The signal was then demodulated, synchronous with the vidicon cathode chopped input. The demodulated video signal was amplified and low-pass filtered to produce baseband video construction, which was converted to a digital signal that formed 832 9-bit words for each of the 700 television lines. The data signal was transmitted to the data automation subsystem (DAS), where it was rate-buffered and formatted for input to the spacecraft's digital tape recorder. There it was stored until it could be played back, at a lower bit rate, to the deep space stations and relayed to the Space Flight Operations Facility to be recorded and reconstructed into a picture. Up to 32 pictures could be stored in the recorder for later transmission to Earth. The 26-m (85-ft) antennas of the Deep Space Network were capable of receiving picture data, but at a much lower bit rate than the 64-m (210-ft) antenna at the Goldstone tracking station. Therefore, most picture playbacks used the 64-m antenna.

In addition to buffering the television data, the DAS provided timing control functions for the television sweep circuits. Figure II-7 shows the 84-s TVS-DAS interface timing between successive frames of a single camera. About 6 s after shuttering, an image was read at the rate of 700 lines/42 s, followed by 14 separate beam retraces to erase residual vidicon charge (29.4 s). The interleaving of camera sequences thus allowed alternating cameras to photograph at a maximum frequency of each 42 s.

3. Automatic Exposure Control

The DAS also selected one of a limited range of shutter speeds for each camera based on an "average" value extracted from the previous picture. This automatic exposure control (AEC) was implemented by summation of the 4 most significant bits of the 9-bit binary words. A sample consisted

TEAM LEADER
H. MASURSKY ^a
DEPUTY
B. SMITH ^a

DISCIPLINE GROUPS

ATMOSPHERIC PHENOMENA	GEODESY/ CARTOGRAPHY	GEOLOGY	VARIABLE SURFACE FEATURES	SATELLITE ASTRONOMY	POLAR PHENOMENA
C. LEOVY	G. de VAUCOULEURS	J. McCUALEY	C. SAGAN	J. POLLACK	B. MURRAY
G. BRIGGS E. SHIPLEY B. SMITH R. WILDEY J. POLLACK A. YOUNG	D. ARTHUR R. BATSON W. BORGESON M. DAVIES R. LEIGHTON A. YOUNG R. WILDEY	M. CARR W. HARTMANN R. SHARP L. SODERBLOM D. WILHELMs J. CUTTS D. MILTON B. MURRAY C. SAGAN	J. CUTTS J. LEDERBERG E. LEVINTHAL J. VEVERKA R. WILDEY A. YOUNG G. BRIGGS M. CARR G. de VAUCOULEURS J. POLLACK B. SMITH	D. MILTON M. DAVIES W. HARTMANN C. SAGAN J. VEVERKA B. SMITH A. YOUNG	J. CUTTS R. LEIGHTON J. LEDERBERG C. LEOVY R. SHARP L. SODERBLOM D. MILTON

TASK GROUPS

HARDWARE	MISSION ANALYSIS	DATA PROCESSING AND PROCESS CONTROL	MISSION OPERATIONS
B. MURRAY	G. BRIGGS	E. LEVINTHAL ^b	B. SMITH
W. BORGESON J. CUTTS R. LEIGHTON B. SMITH R. WILDEY A. YOUNG	W. BORGESON M. DAVIES D. MILTON J. POLLACK C. SAGAN B. SMITH	D. ARTHUR R. BATSON ^b G. BRIGGS ^b J. CUTTS M. DAVIES E. SHIPLEY ^b B. SMITH ^b L. SODERBLOM ^b J. VEVERKA ^b R. WILDEY ^b A. YOUNG ^b	R. BATSON G. BRIGGS M. CARR W. HARTMANN C. LEOVY J. McCUALEY B. MURRAY C. SAGAN

^aEx-officio members of all groups.

^bMember of the Process Control sub-group. A. Young and L. Soderblom are chairmen.

Fig. II-1. Mariner 9 television team matrix.

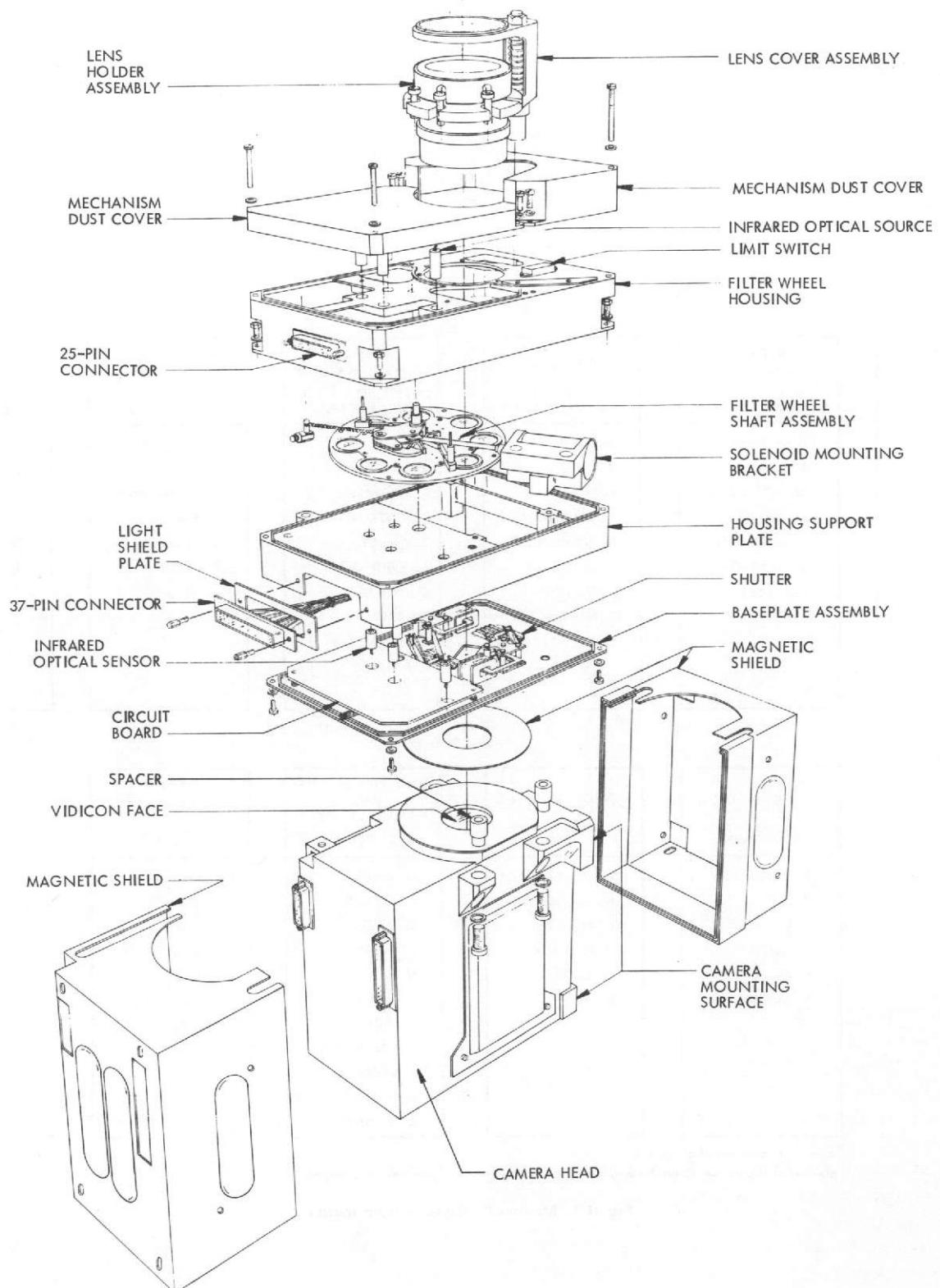


Fig. II-2. Wide-angle camera: exploded view.

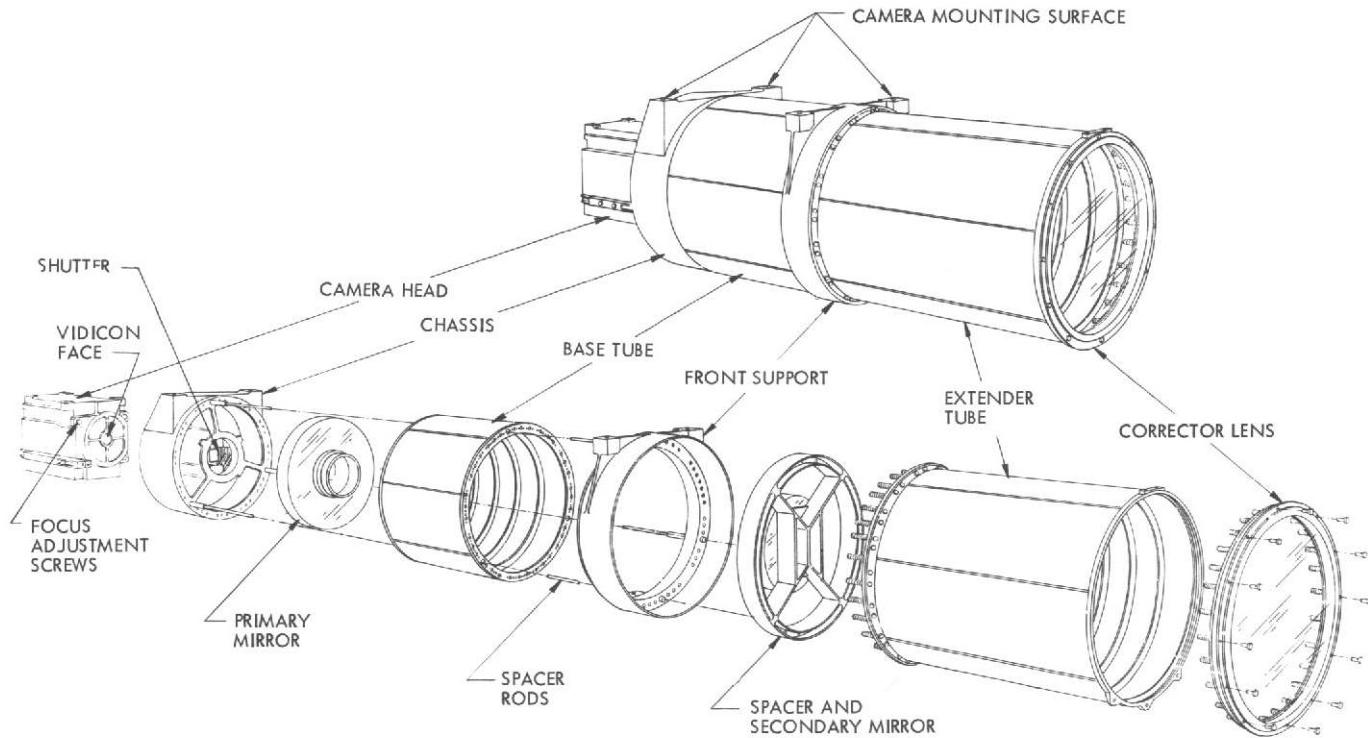


Fig. II-3. Narrow-angle camera: exploded view. The focal plane shutter is mounted directly in the camera chassis.

of 101 pixels from 44 selected television lines located in the top half of a television picture. Initially, the AEC maintained the shutter speed of the wide-angle camera at 96 ms and of the narrow-angle camera at 12 ms, with the ability to substitute one speed above or one speed below these values (wide: 48 or 192 ms; narrow: 6 or 24 ms). A change in shutter speed was desired for a subsequent picture when the sample averages were below $\frac{1}{4}$ (128 DN) or above $\frac{3}{4}$ (383 DN) of the camera's light-transfer scale (Fig. II-8). This plan was implemented by dividing the frame average signal from the wide-angle camera into 15 equal increments. The most desirable linear part of the camera's transfer corresponded to parts 4 through 11, or one-half of the dynamic range of the cameras. If the wide-angle camera were in the 96-ms exposure mode and the output fell in this range, then the AEC would retain 96 ms for the next exposure of the wide-angle camera and 12 ms for the narrow-angle exposure immediately following. With other frame average signals and at other initial exposure settings, different decisions regarding the subsequent exposure time were made as indicated in Fig. II-8. The first frame exposed in a photographic sequence was used to set the AEC and was not usually tape recorded. It was known as the "false-shuttered" frame. The AEC was capable of being overridden by ground command (see Section III-B). It was possible to take one single wide- or narrow-angle picture, wide- and narrow-angle pairs at selected points on the surface, or a mixed sequence of pictures.

4. Camera Performance

The resolution of surface features and of the area in the field of view of each camera was dependent on the slant range from the cameras to the planetary surface. With the cameras pointed vertically at the surface and the spacecraft at an altitude of 1500 km, surface resolution in the wide- and narrow-angle cameras corresponded to about 0.5 and 0.05 km per picture element (pixel), respectively. The picture format consisted of 832 pixels arranged on each of 700 lines (see Table II-1).

The vidicon cameras suffered from many distortions and imperfections. Ground and inflight calibrations were designed to measure these distortions and imperfections, and the ground calibration data also were used to correct or to compensate for them. Images of a flat field (light source of uniform areal intensity) appear in Figs. II-9a and II-9b. These specific frames were recorded on the Mariner 9 tape recorder during ground camera tests, but were played back after launch in a test of the spacecraft's telemetry subsystem. The small black fiducial, or reseau, marks are metallic spots deposited on the faceplate of the vidicon sensor to provide a geometric reference. Geometric distortion of the camera is apparent in the curvature and keystoning of the original linear and orthogonal arrangement of reseau marks. The effect of this distortion when a scene is imaged is shown graphically in the images of the RETMA target (Figs. II-10a and II-10b).

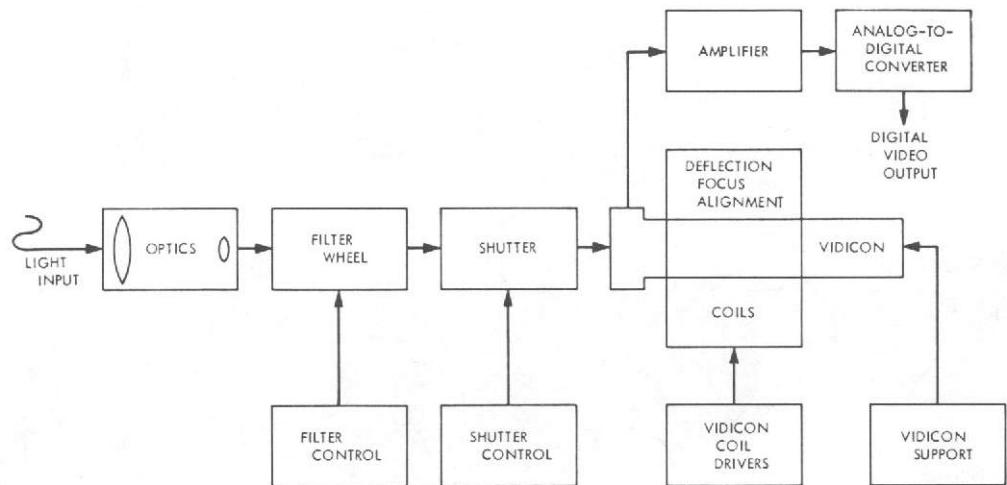


Fig. II-4. Block diagram of slow-scan television subsystem.

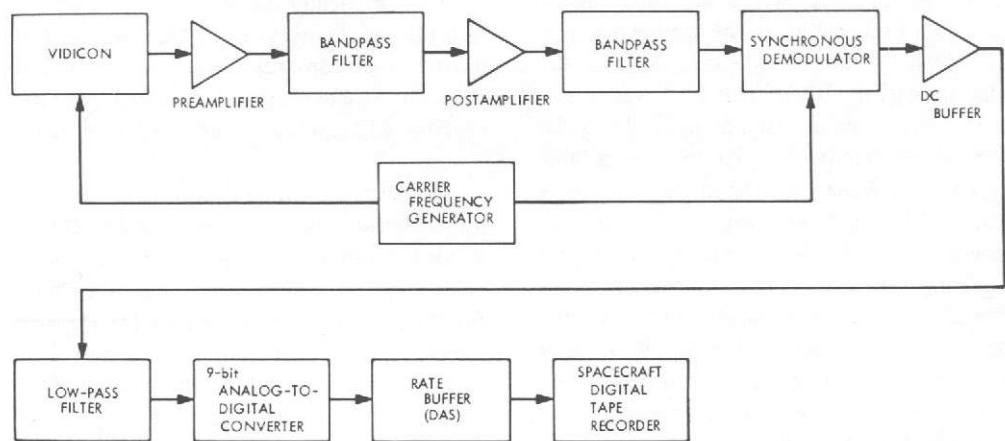


Fig. II-5. Video signal processing.

Table II-1. Optical parameters

Parameters	Wide-angle camera	Narrow-angle camera
Focal length, mm	52.267	500.636
f/number	4.0	2.35
T/number	4.46	3.55
Field of view, deg	13.47 X 10.45	1.41 X 1.09
Target size, mm	9.6 X 12.5	9.6 X 12.5
Number of scan lines	700	700
Number of samples/line	832	832
Readout time, s	42	42
Shutter speeds, s	0.003 to 6.144	0.003 to 6.144
Filters (effective wavelength ^a)		
Filter position (Fp)	2 4 6 8	
Medium bandpass	0.610, 0.545, 0.477, 0.414	
Filter position (Fp)	1 3 5 7	
Broad bandpass	0.560 0.565 0.565 0.565	0.588
Wide-angle camera polarization filter angle with vertical (line) axis	Fp 3 = 0° Fp 5 = 60° Fp 7 = 120°	

^aSolar spectral irradiance.

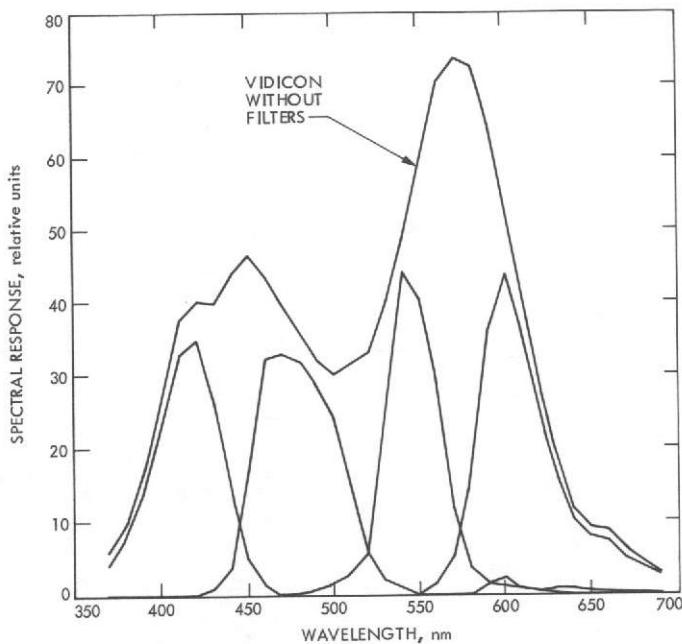


Fig. II-6. Television camera spectral response with color filters, based on component tests.

B. Television Experiment Summary

During the almost 1-yr period that the Mariner 9 television cameras photographed Mars and its satellites, the nature of the imaging data acquired changed in response to the changing scientific and engineering conditions. This flexibility was made possible because the mission had been designed to be adaptive (Refs. II-3 and II-4).

1. Mariner 9 Adaptive Capability

An essential feature of the Mariner 9 adaptive capability was a mission design "language," which streamlined the conversion of scientific requirements into commands actually transmitted to the spacecraft. During previous missions, each sequence of spacecraft commands was carefully verified in ground test to ensure that they violated no spacecraft constraints. For Mariner 9 a modular approach was adopted. Once the modules and the set of rules for combining them were tested, it was possible to execute a variety of data-taking sequences assembled from these modules without performing a test on each sequence. The modular approach also facilitated the recognition of constraints and effective communication between the television team and the mission design engineers.

a. *Spacecraft blocks.* The elementary mission design module was the spacecraft block, which corresponded to a

Table II-2. Spacecraft blocks

TV blocks:

- 1.1 Television mapping
- 1.2 Single BA picture pair
- 1.3 Multiple BA picture pairs
- 1.4 Picture sequence control

Scan platform slew blocks:

- 2.1 Platform slew (one axis)
- 2.2 Platform slew (two axes)

Playback blocks:

- 3.1 Playback: 26-m antenna
- 3.2 Playback: 64-m antenna

Maneuver blocks:

- 4.1 Tandem maneuver
- 4.2 Sequencer/parallel maneuver
- 4.3 Computer maneuver

Science engineering blocks:

- 5.1 Television engineering
- 5.2 Television dark current integration
- 5.3 Science turnon
- 5.4 Science turnoff

Spacecraft engineering blocks:

- 6.1 Battery reconditioning
- 6.2 Stray light
- 6.3 Scan unlatch
- 6.4 Engine vent
- 6.5 Minimum power
- 6.6 Propulsion lines opening
- 6.7 Propulsion lines closing

CC&S verification blocks:

- 7.1 Sequencer load and verify
- 7.2 Memory readout verify
- 7.3 Single word readout verify
- 7.4 Computer check sum verify

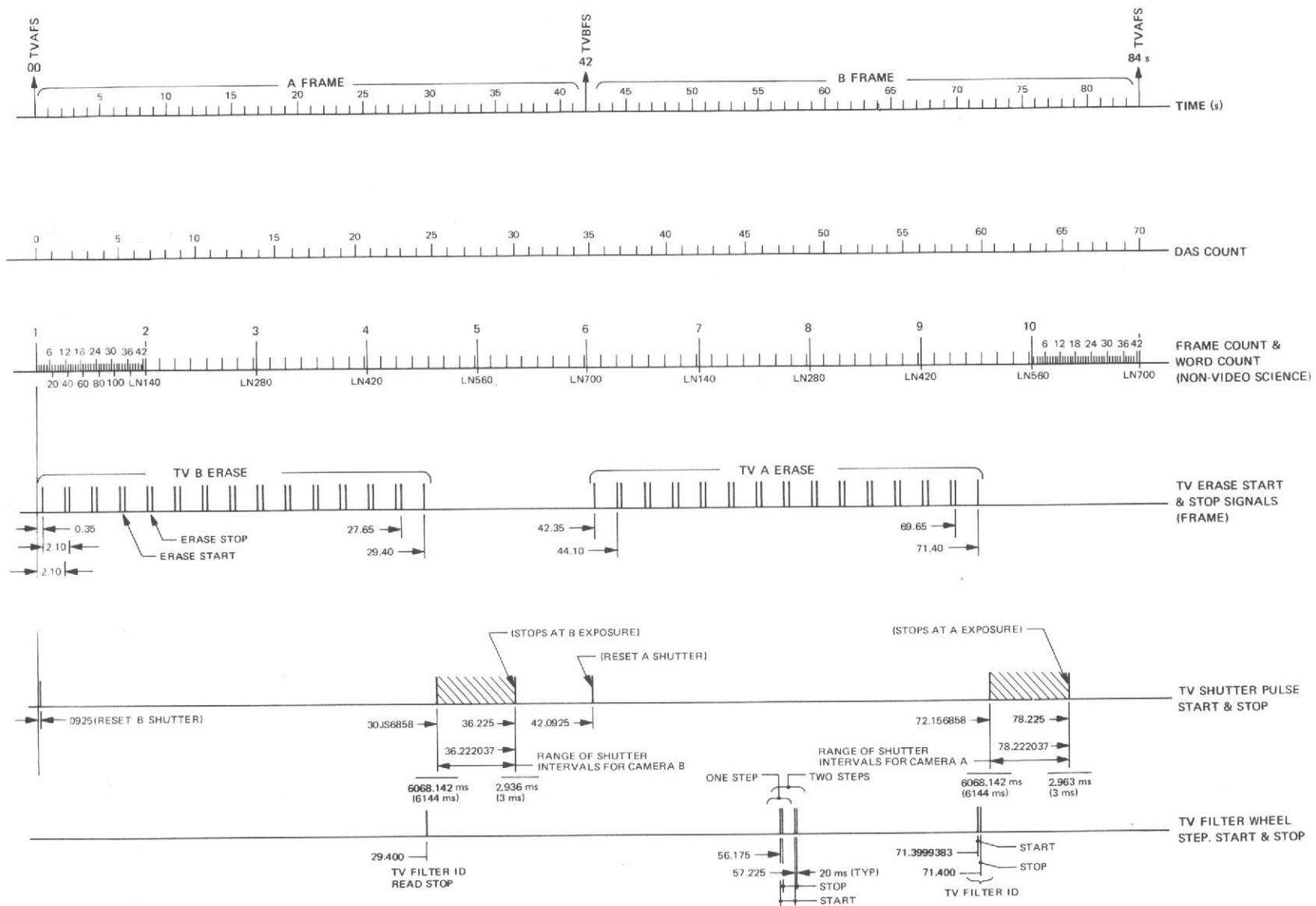


Fig. II-7. Timing parameters for Mariner 9 television cameras, showing interleaving of wide- and narrow-angle cameras during an 84-s interval. After a wide-angle-camera shutter event, an image was read from the vidicon between shutter + 6 s and shutter + 48 s. The read beam subsequently retraced its path 14 times during the next 29 s while the narrow-angle camera began to read its shuttered image.

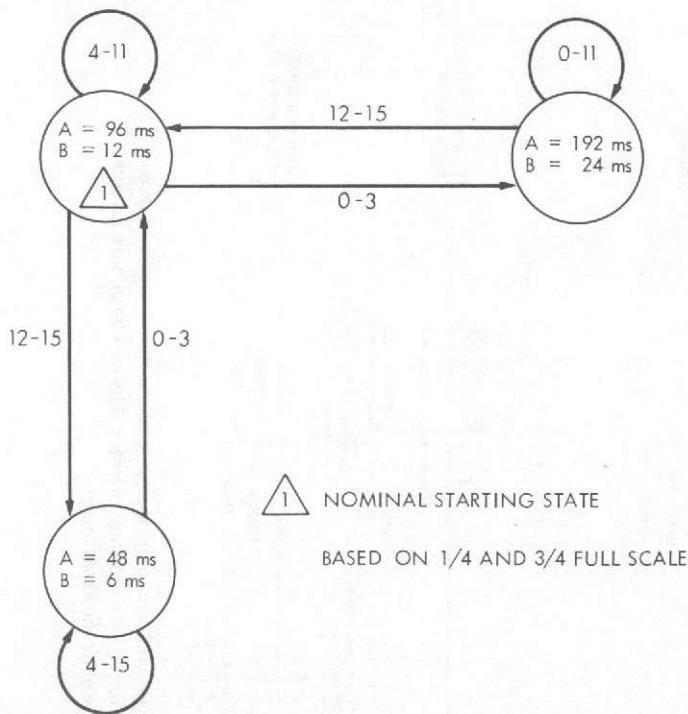


Fig. II-8. Automatic exposure control.

simple set of spacecraft commands yielding a simple predetermined amount of data. A list of spacecraft blocks appears in Table II-2.

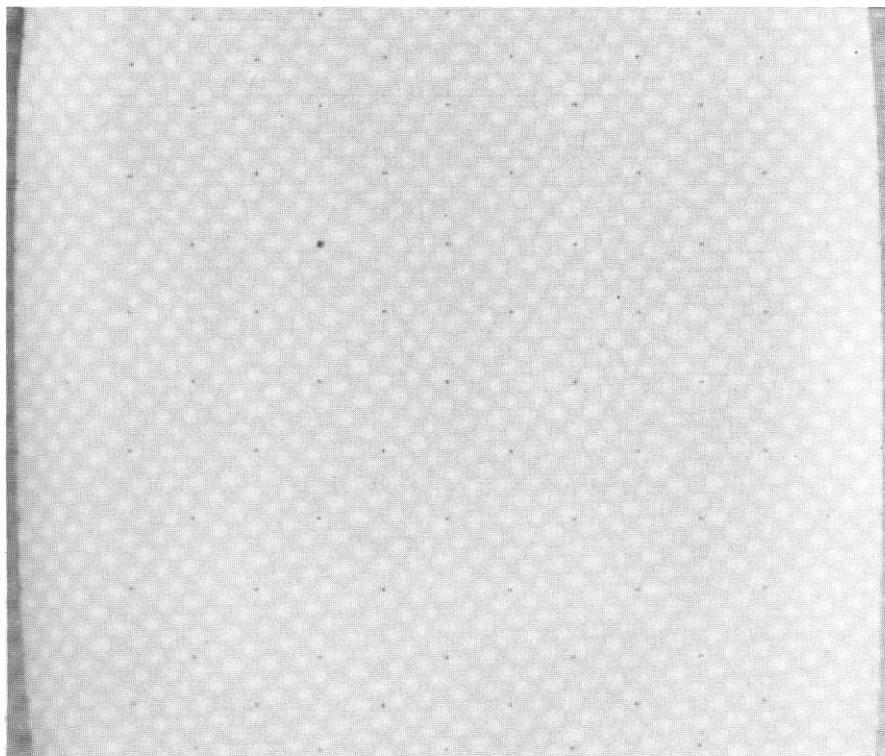
One of the simpler blocks used during science data acquisition was 1.2, the single BA picture pair (see Table II-3). In this block, the spacecraft recorded on the tape recorder one narrow-angle television picture (B); one wide-angle television picture (A); and data from the ultraviolet and infrared spectrometers and infrared radiometer taken during a single 84-s DAS frame. The block was structured so that the spacecraft was taken from a neutral cruise state, conditioned to allow data acquisition, then returned to a neutral cruise state. The time required for this block was 252 s. The block was capable of being initiated immediately upon the end of any other block that left the spacecraft in its required neutral state. Upon its completion, any other block that matched the neutral state could have been started. A complementary block, the picture sequence control block (entry 1.4 in Table II-2) was designed to perform in parallel with this and other television blocks, providing the additional flexibility of instrument pointing changes and selective recording. In combination, blocks 1.2 and 1.4 permitted the execution of a BA pair, single B, and single A, all with or without scan platform slewing. Together with blocks 1.1 and 1.3, television mapping, and multiple BA pairs, this provided all of the basic options desired for the mission.

Table II-3. Block 1.2 single BA pair

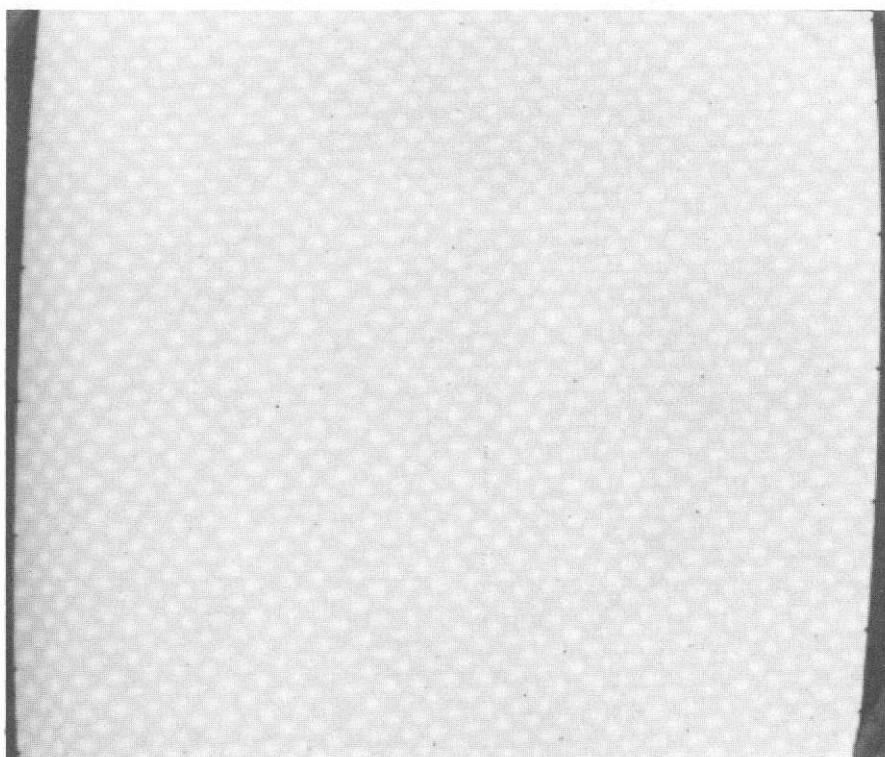
Step	Event	Relative timing, s
1.	B-frame start pulse to CC&S	0
2.	Take television picture pair	0
3.	DAS logic to false shutter state	42+
3.1	Close camera B shutter	78
3.2	Close camera A shutter	120
4.	DAS logic to single picture pair state	126+
5.	Close camera B shutter	162
6.	Data storage subsystem (DSS) start record	167
(7.)	(Step filter in camera A, if required)	(182)
8.	Close camera A shutter	204
9.	DAS logic to stop recorder state	210+
10.	DSS stop record	252

With all television picture blocks, the initial narrow-angle frame was preceded by a wide-angle-camera exposure that normally was not tape recorded (the "false-shuttered" frame used to set the AEC; see Section II-A). However, in certain cases (see Section III), it was desirable to record and transmit the false-shuttered frame. In these cases and generally when AEC was not desired, a direct ground command was used to set camera exposure. No provision existed for including the exposure time required for a given frame in the stored program of camera commands in the central computer and sequencer (CC&S). In a similar fashion, filters could be commanded directly from the ground immediately before picture acquisition.

b. *Science links.* The observational units that emerged from television experiment planning generally were known as "science links." Each science link required the execution of several spacecraft blocks. An example is a dyad, which consisted of two television pictures: one from the wide- and one from the narrow-angle camera (see Fig. II-11). This particular link included an early tape recorder start to ensure recovery

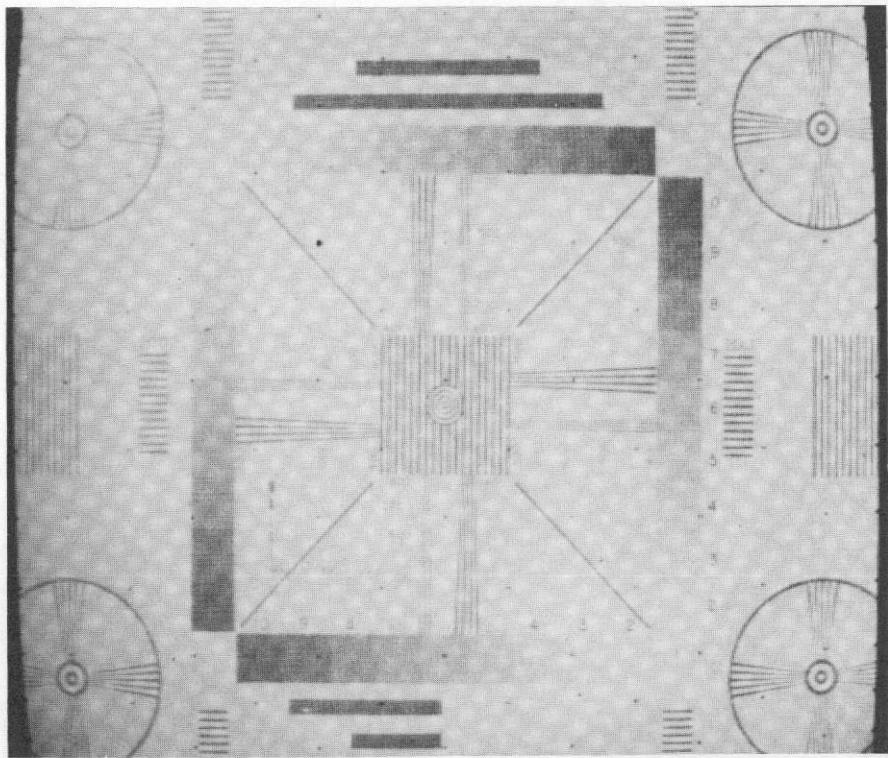


(a) WIDE-ANGLE CAMERA

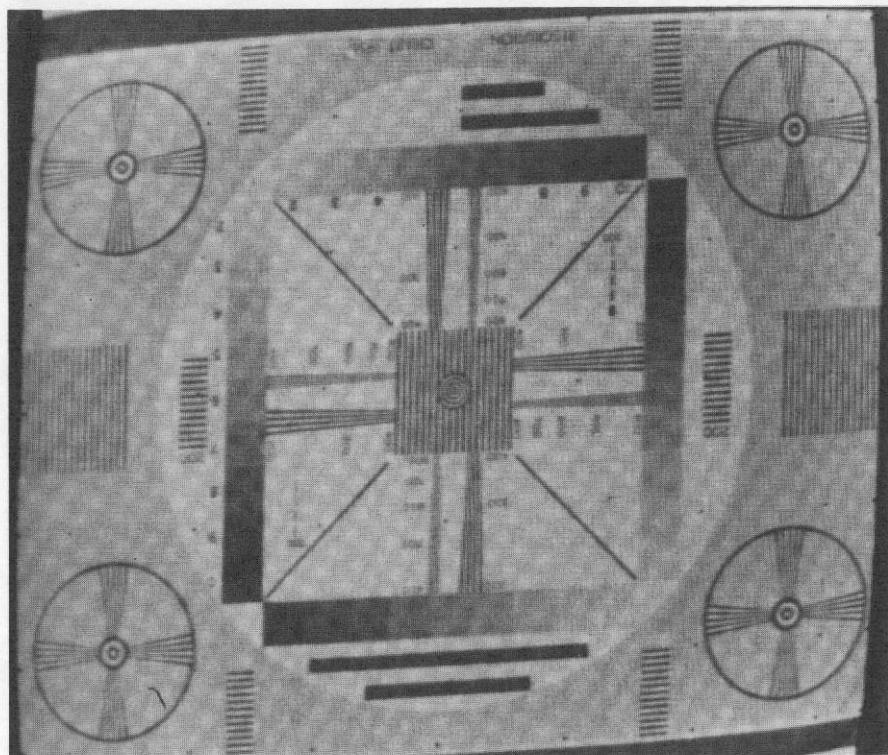


(b) NARROW-ANGLE CAMERA

Fig. II-9. Flat-field targets imaged by Mariner 9 vidicon cameras in ground test, tape recorded, and played back after launch. The small black reseau marks were arranged differently in the two cameras.



(a) WIDE-ANGLE CAMERA



(b) NARROW-ANGLE CAMERA

Fig. II-10. RETMA targets imaged by Mariner 9 vidicon cameras in ground test, tape recorded, and played back after launch. Barrel and keystone distortions are apparent from the geometry of the images.

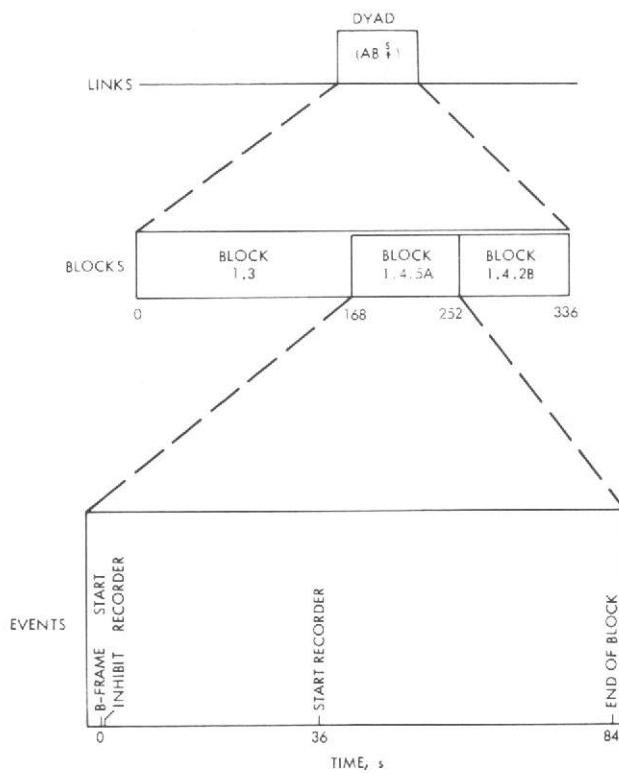


Fig. II-11. Relationship of links and blocks illustrated by the structure of a dyad link.

of a certain segment of spectral data and the initiation of a scan platform slew after shutting the second picture. Block 1.3, multiple picture pairs, was used to command the spacecraft to shutter two BA picture pairs. Blocks 1.4.5A and 1.4.2B were used to control the tape and slews. Other links (triads, tetrads, pentads, and sextads) that consisted of different combinations of wide- and narrow-angle frames were developed in response to the needs of the television experiment.

In order to provide for the orderly and successful acquisition and transmission of data, the various links were combined into a "science linking plan." Linking plans were developed for two successive revolutions (zenith and nadir) comprising a 24-h period. Science data could be recorded only on nadir revolutions because the 64-m Goldstone antenna was not accessible for data transmission. Links providing for real-time high-rate science data communication and tape recorder playback were scheduled for the zenith revolutions when the 64-m antenna was available. Several hours of communication time also were required to reprogram the spacecraft's CC&S with instructions corresponding to a new science linking plan. (Commands to reprogram the 512 words of a 22-bit CC&S memory were sent at a rate of 1 bps.) This was considered acceptable before the arrival at Mars and the discovery that the obscuration produced by the global dust storm invalidated

the linking plans that had been prepared for the first 27 days of orbital operations. At that time, it was realized that the planning of the mission had to be simplified; thus, an additional modularization concept, the standard mission day (SMD), emerged.

c. *Standard mission day.* Because orbital geometry changed slowly, a single linking plan (the SMD) was developed to serve for a number of days with changes permitted in scan platform pointing, but not in the timing of the links. A logical planning period was about 20 days, corresponding to the complete longitudinal coverage achieved with the 9° advance of the ground track on successive nadir (recording) or zenith (transmitting) revolutions (see Fig. II-12). Although it was not possible to make significant revisions to the number and type of pictures taken from different parts of the orbit during one of these planned science cycles, any one link could satisfy different experiment objectives on different revolutions. For example, a link consisting of a group of pictures acquired approximately 30 min before periapsis ($P - 30$ min) on the early revolutions was capable of being targeted at the polar cap on one revolution, at a suspected variable feature in the equatorial region on a second, and at the limb (horizon) of the planet to search for atmospheric phenomena on a third. Thus, each SMD included many links that were retargetable on a daily basis. The CC&S memory was maintained essentially unchanged for the entire 20-day period with all timing events loaded once at the beginning of each period so that the daily updates contained only slew magnitude changes. The retargeting was restricted by the pointing capabilities of the spacecraft (see Figs. II-13 and II-14) and the rate at which the scan platform slewed (1/40/s). A description of how the planning actually was implemented on a daily basis is given in Volume II of this document.

2. The Science Cycles

During the 12 months of operation, the science objectives sought by the six television discipline groups, together with those of the non-television experiments, were woven into a complete mission plan consisting of 12 science cycles. Pre-orbital science is included as one of these cycles, and post-solar occultation television coverage is divided into three cycles on the basis of the star being tracked for spacecraft stabilization. The science cycles were:

- (1) Pre-orbital science.
- (2) Post-orbital insertion mapping, calibration, and phase function cycle (Revs 1-15).
- (3) Interim cycles (Revs 16-23).

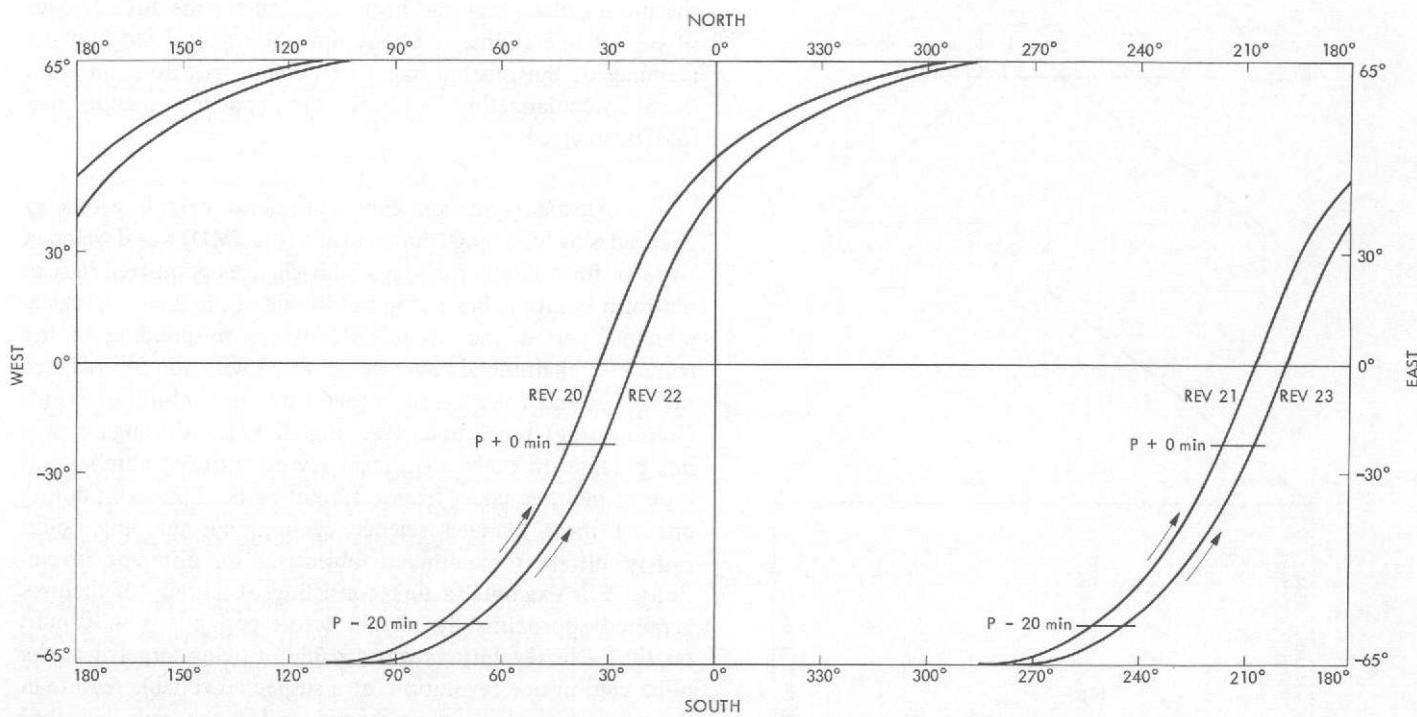


Fig. II-12. Typical ground tracks of Mariner 9, showing the 90° eastward drift on alternate revolutions.

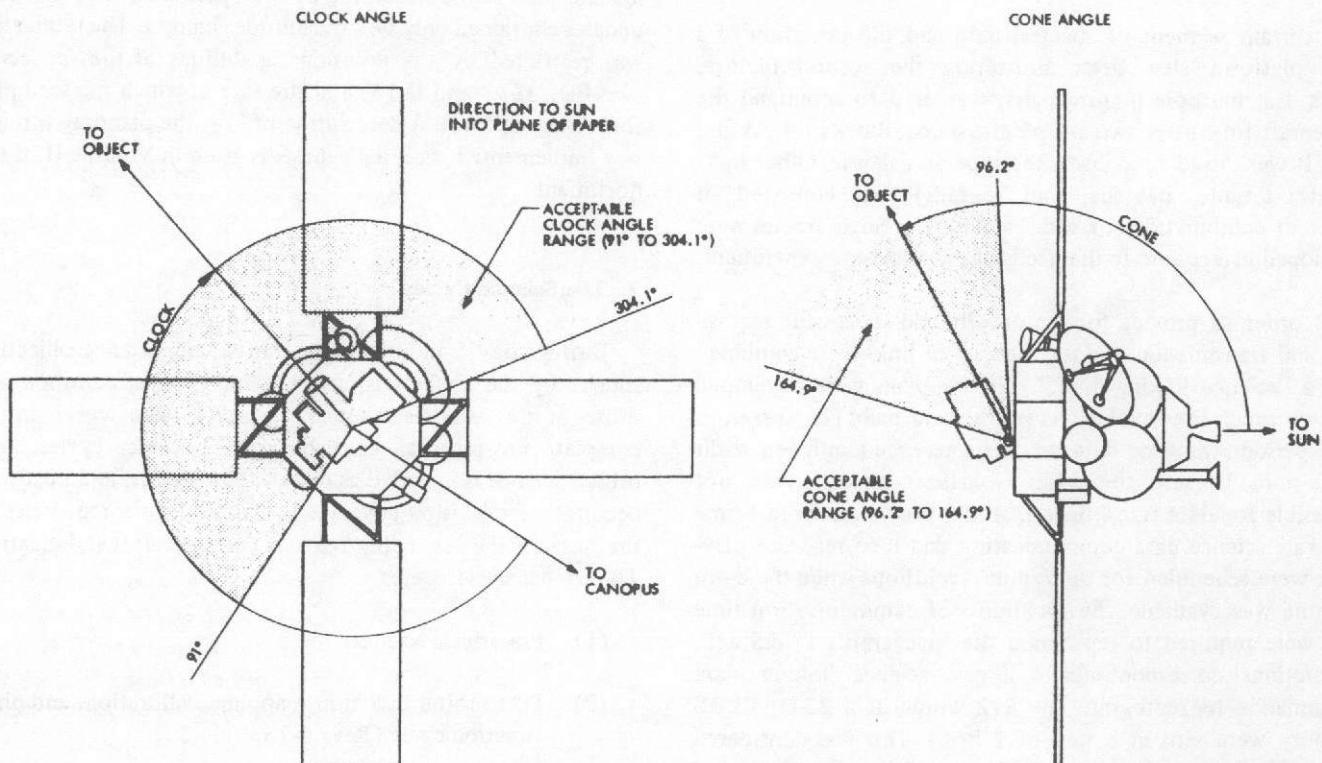


Fig. II-13. Definitions of clock and cone angles.

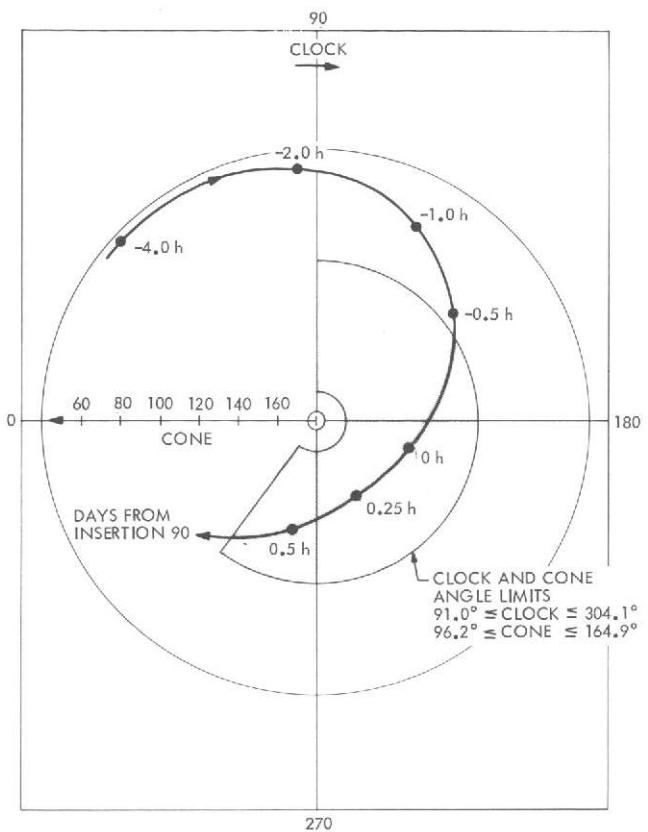


Fig. II-14. Clock and cone angles of the center of Mars are depicted by the heavy curve; the shaded area indicates cone and clock angles accessible to the scan platform. Depending on the star used as reference accessible clock angles could be changed, bringing into view features that were previously outside clock angle limits. The curve shown here is a pre-mission predict using Canopus as the reference star and is intended for illustrative purposes only.

- (4) Recon I (Revs 24–63).
- (5) Recon II (Revs 64–99).
- (6) Mapping Cycle I (Revs 100–138).
- (7) Mapping Cycle II (Revs 139–177).
- (8) Mapping Cycle III (Revs 178–217).
- (9) Extended mission, Phase I (Revs 218–262).
- (10) Extended mission, Phase II: Arcturus (Revs 416–459).
- (11) Extended mission, Phase III: Canopus (Revs 473–533).
- (12) Extended mission, Phase IV: Vega (Revs 667–676).

An overall summary of events during the Mariner 9 mission is given in Section I, and a description of events during

each science cycle is given in Volume II and in the Volume II Addendum. The sections in this Volume that deal with the data acquired in the different science disciplines also include details of the objectives and accomplishments during each science cycle, where appropriate. In the case of the satellite discipline (see Section XII), this breakdown is not relevant as observing conditions for the satellites were not on a 20-day cycle. The subsequent paragraphs describe how the science cycles were developed as the conditions of the mission evolved.

3. Pre-orbital Science

During the cruise phase of the Mariner 9 mission, many data-acquisition sequences were devoted to inflight calibration of the cameras. The data derived during these sequences are described in Section III. The first Mars-oriented pictures taken for exploratory, rather than calibration, purposes began when Mariner was about 3½ days from insertion into orbit. During the next 3 days, three pre-orbital science (POS) sequences (POS-1, POS-2, and POS-3) were executed. They showed no surface detail, but they did reveal structure in the global dust storm that was obscuring the surface of Mars. These picture sequences are described in detail in Section XI.

4. Reconnaissance Coverage

The first four orbital science cycles acquired between Revs 1 and 99 were of a reconnaissance nature because of the dust storm. The last of these cycles, Recon II, shows many of the important aspects of the reconnaissance activity that occurred during this period of the mission. The planning for Recon II began about 2 wk before the cycle actually was executed. It was comprised of several science links. The global TV link consisted of several wide-angle frames of the lighted disk taken at very high altitudes (Fig. II-15). The philosophy was that, by using this low-resolution coverage, “targeted” tetrads made up of four narrow-angle frames (Fig. II-16) would then be targeted on later revolutions into areas becoming clear of the dust obscuration. Global and targeted coverages during Recon II are discussed in more detail in Section XI.

The morning spectral mapping link concentrated data acquisition by the ultraviolet and infrared spectrometers and the infrared radiometer near the morning terminator (Fig. II-17). This non-television link was intended to monitor the composition of the dust and the rate of clearing. A sextad, consisting of three wide- and three narrow-angle frames (Fig. II-18; narrow-angle frames not shown), was usually targeted near the south pole in order to monitor changes in the polar cap.

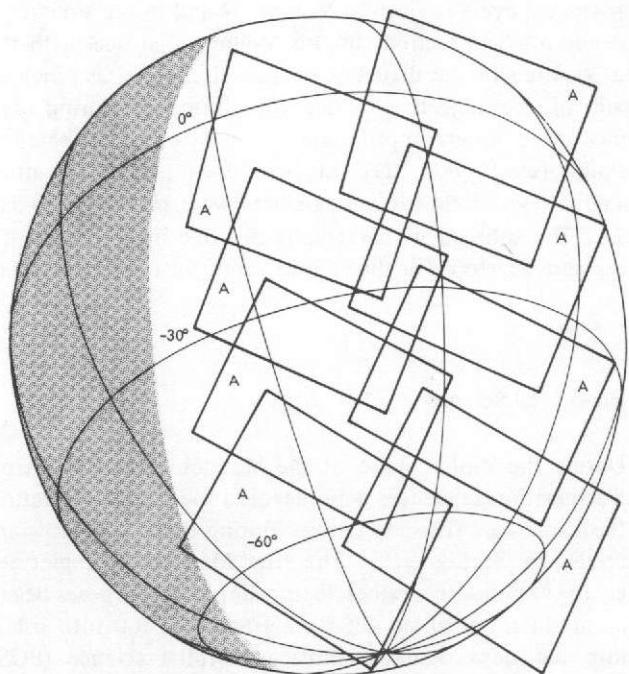


Fig. II-15. Recon II SMD: typical footprints of global TV link (conceptual).

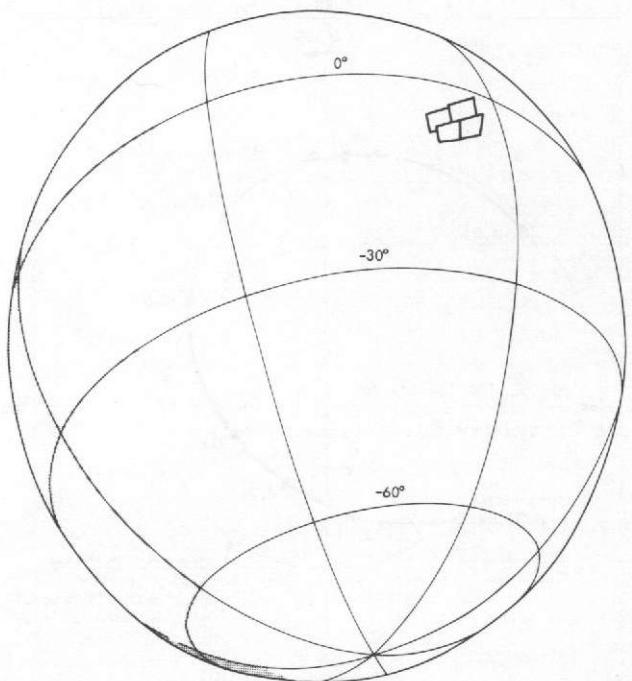


Fig. II-16. Recon II SMD: typical footprints of tetrad (conceptual).

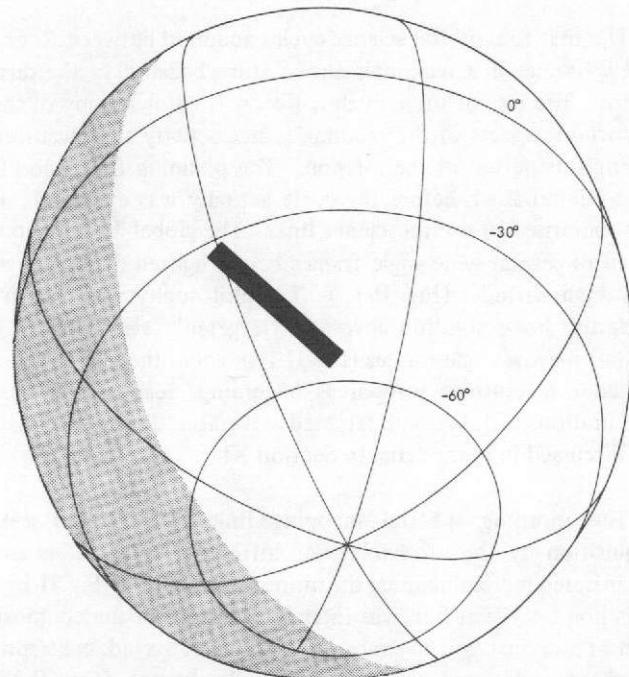


Fig. II-17. Recon II SMD: typical footprint of morning spectral mapping link (conceptual).

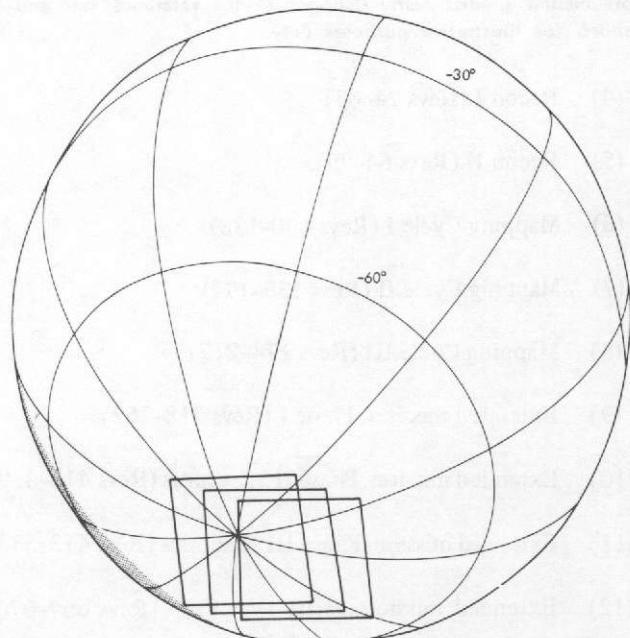


Fig. II-18. Recon II SMD: typical wide-angle-camera footprints of a sextad (conceptual).

The polar coverage from this and from later parts of the mission is described in Section VIII.

The feasibility of starting to map the planet systematically was continually tested by means of a mapping link comprised of several wide- and narrow-angle frames (Fig. II-19). The mapping coverage obtained during this phase of the mission, when the planet was heavily obscured by dust, is presented in Section VII.

Figure II-20 shows the Recon II SMD. The science links were constructed to occur at the same time from periapsis on each revolution, but the pointing of some of the links varied daily throughout the 20-day cycle. Many links used a fixed pointing direction of the scan platform for several consecutive days without changing. The slews for these links were re-optimized a few times during the Recon II cycle to accomplish the desired objectives. About 30 platform slews were required on each revolution.

5. Mapping Coverage

At the same time that Recon II was being implemented, studies were initiated to understand how to accomplish the primary science objectives, including mapping the planet once the dust storm cleared. Many factors were considered in this planning effort, and ultimately led to a decision to change the spacecraft's orbit.

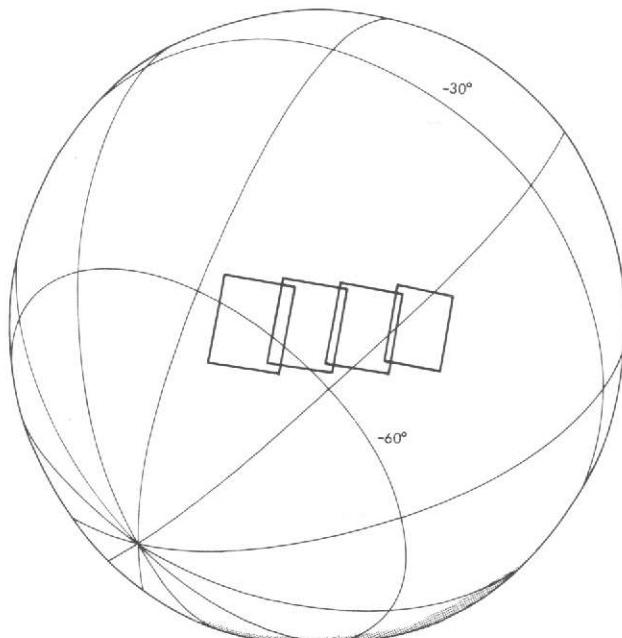


Fig. II-19. Recon II SMD: typical footprints of mapping link (conceptual).

a. Mapping sequence design. A minimum of 40 days was found to be required to map the planet from 65°S to 45°N. (The north polar hood obscured visibility of regions farther north than 45° in latitude.) However, to perform the task in 40 days, almost all of the total pictures available on each revolution would have been required. This was unacceptable because the other key mission objectives involving dynamic phenomena, geodesy, and satellites would have been lost. The spectral experiments also had competing desires for the use of the tape recorder on many revolutions.

It was estimated that, if mapping were extended for a 60-day time period, the number of pictures for mapping of the planet would remain the same. But, as the accumulated total of all pictures would be greater for 60 days than for 40 days, the number of pictures designated for mapping per revolution would decrease. The decrease was not sufficient to accomplish the other experiment objectives on each revolution. It was determined, however, that the mapping "footprint" at 1390 km would not overlap side to side on adjacent tracks of Mapping Cycles I, II, and III near the periapsis latitude of 20°S. A minimum altitude of 1650 km would be necessary to provide a 5% average overlap given the field-of-view characteristics of the wide-angle camera. Raising the periapsis altitude also further decreased the number of wide-angle pictures required for mapping. If the periapsis altitude of the orbit were raised from 1390 km to 1650 km, the number of pictures required for mapping could be decreased even further.

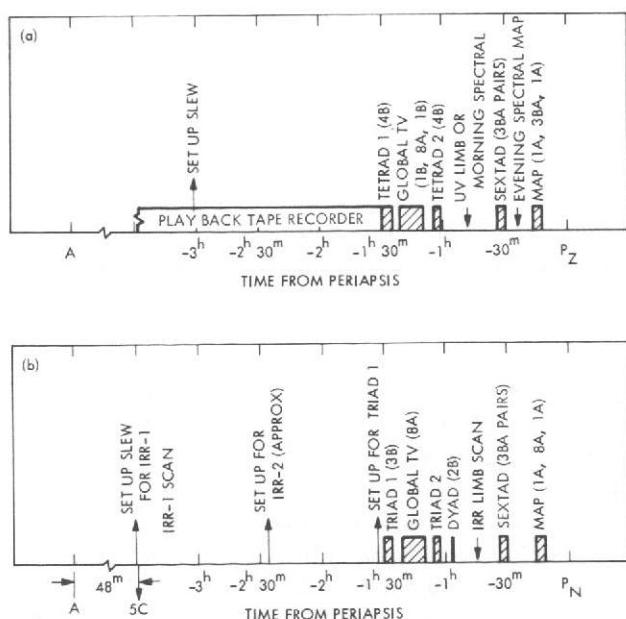


Fig. II-20. Recon II SMD. (a) Goldstone zenith pass. (b) Goldstone nadir pass.

For a periapsis altitude of 1650 km, the number of wide-angle frames required to map the planet could be held to about 10 per revolution for the first 40 days of the 60-day time period. This would permit mapping from 65°S to 25°N latitude with small gaps in the latitude from about 35°S to 0°. About 10 narrow-angle frames per revolution were required so that a narrow-angle picture would be nested inside of each wide-angle picture taken.

For a 32-picture budget, this would leave 12 pictures per revolution for the other experiments for 40 days. For the last 20 days, six wide-angle frames per revolution were needed to fill the gaps in mapping coverage from 35°S to 0° latitude. Six additional pictures per revolution, three wide- and three narrow-angle, were needed to extend the mapping from 25°N to 45°N latitude. Thus, 12 pictures per revolution were needed to map the last 20-day cycle. Figure II-21 shows the wide-angle-camera mapping strategy for the 60-day time period through three 20-day cycles.

The amount of scan platform slewing during the mapping mode also was dependent on the periapsis altitude. More slews were required on each revolution for the lower altitude in order to obtain contiguous forward laps with the wide-angle camera. An absolute minimum number of slews was desired by the ultraviolet spectrometer (UVS) and infrared radiometer (IRR) experimenters because of the difficulty in analyzing these non-television data if the scan platform moved during data acquisition. The number of slews could be decreased to about two per revolution if the altitude were more than 1550 km. Two slews per revolution were consistent with keeping the viewing angle (angle measured at the surface of Mars between local vertical and the optic axis from the spacecraft) less than 25°.

The number of television pictures that could be obtained each day decreased with time. Figure II-22 shows the estimated number of pictures per day vs time after arrival. In Fig. II-22, the total number of pictures per revolution drops below that required for mapping (24 per day for the third 20-day cycle) in early March 1972. Thus, for a 60-day mapping interval, mapping had to be started in early January 1972.

Another problem was the drift rate between the time of periapsis and the time of Goldstone zenith (see Section I). In order to maximize the number of pictures to be played back over Goldstone each day, the science data-acquisition period near periapsis had to occur near the zenith of Goldstone. In this manner, data taken on the nadir revolutions could be played back each day during the first 3 h and 15 min (for 32 pictures) after the appearance of Mars above the horizon as viewed from the Goldstone tracking station (see Fig. I-5). Science data then could be taken immediately after this for the

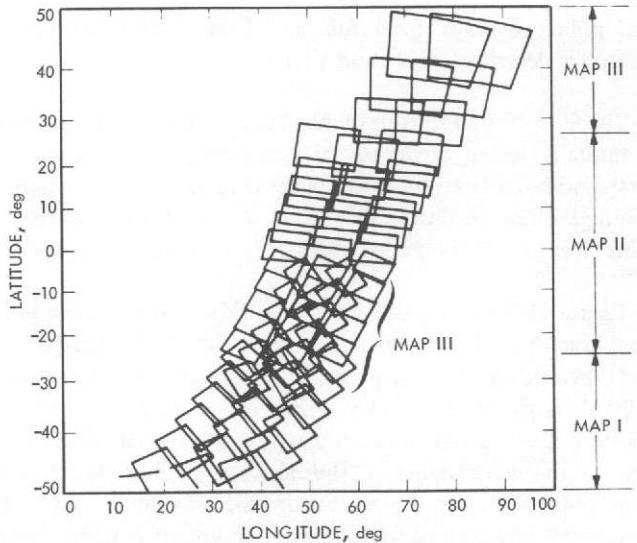


Fig. II-21. Composite of mapping cycles: Mapping Cycles I, II, and III.

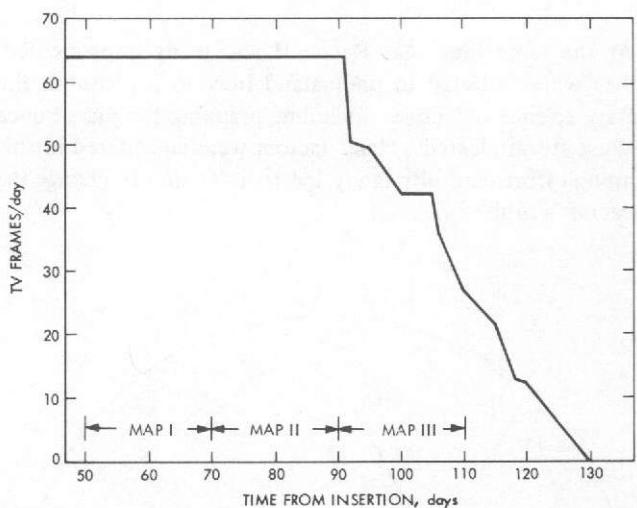


Fig. II-22. Total number of television pictures that could be received per day at the Goldstone tracking station without performing a spacecraft HGAM.

few hours near periapsis and could be played back during the few hours preceding Goldstone set.

The orbital period achieved at the time of the first orbit trim maneuver (November 19, 1971) was in error (too low) by about 31 s per revolution. This deviation was attributed to the large tesseral harmonics of the gravity field of Mars. In one month (to December 19) the accumulated time error would have been 31 min, which meant that the time between periapsis and Goldstone zenith would have drifted apart by that amount,

effectively reducing the time for playing back pictures by the equivalent of four or five frames. Another trim maneuver to correct the shift between Goldstone zenith and the time of periapsis was seen as a permanent solution to this progressively worsening drift problem. The trim maneuver seemed desirable also to increase periapsis altitude and to reduce the number of pictures required for mapping of the planet and the number of associated slews of the scan platform. A single trim maneuver, made before the start of the 60-day mapping mode, solved both problems by slightly changing the orbital period and raising the periapsis altitude (see Section I). A plan was developed to start the systematic mapping of Mars at the beginning of January 1972 after this final trim maneuver.

b. *Detailed science planning.* As an aid to the detailed science planning, the navigation team prepared geometry data using a simple conic program with a plot-generating capability. These data took the form of perspective views of the Martian globe at 10-min intervals near periapsis with scan platform cone angle (target-spacecraft-Sun) and clock angle (angle measured clockwise when looking toward the Sun from the Sun-spacecraft-Canopus plane to the Sun-spacecraft-target plane) grid lines superimposed (see Section III). The experimenters wanted to observe specific Martian features in various latitude bands over a range of longitudes. At a fixed time from periapsis, the same Martian latitude band could be observed by the spacecraft on each revolution; however, the longitudes shifted eastward each day by about 9° (see Fig. II-12). Thus, television pictures that were selected to occur at a particular time from periapsis could survey the same latitude band each day with small shifts in longitude. Over a period of 20 days, all longitude segments could be covered for the specific latitude band. Experimenters looked at the perspective views of the planet and decided what latitude bands were most desirable for viewing. On the basis of this information, a preliminary set of science observations was proposed for Mapping Cycle I. This preliminary set of observations included:

- (1) IRR morning terminator scans.
- (2) Global television coverage.
- (3) Morning spectral mapping.
- (4) UVS bright limb scans.
- (5) Variable surface feature coverage.
- (6) South polar cap coverage.
- (7) Atmospheric coverage.
- (8) Evening spectral mapping.

- (9) Mapping.
- (10) Northern hemispheric reconnaissance.
- (11) Nightside spectral coverage.
- (12) UVS stellar observations.

The mission design team then generated a set of candidate science links for Mapping Cycle I and organized them into a preliminary SMD which included other spacecraft and ground operation events. A few iterations were required to incorporate all of the desires and to make the various tradeoffs. Many links had to be re-optimized to be consistent with the SMD concept. For instance, the slews for the IRR morning terminator scans were constrained to occur at the same time from periapsis each nadir revolution throughout the cycle. This meant that the time of each slew had to be chosen carefully to ensure that the IRR link would satisfy IRR experiment objectives through the duration of Mapping Cycle I. Some science objectives had to be satisfied by a combined single data-acquisition interval due to similar spacecraft-planet geometry requirements. A single link, called a "pentad," consisting of three wide- and two narrow-angle frames, was designed so that simple retargeting allowed the pentad to satisfy observation requirements for variable surface features, the atmosphere, and the south polar cap.

For retargetable science links (links for which the pointing was allowed to change each revolution), targeting constraints were imposed. Two types of constraints imposed by the spacecraft's two-axis scan platform pointing system affected the link retargeting capabilities. The scan platform was limited in the allowable range of pointing angles on each axis. The minimum reachable cone angle was 96° ; the maximum was 165° (see Figs. II-13 and II-14). These constraints automatically precluded planetary observations at specific phase angles. (For example, pointing vertically at the subspacecraft track as it crossed the terminator was not possible.) The clock axis was also constrained to view the planet at angles greater than 90° , but less than 305° . Either or both pointing angle constraints could, throughout the mission, limit planet viewing (see Section I).

The other constraint imposed was maximum platform slewing rate. The maximum rate of change of pointing angle, $\frac{1}{4}^{\circ}/\text{s}$ on each axis, meant that it sometimes took several minutes to accomplish long platform slews. Slew time between science links was an important parameter in deciding the relative timing of the links within the SMD because that timing was to remain constant throughout the cycle. Because executing a UVS bright limb scan and monitoring the south polar cap on the same revolution required excessive slewing

time, one targeting constraint was that UVS bright limb scans could occur only when the pentad was pointed to "high Sun" regions (areas of interest to the atmospheric and variable surface feature disciplines), which were observed with the Sun as near to the zenith as possible. Maximum slew time possible during the cycle also determined the time at which the set-up slew for the pentad was fixed after the bright limb scan. In order to simplify satellite photography, which was usually accomplished by ground commanding the shuttering of the cameras, special slews were placed in the SMD at times that were optimum for most favorable satellite viewing. When no satellite viewing opportunity existed on a revolution, the slew was set to zero.

The preliminary Mapping Cycle I SMD was iterated with the experimenters until an acceptable SMD was selected. This final SMD, together with the targeting constraints and a set of operational guidelines, formed the output of the mission design team. The entire process took about 14 days and was delivered to the operations area 15 days before the beginning of the 20-day Mapping Cycle I.

Some of the science links are:

- | | |
|---------------|--|
| (1) Global TV | Five wide-angle frames to cover as much of the globe as possible. |
| (2) UV BL | Ultraviolet bright limb experiment for which the spectral scan crosses down into the atmosphere and across the planet. |
| (3) Pentad | Three wide- and two narrow-angle frames that could be used to monitor the south polar cap or variable features or to observe the atmosphere. |
| (4) Mapping | Ten wide- and eight narrow-angle frames used for mapping the planet from 65°S to 25°S latitude. |

About 30 platform slews were required for each revolution in order to accomplish all science objectives. Planning for the pointing of targetable links was a daily activity during the 20-day cycle. The Mapping Cycle I science linking plan was designed to be flexible enough to accommodate all science objectives of this first cycle of mapping Mars. Mapping Cycle I was followed successively by Mapping Cycles II and III.

6. Extended Mission

By the end of Mapping Cycle III, the major objective of mapping 70 percent of the planet had been satisfied. The lengthening distance and changing angular relationship between Earth and Mars had caused a progressive lowering in the signal-to-noise ratio, which forced selection of lower playback data rates. By the start of this cycle, approximately 20 pictures could be played back on each zenith revolution and 15 or 16 on each nadir revolution. Near the end of Phase I of the extended mission, this had changed to about 10 on both zenith and nadir revolutions. No data were acquired between Revs 244 and 258 because an apparent malfunction to the spacecraft's CC&S was being investigated.

The linking plans on zenith and nadir revolutions were similar during Phase I of the extended mission. Each consisted of five triads: 1, 2, and 4 comprised three B-frames, and 3 and 5 a single B and an AB pair. Freed from the requirement to perform systematic mapping at a specific time in the orbit, not only the pointing, but also the time at which each triad was executed could be and was modified under the constraint that the five triads remain in the same order without overlap (see Volume II, Tables 6-14 and 6-15). Early in Phase I of the extended mission, when more than 15 pictures were recovered from each zenith and nadir revolution, additional television pictures were acquired either before, after, or between two of the five triads. These frames were not preprogrammed into the spacecraft's computer, but were directly "ground-commanded" and executed immediately on receipt of the command at the spacecraft. Because the one-way radio transmission time from Earth to the vicinity of Mars was about 20 min at this time (Ref. II-5), the ground commands were sent that length of time before execution time at the spacecraft. Ground commanded frames also had been used during early mapping sequences to photograph Phobos and Deimos and to provide targeting flexibility to handle the declining rate of picture return during Mapping Cycle III. Toward the end of Phase I, as the number of pictures per revolution decreased, one or more of the five triads was deleted from the data recorded or played back to the ground station.

Spacecraft operations ceased because of the twice daily solar occultation of the spacecraft on Rev 262 and did not resume until Rev 416. The rest of the mission subsequent to Rev 416 was dedicated to several objectives:

- (1) Monitoring the dynamic state of the Martian atmosphere and selected variable features.
- (2) Systematically mapping the region from 40°N to the north pole, a region previously obscured by the north polar hood, thus completing the mapping of the planet.

- (3) High-resolution imaging of about 25 areas proposed as possible Viking landing sites.

A general relativity test also was performed during the weeks before and after the solar conjunction of Mars on September 7, 1972.

An entirely different framework for data acquisition existed after Rev 416 because it was necessary for the spacecraft to execute a high-gain antenna maneuver (HGAM) before each tape playback in order to reorient the spacecraft away from its celestial reference so that the high-gain antenna was pointed directly at Earth. Even with this maneuver, it was not possible to operate at the signal-to-noise ratio achieved early in the mission because Mars and Mariner 9 were then three times farther from Earth.

Initially, television pictures during the extended mission were taken on a weekly cycle. The cycle began the first week in June 1972 and continued for 9 consecutive weeks. Each weekly cycle began with a CC&S update on Wednesday for a zenith/nadir data-taking pair on Thursday/Friday. The zenith revolution on Friday was used to play the tape-recorder data back to Earth. In order for the spacecraft to perform this playback, it had to execute an HGAM before the tape playback in order to optimally point the HGA toward Earth. After all data were returned, the spacecraft was reoriented to acquire celestial reference. The entire sequence was repeated

for another zenith/nadir pair in the same week beginning with a smaller CC&S update on Saturday and ending with a HGAM on Monday. Both zenith/nadir pairs in a given week were structurally similar (cf Revs 416/417 and 422/423 in the Volume II Addendum). However, even though the order of the links remained the same, the links were allowed to move relative to periapsis from one zenith (or nadir) revolution to the next data-taking revolution in the same week, and some ground-commanded picture sequences could be inserted.

Operations continued at the rate of two CC&S updates, two structurally similar zenith/nadir data-taking pairs, and two high-gain antenna maneuvers each week through the first week in August 1972. From this point until the end of the mission, each week's television sequences were tailored to suit specific objectives.

Three different stars were used for roll axis reference during the extended mission. Data acquisition began after solar occultation with the star Arcturus as the roll reference. This continued until late June 1972 (Revs 416-459). By using Arcturus, the clock angle constraints were eased when viewing Mars near periapsis, and viewing conditions for the north polar region were improved. The star Canopus, which had been the primary roll reference star for the mission, was used to obtain data in July (Revs 473-533). The star Vega was used after superior conjunction in September (Revs 667-676) in order to optimize viewing geometry near periapsis.

References

- II-1. Steinbacher, R. H., and Gunter, S. Z., "The Mariner Mars 1971 Experiments: Introduction," *Icarus*, Vol. 12, p. 3, 1970.
- II-2. Danielson, E. G., Jr., and Montgomery, D. R., "Calibration of the Mariner Mars 1969 Television Cameras," *J. Geophys. Res.*, Vol. 76, p. 418, 1971.
- II-3. Haynes, N. R., Bollman, W. E., and O'Neil, W. J., *The Mariner Mars 1971 Mission Design*, Paper 70-1048, presented at AAS/AIAA Astrodynamics Conference, Santa Barbara, Calif., August 1970.
- II-4. Haynes, N. R., Bollman, W. E., Neilson, R. A., Nock, K. T., and Travers, E. S., *Mariner Mars 1971 Adaptive Mission Planning*, Paper 72-944, presented at AIAA/AAS Astrodynamics Conference, Palo Alto, Calif., September 1972.
- II-5. Webb, W. A., *Mariner Mars 1971 Orbit Design and Characteristics Handbook*, Jet Propulsion Laboratory Internal Report 610-113, 1970.

III. Television Camera Calibration and Data Products

The data products of the Mariner 9 television experiment, consisting of several different types of computer-processed images (see Sections IV through VI) and supporting graphical and numerical data, will continue to be used for the scientific investigation of Mars. Not all data products produced during the Mariner 9 mission were intended for an archival scientific purpose; because Mariner 9 was an adaptive mission, many were temporary products needed to influence and conduct mission planning. An important prerequisite to the production of both temporary and permanent data products was the calibration of the television cameras.

A. Television Camera Calibration

In order to map and measure accurately the surface of Mars and to observe subtle dynamic effects on its surface and in its atmosphere, precise calibrations of camera distortions were necessary. These calibrations were performed before launch using specially designed stimuli. Calibrations also were conducted in flight, but the lack of a suitable stimulus (only Mars, Saturn, and the stars were available) meant that only a verification, rather than a true calibration, was possible.

1. Preflight Calibration

The television cameras suffered from both photometric and geometric distortions, most of which were attributed to the vidicon television sensor and associated electron beam deflection systems rather than to the camera optics.

Photometric distortion occurred because of local variations in the vidicon target material, charge dissipation during vidicon scanning, and electron optical distortion, with the result that the sampled digital DN values varied within an image of a uniformly illuminated scene. As the erasure between successive frames was imperfect, each image also contained a remnant of unerased past exposures. The residual image at a location within the sampled image was a complex nonlinear function of temperature, wavelength of incident light, and brightness of the current and preceding images. The photometric response of the vidicon, as determined by the relationship of data number to input brightness, was nonlinear; it also varied with temperature and with the wavelength of the incident light.

Geometric distortions in the scanned images occurred because of barrel and keystone distortions in the magnetic

systems used to scan the vidicon target and because of the deflection of the scanning beam by the charged vidicon target.

A preflight calibration consisting of 14 camera performance tests, five at room temperature (bench) and nine in a thermal vacuum chamber at different temperatures (environmental), provided the data base for characterizing these distortions. This data base of more than 7000 frames was used to provide correction for camera shading in the earliest picture versions (see Section IV) and, in a process known as "decalibration" (see Section V), to remove photometric and geometric distortions. Camera calibrations are summarized in Table III-1 and are discussed in detail in Ref. III-1.

2. Inflight Camera Performance Verification

Inflight camera performance verification began on September 29, 1971, after playback of calibration pictures that had been tape recorded before launch. The first inflight photographic sequences were directed at star fields. Scan calibrations I and II were special sequences designed to determine the accuracy with which the scientific instruments could be directed toward specific targets. Photography of star fields provided the information necessary to refine camera pointing accuracy, which was critical to later science sequences. These pictures also permitted an assessment of focus, system noise interference, and residual image. Saturn calibration produced images of Saturn with several shutter speeds, at a number of locations within the field of view, which were used to determine shading and light-transfer characteristics of the cameras. Mars calibrations I and II were similar sequences directed toward Mars, while the planet was still small in angular size. These data completed the comparison link between Mariner's Saturn and Mars orbital photography and Earth-based observations of both planets. During orbital operations, repeated photography of isolated Martian regions gave additional information regarding the light-transfer, spectral, and modulation-transfer characteristics of the television cameras. The inflight calibration sequences, which required 270 frames, are summarized in Table III-2 and are discussed in detail in Refs. III-2 and III-3.

B. Camera Performance

Basic attributes of the television cameras and the digital video data that were telemetered to the ground station were studied from preflight calibration data, inflight calibration data, and data from normal science (noncalibration) sequences. Many performance characteristics, which became apparent from study of the Mariner 9 pictures after launch, were sig-

Table III-1. Calibration measurements and their applications

Calibration	Application
Reseau pattern and electronic distortion	Geometric correction for geodesy and cartography; decalibration
Focal length and optical distortion	Geodesy and cartography
Light transfer	Exposure settings; decalibration
Shading	Exposure settings; shading correction of real-time pictures; decalibration
Spectral response	Interpretation of multi-filter pictures; determination of filter position after filter-wheel failure
Stray light	Satellite picture planning; decalibration
Residual image	Decalibration
Modulation transfer	Resolution and focus
Point spread function	Detection threshold in star pictures
Camera alignment	Camera pointing and non-television-instrument offsets
Noise power spectra	Recognition of coherent noise components

nificant in the interpretation of the pictures and in plans for picture-taking sequences.

1. Geometric Characteristics

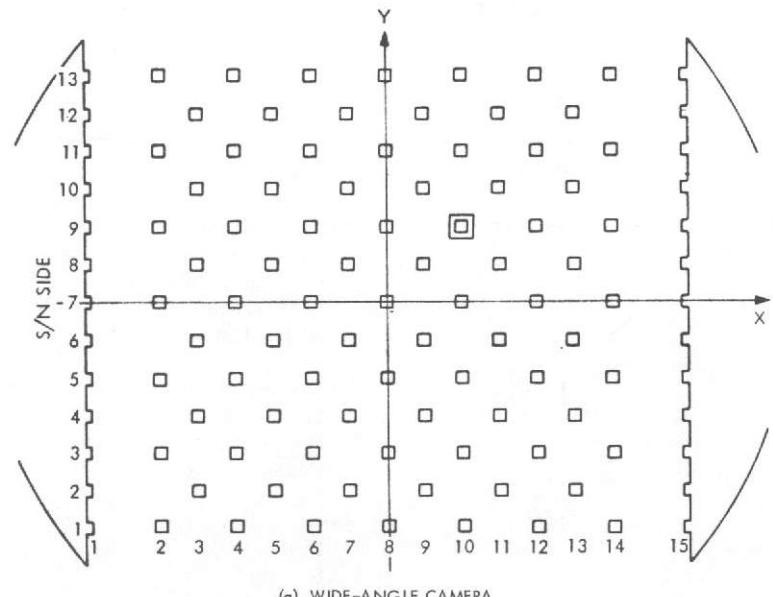
Measurements of camera focal length, alignments, and geometric distortions were taken during preflight calibration (see Ref. III-1). Separate determinations were made of the distortion introduced as the object was focused optically onto the vidicon surface and distortion introduced as this latent image on the vidicon surface was scanned with an electron beam. The electronic distortion was far greater in both cameras; optical distortion was negligible in the narrow-angle camera.

Geometric calibrations were used to generate numerical data on the geometric characteristics of the cameras and to implement corrections to the raw pictures using image processing techniques (Ref. III-4 and Section V).

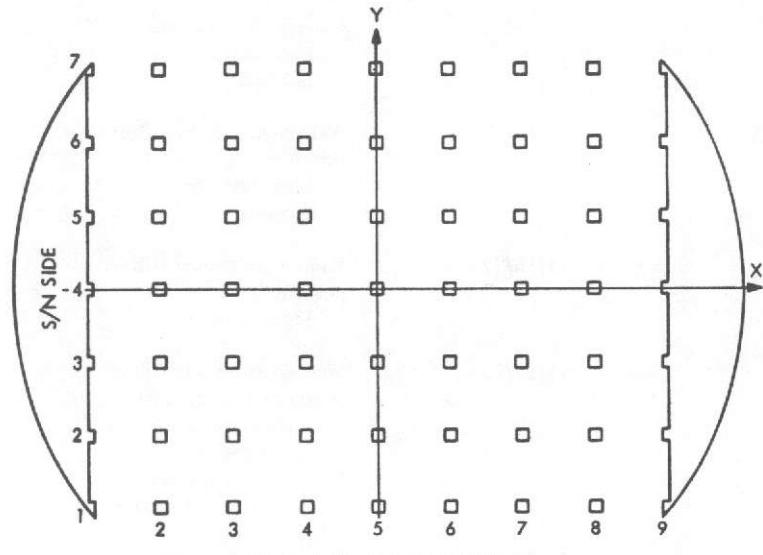
Reseau marks on the faceplates of the vidicon picture tubes (Figs. III-1 and III-2) were instrumental in obtaining accurate

Table III-2. Calibration sequences

Sequence	Date	Description	Number of pictures
AFETR playback	9/29/71	Telemetry test	30
Scan calibration I	10/1/71	Narrow-angle camera Camera alignment Point spread function Power spectra Residual image	31
Scan calibration II	10/8/71	Narrow-angle camera Camera alignment Point spread function Residual image	32
Saturn calibration	11/4/71	Narrow-angle camera Light transfer Shading Residual image	31
Mars calibration I	11/9/71	Narrow-angle camera Light transfer Shading	33
Mars calibration II	11/10/71	Wide-angle camera (filter positions 2 and 8) Light transfer Shading	30
Rev 6	11/16/72	Wide-angle camera (filter position 2) Light transfer	8
Rev 7	11/17/71	Wide-angle camera (filter positions 1, 2, 3, 7, 8) Light transfer Shutter speed Narrow-angle camera Point spread function	21
Rev 72	12/20/71	Narrow-angle camera Point spread function	18
Rev 76	12/22/71	Wide-angle camera (filter position 2) Light transfer	8
Rev 225	3/5/72	Narrow-angle camera Light transfer Wide-angle camera Light transfer	14
			3



(a) WIDE-ANGLE CAMERA



(b) NARROW-ANGLE CAMERA

Fig. III-1. Reseau grids for Mariner 9 television camera vidicons.

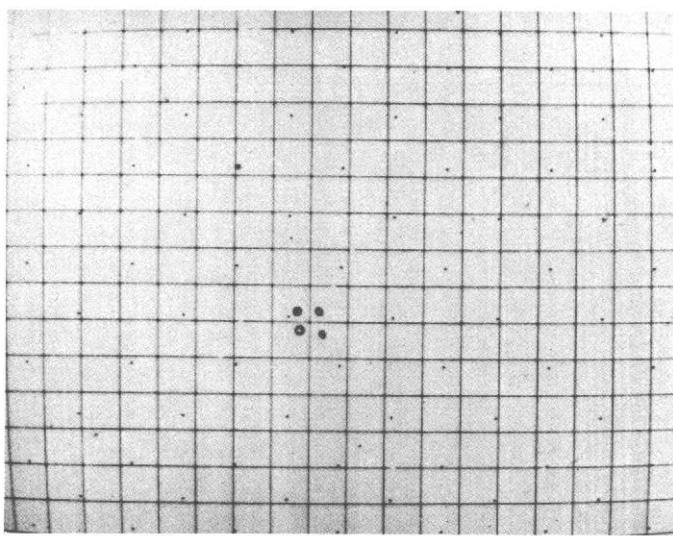


Fig. III-2. Mariner 9 calibration image. The small dark marks represent the reseau pattern on the face of the camera tube. The grid is the image of a target used to determine geometric distortion.

geometric information from the television cameras. Any post-launch shift or distortion of the scanning raster, causing a change in electronic distortion, was evident as a change in position of the reseau marks in the telemetered image. A raster shift, expected to occur as a consequence of leaving Earth's magnetic field, was observed when reseau positions were compared with preflight determinations obtained at equivalent light levels. The displacements, measured in television lines and pixels, are given in Table III-3. During the ground calibration of the spacecraft, it also was observed that the reseau positions in the scanning raster were dependent upon light exposure level. A shift of about 3 pixels to higher line values occurred between threshold and saturation light levels, and is attributed to bending of the read beam by the unscanned area of the vidicon target. Inflight photography revealed similar displacements; Figure III-3 shows wide- and narrow-angle reseau displacements between threshold and saturation signal levels magnified ten times. Geometric distortion calibrations were performed relative to the reseau marks to neutralize the effects of raster shift; geometric errors in decalibrated images (see Section V) are less than 1 pixel (Ref. III-2).

In pictures of star fields used to calibrate scan platform pointing (scan calibrations I and II), the dark reseau marks generally were invisible at low-background light levels, and read-beam deflection of the great charge discontinuities that corresponded to star positions created greater uncertainties with respect to geometric distortion. However, based on the anticipated positions of reseau marks at the lowest light levels (Fig. III-3b), distortion of the geometric patterns of star fields

Table III-3. Approximate displacements of reseau marks in wide- and narrow-angle television cameras

Displacement	Wide-angle camera	Narrow-angle camera
Vertical	2.44 ± 0.01 line	-0.26 ± 0.01 line
Horizontal	-3.61 ± 0.01 pixel	2.78 ± 0.01 pixel
Rotation	0.58 ± 0.1 mR clockwise	3.6 ± 0.1 mR
Scale, enlargement	-0.14%	0.1%

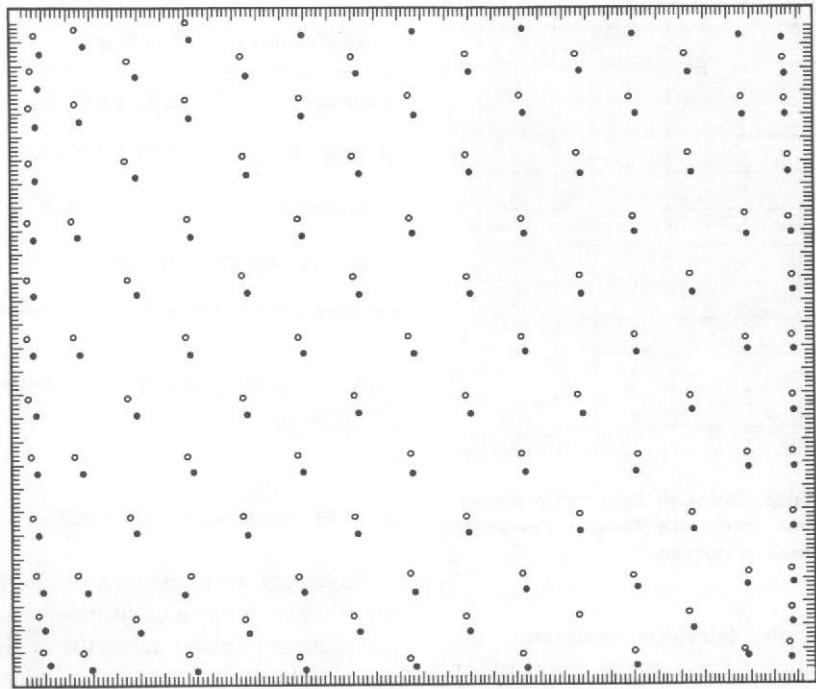
appeared to be within 1 pixel of that predicted from preflight calibrations.

2. Photometric Characteristics

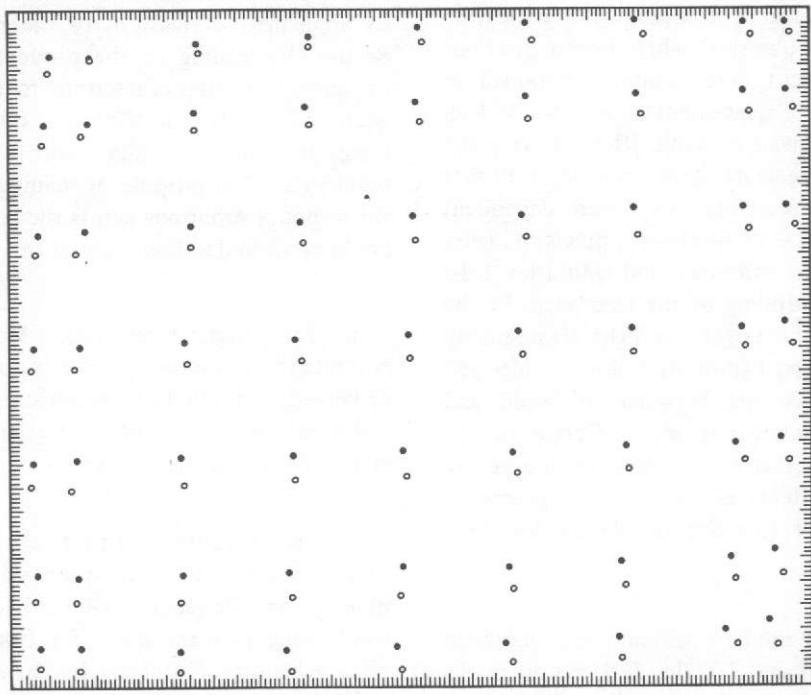
Prelaunch measurements of the photometric properties of the Mariner 9 cameras included light-transfer characteristics, variations in response across the field of view (shading), spectral and polarimetric properties, and blemishes. These photometric calibrations were used to generate graphical and numerical data on the photometric characteristics of the cameras (Ref. III-1), to implement corrections to the data by decalibration (see Section V) leading to the production of the RDR, and to implement shading corrections to the real-time pictures (see Section IV). The decalibration objective was to generate an image in which the data values were proportional to scene luminance. The purpose of shading correction was to correct for response variations across the field of view so that features could be viewed in their correct tonal relationships.

a. *Light-transfer response.* Mariner 9 television inflight photometric response characteristics were consistent to within 25 percent of preflight measurement for the wide-angle camera and to within 15 percent for the narrow-angle camera over the dynamic range of each system.

Five areas (center and four corners) across the field of view of each camera were analyzed using the data from several photographic sequences (Refs. III-2 and III-3). Successive overlapping pictures taken far from periapsis were used to place a feature of constant luminance at these positions. For example, pictures taken in succession during Revs 119-125 show a given surface moving diagonally from left to right across the field of view, and during Revs 250-262 from right to left, with little change in viewing geometry. Mars calibration II also provided useful data for checking preflight light-transfer calibrations at several light levels.



(a) WIDE-ANGLE CAMERA



(b) NARROW-ANGLE CAMERA

Fig. III-3. Displacement of reseau locations between threshold and saturation exposures magnified ten times.

In Fig. III-4, a best estimate of inflight camera performance for each camera at the center of the field of view is compared with values determined from preflight calibrations. The wide-angle-camera data are shown only for filter position 2 (orange). The inflight values relied upon some assumptions regarding the photometric behavior of Mars and Saturn (Ref. III-2). Agreement between inflight and preflight calibration values was good, with the largest fractional deviations occurring at low light levels for the wide-angle camera. These differences were attributed to a decline in camera dark current between launch and the inflight calibration sequences. Changes in shutter speed, which cannot readily be distinguished from changes in dark current, also may contribute to inflight changes in light-transfer characteristics.

The orange filter on the wide-angle camera was used most extensively early in the mission until filter-wheel control was lost on Rev 118; telemetry data and supporting analysis indicated that the filter wheel was locked in position 5, which was the location of one of three polarizing filters. In Fig. III-5, the transfer curve observed in flight for filter position 5 is compared with preflight room temperature calibration (bench). The disparity may be attributed to the fact that the camera was operating at about 5°C, much colder than the temperature for bench calibration. No low-temperature calibration was made for this filter position but, by correcting the bench curve on the basis of temperature variations in vidicon sensitivity for filter position 1, reasonable agreement was shown with preflight values (see Fig. III-5). Spectral response also conformed to preflight calibration values according to the analysis of Ref. III-2.

It is important to note that decalibration of data from the wide-angle camera taken through the three polarizing filters (see Section V) was performed using bench data and was not adjusted for the differential between the bench calibration and actual flight temperatures. Thus, the decalibrated luminosity values on the RDR data were consistently about 29 percent too low. The photometric reliability of the Mariner 9 RDR was questioned on other grounds, especially resulting from analyses of dust-speck shadows on the vidicon faceplates (Ref. III-5).

In pictures from both cameras, several dark circular features were observed that were suggestive of shadows produced by dust specks in the optical systems. Calculations indicated that dust specks on the vidicon faceplates would produce shadows of the sizes observed. However, it was also found that the apparent contrast of the shadows depended on light level (Ref. III-5). Apparent contrast was determined from brightness values calculated from raw DN values using the preflight light-transfer curve. These measurements cast some doubt on the

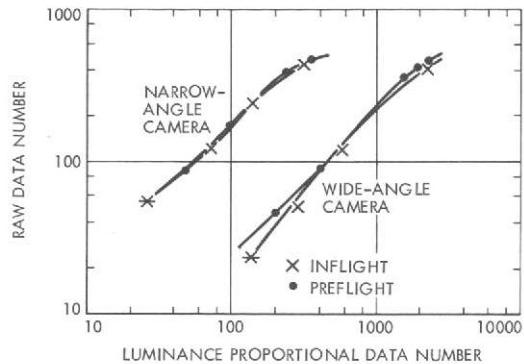


Fig. III-4. Light-transfer response of wide- and narrow-angle cameras, comparing preflight and inflight determinations for the center of the field of view and for filter position 2 in the case of the wide-angle camera.

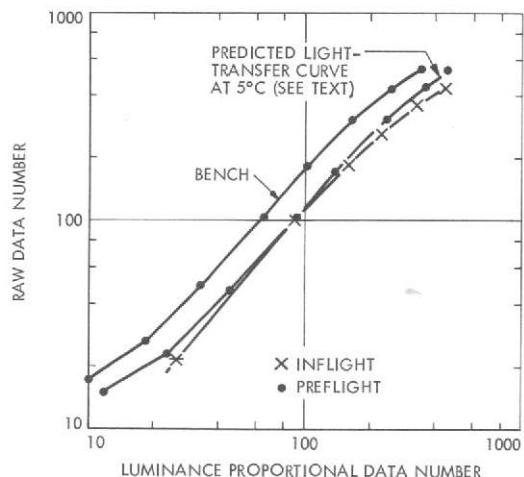


Fig. III-5. Light-transfer response of wide-angle camera: filter position 5.

applicability of preflight photometric calibrations to the data acquired in the vicinity of Mars (Ref. III-5).

Star sequences also gave an indication of the light-transfer response of the cameras for point sources (Ref. III-6). However, there was a large data dispersion, partly attributable to the large and somewhat uncertain effect of image motion (smear); the usefulness of these data as applied to extended sources is questionable.

Changes in camera response between launch and arrival at Mars, uncertainties and variations in the photometric characteristics of Mars, and limitations in the effectiveness of the automatic exposure control (AEC) had an effect on Mariner 9 operational procedures. Because of the dust storm, Mars was

brighter than predicted for the early revolutions in orbit. The shortest exposures available with the AEC led to excessive exposure on the brightest parts of the planet. The failure of the filter wheel on Rev 118 created a similar problem because the AEC was optimized for the orange filter, whereas the polarizing filter had greater transparency. Consequently, shutter speeds were ground commanded when necessary to obtain appropriate exposures.

Ground command of the shutter speeds also was used in other circumstances when the AEC produced undesirable results. In pictures including the limb or terminator of Mars, the AEC sampled black space or large luminance differences, which often caused an unsuitable exposure setting for the subsequent wide- and narrow-angle frames. The low transmission of the violet filter, relative to the orange filter, caused violet frames to be underexposed and orange frames to be overexposed in the automatic filter mode. The usual solution was a single shutter speed for all filters commanded from the ground. Problems also arose when the camera was slewed between successive exposures, changing the luminance geometry and especially the distance from the terminator. In these cases, an empirical relationship between signal and illumination geometry (Fig. III-6) was used to predict the correct shutter speed of the wide-angle camera, which then could be implemented by ground command. Optimal photography should have placed this signal in the mid-range of data numbers. If it fell outside the upper and lower limits of the AEC, then an exposure time transition was likely if the camera were operating in the AEC mode. The range of scene luminance within the frame also was important and is shown as a function of orbital altitude in the small inset diagram. The two diagrams were used effectively to select exposure times that provided a satisfactorily high signal without saturation in any part of the field.

As the AEC did not change exposure until the signal reached $\frac{3}{4}$ scale, the ground command frequently was required with the narrow-angle pictures to provide acceptable data because exposures much in excess of $\frac{1}{2}$ scale in the narrow-angle camera caused a degradation in resolution (see Section III-A-3). Ground commands had to be sent from the Goldstone tracking station to the spacecraft, which meant that they could not be implemented during data acquisition on nadir (odd) revolutions. There also was some risk attached to the use of the ground command, and on Revs 146, 201, 219, and 221, command errors caused erroneous shutter speeds. An error in the CC&S also caused exposure errors during Revs 224 and 233.

b. Shading. In preflight calibration, the response of the upper-left corner of the wide-angle camera's field of view was significantly higher than elsewhere. The narrow-angle camera had similar characteristics (see Ref. III-1). Inflight calibrations

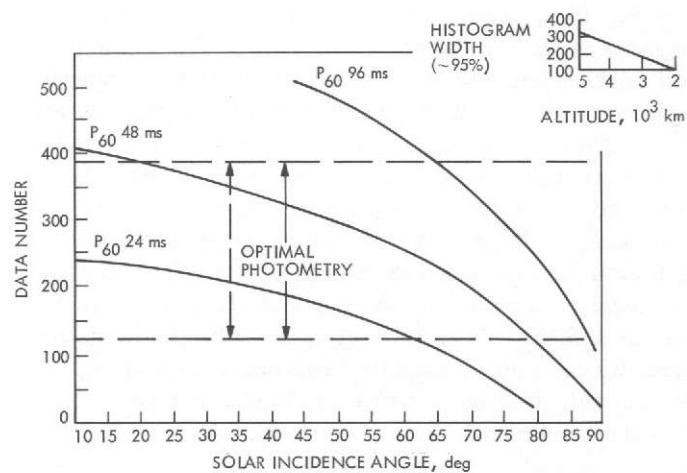


Fig. III-6. Graphical guide to optimal photography: filter position 5. P₆₀ denotes polarizing filter with a 60° orientation relative to the camera scan lines (Ref. III-1).

indicated some change in this shading characteristic (Ref. III-2). The right side of the wide-angle pictures appeared less sensitive than predicted, relative to the left side. This response change was attributed to a residual charge buildup from the normal photographic mode, which always placed the right side of the picture closest to the Martian terminator. No change was reported in the shading characteristics of the narrow-angle camera. Shading correction of the real-time pictures (see Section IV) and decalibration of the raw image data for the RDR were based on preflight calibration data.

c. Residual image. Each image acquired by the Mariner 9 television cameras consisted of a percentage of the previous frame. If the previous frame were dark, little difficulty was presented. If, however, the image were well exposed, with high contrast detail, the residual image was apparent as an overall increase in the apparent scene brightness of the subsequent frame and a subdued record of the actual scene detail. Calibrations of the amount of residual image, performed on the ground (see Ref. III-1), showed that the residual image was somewhat larger in the wide-angle camera, and that it varied between 5 and 15 percent, depending on the exposure of the current and previous frames. These calibrations were used for a residual image correction for the RDR.

The fact that residual image was a significant problem with the wide-angle-camera pictures was evident after the acquisition of six wide-angle frames of Mars taken during the late stages of approach during POS-3 (see Section XI). A new residual formed as each of these frames was taken; each residual was in a slightly different place in the frame because of the motion of the planetary image between frames. Many of the residuals were still apparent in the first few sequences of orbital

photography. The assumption that the residual depended only on the exposure in the previous frame was obviously not appropriate to high-contrast scenes such as the limb (horizon) of the planet.

Several unanticipated operational procedures were implemented because of the persistent residual image left by the limb of the planet in wide-angle pictures. Two procedures were adopted to minimize the residual. The first procedure was applied when there was an attempt to record an image of the limb as part of the science objectives of the atmospheric discipline group. In that case, the limb image was followed by an intentionally overexposed and unrecorded picture that did not include the limb in order to "light flood" the vidicon. This procedure effectively removed the limb residual by creating a spatially uniform residual image. The more frequently used procedure was applied when there was no limb picture actually to be recorded, but when the false-shuttered picture (see Section II), which initiated a photographic sequence, contained the limb. As a remedy, both cameras were left in the 6-ms shutter mode after a revolution's photography until the limb was crossed on the next revolution. This prevented an unwanted residual image because it led to underexposure of the wide-angle picture taken as the limb was crossed. However, it had a disastrous effect on Rev 201 when the ground command to return the shutter to the automatic mode was missed and all the pictures from that revolution were underexposed.

Another modification to the planned sequences was the added capability to record the false-shuttered picture used to control the exposure of the first wide- and narrow-angle pictures of a sequence. This was desirable in many instances to prevent an unknown residual image from affecting decalibration of a targeted picture. False-shutter recording was included as an optional sequence after Rev 70 and was used frequently throughout the mission.

d. Blemishes. In addition to several dark circular features attributable to dust specks on the camera vidicons, many star-like specks are apparent on contrast-enhanced flight pictures. Table III-4 lists the observed blemish positions and amplitudes for the wide- and narrow-angle cameras. The major dark blemishes measured about 30 pixels and appeared to be dust-speck shadows (see Section III-B-2). The bright specks appeared primarily on wide-angle pictures of long exposure (star photography) and were normally less than 5 pixels in diameter.

In each corner of the wide-angle frames are bright defects that appear to be segments of a circle whose diameter is somewhat less than the corner-to-corner dimensions of each frame. These defects probably were caused by scattering in the

Table III-4. Blemishes on camera vidicons (Reduced Data Record locations in parentheses)

Wide-angle camera			
Dust shadows			
Line	Sample	Size, pixels	Amplitude
120 (155)	165 (195)	30	2%
240 (285)	760 (865)	30	3%
485 (550)	130 (155)	30	6%
Narrow-angle camera			
Dust shadows			
Line	Sample	Size, pixels	Amplitude
425 (475)	645 (750)	40	<1/2%
535 (590)	275 (320)	40	1%
690 (755)	330 (395)	50	1-1/2%
Black and white spots			
Line	Sample	Size, pixels	Amplitude
50 (70)	320 (355)	15	+60 DN, -30 DN
187	195	10	+20 DN, -20 DN
240	148	10	+30 DN, -20 DN
118	725	10	+20 DN, -20 DN
322	770	10	+10 DN, -15 DN
522	758	10	+20 DN, -15 DN

Note: There are about a half dozen blemishes, several pixels across, on the wide-angle frames which, under certain conditions, might be mistaken for small craters. The best check on small features is to look at the same location in several frames to verify that the feature is on Mars and not on the vidicon. The narrow-angle vidicon defects are listed in the table because they are large and occur as black and white spots identical to small sharp craters.

electron optics. However, persistent scanning could have imposed them as a fixed pattern on the vidicon target material. Dust specks, blemishes, and these circular defects were generally low-contrast features that were seen easily only when the data were highly enhanced (see Section IV).

3. Resolution and Focus

Preflight determinations of the Mariner 9 camera resolutions were performed using a sine wave resolution target, and the modulation-transfer function (MTF) of the television subsystem was generated. The MTF of each camera was determined in flight by using Fourier transforms of edge tracings across moderate- and high-contrast features (wide-angle camera) and point source images (narrow-angle camera).

Pre-orbital wide-angle pictures of Mars with a scale of about 300 km per pixel provided the high-contrast test targets for

MTF verification. Any significant blurring of the edge of the planet had to be a camera effect in these pictures because atmospheric scattering was limited to altitudes below 50 km. Images of the edge of the polar cap provided a test target of moderate contrast, which was comparable to targets used in ground calibrations. Figure III-7a indicates good agreement between preflight and inflight calibrations for two different filter positions.

For the narrow-angle camera, both preflight and inflight calibrations indicated a loss of resolution when data numbers were above mid-scale. This was a readily noticeable effect, which is of great importance to many users of the imaging data in comparing small features in two different narrow-angle pictures with different exposure levels. Users should be cautious in their conclusions.

Resolution degradation of the narrow-angle-camera vidicon at high exposure proved especially noticeable during the extended mission, when photography of selected targets often occurred far from the terminator. It also was evident on nadir revolutions when only a single shutter speed of the narrow-angle camera was possible because shutter speed changes could not be ground commanded (see Section III-B-2-a). Figure III-8 compares two narrow-angle frames with approximately the same distribution of luminance values (histogram shape), and within the same shutter speed AEC range. The loss in resolution is evident from blurring of picture detail and increase in size of the reseau marks. In some cases, during the extended mission, targets were considered inaccessible because of this effect and, as already indicated, exposure times were ground commanded on zenith (even) revolutions, instead of using the AEC, to ensure a suitable narrow-angle camera exposure for many targets.

4. Noise Level

Noise levels in the Mariner 9 television data were determined from preflight and inflight calibrations; the computed power spectra showed no significant difference between the two sets of data. Measured values of random noise were 0.6 DN RMS for the wide-angle camera and 1.2 DN RMS for the narrow-angle camera. This was presumed to be preamplifier noise, as the analysis technique excluded fixed pattern noise (blemishes) on the vidicon surface, and the contribution of telemetry errors was avoided by selecting high signal-to-noise data.

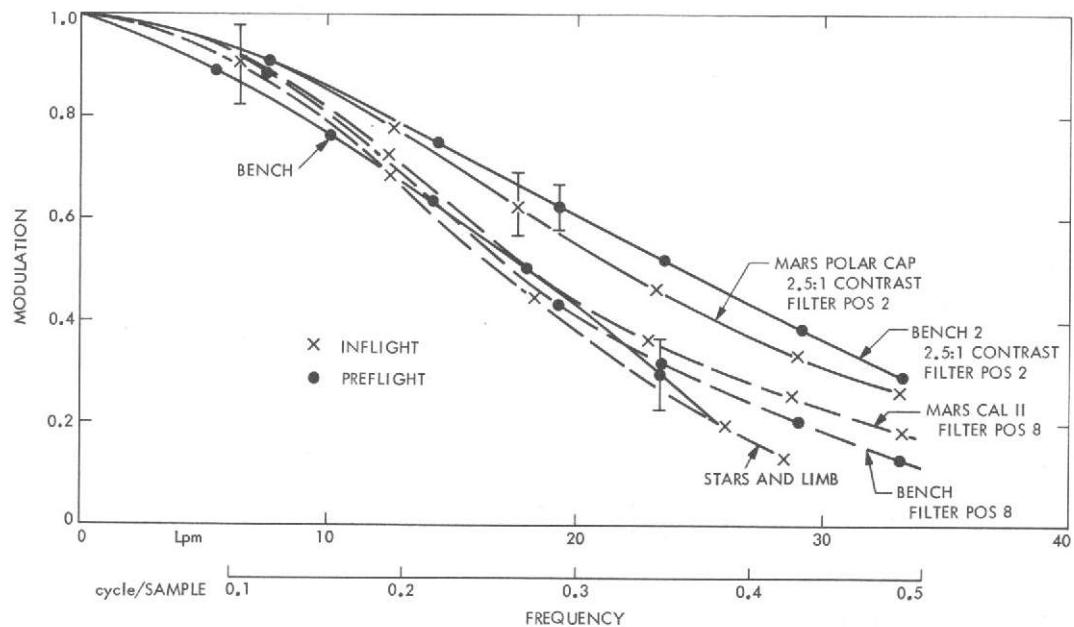
Typical contrast-enhanced flight pictures (see Section IV) revealed coherent noise as vertical bars with an amplitude of about 2 DN peak to peak (about 0.7 DN RMS). It was

attributed to a beat frequency of the carrier (28.8 kHz) with a harmonic of the spacecraft's power frequency (2.4 kHz). Image processing with a vertical filter (see Sections IV and V) reduced the visibility of the noise pattern. Figure III-9a is an example of a wide-angle image showing coherent noise.

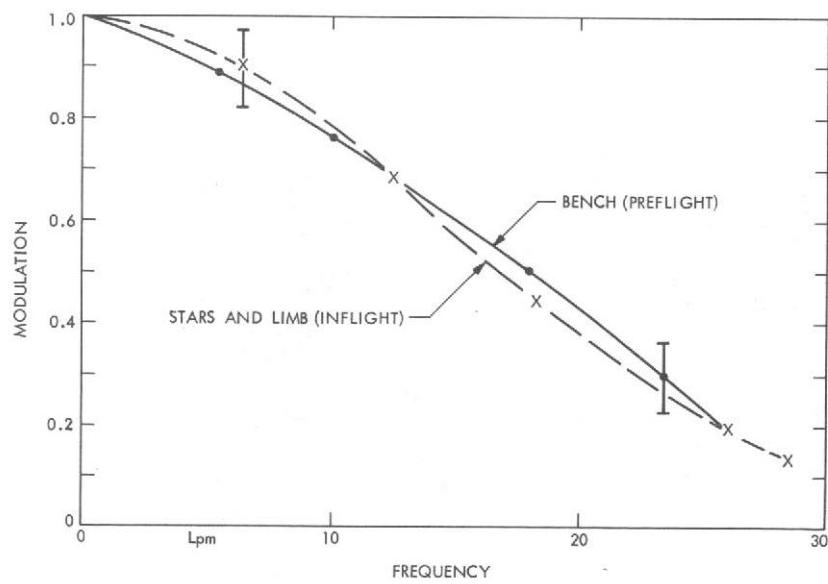
Complex noise patterns were visible in many wide-angle frames with an amplitude of from 5 to 30 DN (Fig. III-9b). The noise was produced by mechanical vibrations of the ultraviolet spectrometer (UVS) mirror, transmitted to the television cameras through the scan platform, and resulted in spasms of microphonic noise during periods of UVS operation. This interference was the only new noise component detected after the launch of Mariner 9. Image processing techniques were developed to remove it, but were not routinely applied to the picture data.

Although not a source of noise intrinsic to the television subsystem, telemetry errors had a significant effect on picture quality. Telemetry quality was most easily recognized in picture data by the number of noise "spikes" and line drop-outs on the picture label (see Section IV). Errors in the line synchronization code (dropouts) and in the 4 most significant bits of a pixel word were a function of telemetry signal-to-noise ratio (SNR). For the available telemetry transmission rates, specific SNR thresholds were defined to initiate spacecraft commands to transmit data at a lower rate. The observed SNR was monitored by the telecommunication station's block decoder assembly; variations occurred as a result of the increasing distance of the spacecraft from Earth, the elevation of Mars above a station's local horizon at the time of transmission, and ground equipment performance. Figure III-10 is a typical SNR variation during Revs 93 and 94 at the Goldstone tracking station, showing how the science data rates were switched to achieve optimum performance.

Imposed on the diurnal variation of the SNR was the longer-term change caused by the varying range of Mariner 9 from Earth and the Earth-Mars-Sun geometry. Figure III-11 shows the variation in predicted bit-error rate (BER) during the extended mission. By Rev 280, the Mars-Earth distance was too great to transmit data using 16.2 kbps at an SNR of 3 dB (5×10^{-3} BER), and by Rev 520 it was anticipated that threshold tolerances would have been reached by the television cameras and the infrared interferometer spectrometer (IRIS). Two options were available: play back television pictures at 4.05 kbps (20 min per picture) and lose the IRIS data or switch to the spacecraft's radio backup exciter (exciter 1). The latter option was selected and was implemented on May 30, 1972. The effect of telemetry quality on the quality of the enhanced images is illustrated in Fig. III-12.

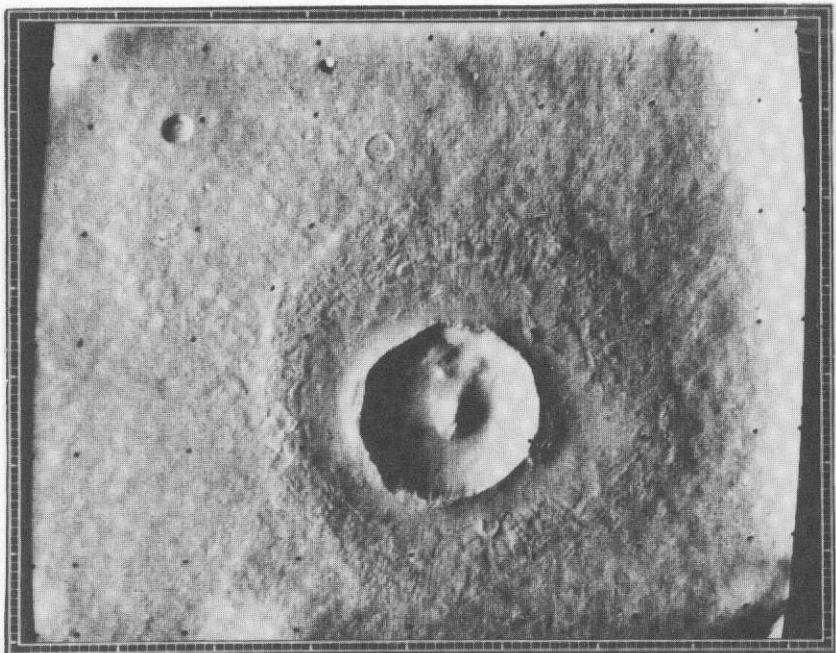


(a) WIDE-ANGLE CAMERA

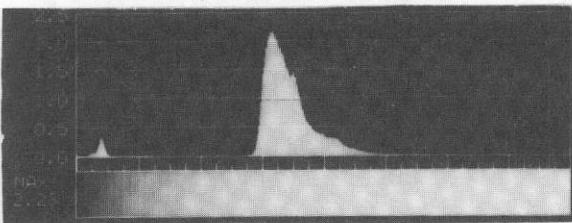


(b) NARROW-ANGLE CAMERA

Fig. III-7. Modulation-transfer function of cameras from preflight and inflight calibrations.

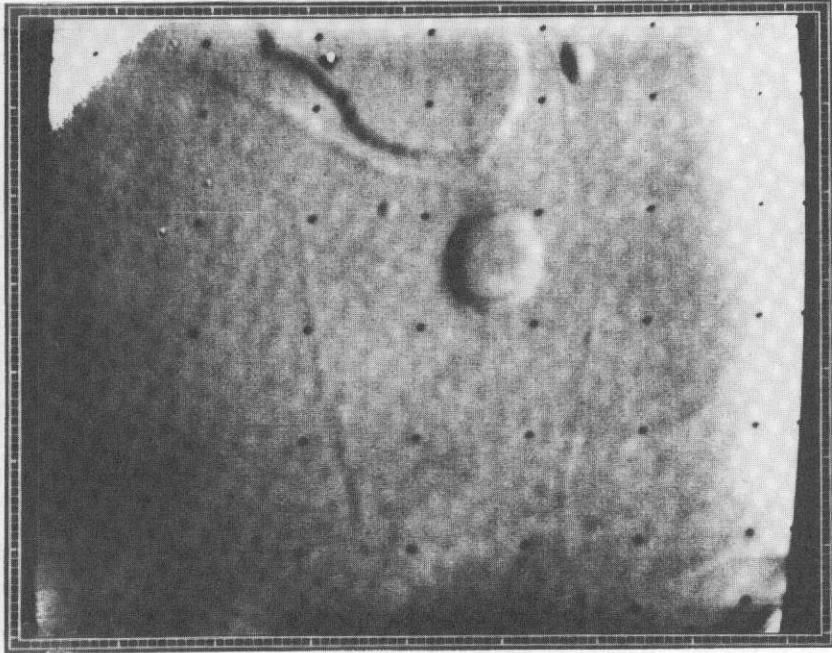


ENHANCED (SHADING-CORRECTED) IMAGE

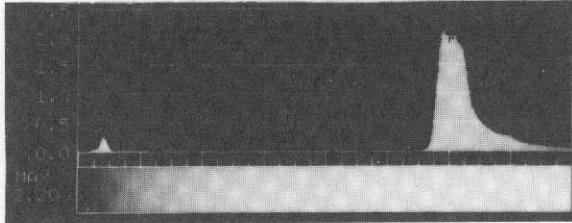


HISTOGRAM
OF RAW
DATA

(a) DAS 08623029



ENHANCED (SHADING-CORRECTED) IMAGE



HISTOGRAM
OF RAW
DATA

(b) DAS 08657469

Fig. III-8. Resolution vs light level for narrow-angle camera. In (b) the camera was exposed to 3/4 of full scale, the reseau marks are increased in size, and scene detail in the enhanced image is blurred.

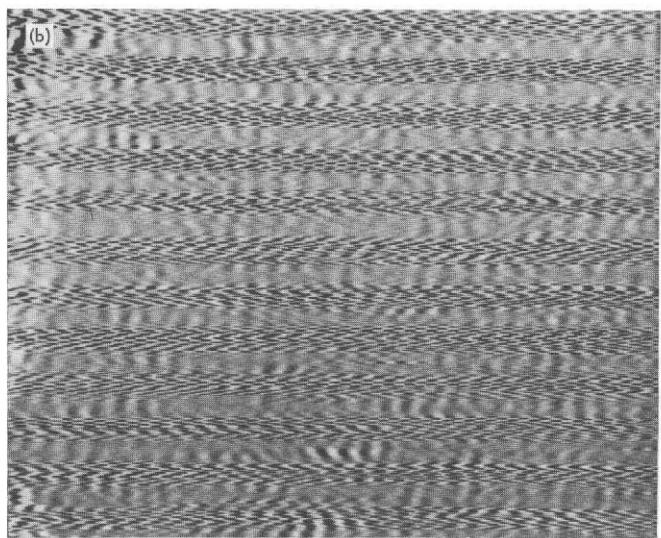
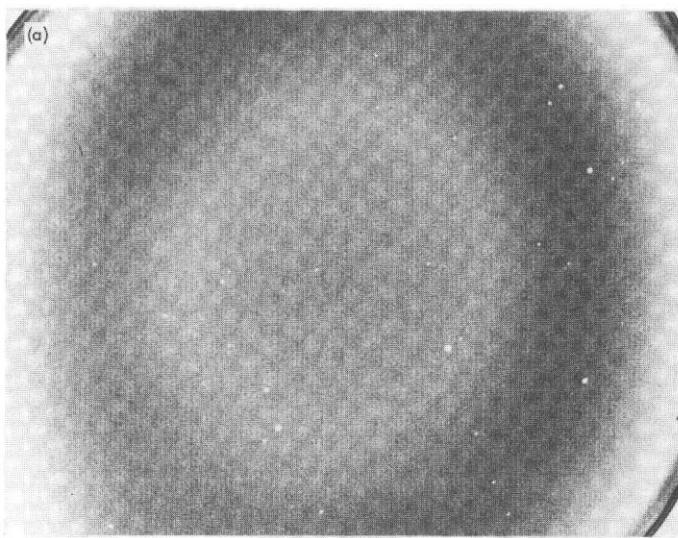


Fig. III-9. (a) Coherent noise in a narrow-angle picture of a star field. Several different frequencies contribute to the pattern, providing an overall amplitude of about 2 DN peak to peak (about 0.7 DN RMS). Random noise, which is also present in this picture, has an amplitude of about 1.2 DN RMS. Contrast is exaggerated by about a factor of 10. (b) Complex noise pattern in the wide-angle camera. The noise pattern, produced by mechanical vibrations of the UVS, has been separated from image detail by bandpass filtering. Contrast is exaggerated by an uncertain factor.

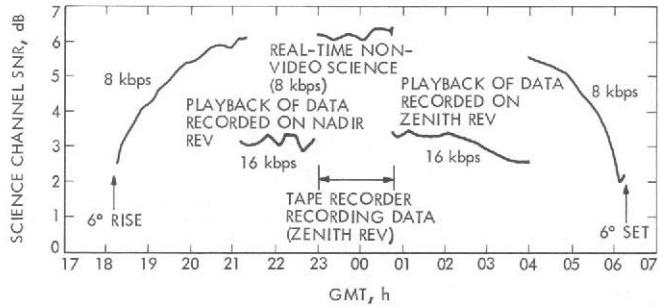


Fig. III-10. Mariner 9 SNR for science data transmitted on Revs 93 and 94 and received at the Goldstone, California, tracking station.

C. Television Experiment Data Processing

The 26 television experimenters comprising the television team participated in the plans for television data acquisition and were the immediate users of the data recovered. The rapid production and distribution of television data enabled the mission to be highly adaptive. Some members of the team monitored the quality of the incoming data; others performed preliminary analyses; and some participated in daily science recommendation team and mission analysis meetings to plan future science operations.

Data made available to the television team for monitoring, analyzing, and planning purposes were composed of video data

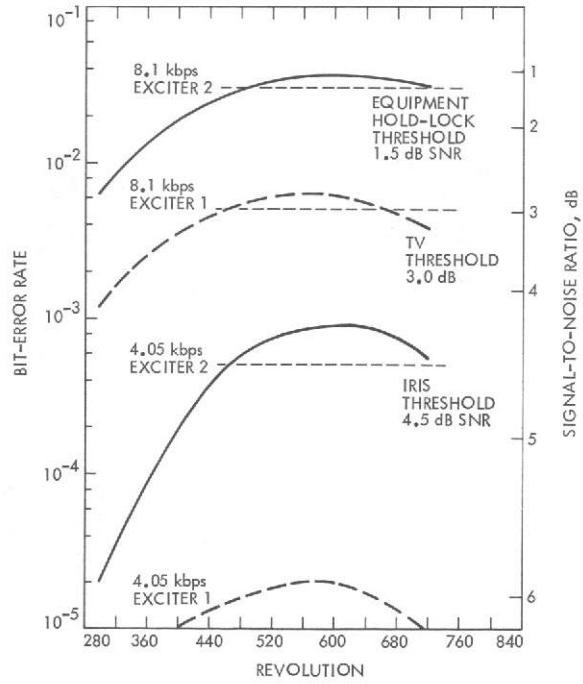


Fig. III-11. Science BER during extended mission.

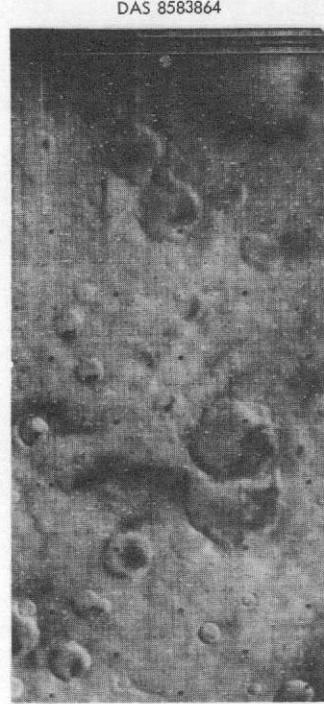
processed in various ways to meet various needs on various time scales. Supporting data, defining the conditions under which pictures were taken, also were generated and were upgraded on several occasions as information regarding the



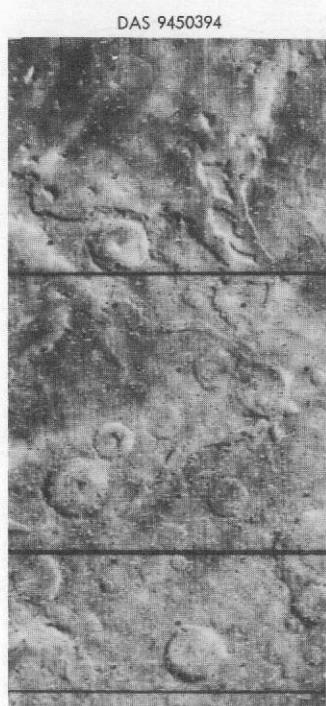
BER: 10^{-4} SNR: 6 dB
RATE: 8.1 kbps



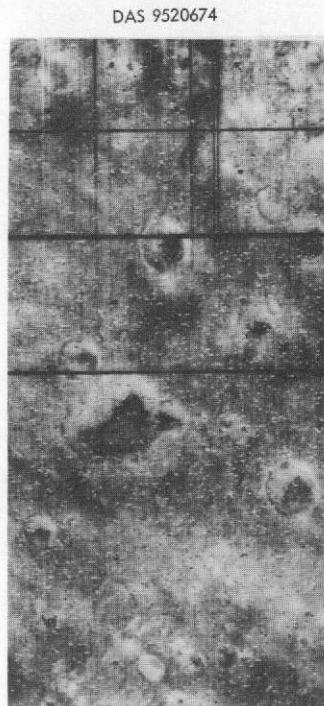
BER: 10^{-3} SNR: 4.5 dB
RATE: 8.1 kbps



BER: 2×10^{-3} SNR: 3.8 dB
RATE: 8.1 kbps



BER: 5×10^{-3} SNR: 3 dB
RATE: 8.1 kbps



BER: 10^{-2} SNR: 2.5 dB
RATE: 8.1 kbps



BER: 5×10^{-4} AND 10^{-2}
SNR: 5 dB AND 2.5 dB
RATE: 8.1 kbps

Fig. III-12. BER examples. Subcaptions describe the noise characteristics.

orbit of Mariner 9 was refined. Video and supporting data were delivered to the experimenters in the form of volatile television monitor displays (as the data were received); hard-copy photographic products including prints, negatives, and positive transparencies; duplicate tapes; and computer listings. Microfiche copies of many of these materials also were produced, but generally much later than the primary data. These products are described in more detail in Tables III-5 through III-7.

1. Video Data Products (See Table III-5)

The television telemetry data received from Mariner 9 were processed in real time to provide a raw image and two or three enhancements which were displayed immediately on television monitors. Some hours later, photographic film records of the same data were completed. These early data products were vital to the planning of the Mariner 9 mission, but remained useful for long-term science analyses (see Section IV). Computer processing of these real-time pictures was performed by the mission test computer (MTC); photographic film processing was performed by the mission test video system (MTVS). The MTC also produced the Experiment Data Record (EDR), which was the highest-quality digital video data available after the merger of the real-time data with tape recordings made at the tracking station.

Correction of photometric and geometric distortions was part of second-generation processing (see Section V) conducted by the JPL Image Processing Laboratory (IPL) and led to the production of the RDR. Additional processing of a subset of the Mariner 9 data at the IPL led to the production of rectified and scaled (R&S) pictures, which were mapping projections designed primarily for incorporation into semi-controlled and controlled photomosaics at 1:5,000,000 and larger scales (see Section VI). Specially processed television data meeting the needs of individual and small groups of experimenters were produced at the IPL and also by the Artificial Intelligence Laboratory (AIL) of Stanford University (Ref. III-7).

2. Picture Summaries and Navigation Data (See Table III-6)

Detailed summaries of the various processed forms of data available for specific pictures appear in a series that is available as computer printouts and microfiche cards (Fig. III-13). The summaries identify the photographic film products by roll and file number and the digital imaging data by magnetic tape and file for each picture. The Real-Time Picture Data Summary includes real-time picture products and the EDR. The IPL

Enhancement Summary lists all processed imaging data produced at the IPL, including the RDR, R&S pictures, and special experiment support enhancements. The subset of data from the IPL Enhancement Summary that constitutes the RDR appears in the RDR Data Summary. Summaries of R&S data also have been generated.

The picture summaries provide no information about what part of Mars is included in a particular picture or about the geometry of picture acquisition (range, lighting, viewing, etc.) This type of supporting information is derived from a separate file of navigation data termed the Supplementary Experiment Data Record (SEDR). The final version of the SEDR was produced by a sequence of computer programs called "Mini-LIBSET." The most widely distributed hard-copy version of data derived from the SEDR is shown in Fig. III-14. Data extracted from the SEDR are also used in the Microfiche Catalog Index for both real-time and RDR data (see Fig. III-15).

In both the picture summaries and the SEDR, the primary identification for a specific picture is an eight-digit number called the DAS time, or DAS count. This number was generated by a spacecraft clock that counted in increments of 1.2 s. There were, therefore, 35 increments of the DAS time during the fixed time span of 42 s required for shuttering a picture, reading the image from the vidicon, and tape recording it. The most significant DAS time in the operation of the television camera corresponded to camera shuttering, which exposed the sensitive target of the vidicon. Most exposures were shorter than the 1.2-s DAS time increment, so that the time at which exposure occurred was adequately approximated by the opening time of the shutter.

The DAS time corresponding to the shutter opening was not included in the video data stream, although the DAS time corresponding to the readout of each line of data from the cameras was included in the telemetry. The DAS time that appears on picture labels and identifies these pictures in the picture summaries was derived directly from these telemetry data. The picture label DAS time corresponds to the readout time of the first line of data successfully reconstructed into an image. When a picture was successfully received, the picture label DAS time was five units larger than the DAS shutter time. Some lines at the top of the frame were missing in about 5 percent of the pictures, and the DAS time on the picture label and in the picture summaries was up to 30 units larger than the DAS shutter time. In about 20 pictures, because of telemetry errors, the DAS time was erroneous and bears no simple relationship to the DAS shutter time. In the SEDR and also in the Microfiche Catalog Indexes (see Fig. III-15), the DAS shutter time is used to identify pictures.

Table III-5. Video data products used by experimenters

Data type	Data product	Institutional availability			
		NSSDC	JPL	USGS	Other ^a
Real-time pictures (see Section IV)	16-mm microfilm	Yes ^{b,c}	No	No	
	Microfiche	Yes ^{b,c}	Yes ^b	Yes ^b	
	Caltech microfiche	Yes ^{b,c}	No	No	Caltech
	70-mm positive transparency (master)	No	Yes ^b	No	Caltech
	70-mm negative	Yes ^{b,c}	Yes ^b	Yes ^b	
	70-mm strip contact print	Yes ^c	Yes ^b	Yes ^b	
	20-by 25-cm (8- by 10-in.) prints	Yes ^c	Yes ^b	Yes ^b	
Experiment Data Record (see Section IV)	Prints, film dupes, and slides (standard sizes)	Yes ^c	No	No	
	Duplicate tape				
Reduced Data Record (see Section V)	PTV Preliminary unprocessed video or TVE Final unprocessed video	No	Yes ^b	Yes ^b	Stanford U., Cornell U.
	Microfiche	Yes ^{b,c}	Yes ^b	Yes ^b	
	70-mm positive transparency (master)	No	Yes ^b	Yes ^b	
	70-mm negative (original)	No	Yes ^b	No	
	70-mm negative (duplicate)	Yes ^{b,c}	Yes ^b	Yes ^b	
	70-mm strip contact print	Yes ^c	Yes ^b	Yes ^b	
	20- by 25-cm (8- by 10-in.) prints	Yes ^c	Yes ^b	Yes ^b	
Rectified and scaled pictures (see Section VI)	Prints, film dupes, and slides (standard sizes) ^d	Yes ^c	No	No	
	Duplicate tape of reduced and decalibrated data	Yes ^c	Yes ^b	Yes ^b	Stanford U., Cornell U.
	70-mm positive transparency (master)	Yes ^b	Yes ^b	Yes ^b	
	70-mm negative (original)	No	Yes ^b	No	
	70-mm negative (duplicate)	Yes ^{b,c}	Yes ^b	Yes ^b	
Limb microfiche	20- by 25-cm (8- by 10-in.) prints	Yes ^c	Yes ^b	Yes ^b	
	High geometric fidelity prints	No	No	Yes ^b	
	Prints, film dupes, and slides (standard sizes)	Yes ^c	No	No	
	Duplicate tape	No	Yes ^b	Yes ^b	
	Microfiche	Yes ^{b,c}	Yes ^b	No	
Specially processed television data for experimenter analysis support	70-mm negative (original)	No	Yes ^b	No	Experiment team members retain some original negatives and prints
	20- by 25-cm (8- by 10-in.) prints	No	Yes ^c	Yes ^b	

^aData in this column are incomplete and therefore subject to change.

^bReference copy available at the Institution.

^cReproduction copy available upon request.

^dSee available formats in Data Announcement Bulletin, NSSDC 74-05, March 1974.

NSSDC National Space Science Data Center, Code 601, Goddard Space Flight Center, Greenbelt, Md.

JPL Jet Propulsion Laboratory, Pasadena, Calif.

USGS U. S. Geological Survey, Flagstaff, Arizona.

Caltech Space Photography Laboratory, Division of Geological and Planetary Sciences, Pasadena, Calif.

Stanford U. Artificial Intelligence Laboratory, Stanford, Calif.

Cornell U. Laboratory for Planetary Studies, Center for Radiophysics and Space Research, Ithaca, N. Y.

Table III-6. Television data summaries

Data type	Data product	Institutional availability			
		NSSDC	JPL	USGS	Other ^a
Picture enhancement summaries and indexes (see Fig. III-13)					
<u>Real-Time Picture Data Summary.</u> Listings of roll and frame identifications of all real-time picture versions and tape and file numbers for EDR. Two separate catalogs: one arranged in ascending order of DAS time; the other in ascending order of roll number	Computer printout 16-mm microfilm	No No	Yes ^b No	Yes ^b No	
<u>IPL Enhancement Summary.</u> Listings of all processed versions of each Mariner 9 picture produced at the IPL. Includes the RDR, R&S data, limb microfiche, and experimenter analysis support data. Two separate catalogs: one arranged in ascending order of DAS time; the other in ascending order of roll number. Includes the RDR as a subset	Computer printout 16-mm microfilm 25- by 36-cm (10- by 14-in.) prints	No No No	Yes ^b No No	Yes ^b No No	
<u>RDR Data Summary.</u> Listings of roll and frame identifications of the two film versions and the tape and file numbers of basic digital data for the RDR. Two separate catalogs: one arranged in ascending order of DAS time; the other in ascending order of roll number	Computer printout 16-mm microfilm	No No	Yes ^b No	Yes ^b No	
Picture geometry data					
<u>Supplementary Experiment Data Record.</u> Numerical information on latitude, longitude, solar illumination angle, etc. Complete data set available only on magnetic tape (see Ref. III-8 for format)	Computer printout (see Fig. III-14) Microfiche 22- by 28-cm (8½ by 11-in.) prints Magnetic tape	No Yes ^{b,c} No Yes ^c	Yes No No Yes	No No No Yes ^c	
<u>Latitude and Longitude Index.</u> Pictures sorted by latitude center point and longitude center	Computer printout 16-mm microfilm	No Yes ^{b,c}	Yes ^b No	Yes ^b No	
<u>Special Indexes.</u> Pictures sorted by DAS time, MTVS roll and file number, and by IPL roll and processing time	16-mm microfilm	Yes ^{b,c}	No	No	
Microfiche catalogs					
Summaries of picture data in microfiche or microfilm form (see Table III-5). Includes identification of different picture versions (but not tapes) and picture geometry numerical data					
<u>Real-Time Microfiche</u>	Microfiche (with images)	Yes ^{b,c}	Yes ^b	No	
<u>Reduced Data Record Microfiche</u>	Microfiche	Yes ^{b,c}	Yes ^b	Yes ^b	

^aData in this column are incomplete and therefore subject to change.

^bReference copy available at the Institution.

^cReproduction copy available upon request.

NSSDC National Space Science Data Center, Code 601, Goddard Space Flight Center, Greenbelt, Md.

JPL Jet Propulsion Laboratory, Pasadena, Calif.

USGS U. S. Geological Survey, Center of Astrogeology, Flagstaff, Ariz.

Table III-7. Graphical data, photomosaics, and maps used by experimenters

Data type	Data product	Institutional availability			
		NSSDC	JPL	USGS	Other ^a
Graphical data					
<u>Footprint Charts.</u> Computer-generated plots showing the outline of coverage for various subsets of Mariner 9 television pictures plotted on Mercator or Polar Stereographic coordinate grids (see Addendum)	1:5,000,000-or 1:25,000,000-scale (full size) reproductions Prints, film dupes, and slides (standard sizes)	Yes ^b Yes ^{b,c}	Yes ^b No	No No	Cornell U.
<u>Overlays.</u> Computer-produced data sheets that are suitably scaled for overlays on real-time pictures to show: (1) latitude and longitude grid lines relevant to each picture, and (2) Sun elevation and viewing angle contours	22- by 28-cm (8½- by 11-in.) prints 22- by 28-cm (8½- by 11-in.) transparencies Prints, film dupes, and slides (standard sizes)	Yes ^{b,c} No Yes ^c	Yes ^b Yes ^b No	Yes ^b No No	
Photomosaics					
<u>JPL Mosaics.</u> One of 96 mosaic boards of selected areas on the Martian surface grouped according to geographic area	Original boards 22- by 28-cm (8½- by 11-in.) prints 10- by 13-cm (4- by 5-in.) negatives Prints, film dupes, and slides (standard sizes)	No Yes ^{b,c} Yes ^b Yes ^c	No Yes ^b Yes ^b No	Yes Yes ^b Yes ^b No	
<u>USGS Mosaics.</u> 1:5,000,000-scale mosaics of 30 areas of planet. Two types produced: semi-controlled and controlled. Only semi-controlled mosaics are available for general distribution. Mosaics at 1:1,000,000 scale for selected areas including Viking landing sites	Original mosaics Duplicates at 1:5,000,000 scale 10- by 13-cm (4- by 5-in.) negatives Prints, film dupes, and slides (standard sizes)	No No Yes ^b Yes ^c	No Yes ^b No No	Yes ^b Yes ^{b,c} Yes ^b No	
<u>Globe Mosaics.</u> Rectified and scaled Mariner 9 pictures mosaicked onto 1.2-m (4-ft) globe	Original globes 10- by 13-cm (4- by 5-in.) negatives of entire globe 10- by 13-cm (4- by 5-in.) negatives of contiguous sectors Prints and slides (standard sizes)	No Yes ^b Yes ^b Yes ^c	Yes ^b Yes ^b Yes ^b No	No No No	
Maps					
<u>USGS Shaded Relief Maps.</u> Airbrushed topographic maps based on controlled photomosaics	Original maps Duplicates at 1:25,000,000, 1:5,000,000, and 1:1,000,000 scales	No No	No Yes ^b	Yes ^b Yes ^{b,c}	
<u>Albedo Maps.</u> Produced at the University of Texas	Photographic prints Duplicates at 1:5,000,000 scale	Yes ^c No	No Yes ^c	No Yes ^c	U. of Texas

^aData in this column are incomplete and therefore subject to change.

^bReference copy available at the Institution.

^cReproduction copy available upon request.

NSSDC National Space Science Data Center, Code 601, Goddard Space Flight Center, Greenbelt, Md.

JPL Jet Propulsion Laboratory, Pasadena, Calif.

USGS U. S. Geological Survey, Center of Astrogeology, Flagstaff, Ariz.

Cornell U. Laboratory for Planetary Studies, Center for Radiophysics and Space Research, Ithaca, N. Y.

U. of Texas Department of Astronomy, Austin, Texas.

(a) MARINER 9 -- REAL-TIME PICTURE SUMMARY

JUL 19, 1973

DAS TIME	GMT	REV	CAM NO.	D	EXP	FILT	MTVS	MTC	INPUT	FILE	COMMENTS
		NO.	IN	S	TIME	POS	ROLL	FILE	ENHC	TAPE	NO
			REV	P	(MS)			R	S	F	
01320992	313.03.29.14	A	10	C	24MS	1	4000--009 X	PTV-0040	12	IMAGE BELOW CENTER	MARS CAL I
	313.03.29.14	A	10	C	24MS	1	4000--010 X	PTV-0040	12		
	313.03.29.14	A	10	C	24MS	1	4000--011 X	PTV-0040	12		

(b) MARINER 9 -- IPL ENHANCEMENT SUMMARY

SEP 13, 1973

DAS TIME	PRC	PRC	ROLL	ENHC	ENHC	ENHC	ENHC	ENHC	ENHC	OUTPUT	TAPE	REMARKS
	TIME	DATE	NC#	1	2	3	4	5	6	7	TAPE	FILE
01320992	07/01/72	NCF	1803	0015							TVR-1054	01
	211123		1803	0015	CSL							
	211451		1803	0015	MD16							
11/10/72	152933		0055	PS2						-	-	MARS CAL 1

(c) RDR SUMMARY

JUN 8, 1973

DAS TIME	REV	CAM	NC.	TOTL	D	CML	ROLL	PRCC	ENHC	ENHC	RDR	
	NO.		IN	PICS	S	PIC.	NO.	TIME	1	2	STATUS	
			REV	IN	P	NO.						
01320992	A	10	C	1803	NONF		0015					
	A	10	C	1803	211123		0015	CSL		OK		
	A	10	C	1803	211451		0015	MD16		OK		

Fig. III-13. Sample picture summaries for DAS 01320992.

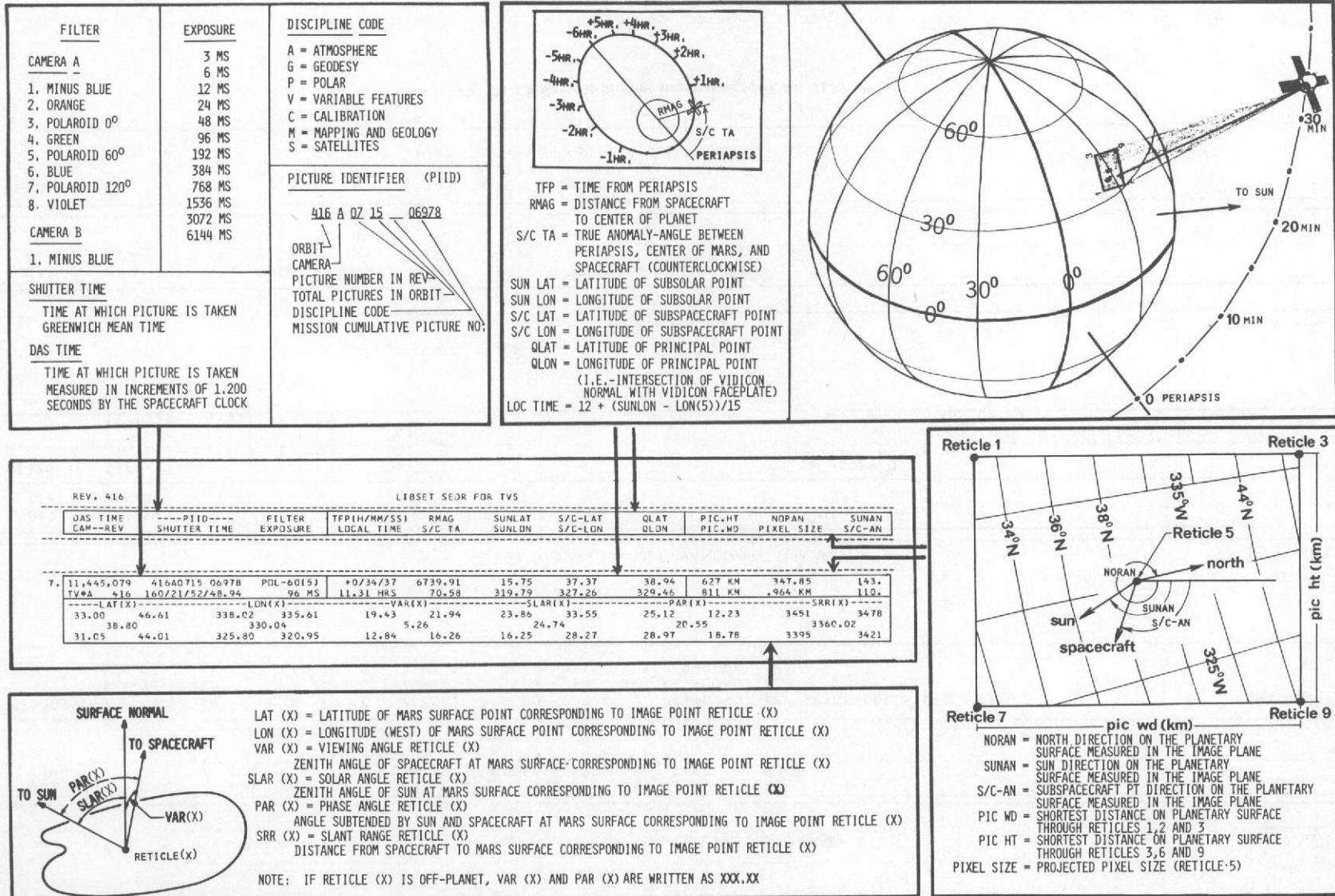


Fig. III-14. Explanation of SEDR data.

SHOWN BELOW IS THE INDEX HEADING AND AN EXAMPLE OF THE THREE LINES OF DATA THAT DESCRIBE EVERY PICTURE IN THE CATALOG. TWO VERSIONS OF EACH PICTURE APPEAR IN THE MICROFICHE CATALOG. THEIR LOCATION IN THE MICROFICHE CATALOG AND THE ROLL AND FILE NUMBER OF THE SAME DATA STORED ON 70MM FILM IS ALSO GIVEN. PICTURE IDENTIFICATION NUMBERS AND CAMERA FILTER INFORMATION ALSO APPEAR. BASIC RANGE, VIEWING ILLUMINATION AND COVERAGE INFORMATION IS TABULATED AND EXPLAINED BY THE ASSOCIATED DIAGRAMS.

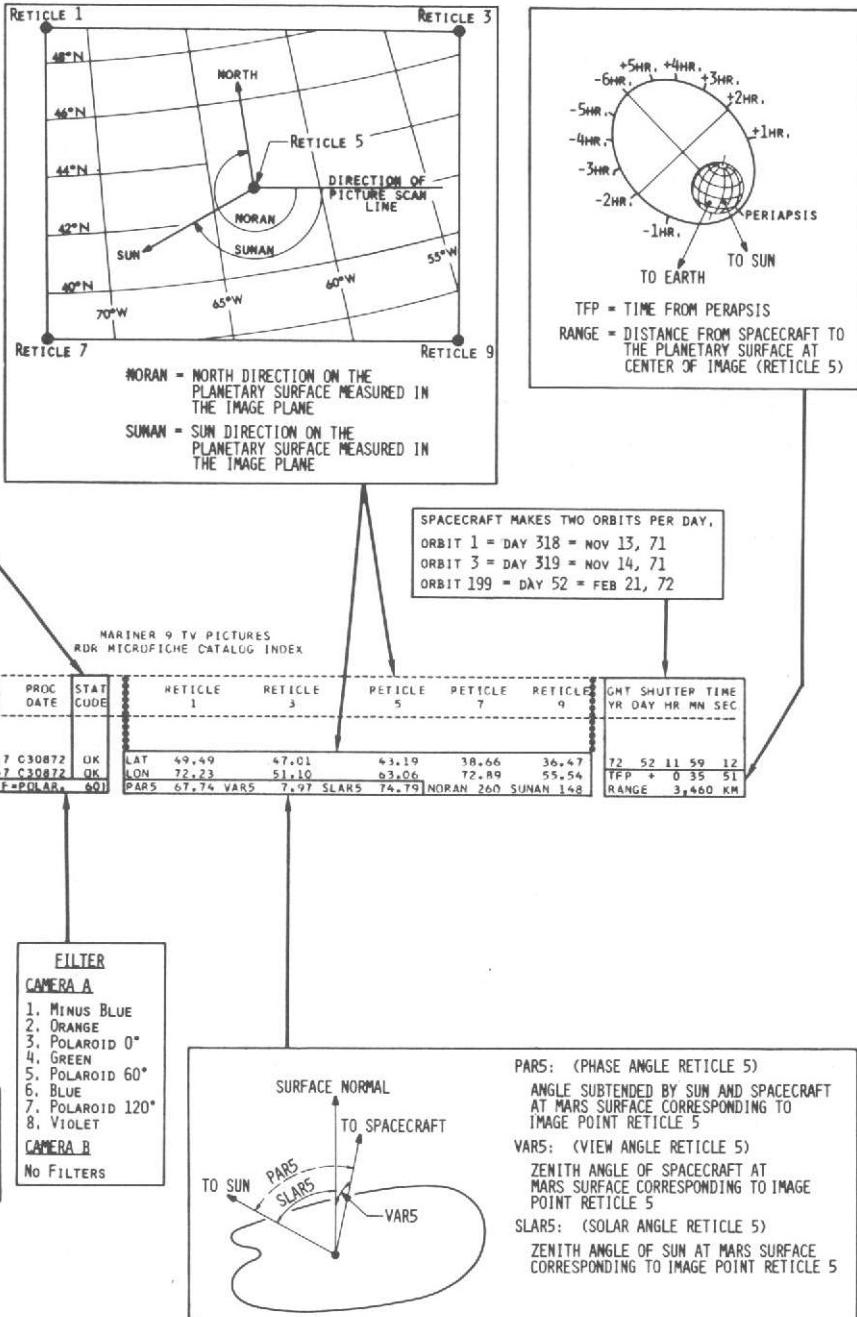


Fig. III-15. Explanation of data on Microfiche Catalog Index.

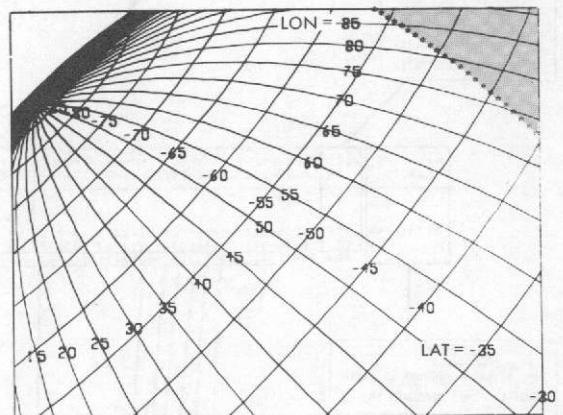
In searching for the navigation data corresponding to a specific picture, or vice versa, the characteristics of the DAS time identification scheme must be clearly understood. Data acquired by other boresighted instruments on the spacecraft's scan platform also used the DAS time for identification. For these other instruments, acquisition and readout times were identical.

Although the DAS time is the primary identification number and the only one that appears reliably on the pictures, other forms of identification have been used. The format of the Principal Investigator Identification (PIID; see Fig. III-14) suffers from the disadvantage of never appearing on real-time pictures and only irregularly on the RDR and R&S pictures. It also is long and cumbersome. In this volume and in Volume II, pictures listed in the tables are identified by revolution and frame number as well as by DAS time. This former notation is brief and is more immediately informative regarding when during the mission and at what stage during a revolution a specific picture was taken. It does not, however, appear on the pictures but is assigned by a computer program that scans the SEDR data. Some deletions have been made from the SEDR files (see next paragraph), causing changes in the picture sequence numbers. For these reasons, the DAS time is considered the more reliable.

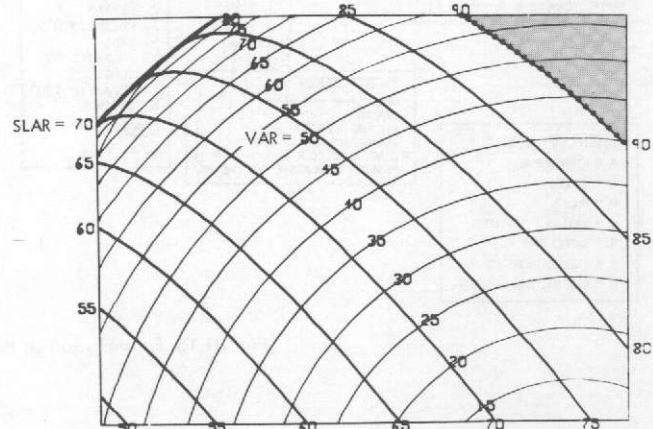
Some pictures planned to be taken by Mariner 9 were not obtained because of spacecraft or command problems. In other cases the pictures were taken, but the data were never transmitted or were not recovered by the ground station. In many more cases, parts of a picture were recovered, but varied numbers of lines from the picture were lost. Sometimes these data were recoverable because they had been received at the Goldstone station, but were lost in the real-time transmission from Goldstone to the MTC at JPL. In the SEDR there is no direct indication of the data recovered from a picture-taking sequence, and in early versions many pictures were listed for which no actual image was received. In the final SEDR dated June 30, 1973, all entries were deleted for which no film hard-copy image consisting of more than ten lines existed. This version of the SEDR was also used for most of the tables presented in this volume; a similar set of data was used in the Volume II Addendum. Between the publication of Volume II (December 15, 1972) and the Addendum to Volume II, 215 frames were either added to or deleted from the SEDR file. About 35 frames were deleted between then and the production of the final SEDR. For both of these supplementary experiment data systems, the MARK IV Data Management System was used as the final storage and output technique for data. This permitted data to be sorted and formatted according to various criteria (Ref. III-8). The MARK IV System also was used in the production of many tables in this volume.

3. Graphical Data, Photomosaics, and Maps (see Table III-7)

a. Graphical data. Graphical data were extremely important to science analysis and mission planning. Overlays were transparent computer-produced sheets scaled to the real-time 20- by 25-cm (8- by 10-in.) copies of television pictures. They showed either latitude and longitude grid lines relevant to each picture or Sun elevation and spacecraft viewing angle contours (Fig. III-16). Footprint charts were computer-generated plots showing the outline of coverage for various subsets of Mariner 9 television pictures on Mercator or Polar Stereographic coordinate grids (Fig. III-17). Charts were generated at both 1:5,000,000 and 1:25,000,000 scales (see Addendum to this volume). Footprint plots at much smaller formats also were used for mission planning. The SCOUT program was used to generate mapping projections and perspective views with superimposed footprints and was used with graphics terminals in the Space Flight Operations Facility to provide both volatile and permanent displays for planning purposes (see Fig. III-18). A more accurate display was provided by the more sophisticated



(a) FOR LATITUDE (LAT) AND LONGITUDE (LON) GRID LINES



(b) FOR LIGHTING ANGLE (SLAR) AND VIEWING ANGLE (VAR) CONTOURS

Fig. III-16. Examples of overlays for DAS 03247830.

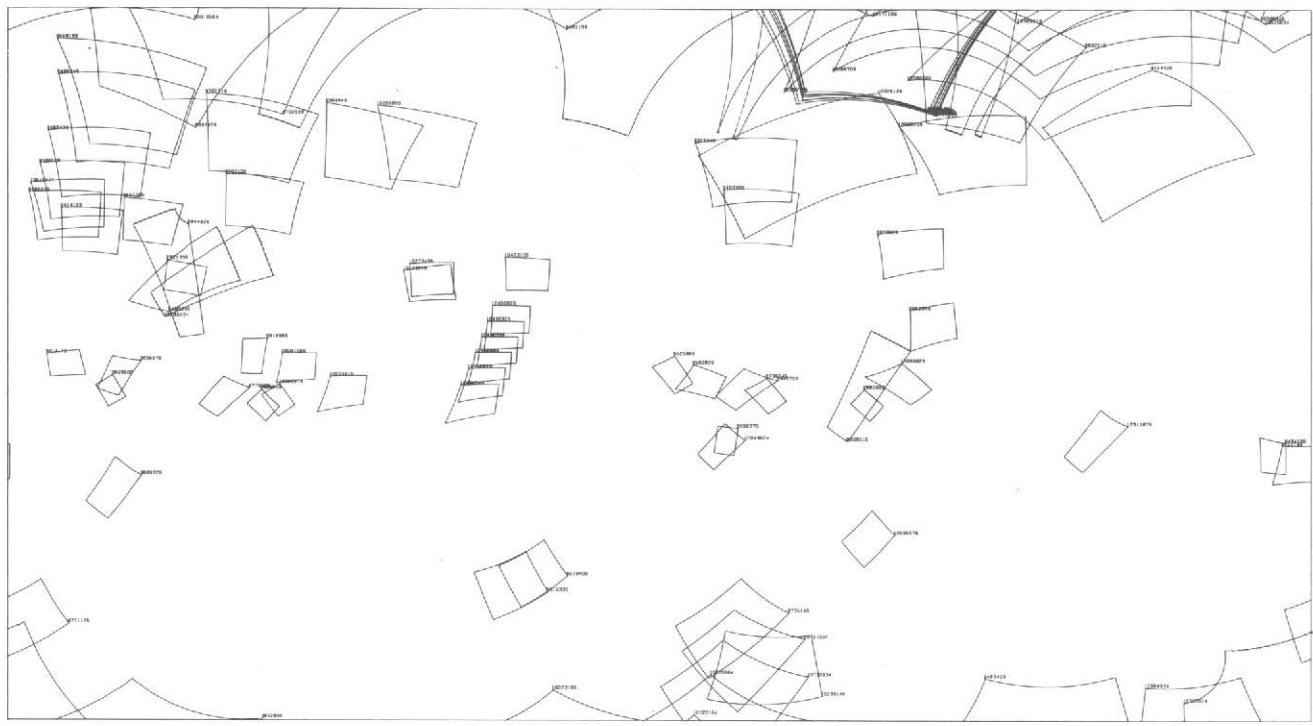


Fig. III-17. Examples of footprint plots for wide-angle frames from Phase I of the extended mission: Revs 247-262. The original is a 1:25,000,000-scale Mercator Projection.

program, POGASIS, which was used for the final version of a sequence plan. POGASIS contained the mission constraints for Mariner 9 and could plan portions of a data-acquisition sequence given initial conditions by the operator.

b. Photomosaics. During the mapping phase of the orbital operations, variable-scale mosaics were assembled on a real-time basis by personnel of the U.S. Geological Survey, and copies were distributed (Ref. III-9). These mosaics consisted of photographic "chips" cut from strip contact prints, which were pasted onto latitude and longitude grids that were specially designed to accept the unscaled pictures. One set of variable-scale mosaics (16 mosaic boards) contained spatially filtered versions of the Mariner 9 pictures; the other set used the shading-corrected (albedo) version.

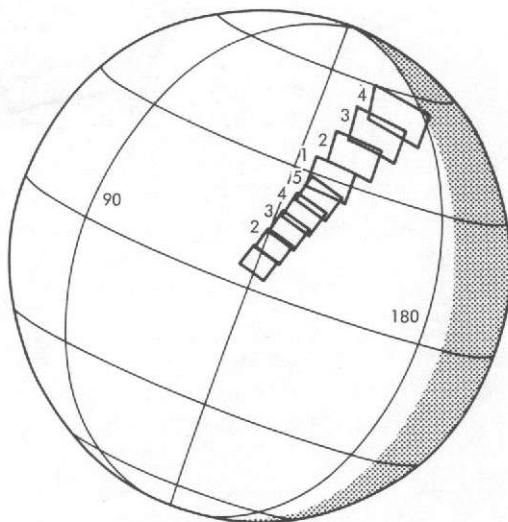
Groups of special mosaics containing three or four contiguous wide-angle frames were mounted for display during the early exploratory phase of the mission. Later, similar mosaics of contiguous narrow-angle frames were assembled showing interesting landforms. Copies of these mosaics were distributed.

At the U.S. Geological Survey, Flagstaff, Arizona, uncontrolled photomosaics were made at 1:5,000,000 scale, and copies were sent to JPL for distribution. These mosaics used scaled, but unrectified, pictures assembled onto Mercator,

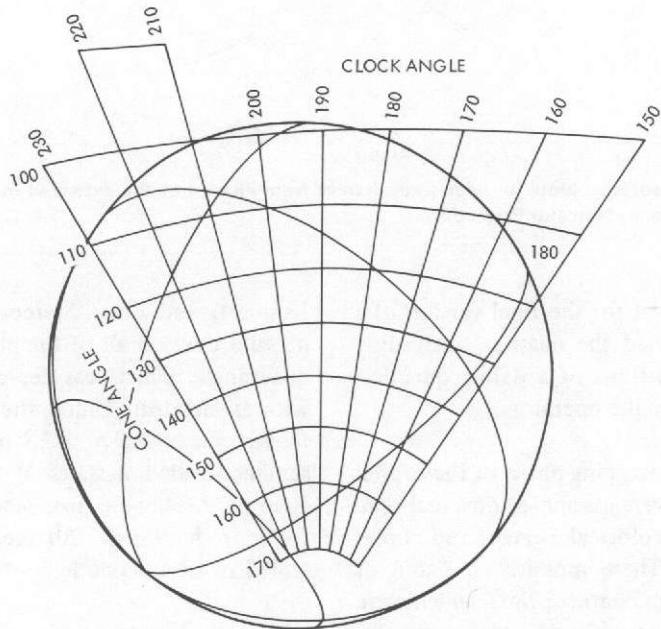
Lambert, and Polar Stereographic grids. Twenty-nine such mosaics covered all of the planet, except for the Mare Boreum quadrangle, which was depicted by a shaded relief map made with an airbrush. Unlike the other 28 mosaics, the north polar mosaic made use of R&S pictures (see Section VI). Thirty semi-controlled mosaics at 1:5,000,000 scale, comprised of R&S pictures, were produced later (see Sections VII and VIII for reproductions). All pictures used in these mosaics were scaled to fit a geodetic control network of reference locations.

Rectified pictures also were mosaicked on a 1.2-m (4-ft) globe (see Section VI). Copies of this globe have been made using a novel technique. The original globe was photographed in 452 approximately rectangular segments. The location of each photograph was defined by a mask. It is possible to create a reproduction of the original globe at any desired scale by reproducing and assembling these small-scale photographic segments.

A set of 96 picture boards containing picture chips from the 70-mm strip contact prints, sorted for various sectors of the planet, also were produced by the U.S. Geological Survey. These boards were divided into three groups: narrow-angle frames taken during mapping runs, wide- and narrow-angle frames not taken during mapping runs, and geodesy frames. For the most part, these pictures were not mosaickable, but



(a) REV 200: POSSIBLE TARGETS



(b) REV 140: P - 10 min

Fig. III-18. SCOUT program plots used in mission sequence planning.

were arranged on the boards in columns, each column related to a revolution. Copies were produced by the MTVS at JPL and were distributed.

c. Maps. Final mapping products include an updated 1:25,000,000-scale shaded relief rendition of topographic features using a Mercator Projection for the latitude range of

65°N to 65°S and Polar Stereographic Projections from 60°N to 90°N and 60°S to 90°S. Similar maps that show the planet's albedo features also were produced.

A 1:16,700,000-scale 40-cm-diameter (16-in.-diameter) cartographic globe also has been produced under the direction of members of the Mariner 9 television team (see Ref. III-10).

References

- III-1. Snyder, L.M., *Mariner 9 TV Subsystem Calibration Report*, Jet Propulsion Laboratory Internal Report 610-202, 1971.
- III-2. Thorpe, T.E., "Verification of Performance of the Mariner 9 Television Cameras," *Applied Optics*, Vol. 12, p. 1775, 1972.
- III-3. Thorpe, T.E., *Mariner 9 Television Imaging Performance Evaluation, Vol. II (Mariner 9 TV Subsystem Calibration Report)*, Jet Propulsion Laboratory Internal Report 610-237, 1972.
- III-4. Kreznar, J.E., *User and Programmer Guide to the MM71 Geometric Calibration and Decalibration Programs*, Jet Propulsion Laboratory Internal Report 900-575, 1973.
- III-5. Young, A.T., "Television Photometry: The Mariner 9 Experience," *Icarus*, Vol. 21, p. 262, 1974.
- III-6. Thorpe, T.E., "Mariner Star Photography," *Applied Optics*, Vol. 12, p. 359, 1973.
- III-7. Levinthal, E.C., Green, W.B., Cutts, J.A., Jahelka, E.D., Johansen, R.A., Sander, M.J., Seidman, J.B., Young, A.T., and Soderblom, L.A., "Mariner 9-Image Processing and Products," *Icarus*, Vol. 18, p. 75, 1973.
- III-8. *Mariner Mars 1971 Science Data Team Final Report*, Jet Propulsion Laboratory Internal Report 610-239, 1973.
- III-9. Batson, R.M., "Cartographic Products From the Mariner 9 Mission," *J. Geophys. Res.*, Vol. 78, p. 4424, 1973.
- III-10. *Globe Supplement to The Many Faces of Mars*, Technical Memorandum 33-564, Jet Propulsion Laboratory, Pasadena, Calif., 1973.

IV. Real-Time Pictures

Real-time picture processing for Mariner 9 provided:

- (1) A raw image and histogram that could be used to verify that the cameras were working normally, that the pictures were suitably exposed, and that the data error rate was acceptable (see Section III).
- (2) Enhancements with excellent renditions of low-contrast detail so that mission planning decisions could be based on features visible in the pictures.
- (3) Data in a form suitable for the production of planning mosaics and first-order scientific analyses.

Computer processing for these real-time products was limited to the time period between the receipt of successive pictures, but was sufficient for the production of three or four versions of each picture. As the mission progressed, more sophisticated algorithms were introduced to improve the quality and usefulness of the real-time pictures.

A. Mission Test Computer and Mission Test Video System

Two facilities at JPL were involved in real-time processing and display of television pictures from Mariner 9. The mission test computer (MTC) provided the formatted television images to the mission test video system (MTVS) for film recording and hard-copy generation. The MTC extracted imaging and engineering data from the incoming telemetry stream and provided various displays of the extracted data. The overall flow of imaging data through the MTC is shown in Fig. IV-1 and is discussed in Refs. IV-1 and IV-2. Figure IV-2 shows the MTVS processing and indicates the multiple film products generated for each image received.

The first task performed by the MTC was to establish line and frame synchronization within the incoming telemetry stream using "markers" placed within the telemetry stream by the spacecraft's data automation subsystem (DAS). These markers indicated the start of a block of data containing one

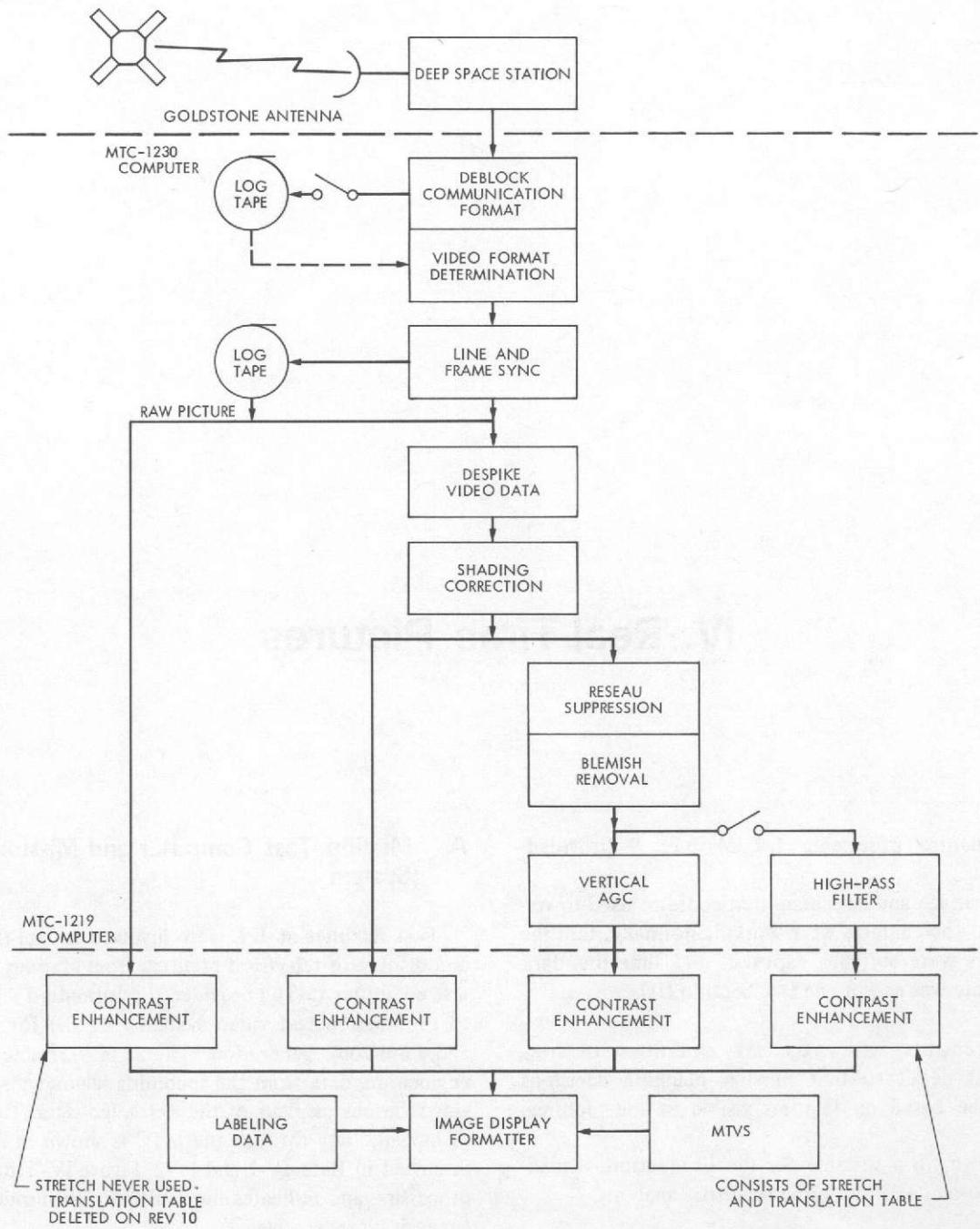


Fig. IV-1. MTC data flow: real-time processing.

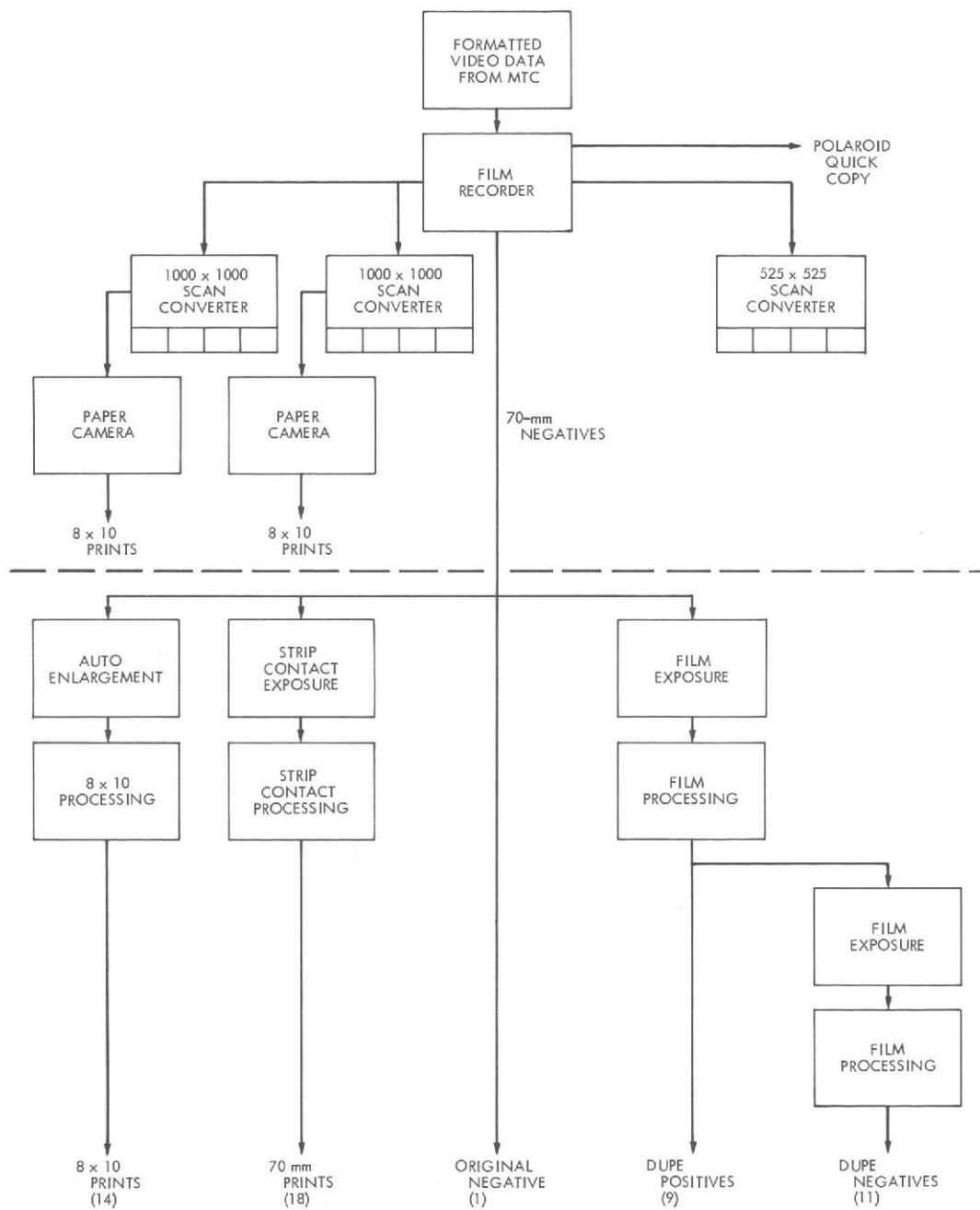


Fig. IV-2. MTVS data flow and products.

line of a television image, selected data from non-imaging science instruments, and engineering telemetry. The algorithms used to establish synchronization were changed during the 90-day standard mission to accommodate the increasing bit-error rate (BER) in the incoming telemetry. Provisions also were added to correct isolated bit-error spikes within the television data as the BER increased.

Once a television frame had been identified and extracted from the telemetry stream, the raw frame was formatted for film-recorder playback. The MTC framed the actual image that had been acquired by the Mariner 9 cameras with step wedges, histograms, and a label identifying the picture and providing supporting numerical information (Fig. IV-3). Two or three enhanced versions also were generated; these were framed with step wedges, histograms, and labels (Fig. IV-4).

to identify picture lines in the incoming data stream. Up to three or four errors were permitted in this pseudonoise (PN) code before it was unable to detect the start of a line, and consequently the end of the preceding line. The total number of PN code errors detected appears in the picture label as PN errors; there are 121 in Fig. IV-3. Also appearing in the picture label are the number of full lines (F), partial lines (P), and missing lines (M). A full line had an acceptable synchronization code at both ends and was included in the image. Partial lines with a poor synchronization code on one side and missing lines with poor synchronization codes on both sides were deleted from the picture and are known as "dropouts." (There are two partial-line dropouts in Fig. IV-3.) During replays of the data from original tapes held at the tracking station, it was possible to accept PN errors as high as six. The Experiment Data Record (EDR) is a permanent record of the digital imaging data produced from these replays and contains fewer dropouts (Ref. IV-3) than the preliminary records.

B. Picture Supporting Information

Some of the information that frames the real-time pictures is common to all versions of a given frame. Other information, specifically that relating to the image processing involved in producing different enhancements, differs from version to version.

1. Picture Identification

The primary picture identification is the DAS time, which appears in the lower-right part of the label (Fig. IV-3). This eight-digit number identifies the time at which readout of the first line in the picture occurred and normally differs from the DAS shutter time by five units (see Section III for details). Also on the picture label is the revolution (orbit) number on which the data were acquired and a picture sequence number in that revolution which, in many cases, is erroneous and not useful as picture identification.

2. Picture Geometry Predicts

The alphanumeric information in the upper-right part of the label includes picture-taking geometry based on predicts provided by the science data team. All of these data are obsolete, and although some of the picture label data that pertain to geometry are approximately correct, some are grossly inaccurate and potentially misleading to the user. Catalogs of accurate data on picture geometry are identified in Section III.

3. Telemetry Errors

a. *Dropouts.* Preceding each line in the picture telemetry was a 32-bit synchronization code, which was a marker used

b. *Spikes.* Errors in the synchronization code were easily determined because the code was explicitly defined before launch and was the same for each line in all pictures. However, errors in the imaging data were more difficult to recognize because each image, as read from the vidicon, was an original and unique set of data. It was possible, however, to detect many errors in single pixels (spikes) of the imaging data telemetry. Limitations in the inherent resolution of the vidicon precluded large transitions in data number between two adjacent pixels. Thus, it was established by camera tests that a pixel value 40 DN lighter or darker than the surrounding pixels had to be caused by a telemetry error. For automatic detection of these spikes, each pixel in a line was compared with the preceding and succeeding pixels; if the difference in both cases exceeded 40 dB in the same direction, it was recorded as a pixel spike. In versions other than the raw picture (see Fig. IV-1), the pixel was replaced by the average of the contiguous pixels. The total number of spikes appears in the label (see Fig. IV-3). Errors in contiguous pixels in the same line were not necessarily detected, and spike removal then was not effective.

When the number of pixel and PN errors reached a specific limiting level, set at about 10,000 and 250, respectively, the quality of the imagery deteriorated to such an extent that the spacecraft was commanded to transmit data at a lower rate (see Section II). In some cases, especially late in the mission, a 4.05-kbps data rate was used, although an 8.1-kbps data rate would have provided acceptable imagery. However, other instruments using the same data stream (e.g., the infrared interferometer spectrometer) required much lower error rates for usable data than did the television cameras.

4. Electronic Gray Scale

In each picture version is a nine-element gray scale. This scale, which was used in control of the photographic film processing, was generated digitally and was identical in each picture version.

C. Image Processing

Three or four different versions of each Mariner 9 picture were produced routinely by the MTC/MTVS. Examples of raw, shading-corrected, vertical automatic gain control (VAGC), and high-pass filtered (HPF) versions appear in Fig. IV-4. The four versions were produced sequentially, and processed versions of all data acquired from a revolution were recorded on a single roll of film. Processed frames are identified by a roll and frame number of the form xxxx-xx, which increments by one unit for each successive version.

1. Digital Processing

Each of the processed picture versions was subjected to several different digital processing steps (Fig. IV-1), culminating in the contrast enhancement that was applied before processed digital data were transferred to a film recorder. The final enhancement consisted of two parts:

- (1) A linear "stretch" to expand the 8-bit data resulting from the previous processing across the desired range from black (0) to white (255).
- (2) A nonlinear "translation" which optimally matched the final digital data to the film recorder characteristics.

Different stretch algorithms were employed with the different picture versions. Only one translation table, selected after premission evaluation of various alternatives, was used.

The two histograms that appear beneath each enhancement (see Fig. IV-4) provide statistical information on the data numbers in the image before and after contrast enhancement. The data input histogram shows the characteristics of the data immediately before contrast enhancement. However, this histogram does reflect the effect of every other digital processing step such as spike removal, blemish removal, reseau suppression, shading correction, and filtering. The film output histogram shows the distribution of the data after contrast enhancement in the form in which it was supplied to the film recorder. Except for the raw pictures, these film output histograms are asymmetric in form because of the action of the translation table. The horizontal scale of data numbers on each

histogram corresponds to increments of eight data numbers. Input data range from 0 to 255 DN (8 bits); film output ranges from 0 to 63 (6 bits).

Beneath each histogram is a panel of smoothly varying gray tone values bearing a one-to-one correspondence with the horizontal scale of DN values associated with the histogram. The panel beneath the film output histogram indicates the correspondence between gray levels in the image and the digital values supplied to the film recorder that produced that gray level. Similarly, the panel beneath the data input histogram shows the correspondence between image gray levels and digital data values before contrast enhancement. Thus, by comparing the photographic density in the image with that in the panel, it is possible to make rough estimates of numerical DN values for the different enhancements. A feature of the data input panels for the enhanced pictures is the abrupt change from black to white with an extremely narrow band of intermediate gray. This characteristic is an indication of the extreme contrast stretch applied to the data.

The real-time processing system was designed to produce each enhancement automatically without manual intervention. However, all pictures were not handled identically. Through the use of automatic contrast stretch algorithms, for example, low-contrast scenes were enhanced by a greater amount than were high-contrast scenes. Several improvements also were made in the early phases of the mission as the characteristics of the imaging data were better understood (see Table IV-1).

2. Enhancement Details

The raw version and two or three enhanced versions were subjected to a series of processing steps (see Fig. IV-1), which are discussed in the subsequent paragraphs.

a. *Raw picture version.* The raw picture version of each frame received minimal digital processing; the only significant alteration of incoming data was the conversion of 512 digital levels in the input to 64 levels in the data transferred to the film recorder. The two histograms in the raw picture example in Fig. IV-4 reflect the simplicity of this processing, as they are the same shape and differ only in the smaller number of discrete levels in the film output histogram. In some early versions of the raw picture (see Table IV-1), the translation table was used as part of the final contrast-enhancement step; this procedure was discontinued after Rev 10.

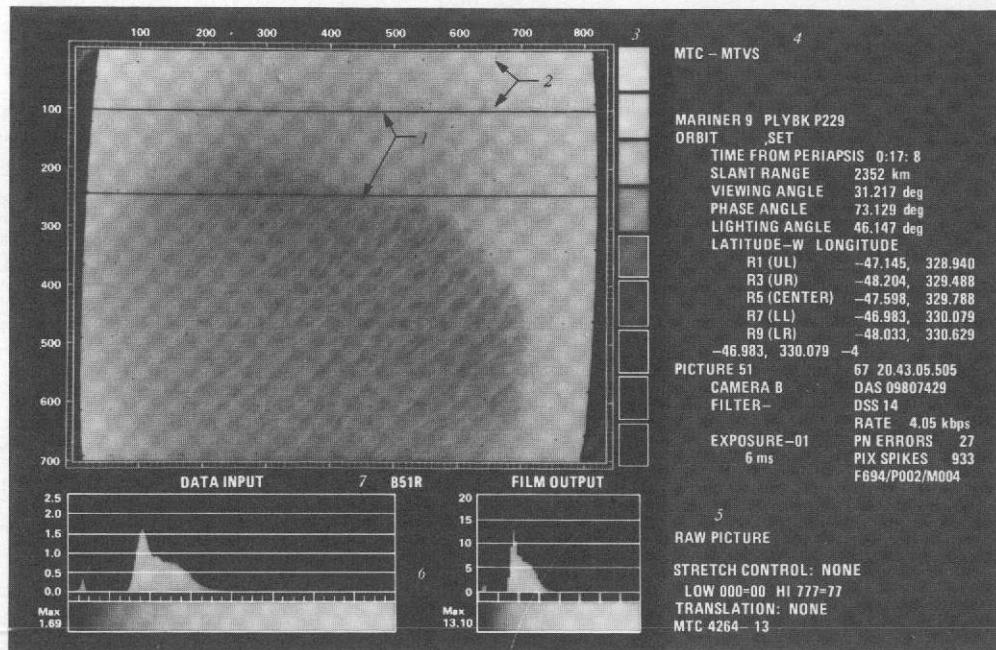
b. *Shading-corrected picture version.* The first step in the production of the shading-corrected picture version was the removal of spikes (pixels either much darker or lighter than surrounding pixels because of telemetry error). Spikes were

1 MISSING OR PARTIAL LINES

2 RESEAU MARKINGS

3 ELECTRONIC NINE-ELEMENT GRAY SCALE

PICTURE
LINE
NUMBER



4 PICTURE IDENTIFICATION,
NAVIGATION DATA AND
RAW IMAGES DATA
CHARACTERISTICS

5 IMAGE PROCESSING
INFORMATION AND
PICTURE VERSION

6 DATA INPUT AND
FILM OUTPUT
HISTOGRAMS

7 PICTURE IDENTIFICATION

MARINER 9 PLYBK P229
ORBIT , SET

TIME FROM PERIAPSIS 0:17:8

SLANT RANGE 2352 km

VIEWING ANGLE 31.217 deg

PHASE ANGLE 73.129 deg

LIGHTING ANGLE 46.147 deg

LATITUDE-W LONGITUDE

R1 (UL)	-47.145, 328.940
R3 (UR)	-48.204, 329.488
R5 (CENTER)	-47.598, 329.788
R7 (LL)	-46.983, 330.079
R9 (LR)	-48.033, 330.629

-46.983, 330.079 -4

PICTURE 51 67 20.43.05.505

CAMERA B DAS 09807429

FILTER- DSS 14

EXPOSURE-01 RATE 4.05 kbps

6 ms PN ERRORS 27

PIX SPIKES 933 F694/P002/M004

PICTURE EXPOSURE TIME

REVOLUTION ON WHICH PICTURE WAS TAKEN

GIVEN IN h, min, s; + = AFTER PERIAPSIS

RANGE, VIEWING AND ILLUMINATION GEOMETRY
FOR CENTER OF PICTURE

LATITUDES AND LONGITUDES CORRESPONDING
TO RESEAU MARKS

RESEAU 1 = UPPER-LEFT CORNER

RESEAU 3 = UPPER-RIGHT CORNER

RESEAU 5 = CENTER

RESEAU 7 = LOWER-LEFT CORNER

RESEAU 9 = LOWER-RIGHT CORNER

DATA ERRONEOUS

PICTURE SEQUENCE No., PERIAPSIS
DAY AND TIME

CAMERA ID, DAS TIME MARKER

FILTER ID, TRACKING STATION ID

DATA RATE

DATA ERRORS

694 FULL LINES

2 PARTIAL LINES

4 MISSING LINES

Fig. IV-3. Explanation of information in picture label 1: picture identification, navigation data, and raw image data characteristics.

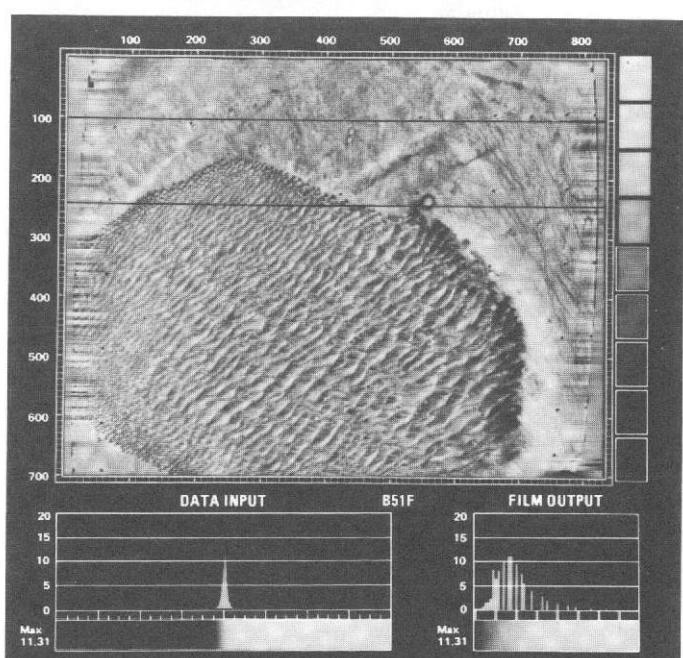
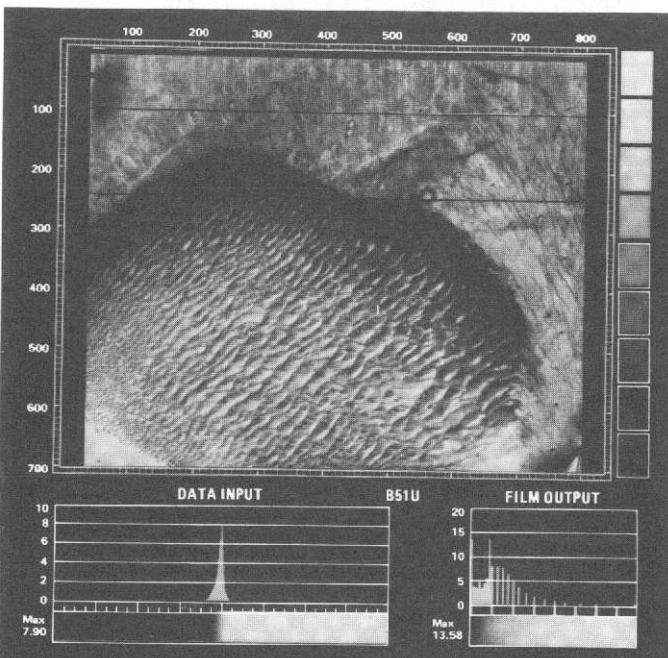
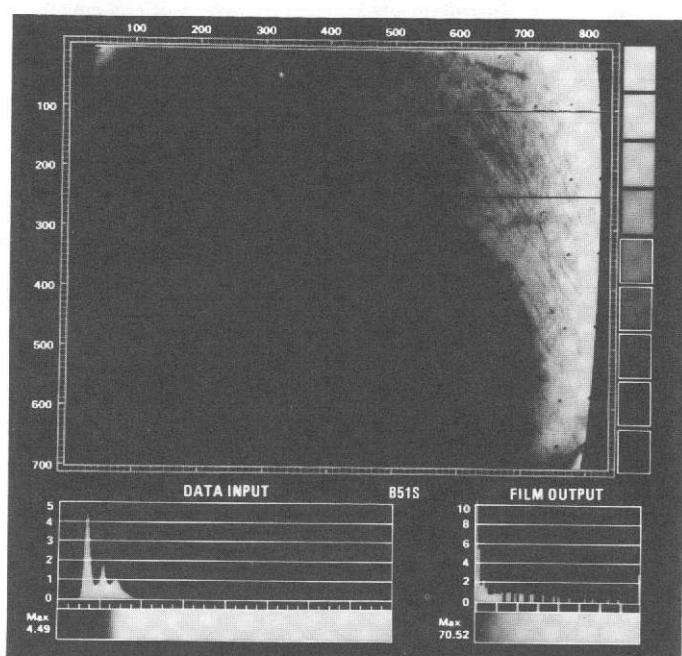
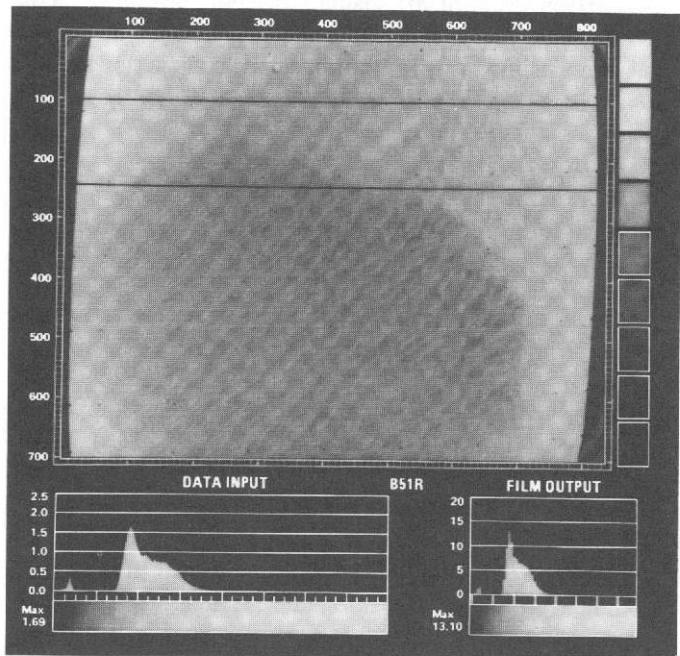


Fig. IV-4. Raw, shading-corrected, and two filtered versions of a Mariner 9 narrow-angle picture.

Table IV-1. Improvements in image processing of real-time MTC/MTVS pictures^a

Sequence	Improvements
POS-1	Raw pictures and most significant bit truncated pictures (two versions) were produced. The latter replaced a shading-corrected picture. Data for both versions were conditioned for film processing, with TT3 selected during simulations.
POS-2	50-line HPF added as third picture version and alternated with shading-corrected stretched version.
Rev 1	First orbital pictures. Raw pictures remained the same. Shading-corrected version replaced most significant bit truncated version. 150-line HPF was third version.
Rev 10	TT3 taken out of raw picture to simplify analysis of engineering data.
Rev 109	VAGC introduced as Roll 4133. Revs 97-108 (Rolls 4118-4132) originally processed with the HPF rerun during solar occultation as Rolls 5000-5014. VAGC incorporated reseau removal. Automatic stretch determined end points by scanning from the center of the histogram out (Auto-CS).
Rev 147	Blemish removal introduced in VAGC version.
Rev 148	Auto-CS stretch control introduced in VAGC version.
Rev 199	Fourth picture version, similar to pre-Rev 109 HPF version, introduced as falling data rate made additional processing time available. This version incorporated reseau removal not used previously with this algorithm.

^aTable indicates only the most significant improvements. Many minor changes in parameters were also made, but were not recorded.

removed or made less noticeable by replacing the erroneous pixel with the average of the values of the nearest pixels.

Spatial nonuniformity in the photometric response of the vidicon camera was compensated for by using a set of coefficients based on preflight calibration data (see Section III). This shading correction provided only a first-order correction to the camera shading and was not intended to provide data with photometric linearity. It did remove anomalous bright and dark areas near the edge of the frame.

The effectiveness of the shading correction is not well illustrated by Fig. IV-4, where the high contrast of true scene detail overwhelms the effects of camera shading. However, in images where the original scene was uniformly bright, the effectiveness of shading correction is best exhibited by a comparison of the data input histograms for raw and shading-corrected pictures. The histogram in the shading-corrected picture is more sharply peaked and without the wings of the histogram for the corresponding raw picture.

Contrast enhancement of shading-corrected data did not take place until the entire frame of data had been processed and a histogram generated (see Fig. IV-1). A histogram of shading-corrected data was scanned to determine the parameters for an appropriate contrast enhancement. The objective of this contrast enhancement was to expand the relatively narrow range of data numbers, and hence shades of gray, in the shading-corrected image over the entire range from black to white available in the 64-level, 6-bit output display system. The implementation of the automatic external scan (Auto-ES) contrast-enhancement algorithm is shown by Fig. IV-5 (also see Ref. IV-2).

The algorithm was designed to establish the data numbers (LOW and HI) bounding the darkest (5%) and the brightest (2%) pixels in the scene viewed. The starting points for scanning the histogram to determine the low (LOW) and high (HI) were chosen to exclude spurious dark areas such as reseau marks. Data numbers in the scene between LOW and HI were then expanded or stretched linearly over the range 0 to 63. The values of LOW and HI used in this stretching procedure are listed in octal notation (number system with base 8) beneath the shading-corrected image (Fig. IV-4). The final stage of contrast enhancement of the shading-corrected image involved the application of the translation table stretch, which preceded the transfer of data to the volatile displays and film recorder. The choice of this translation table is discussed in Section IV-C.

With some of the early shading-corrected pictures, a non-automatic (MANUAL) contrast stretch replaced Auto-ES. In those cases, LOW and HI were pre-selected without any reference to the data actually acquired.

c. *HPF picture version.* Although the shading-corrected version of each Mariner 9 picture with contrast stretch revealed many subtle tonal differences that were not evident in the raw picture version, in many cases it was not adequate for scientific interpretation. The characteristic that precluded this is shown in Fig. IV-4 where the sharp boundary between lighter and darker areas on the planet is apparent, but where little detail can be discerned away from the boundary because of light and dark saturations of the image. Two other picture versions were designed to display fine detail in all parts of this

type of scene: the HPF and the VAGC. In both of these versions, fine (high spatial frequency) detail was enhanced at the expense of large-scale (low spatial frequency) brightness variation.

The early Mariner 9 pictures were enhanced with only the HPF, which was implemented by replacing each pixel with its own value minus a running average of pixels along a horizontal line.

$$Y_K = X_K - \bar{X}_K + C \quad (1)$$

where

$$\bar{X}_K = \frac{\ell = +M}{\ell = -M} \sum X_K + \ell \quad (2)$$

and

X_K = DN values of pixels input to HPF

\bar{X}_K = running average of pixel values

Y_K = DN values of pixels output by HPF

M = integer representing half-width of filter ($M = 75$ in most Mariner 9 real-time pictures)

C = bias value nominally set to 255 to distribute filtered data values on both sides of mid-scale

The result of this operation was a frame of data without gross brightness variations, as indicated in the narrow data input histogram with the HPF picture in Fig. IV-4. The wings of this histogram correspond to local fine-scale variations in scene brightness.

Just as the shading-corrected data required contrast enhancement to render features clearly visible, the filtered data also required contrast enhancement. However, in this case, a different algorithm, the automatic center scan (Auto-CS), was used during most of the mission. This algorithm (see Fig. IV-6) was designed to take advantage of the fact that the mean value of filtered data numbers was equal to C (see Eq. 1) and nominally set to 255. Auto-CS allowed the contrast of the filtered data to be expanded to varying extents, depending upon the width of the input data histogram. However, the mean value of these contrast-enhanced pictures was

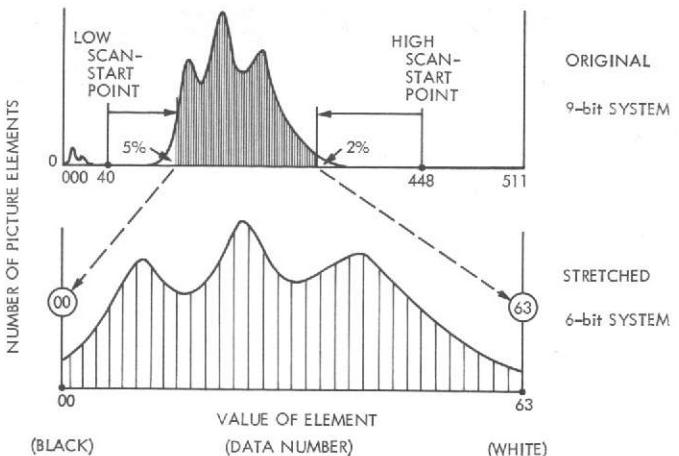


Fig. IV-5. Contrast stretching of shading-corrected data (Auto-ES).

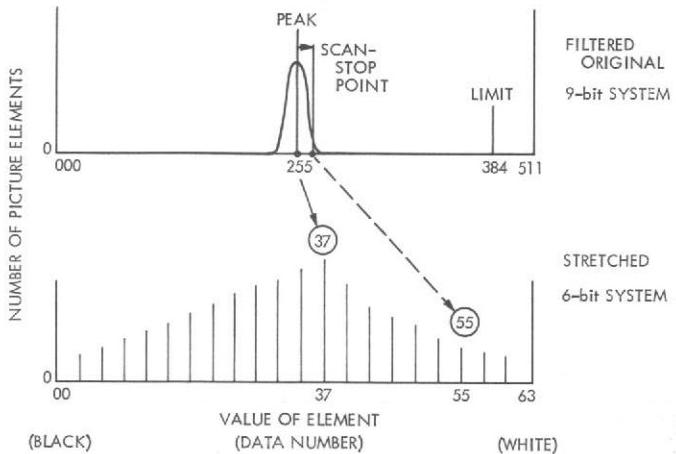


Fig. IV-6. Stretching of filtered data (Auto-CS).

always the same so that the filtered and contrast-enhanced data gave pictures with a constant average tonal level. The Auto-ES (see Fig. IV-5) was used with the HPF version earlier in the Mariner 9 mission, but was superseded because it produced enhancements with highly variable average tonal level. The effect of high-pass filtering followed by contrast enhancement is shown in Fig. IV-4. By comparing this version with the shading-corrected version, it is evident that the broad areas of light and dark saturation have been replaced by a scene with a uniform gray cast where fine detail in areas formerly in light and dark saturation is rendered in moderate to high contrast.

The HPF version of Fig. IV-4 incorporates several additional processing steps to those indicated by Eqs. (1) and (2). The reasons for incorporating additional processing can be understood from the examination of an HPF version produced

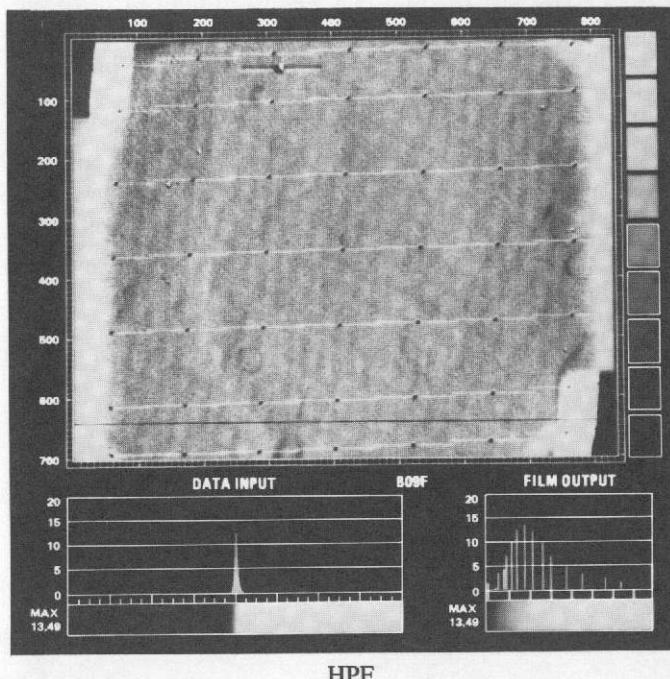
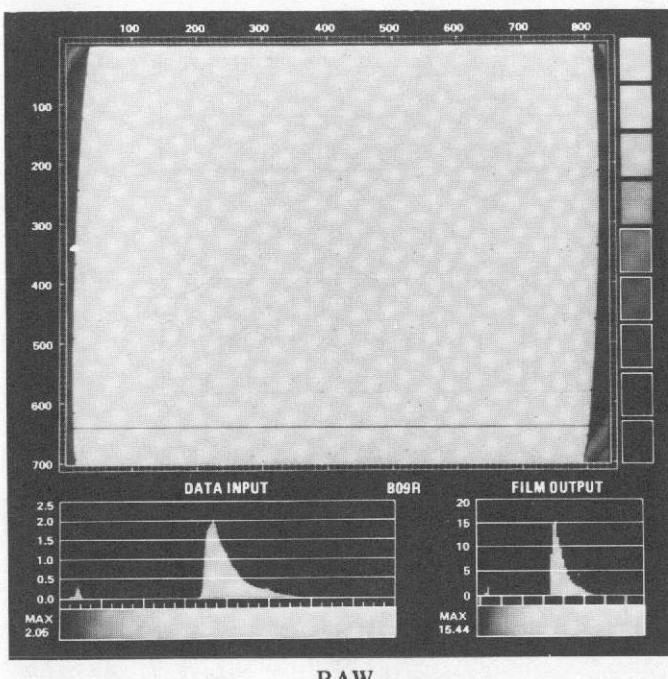


Fig. IV-7a. Raw and HPF versions of pictures received early in the mission. In the HPF version, the blemish and reseau marks produced horizontal bright wings on either side of the features, and a band of saturation developed contiguous with the curved vidicon mask.

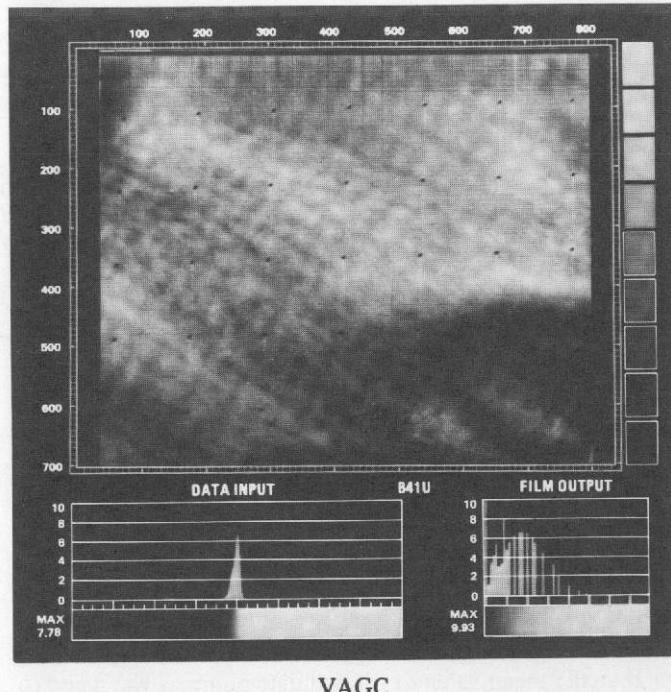
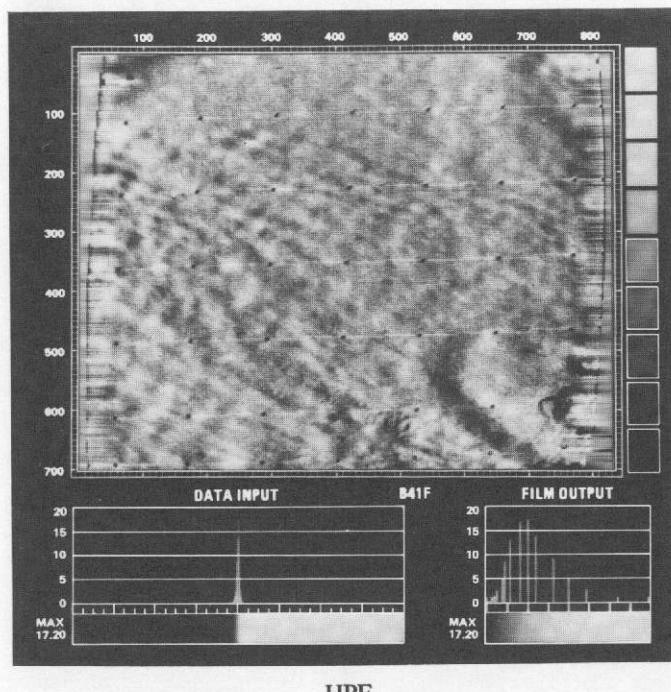


Fig. IV-7b. Blemish removal, reseau suppression, and extrapolation across the black mask area suppressed artifacts produced during high-pass filtering. In the VAGC version, the black mask area was squared off and the vertical filtering suppressed periodic noise.

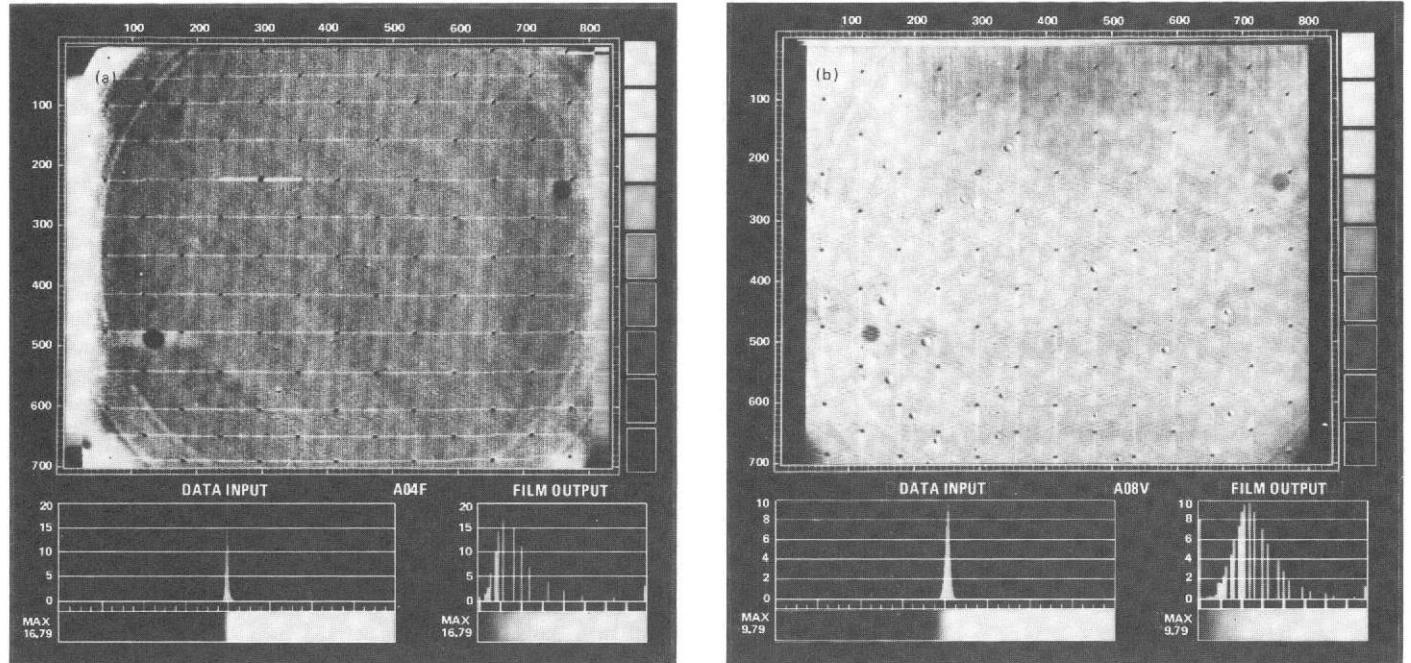


Fig. IV-8. (a) HPF version of wide-angle picture from Rev 10 without reseau suppression. Three major dark blemishes caused by dust specks on the camera optics are visible as an artifact attributed to the target ring of the vidicon (see text). (b) VAGC version of wide-angle picture from Rev 198 with reseau suppression. A complex pattern of noise caused by the ultraviolet spectrometer is discernible in the horizontal bands.

early in the mission (Fig. IV-7) with only the algorithms described in the preceding paragraphs. These frames show distracting bright artifacts, formed where the HPF interacted with the black mask at each side of the frame, reseau marks, and blemishes within the image. Additional algorithms were added to the HPF (see Table IV-1) to suppress some of these effects. However, in *highly* contrast-enhanced, filtered versions of the later images, bright wings can be seen on each side of the reseau marks, and linear artifacts appear at the boundary of the black mask.

The enhanced versions of Figs. IV-7 and IV-8 illustrate blemish removal in Mariner 9 television data (see Section II). The techniques used to remove some of these blemishes from the filtered images differ significantly from those used to suppress the reseau marks. Blemishes were assumed to lie within a specific rectangular area in the raster, and were removed by replacing that rectangular area with mean values of adjacent pixels. However, no assumptions were made regarding the positions of reseau marks for their suppression. The suppression algorithm detected the reseau position by searching for dark areas within the frame as the filtering was being performed. Table IV-1 summarizes the improvements made to the HPF data.

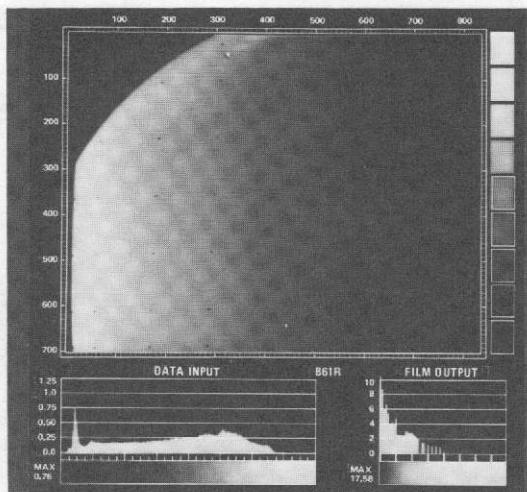
d. VAGC picture version. This picture was originally developed as an improvement over the HPF version. A strong vertical component of noise was apparent in the Mariner 9 pictures (Fig. IV-7). When the detail in the pictures was extremely low in contrast, as it was over the entire planet during the dust storm, this noise was exaggerated by the horizontal scanning of the HPF.

By performing the filtering vertically, it was possible to suppress the vertical noise. For this reason, the horizontal filter was replaced after Rev 109 by the vertical filter. However, in many pictures with high contrast detail, in which noise is no problem (e.g., in Fig. IV-4), the VAGC and HPF versions are complementary and both versions were produced after Rev 199 when falling spacecraft data rates permitted more time between frames for digital processing.

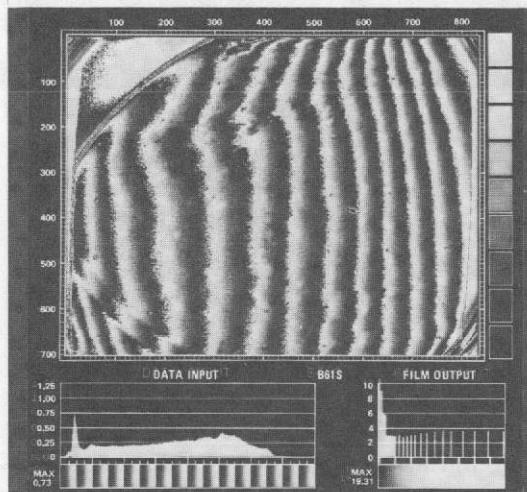
The algorithm used in the VAGC version is not a "rotated" version of the HPF. Because data were read into the computers a line at a time and the number of lines that could be stored at any one time was limited, an alternate function was sought. The symbols in the algorithm mathematically expressed by

$$Y_K = X_K \cdot \bar{X}_K + 255 \quad (3)$$

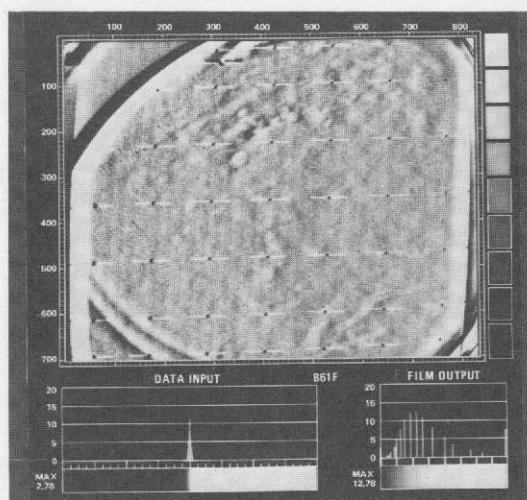
$$\bar{X}_K = \left[\frac{M\bar{X}_{K-1} + X_K}{M + 1} \right] \quad (4)$$



(a) RAW



(b) CONTOURED



(c) HPF

have the same significance as they did for the HPF, except that here K increases vertically down a column rather than horizontally along a line. This method has the advantage of extreme simplicity and effectively removes vertical scene noise near the reseau marks (Fig. IV-7). As with the HPF pictures, bright artifacts appear and extend downward from the reseau marks as a consequence of the asymmetrical form of the processing function. This asymmetry in the processing can cause small displacements in the locations of image detail. This filter was named "vertical automatic gain control" because of the resemblance to an electronic analog filtering circuit that responds only to time signals in the past, and not to those in the future.

Reseau and blemish suppression implemented with the VAGC were similar to those used with the HPF. However, processing problems at the black masks led to digital "squaring off" of the pictures with a small loss of scene area.

e. *Contoured picture version.* In addition to these four principal picture versions, a contoured version of the raw data was produced using only POS pictures. This version was generated by removing 2, 3, or 4 of the most significant bits from the 9-bit data number in the raw image data. This type of processing revealed features in the data that were not visible in the raw image (see Figs. IV-9a and IV-9b), but generally did not reveal them as effectively as the filtered image (Fig. IV-9c).

3. Experiment Data Record

The EDR, which represented an archival digital tape record of the best available raw imaging data, also was generated by the MTC digital processing system. The EDR contained television picture data and a limited amount of additional science and engineering data (Ref. IV-3). This EDR tape was used for replays of real-time processing of pictures when the recalled data were of significantly higher quality than the real-time

Fig. IV-9. Raw, contoured, and HPF versions of a POS-3 picture. The contoured version was produced from the raw data by truncation of the 4 most significant bits from these data, and the effect of this processing is reflected in the data input histogram and the gray scale panel beneath it. The HPF version was produced with a much shorter filter length than was used with most of the later pictures.

data (see Section III) and was the primary data source for the production of the RDR and other more sophisticated digital processing of the Mariner 9 data. Other engineering measurements extracted from the Mariner 9 telemetry were incorporated into a LIBSET tape used in the creation of the SEDR (see Section III).

D. Image Display and Film Processing

Visual displays of raw and enhanced digital data included volatile television displays by means of scan converters and a permanent film copy produced by the MTVS film recorder (see Fig. IV-2).

1. Negatives and Film Transparencies

The primary product, and the only one actually produced on the film recorder, was the first-generation 70-mm negative. Second-generation positive transparencies and contact prints and third-generation negative transparencies were produced on an automatic contact printer. Enlargements produced from the first-generation negative also were used for mission planning and scientific interpretation. Additional duplicate negatives were needed for distribution so that other enlargements could be produced at other institutions as needed.

An early requirement on the film processing was for a duplicate third-generation negative (see Fig. IV-2) that accurately reproduced the tones and contrasts of the original first-generation negative. Carefully controlled film processing procedures were devised to meet these essential properties of reproducibility. In Fig. IV-10, density measurements of the electrical gray scale (EGS), for first-, second-, and third-generation transparencies, show that it was possible to achieve a close match between the characteristics of the duplicate and original negatives.

This procedure for precise replication of the original negative was not completely satisfactory, as it was necessary to produce the second-generation positive and third-generation negative with low average densities. High-density processing produced better reproduction of the transfer curve and satisfactory contact copies, but the high density caused high fog level in enlargements and provided images too dark for normal projector viewing. For these reasons, the second- and third-generation transparencies were printed at somewhat lower densities than originally planned.

2. Contact Prints and Enlargements

The most widely used photographic materials for science analyses and mission planning were positive paper prints. Both

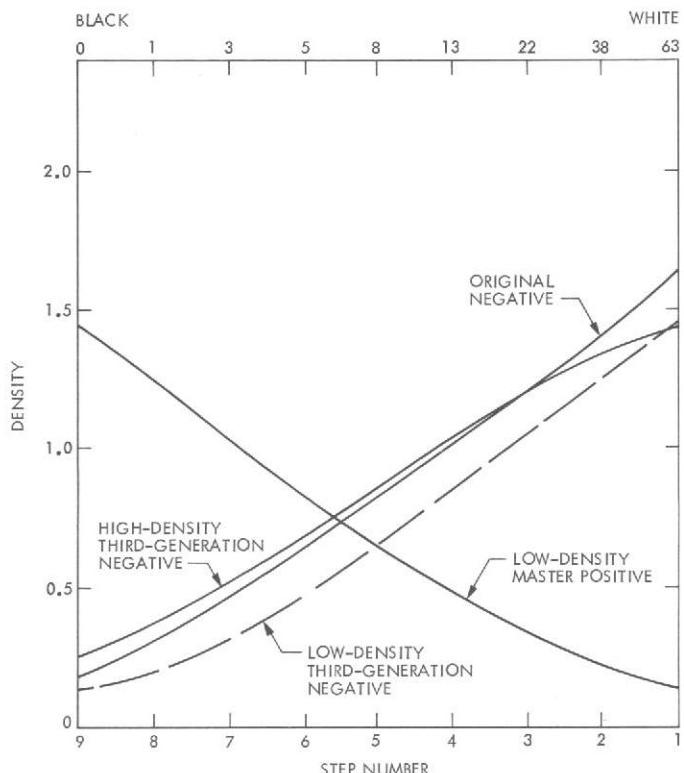


Fig. IV-10. MTVS film processing of first-, second-, and third-generation 70-mm film transparencies.

70-mm contact prints and 20- by 25-cm (8- by 10-in.) enlargements were routinely produced; typical transfer curves for these materials, based on measurements made using a reflection densitometer, are shown in Fig. IV-11.

3. Optimal Display of Film Copies

The final step of digital processing of Mariner 9 real-time enhancement data was a nonlinear modification of the processed data to match the transfer characteristics of the film recorder so that the data were optimally displayed on film. This modification was implemented with a translation table that was applied after linear contrast enhancement with the Auto-CS or Auto-ES algorithms had been completed. Several translation tables were created (see Fig. IV-12a), and one was selected so that equal increments in data number before translation were equally discriminable as density differences on film across the entire range of DN values.

Under conditions of moderate illumination where background brightness is comparable to scene brightness, the minimum visually discernible change in film density is about 0.05 and is independent of density in the range of 0.3 to 1.7 (Ref. IV-3). As can be seen in Fig. IV-12b without the transla-

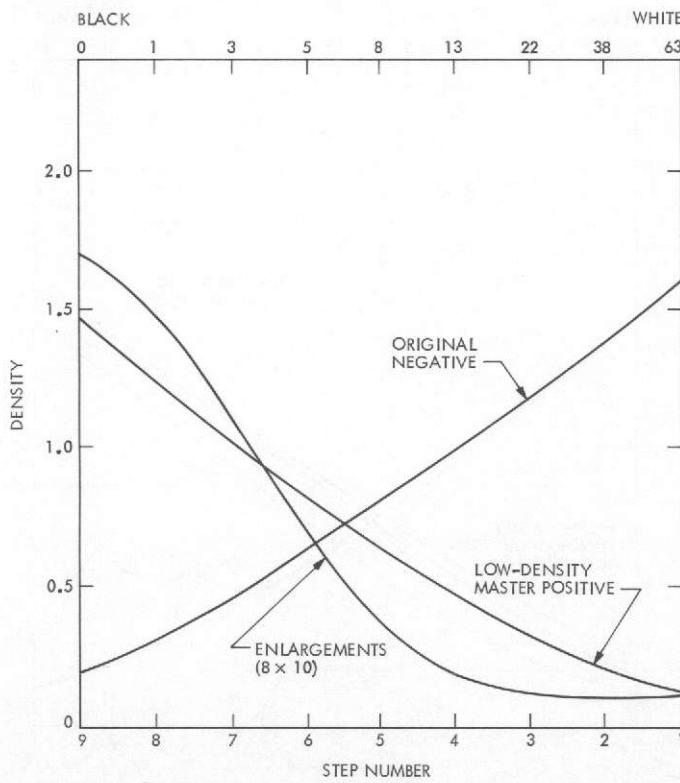


Fig. IV-11. Transfer curves for 20- x 25-cm (8- x 10-in.) enlargements and positive transparency data.

tion table, equal increments in processed data numbers do not provide equal increments in density at all data levels and therefore are not equally discriminable. However, with translation table TT3, this situation was substantially corrected for film transparencies and produced adequate correction with enlargements (Fig. IV-12b). This particular translation table was implemented with all enhancements, but not with the raw image.

Many users of the Mariner data are concerned whether the raw image provides an authentic rendition of Martian surface contrasts. In Fig. IV-12d, the reflectivity or transmissivity calculated from the density (Fig. IV-12b) of a Mariner 9 image is plotted against the scene brightness. It is apparent that, when no translation is used, and except for the special case of low DN values, Mariner 9 raw pictures underestimate the contrast of surface detail on Mars.

* Mariner 9 produced many observations of the horizons of Mars, which included a low-brightness, detached haze layer. Nonlinear transfer characteristics of the raw image

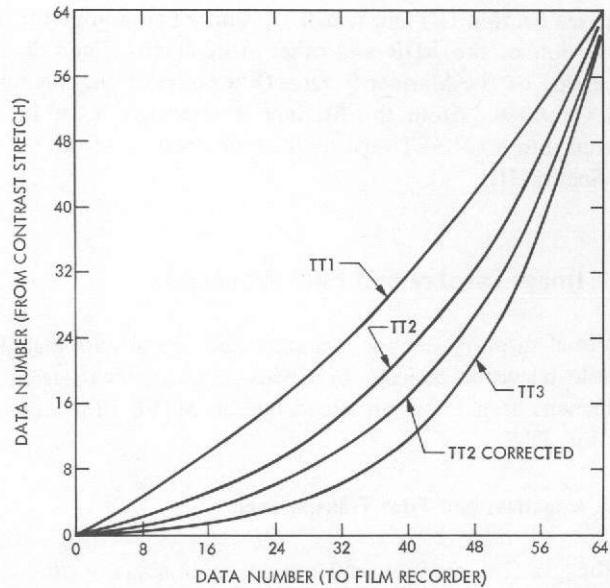


Fig. IV-12a. MTC translation tables.

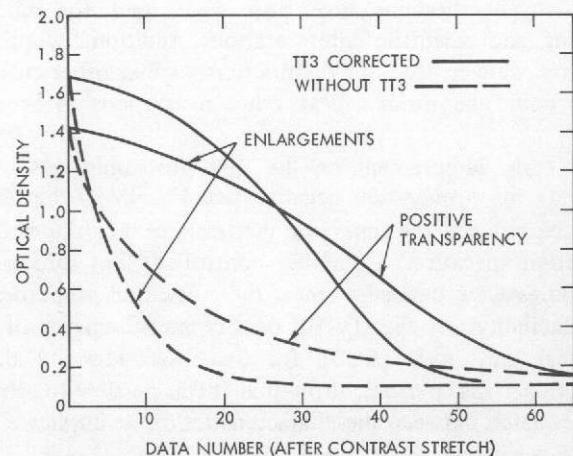


Fig. IV-12b. Optical density vs input data number for positive transparencies and enlargements.

(Figs. IV-11c and IV-11d) were almost ideally suited for presentation of these haze layers and were retained for this reason.

In the Mariner 9 picture of the Martian surface shown in Fig. IV-4, the brightness is lower than mid-scale; the raw image is also of satisfactory contrast and approximates the true contrast that would be perceived in that part of Mars. However, in most pictures where brightness was mid-scale or higher, the contrast, and therefore the quality, of the raw image was compromised by the lack of a translation table in the processing.

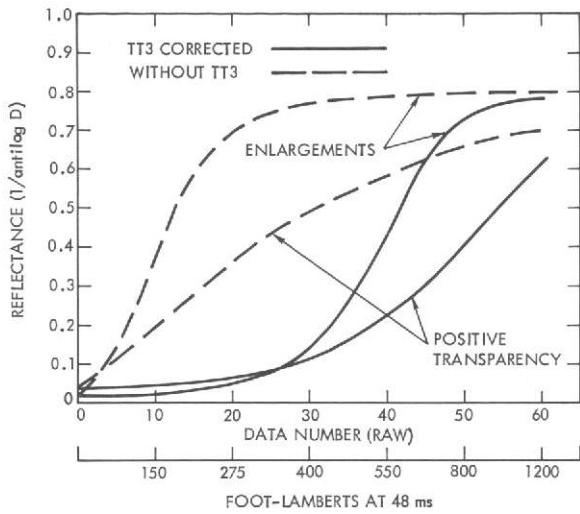


Fig. IV-12c. Reflectivity vs data number (same data as in Fig. IV-11b). The original scene brightness equivalent to a specific raw data number is shown based on camera transfer curves of Section III.

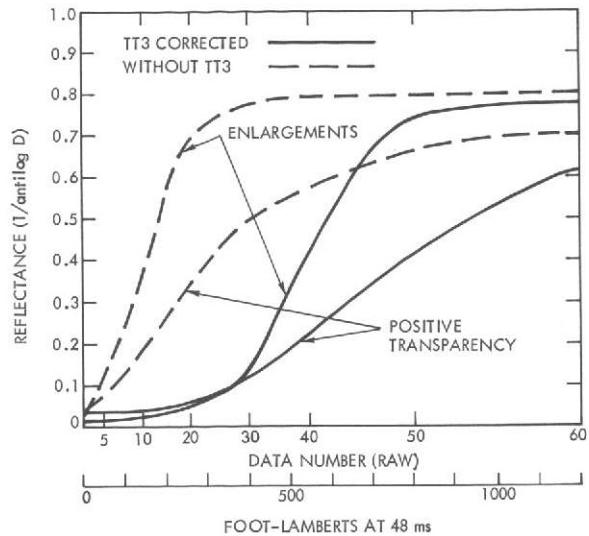


Fig. IV-12d. Reflectivity vs original scene brightness (same data as in Fig. IV-12c with the original scene brightness scale linearized).

References

- IV-1. Levinthal, E. C., Green, W. B., Cutts, J. A., Jahelka, E. D., Johansen, R. A., Sander, M. J., Seidman, J. B., Young, A. T., and Soderblom, L. A., "Mariner 9 — Image Processing and Products," *Icarus*, Vol. 18, p. 75, 1973.
- IV-2. Stott, R. F., *Mariner Mars 1971 Real-Time Video Data Processing*, Jet Propulsion Laboratory Internal Report 610-230, 1972.
- IV-3. *Mariner Mars 1971 Science Data Team Final Report*, Jet Propulsion Laboratory Internal Report 610-239, 1973.

V. Reduced Data Record

The Mariner 9 real-time pictures represented an essentially qualitative form of the television data and exhibited photometric and geometric distortions. For quantitative analysis of the imaging data, digital processing was used to remove the camera-induced distortion. This removal processing, used on the best version of the raw picture data (the EDR), was performed by the Image Processing Laboratory (IPL) using calibration data measured during prelaunch testing of the cameras. The set of data resulting from this process is the Reduced Data Record (RDR). The RDR has as its principal elements:

- (1) Numerical image data on magnetic tape.
- (2) Photographic data reproduced from the numerical data consisting of two enhanced versions of each television picture.

A detailed description of the RDR is given in Ref. V-1.

Examples of the two enhanced versions of RDR photographic data appear in Fig. V-1. These RDR picture versions and the real-time picture version of Fig. IV-4 were derived from the same Mariner 9 television frame. The first RDR version in Fig. V-1, the contrast-stretched or albedo version, received similar enhancement processing to that applied to the shading-corrected version of the real-time pictures (Fig. IV-4). The second RDR version, the high-pass filtered (HPF) version, received similar, but not identical, enhancement processing to the real-time HPF version. The primary difference is that the filtering was performed vertically in the RDR HPF version and was performed horizontally in the real-time version.

The alphanumeric information beneath the pictures (see Fig. V-1) includes a histogram of the output data, information on camera-pointing conditions and region covered, and details of processing performed on the pictures. Explanations and cautions regarding the information provided are presented in Ref. V-1.

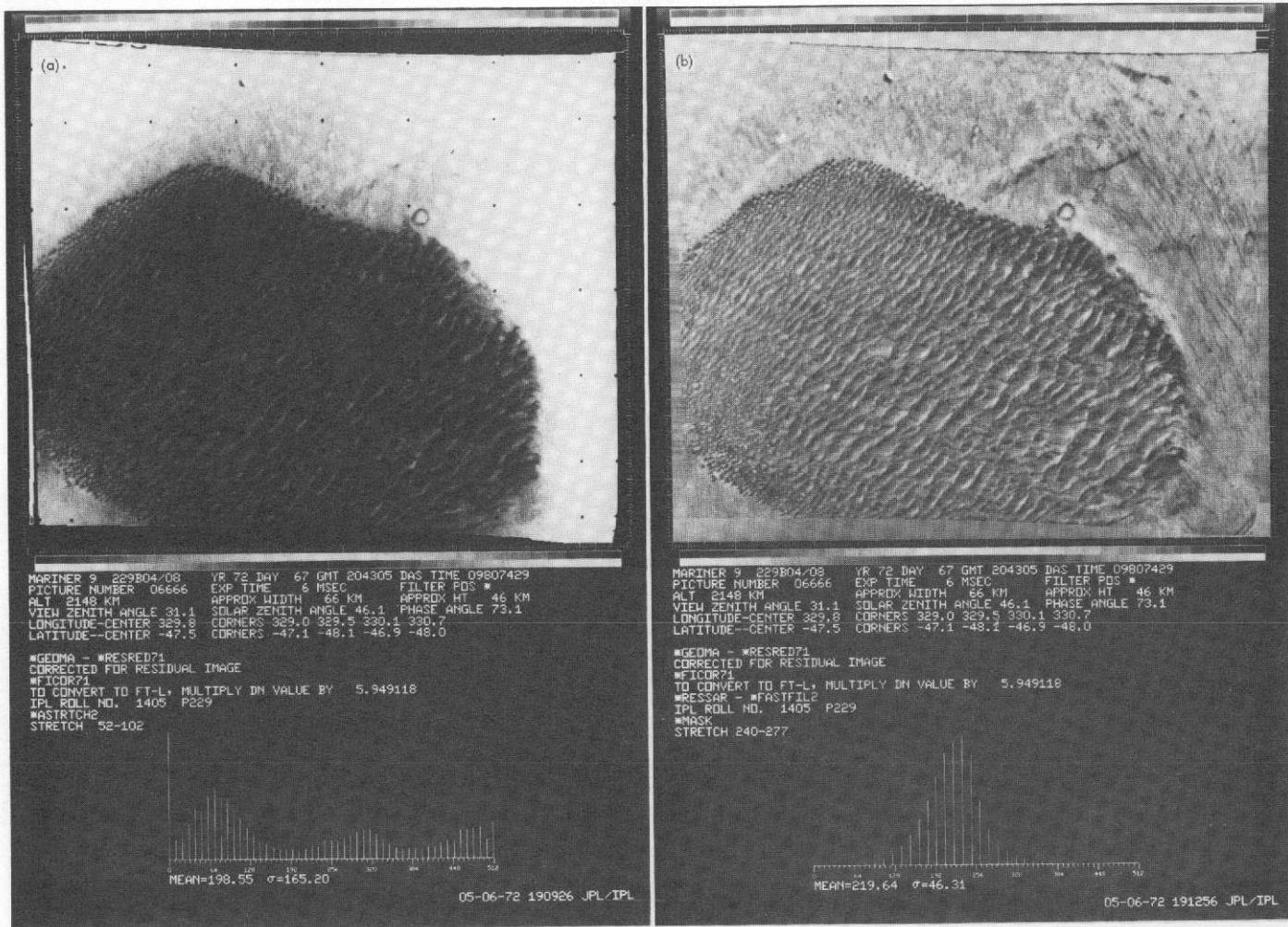


Fig. V-1. Photographic versions of RDR data. (a) Contrast-stretched or albedo version shows the RDR data with relative brightness exaggerated in a linear fashion, but not distorted. (b) This version shows large-scale variations in brightness suppressed and enhanced contrast of smaller features. Histograms of the enhanced numerical data corresponding to each picture (picture location, lighting and viewing data, and picture-processing mnemonics) are reproduced beneath each picture.

The RDR photographic data are being distributed in microfiche form (see Fig. III-15). The index supplied with the microfiche provides information from the SEDR and identification numbers necessary to order enlargements of specific pictures.

It must be emphasized that quantitative photometry should be attempted only through analysis of the numerical data. The enhancement processing and subsequent film processing used to create hard-copy film products almost totally obscure the absolute brightness units of the RDR. Thus, densitometry of film products should never be used for precise photometric analysis. Caution also is necessary in the use of RDR film products for precise photogrammetric analysis. Distortion in the film converter used to produce the RDR photographic data

is not negligible. Therefore, when performing photogrammetry, measurements of position should be in terms of the discrete picture elements (pixels) which can be seen when a picture is enlarged or magnified. If this is not feasible, numerical data should be reprocessed and reproduced on a precise photomechanical device.

It also should be recognized by those desiring to use the RDR numerical data quantitatively that the goal of decalibration has been approached, but not achieved. The accuracy of the RDR data is limited by the accuracy and completeness of the calibration data and by the accuracy of the assumptions on which the correction algorithms are based. At this time it would be premature to attempt a realistic estimate of the accuracy of the RDR.

For about 850 pictures of the Martian limb, the RDR numerical data have been additionally processed to produce plots of data number vs position along straight lines perpendicular to the limb. These plots, along with two enhanced versions of each picture, have been collected and photographed onto

microfiche to comprise the Limb Profile Microfiche Library. This Library, described in Ref. V-1, is available from the National Space Science Data Center, Greenbelt, Maryland. Examples of the limb data available in this Library are shown in Section XI of this document.

Reference

- V-1. Seidman, J. B., Green, W. B., Jepsen, P. L., Ruiz, R. M., and Thorpe, T. E., *A User's Guide to the Mariner 9 Television Reduced Data Record*, Technical Memorandum 33-628, Jet Propulsion Laboratory, Pasadena, Calif., 1973.

VI. Rectified and Scaled Picture Data

Geometrically precise rectified and scaled (R&S) projections of Mariner 9 pictures were produced at the Image Processing Laboratory using the RDR and the SEDR as data sources. The set of R&S versions included:

- (1) Conformal mapping projections of wide-angle pictures obtained in the Mariner 9 mapping mode, providing complete coverage of the planet at 1-km resolution (about 1500 frames).
- (2) Mapping projections of a limited number of wide-angle pictures processed with an empirical photometric function designed to normalize scene reflectance to the conditions of vertical illumination and viewing.
- (3) Orthographic projections of narrow-angle pictures (not including those that show the limb of Mars) taken after Rev 100 (about 1850 frames).

These items were used in the production of:

- (a) High-quality photomosaics at 1:5,000,000 scale for each of the 30 quadrangles or areas into which the planet was divided. These photomosaics are used as base control for 1:5,000,000-scale geologic maps of Mars planned by the Mariner 9 science experimenters. The photomosaics were assembled from wide-angle mapping projections (item 1) using controls derived by analytical photogrammetric measurements (see Section IX).
- (b) Photomosaics at 1:1,000,000; 1:250,000; and other scales for special areas of geologic interest (items 1 and 3).
- (c) A photomosaic of wide-angle pictures on a spherical globe about 1 m in diameter. The global presentation

- is valuable in depicting the terrain distribution in areas where flat mapping projections overlap (item 1).
- (d) Photomosaics at 1:5,000,000 scale for a limited number of quadrangles displaying normalized planetary reflectance or albedo (item 2).

A. Processing Details

The digital processing of R&S pictures was designed to provide a tonal match between pictures in mosaics as well as a precise geometric match. The most extensively used approach was the use of the HPF algorithm (see Section V) to remove gross brightness variations between different parts of each Mariner 9 picture. The production of an HPF mapping projection is illustrated in Figs. VI-1a, VI-1b, and VI-1c. The effectiveness of high-pass filtering in the suppression of distracting edge effects between pictures in a mosaic is shown in Fig. VI-2. High-pass filtering was used in the production of the individual mapping projections described in items 1 and 3 and in a, b, and c. This type of processing generally provided excellent rendition of topographic detail, but large-scale tonal differences between different parts of the planetary surface were suppressed (Fig. VI-3).

Another approach to suppression of edge effects between pictures in photomosaics (see items 2 and d) was to remove brightness differences in individual pictures, which are caused by variations in solar illumination and camera viewing geometry. In the production of product c (see Figs. VI-1d, VI-1e, and VI-1f), an empirical function was used to normalize the planetary brightness to anticipated values for vertical illumination and viewing. This provided suppression of edge effects between the pictures in a photomosaic and an approximate delineation of light and dark (albedo) markings on the Martian surface (Fig. VI-4). Photomosaics produced in this way should not, however, be considered true albedo maps because surface reflectance was only inferred from assumed photometric scattering properties of the surface. A limited number of Mariner 9 pictures received this type of processing.

Geodetic information for all R&S projections was based on the SEDR C-matrix, which provided camera-pointing information relative to the spacecraft's celestial reference and the spacecraft-planet centerline. Planetocentric latitudes and longitudes were computed using these basic data for points appearing in the field of view of the camera (see Refs. VI-1

and VI-2). The television picture then was geometrically transformed to an orthographic projection or one of three mapping projections (Mercator, Lambert Conformal, or Polar Stereographic), using the computer program MAP2 (see Ref. VI-3; projection equations are also given in Ref. VI-4). Computations of planetocentric latitude and longitude were based on a spheroidal planet; for the projections, the planet was assumed to be spherical. MAP2 implemented the projections by dividing the format of the projected picture into 361 (19 by 19) similar rectangles. The corner points of these rectangles projected exactly, and intervening points were bilinearly interpolated. Thus, for oblique frames, there is a possibility of significant error in the projection. The successful mosaicking of the mapping projections for the 30 mapping quadrangles, performed at the U.S. Geological Survey, Flagstaff, demonstrated that the projections were adequate for the mapping program.

Before rectification and scaling were performed, blemishes and reseau marks were removed from the RDR data. A fixed contrast stretch was used to prepare the data for printing. A stretch dependent on Sun-elevation angle was considered to compensate for contrast variations dependent on Sun-elevation angle, but was rejected for production processing because of its complexity. The scale of the projection was chosen from ten possible scales so that the maximum area of image detail was included within the output raster. The coordinates of the reseau corner points were computed and printed on the picture label.

For cartographic use, video tapes were converted to positive geometrically precise hard copies on a photomechanical film converter at the Astrogeology Branch of the U.S. Geological Survey, Flagstaff. These copies were used in the photomosaics displayed in Figs. VI-3 and VI-4a, and also are presented in Section VII.

For mosaicking pictures on the globe (Fig. VI-3), the orthographic projection was appropriate. However, standard mapping projections are conformal and very close to orthographic projection over limited areas. Before the standard mapping pictures were mosaicked on the globe, scale variations with latitude were adjusted photographically.

Mapping projections for the 30 charts in which topographic information was emphasized were given priority; consequently, only a few pictures corrected for Sun-elevation angle were produced. The only mosaic made using these pictures is shown in Fig. VI-4b. Figure VI-5 contains some examples of long-range pictures that were processed with the Sun-elevation correction to emphasize albedo features.

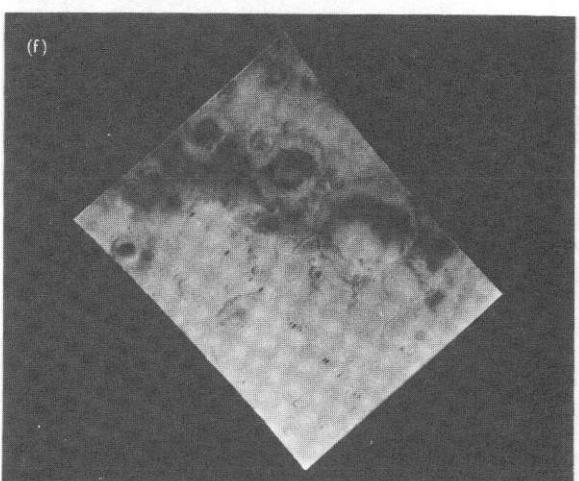
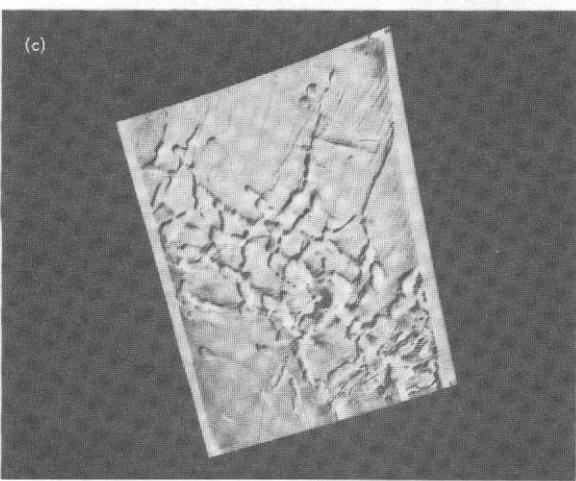
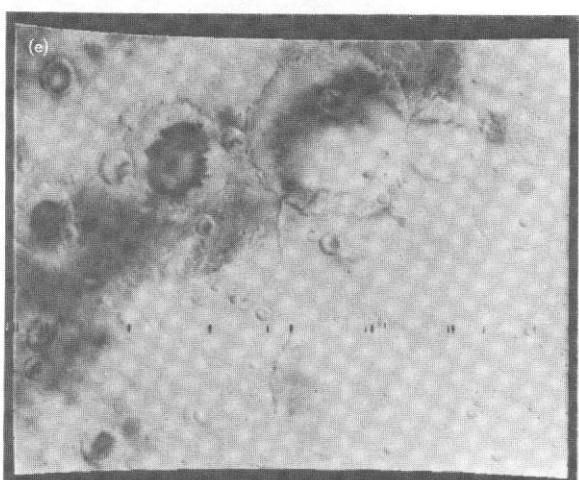
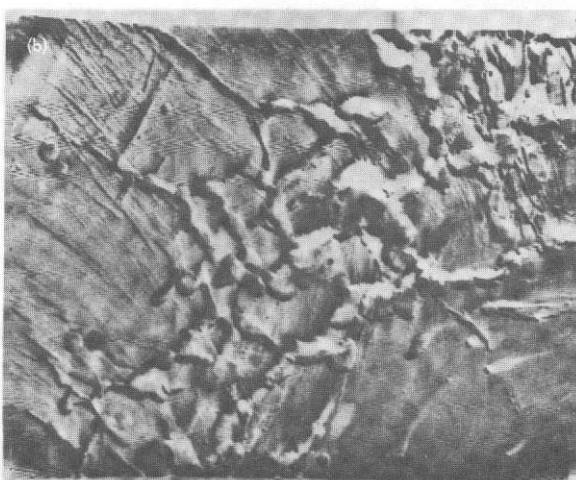
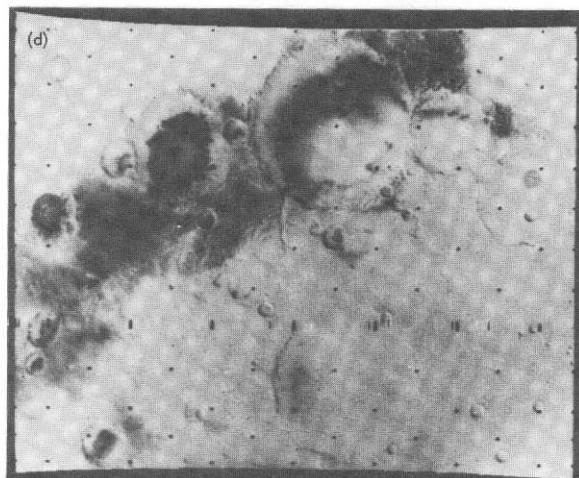
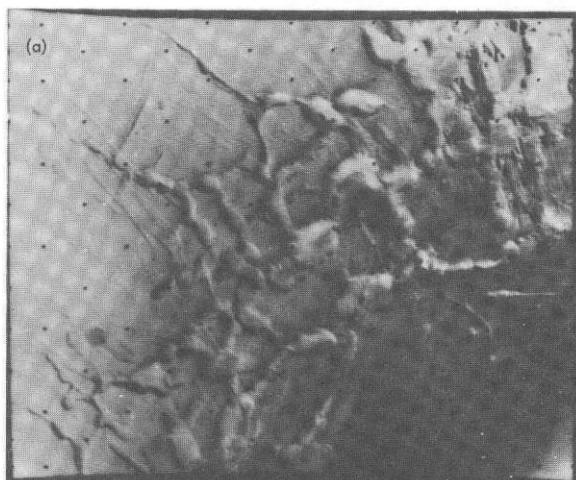


Fig. VI-1. (a, b, c) Contrast-stretched, HPP, and HPF R&S versions of RDR data for a wide-angle picture in the Phoenicis Lacus region. (d,e,f) Contrast-stretched, Sun-elevation-angle-corrected, and Sun-elevation-angle-corrected R&S versions of RDR data for a wide-angle picture in the Sinus Sabaeus region.

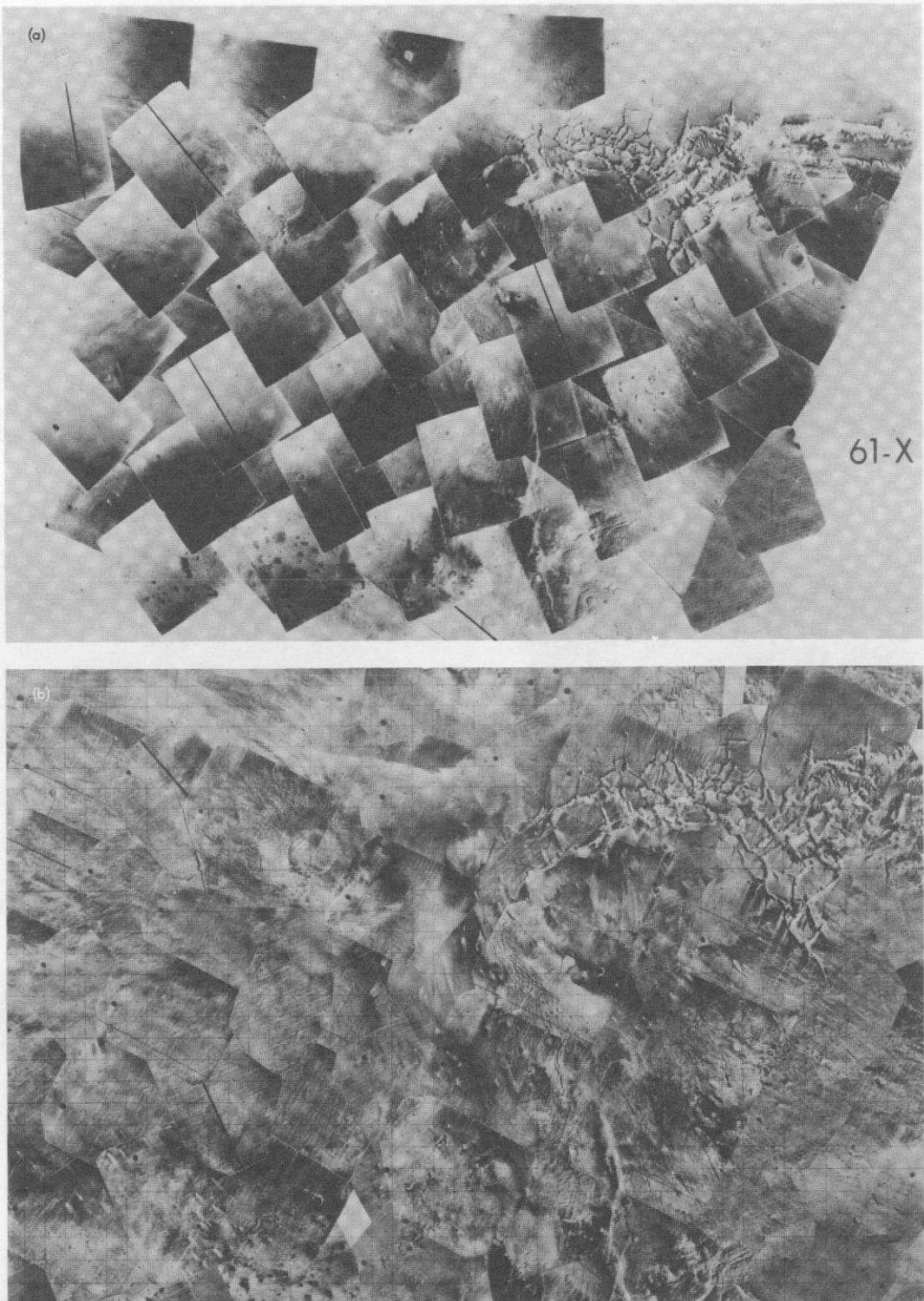


Fig. VI-2. (a) Photomosaic of pictures in the Phoenicis Lacus region. Pictures were subjected to minimal image processing. Only a contrast stretch was applied to the raw spacecraft data to enhance detail. Note the substantial geometric and photometric mismatch among the individual pictures that form this mosaic. (b) Photomosaic of the same region. Pictures were photometrically and geometrically decalibrated, high-pass filtered, and then transformed into mapping projections. Geometric and photometric interlocking of the elements of this mosaic is vastly improved over those in Fig. VI-2a. After transformation, the pictures in the mosaic may be considered map fragments, rather than perspective views of the planet, so that the photomosaic is in fact a geometrically accurate photomap. This mosaic is one of 30 that cover the entire planet.

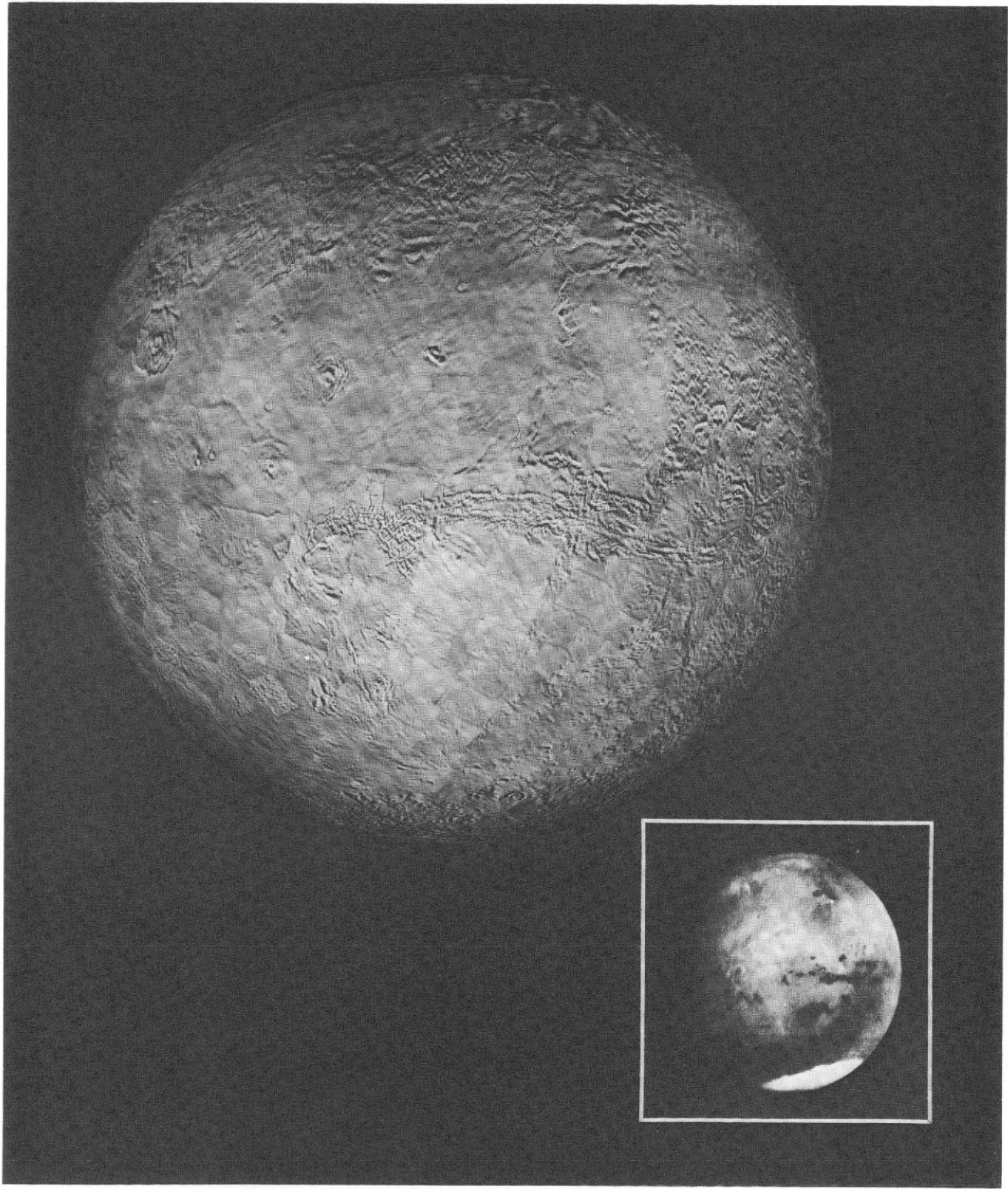


Fig. VI-3. A 1.3-m (4-ft) global mosaic of Mars assembled from Mariner 9 HPF R&S pictures. The continental scale light and dark markings that occur on this face of the planet (see Mariner 7 picture inset) were suppressed by the computer processing.

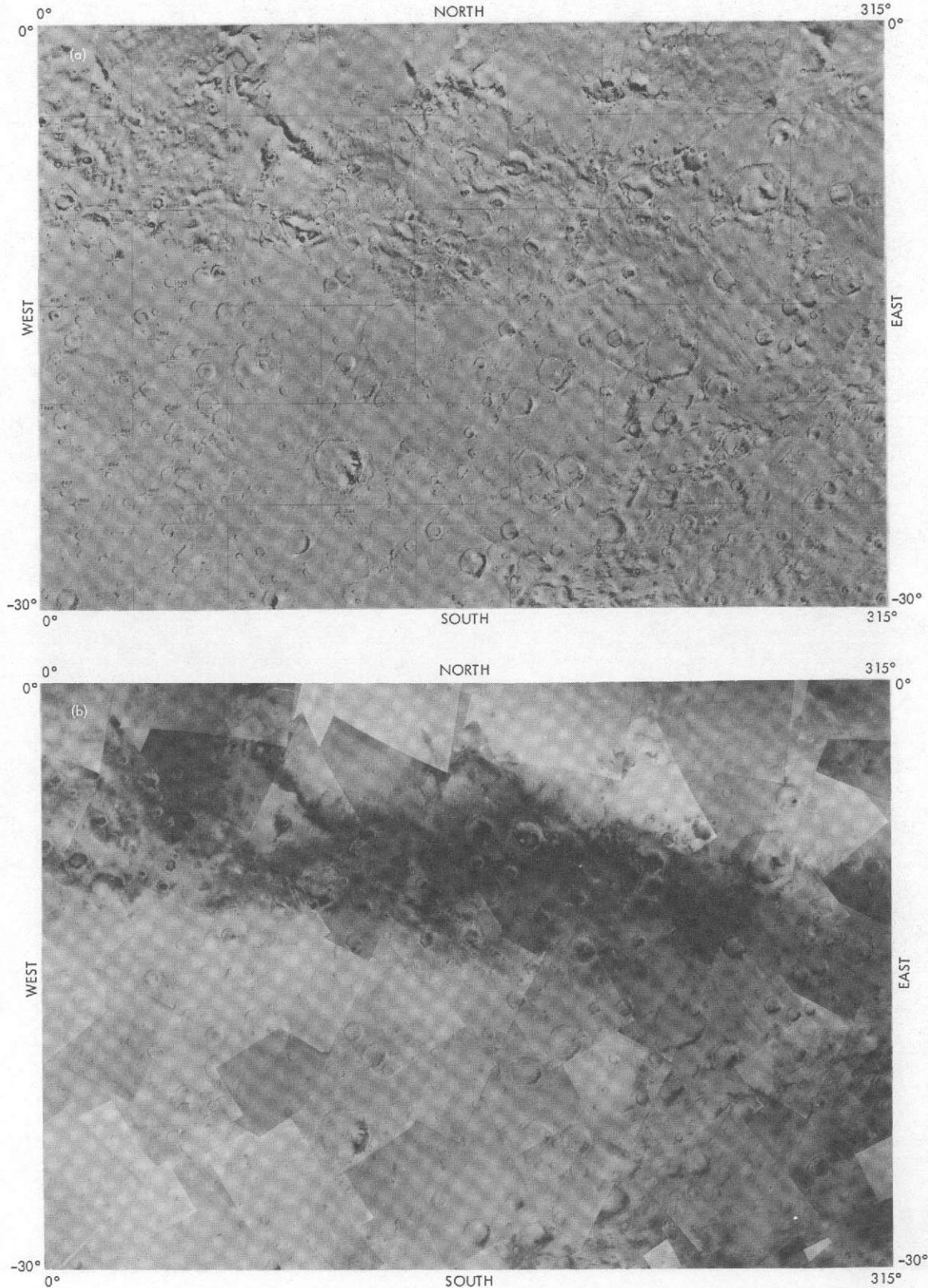


Fig. VI-4. Comparison of (a) R&S filtered pictures and (b) Sun-elevation-angle-corrected pictures in the Sinus Sabaeus region. Both mosaics show minimal edge effects. The filtered mosaic shows good topographic detail, but no large-scale albedo features.

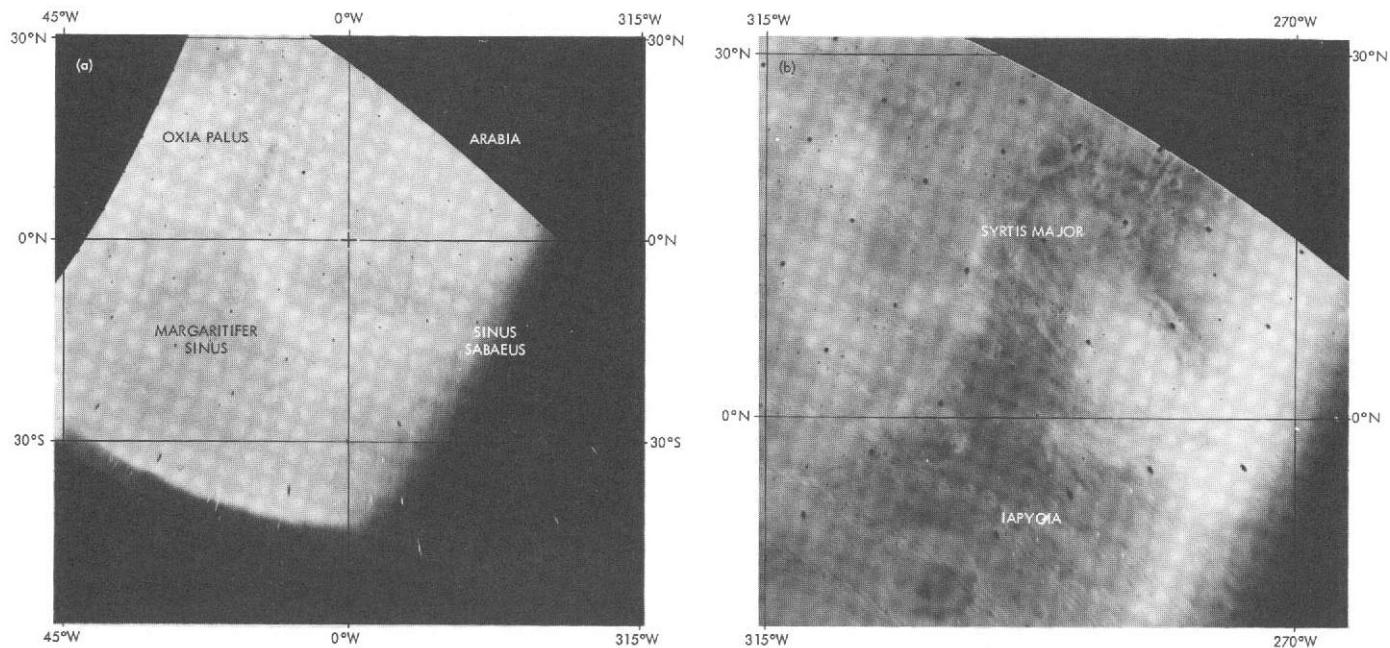


Fig. VI-5. Sun-elevation-angle-corrected R&S versions of global pictures taken late in the Mariner 9 mission. (a) Meridiani Sinus region during Rev 667. (b) Syrtis Major region during Rev 675.

References

- VI-1. *Computer Cartographic Projections for Planetary Mosaics Final Report. Volume I: Task Summary*, Jet Propulsion Laboratory Internal Report 900-639, 1973.
- VI-2. *Computer Cartographic Projections for Planetary Mosaics Final Report. Volume II: MAP2 Program Mathematical Development*, Jet Propulsion Laboratory Internal Report 900-639, 1973.
- VI-3. *Computer Cartographic Projections for Planetary Mosaics Final Report. Volume III: MAP2 Program User's Guide*, Jet Propulsion Laboratory Internal Report 900-639, 1973.
- VI-4. Batson, R.M., "Cartographic Products From the Mariner 9 Mission," *J. Geophys. Res.*, Vol. 78, p. 4424, 1973.

VII. Photographic Mapping, Geology, and Cartography

Before the Mariner 9 mission, only about 20 percent of Mars had been photographed with the resolution necessary to resolve topographic forms. Most of this coverage was obtained in 1969 when Mariner 6 made an equatorial flyby of the planet and when Mariner 7, 5 days later, photographed the south polar cap at close range. The Mariner 6 and 7 pictures revealed a somewhat disappointing landscape, studded with large impact craters similar to those observed on the Moon. Only the limited areas of "chaotic terrain" (see Ref. VII-1) suggested significant internal activity on the planet.

Mariner 9 inherited the basic design of the Mariner 6 and 7 television subsystem, although significant improvements were made in their electronic capabilities (see Section II). A fixed-feature investigation was structured around these cameras with the objective of defining the geology and topography of at least 70 percent of the surface of the planet at a resolution consistent with the attainment of contiguous coverage (Ref. VII-2). The pictures thus acquired indicated that Mars is not a geologically dead world, but a volcanically active planet whose surface is marked by wind action and mysterious fluvial processes.

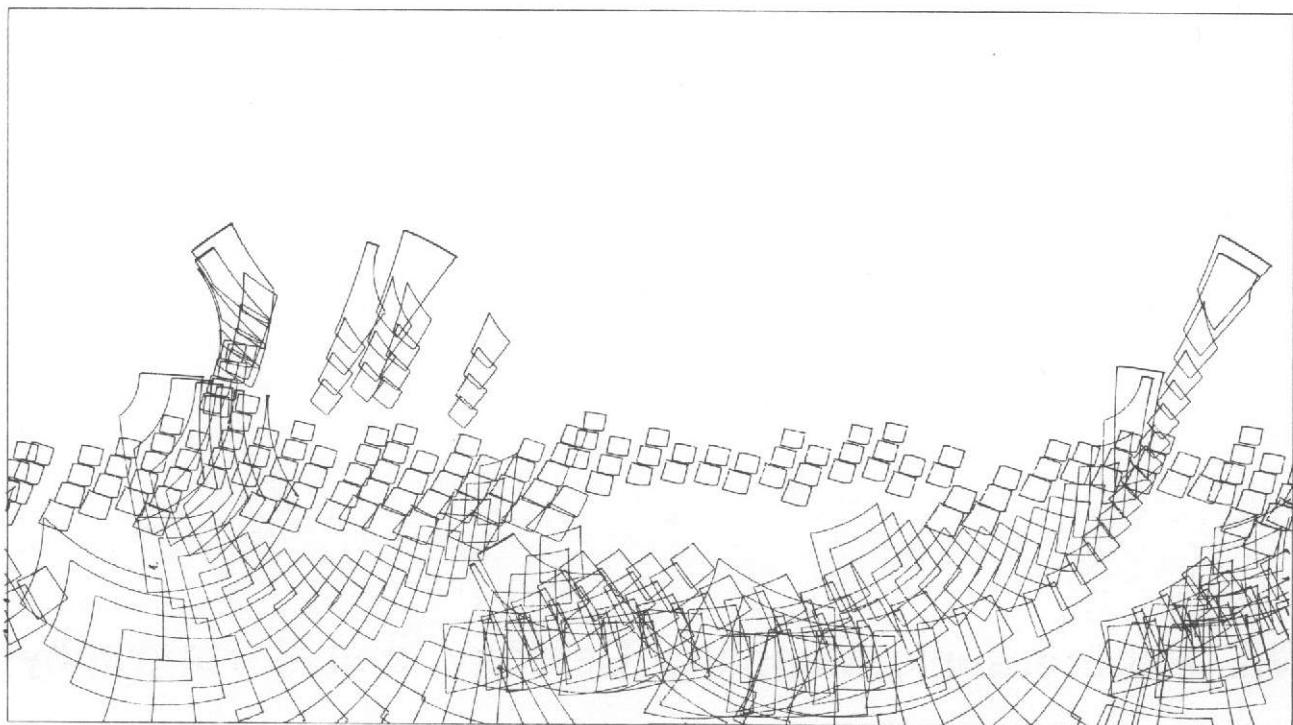
Studies of the fixed features on Mars were conducted using the wide-angle camera to acquire medium-resolution coverage of the entire planet, and the narrow-angle camera, with

ten times the resolution but only 1 percent of the coverage of the wide-angle camera, to systematically "sample" the planet's surface at a resolution sufficient to study in detail landforms of fundamental geological, geochemical, and geophysical significance. Mosaickable groups of high-resolution pictures and stereoscopic coverage of features recognized in the wide-angle pictures also were acquired for this purpose.

A. Photographic Mapping (Wide-Angle Pictures)

1. The Dust Storm

The loss of Mariner 8 and the dust storm that almost totally obscured the surface of Mars during the first several weeks of Mariner 9 orbital operations significantly affected the way in which mapping was performed. Before the loss of Mariner 8, it was planned to conduct the mapping mission from an 80° inclination orbit, and to take the mapping pictures vertically and close to the evening terminator of Mars. After the loss of Mariner 8, a compromise orbit with an inclination of 65° was chosen for the remaining spacecraft. The orbit permitted vertical photography between the 65° parallels, but required oblique and longer-range photography in the polar regions. The variation in lighting angles was increased in



REVS 24-99

Fig. VII-1. Wide-angle mapping frames acquired during the Martian dust storm.

the 65° orbit during the early parts of the mission because the ground track made a steeper angle with the terminator.

As Mariner 9 approached Mars, it became increasingly evident that the dust storm obscuring the planet's albedo features, which had been observed telescopically from Earth, would interfere with medium- and high-resolution photography of the surface by the Mariner 9 television cameras. This assessment was confirmed when pre-orbital pictures showed little detail and when early orbital pictures showed only the vaguest outlines of surface topographic features. As a consequence, no attempt was made to immediately implement the preflight plan of laying down contiguous swaths of wide-angle pictures for meeting the mapping objective. Instead, picture sequences were redirected to observe the polar region, where the atmosphere was much clearer than over the rest of the planet (see Section VIII) and to conduct observations of, and probe the transparency of the atmosphere (see Section XI). However, a limited number of frames on each revolution was devoted to photographing the planet at the range, lighting, and viewing conditions originally planned for mapping photography. Few of these pictures showed more than the vaguest outlines of the larger craters on the Martian surface (see Fig. VII-1 for footprint plots showing the areas covered by these frames).

2. Mapping Sequence Design

After about 40 days (80 revolutions) of orbital picture taking, there were some indications that the clarity of the atmosphere was improving, although much surface detail was still obscured. However, the mapping could not be delayed if medium-resolution pictures of 70 percent of the planet were to be obtained. Soon after Rev 200, Earth would move away from the principal lobe of the high-gain antenna, fixed immovably to the spacecraft; thus, falling signal strength would reduce the number of frames that could be recovered each day (see Section II-B-5). By Rev 262, the spacecraft, if it survived that long, would be occulted from the Sun by Mars for such a great part of each day that sufficient electrical power would not be available to continue science operations.

The brief firing of the spacecraft's rocket motor on Rev 96 increased the height of periapsis from 1385 to 1650 km, thus reducing the number of pictures required for complete coverage of the planet. The way in which mapping coverage was developed with this new orbit required modifications to the previous plan (see Section II-B-5). However, the new plan still encompassed the fundamental feature of the first plan, which took advantage of a fortunate relationship between the rotational periods of Earth and Mars. The orbital

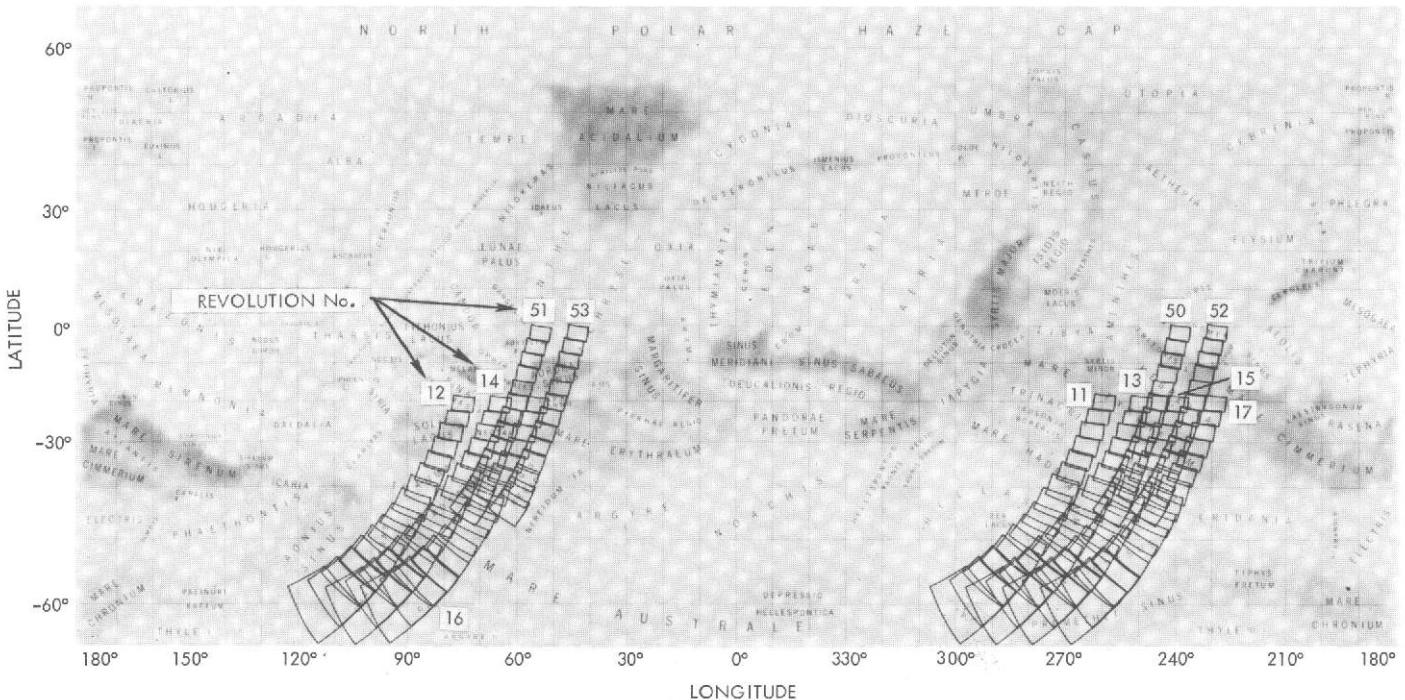


Fig. VII-2. Typical wide-angle-camera footprints for surface mapping according to the mission plan devised after the loss of Mariner 8. Corresponds to orbital inclination of 65° , period of 11.98 h, and periapsis altitude of 1250 km. Because of the dust storm, the mapping sequences were deferred almost 50 days and, to reduce the number of pictures needed, were acquired from an altitude of about 1600 km. This figure shows the concept of building contiguous coverage in a given latitude band on successive revolutions and the manner of extending coverage to more northerly latitudes and filling gaps after an interval of 39 revolutions.

period of Mariner 9 was closely synchronized with that of Earth so that data playbacks could be made from the same part of the Mariner 9 orbit each day. Because Mars took 43 min longer to rotate than did Earth, the ground track of each successive odd (nadir) or even (zenith) revolution was displaced by about 9° . Consequently, ground tracks gradually proceeded eastward (see Fig. VII-2), and the ground tracks of Rev 139 almost exactly retraced those of Rev 100. Therefore, mapping photography logically was divided into cycles 39 revolutions long. During a cycle, it was possible to cover a given latitude band so that corresponding pictures on each revolution had similar coverage and viewing and lighting geometry. On subsequent cycles, a different latitude band could be photographed, or gaps between the original mapping swaths could be filled (see Volume II).

The latitude band from 65°S to 25°S was covered in Mapping Cycle I (Fig. VII-3a) and from 25°S to 25°N in Mapping Cycle II (Fig. VII-3b). In Mapping Cycle III (Fig. VII-3c) gaps in latitudes 30°S to 0° were filled,¹ and mapping

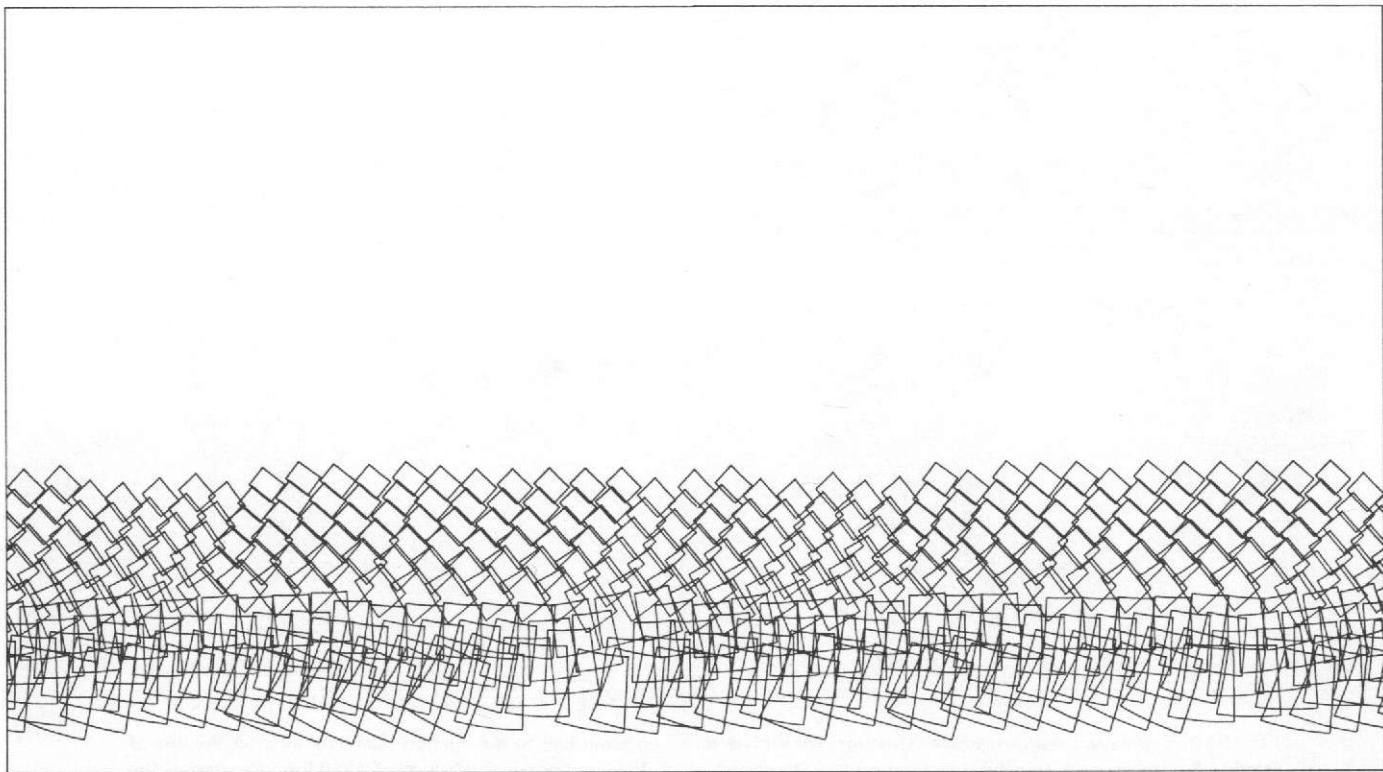
was extended from 25°N to 45°N . At that time, the edge of the north polar hood, or haze layer, extended between 40°N and 45°N , and the pictures acquired north of these latitudes contained little information regarding the surface.

Continued operation of Mariner 9 after the end of the standard mission made it possible to perform exploratory photography of the haze-covered north polar region (Mare Boreum quadrangle) and to fill gaps south of 45°N . In the period between Revs 217 and 262 (extended mission, Phase I), the rephotographing of the south polar region (Mare Australe quadrangle) was also completed (see Section VIII).

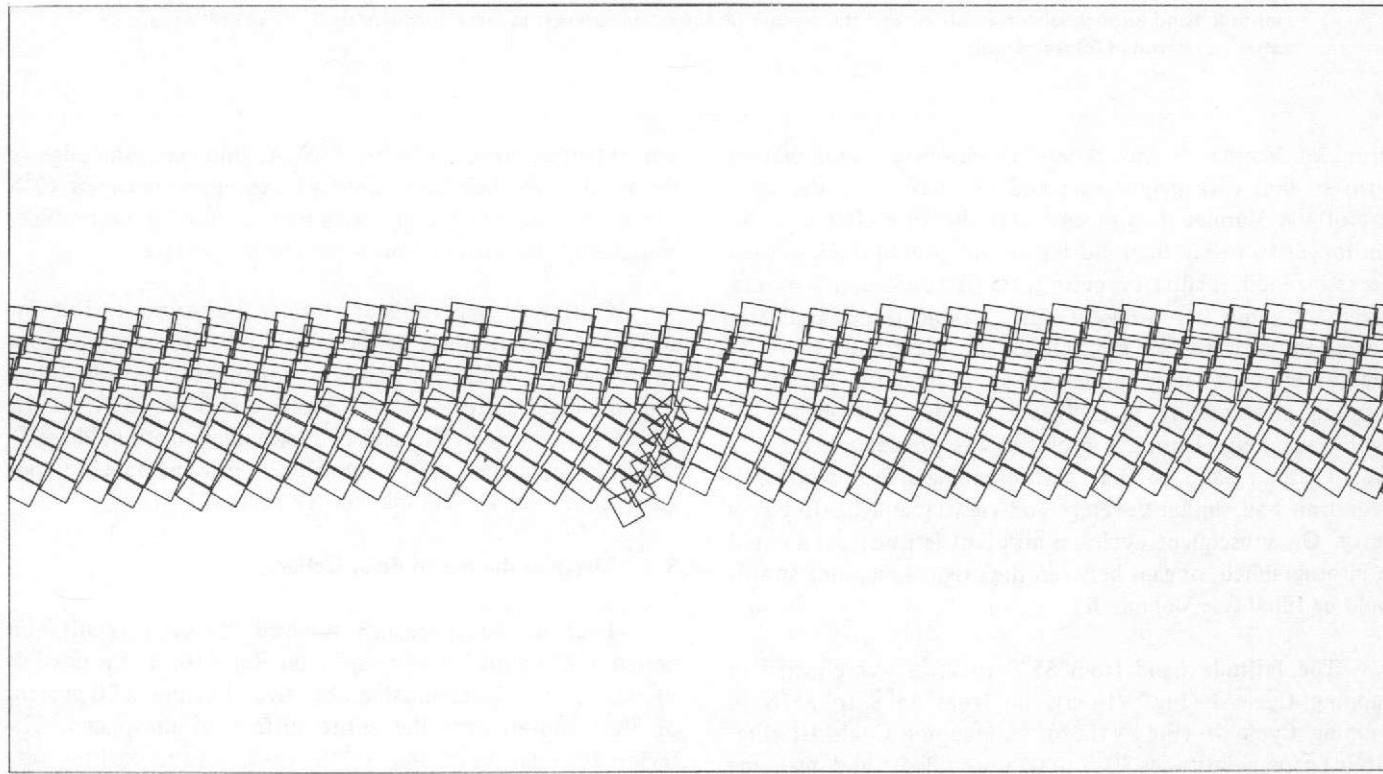
3. Mapping the North Polar Collar

Because the spacecraft survived the solar occultation period and resumed photography on Rev 416, it was possible to exceed the original mission objective of mapping 70 percent of Mars and to map the entire surface of the planet. The region between 45°N and 65°N , which was marked by haze before Rev 262, was found to be clear of haze cover on Rev 416. Mapping of the "north polar collar" was performed between Revs 416 and 459; during this period Arcturus was

¹ The latitude range in which the spacecraft was closest to Mars and television pictures covered the least area.

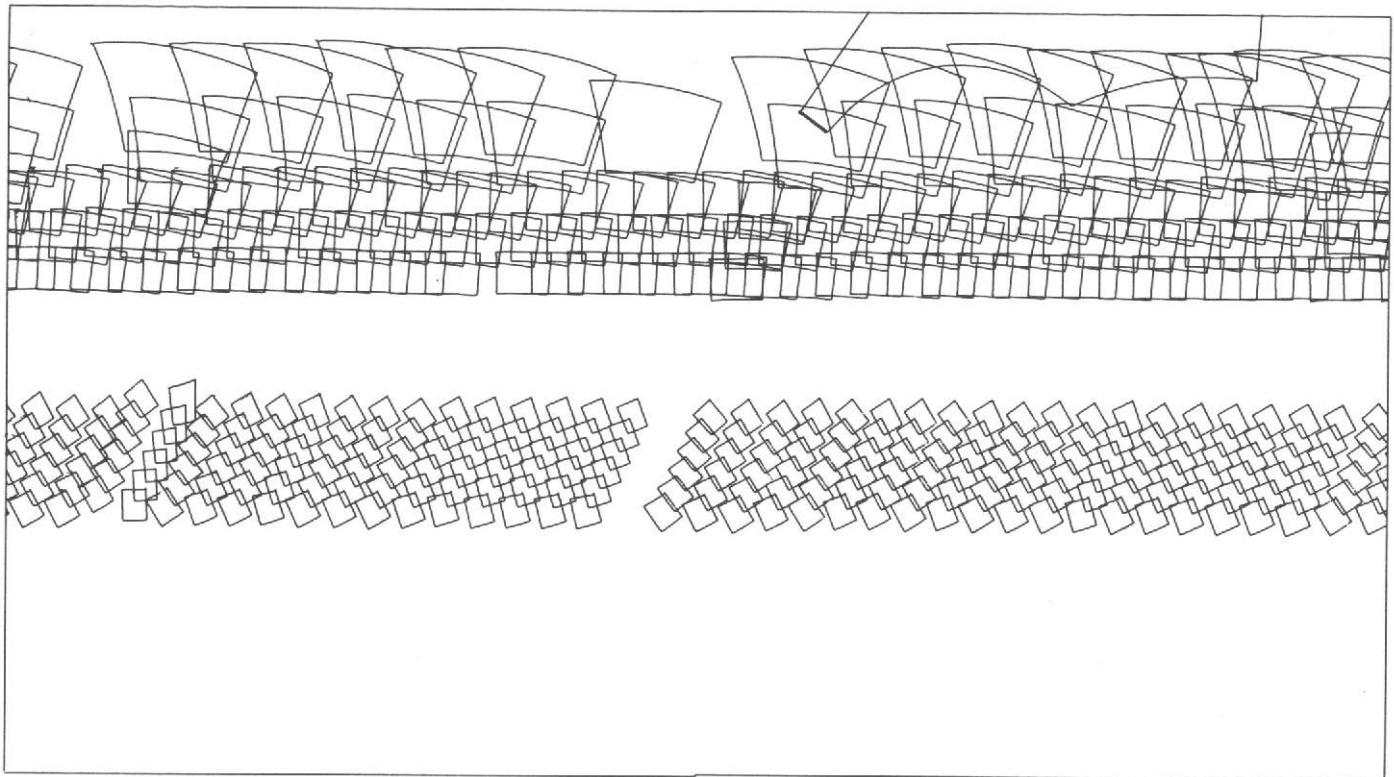


(a) REVS 100—138

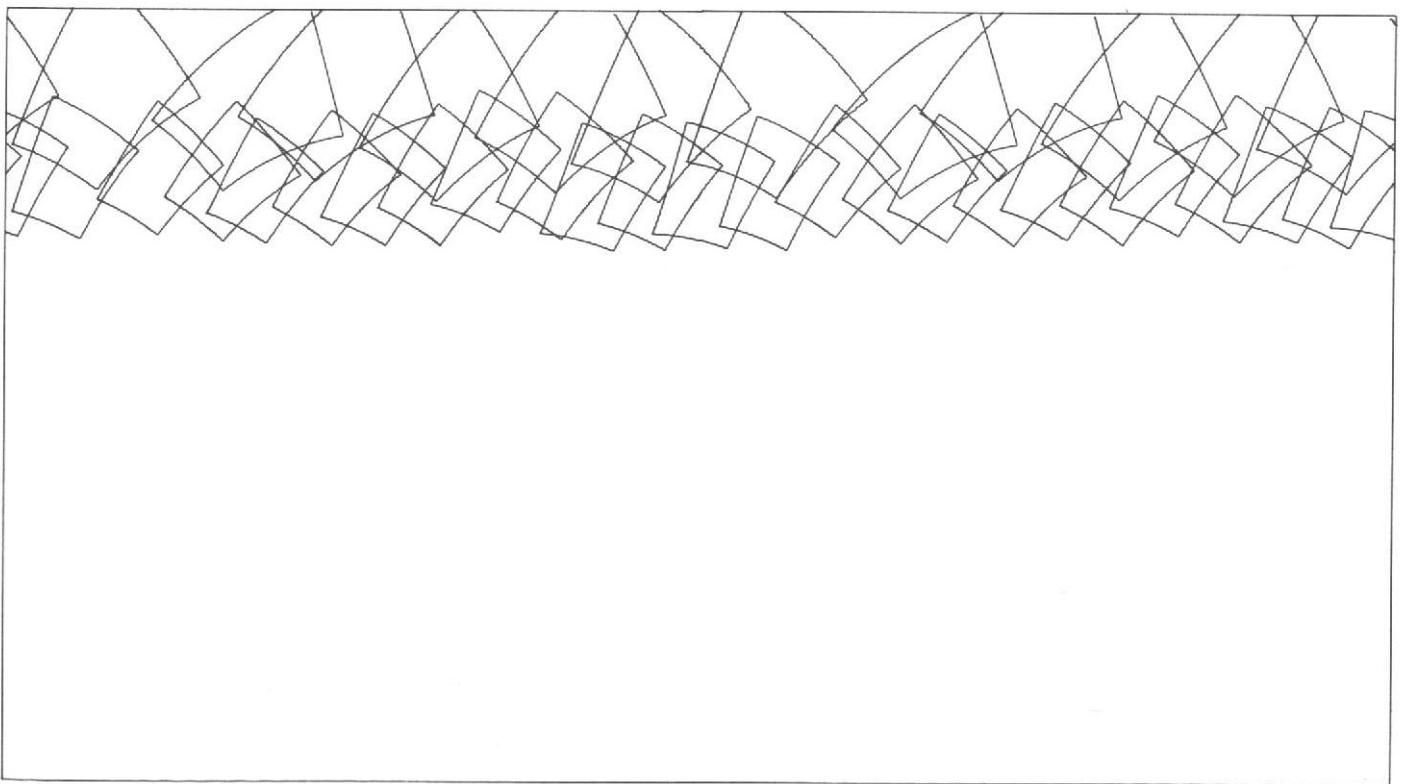


(b) REVS 138—178

Fig. VII-3. Wide-angle mapping frames. (a) Mapping Cycle I. (b) Mapping Cycle II. (c) Mapping Cycle III. (d) Extended mission, Phase I.



(c) REVS 179—217



(d) REVS 416—451

Fig. VII-3. (contd.).

Table VII-1. Picture coverage for systematic mapping and geology

Revs	Phase	Orbital science links		Coverage
		Zenith pass (even revolutions)	Nadir pass (odd revolutions)	
		Systematic mapping and geology		
1-15	Post-orbital insertion mapping calibration and phase function	16BA + 1B on most revolutions	16BA + 1B on most revolutions	Variety of ranges and locations
16-23	Interim sequence	3A, 8BA	4A, 5BA	Latitude band: -60° to 0°
24-63	Recon I	2 + BA	4BA ^a	Latitude band: -40° to -10°
64-99	Recon II	1A, 3BA, 1B	1A, 4BA	Variety of latitude ranges
100-138	Mapping Cycle I	TV mapping 1 (1A, 3BA) TV mapping 2 (1A, 5BA)	Same as zenith Same as zenith	Latitude band: -65° to -48° Latitude band: -50° to -25°
139-177	Mapping Cycle II	TV mapping 1 (1A, 4BA, 1B) TV mapping 2 (5BA)	Same as zenith	Latitude band: -25° to -5° Latitude band: -5° to 20°
178-217	Mapping Cycle III	TV mapping 1 (2A, 1B, 2A, 1B, 2A) TV mapping 2 (5AB)	TV mapping 1 (2A, 1B, 4A) TV mapping 2 (3AB)	Latitude band: -30° to -5° Latitude band: 25° to 65°N
218-262	Extended mission, Phase I	No systematic coverage. Some filling of gaps	Same as zenith	
416-459	Extended mission, Phase II: Arcturus	North collar mapping; Six revolutions, 6AB parts per revolution	Same as zenith	Latitude band: 45° to 65°
613-673	Extended mission, Phases III and IV	No systematic coverage	Same as zenith	
Targeted narrow-angle frames for geology				
100-138	Mapping Cycle I		TLR (1B) -37 min, 54 s	
139-177	Mapping Cycle II	Single B-frame (1B) 19 min, 42 s Single B-frame (1B) -14 min, 6 s	Single B-frame (1B) -19 min, 42 s Single B-frame (1B) -14 min, 6 s	
178-217	Mapping Cycle III	Dyad 1 (2B) -24 min, 54 s ^b Tetrad 2 (4B) -11 min, 18 s TEC (1B) 6 min, 56 s	Dyad 1 (2B) -24 min, 54 s Dyad 2 (2B) -8 min, 30 s	
218-262	Extended mission, Phase I	Triad 2 (3B) Triad 4 (3B)	Triad 2 (3B) Triad 4 (3B)	
416-459	Extended mission, Phases II, III, IV	Targets of opportunity on Viking sites and significant geologic features	Same as zenith	

^aThe links listed in this table were used extensively for geology as opposed to targeted frames used for atmospheric studies. Those picture links containing only narrow-angle frames are assumed to fall into this category: picture links, which contained wide- and narrow-angle frames and which were used sometimes for geologic coverage, are listed in Table VIII-2.

^bThese links were used on some orbits for photographing features in the Mare Australis quadrangle below 65°S (see Table VIII-1).

used as the reference star for stabilizing the spacecraft. Wide-angle frames of the north polar collar were acquired from significantly greater range than other mapping frames and are of lower resolution. Partly because of the greater range and partly because of the high latitude, data on only about 20 percent of the revolutions between 416 and 459 were necessary to obtain complete contiguous coverage. Mapping of the region north of 65°N was also accomplished between Revs 416 and 459 (see Section VIII). A detailed summary of the mapping coverage by Mariner 9 (except for coverage in the polar regions) is given in Table VII-1.

4. Quality of the Mapping Pictures

An ideal mapping mission would consist of the acquisition of images from a constant altitude, viewing vertically and at a constant solar elevation angle. Pictures taken under such conditions are most convenient for compilation into maps and

permit reliable comparisons of features appearing in several different pictures. Constant illumination conditions cannot be obtained at all latitudes by an orbiting spacecraft, although constant range and vertical viewing are, in principle, attainable. The pointing of the Mariner 9 cameras was adjusted so that two pictures in each mapping swath were aimed vertically (see Section II-B-5-a). The resolution of the pictures is highest near the periapsis altitude (20°S) and generally is better in the southern than in the northern hemisphere.

Factors such as high lighting angles and residual obscuration from the dust storm offset the higher resolution of southern hemisphere photography. During Mapping Cycle I, when the latitude belt between 65°S and 25°S was systematically photographed, there was still considerable muting of surface detail because of suspended aerosols. Because of the prolonged delay in starting the mapping, the ground track of the spacecraft had migrated a considerable distance from the termi-

nator. Lighting angles lay in the range of from 40° to 50°, but did not vary significantly along the ground track.

B. Geology (Narrow-Angle Pictures)

1. Systematic Sampling

The systematic narrow-angle coverage obtained in conjunction with the mapping sequences is presented in Figs. VII-4a and VII-4b. Resolution and viewing of the narrow-angle frames varied with latitude in the same way as did the accompanying wide-angle frames. The density of narrow-angle-frame sampling (number of frames/10⁶km²) is variable, although this is distorted in the Mercator Projections of Fig. VII-4. Most latitude bands are fairly well sampled, but there are significant gaps between 45°S and 53°S, 15°N and 30°N, and 60°N and 70°N.

2. Special Targets and Stereo Coverage

Features of particular interest that were recognizable in both wide- and narrow-angle frames were selected for additional high-resolution coverage with the narrow-angle camera. These features were difficult to photograph because of uncertainties in camera pointing, feature location, and planetary spin axis. Some redundant frames were taken so that particularly significant features² were included in the field of view of at least one frame. During most of the standard mission, however, targeting reached an unanticipated level of precision.

Targeted narrow-angle frames of geologic interest acquired between Revs 100 and 676 are plotted in Fig. VII-4c. Pictures taken specifically for viewing variable surface features, but within a viewing range and resolution that make them useful in geologic interpretations, are included. Many narrow-angle frames were acquired in sequences that also included a wide-angle frame, which is not plotted.

Some sequences were designed to photograph the surface with a range of viewing angles suitable for stereoscopic studies of topographic relief. The rapid slewing rates necessary placed some limitations on the locations that could be studied in this way. Areas that have been examined stereoscopically include Valles Marineris (Coprates Canyon: 5°S to 15°S, 45°W to 95°W),² Arsia Mons (South Spot: 11°S, 119°W), Olympus Mons (Nix Olympica: 17°N, 133°W), and the residual south polar cap (Refs. VII-3 and VII-4).

3. Viking Landing Sites

Mariner 9 pictures of several candidate sites were obtained for the two Viking spacecraft scheduled to land on Mars in 1976 (Ref. VII-5). Neither very high nor very low regions were considered accessible to Viking, and surface roughness was another consideration. Radar, wide-angle photography, and systematic narrow-angle frames gave some idea of regional variations in roughness and allowed apparently smooth areas to be isolated. However, narrow-angle pictures, targeted exactly on the potential landing sites, also were required to confirm these judgements and to choose between different landing sites.

The equatorial landing sites considered are given in Table VII-2, and the special narrow-angle pictures taken at these sites are indicated in Fig. VII-4d. But for the interest of Viking, most of these areas would not have been photographed. They are generally smooth and devoid of topographic detail, whereas most of the areas of special targeting are rougher regions with varied and complex topographic features. Candidate landing sites in polar and intermediate latitudes were selected after the end of the Mariner 9 mission, and therefore no narrow-angle special frames were specifically targeted for those landing sites.

C. Cartography

The medium-resolution coverage discussed in Section VII-A was obtained for cartographic purposes. Decalibrated pictures (see Section V) rectified to standard mapping projections (see Section VI) at the JPL Image Processing Laboratory were assembled into 1:5,000,000-scale mosaics at the U. S. Geological Survey, Center of Astrogeology, Flagstaff, Arizona (Ref. VII-6). These photomosaics display many of the planet's major physiographic features and provide a valuable basis for the systematic study of the geology of Mars. They also provide a suitable way of displaying the results of the mapping photography. Thirty mosaics were required to cover the entire planet; identification codes and names for these 30 quadrangles are presented in Fig. VII-5. Twenty-eight of the 30 mosaics are presented as Fig. VII-6 (northern hemisphere) and Fig. VII-7 (southern hemisphere), which have been reduced from the original 1:5,000,000-scale photomosaics.

Each wide-angle frame in the photomosaics is identified and listed. Predicted locations for the systematic narrow-angle pictures, individually targeted frames, and Viking landing sites are also shown. The narrow-angle pictures are reproduced adjacent to the mosaic in which they appear; they are organized into arrays so that the pictures appear in their appropriate relative locations in the mosaic. There has been no attempt to show which frames overlap.

² Names are those recently assigned by the International Astronomical Union. Informal names used in earlier publications and in other sections of this volume and the approximate coordinates are given in parentheses.

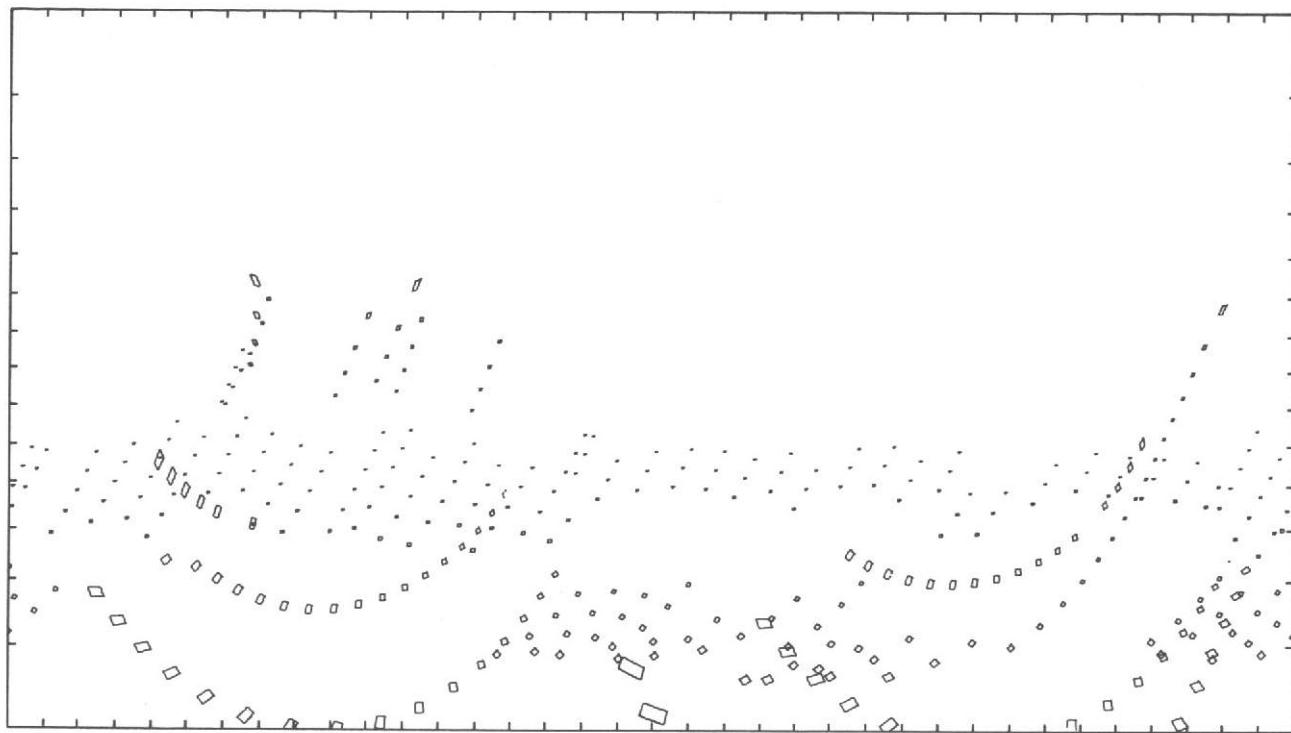
Numerical information regarding picture geometry for these frames appears in Tables VII-3 and VII-4, indexed by the same numbers used to identify the pictures in the photo-mosaics and the reproductions. This is only a subset of information available in the Supplementary Experiment Data Record (SEDR; see Section III). For an estimate of the sizes of visible features, the narrow-angle pictures of Figs. VII-6 and VII-7 can be used in conjunction with the data given in Tables VII-3 and VII-4 and in Fig. VII-8. More precise values of feature dimensions in the order of increasing precision are the SEDR listings that provide picture height and width, transparent overlays of latitude and longitude (see Section III), and the rectified and scaled pictures (see Section VI). The user could also derive scale and any other detailed information on picture geometry by processing the SEDR with his own computer programs.

The 1:5,000,000-scale photomosaics have been used as the basis for 1:5,000,000-scale shaded relief maps showing the major topographic features on Mars (Ref. VII-7) and a limited number of albedo charts (Ref. VII-8). A 1:25,000,000-scale shaded relief map that covers almost the entire planet is reproduced in Appendix A. The division of the planet into a southern hemisphere of heavily cratered terrains and a northern hemisphere largely occupied by smooth plains is obvious.

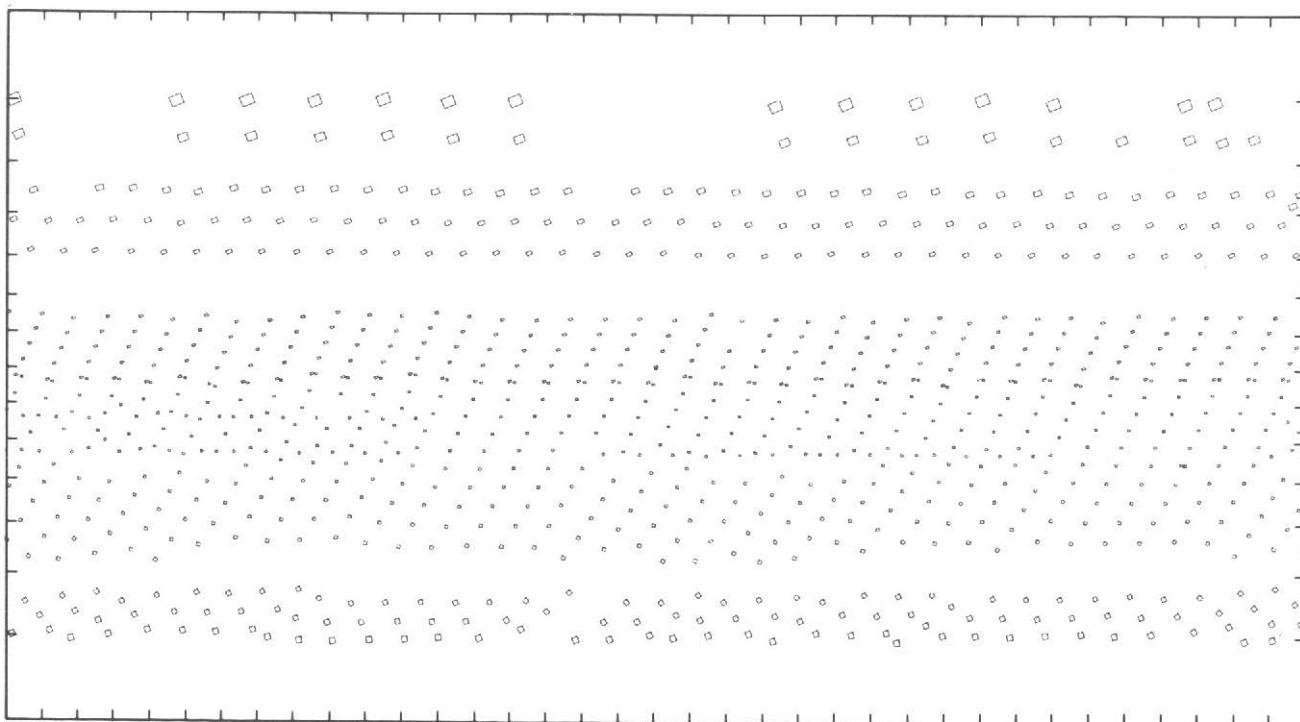
Along the margins of the cratered terrains, other more complex terrains can be seen. These include the chaotic terrains near 50°N latitude and the fretted terrains, which bound the greatest northern extent of cratered terrain between 0° and 270°W longitude (see Ref. VII-1). Several impact basins appear in the heavily cratered southern part of Mars (Ref. VII-9).

The western hemisphere of Mars has the most spectacular individual features. Most dominant are the shield volcanoes of Olympus Mons and Tharsis Montes (the Tharsis ridge: 12°S to 16°N, 101°W to 125°W), but centered on this volcanic complex is a radial fracture system that extends for thousands of kilometers in all directions. Some of these fractures have developed into troughs, the largest of which is Valles Marineris, which extends from east to west a few degrees south of the equator. More complex fracture systems have developed into the Labyrinthus Noctis (Chandeler: 5°S to 8°S, 92°W to 110°W) at the western end of Valles Marineris. Surrounding the Olympus Mons shield structure is an aureole of structured terrain (Ref. VII-10).

Mars will be explored in much greater detail before even this decade ends, but the basic physiographic framework provided by the Mariner 9 mapping pictures will not be superseded.



(a) REVS 24 - 99



(b) REVS 100 - 216

Fig. VII-4. Narrow-angle mapping and special coverage frames. (a) Mapping frames during the Martian dust storm: Recon I and Recon II. (b) Mapping Cycles I, II, and III. (c) Special coverage frames. (d) Viking landing sites.

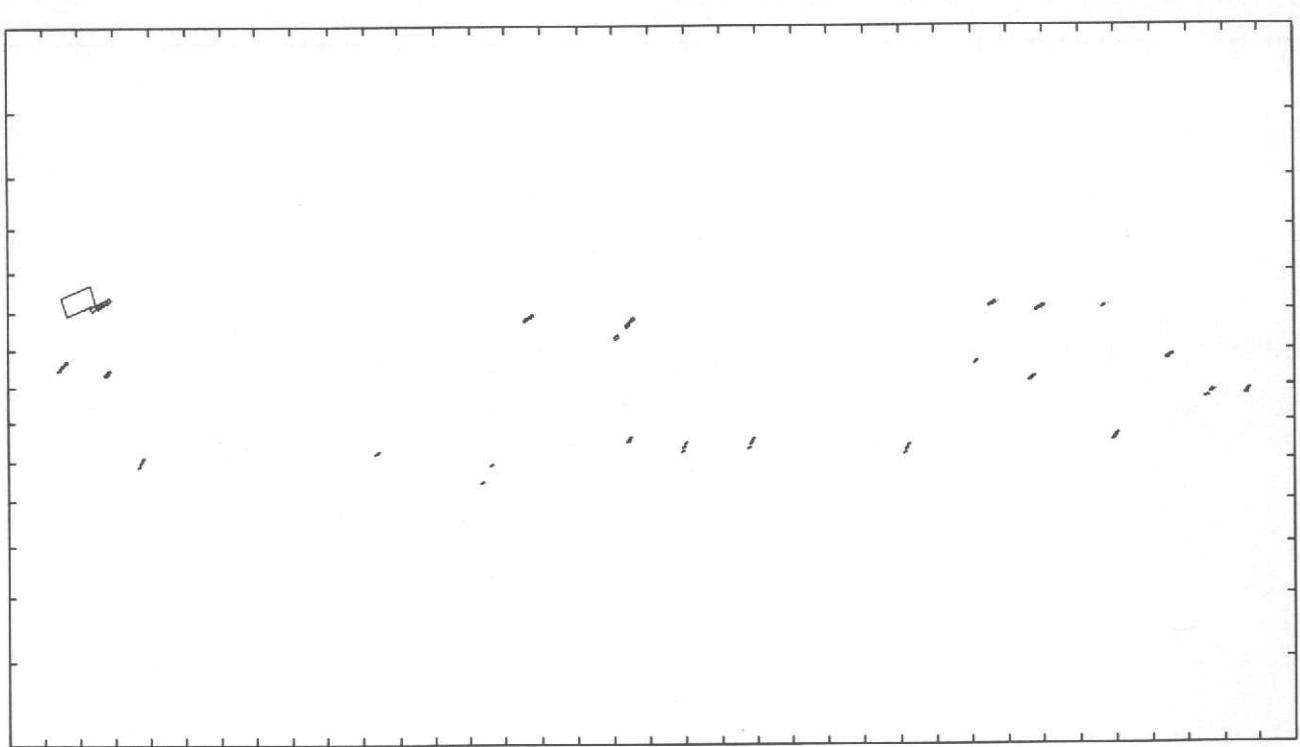
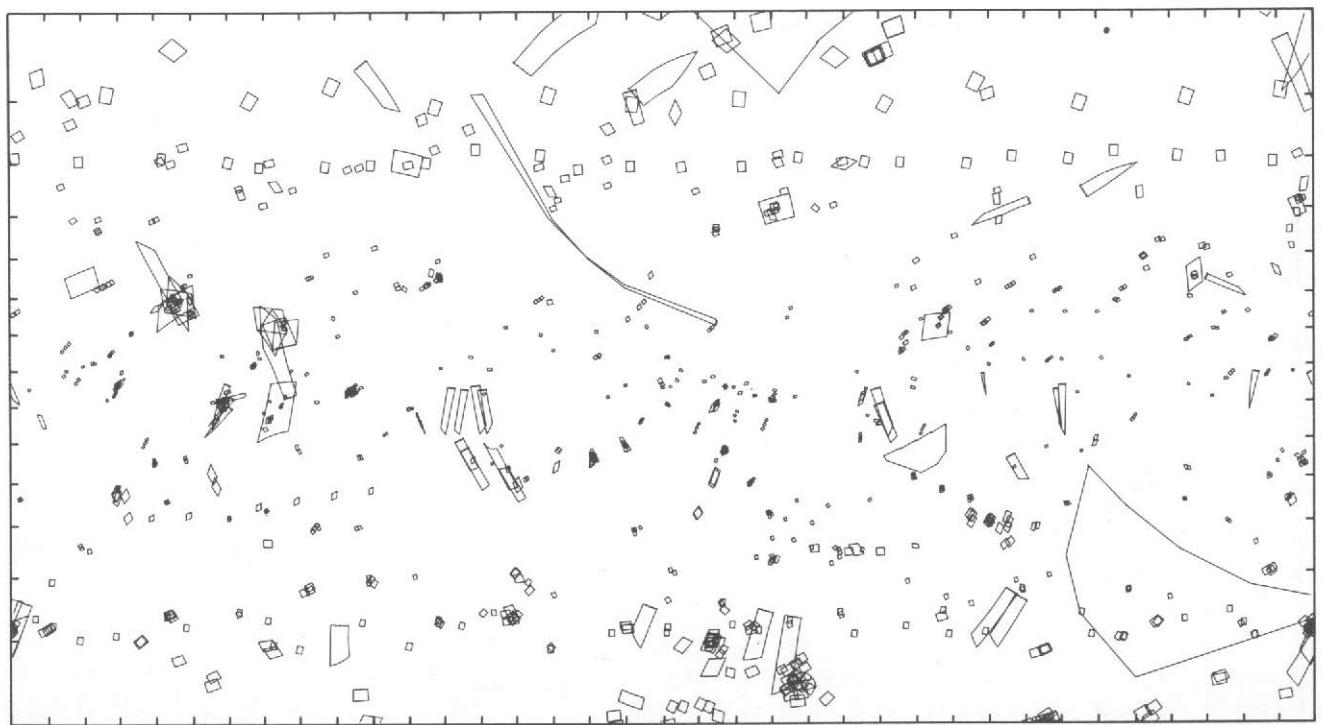


Fig. VII-4. (contd).

Table VII-2. Locations of candidate Viking landing sites

Site	Latitude	Longitude	Site	Latitude	Longitude
1 ^a	15.0°S	5.9°W	19	8.0°N	207.0°W
2	22.0°N	27.0°W	20 ^a	8.0°N	215.0°W
3	21.6°N	40.0°W	21	1.3°N	221.4°W
4 ^a	18.6°N	34.0°W	22 ^a	14.0°S	230.0°W
5 ^a	21.4°S	44.5°W	23 ^a	21.5°N	232.5°W
6	2.0°S	63.7°W	24	21.0°N	245.0°W
7 ^a	18.2°S	76.3°W	25	16.0°N	250.0°W
8	21.5°N	75.5°W	26	22.0°S	251.0°W
9 ^a	20.5°S	142.5°W	27 ^a	21.0°N	251.0°W
10	2.5°S	147.0°W	28 ^a	1.9°N	253.4°W
11 ^a	4.0°N	152.0°W	29 ^a	22.0°N	264.0°W
12 ^a	23.0°N	153.0°W	30 ^a	6.2°N	268.8°W
13 ^a	5.5°N	164.3°W	31	10.0°N	275.0°W
14	11.3°S	169.0°W	32 ^a	17.5°S	288.3°W
15	—	—	33	—	—
16	7.0°S	187.0°W	34 ^a	16.0°S	331.8°W
17 ^a	3.0°S	191.0°W	35 ^a	17.4°S	350.2°W
18	2.0°S	203.0°W			

^aPhotographed by Mariner 9.

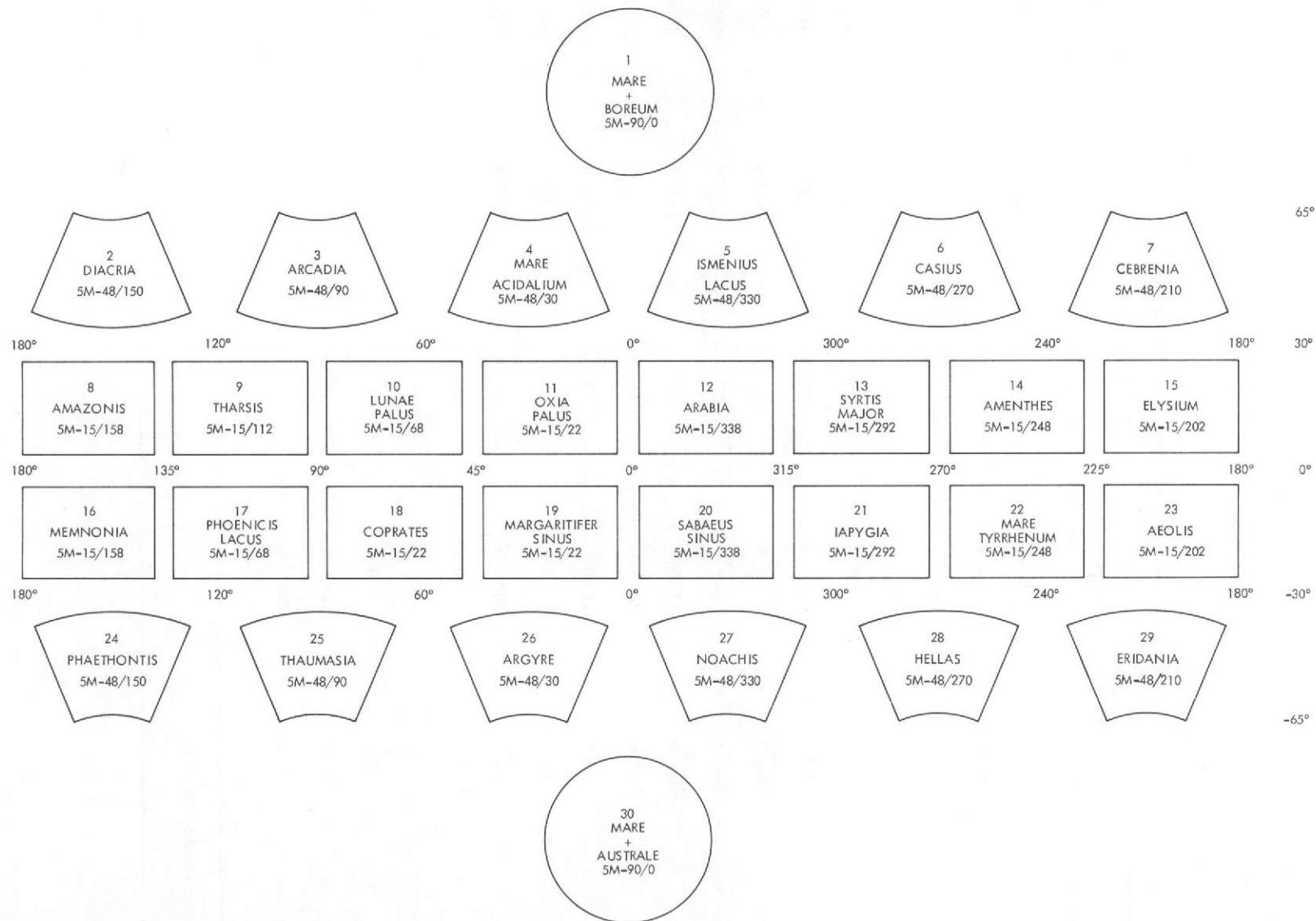
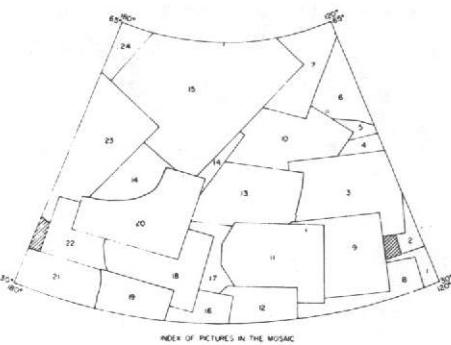
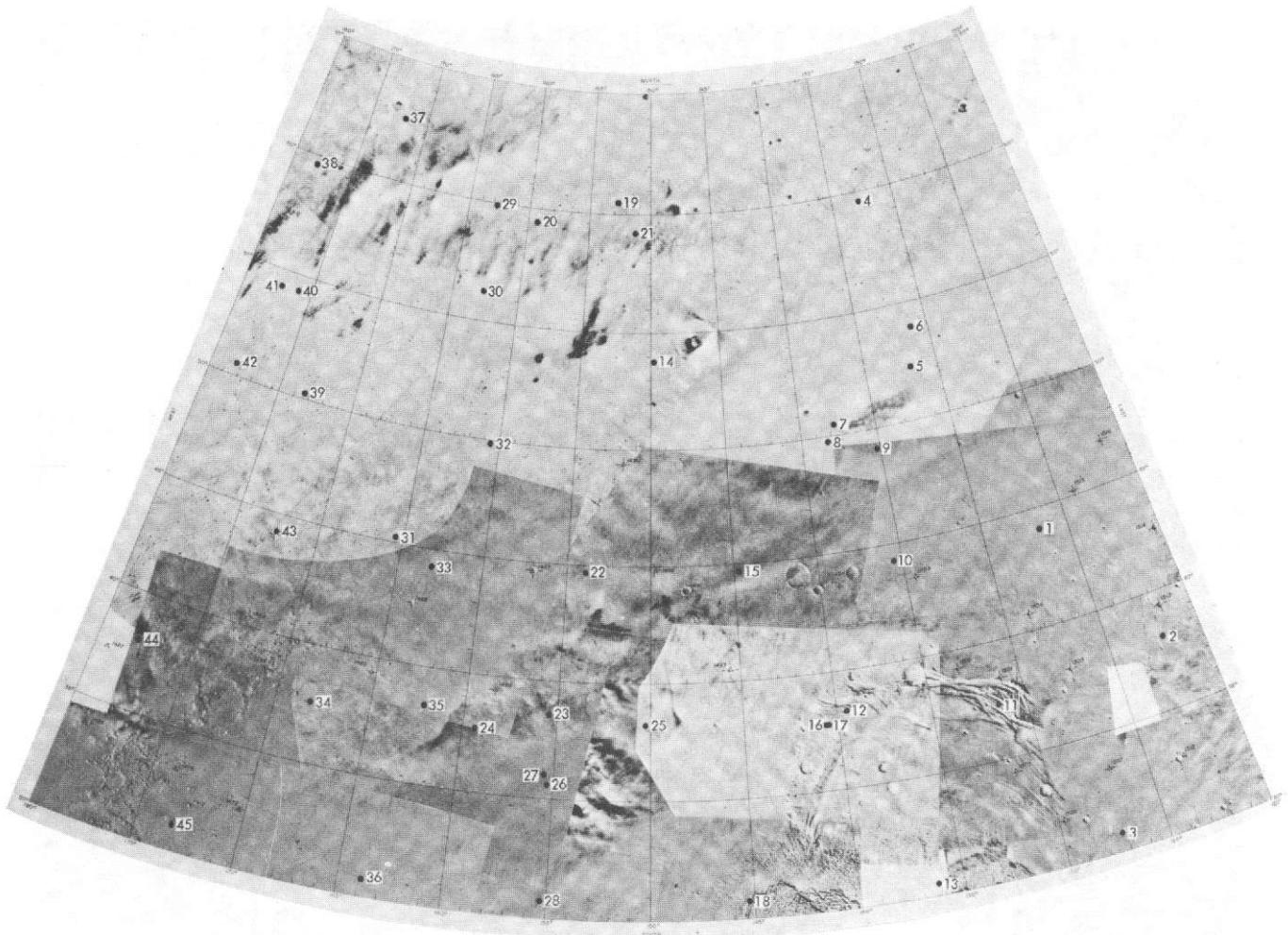


Fig. VII-5. Quadrangle layout for 1:5,000,000-scale map of Mars showing quadrangle names and identifying codes. A working set of numbers from 1 to 30 was used during the Mariner 9 mission, and is also shown in the quadrangle layout.



IDENTIFICATION NUMBERS OF PICTURES IN THE MOSAIC

Index No.	DAS No.	Index No.	DAS No.
1	8370649	13	8083713
2	8370989	14	12328127
3	8370939	15	12328407
4	8259099	16	8083933
5	11658395	17	8083073
6	11482109	18	8011183
7	8298819	19	8011141
8	8298819	20	9342376
9	8269999	21	9342099
10	8155033	22	9342239
11	11481619	23	12327981
12	8154693	24	12152682

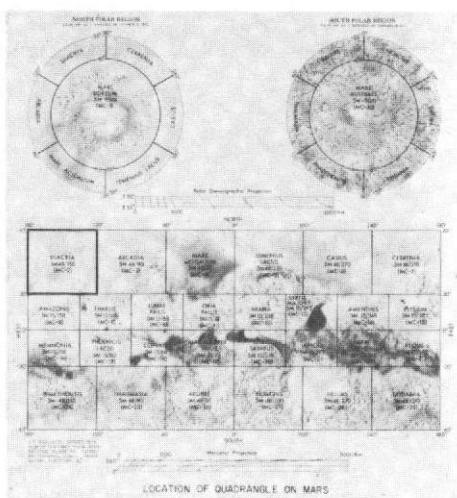


Fig. VII-6a. The Diacria quadrangle (MC-2). Photomosaic of wide-angle mapping frames in Lambert Projection serving as index map for locations of narrow-angle frames. Index numbers on the photomosaic correspond to those for the accompanying narrow-angle frames and the data listings of Table VII-3a, and not to the charts and tables directly below the photomosaic.

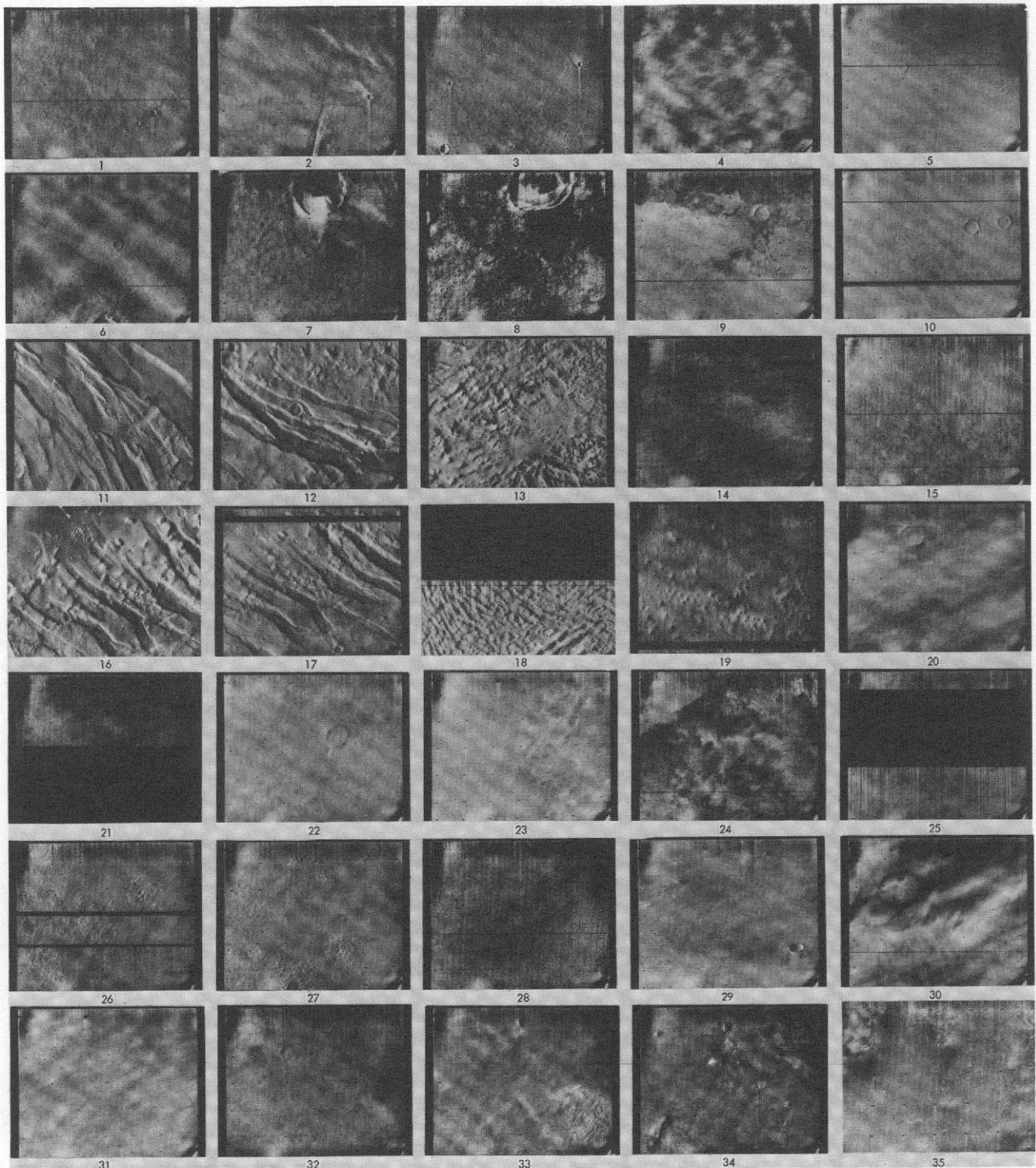


Fig. VII-6a. (contd). Narrow-angle frames (VAGC versions) that lie in the Diacria quadrangle: Revs 100–676; viewing angles less than 80°. Index numbers correspond to those on the photomosaic of this quadrangle and to Table VII-3a.

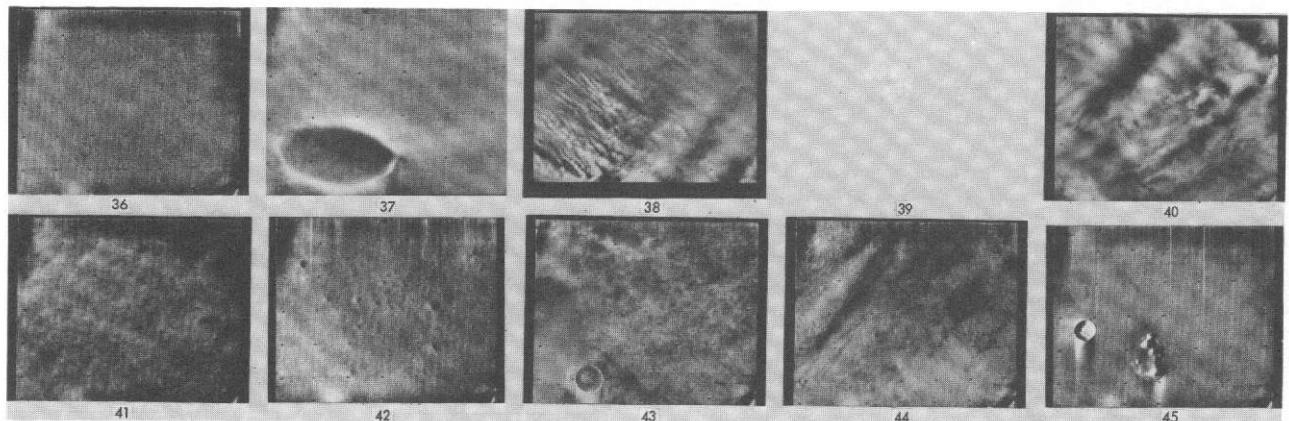
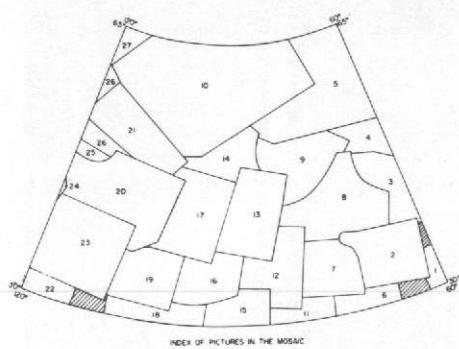
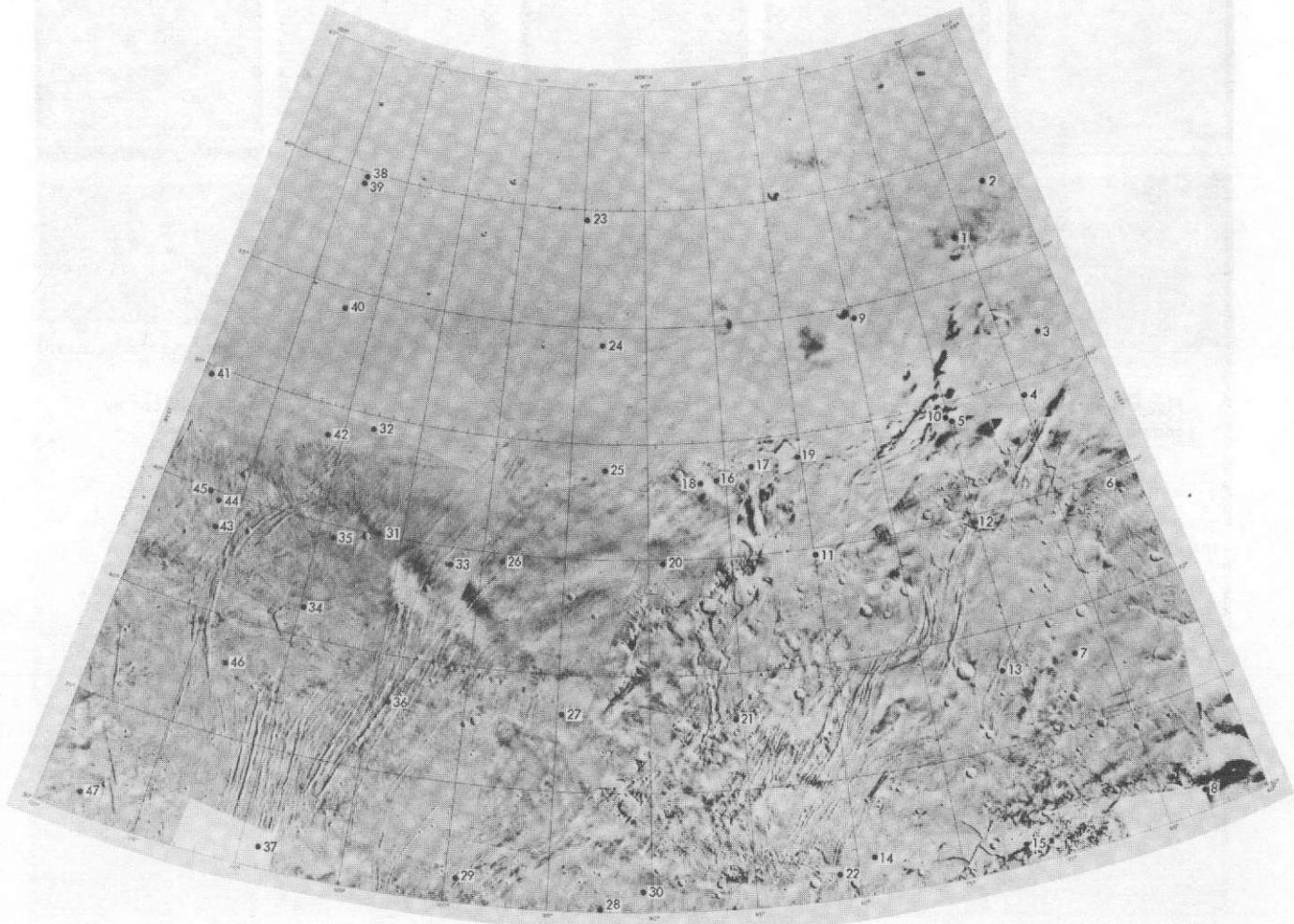


Fig. VII-6a. Narrow-angle frames in the Diacria quadrangle (contd). Index No. 39 is a wide-angle frame introduced by computer error.



IDENTIFICATION NUMBERS OF PICTURES IN THE MOSAIC

Index No.	DAS No.	Index No.	DAS No.
1	8074779	15	8566969
2	8710969	16	8514979
3	8731139	17	8443159
4	1183576	18	8514039
5	1323319	19	8520139
6	8730559	20	8371129
7	8658969	21	11658195
8	8659109	22	8370549
9	1153709	23	8370989
10	1165888	24	8227139
11	8658829	25	8299999
12	8658929	26	11481159
13	9315119	27	11492709
14	11658535		

INDEX OF PICTURES IN THE MOSAIC

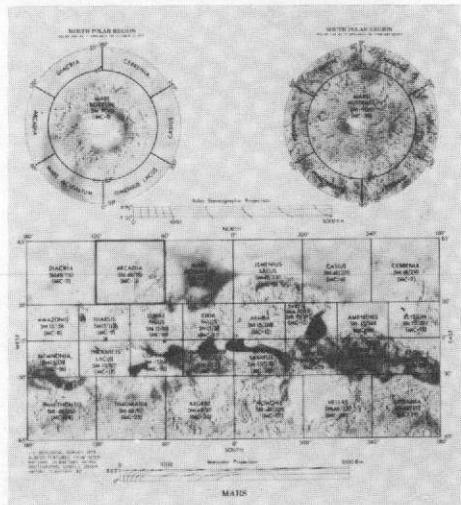


Fig. VII-6b. The Arcadia quadrangle (MC-3). Photomosaic of wide-angle mapping frames in Lambert Projection serving as index map for locations of narrow-angle frames. Index numbers on the photomosaic correspond to those for the accompanying narrow-angle frames and the data listings of Table VII-3b, and not to the charts and tables directly below the photomosaic.

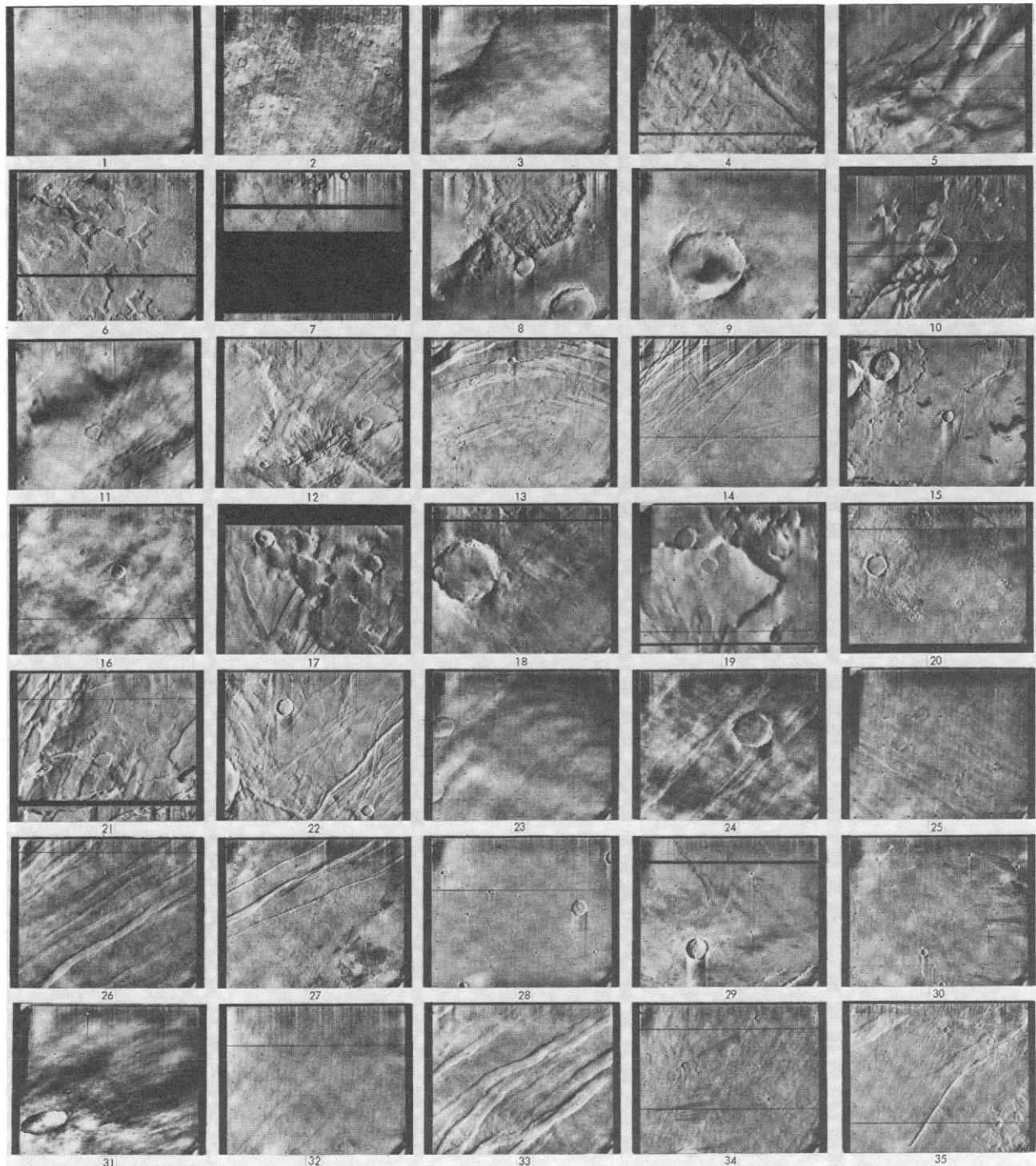


Fig. VII-6b. (contd). Narrow-angle frames (VAGC versions) that lie in the Arcadia quadrangle: Revs 100–676; viewing angles less than 80° . Index numbers correspond to those on the photomosaic of this quadrangle and to Table VII-3b.

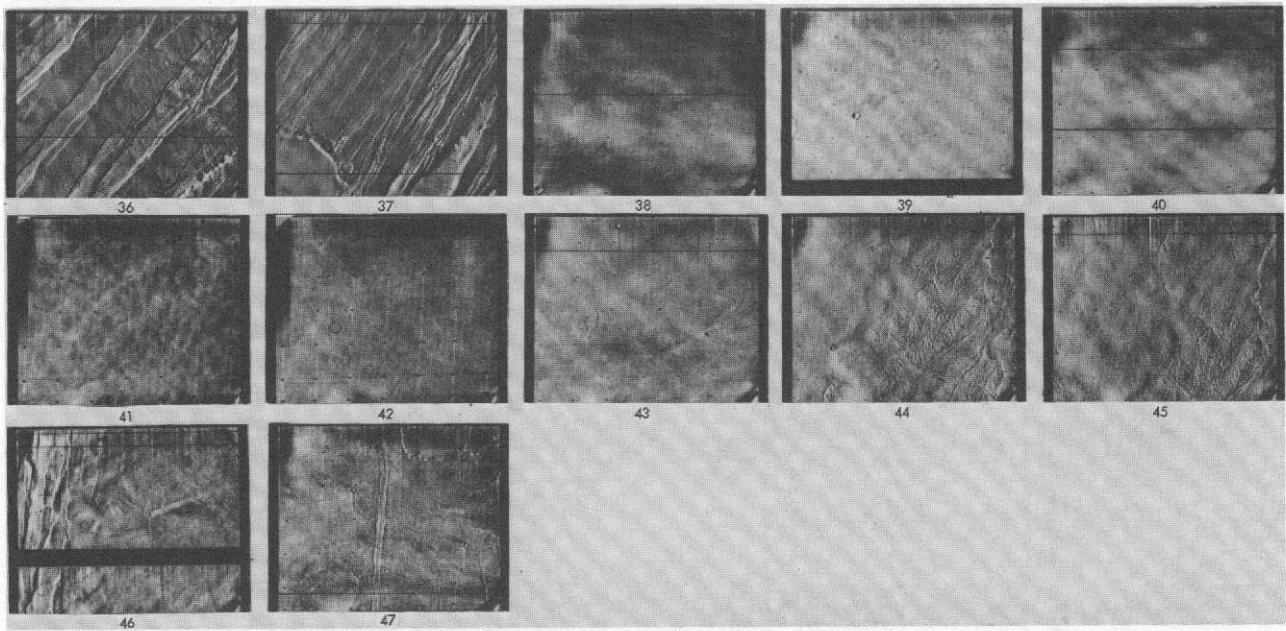
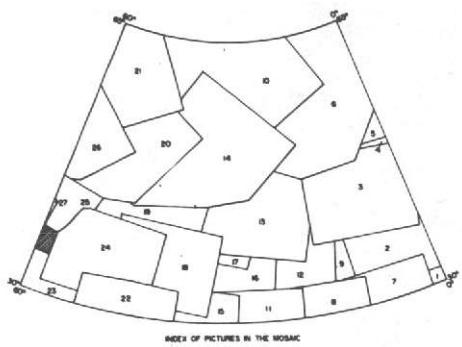


Fig. VII-6b. Narrow-angle frames in the Arcadia quadrangle (contd).



IDENTIFICATION NUMBERS OF PICTURES IN THE MOSAIC

Index No.	DAS No.	Index No.	DAS No.
1	9206119	15	9010559
2	9234369	16	9010699
3	9162619	17	12188372
4	9234529	18	8946209
5	9218231	19	8946259
6	12186792	20	12012564
7	9234229	21	11835986
8	9162519	22	8946249
9	9162679	23	89474779
10	12012984	24	8974919
11	9090449	25	8731139
12	9090489	26	11835706
13	8946949	27	8902953
14	12012704		

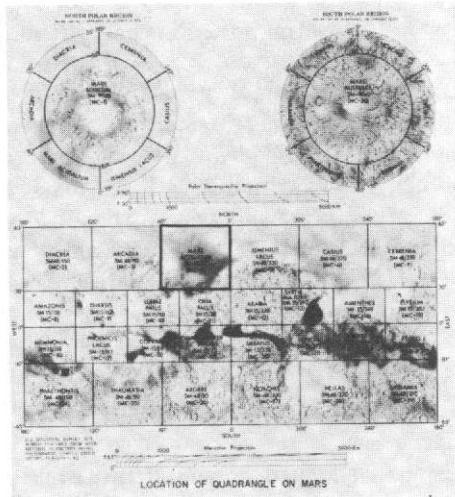


Fig. VII-6c. The Mare Acidalium quadrangle (MC-4). Photomosaic of wide-angle mapping frames in Lambert Projection serving as index map for locations of narrow-angle frames. Index numbers on the photomosaic correspond to those for the accompanying narrow-angle frames and the data listings of Table VII-3c, and not to the charts and tables directly below the photomosaic.

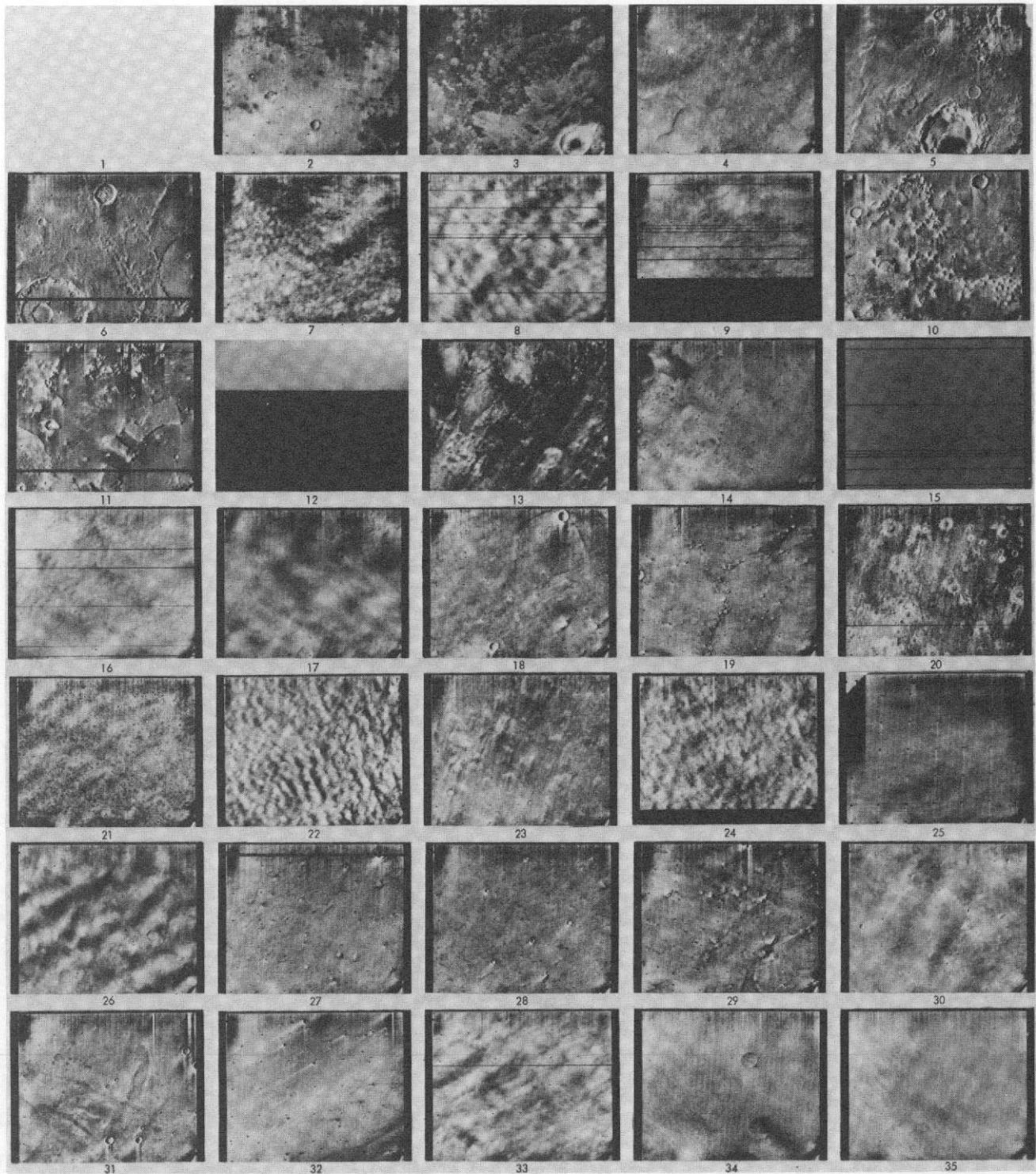


Fig. VII-6c. (contd). Narrow-angle frames (VAGC versions) that lie in the Mare Acidalium quadrangle: Revs 100-676; viewing angles less than 80° . Index numbers correspond to those on the photomosaic of this quadrangle and to Table VII-3c. Images with little detail may have been underexposed (see histograms in original data and Section IV). Blanks denote pictures planned but not recovered.

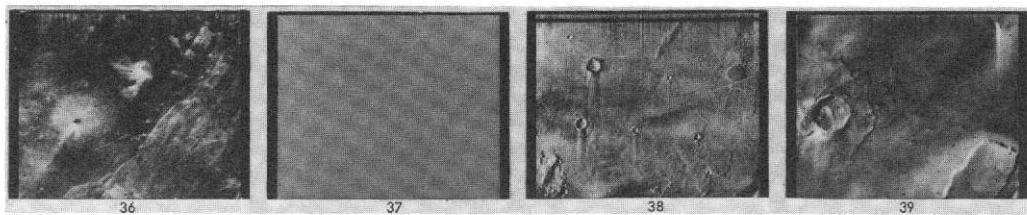
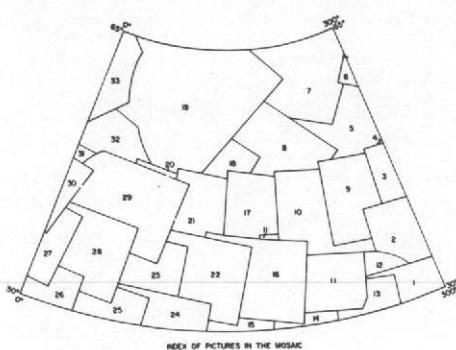


Fig. VII-6c. Narrow-angle frames in the Mare Acidalium quadrangle (contd.).



Index No.	DAS No.	Index No.	DAS No.
1	8334869	18	12364031
2	8335049	19	12364111
3	8335149	20	7975343
4	11622415	21	8047303
5	11446129	22	8047163
6	11622905	23	8047149
7	12521105	24	8047023
8	11445639	25	7975063
9	8263119	26	9306119
10	8191019	27	9306109
11	8191019	28	9306259
12	8262979	29	9306399
13	8262839	30	9162619
14	818913	31	9162699
15	8118913	32	1236381
16	8119053	33	12168792
17	8119193		

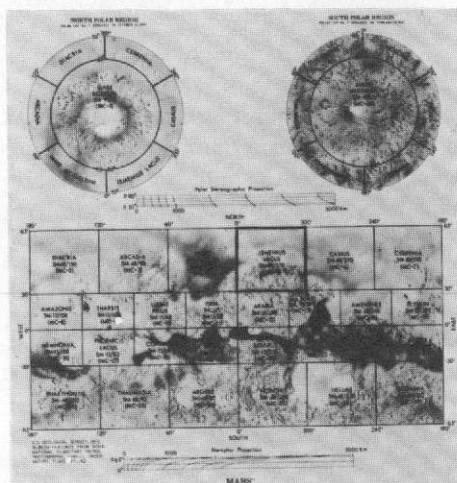


Fig. VII-6d. The Ismenius Lacus quadrangle (MC-5). Photomosaic of wide-angle mapping frames in Lambert Projection serving as index map for locations of narrow-angle frames. Index numbers correspond to those for the accompanying narrow-angle frames and the data listings of Table VII-3d, and not to the charts and tables directly below the photomosaic.

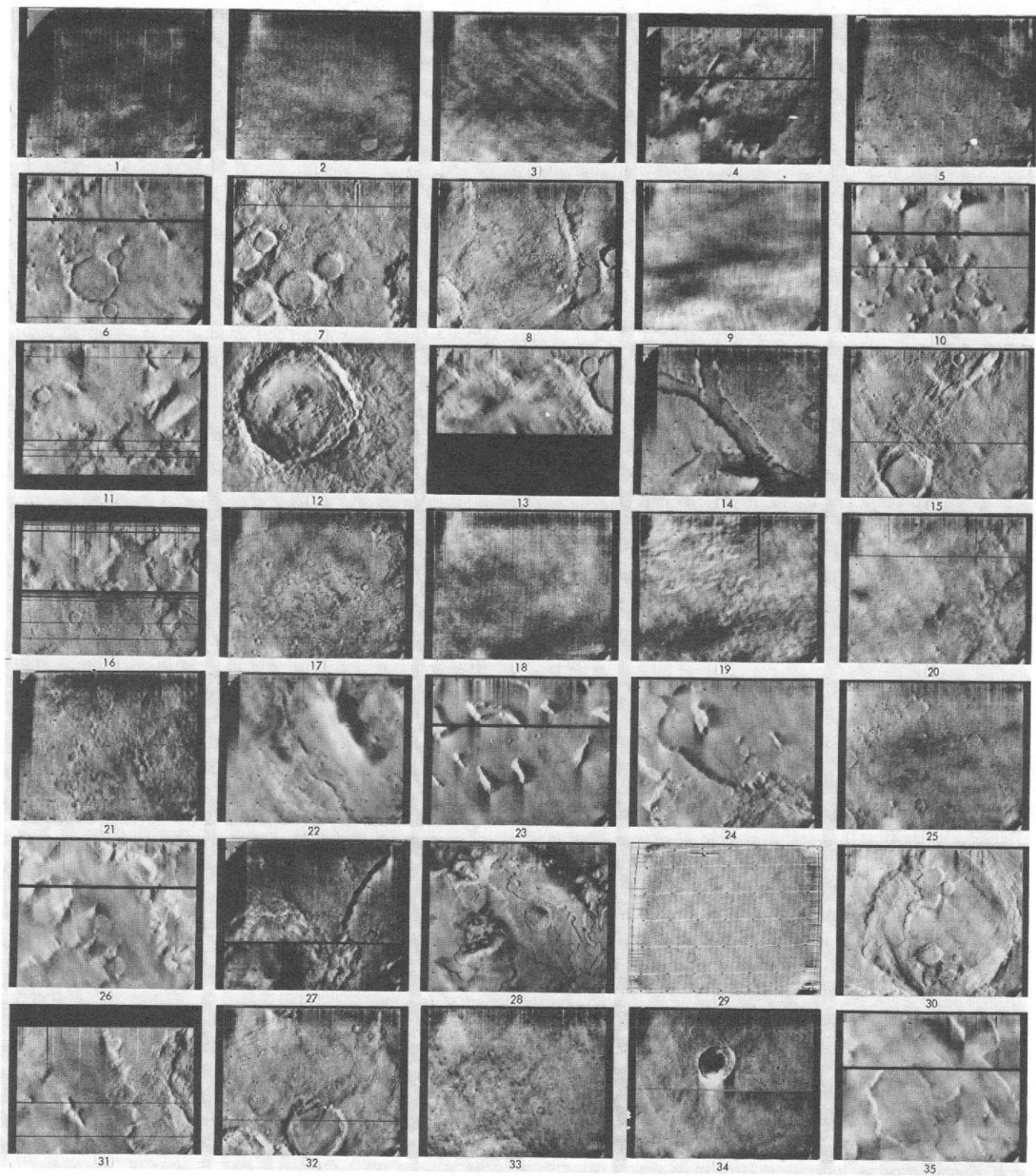


Fig. VII-6d. (contd). Narrow-angle frames (VAGC versions) that lie in the Ismenius Lacus quadrangle: Revs 100–676; viewing angles less than 80° . Index numbers correspond to those on the photomosaic of this quadrangle and to Table VII-3d.

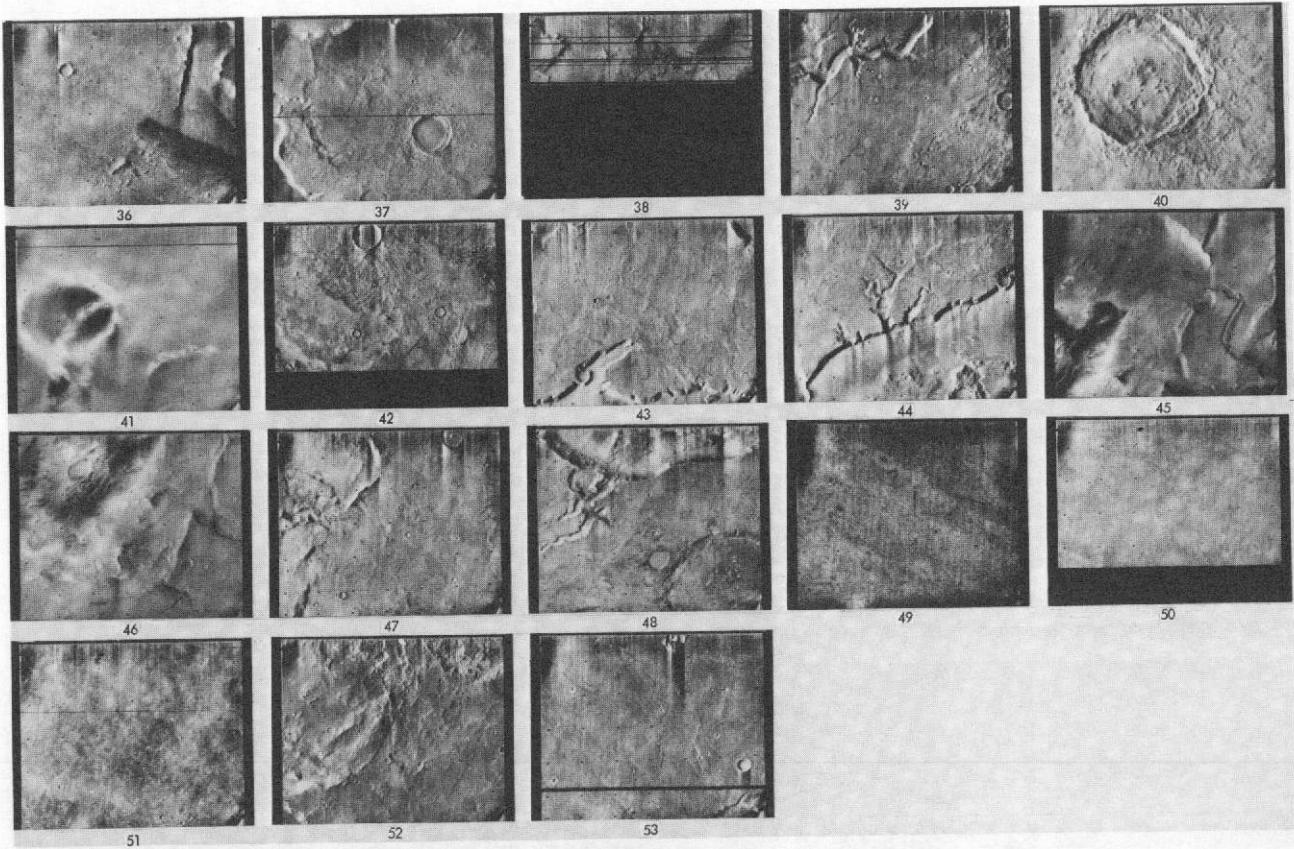
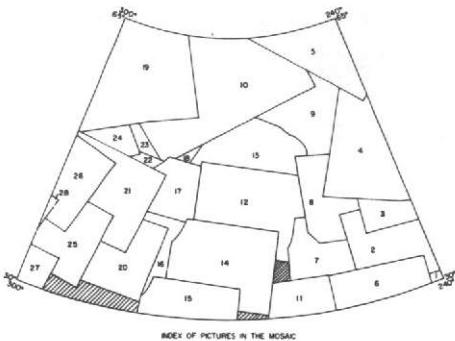
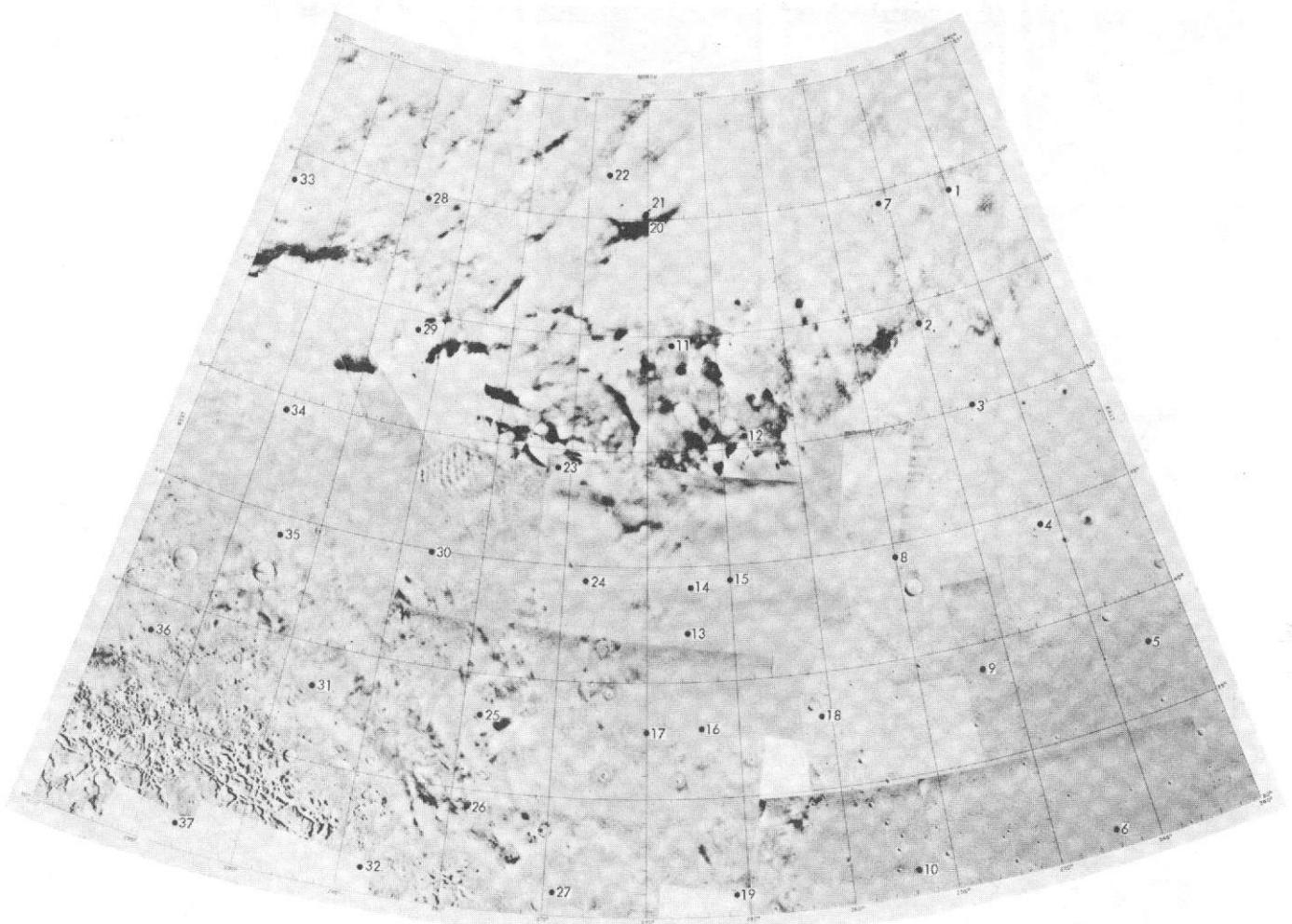


Fig. VII-6d. Narrow-angle frames in the Ismenius Lacus quadrangle (contd).



IDENTIFICATION NUMBERS OF PICTURES IN THE MOSAIC

Index No.	DAS No.	Index No.	DAS No.
1	8838799	15	8550889
2	8766979	16	8478999
3	8771119	17	8479139
4	11975568	18	11622552
5	11800146	19	11466129
6	8766839	20	8406959
7	869119	21	8315149
8	8696159	22	8407109
9	11800006	23	11622415
10	11622905	24	11465779
11	8691179	25	8335099
12	8511169	26	8263119
13	11799586	27	8334874
14	9551029	28	8262894

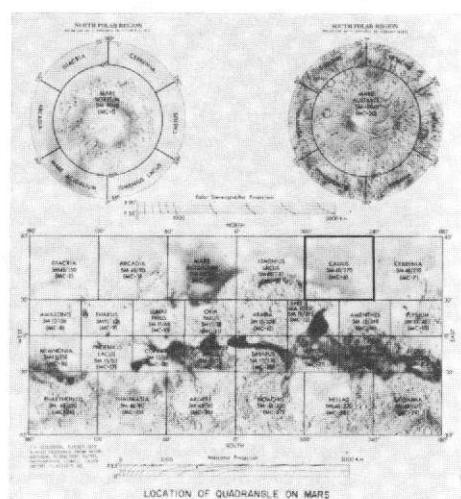


Fig. VII-6e. The Casius quadrangle (MC-6). Photomosaic of wide-angle mapping frames in Lambert Projection serving as index map for locations of narrow-angle frames. Index numbers on the photomosaic correspond to those for the accompanying narrow-angle frames and the data listings of Table VII-3e, and not to the charts and tables directly below the photomosaic.

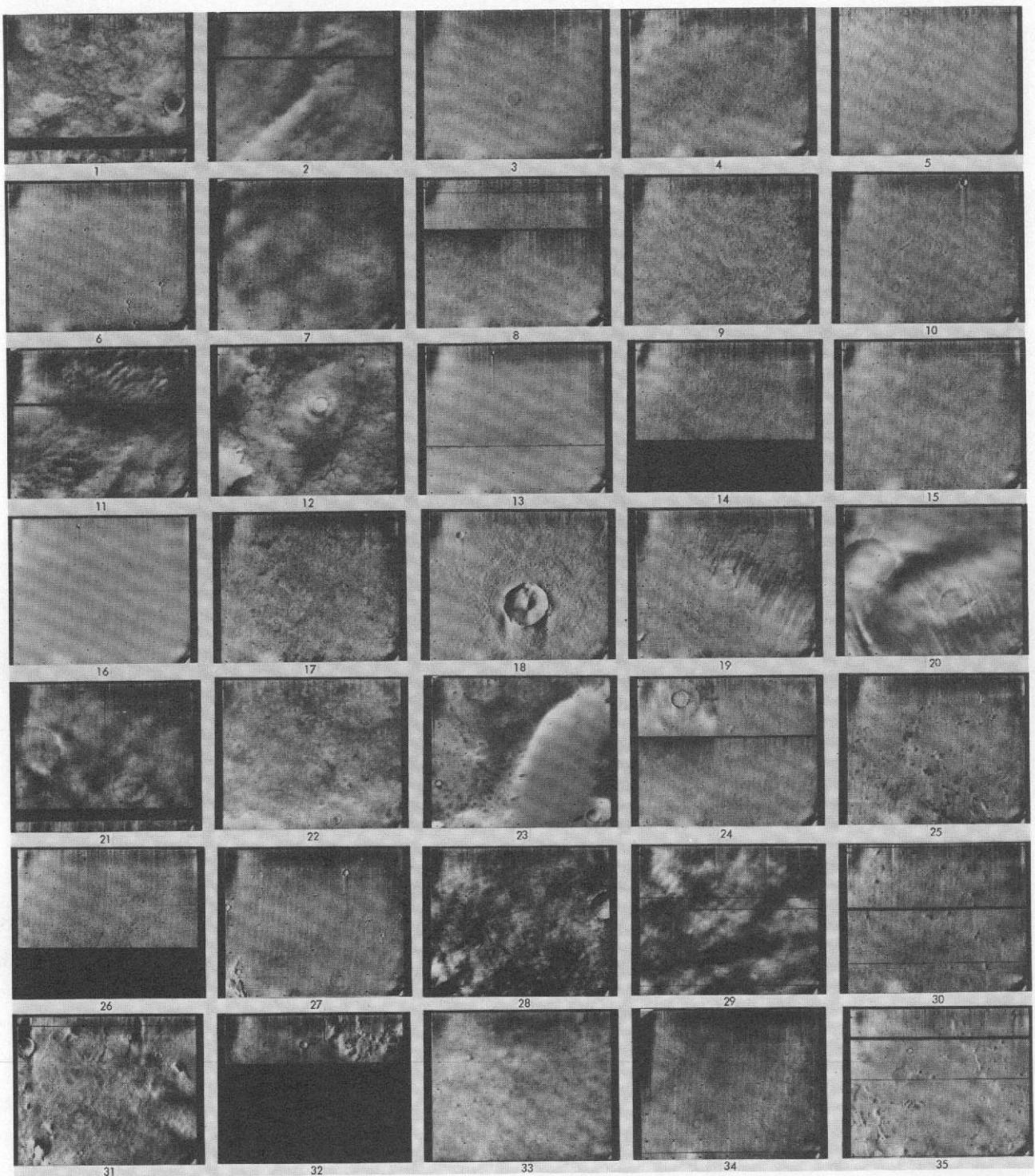
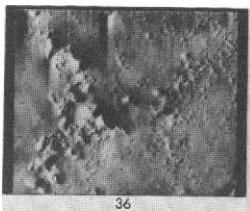
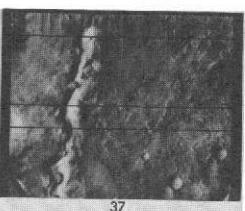


Fig. VII-6e. (contd). Narrow-angle frames (VAGC versions) that lie in the Casius quadrangle: Revs 100-676; viewing angles less than 80°. Index numbers correspond to those on the photomosaic of this quadrangle and to Table VII-3e.

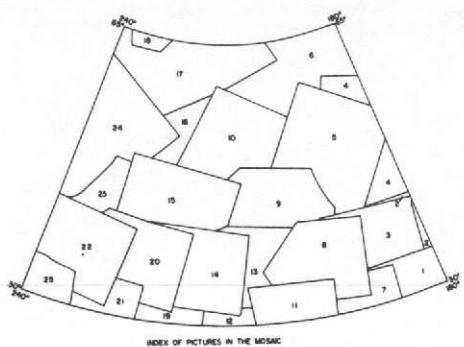
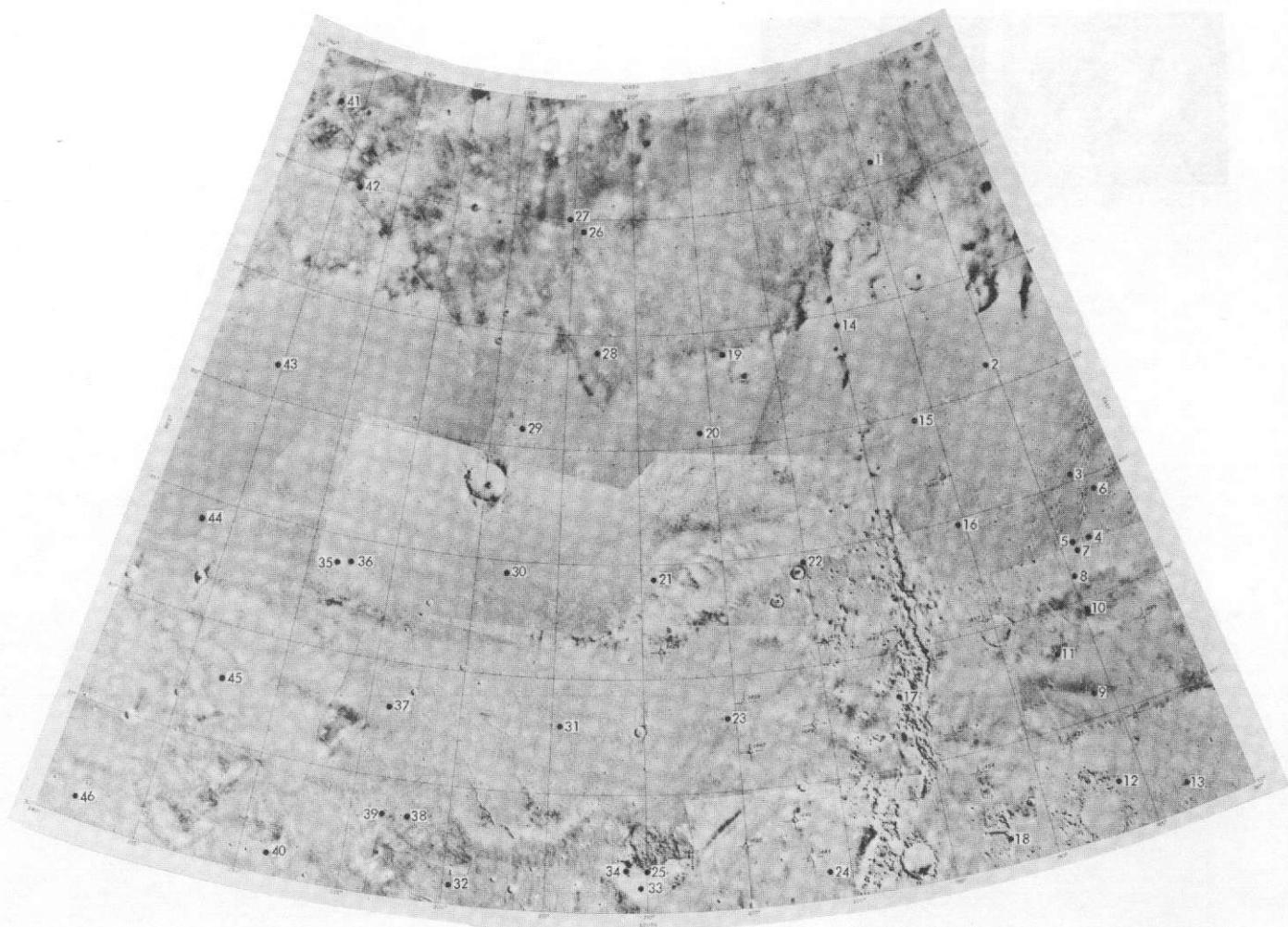


36



37

Fig. VII-6e. Narrow-angle frames in the Casius quadrangle (contd.).



IDENTIFICATION NUMBERS OF PICTURES IN THE MOSAIC

Index No.	DAS No.	Index No.	DAS No.
1	9270009	14	885788
2	9270349	15	8839079
3	9198459	16	11976724
4	12327981	17	11972004
5	12152602	18	1082544
6	12252322	19	882549
7	9198319	20	891069
8	9126569	21	8910829
9	8962929	22	8839739
10	12151662	23	8267119
11	9126429	24	11976584
12	9054539	25	8838799
13	9054679		

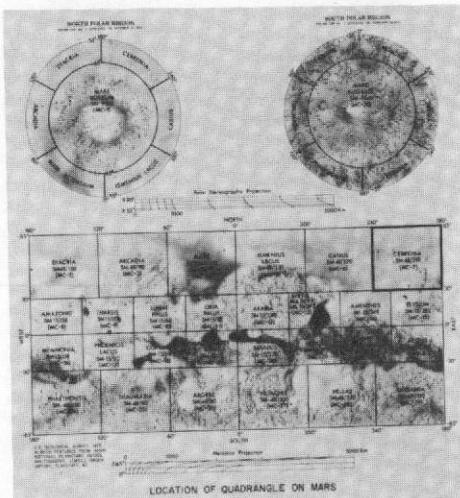


Fig. VII-6f. The Cebrenia quadrangle (MC-7). Photomosaic of wide-angle mapping frames in Lambert Projection serving as index map for locations of narrow-angle frames. Index numbers on the photomosaic correspond to those for the accompanying narrow-angle frames and the data listings of Table VII-3f, and not to the charts and tables directly below the photomosaic.

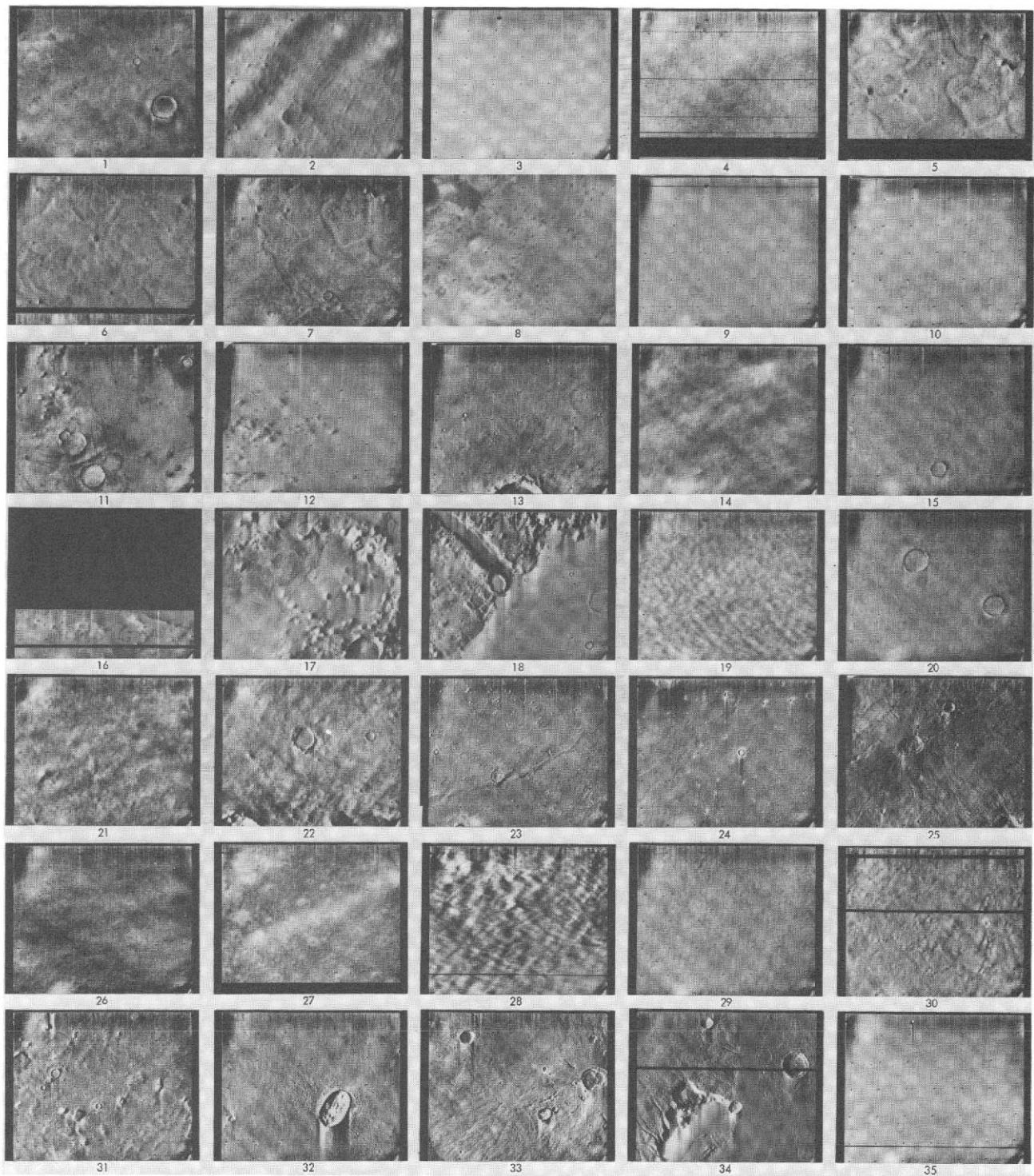


Fig. VII-6f. (contd). Narrow-angle frames (VAGC versions) that lie in the Cebrenia quadrangle: Revs 100–676; viewing angles less than 80° . Index numbers correspond to those on the photomosaic of this quadrangle and to Table VII-3f.

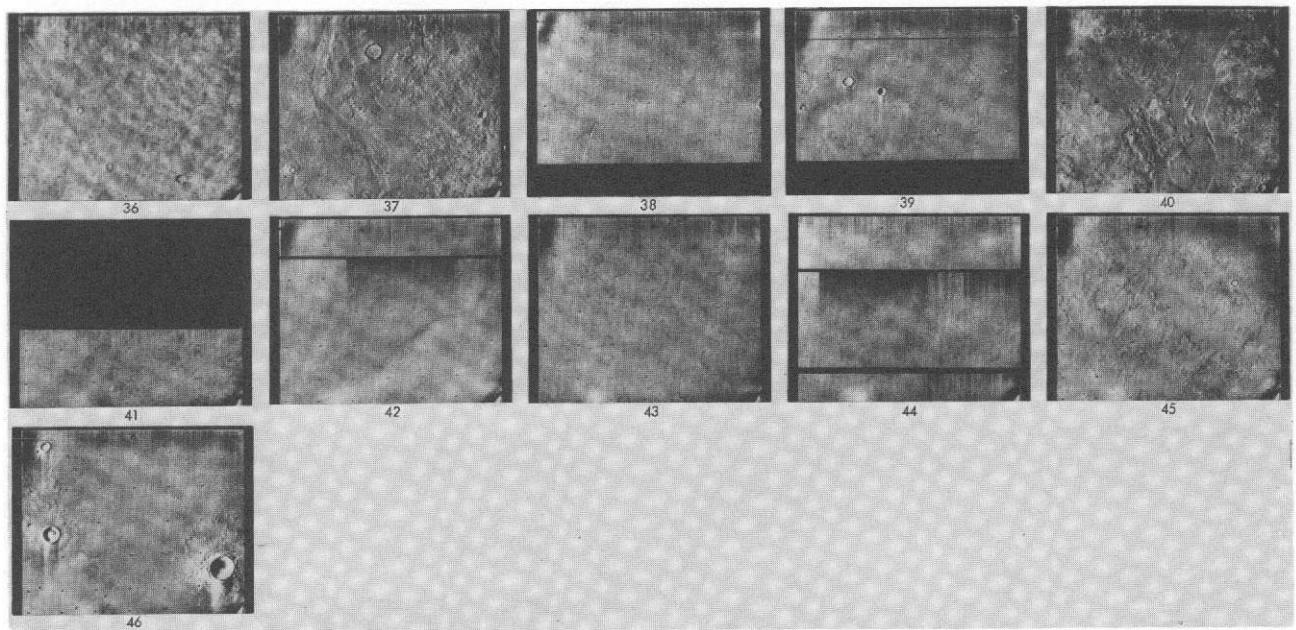
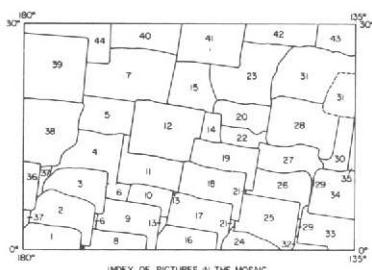
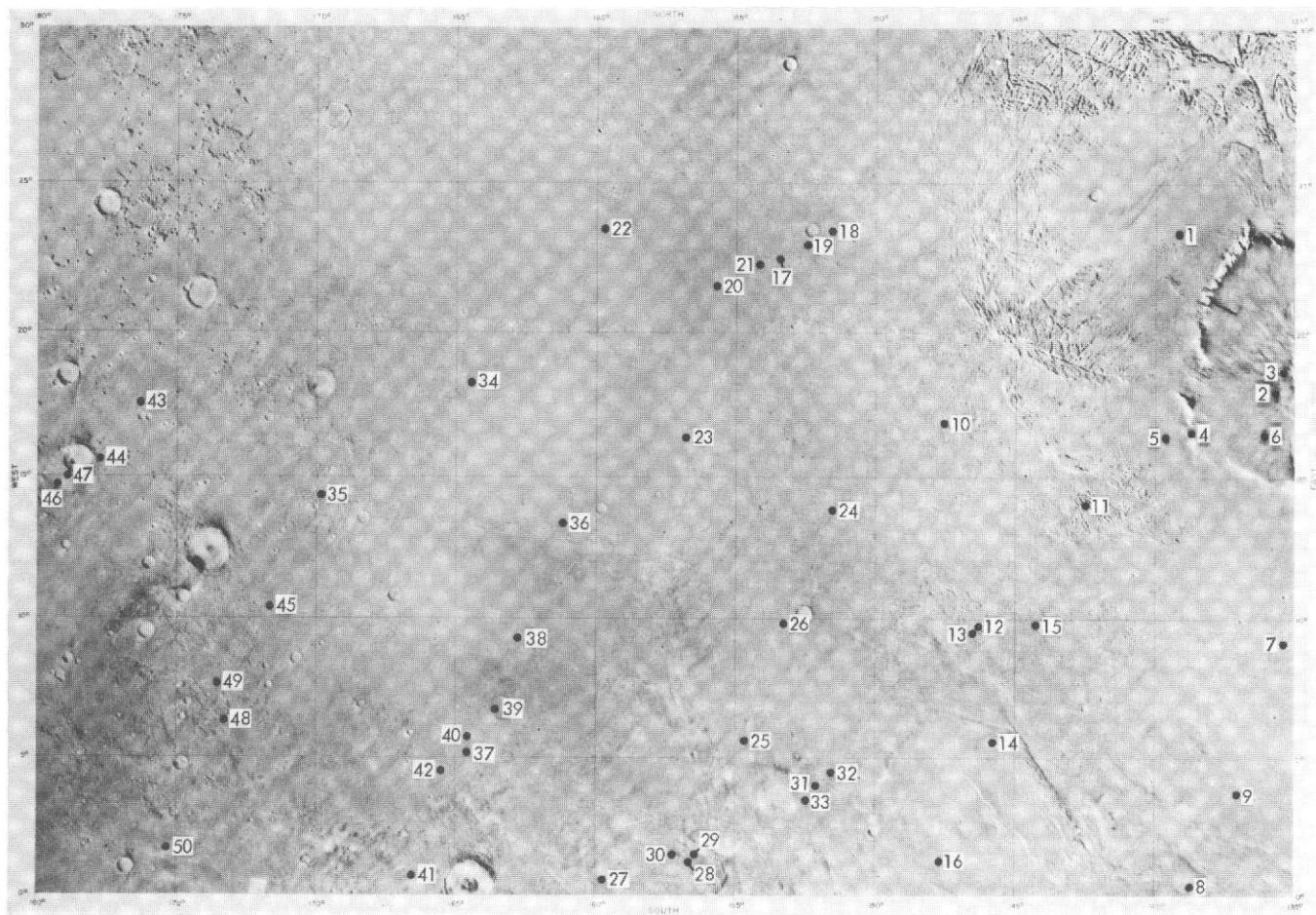


Fig. VII-6f. Narrow-angle frames in the Cebrenia quadrangle (contd).



INDEX No.		DAS No.		INDEX No.		DAS No.	
1	0660713R	23	0675181R	2	0660714R	24	0682310R
3	0660747R	25	0682321R	4	0660754R	26	0682328R
5	0660761R	27	0682335R	6	0660769R	28	0682339R
7	0660798R	29	0682343R	8	0667923R	30	0682370R
9	0667933R	31	0682374R	10	0667936R	32	0682376R
11	0667943R	33	0684917R	12	0667950R	34	0685924R
13	0667953R	35	0685925R	14	0667970R	36	0723052R
15	0667965R	37	0723057R	16	0675119R	38	0723075R
17	0675120R	39	0723076R	18	0675132R	40	0801114R
19	0675139R	41	0807253R	20	0675143R	42	0812154R
21	0675167R	43	0822164R	22	0675174R	44	0934210R

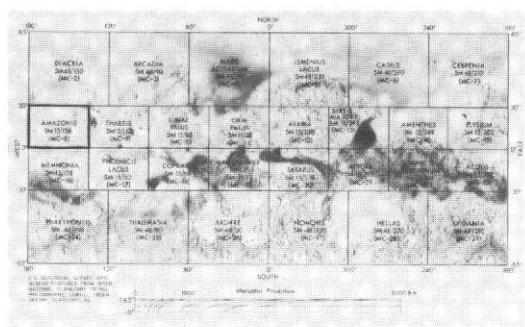


Fig. VII-6g. The Amazonis quadrangle (MC-8). Photomosaic of wide-angle mapping pictures in Mercator Projection serving as index map for locations of narrow-angle frames. Index numbers on the photomosaic correspond to those for the accompanying narrow-angle frames and the data listings of Table VII-3g, and not to the charts and tables directly below the photomosaic.

REPRODUCIBILITY OF FIG.
ORIGINAL PAGE IS POOR

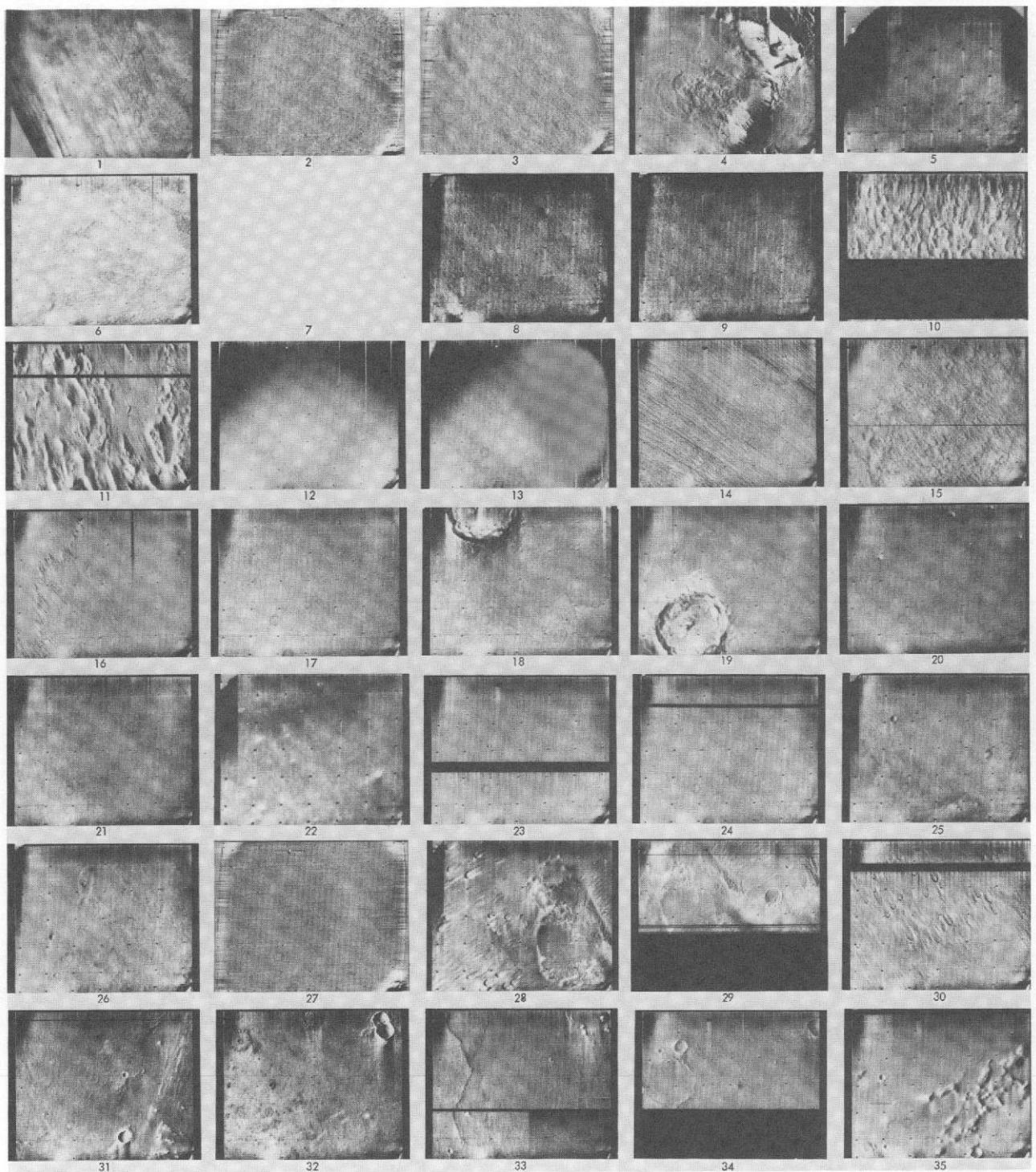


Fig. VII-6g. (contd). Narrow-angle frames (VAGC versions) that lie in the Amazonis quadrangle: Revs 100–676; viewing angles less than 80° . Index numbers correspond to those on the photomosaic of this quadrangle and to Table VII-3g. Blanks denote pictures planned but not recovered.

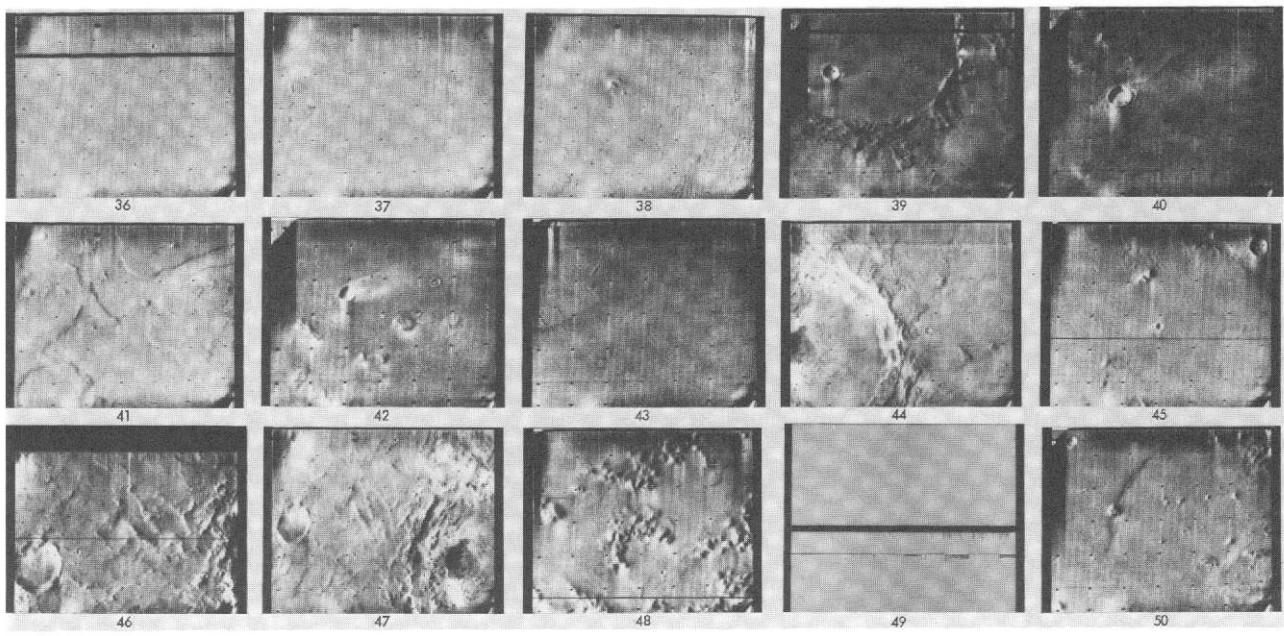
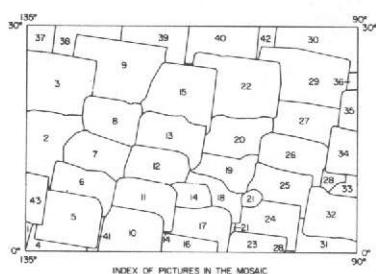
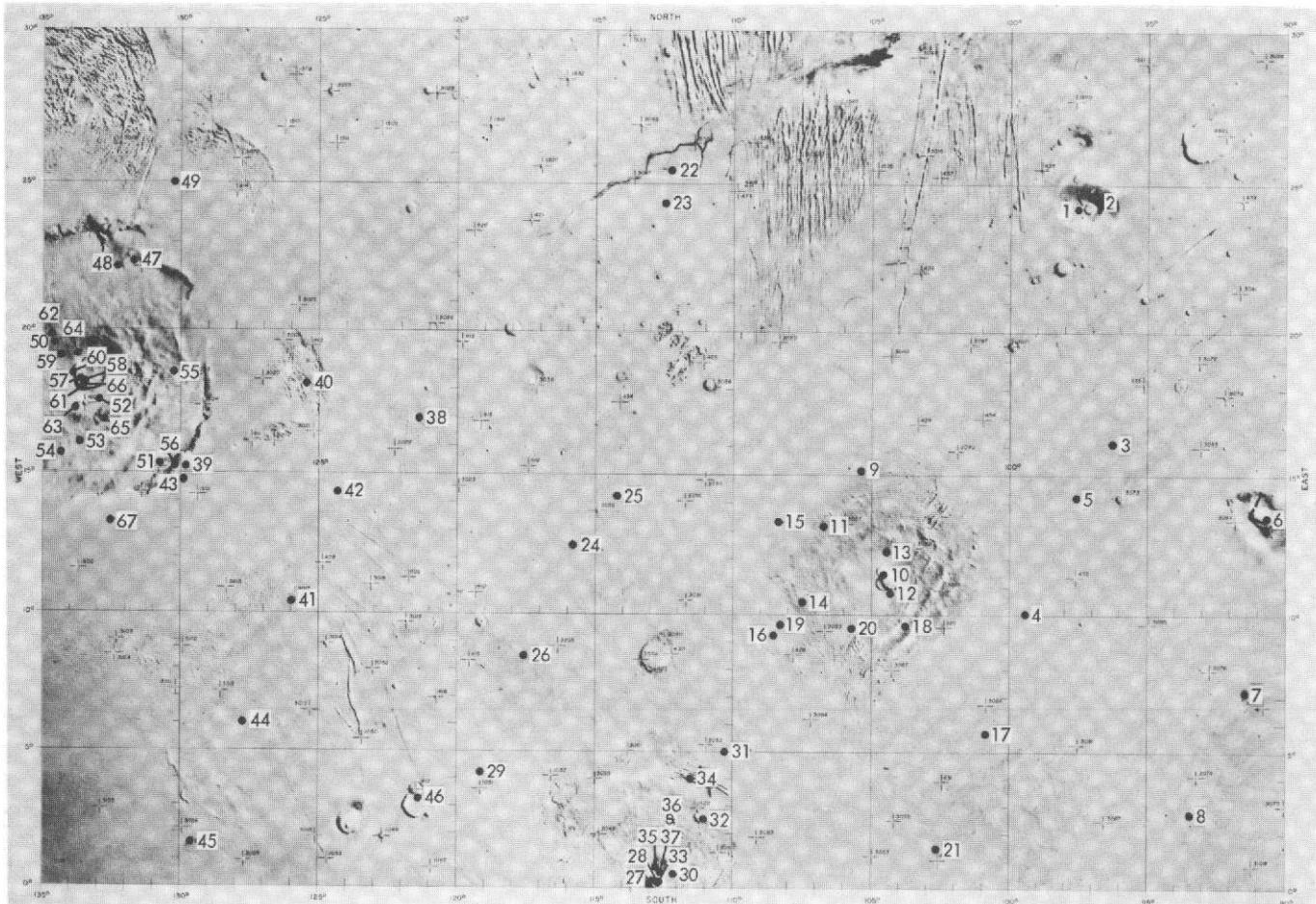


Fig. VII-6g. Narrow-angle frames in the Amazonis quadrangle (contd). Images with little detail may have been under-exposed (see histograms in original data and Section IV).



IDENTIFICATION NUMBERS OF PICTURES IN THE MOSAIC

Index No.	D&S No.	Index No.	D&S No.
1	06895738	23	07181586
	06895668	24	07181587
3	06895738	25	07182362
4	06896728	26	07183448
	06896720	27	07183449
6	068967278	28	07183548
7	068967348	29	07183706
	068967340	30	07183707
9	068967768	31	07251801
	07039168	32	07252002
11	07039170	33	07252003
	07039308	34	07253635
13	07039378	35	07255468
14	07039506	36	07260180
15	07039526	37	07260181
	07111178	38	08280202
17	07111198	39	08280754
	07111288	40	08280755
19	07111308	41	08280756
	07211106	42	08511846
21	07211168	43	08511847
	07211170	44	08511848

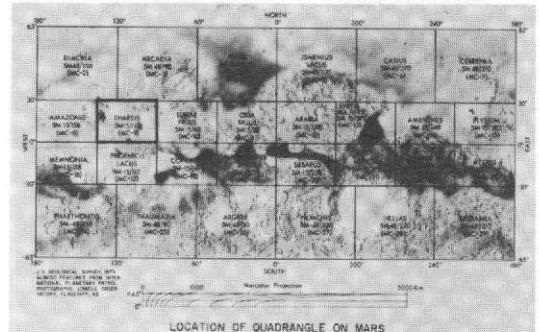


Fig. VII-6h. The Tharsis quadrangle (MC-9). Photomosaic of wide-angle mapping pictures in Mercator Projection serving as index map for locations of narrow-angle frames. Index numbers on the photomosaic correspond to those for the accompanying narrow-angle frames and the data listings of Table VII-3h, and not to the charts and tables directly below the photomosaic.

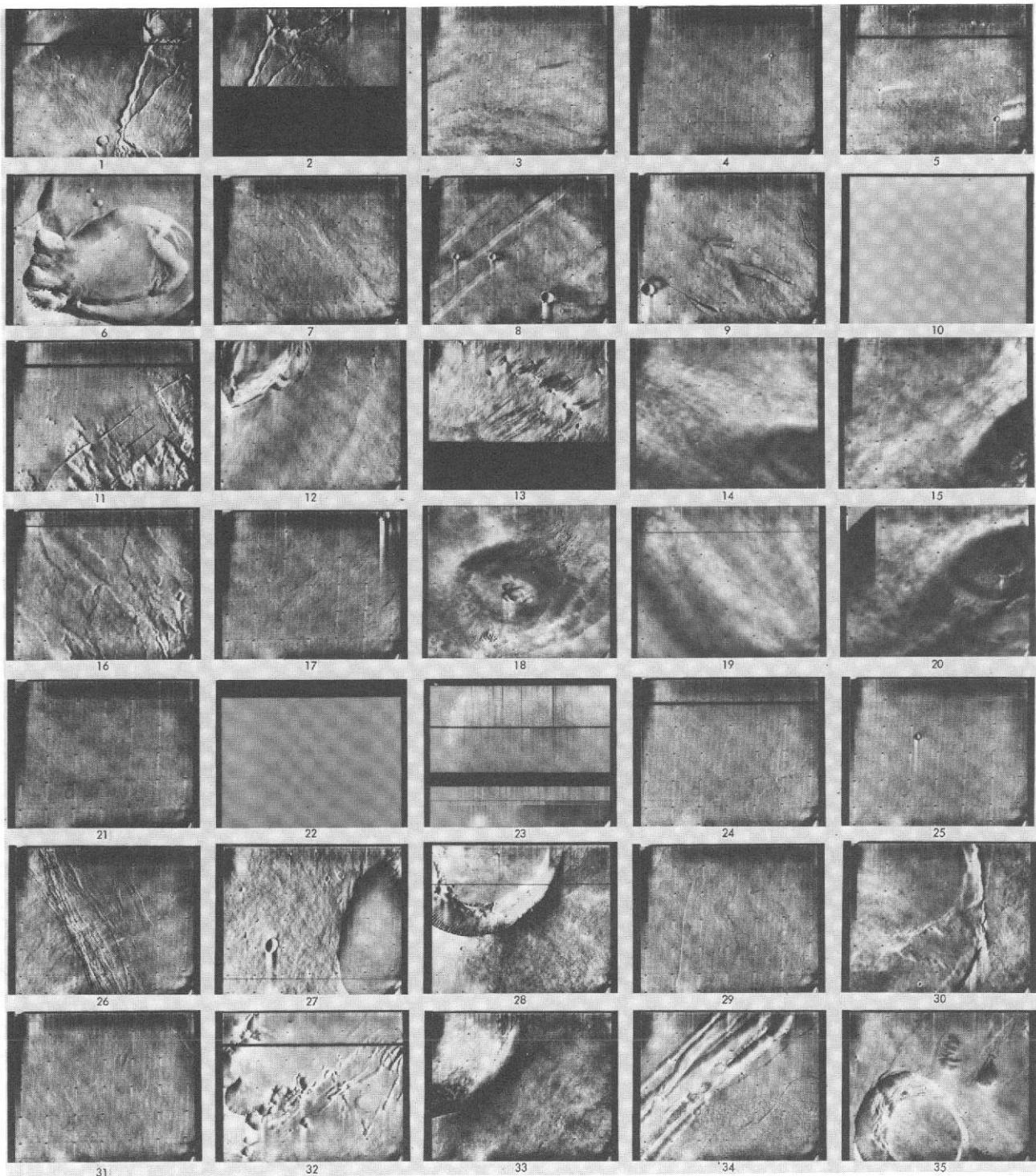


Fig. VII-6h. (contd). Narrow-angle frames (VAGC versions) that lie in the Tharsis quadrangle: Revs 100–676; viewing angles less than 80° . Index numbers correspond to those on the photomosaic of this quadrangle and to Table VII-3h. Images with little detail may have been underexposed (see histograms in original data and Section IV).

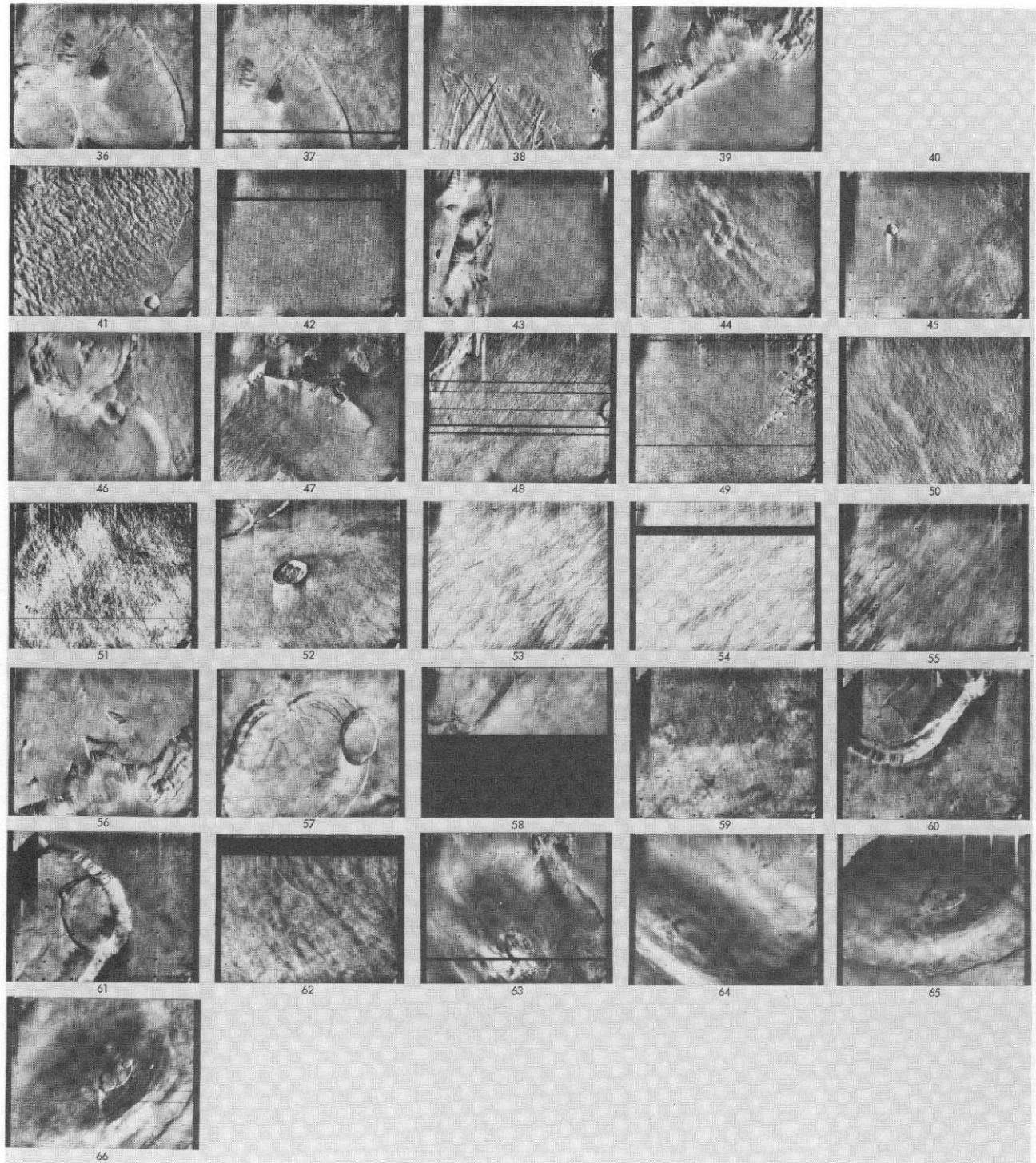
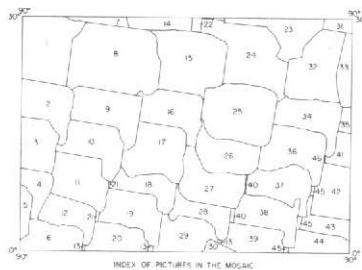
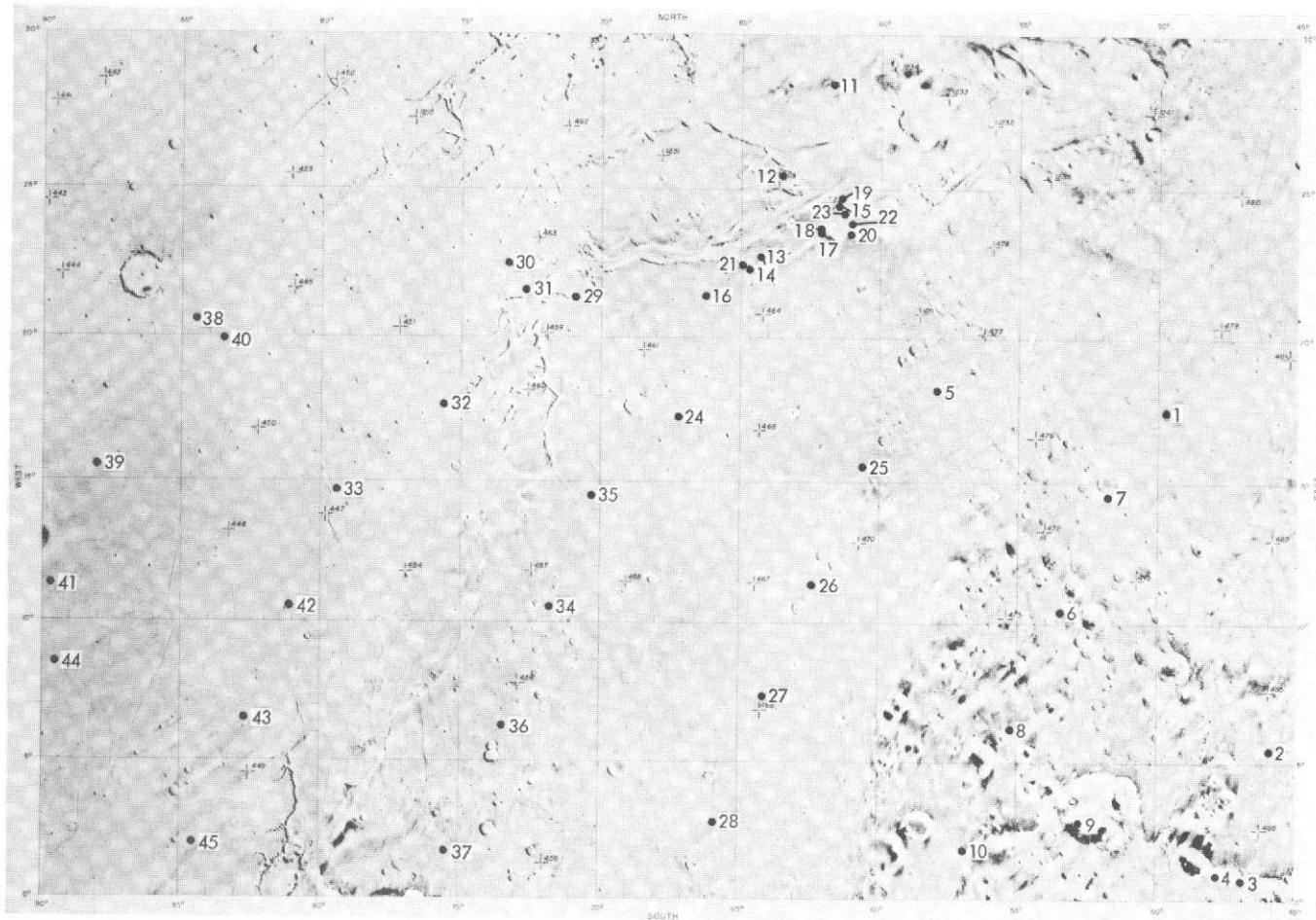


Fig. VII-6h. Narrow-angle frames in the Tharsis quadrangle (contd). Blanks denote pictures planned but not recovered.



IDENTIFICATION NUMBERS OF PICTURES IN THE MOSAIC

Index No.	DAS No.	Index No.	DAS No.
1	7255813	24	7471693
2	7255463	25	7471343
3	7255393	26	7471273
4	7255673	27	7471203
5	7255253	28	7471133
6	7327143	29	7471063
7	7255793	30	6137933
8	7327773	31	2098469
9	7327423	32	7543563
10	7327353	33	7615473
11	7327263	34	7615133
12	7327113	35	7615123
13	7380493	36	7543163
14	8730059	37	7543093
15	7399733	38	7543023
16	7399753	39	7543053
17	7399313	40	7471553
18	7399243	41	7615063
19	7399173	42	7614983
20	7327393	43	7614913
21	7327633	44	7614943
22	8802819	45	7543443
23	8874279	46	7613513

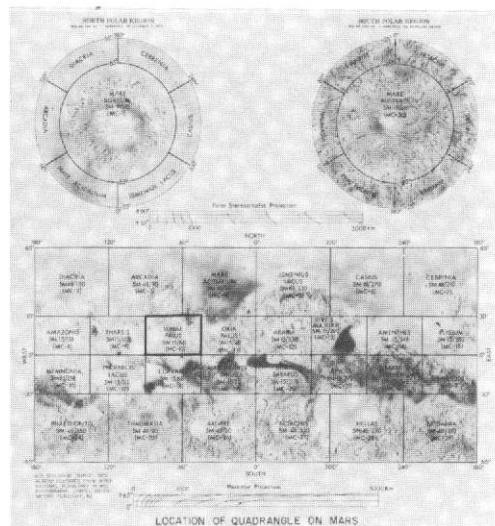


Fig. VII-6i. The Lunae Palus quadrangle (MC-10). Photomosaic of wide-angle mapping frames in Mercator Projection serving as index map for locations of narrow-angle frames. Index numbers on the photomosaic correspond to those for the accompanying narrow-angle frames and the data listings of Table VII-3i, and not to the charts and tables directly below the photomosaic.

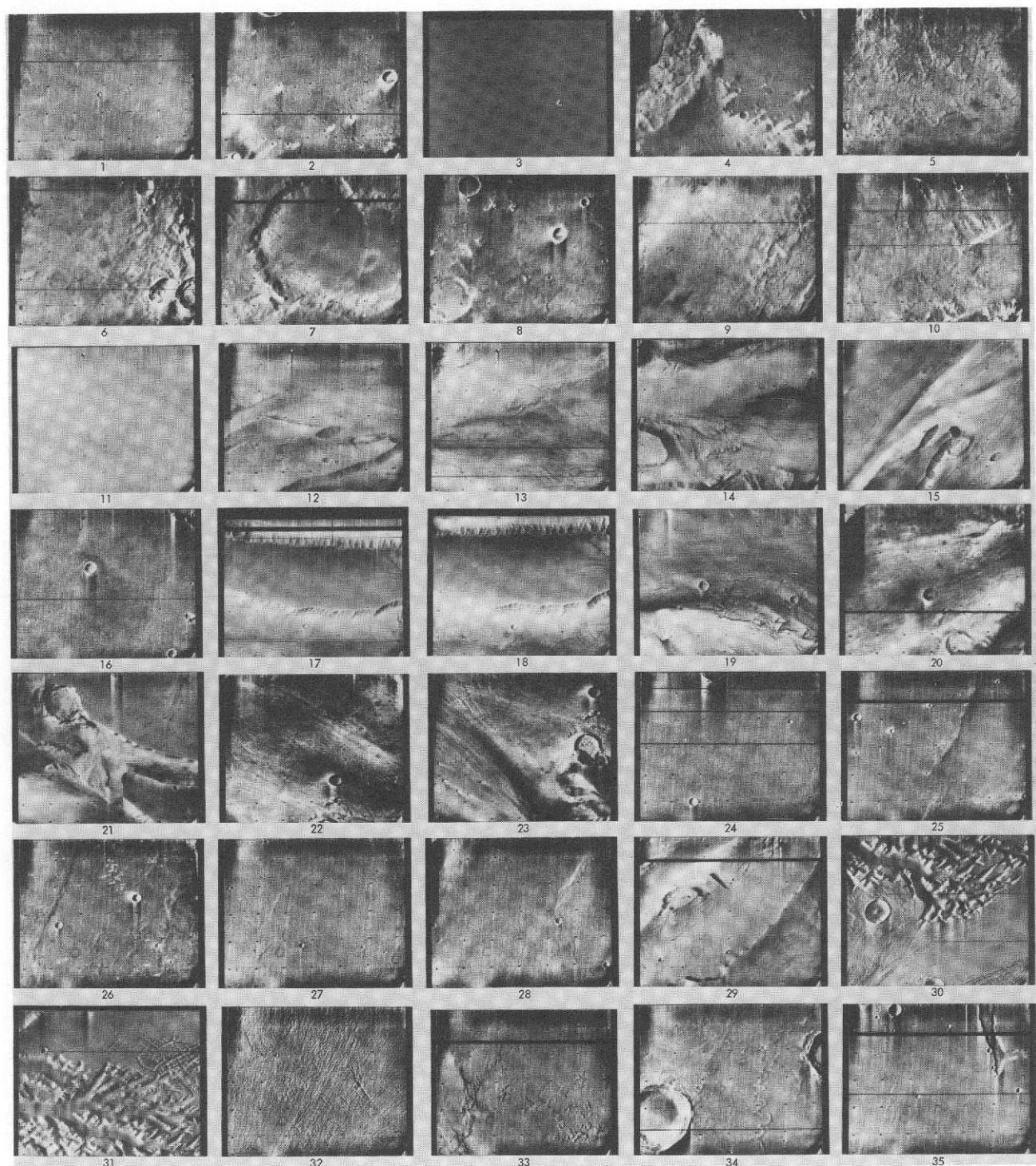


Fig. VII-6i. (contd). Narrow-angle frames (VAGC versions) that lie in the Lunae Palus quadrangle: Revs 100–676; viewing angles less than 80° . Index numbers correspond to those on the photomosaic of this quadrangle and to Table VII-3i. Images with little detail may have been underexposed (see histograms in original data and Section IV). Index No. 3 is a satellite frame introduced by computer error.

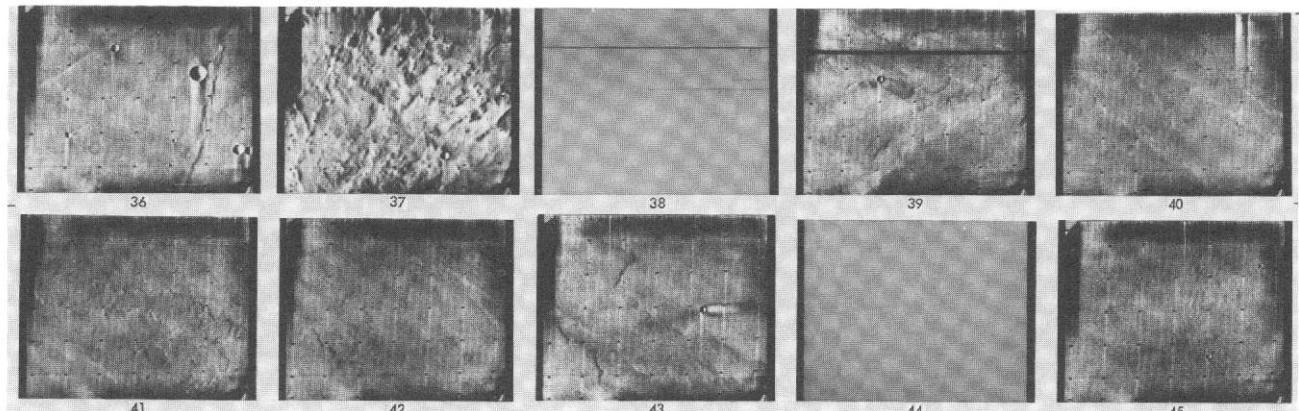
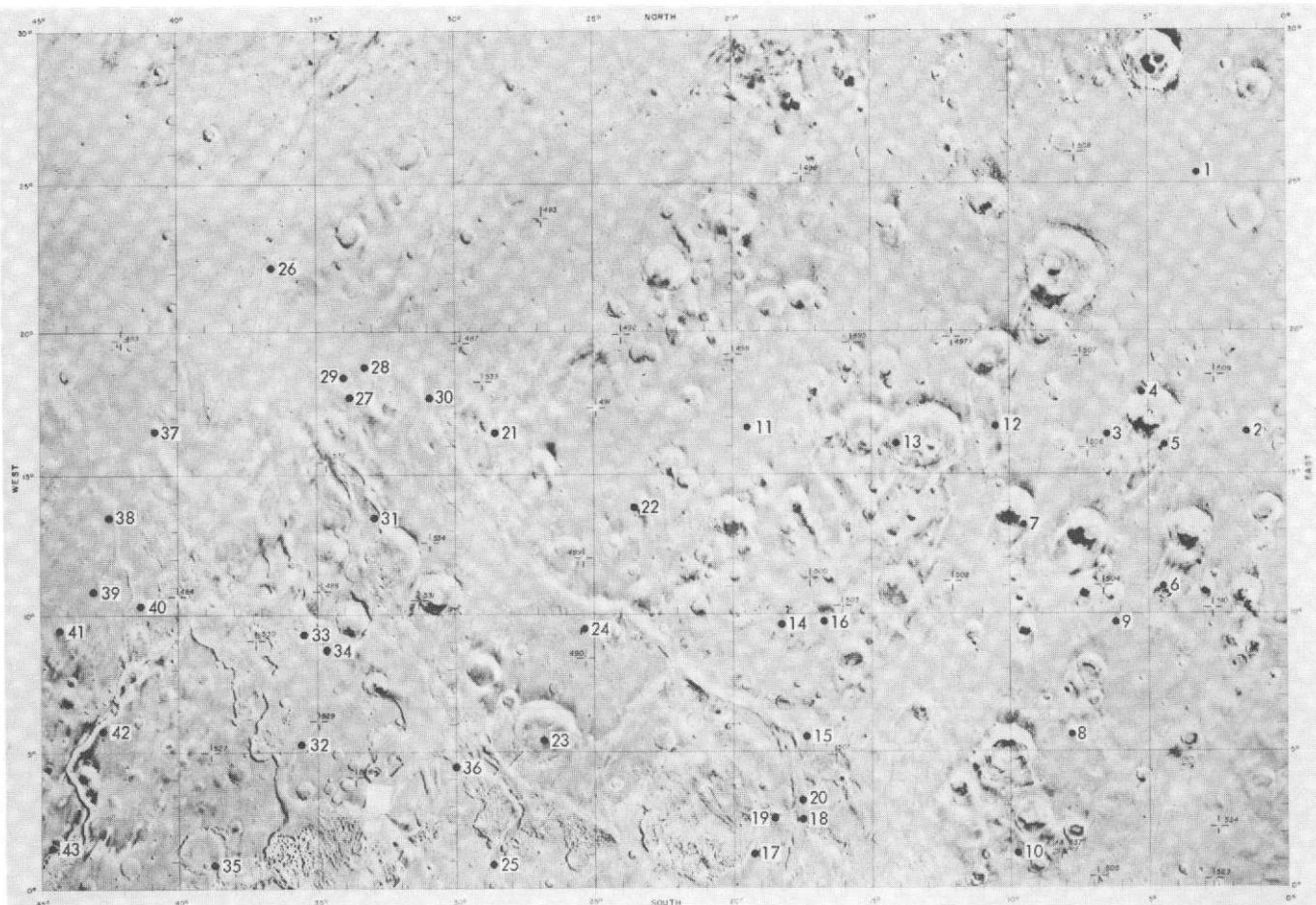


Fig. VII-6i. Narrow-angle frames in the Lunae Palus quadrangle (contd). Images with little detail may have been under-exposed (see histograms in original data and Section IV).



IDENTIFICATION NUMBERS OF PICTURES IN THE MOSAIC					
Index No.	DAS No.	Index No.	DAS No.	Index No.	DAS No.
1	8546699	18	9090449	35	9306119
2	7615473	19	9162359	36	7903035
3	7615125	20	7758252	37	7903036
4	7615124	21	7758253	38	7837013
5	7619083	22	7758833	39	7962613
6	7614913	23	7758763	40	7902543
7	8018585	24	6876227	41	7837012
8	10451609	25	7758254	42	7902542
9	7615474	26	7758263	43	7750983
10	7154013	27	9342929	44	7902403
11	7687013	28	7831145	45	6571565
12	7686943	29	7830795	46	7902893
13	7686942	30	7830796	47	7902893
14	7686553	31	7759113	48	6571443
15	7615333	52	7830563	49	6571353
16	7686753	53	7830563		

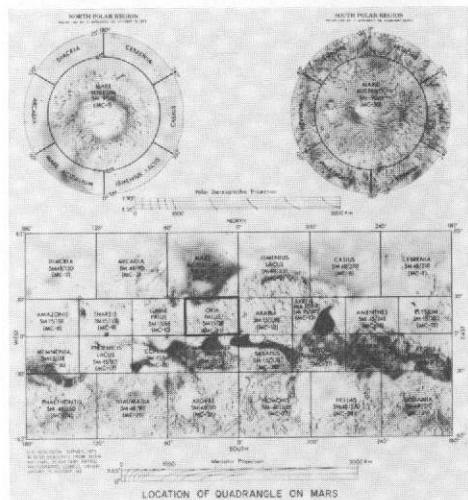


Fig. VII-6j. The Oxia Palus quadrangle (MC-11). Photomosaic of wide-angle mapping frames in Mercator Projection serving as index map for locations of narrow-angle frames. Index numbers on the photomosaic correspond to those for the accompanying narrow-angle frames and the data listings of Table VII-3j, and not to the charts and tables directly below the photomosaic.

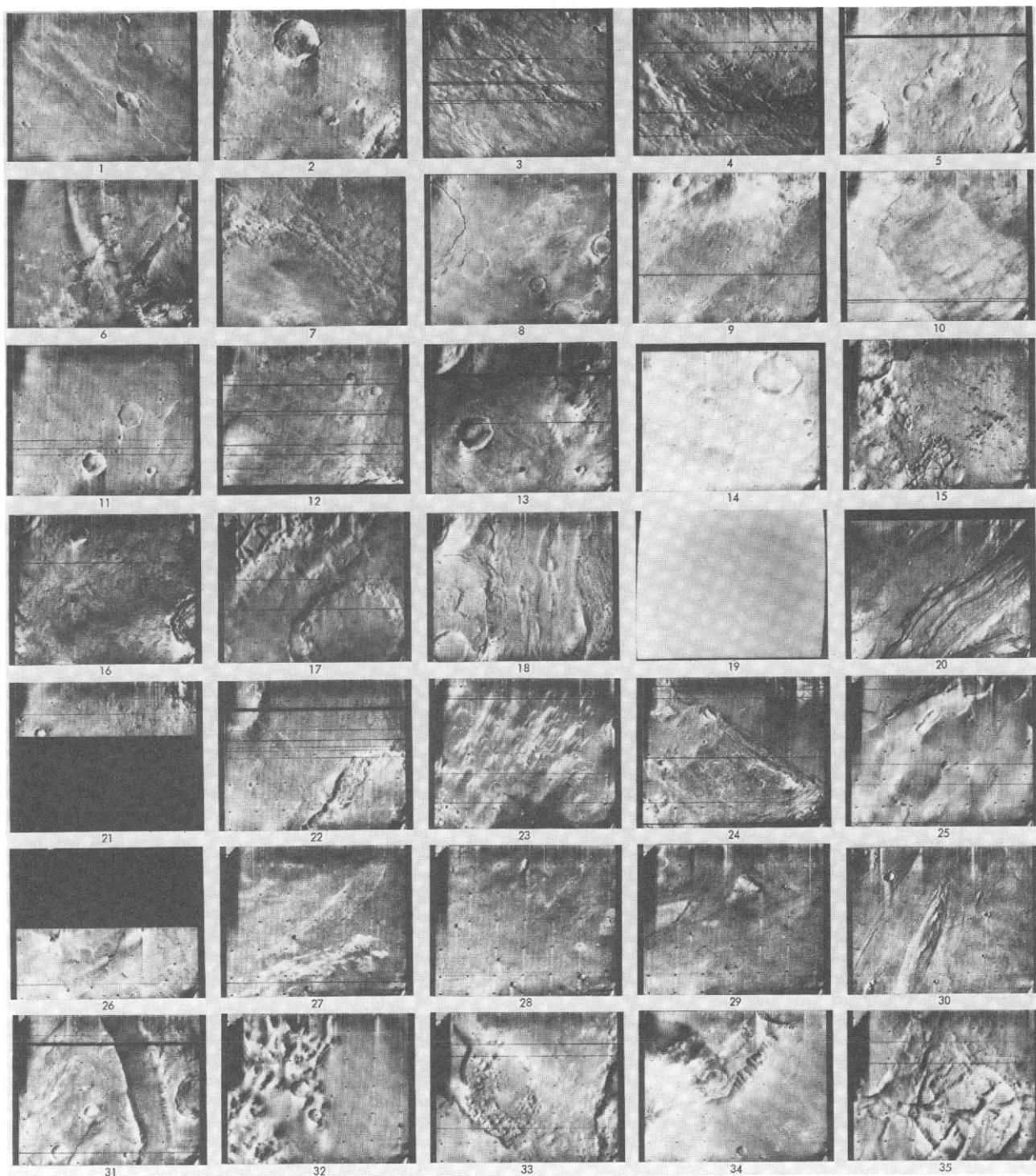


Fig. VII-6j. (contd). Narrow-angle frames (VAGC versions) that lie in the Oxia Palus quadrangle: Revs 100–676; viewing angles less than 80° . Index numbers correspond to those on the photomosaic of this quadrangle and the data listings of Table VII-3j, and not to the charts and tables directly below the photomosaic. Images with little detail may have been underexposed (see histograms in original data and Section IV).

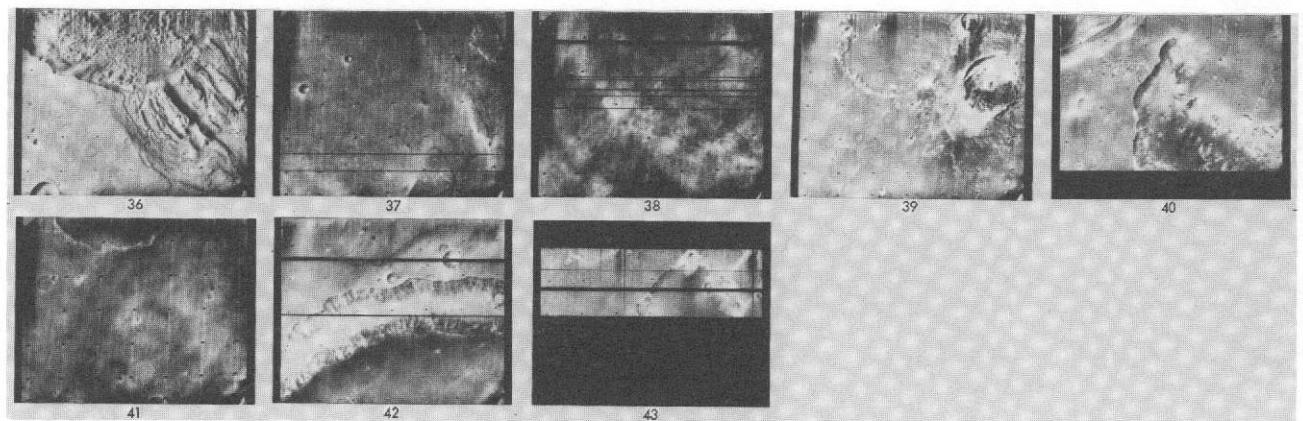
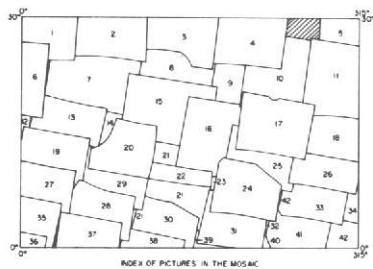
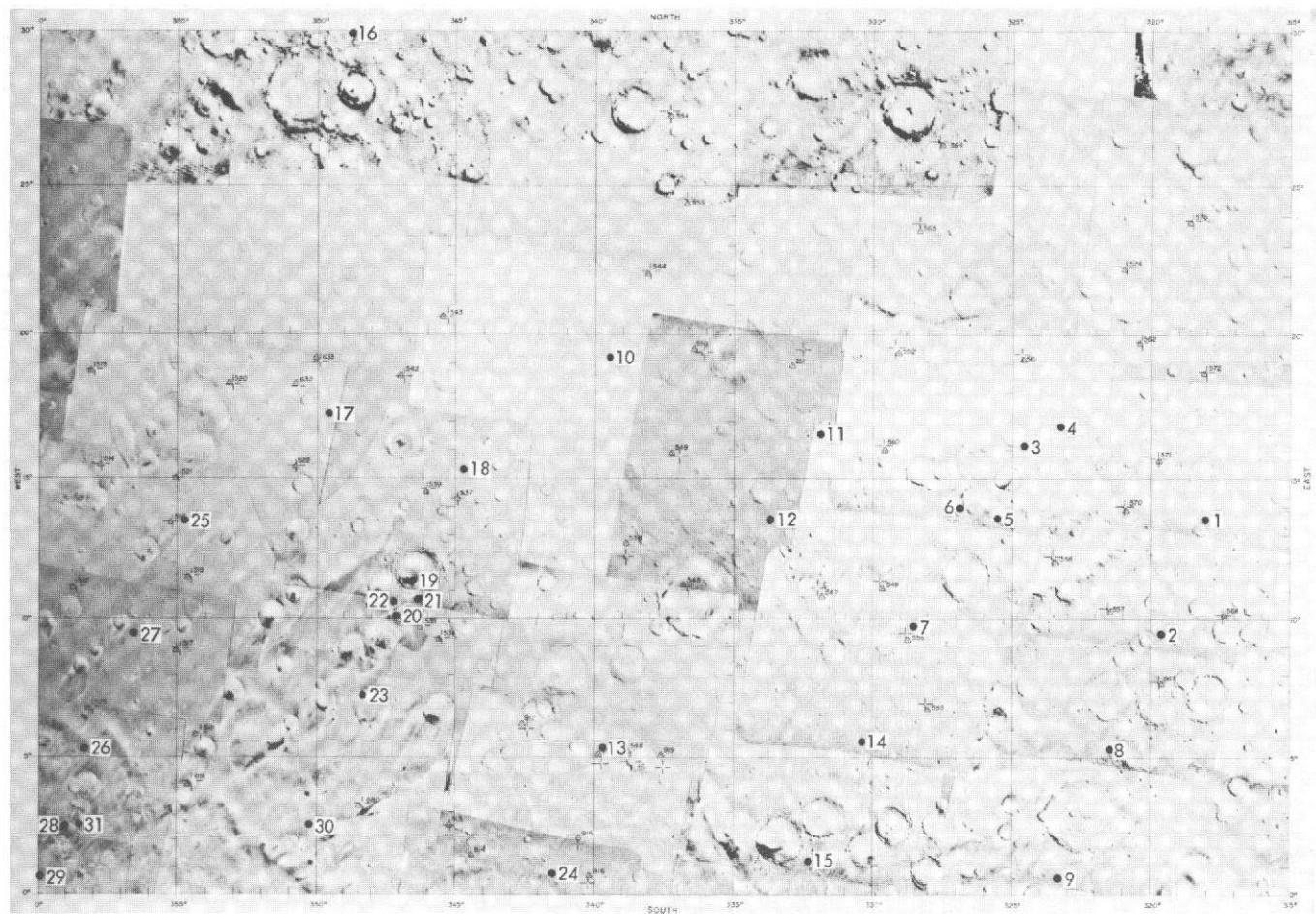


Fig. VII-6j. Narrow-angle frames in the Oxia Palus quadrangle (contd).



IDENTIFICATION NUMBERS OF PICTURES IN THE MOSAIC

Index No.	DAS No.	Index No.	DAS No.
1	9300116	22	67152431
2	9378009	23	67287303
3	8047023	24	67287305
4	8118913	25	67732702
5	8620382	26	67732703
6	7902033	27	67514230
7	6571393	28	66433173
8	6641943	29	66434539
9	6715243	30	67287304
10	6787793	31	67927530
11	6859573	32	67876536
12	7902683	33	66436230
13	6643623	34	66436231
14	6643593	35	67142326
15	6643373	36	65713131
16	6715765	37	66433171
17	6643373	38	66433172
18	6585403	39	67872631
19	6571563	40	66591713
20	6643523	41	66591714
21	6643523	42	66591715

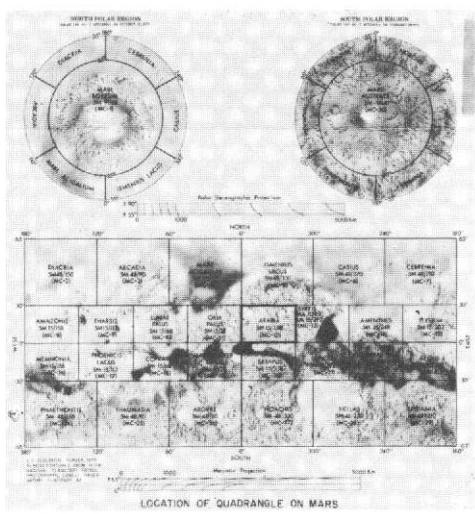


Fig. VII-6k. The Arabia quadrangle (MC-12). Photomosaic of wide-angle mapping frames in Mercator Projection serving as index map for locations of narrow-angle frames. Index numbers on the photomosaic correspond to those for the accompanying narrow-angle frames and the data listings of Table VII-3k, and not to the charts and tables directly below the photomosaic.

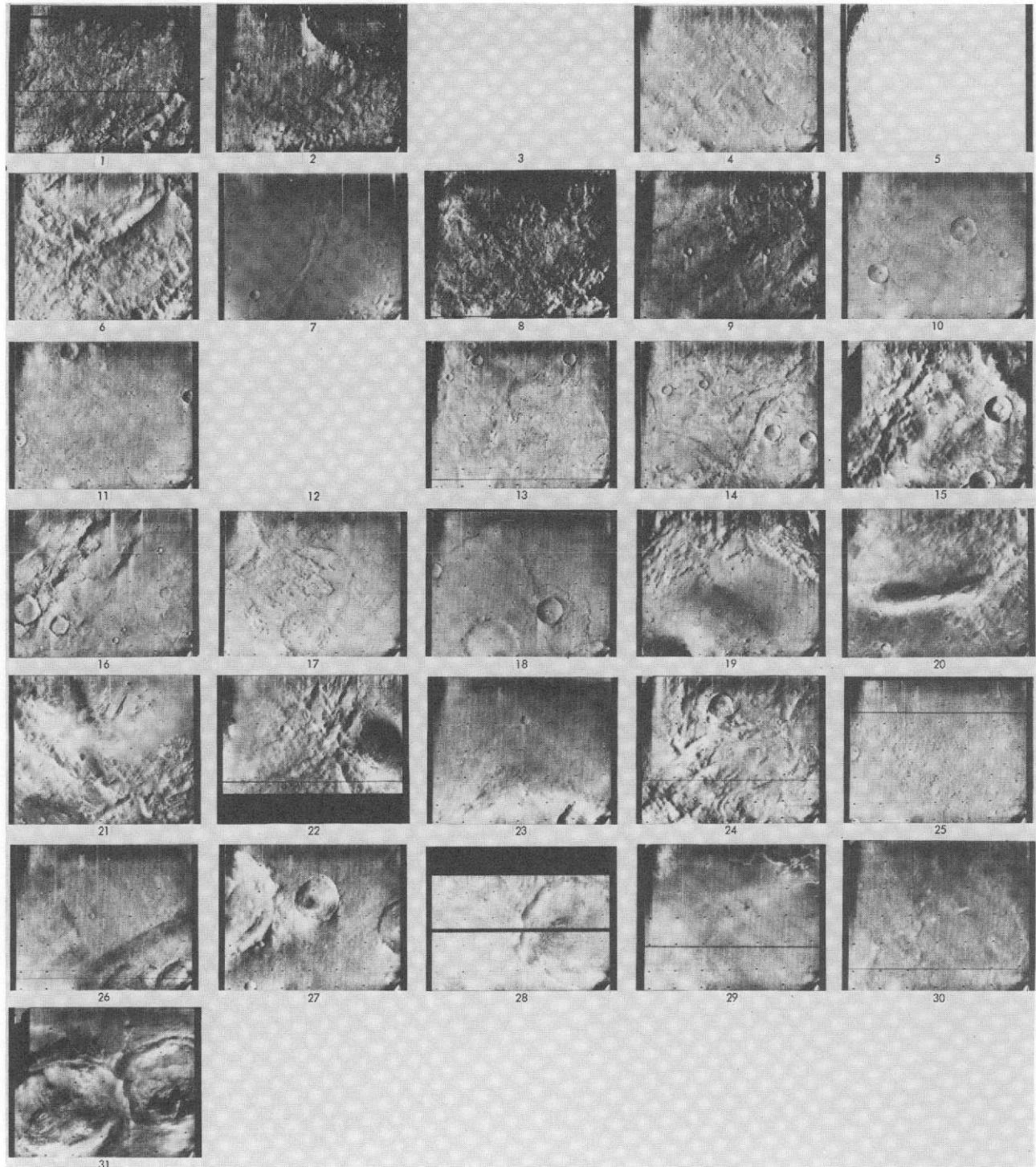
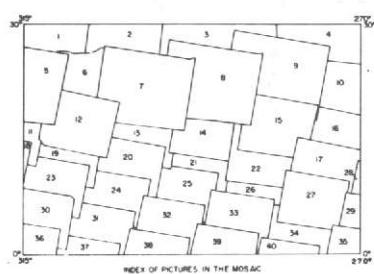
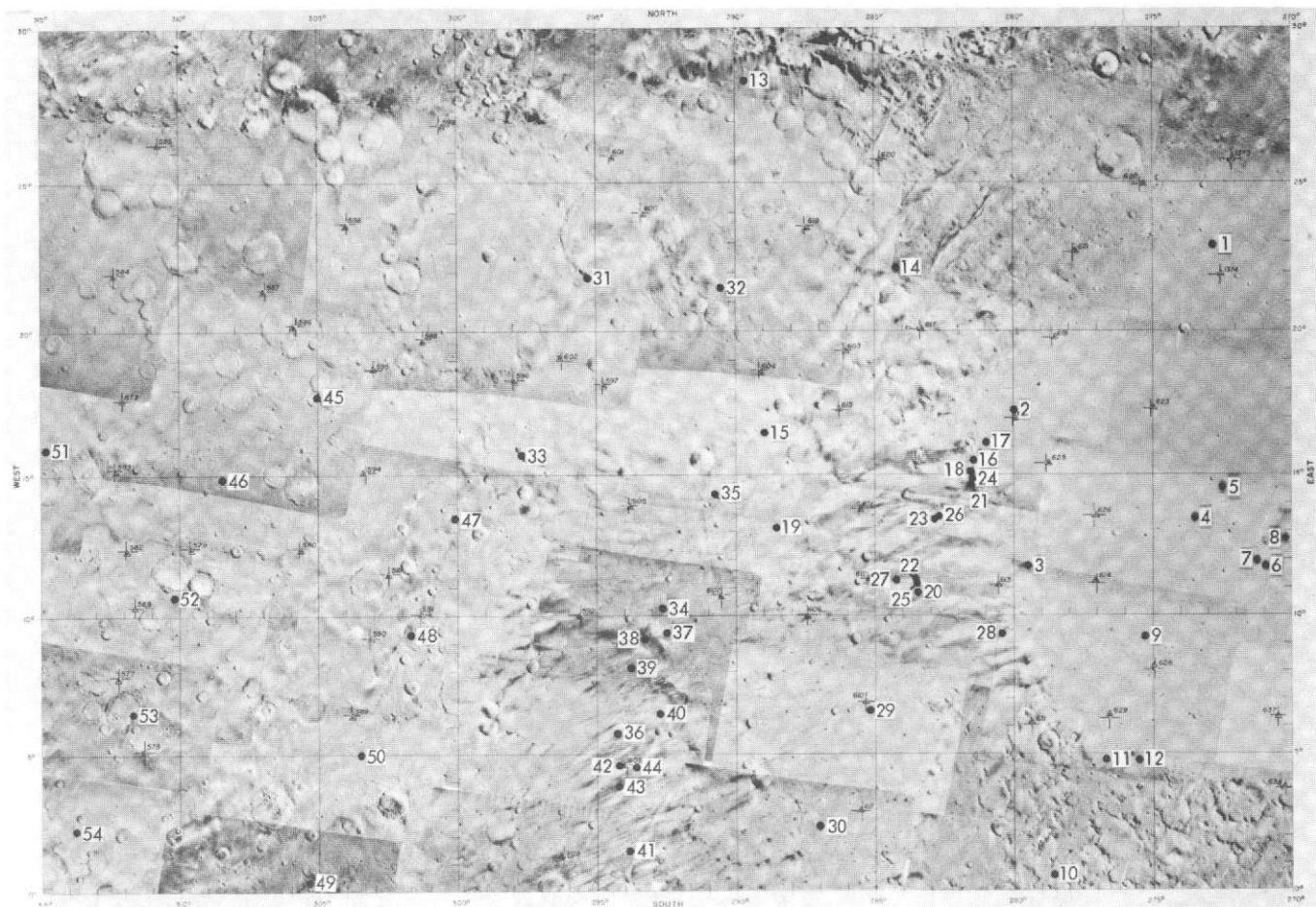


Fig. VII-6k. (contd). Narrow-angle frames (VAGC versions) that lie in the Arabia quadrangle: Revs 100–676; viewing angles less than 80° . Index numbers correspond to those on the photomosaic of this quadrangle and the data listings of Table VII-3k, and not to the charts and tables directly below the photomosaic. Blanks denote pictures planned but not recovered.



IDENTIFICATION NUMBERS OF PICTURES IN THE MOSAIC

Index No.	DAS No.	Index No.	DAS No.
1	8246939	21	7015153
2	6334869	22	7147283
3	9953829	23	6931793
4	8550689	24	7003253
5	6859753	25	7147283
6	6931793	26	7147283
7	7003253	27	7219273
8	7075773	28	7291303
9	7147803	29	7291233
10	7147803	30	7003183
11	6855403	31	7003183
12	6931433	32	7075213
13	7003393	33	7147243
14	7147803	34	7291163
15	7147453	35	7291163
16	7219413	36	6931153
17	7219343	37	7003113
18	6855403	38	7003133
19	6931363	39	7147173
20	7003323	40	7219133

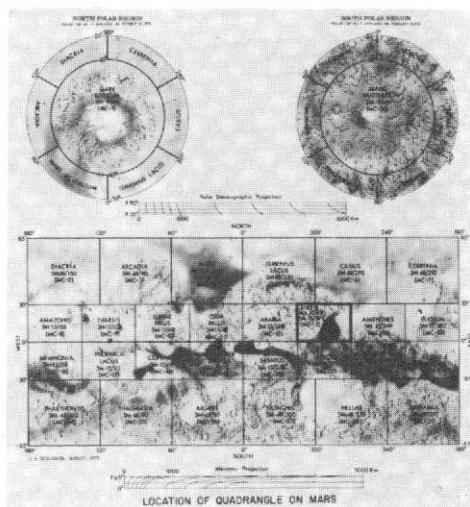


Fig. VII-6I. The Syrtis Major quadrangle (MC-13). Photomosaic of wide-angle mapping frames in Mercator Projection serving as index map for locations of narrow-angle frames. Index numbers on the photomosaic correspond to those for the accompanying narrow-angle frames and the data listings of Table VII-3I, and not to the charts and tables directly below the photomosaic.

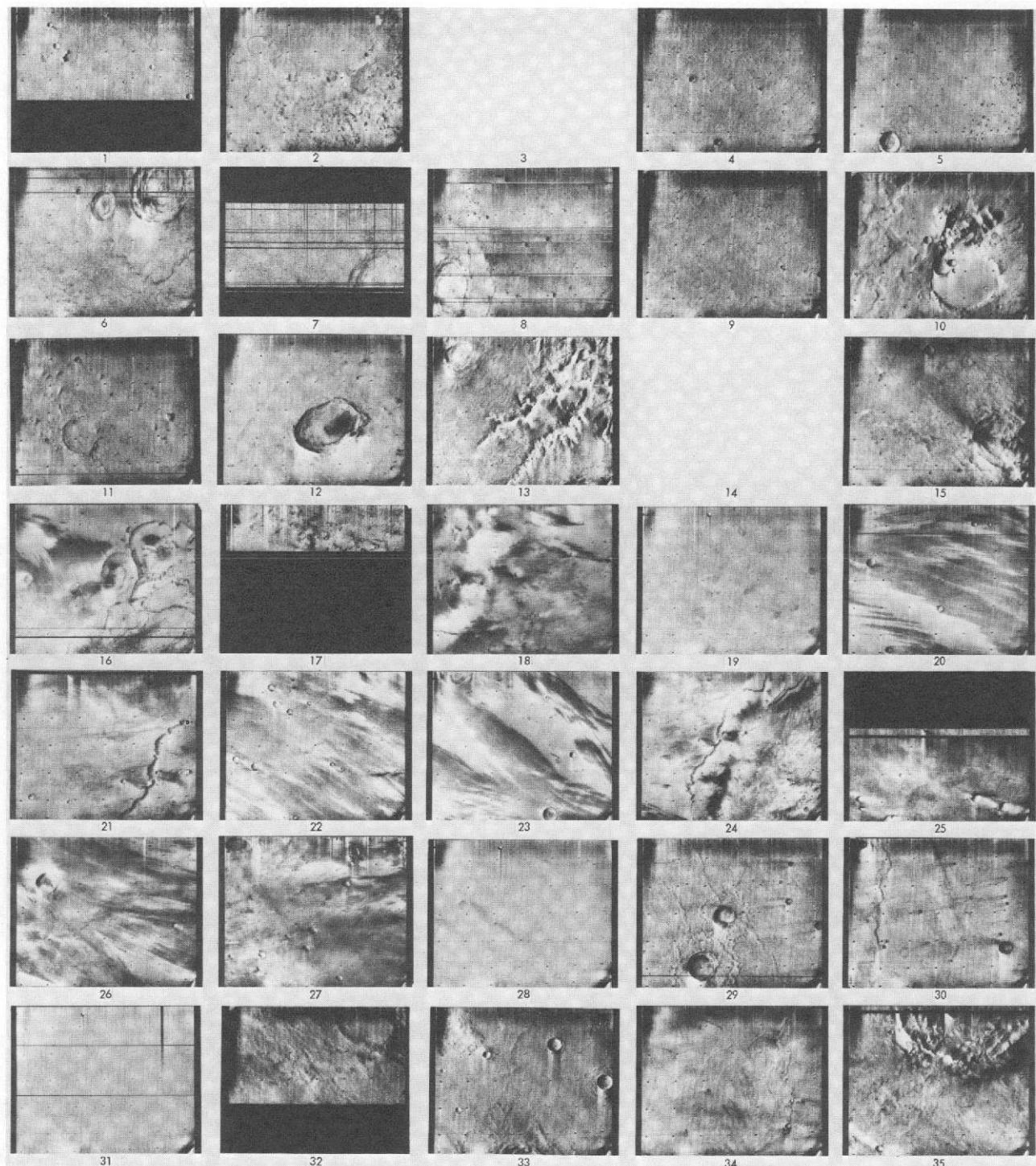


Fig. VII-6I. (contd). Narrow-angle frames (VAGC versions) that lie in the Syrtis Major quadrangle: Revs 100–676; viewing angles less than 80° . Index numbers correspond to those on the photomosaic of this quadrangle and to Table VII-3I. Images with little detail may have been underexposed (see histograms in original data and Section IV). Blanks denote pictures planned but not recovered.

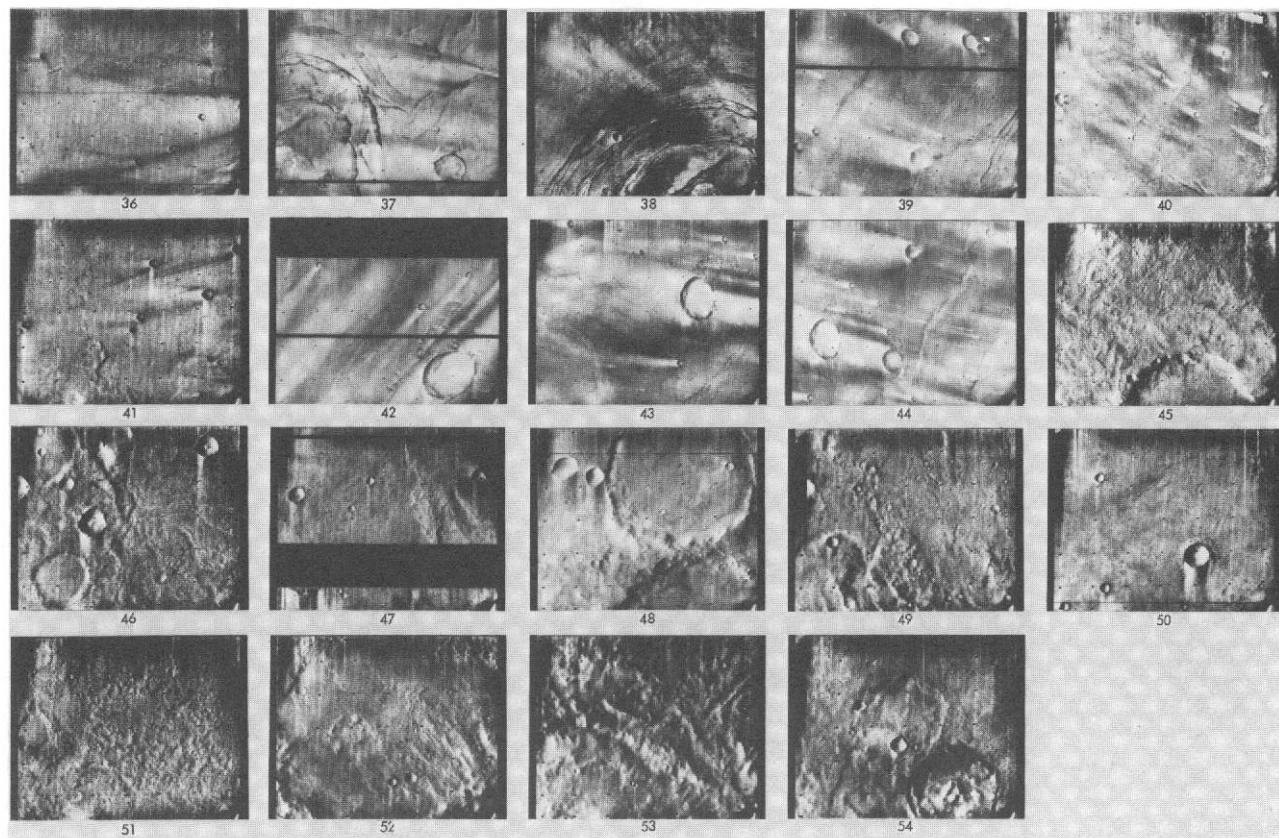
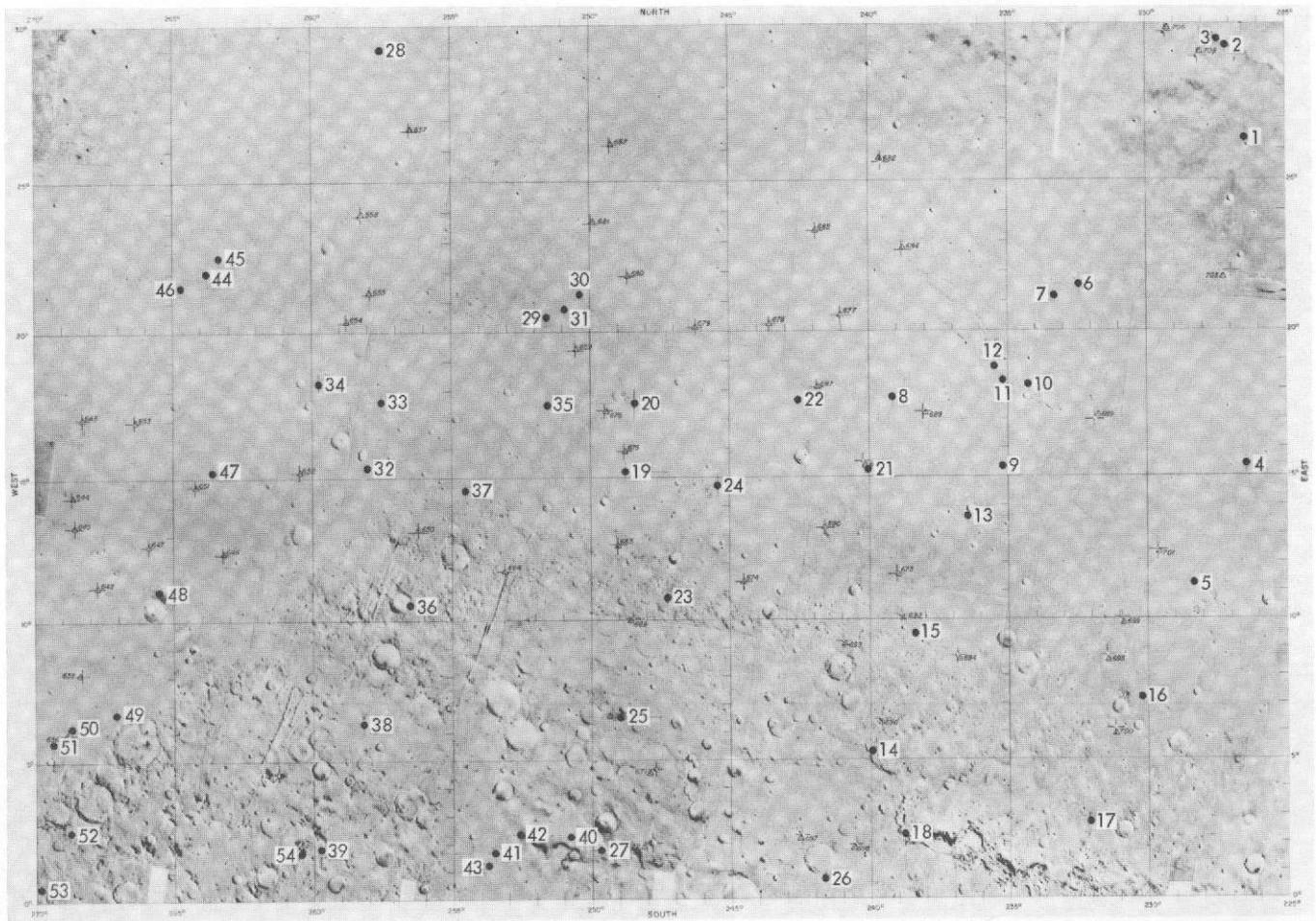


Fig. VII-6I. Narrow-angle frames in the Syrtis Major quadrangle (contd.).



IDENTIFICATION NUMBERS OF PICTURES IN THE MOSAIC			
Index No.	DAS No.	Index No.	DAS No.
1	8652849	23	736263
2	8664879	24	7435223
3	8863839	25	7511113
4	8838739	26	0550089
5	7507748	27	759073
6	7219763	28	7291233
7	7343753	29	7521553
8	7435713	30	7361193
9	7435713	31	7363613
10	7507603	32	7435153
11	7291443	33	7435373
12	7363333	34	7506243
13	7435363	35	7579003
14	7507253	36	7650893
15	7579213	37	7291163
16	7363333	38	7506233
17	7291373	39	7435083
18	7363333	40	7506973
19	7435293	41	7578937
20	7579133	42	7579423
21	7579143	43	7650823
22	7291303		

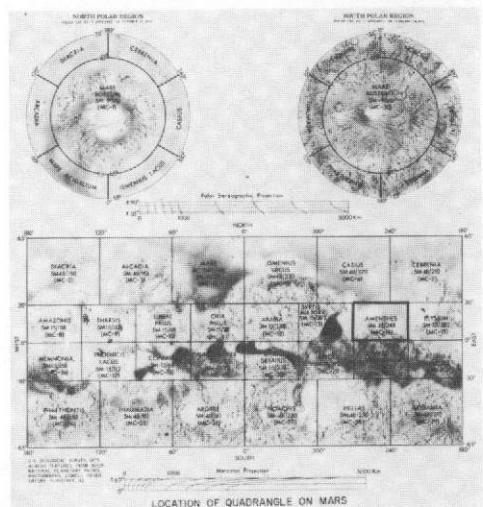


Fig. VII-6m. The Amenthes quadrangle (MC-14). Photomosaic of wide-angle mapping frames in Mercator Projection serving as index map for locations of narrow-angle frames. Index numbers on the photomosaic correspond to those for the accompanying narrow-angle frames and the data listings of Table VII-3m, and not to the charts and tables directly below the photomosaic.

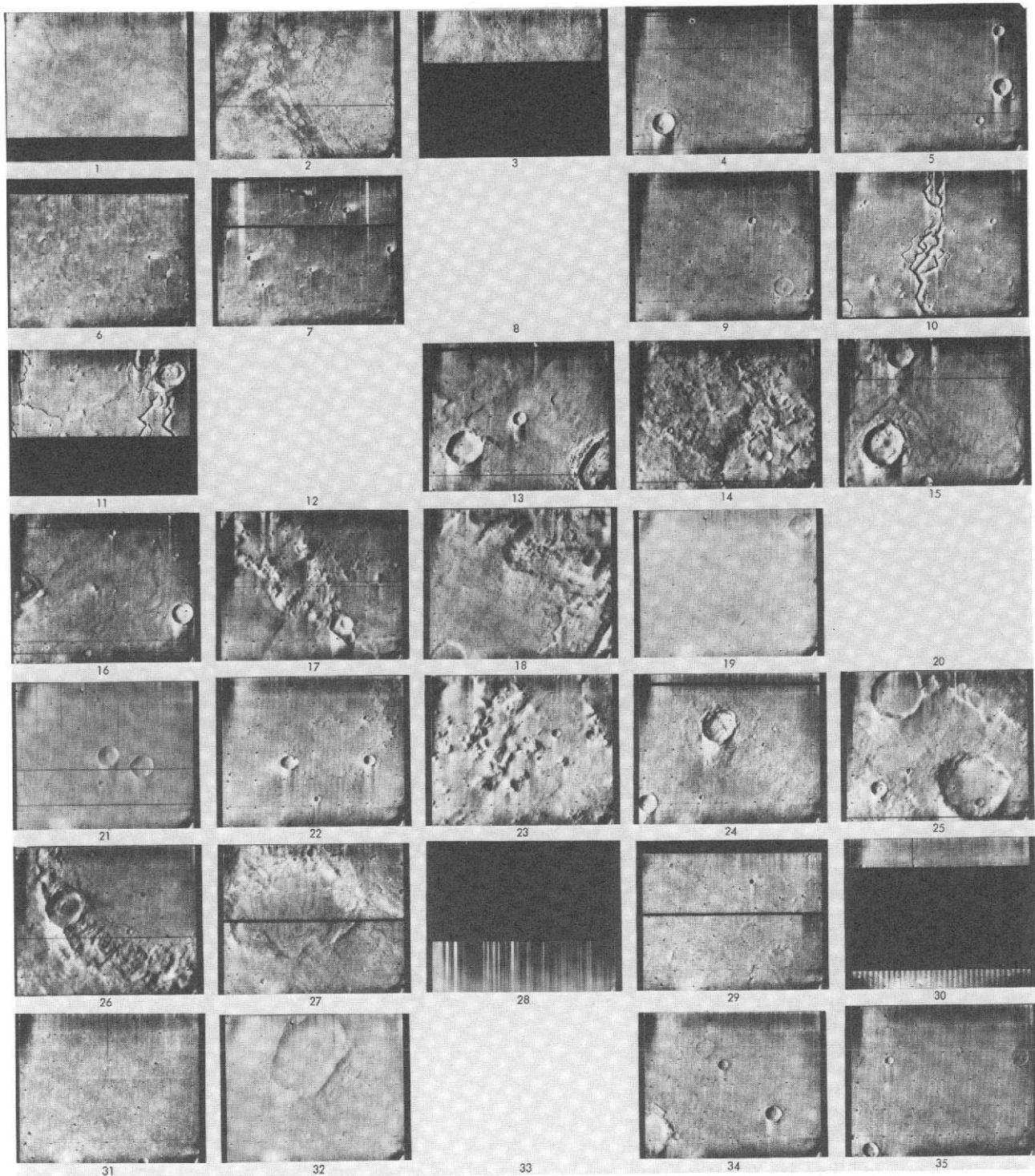


Fig. VII-6m. (contd). Narrow-angle frames (VAGC versions) that lie in the Amennes quadrangle: Revs 100-676; viewing angles less than 80° . Index numbers correspond to those on the photomosaic of this quadrangle and the data listings of Table VII-3m, and not to the charts and tables directly below the photomosaic. Images with little detail may have been underexposed (see histograms in original data and Section IV). Blanks denote pictures planned but not recovered.

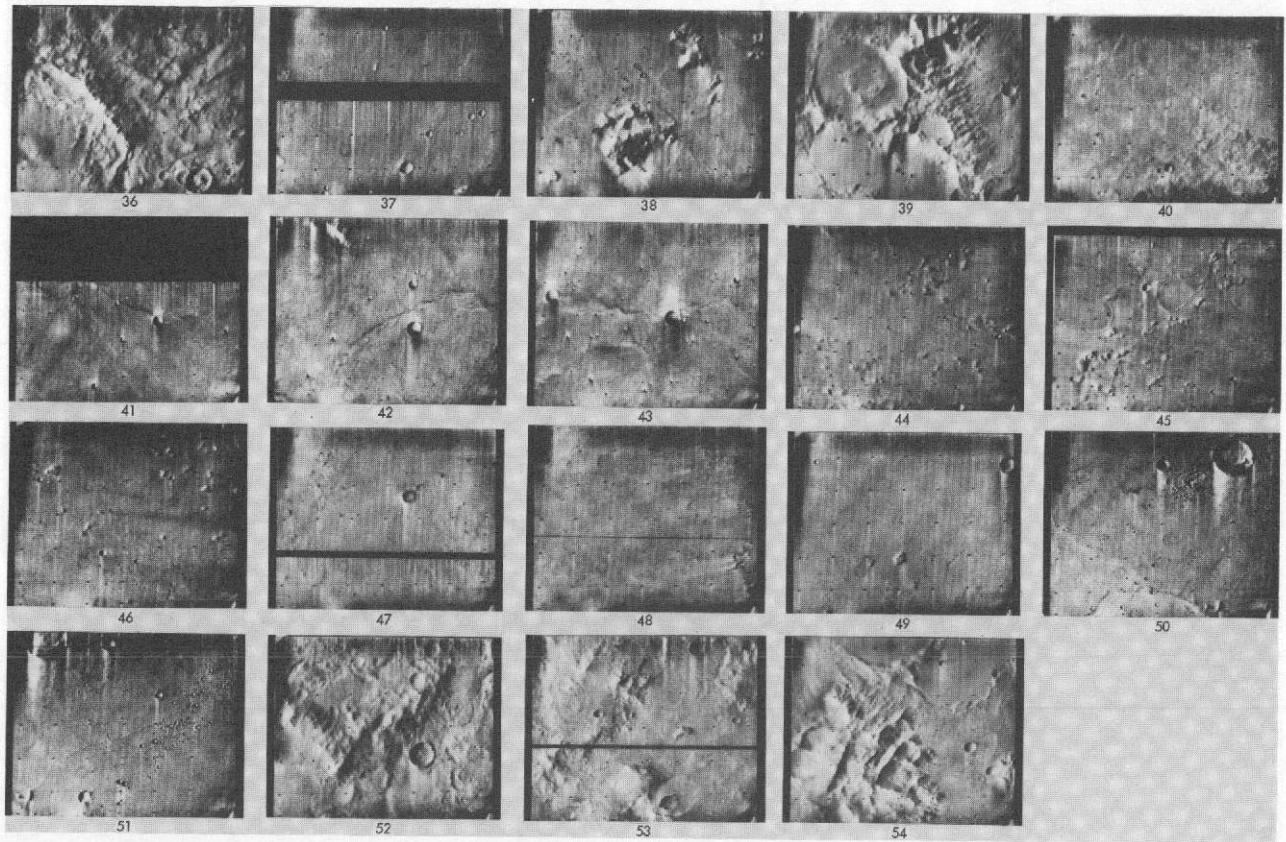
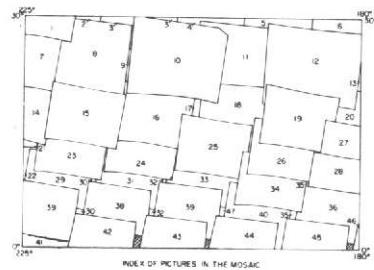
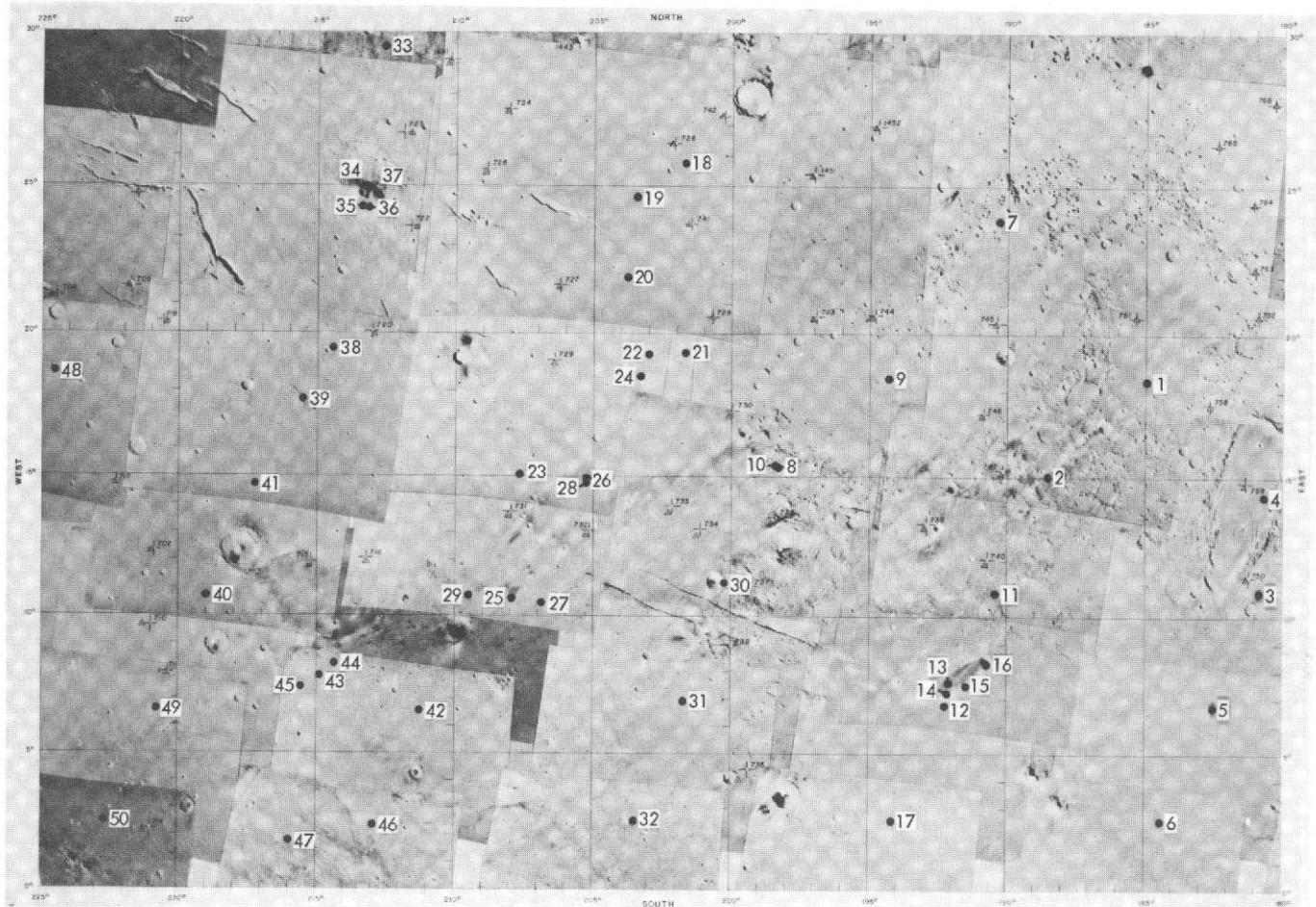


Fig. VII-6m. Narrow-angle frames in the Ammenthes quadrangle (contd).



IDENTIFICATION NUMBERS OF PICTURES IN THE MOSAIC

Index No.	DAS No.	Index No.	DAS No.
1	7579708	25	7794813
2	8826429	26	7866703
3	9054539	27	7794893
4	9126429	28	7938523
5	9198319	29	7650963
6	9270209	30	7651313
7	7579853	31	7794993
8	7651453	32	7723203
9	7651593	33	7794743
10	7723343	34	7866633
11	7723353	35	7794963
12	7867123	36	7738453
13	7939013	37	7650893
14	7579213	38	7722783
15	7651101	39	7794673
16	7722993	40	7794563
17	7723773	41	7550823
18	7794683	42	7722713
19	7938673	43	7794633
20	7938663	44	7794543
21	7579143	45	7938383
22	7579423	46	6607333
23	7651033	47	7795093
24	7722923		

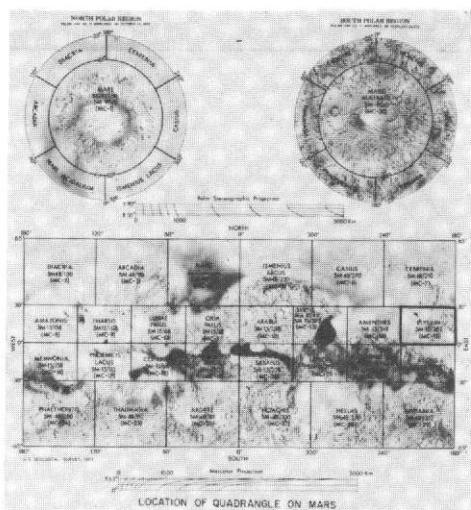


Fig. VII-6n. The Elysium quadrangle (MC-15). Photomosaic of wide-angle mapping frames in Mercator Projection serving as index map for locations of narrow-angle frames. Index numbers on the photomosaic correspond to those for the accompanying narrow-angle frames and the data listings of Table VII-3n, and not to the charts and tables directly below the photomosaic.



Fig. VII-6n. (contd). Narrow-angle frames (VAGC versions) that lie in the Elysium quadrangle: Revs 100–676; viewing angles less than 80°. Index numbers correspond to those on the photomosaic of this quadrangle and to Table VII-3n. Images with little detail may have been underexposed (see histograms in original data and Section IV). Blanks denote pictures planned but not recovered.

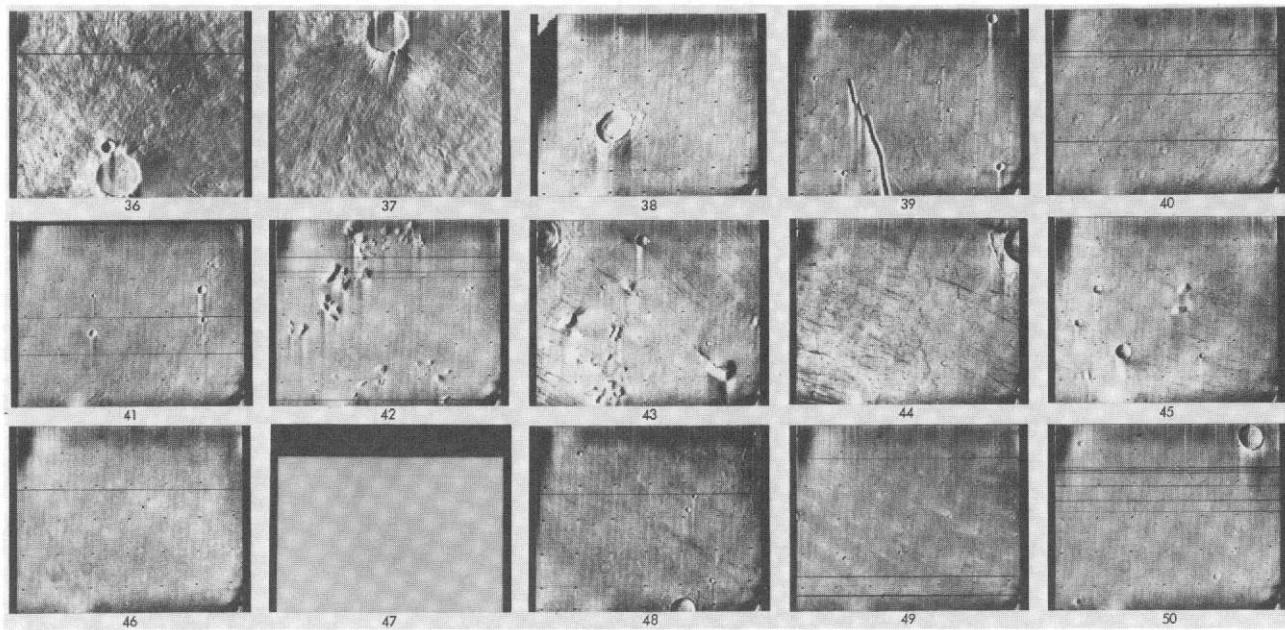
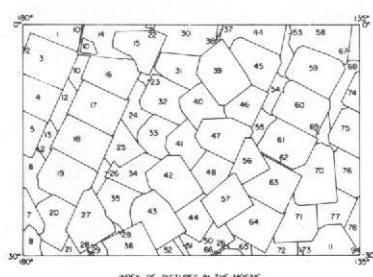
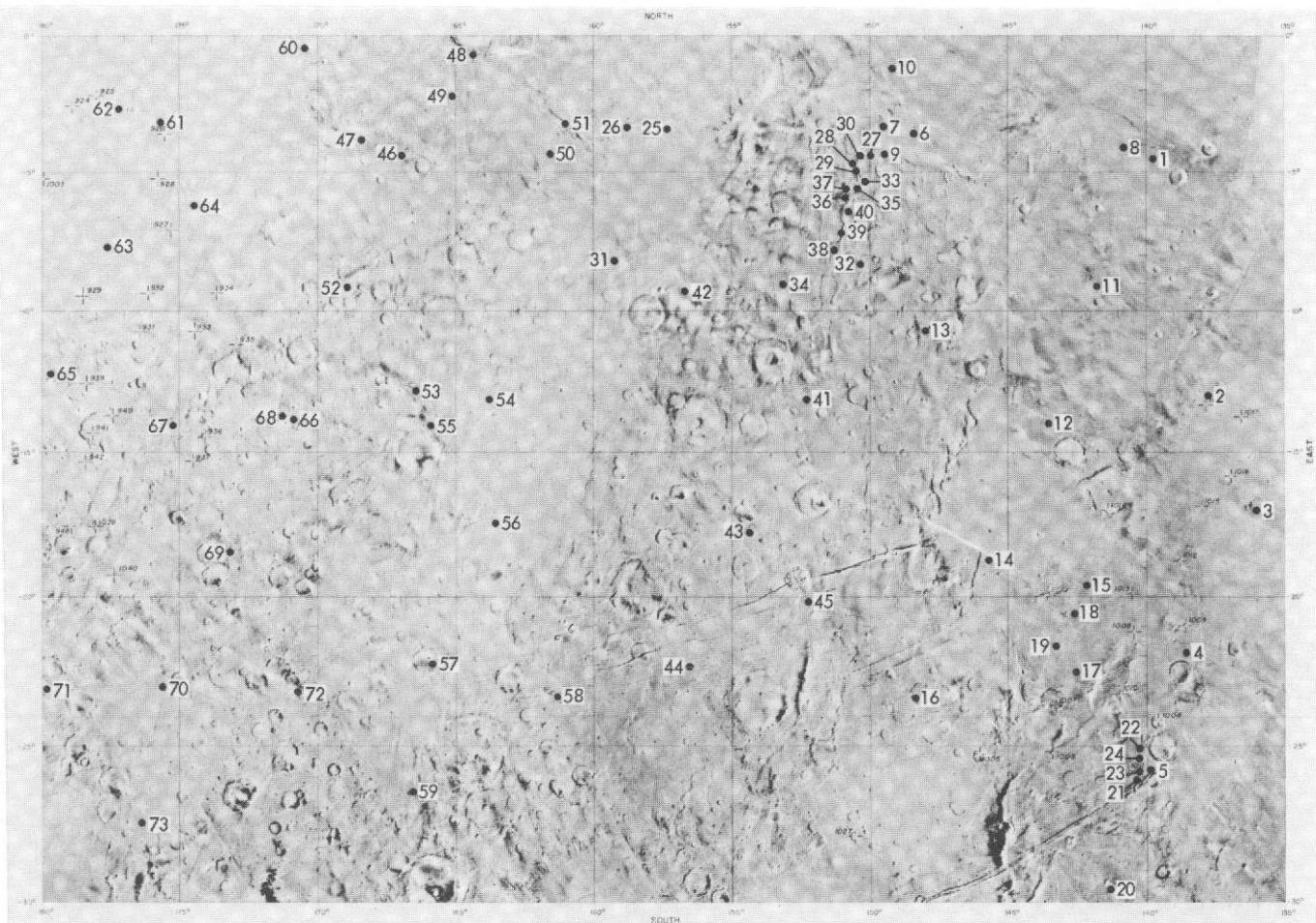


Fig. VII-6n. Narrow-angle frames in the Elysium quadrangle (contd). Images with little detail may have been under-exposed (see histograms in original data and Section IV).



IDENTIFICATION NUMBERS OF PICTURES IN THE MOSAIC					
Index No.	DAS No.	Index No.	DAS No.	Index No.	DAS No.
1	6607333	27	8153353	53	R297629
2	5920773	28	8153713	54	R297559
3	6605363	29	5347381	55	R297479
4	6608913	30	6751183	56	R297479
5	6606943	31	7510833	57	R297349
6	8081463	32	6750763	58	R295173
7	7523103	33	7510793	59	R294673
8	5753173	34	6750623	60	R294673
9	5635253	35	6751053	61	R294673
10	8081673	36	6725249	62	R424143
11	8441269	37	8225079	63	R494143
12	2008173	38	6725173	64	R394173
13	9061533	39	8225099	65	R491253
14	6679223	40	8225299	66	R491183
15	7153913	41	8225459	67	R491149
16	6678773	42	8225099	68	R365219
17	6678803	43	8225319	69	R365379
18	6678733	44	6823143	70	R365239
19	6678663	45	8227793	71	R365159
20	6678693	46	6823173	72	R365069
21	8153363	47	6922652	73	R563213
22	6679293	48	6822583	74	R960713
23	8153633	49	6822513	75	R966463
24	8153453	50	6822579	76	R965753
25	8153493	51	5419293	77	R966503
26	6708473	52	5419223	78	R441339

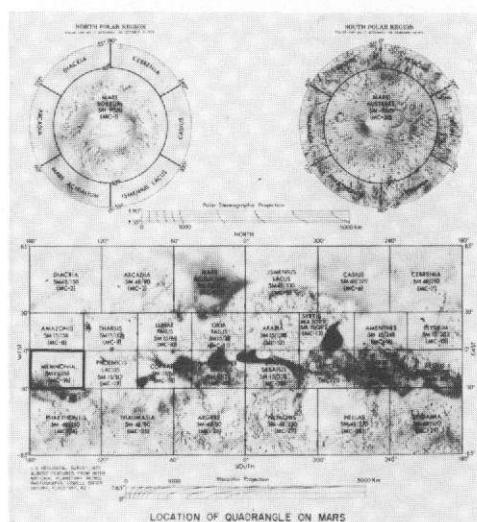


Fig. VII-7a. The Memnonia quadrangle (MC-16). Photomosaic of wide-angle mapping frames in Mercator Projection serving as index map for locations of narrow-angle frames. Index numbers on the photomosaic correspond to those for the accompanying narrow-angle frames and the data listings of Table VII-4a, and not to the charts and tables directly below the photomosaic.

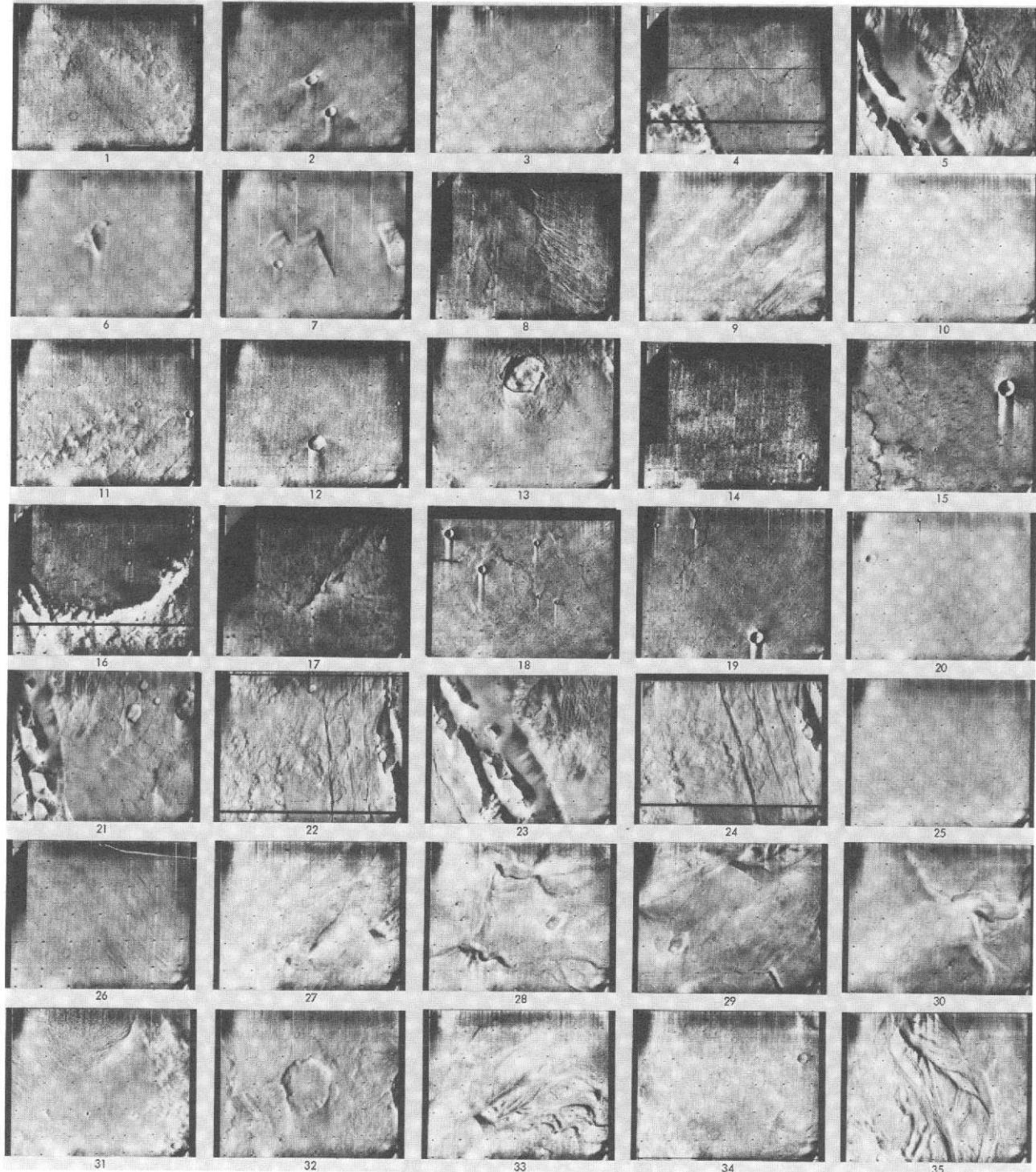


Fig. VII-7a. (contd). Narrow-angle frames (VAGC versions) that lie in the Memnonia quadrangle: Revs 100-676; viewing angles less than 80°. Index numbers correspond to those on the photomosaic of this quadrangle and to Table VII-4a.

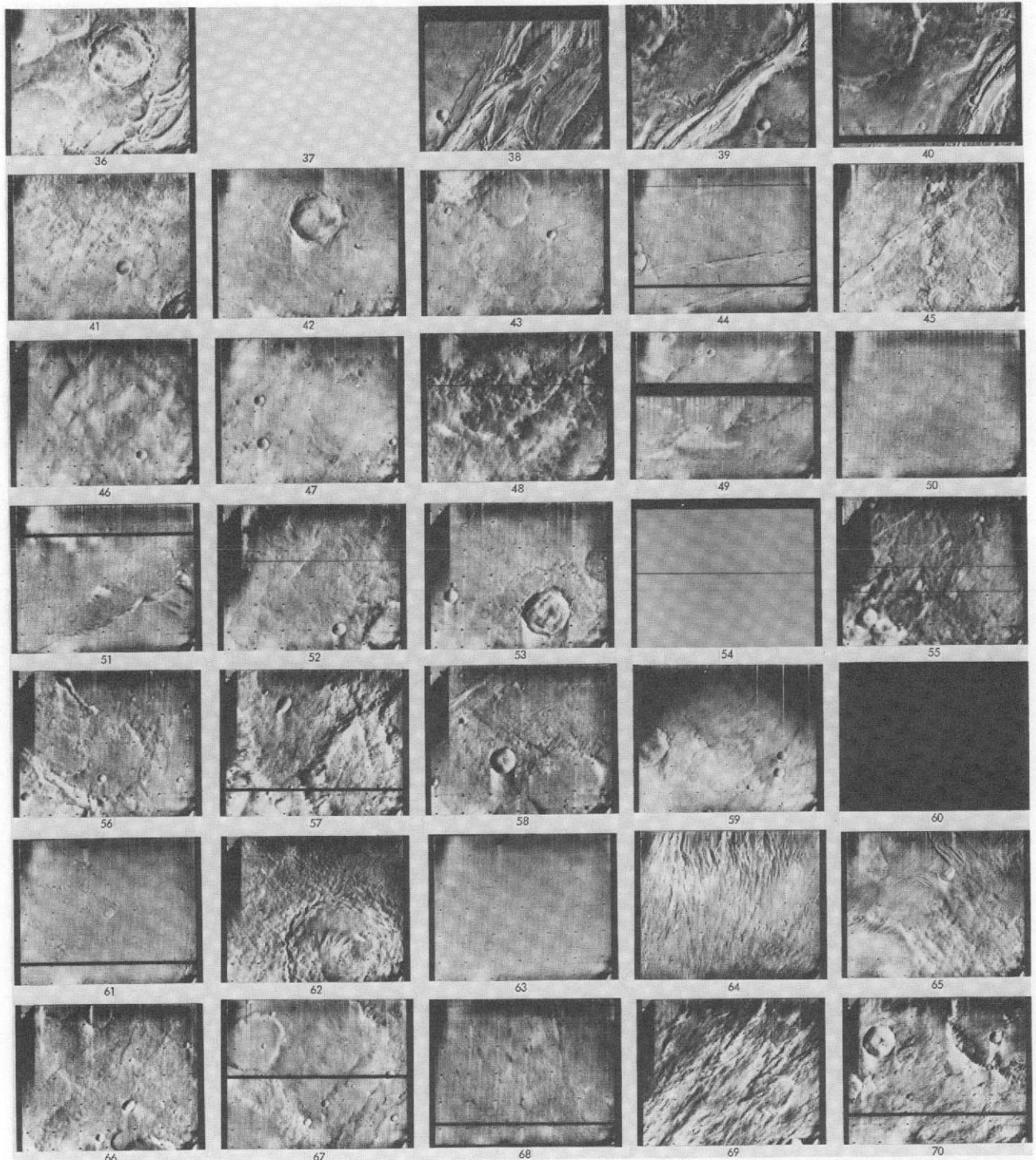


Fig. VII-7a. Narrow-angle frames in the Memnonia quadrangle (contd.). Images with little detail may have been underexposed (see histograms in original data and Section IV). Blanks denote pictures planned but not recovered.

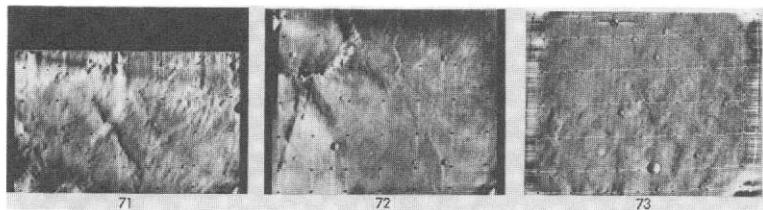
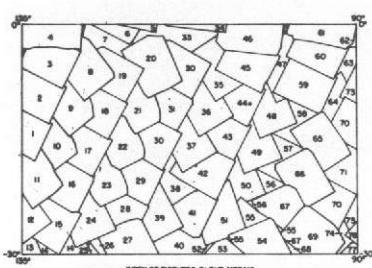


Fig. VII-7a. Narrow-angle frames in the Memnonia quadrangle (contd).



IDENTIFICATION NUMBERS OF PICTURES IN THE MOSAIC					
Index No.	Revolution No.	DAS No.	Index No.	Revolution No.	DAS No.
1	150	6966643	27	195	8585259
2	150	6966713	28	714	7110493
3	150	6966783	29	714	7110563
4	150	6967133	30	714	7110633
5	152	7036153	31	714	7110703
6	153	8513859	32	714	7110773
7	152	7039093	33	714	7111123
8	191	8441619	34	714	7111193
9	191	8441649	35	195	8585193
10	191	8441679	36	195	8585539
11	191	8441409	37	195	8585469
12	191	8441339	38	195	8585399
13	191	8441269	39	195	8585329
14	193	8513229	40	117	5779373
15	152	7038463	41	156	7182523
16	152	7039553	42	156	7182593
17	152	7039563	43	156	7182663
18	152	7036673	44	156	7182733
19	152	7038743	45	156	7182803
20	193	8513579	46	195	8585173
21	193	8513609	47	197	8585369
22	193	8513439	48	197	8585499
23	193	8513369	49	197	8585429
24	193	8513999	50	197	8585459
25	115	5707203	51	197	8585789
26	115	5707273	52	197	8585219

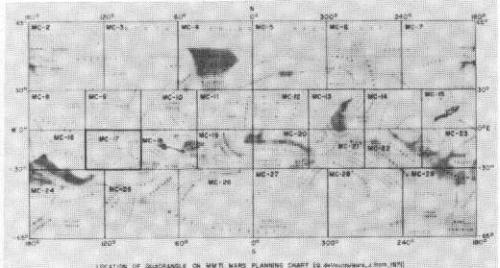


Fig. VII-7b. The Phoenicis Lacus quadrangle (MC-17). Photomosaic of wide-angle mapping frames in Mercator Projection serving as index map for locations of narrow-angle frames. Index numbers on the photomosaic correspond to those for the accompanying narrow-angle frames and the data listings of Table VII-4b, and not to the charts and tables directly below the photomosaic.

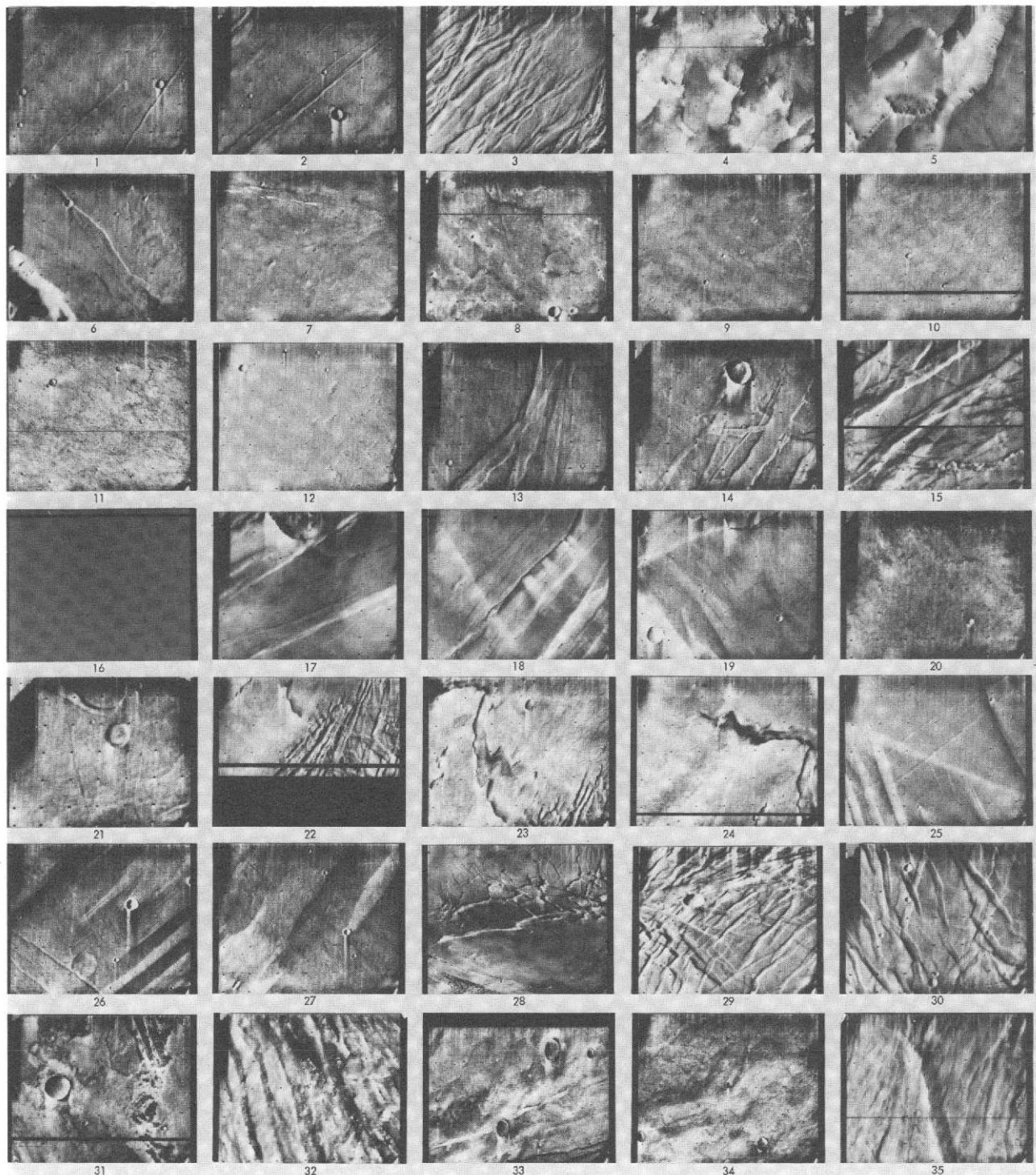


Fig. VII-7b, (contd). Narrow-angle frames (VAGC versions) that lie in the Phoenicis Lacus quadrangle: Revs 100–676; viewing angles less than 80° . Index numbers correspond to those on the photomosaic of this quadrangle and to Table VII-4b. Images with little detail may have been underexposed (see histograms in original data and Section IV).

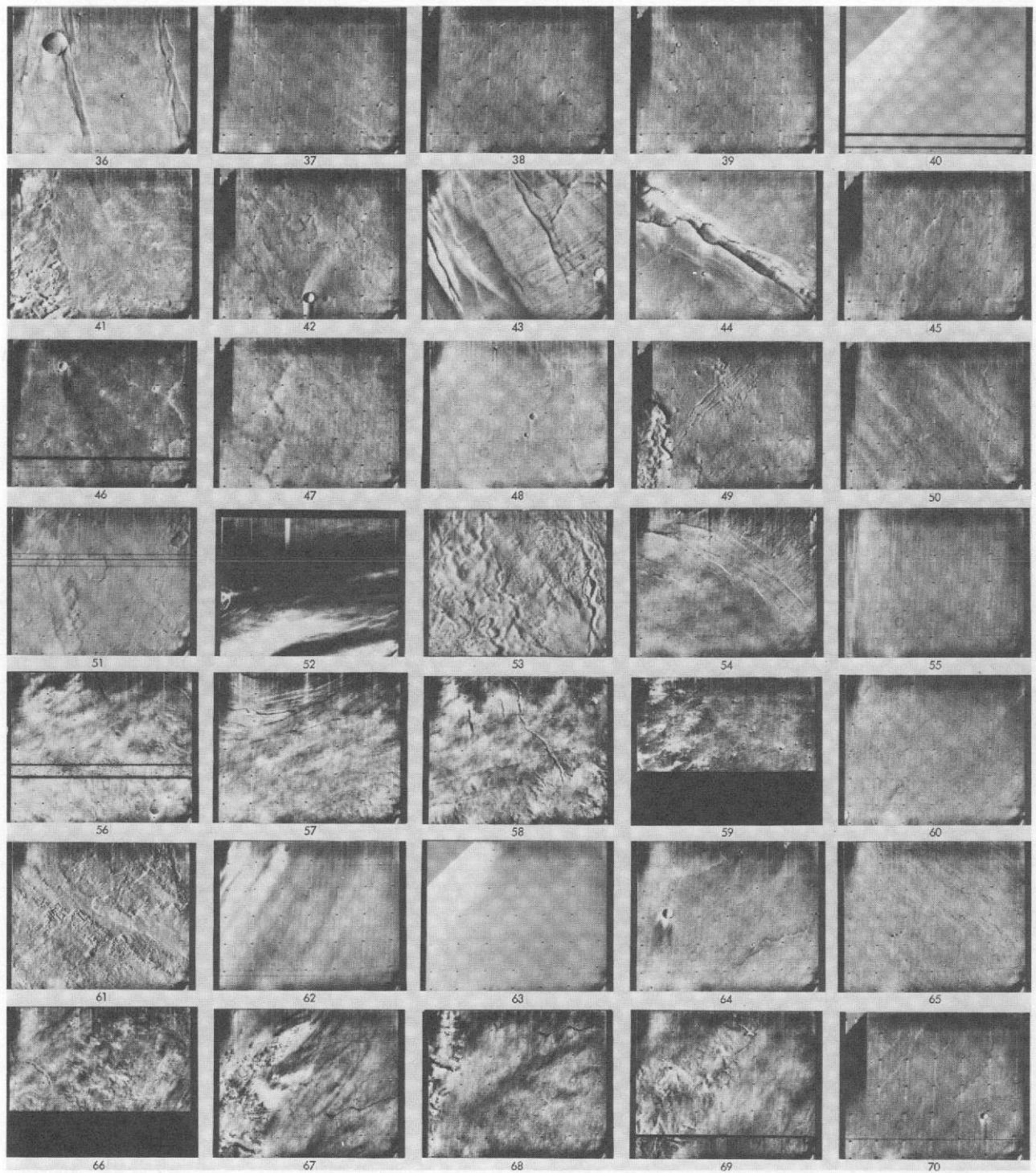


Fig. VII-7b. Narrow-angle frames in the Phoenicis Lacus quadrangle (contd).

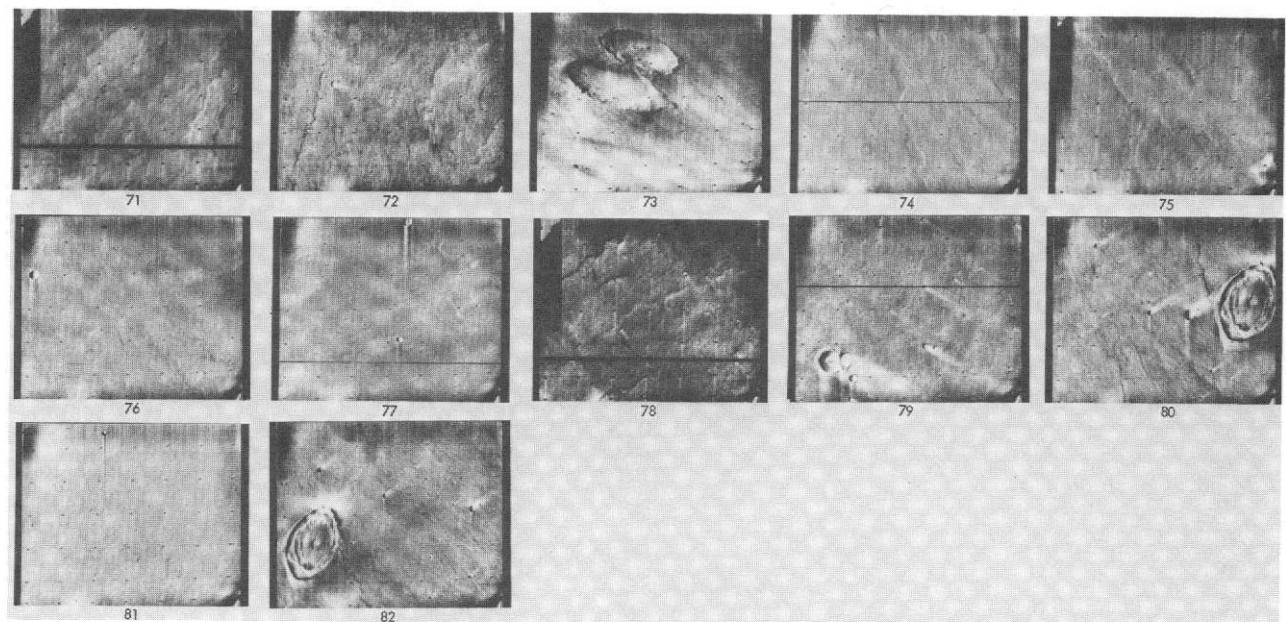
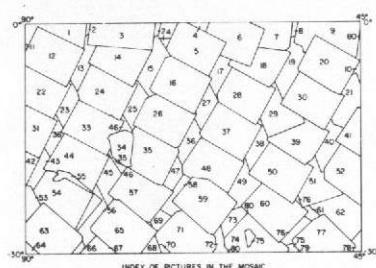
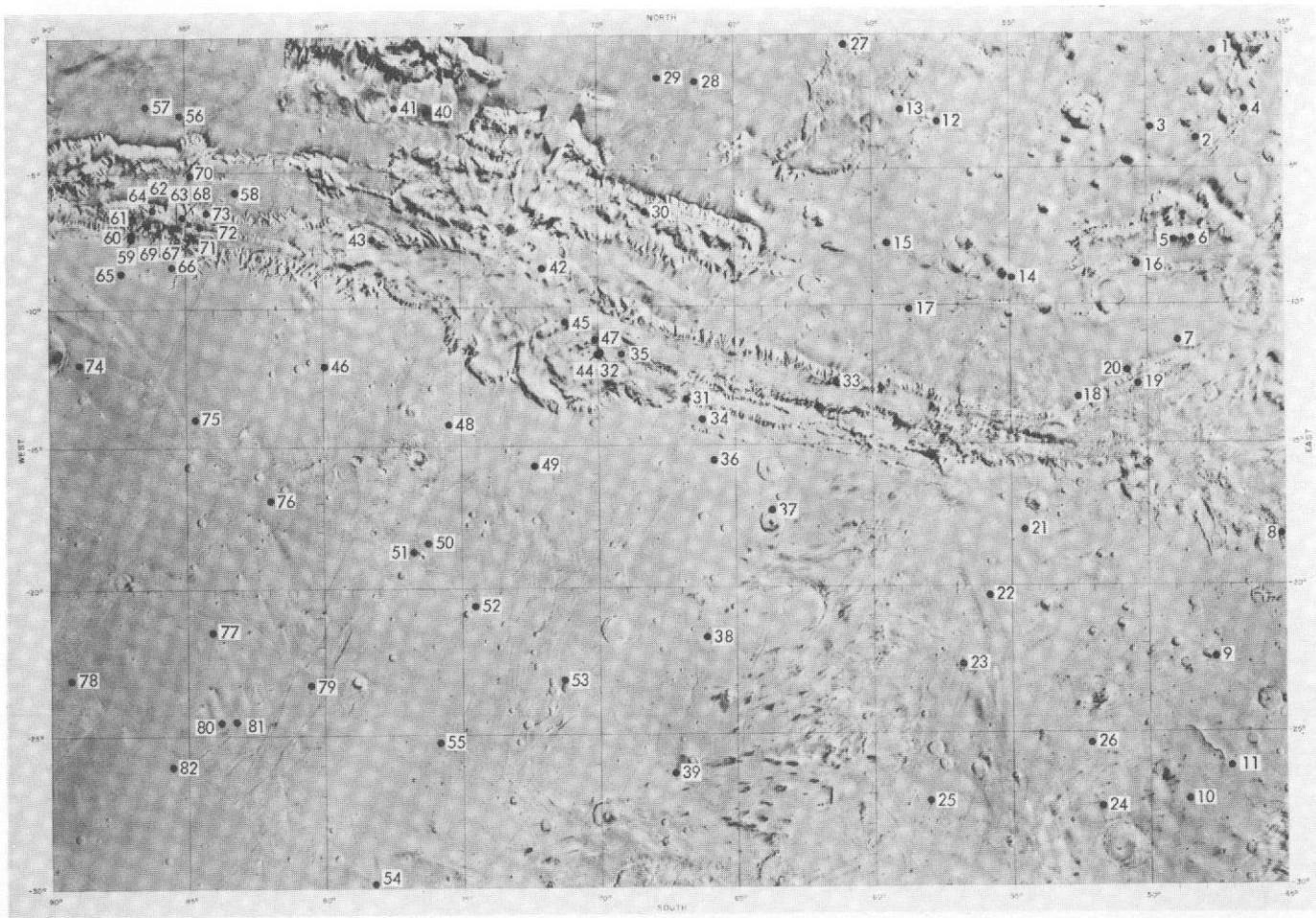


Fig. VII-7b. Narrow-angle frames in the Phoenicis Lacus quadrangle (contd).



IDENTIFICATION NUMBERS OF PICTURES IN THE MOSAIC					
Index No.	DAS No.	Index No.	DAS No.	Index No.	DAS No.
1	7327143	28	7542533	55	5995393
2	5380793	29	9017229	56	8873239
3	7389103	30	7614423	57	6026353
4	7410713	31	7614423	58	5954253
5	7410713	32	8801419	59	6139243
6	6139733	33	7398613	60	6211133
7	7542953	34	12010324	61	7686103
8	6232053	35	7614423	62	6495323
9	7614843	36	8945269	63	5995323
10	9039183	37	7542463	64	5995253
11	8729593	38	9017159	65	6067293
12	7326793	39	7614423	66	6495369
13	6881493	40	9089949	67	6067213
14	7398753	41	7686243	68	8945059
15	8873519	42	7326583	69	8945129
16	7476643	43	9061949	70	7686103
17	9089753	44	7398543	71	6139173
18	7542603	45	8873309	72	9016952
19	9017293	46	8873379	73	9017019
20	7614493	47	8945269	74	4211173
21	9089753	48	7542533	75	9068839
22	7326723	49	9017089	76	9068909
23	5801493	50	7614293	77	9282953
24	7398683	51	9089795	78	9160729
25	8873583	52	7614423	79	8711913
26	7476573	53	8801279	80	5524783
27	8545339	54	7398473		

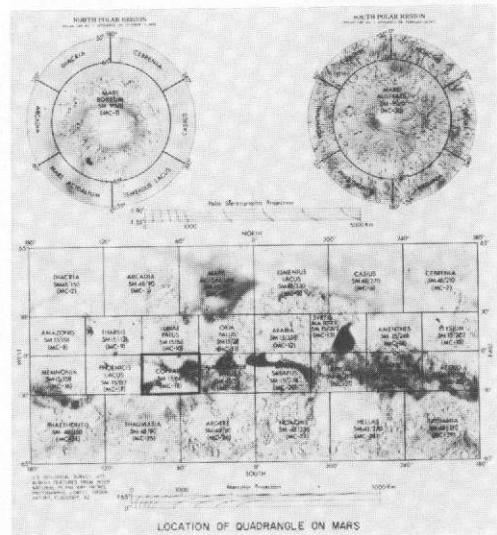


Fig. VII-7c. The Coprates quadrangle (MC-18). Photomosaic of wide-angle mapping frames in Mercator Projection serving as index map for locations of narrow-angle frames. Index numbers on the photomosaic correspond to those for the accompanying narrow-angle frames and the data listings of Table VII-4c, and not to the charts and tables directly below the photomosaic.

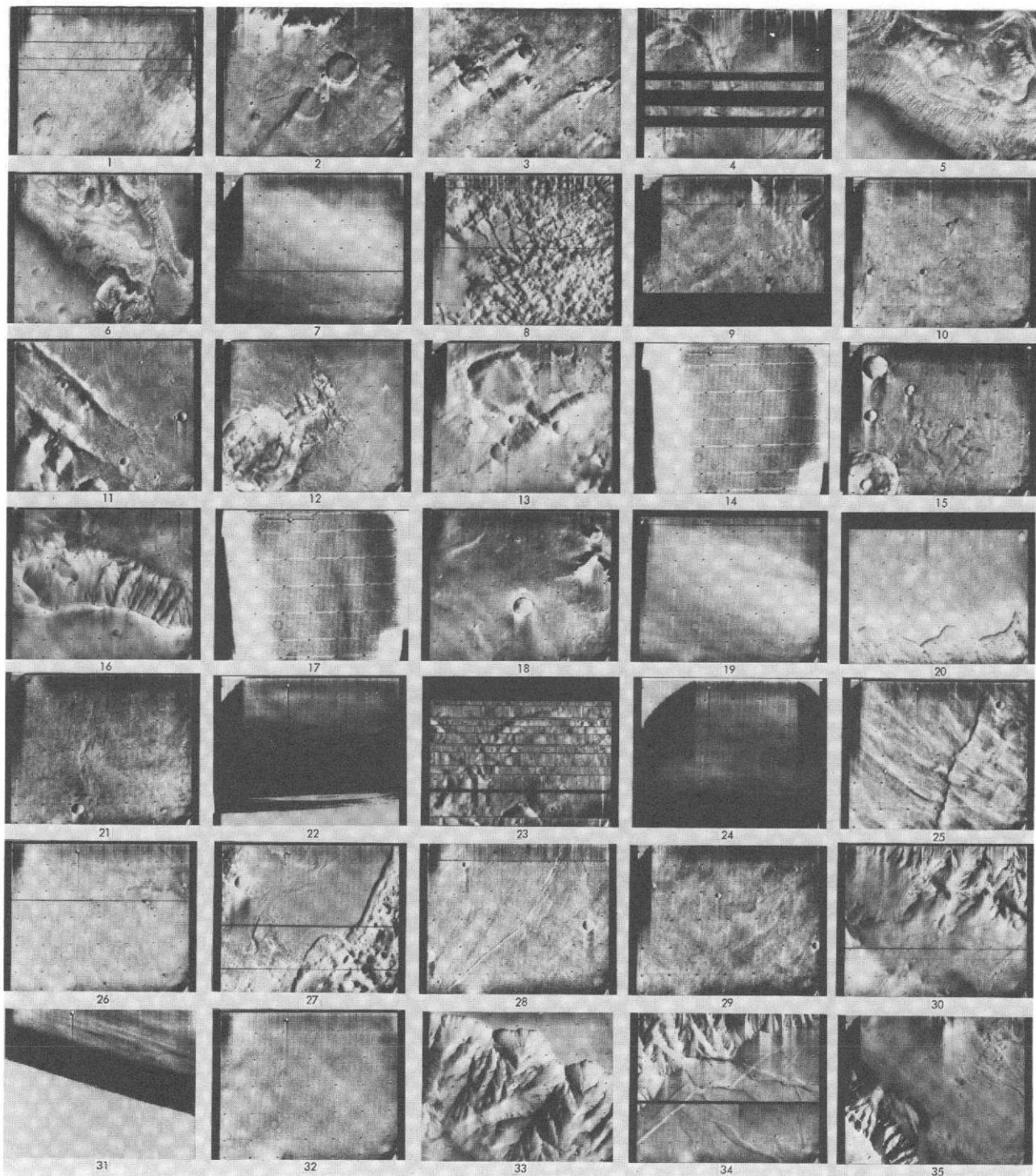


Fig. VII-7c. (contd). Narrow-angle frames (VAGC versions) that lie in the Coprates quadrangle: Revs 100–676; viewing angles less than 80° . Index numbers correspond to those on the photomosaic of this quadrangle and to Table VII-4c.

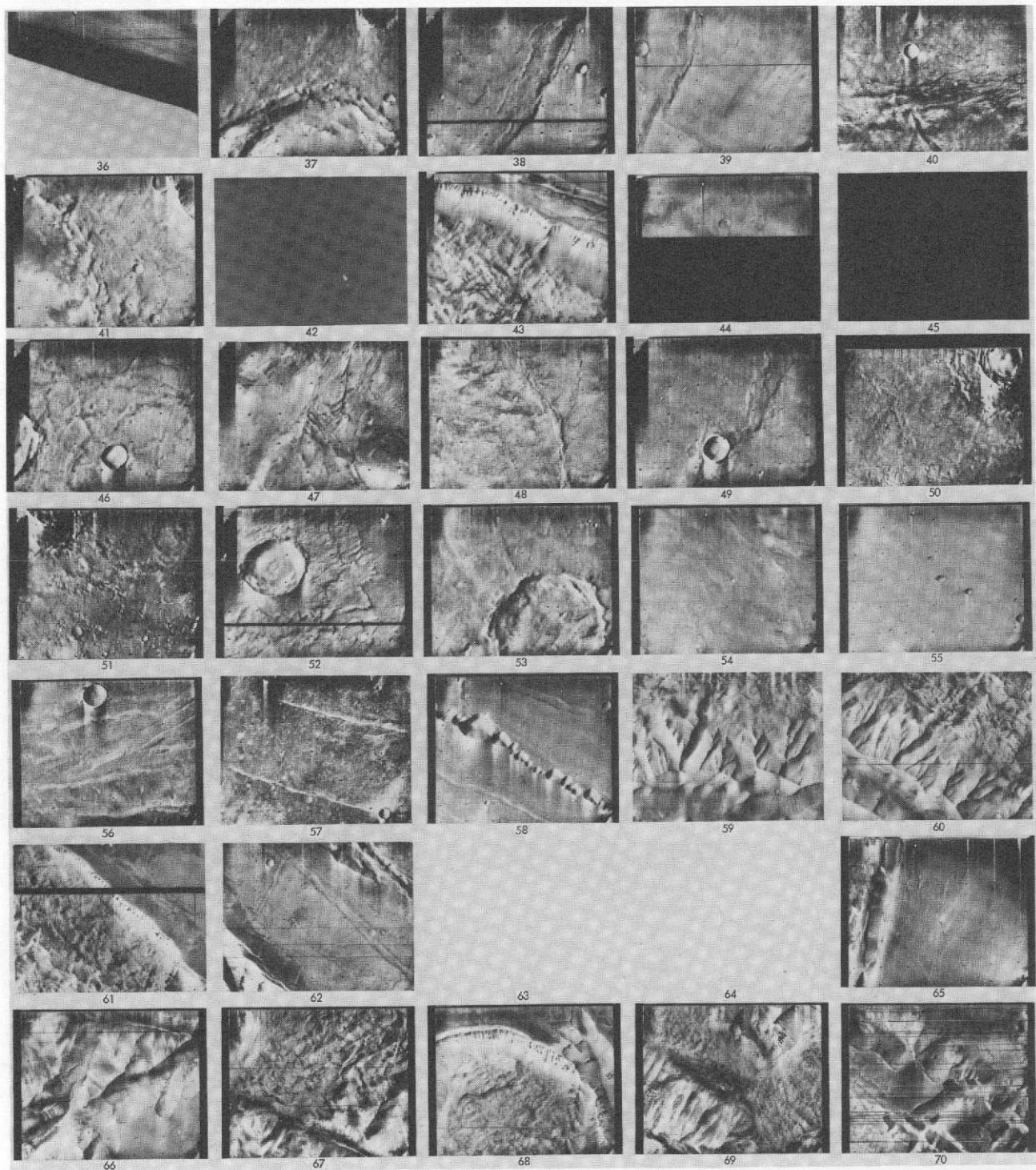


Fig. VII-7c. Narrow-angle frames in the Coprates quadrangle (contd). Images with little detail may have been underexposed (see histograms in original data and Section IV). Blanks denote pictures planned but not recovered. Index No. 42 is a satellite frame introduced by computer error.

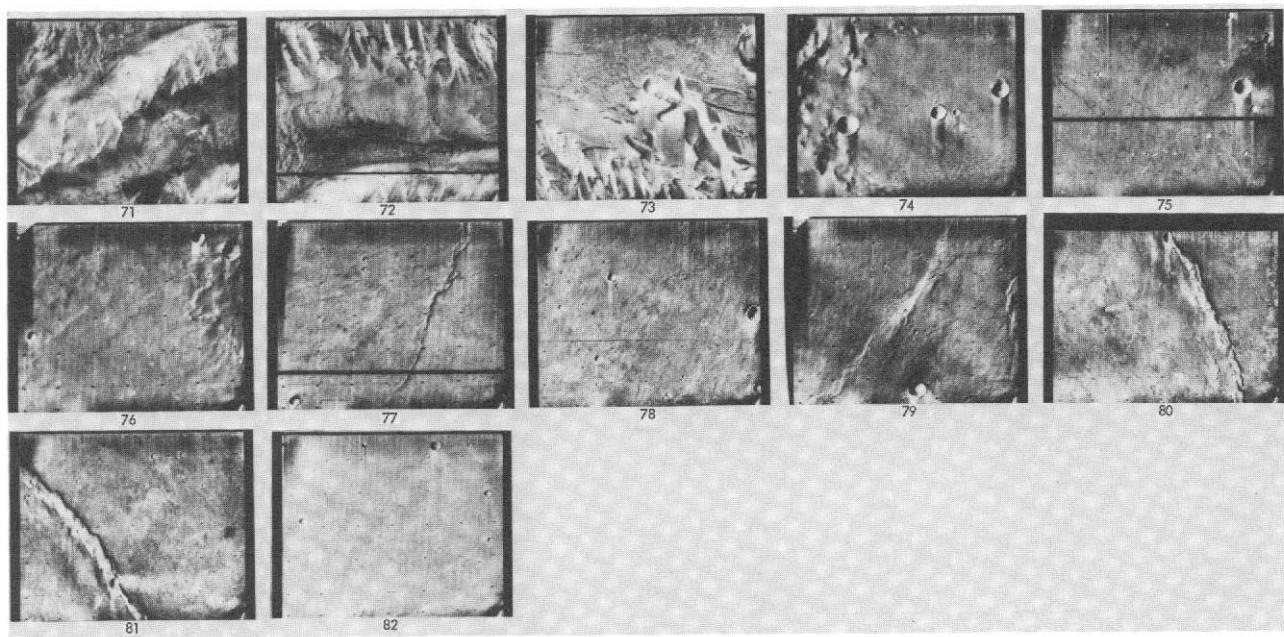
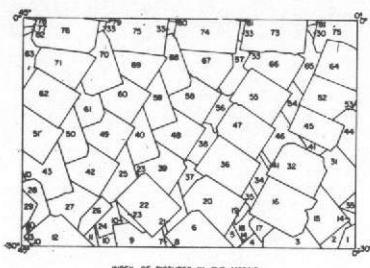
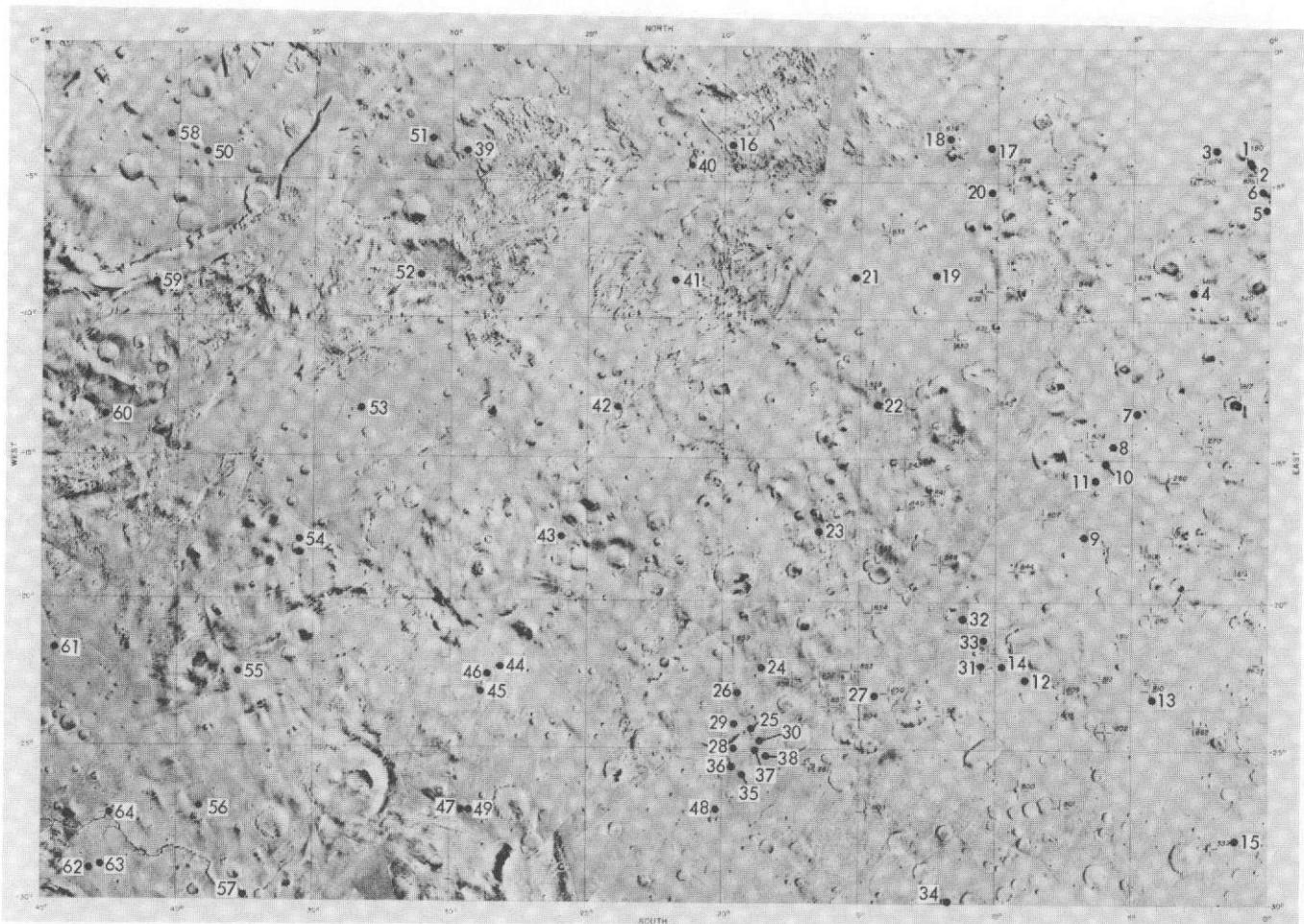


Fig. VII-7c. Narrow-angle frames in the Coprates quadrangle (contd).



IDENTIFICATION NUMBERS OF PICTURES IN THE MOSAIC

Index No.	DAS No.	Index No.	DAS No.	Index No.	DAS No.
1	6117603	29	6791053	57	9305559
2	52719393	30	5894793	58	9310559
3	8045413	31	8045553	59	9320559
4	51674313	32	6577973	60	7158203
5	7971553	33	5317953	61	6161079
6	6498673	34	7973593	62	7684313
7	5740671	35	6647673	63	9089189
8	6486773	36	7901053	64	6571703
9	9336459	37	9304649	65	7782053
10	5668773	38	9304719	66	7902053
11	9336459	39	7920953	67	7830163
12	6354043	40	9320953	68	9089189
13	9160729	41	5956753	69	7758273
14	51674313	42	7758263	70	9161079
15	8045413	43	9161079	71	7684313
16	6570723	44	8045623	72	6571353
17	6167503	45	6570963	73	7920403
18	6496693	46	7901053	74	7684313
19	6496693	47	7901183	75	7684313
20	7901773	48	7830621	76	7684313
21	6167503	49	7758111	77	7615133
22	6426803	50	9161079	78	7615133
23	7920983	51	7686743	79	7684603
24	6570723	52	6570933	80	7758273
25	9337759	53	9089189	81	7830583
26	6354513	54	7973733	82	10432703
27	7757993	55	7901983		
28	9160799	56	9304789		

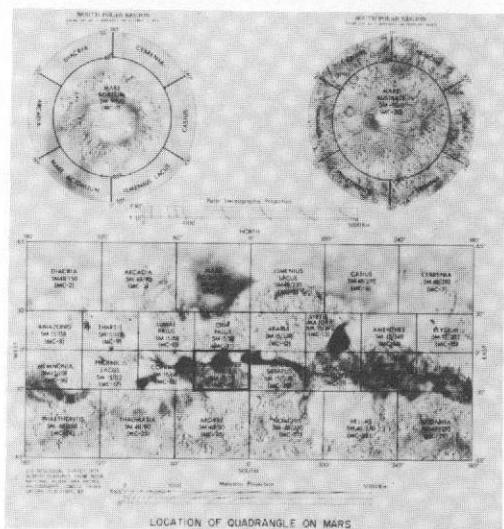


Fig. VII-7d. The Margaritifer Sinus quadrangle (MC-19). Photomosaic of wide-angle mapping frames in Mercator Projection serving as index map for locations of narrow-angle frames. Index numbers on the photomosaic correspond to those for the accompanying narrow-angle frames and the data listings of Table VII-4c, and not to the charts and tables directly below the photomosaic.

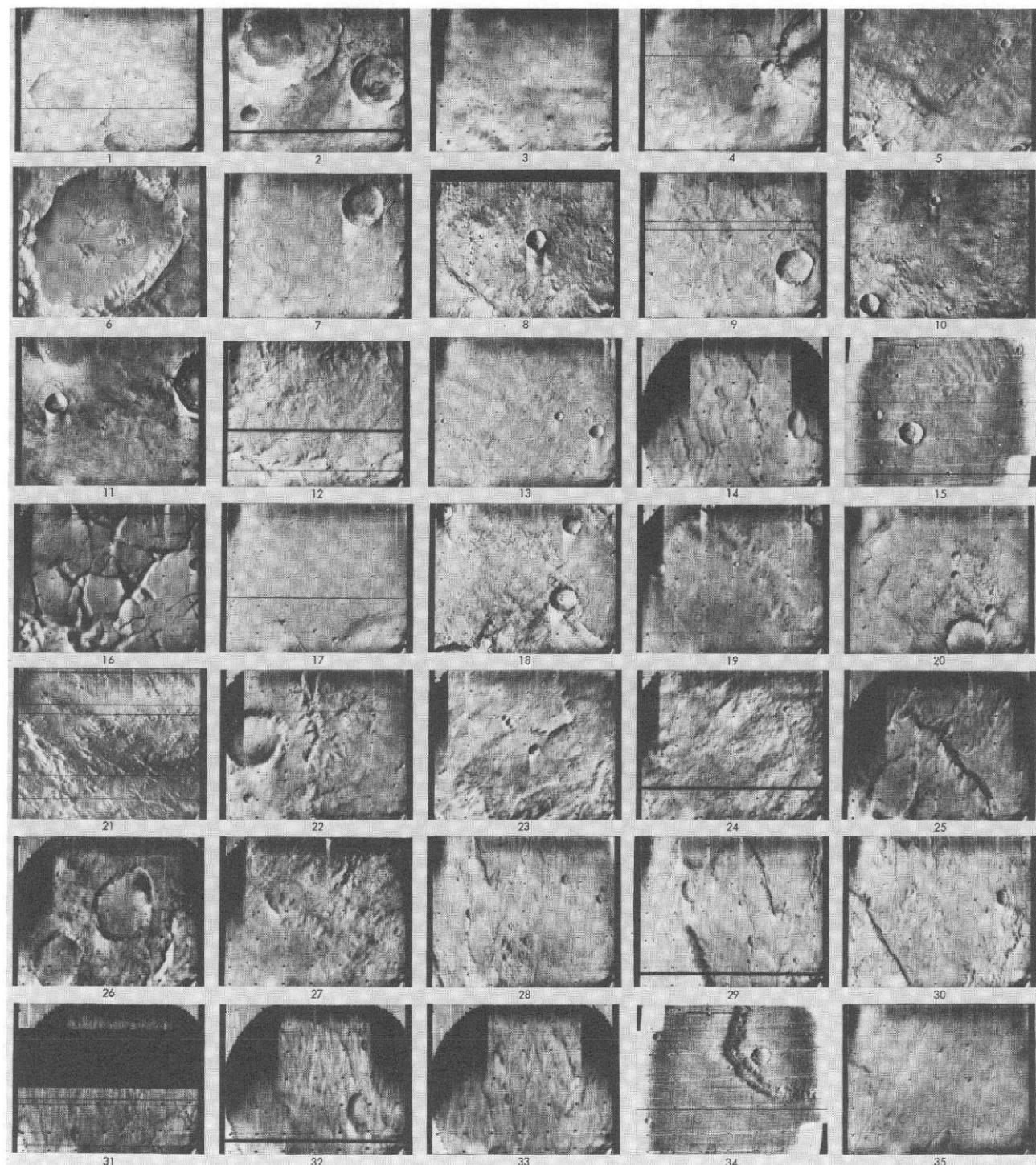


Fig. VII-7d. (contd). Narrow-angle frames (VAGC versions) that lie in the Margaritifer Sinus quadrangle: Revs 100–676; viewing angles less than 80° . Index numbers correspond to those on the photomosaic of this quadrangle and to Table VII-4d.

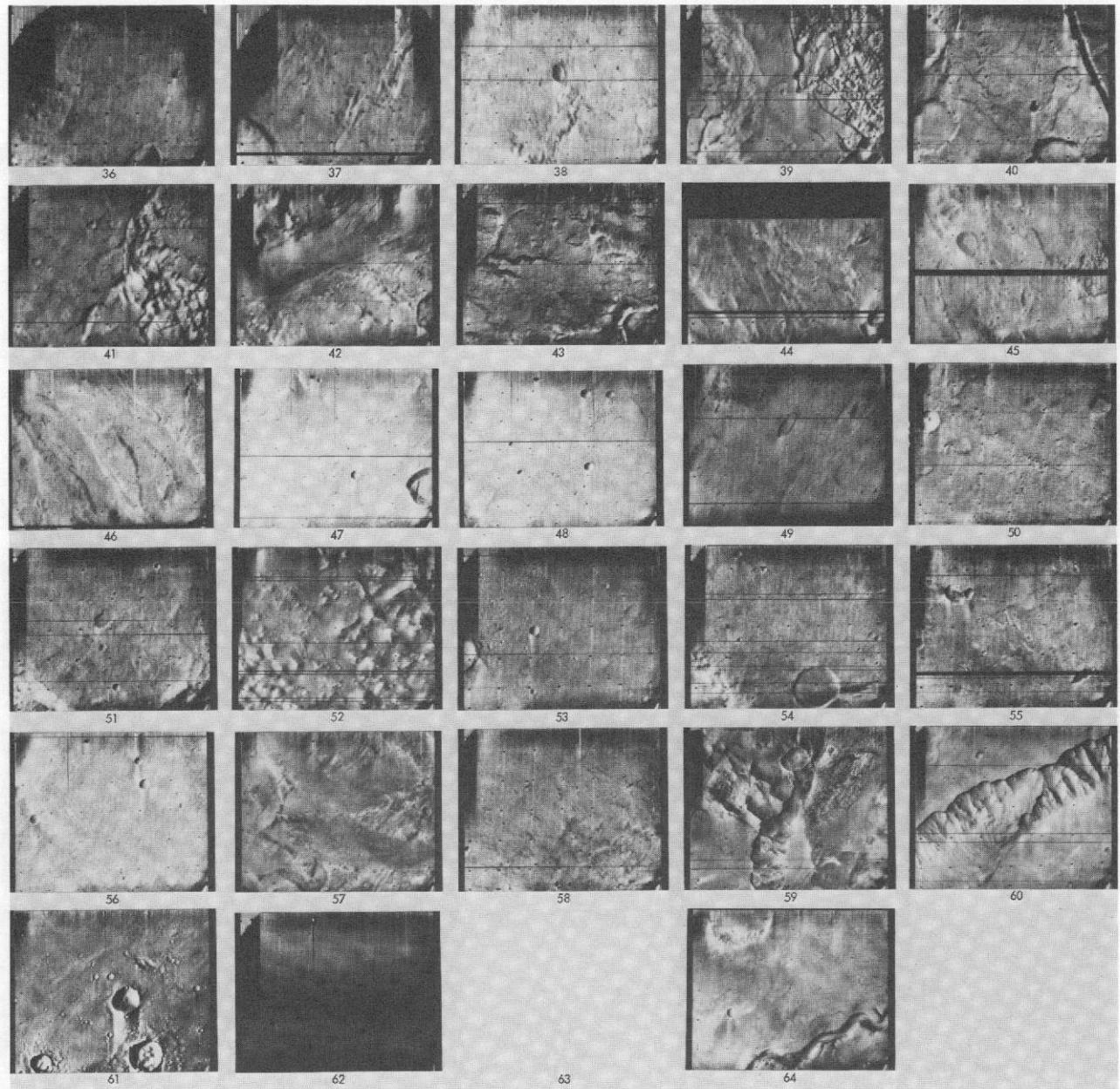
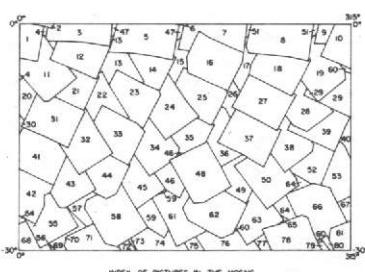


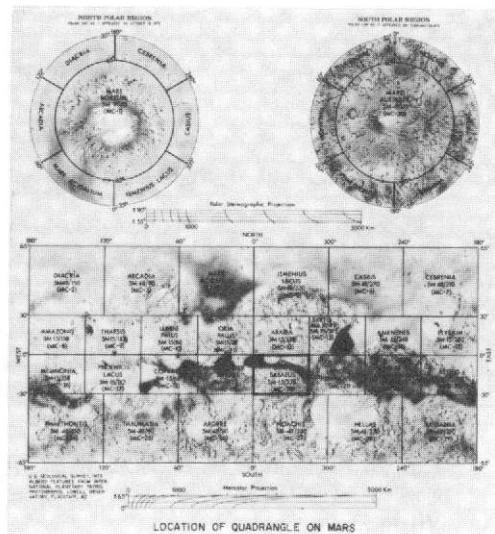
Fig. VII-7d. Narrow-angle frames in the Margaritifer Sinus quadrangle (contd). Images with little detail may have been underexposed (see histograms in original data and Section IV). Blanks denote pictures planned but not recovered.



IDENTIFICATION NUMBERS OF PICTURES IN THE MOSAIC

Index No.	03-36	05-36	05-36	05-36
1	657153	28	423539	55
2	657142	29	423023	56
3	6647113	30	4045623	57
4	6715209	31	4045623	58
5	6715203	32	4117613	59
6	6715273	33	6114713	60
7	6727183	74	4208679	71
8	6727173	75	4208679	72
9	6931153	36	3241459	83
10	6930903	37	4266113	64
11	6930813	38	4266113	65
12	6442973	39	4336663	66
13	6117653	40	4045623	67
14	6117653	41	4045623	68
15	6118619	42	4447013	69
16	6726813	43	4117613	70
17	6727179	44	4114443	71
18	6588773	45	4109003	72
19	6333639	46	4266463	73
20	6333639	47	4266463	74
21	6333639	48	4266463	75
22	6117583	49	4336663	76
23	6117583	50	4333399	77
24	6714783	51	4333399	78
25	6786743	52	4336593	79
26	6261509	53	4405329	80
27	6050303	54	5239463	81

INDEX OF PICTURES IN THE MOSAIC



LOCATION OF QUADRANGLE ON MARS

Fig. VII-7e. The Sinus Sabaeus quadrangle (MC-20). Photomosaic of wide-angle mapping frames in Mercator Projection serving as index map for locations of narrow-angle frames. Index numbers on the photomosaic correspond to those for the accompanying narrow-angle frames and the data listings of Table VII-4e, and not to the charts and tables directly below the photomosaic.

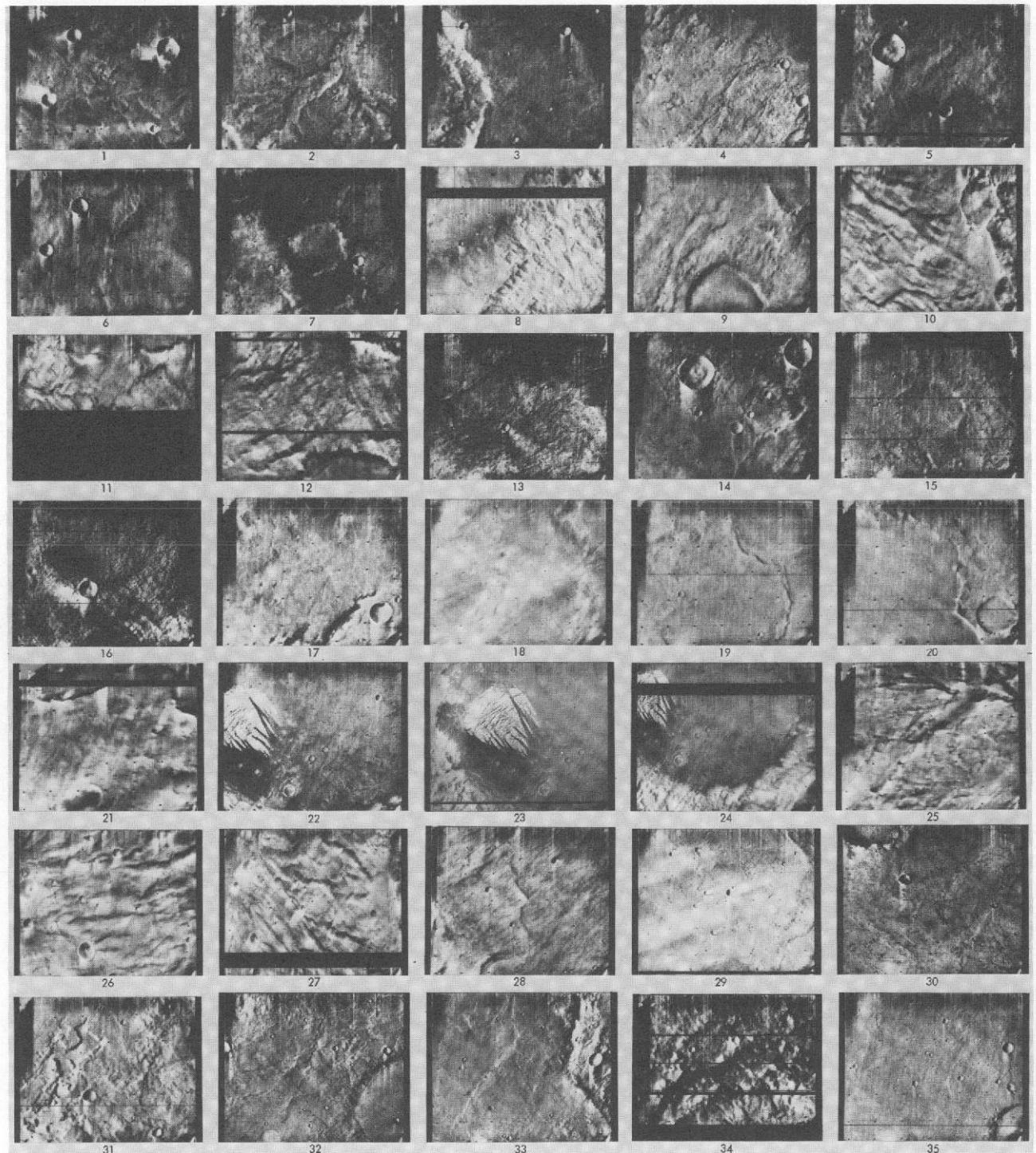


Fig. VII-7e. (contd). Narrow-angle frames (VAGC versions) that lie in the Sinus Sabaeus quadrangle: Revs 100–676; viewing angles less than 80°. Index numbers correspond to those on the photomosaic of this quadrangle and to Table VII-4e.



Fig. VII-7e. Narrow-angle frames in the Sinus Sabaeus quadrangle (contd).

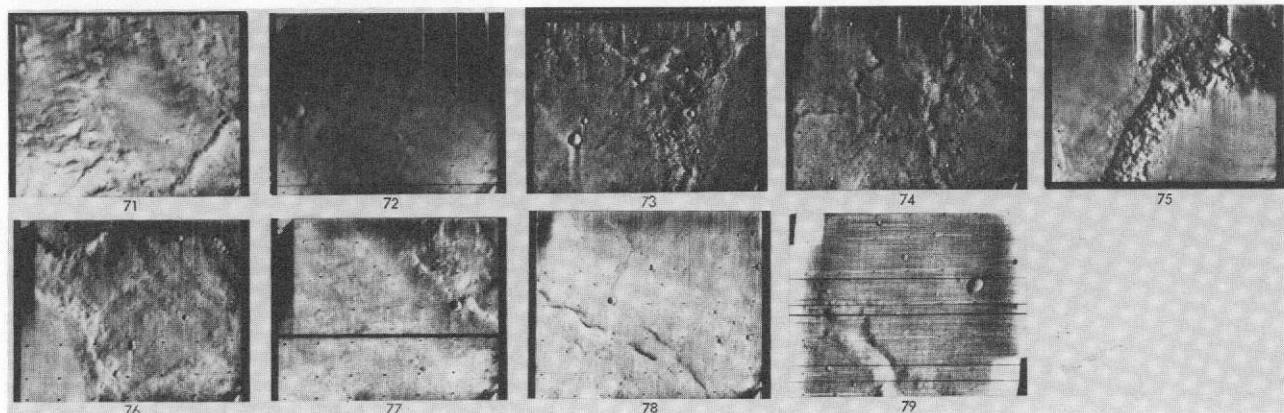
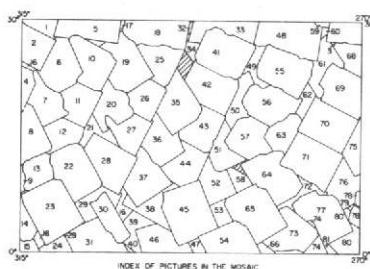
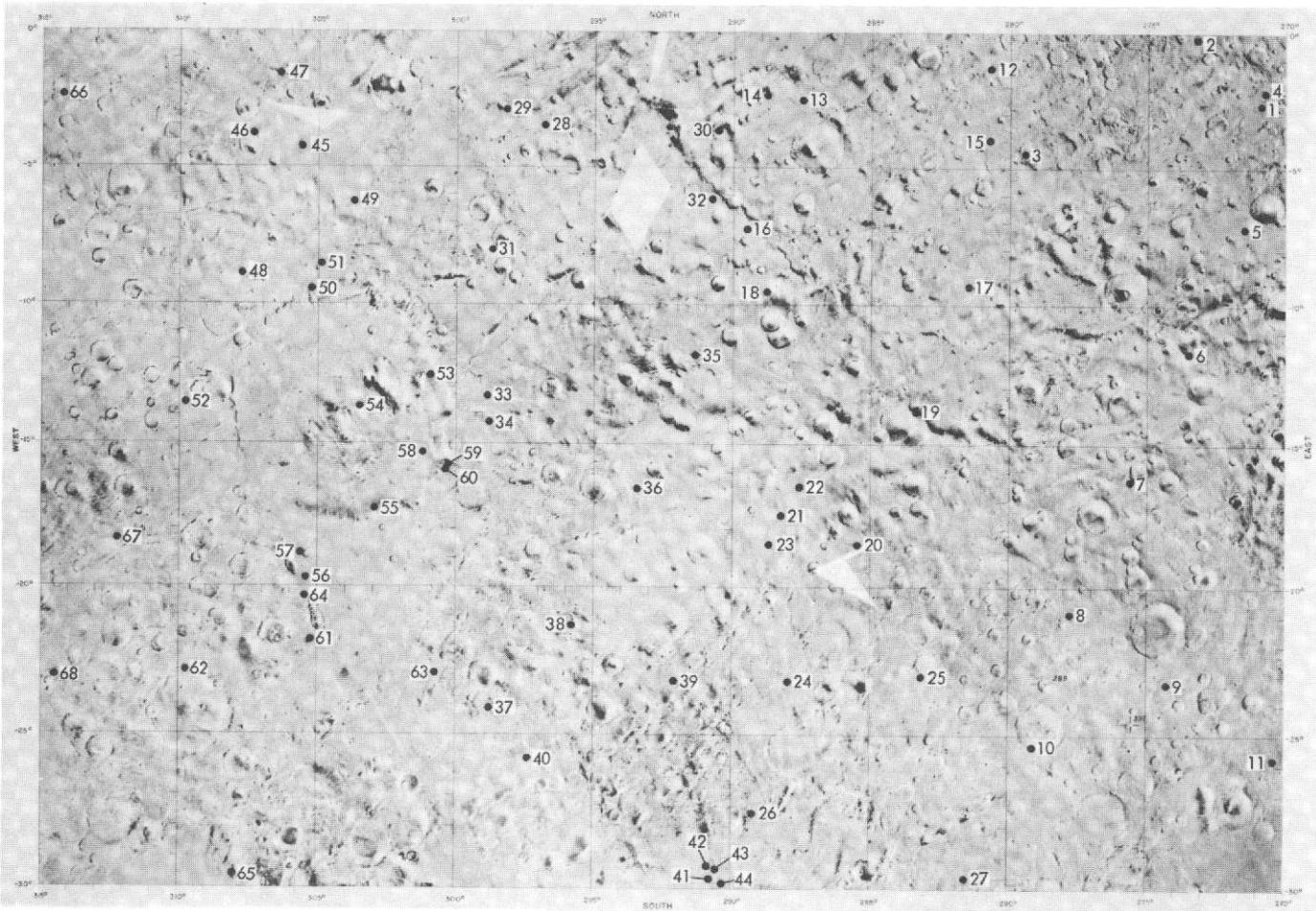


Fig. VII-7e. Narrow-angle frames in the Sinus Sabaeus quadrangle (contd.).



IDENTIFICATION NUMBERS OF PICTURES IN THE MOSAIC

Index No.	DAS No.	Index No.	DAS No.	Index No.	DAS No.
1	631113	38	7074593	65	7219753
2	630803	29	7074513	56	7218733
3	527293	30	8549349	57	7218643
4	630733	31	8549279	58	7218573
5	630733	32	7075213	59	7218203
6	8405569	33	710173	60	7218203
7	8405499	34	8549629	61	8693619
8	8405429	35	8549559	62	8693549
9	8405429	36	8549409	63	8693479
10	700783	37	8549119	64	8693399
11	700693	38	5743463	65	8693339
12	7002623	39	5743393	66	5867313
13	7002623	40	5743323	67	7291163
14	7002483	41	7146729	68	7290123
15	8477243	42	7146753	69	7290143
16	6460173	43	7146663	70	7290773
17	7075133	44	7146613	71	7290603
18	7075143	45	8549109	72	8693333
19	8477593	46	8621239	73	5887383
20	8477529	47	5815353	74	8765229
21	8477529	48	7219113	75	8765439
22	8477389	49	8571589	76	8765239
23	8477319	50	8621519	77	8765299
24	5671223	51	8621449	78	7367493
25	7074733	52	8621379	79	5959413
26	7074733	53	5815423	80	5959413
27	7074653	54	8693269	81	5959273

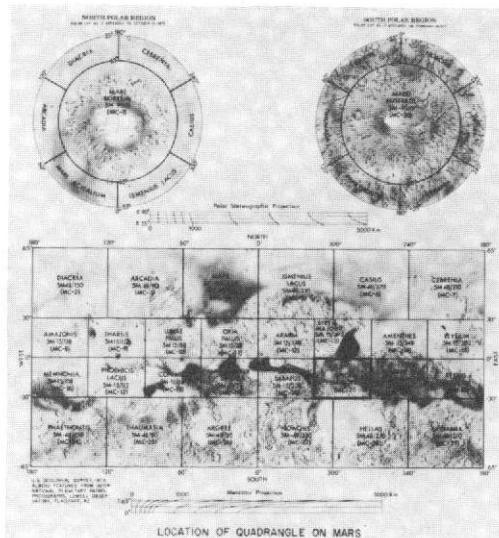


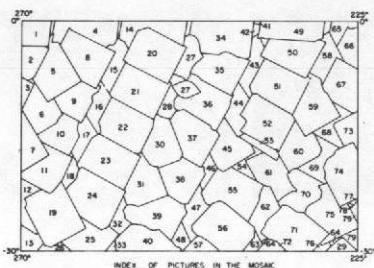
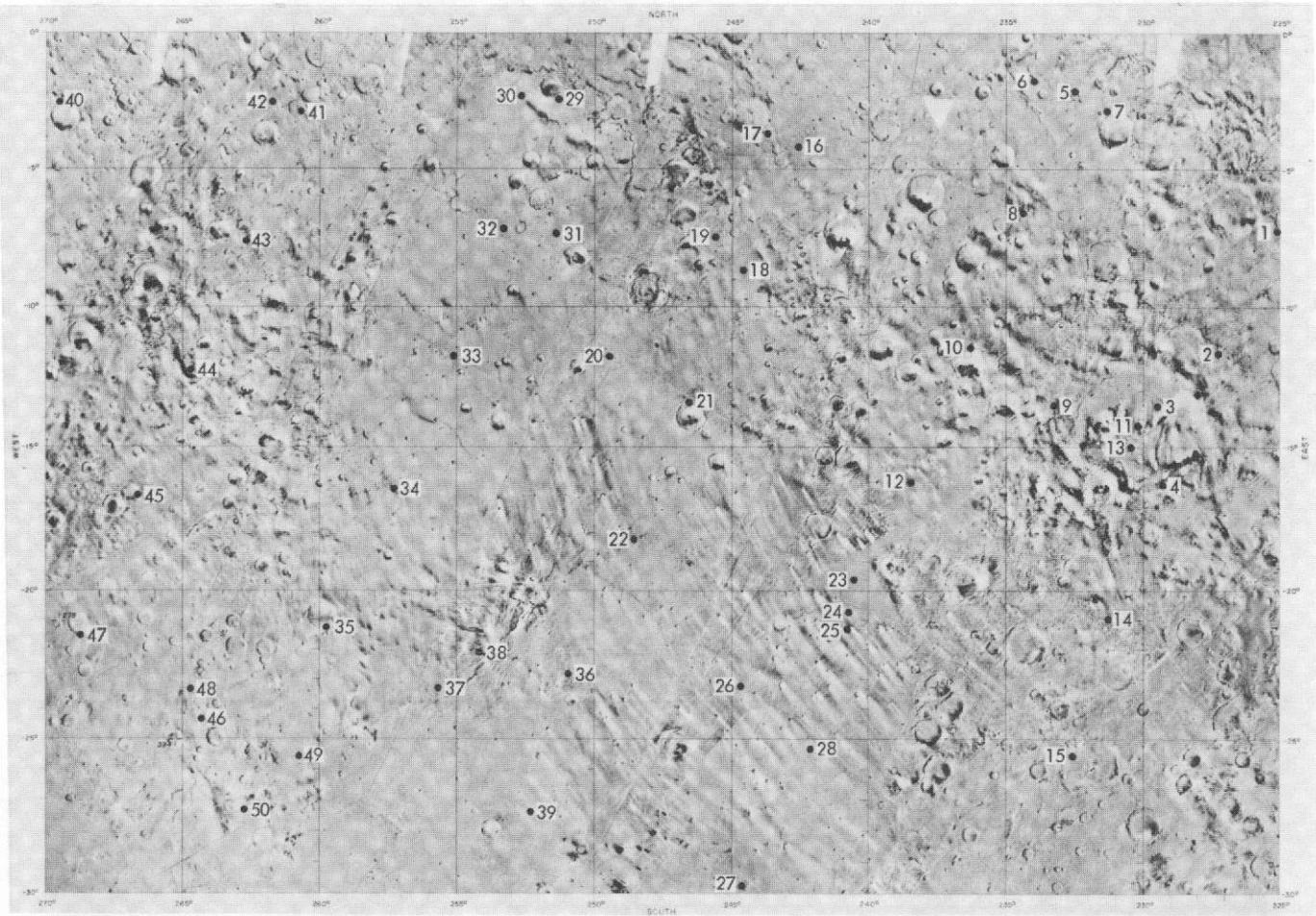
Fig. VII-7f. The Iapygia quadrangle (MC-21). Photomosaic of wide-angle mapping frames in Mercator Projection serving as index map for locations of narrow-angle frames. Index numbers on the photomosaic correspond to those for the accompanying narrow-angle frames and the data listings to Table VII-4f, and not to the charts and tables directly below the photomosaic.



Fig. VII-7f. (contd). Narrow-angle frames (VAGC versions) that lie in the lapygia quadrangle: Revs 100–676; viewing angles less than 80°. Index numbers correspond to those on the photomosaic of this quadrangle and to Table VII-4f. Images with little detail may have been underexposed (see histograms in original data and Section IV). Index No. 2 is a satellite frame introduced by computer error.



Fig. VII-7f. Narrow-angle frames in the lapygia quadrangle (contd).



IDENTIFICATION NUMBERS OF PICTURES IN THE MOSAIC

Index No.	DAS No.	Index No.	DAS No.	Index No.	DAS No.
1	7291365	28	8090359	55	7578303
2	7290813	29	6131863	56	6171533
3	7290743	30	8092039	57	6175083
4	7290743	31	8092040	58	6175084
5	8765579	32	8090149	59	9053209
6	8765509	33	8090797	60	9053139
7	8765459	34	7506973	61	9053069
8	8765459	35	8090798	62	9053070
9	7362703	36	7506553	63	9052929
10	7362653	37	7506483	64	5488663
11	7362563	38	7506413	65	7605233
12	8765459	39	7506414	66	7605234
13	8871389	40	6103793	67	7605403
14	7345083	41	7507043	68	7605333
15	8765309	42	8091139	69	7605193
16	8765469	43	8891139	70	7605193
17	8765399	44	8891139	71	6274043
18	8637329	45	8891139	72	6246973
19	8637329	46	8891139	73	6246973
20	7434733	47	8891139	74	9142959
21	5464665	48	8891033	75	9124889
22	5445993	49	7578933	76	9124819
23	5445993	50	7578933	77	9124819
24	5445433	51	7578513	78	5704753
25	6032303	52	5728443	79	6318933
26	6032303	53	5728443	80	6318933
	8090798	54	5728703	81	6318933

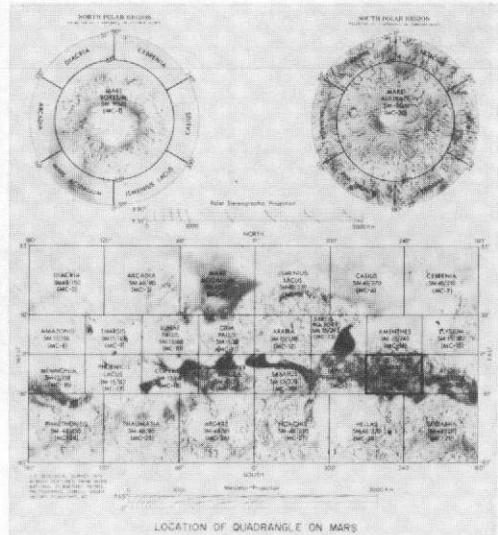


Fig. VII-7g. The Mare Tyrrhenum quadrangle (MC-22). Photomosaic of wide-angle mapping frames in Mercator Projection serving as index map for locations of narrow-angle frames. Index numbers on the photomosaic correspond to those for the accompanying narrow-angle frames and the data listings of Table VII-4g, and not to the charts and tables directly below the photomosaic.

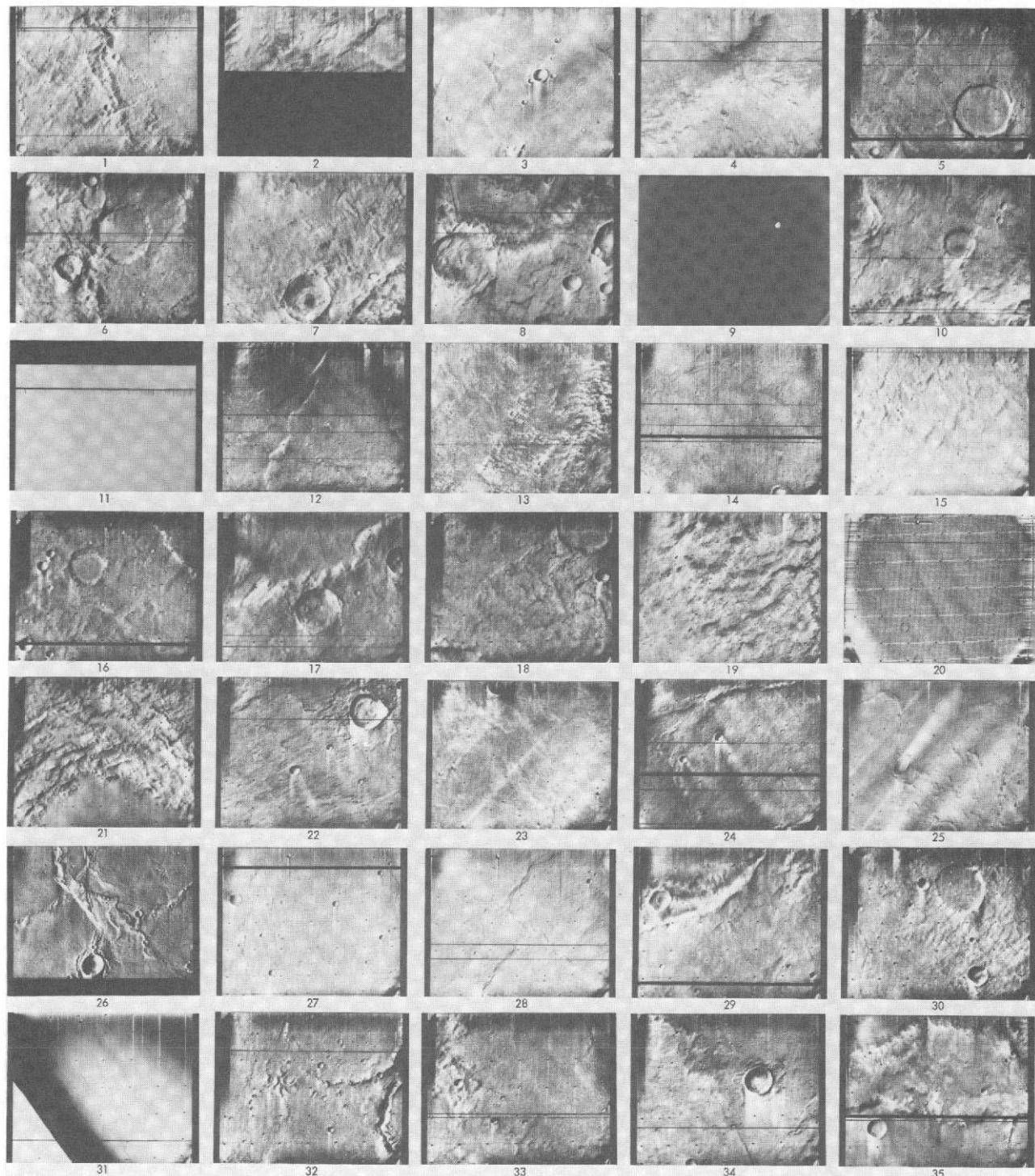


Fig. VII-7g. (contd). Narrow-angle frames (VAGC versions) that lie in the Mare Tyrrhenum quadrangle: Revs 100–676; viewing angles less than 80°. Index numbers correspond to those on the photomosaic and to Table VII-4g. Images with little detail may have been underexposed (see histograms in original data and Section IV). Index No. 9 is a satellite frame introduced by computer error.

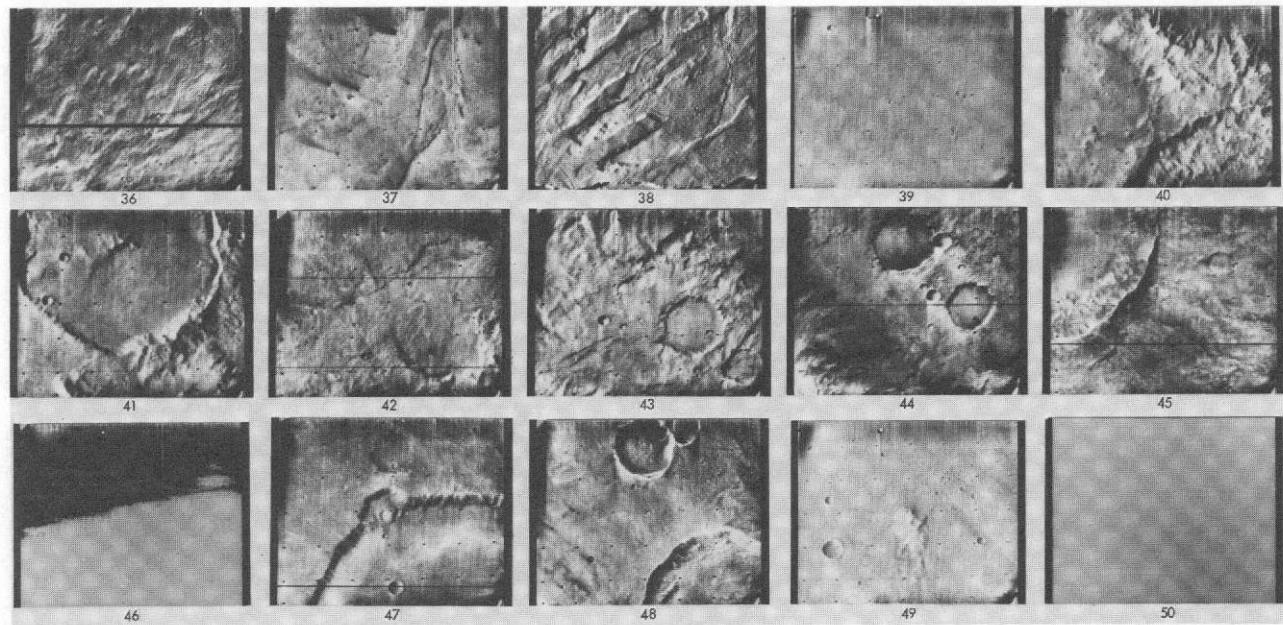
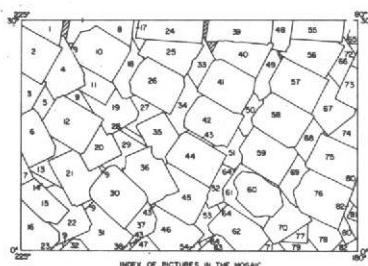
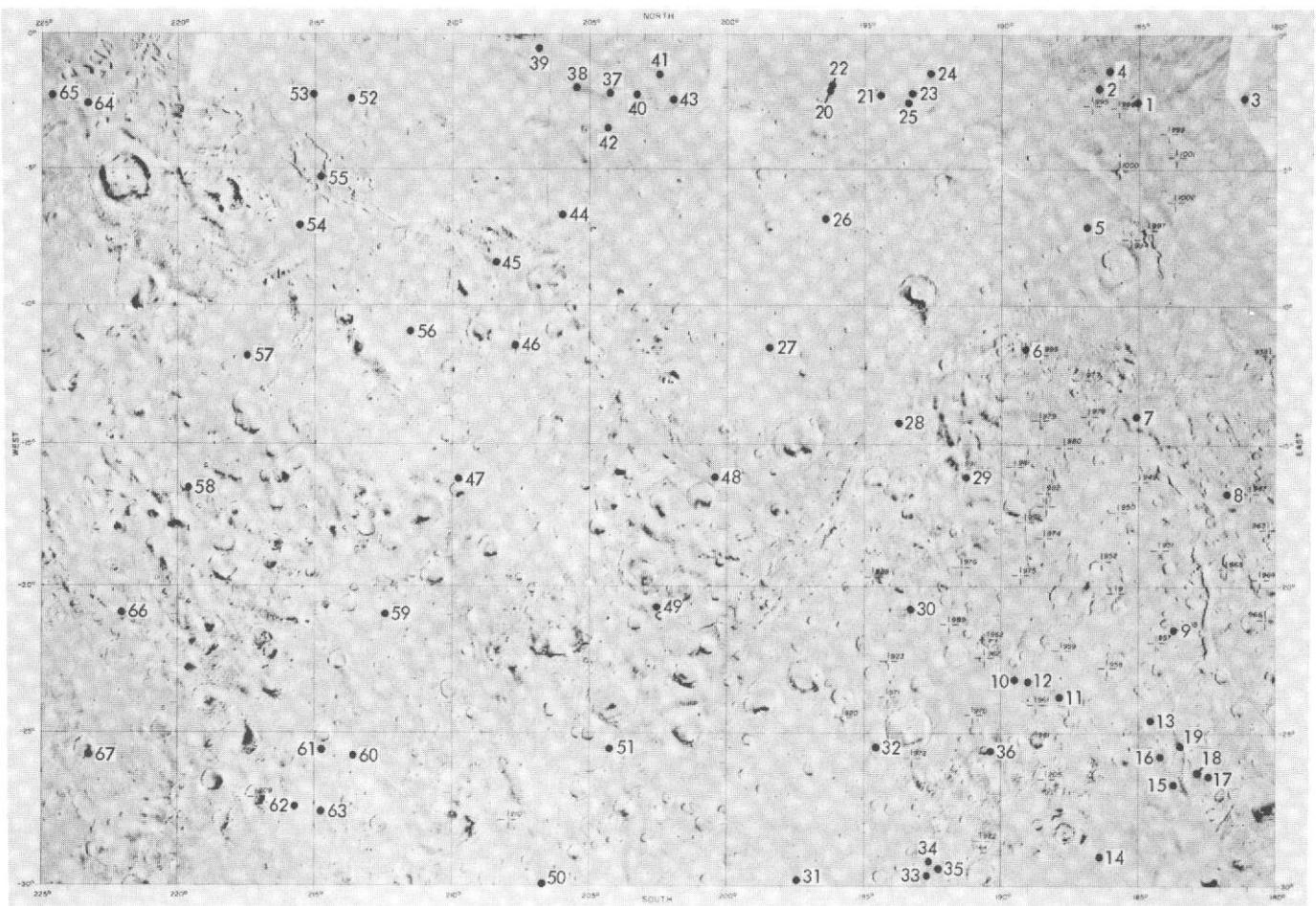


Fig. VII-7g. Narrow-angle frames in the Mare Tyrrhenum quadrangle (contd). Images with little detail may have been underexposed (see histograms in original data and Section IV).



IDENTIFICATION NUMBERS OF PICTURES IN THE MOSAIC

Index No.	DAS No.	Index No.	DAS No.	Index No.	DAS No.
1	7650823	29	7794043	57	7937963
2	7650473	30	6390893	58	7937893
3	7650103	31	6390833	59	7937833
4	9125169	32	6390753	60	6534673
5	9125099	33	9269949	61	7937753
6	9125029	34	9268879	62	6534603
7	9125059	35	9268879	63	6534533
8	7727713	36	9268739	64	5920773
9	5632793	37	9268669	65	6607333
10	7722363	38	9268599	66	8009783
11	7722353	39	7866133	67	8009733
12	7722223	40	7866143	68	8009643
13	7722153	41	7866073	69	8009573
14	7722083	42	7866003	70	8009503
15	6318900	43	5865933	71	8009433
16	6318933	44	7865933	72	6606393
17	5704753	45	7865863	73	6606913
18	9157059	46	6462713	74	6606843
19	9156989	47	6462713	75	8009753
20	9156519	48	13265301	76	6606703
21	9156849	49	9340639	77	9484199
22	9156779	50	9340769	78	5203483
23	9156709	51	9340769	79	5203413
24	7794203	52	9340659	80	8003393
25	7794253	53	9340559	81	6678593
26	7794183	54	9340489	82	9412799
27	7794113	55	7939383		
28	5757683	56	7938033		

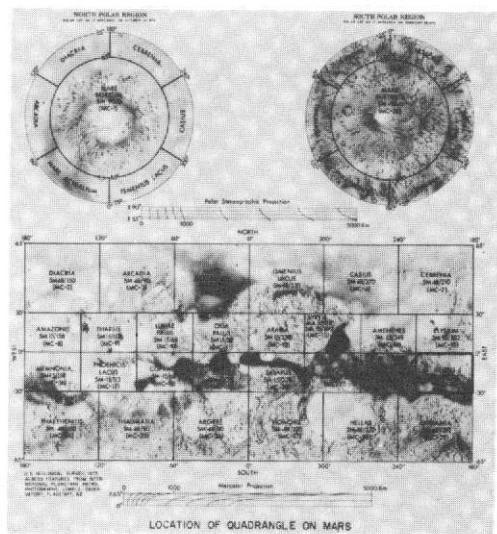


Fig. VII-7h. The Aeolis quadrangle (MC-23). Photomosaic of wide-angle mapping frames in Mercator Projection serving as index map for locations of narrow-angle frames. Index numbers on the photomosaic correspond to those for the accompanying narrow-angle frames and the data listings of Table VII-4h, and not to the charts and tables directly below the photomosaic.

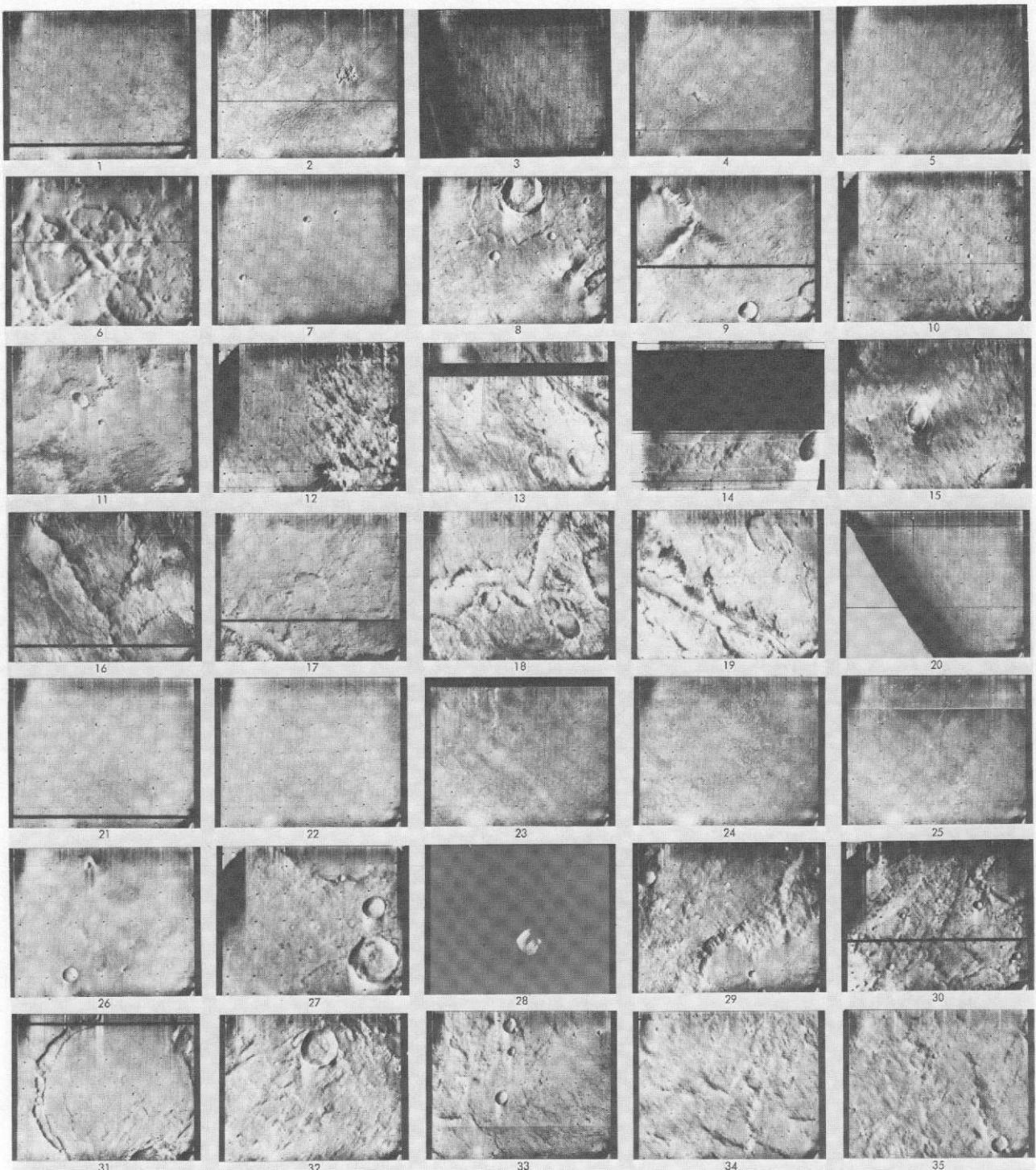


Fig. VII-7h. (contd). Narrow-angle frames (VAGC versions) that lie in the Aeolis quadrangle: Revs 100–676; viewing angles less than 80° . Index numbers correspond to those on the photomosaic of this quadrangle and to Table VII-4h. Index No. 28 is a satellite frame introduced by computer error.

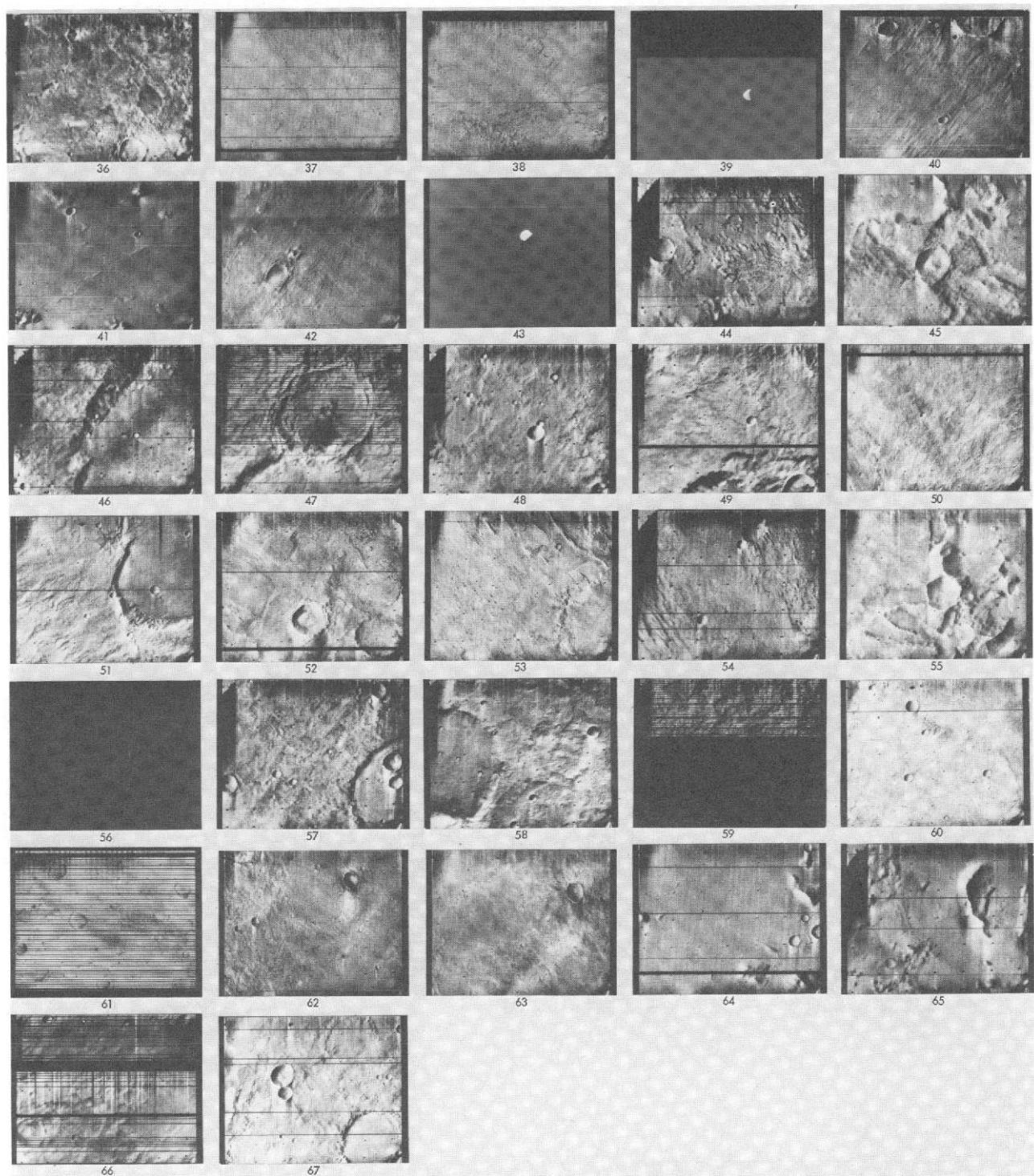


Fig. VII-7h. Narrow-angle frames in the Aeolis quadrangle (contd). Images with little detail may have been underexposed (see histograms in original data and Section IV). Index Nos. 39 and 43 are satellite frames introduced by computer error.

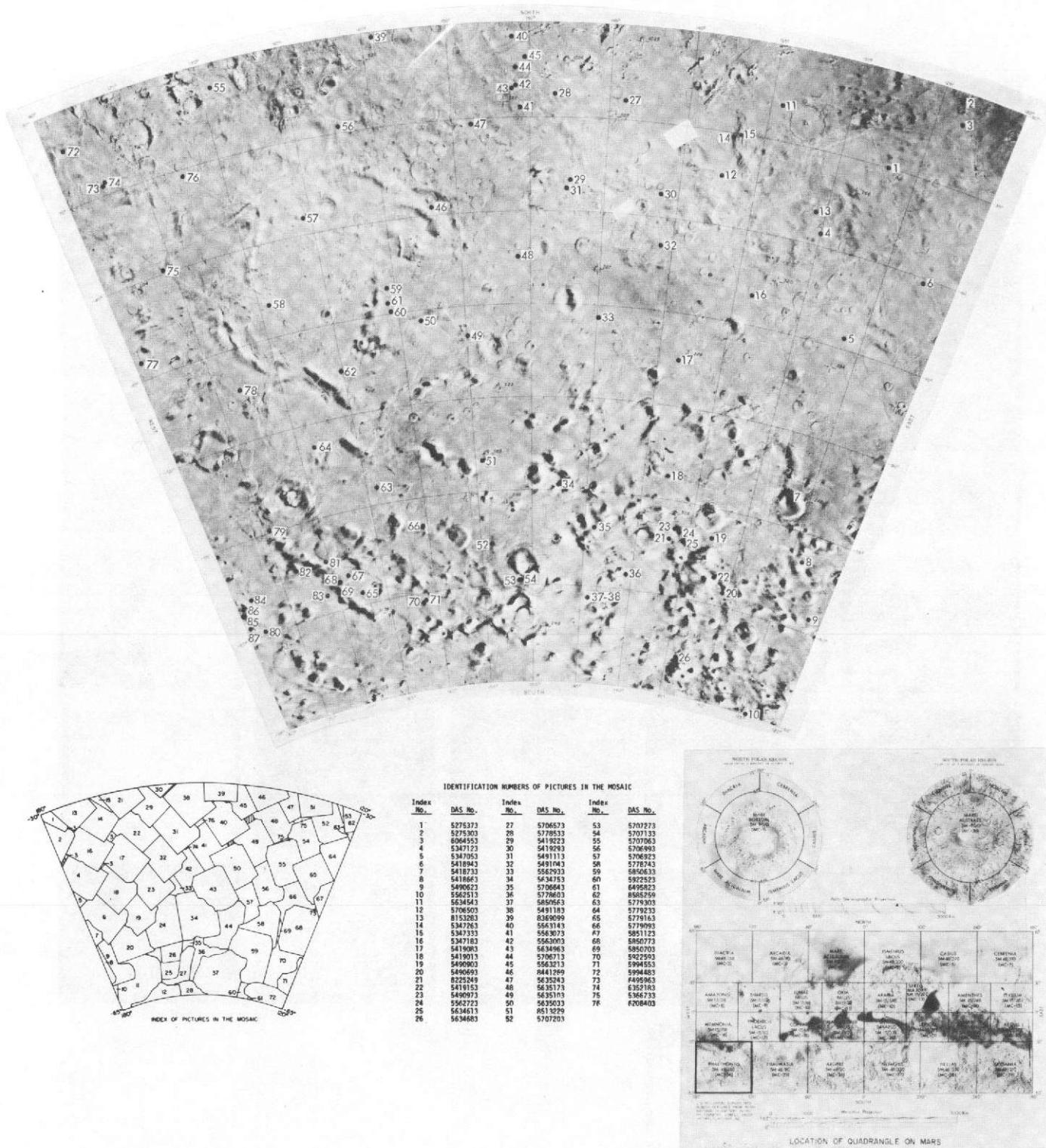


Fig. VII-7i. The Phaethontis quadrangle (MC-24). Photomosaic of wide-angle mapping frames in Lambert Projection serving as index map for locations of narrow-angle frames. Index numbers correspond to those for the accompanying narrow-angle frames and the data listings of Table VII-4i, and not to the charts and tables directly below the photomosaic.

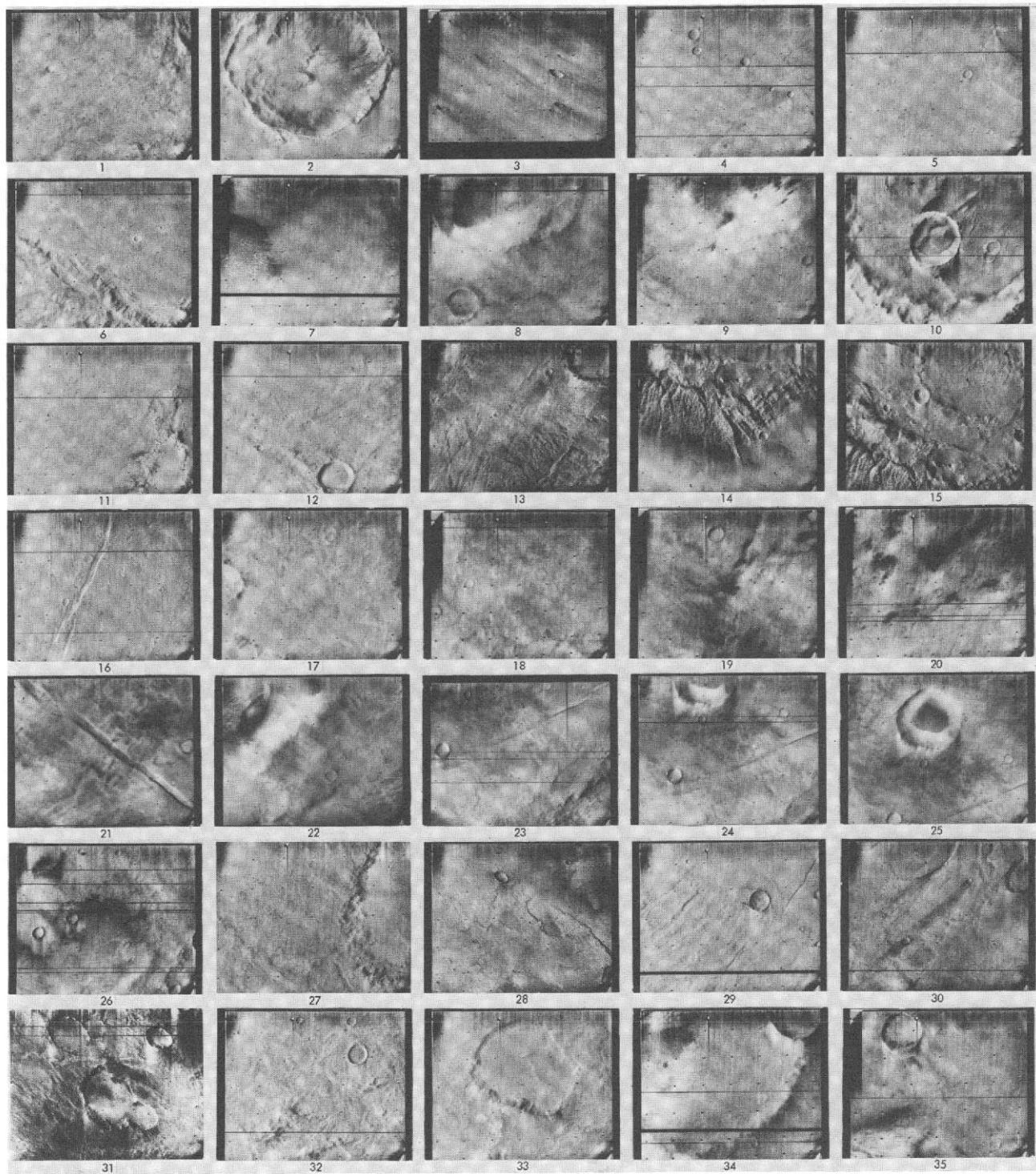


Fig. VII-7i. (contd). Narrow-angle frames (VAGC versions) that lie in the Phaethontis quadrangle: Revs 100-676; viewing angles less than 80°. Index numbers correspond to those on the photomosaic of this quadrangle and to Table VII-4i.

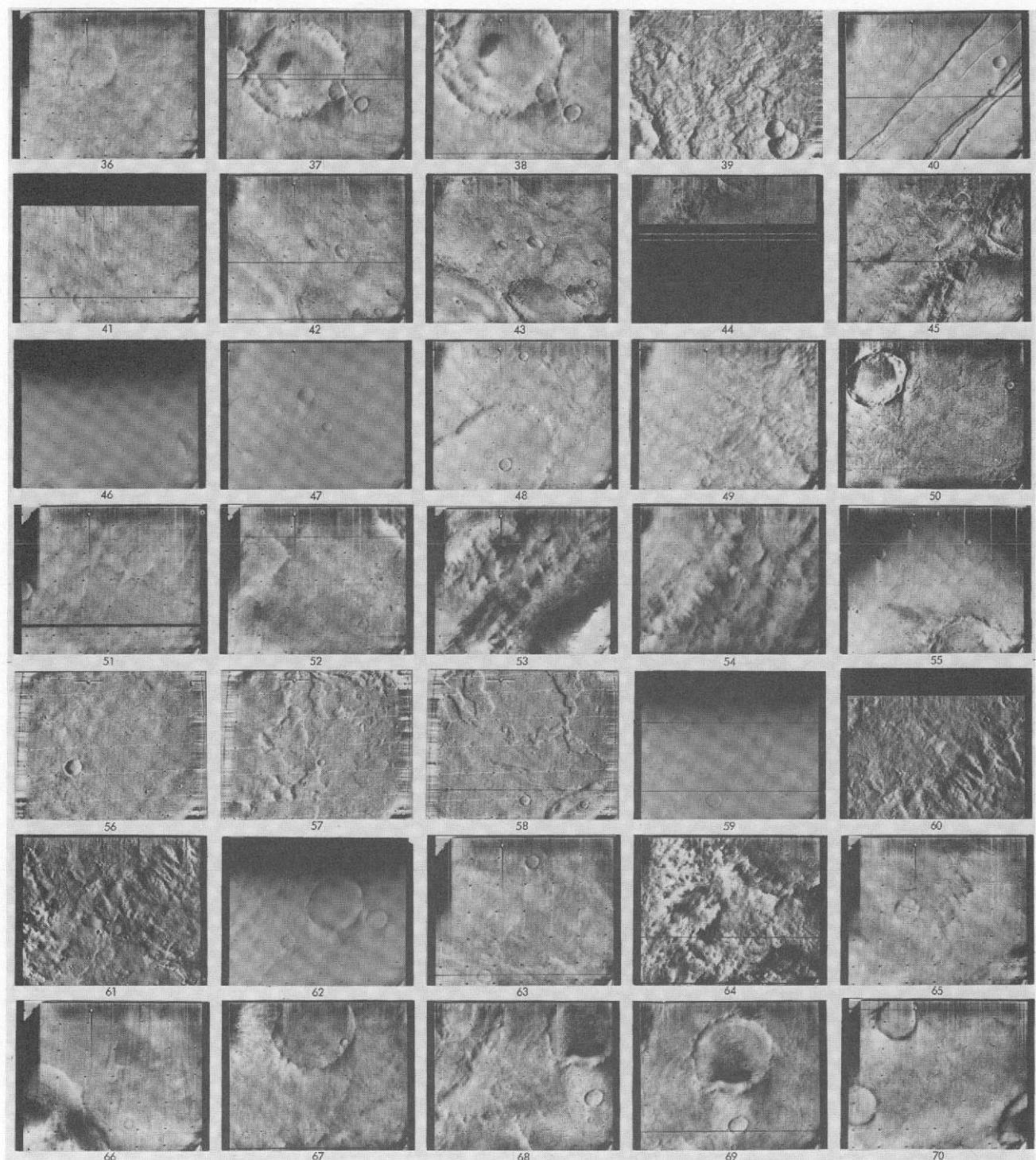


Fig. VII-7i. Narrow-angle frames in the Phaethontis quadrangle (contd).

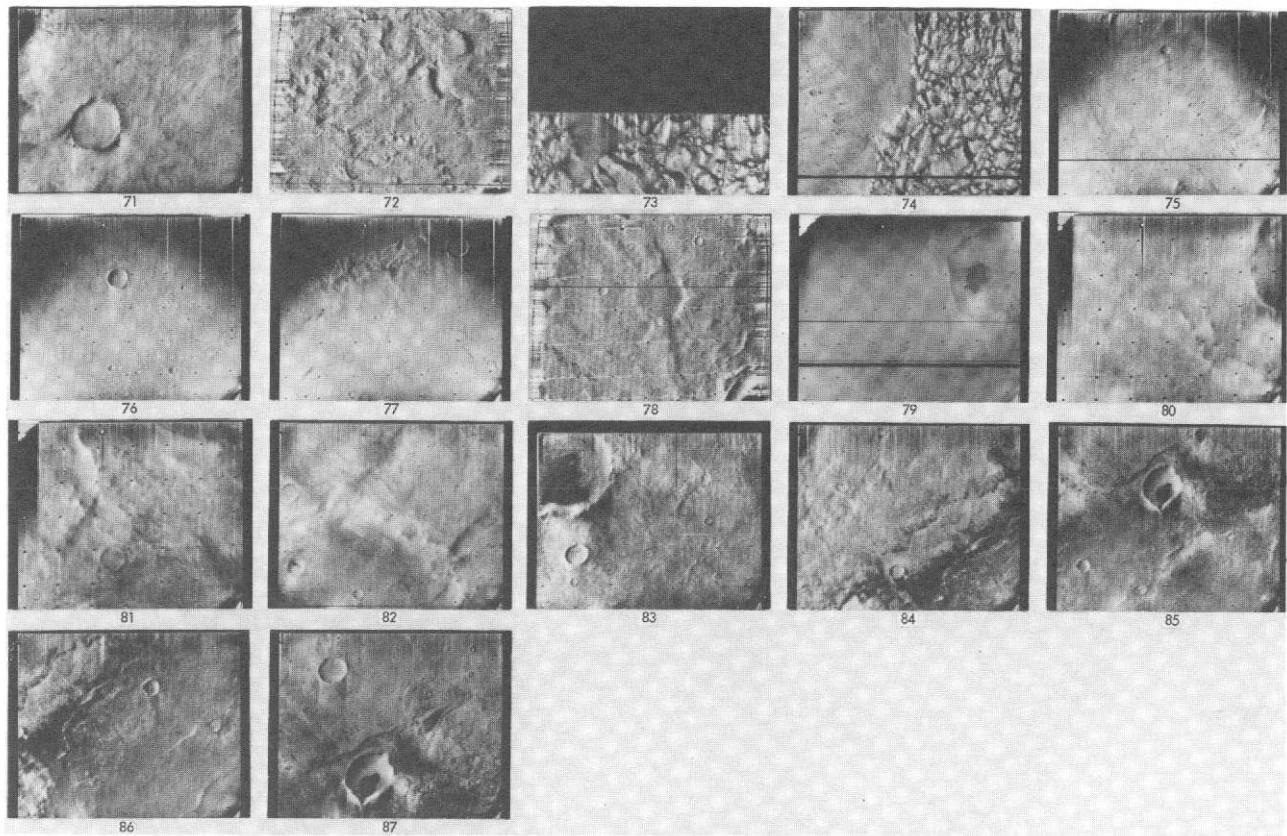
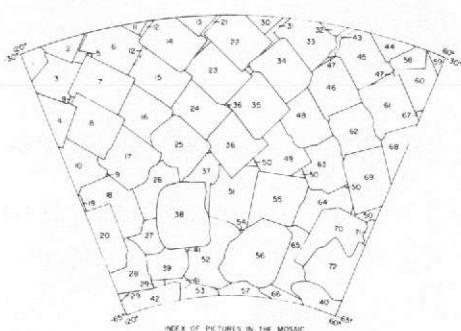
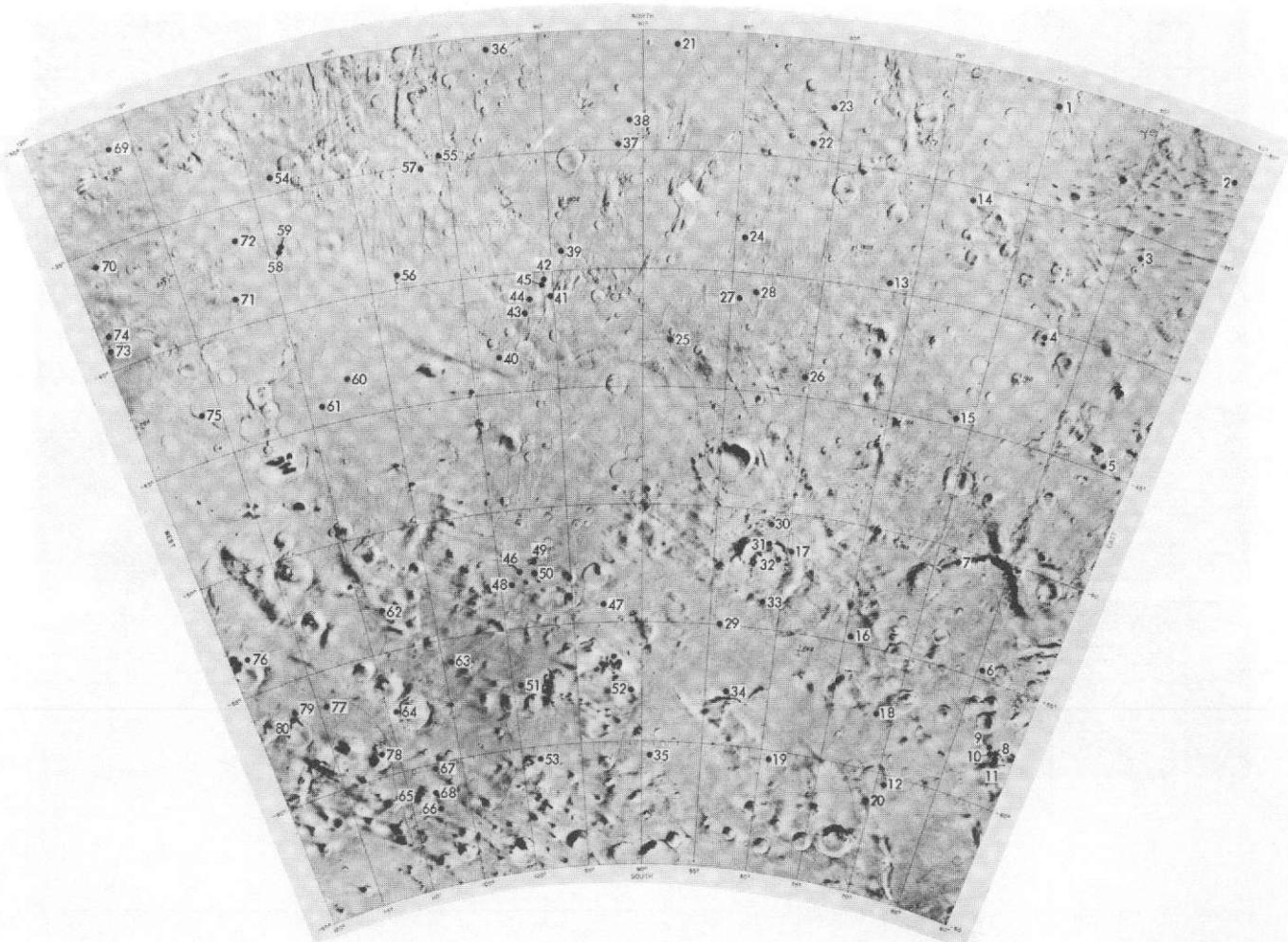


Fig. VII-7i. Narrow-angle frames in the Phaethontis quadrangle (contd).



IDENTIFICATION NUMBERS OF PICTURES IN THE MOSAIC

Index No.	IANS No.	Index No.	IANS No.	Index No.	IANS No.
1	8585259	25	5995043	49	6138895
2	5236873	26	5995044	50	6138896
3	5775350	27	5994623	51	6138545
4	5779233	28	5994553	52	6210293
5	8657219	29	6066443	53	6282113
6	5851163	30	6066444	54	6282135
7	5851163	31	8873169	55	6210433
8	5851193	32	6067283	56	6282183
9	5236873	33	6067215	57	6354603
10	5851163	34	6067216	58	6354649
11	5851403	35	6067073	59	6211063
12	8729240	36	6067003	60	6210993
13	5923363	37	6066653	61	6210223
14	5923363	38	6066654	62	6210853
15	5923223	39	6066513	63	6210785
16	5923153	40	6497783	64	6282323
17	5923083	41	6138403	65	6354073
18	5923083	42	6138404	66	6354083
19	5850773	43	8945059	67	6282813
20	5922663	44	6139173	68	6282745
21	8585153	45	8139173	69	6282775
22	5995153	46	8139153	70	6354143
23	5995183	47	5452683	71	6426633
24	5995113	48	6138963	72	6425963

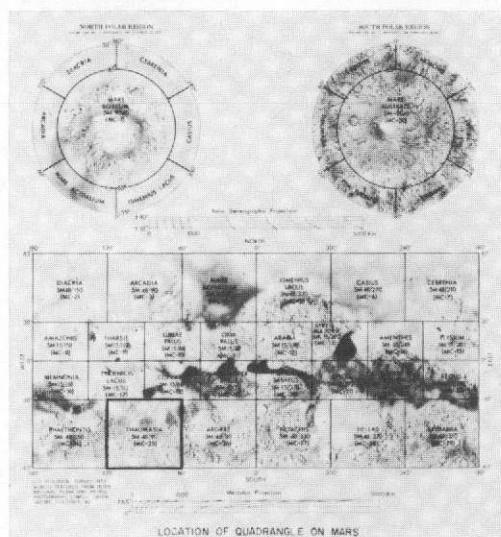


Fig. VII-7j. The Thaumasia quadrangle (MC-25). Photomosaic of wide-angle mapping frames in Lambert Projection serving as index map for locations of narrow-angle frames. Index numbers correspond to those for the accompanying narrow-angle frames and the data listings of Table VII-4j, and not to the charts and tables directly below the photomosaic.

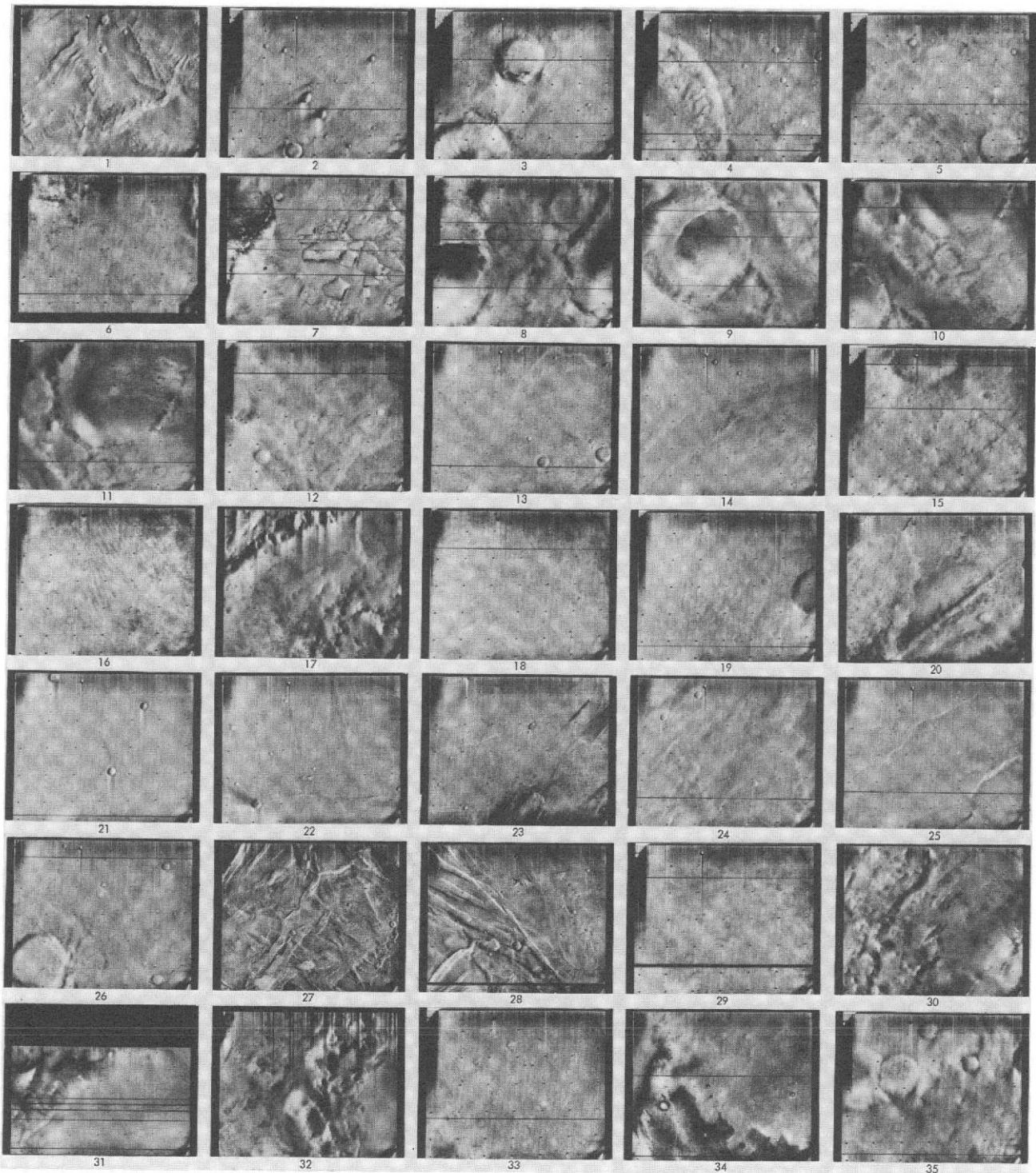


Fig. VII-7j. (contd). Narrow-angle frames (VAGC versions) that lie in the Thaumasia quadrangle: Revs 100–676; viewing angles less than 80° . Index numbers correspond to those on the photomosaic of this quadrangle and to Table VII-4j.

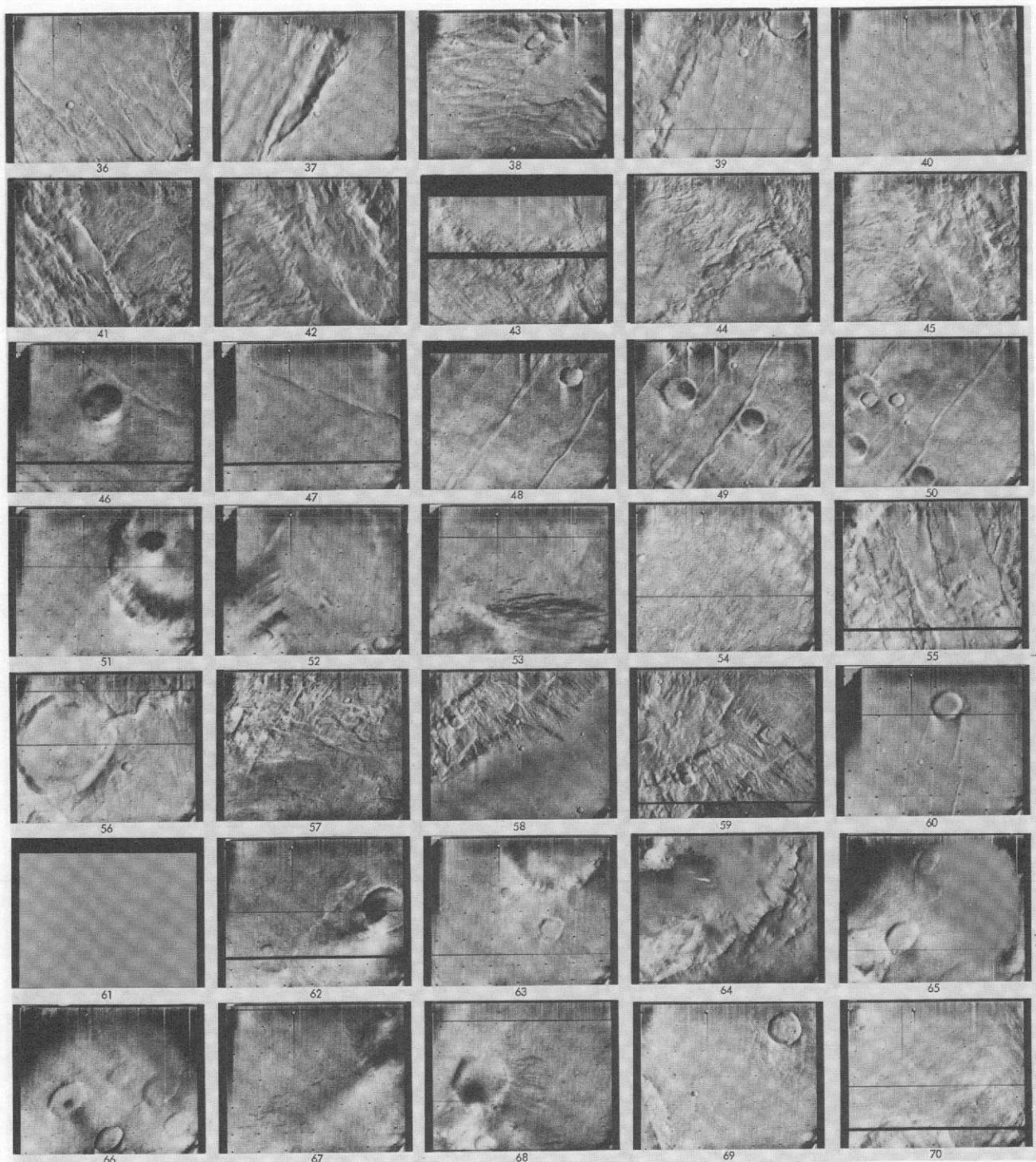


Fig. VII-7j. Narrow-angle frames in the Thaumasia quadrangle (contd). Images with little detail may have been underexposed (see histograms in original data and Section IV).

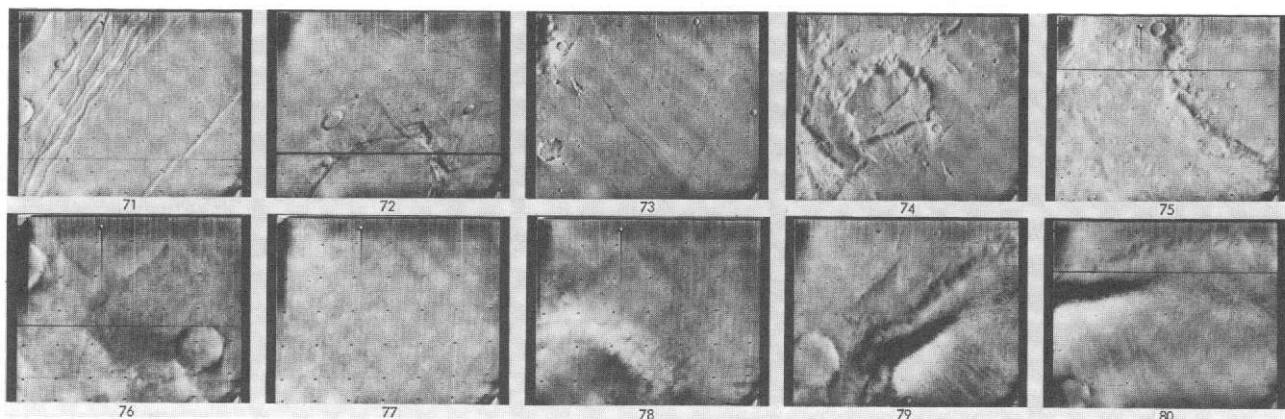
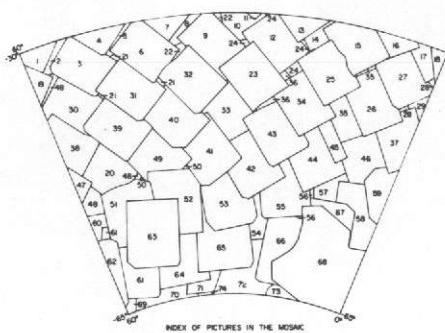


Fig. VII-7j. Narrow-angle frames in the Thaumasia quadrangle (contd.).



IDENTIFICATION NUMBERS OF PICTURES IN THE MOSAIC

Index No.	DAS No.	Index No.	DAS No.	Index No.	DAS No.
1	6211063	26	6239253	51	6476103
2	6208839	27	6239313	52	6476191
3	6238373	28	6239323	53	5164943
4	6287953	29	5311213	54	5238633
5	9160729	30	6239213	55	5238603
6	6239233	31	6239223	56	5954413
7	6354843	32	6426593	57	5310883
8	9232619	33	6426413	58	5327533
9	6234213	34	6117223	59	5327553
10	9304529	35	6209573	60	6476033
11	6426733	36	5817673	61	6476253
12	6468553	37	6111133	62	6476263
13	6468523	38	6297747	63	6476293
14	7973453	39	6354633	64	5166003
15	5167433	40	6426523	65	5238703
16	6083133	41	6209523	66	5327573
17	5239383	42	6167153	67	5328683
18	117303	43	5167223	68	7432703
19	6239213	44	5239113	69	6476123
20	6354563	45	5239103	70	5094703
21	5596673	46	5311173	71	6238693
22	5596713	47	6239173	72	5327543
23	6083133	48	5526603	73	5454503
24	5812693	49	6426453	74	5740523
25	5167353	50	6856743		

INDEX OF PICTURES IN THE MOSAIC

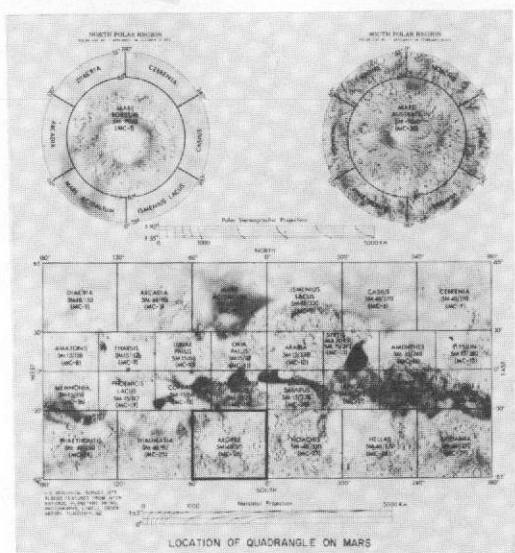


Fig. VII-7k. The Argyre quadrangle (MC-26). Photomosaic of wide-angle mapping frames in Lambert Projection serving as index map for locations of narrow-angle frames. Index numbers correspond to those for the accompanying narrow-angle frames and the data listings of Table VII-4k, and not to the charts and tables directly below the photomosaic.

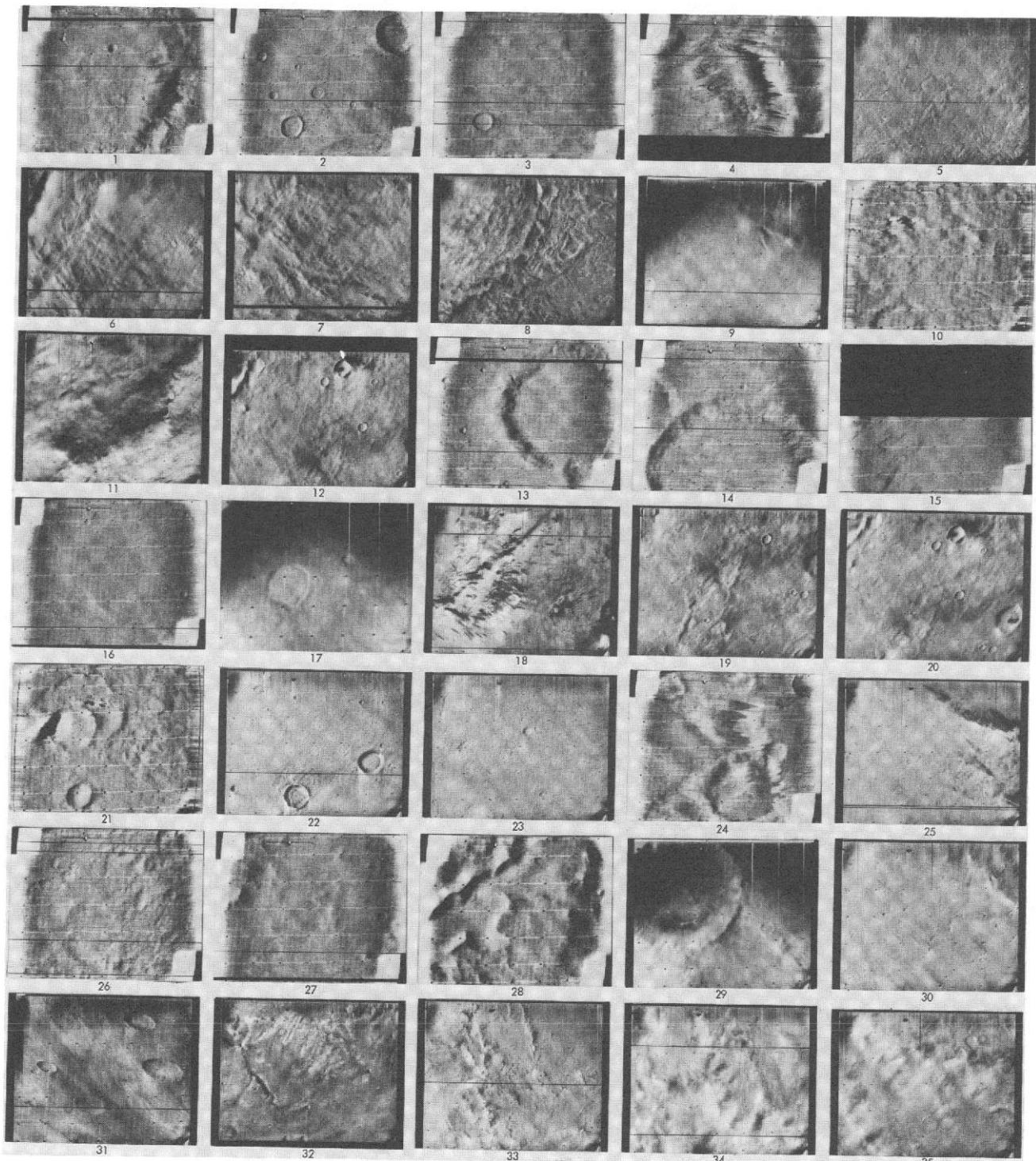


Fig. VII-7k. (contd). Narrow-angle frames (VAGC versions) that lie in the Argyre quadrangle: Revs 100–676; viewing angles less than 80° . Index numbers correspond to those on the photomosaic of this quadrangle and to Table VII-4k.

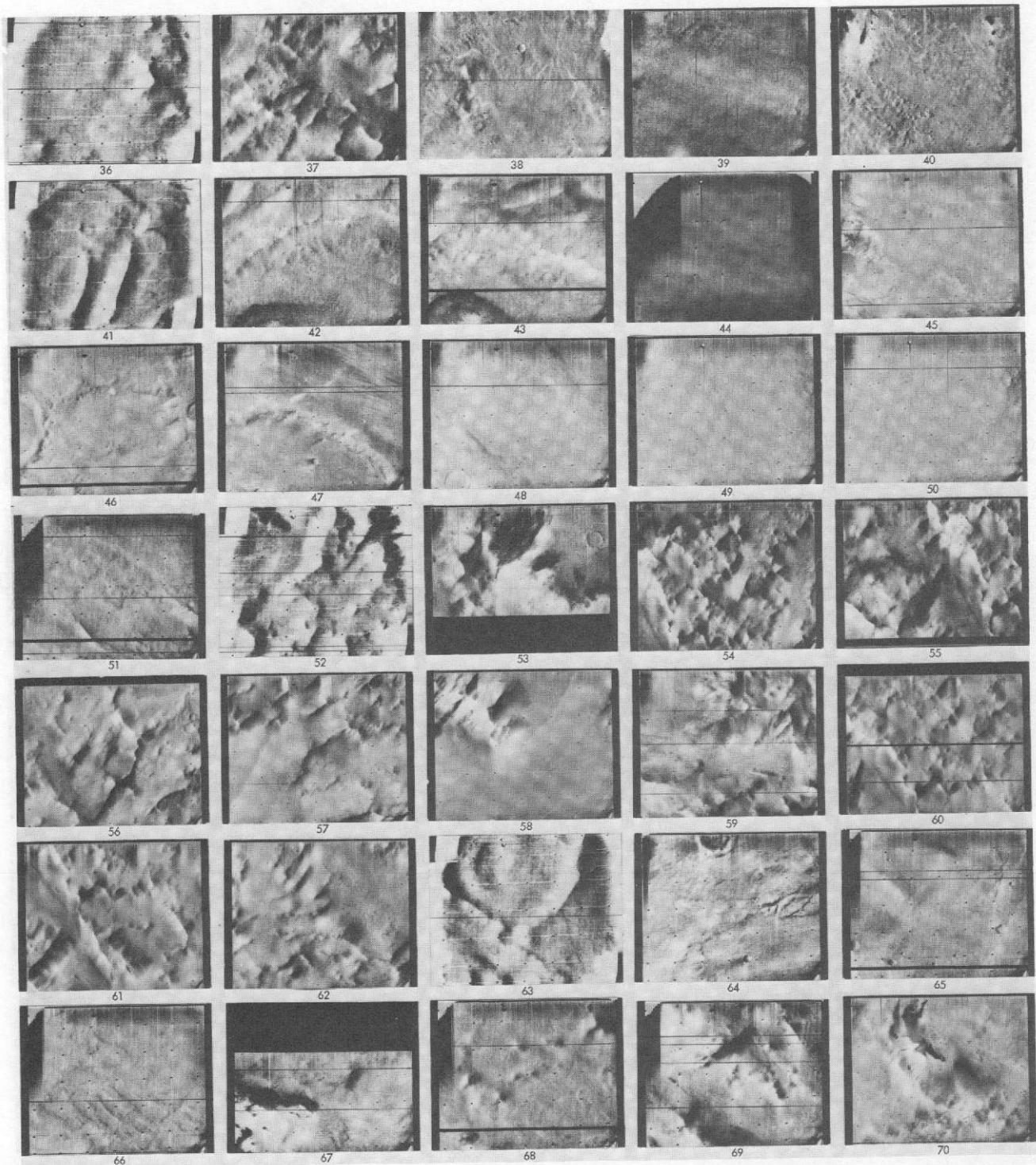


Fig. VII-7k. Narrow-angle frames in the Argyre quadrangle (contd).

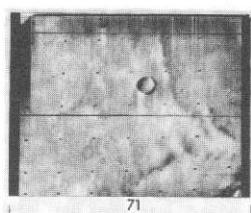
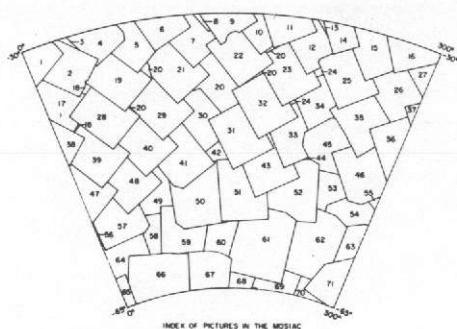
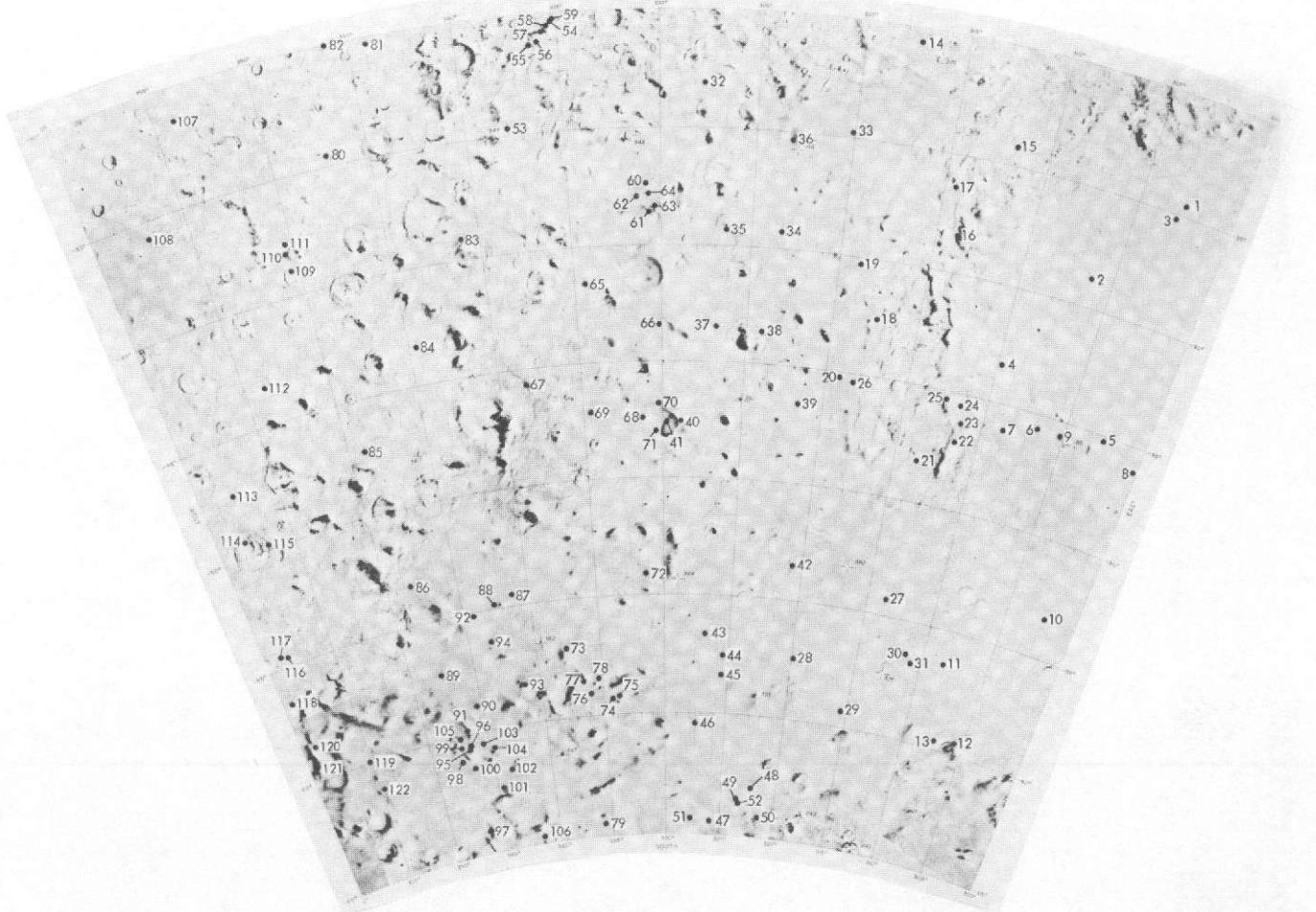


Fig. VII-7k. Narrow-angle frames in the Argyre quadrangle (contd).



IDENTIFICATION NUMBERS OF PICTURES IN THE MOSAIC

Index No.	DAS No.	Index No.	DAS No.	Index No.	DAS No.
1	811793	26	541113	49	5539743
2	544233	27	5743253	50	5536703
3	5311353	27	5743123	51	5670733
4	6108269	28	5363103	51	5742763
5	5302129	29	5402163	53	5670723
6	6261129	30	5527023	53	5686463
7	5455203	31	5598983	55	5686753
8	5454203	32	5598993	56	5686443
9	8333259	33	5671013	57	5454713
10	5527273	34	5671063	58	6526773
11	5411119	36	5311103	59	5670793
12	5598913	36	5015143	60	5742723
13	5599263	37	5015213	61	5614563
14	5477248	38	5311143	62	5601113
15	5423123	39	5383133	63	5958573
16	8549279	40	5454993	64	6526603
17	5454993	41	5598993	65	5526633
18	6030578	42	5598913	66	5670523
19	5363173	43	5670943	67	5742553
20	6243308	44	5670979	68	5611113
21	5453173	45	5743113	69	5958544
22	5527163	46	5815073	70	5686503
23	5598913	47	5828953	71	6030464
24	6640508	48	5454923		

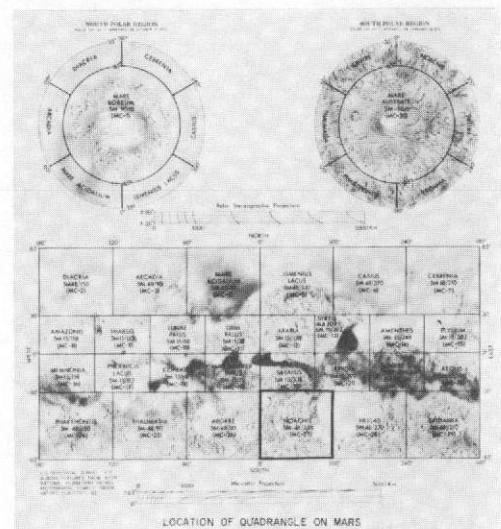


Fig. VII-71. The Noachis quadrangle (MC-27). Photomosaic of wide-angle mapping frames in Lambert Projection serving as index map for locations of narrow-angle frames. Index numbers correspond to the accompanying narrow-angle frames and the data listings of Table VII-41, and not to the charts and tables directly below the photomosaic.



Fig. VII-7I. (contd). Narrow-angle frames (VAGC versions) that lie in the Noachis quadrangle: Revs 100–676; viewing angles less than 80° . Index numbers correspond to those on the photomosaic of this quadrangle and to Table VII-4I. Images with little detail may have been underexposed (see histograms in original data and Section IV).

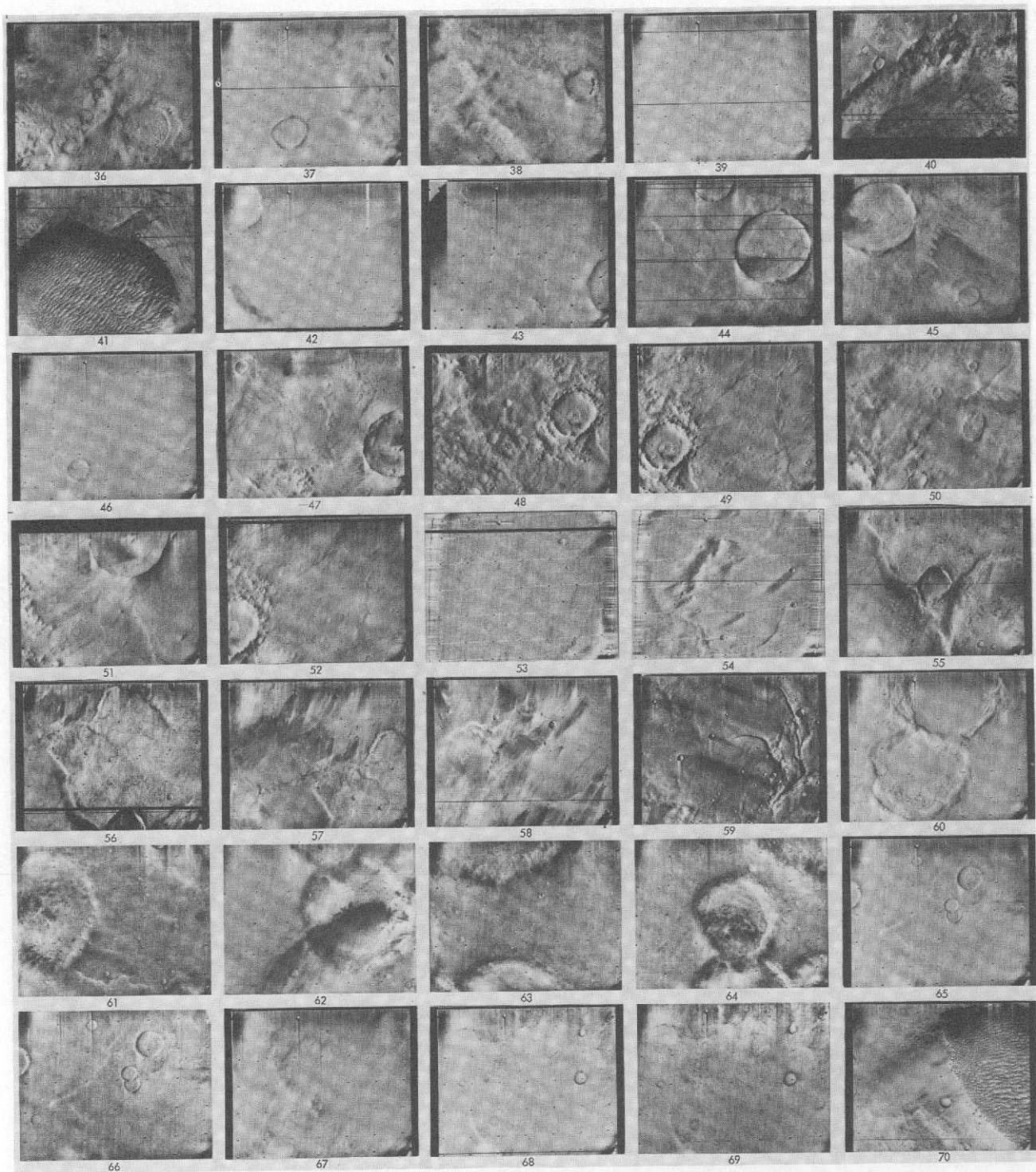


Fig. VII-7I. Narrow-angle frames in the Noachis quadrangle (contd).

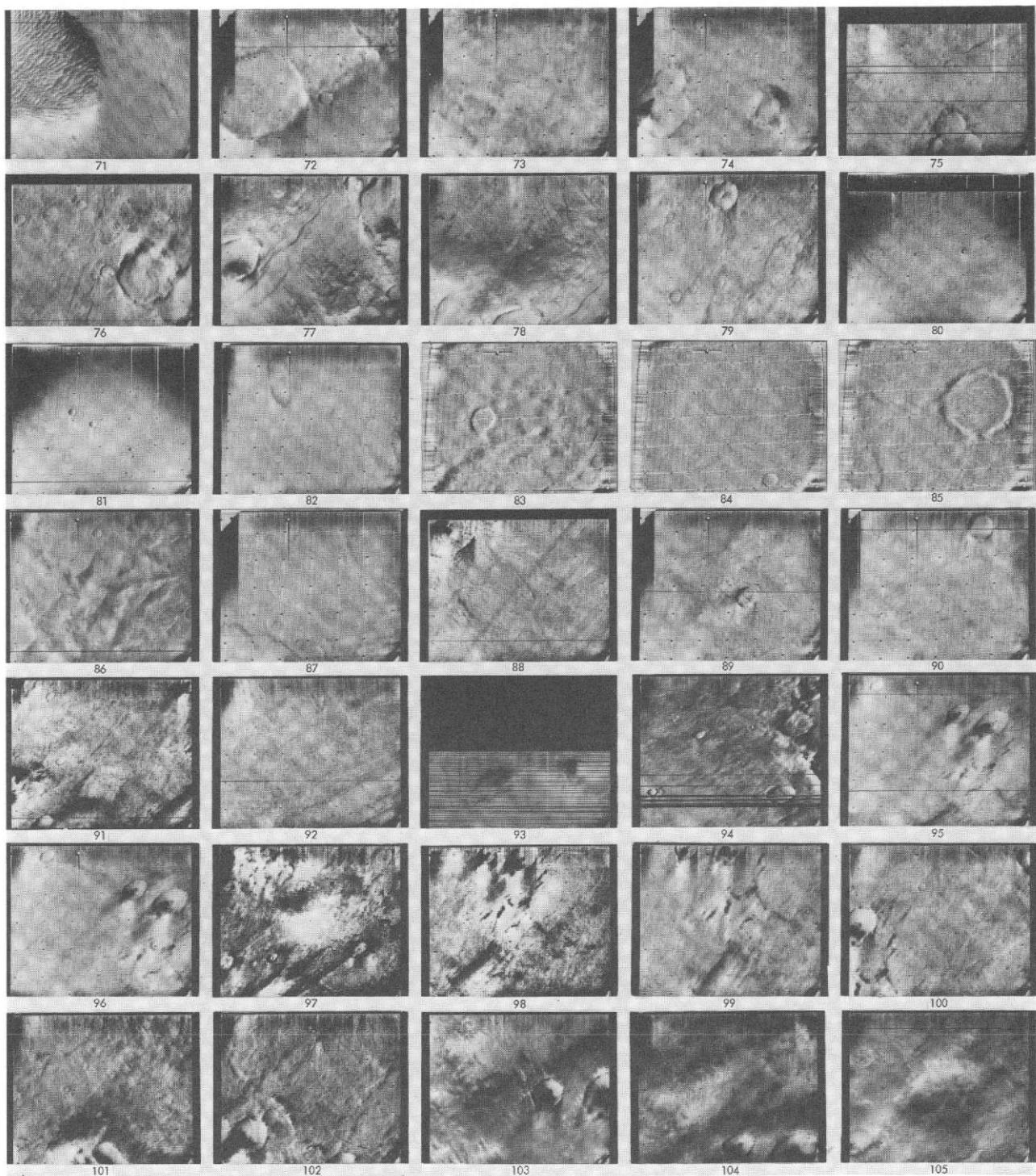


Fig. VII-7I. Narrow-angle frames in the Noachis quadrangle (contd).

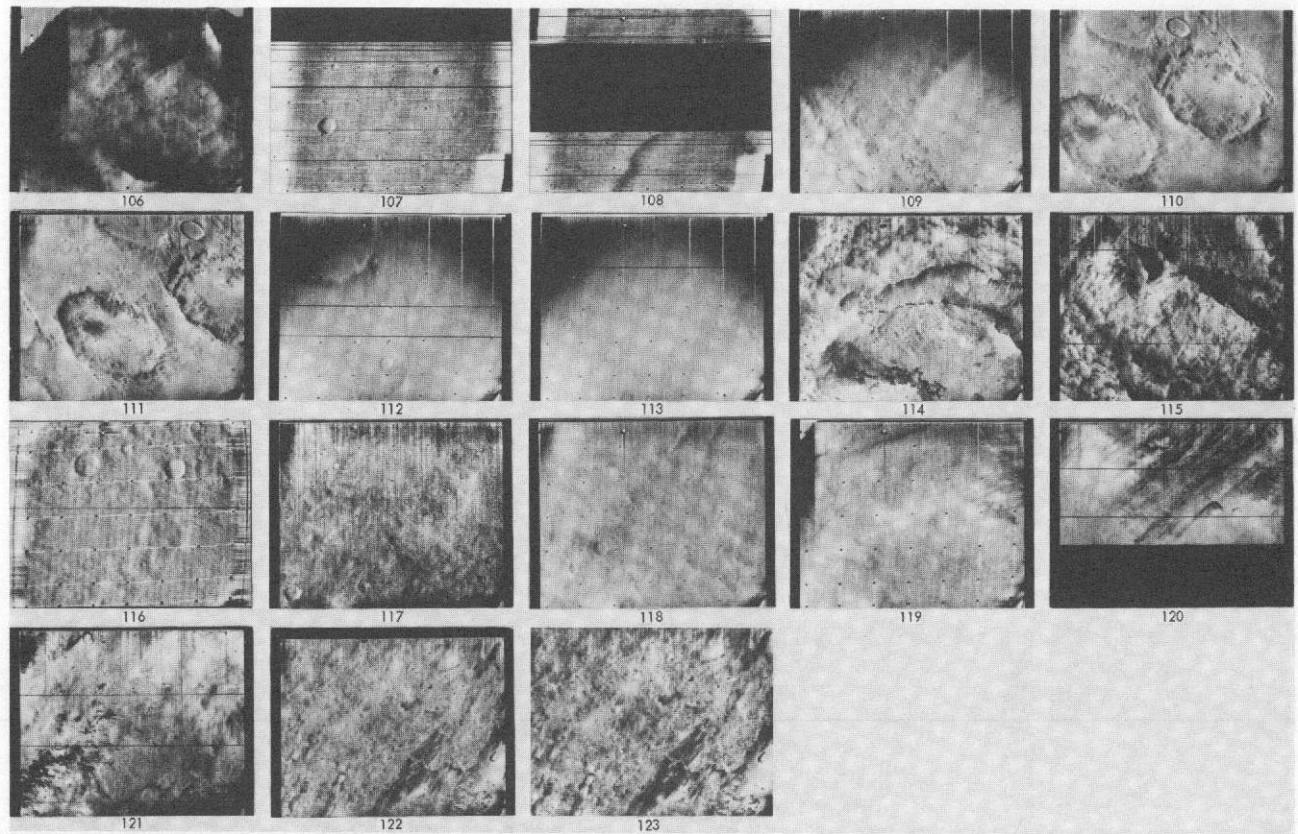
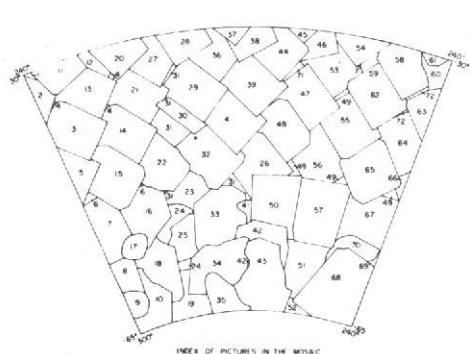
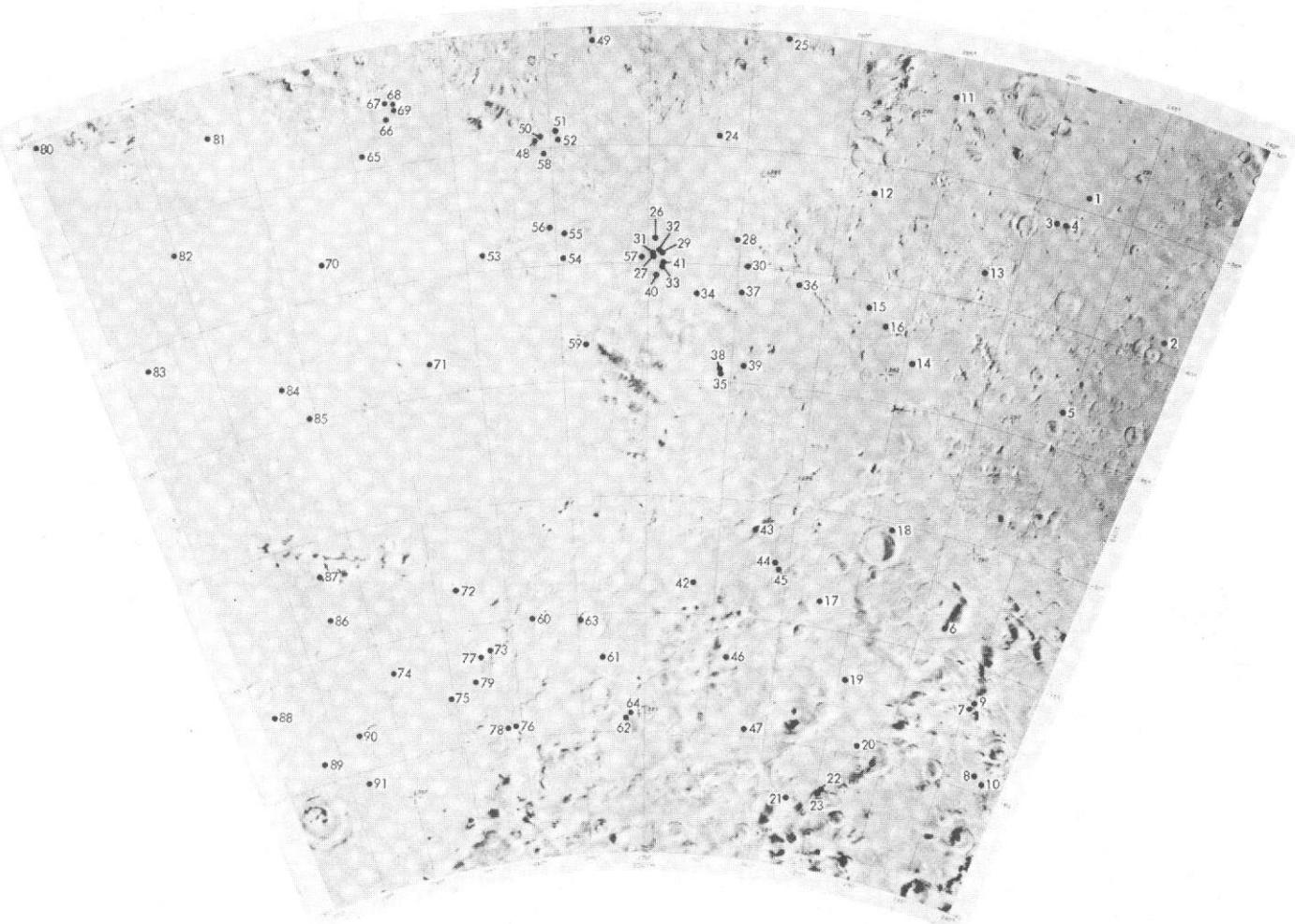


Fig. VII-71. Narrow-angle frames in the Noachis quadrangle (contd).



Index No.	DAS No.	Index No.	DAS No.	Index No.	DAS No.
1	5743393	25	6102493	49	5488593
2	5813323	26	6102913	50	6318573
3	5815213	27	5897313	51	6318163
4	5200893	28	8765229	52	6389983
5	5813293	29	9499229	53	6103133
6	6531473	30	5895133	54	6103193
7	5896683	31	5272788	55	6174943
8	5958573	32	6131023	56	6174873
9	6039353	33	6131023	57	6246833
10	6102353	34	6246203	58	6175063
11	8621239	35	6245713	59	8981039
12	5815353	36	5954973	60	9052929
13	5813293	37	6131023	61	6131023
14	5887173	38	8837189	62	6175013
15	5887103	39	6031163	63	6246903
16	5958713	40	6031093	64	6246833
17	5896543	41	6131023	65	6246833
18	6030533	42	6246213	66	6318653
19	6174313	43	6318093	67	6318303
20	8693269	44	6031233	68	6461873
21	5887143	45	6031233	69	6318053
22	5959063	46	8909079	70	6390053
23	6030673	47	6103053	71	5344743
24	6030603	48	6102983	72	5416703

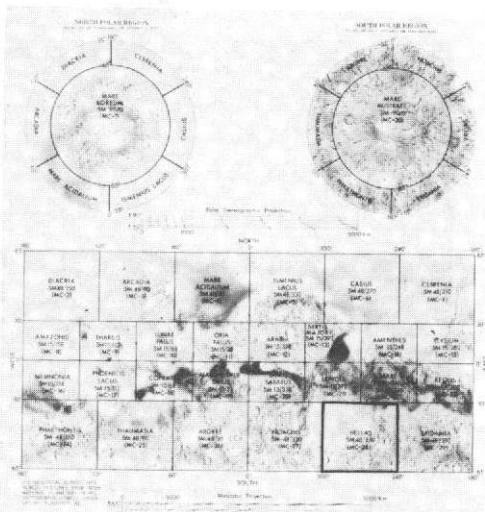


Fig. VII-7m. The Hellas quadrangle (MC-28). Photomosaic of wide-angle mapping frames in Lambert Projection serving as index map for locations of narrow-angle frames. Index numbers correspond to those for the accompanying narrow-angle frames and the picture data listings of Table VII-4m, and not to the charts and tables directly below the photomosaic.

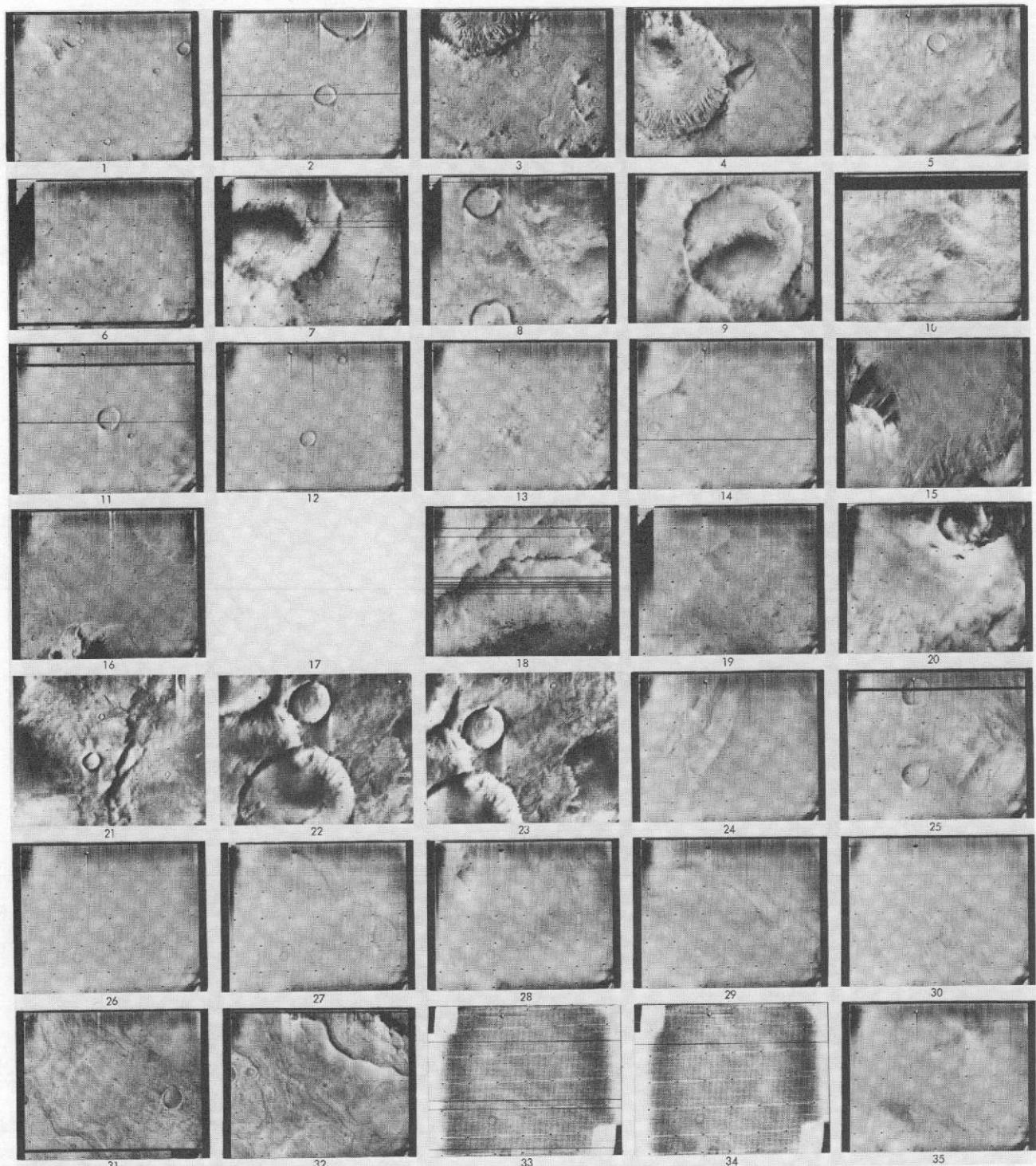


Fig. VII-7m. (contd). Narrow-angle frames (VAGC versions) that lie in the Hellas quadrangle: Revs 100–676; viewing angles less than 80° . Index numbers correspond to those on the photomosaic of this quadrangle and to Table VII-4m. Blanks denote pictures planned but not recovered.

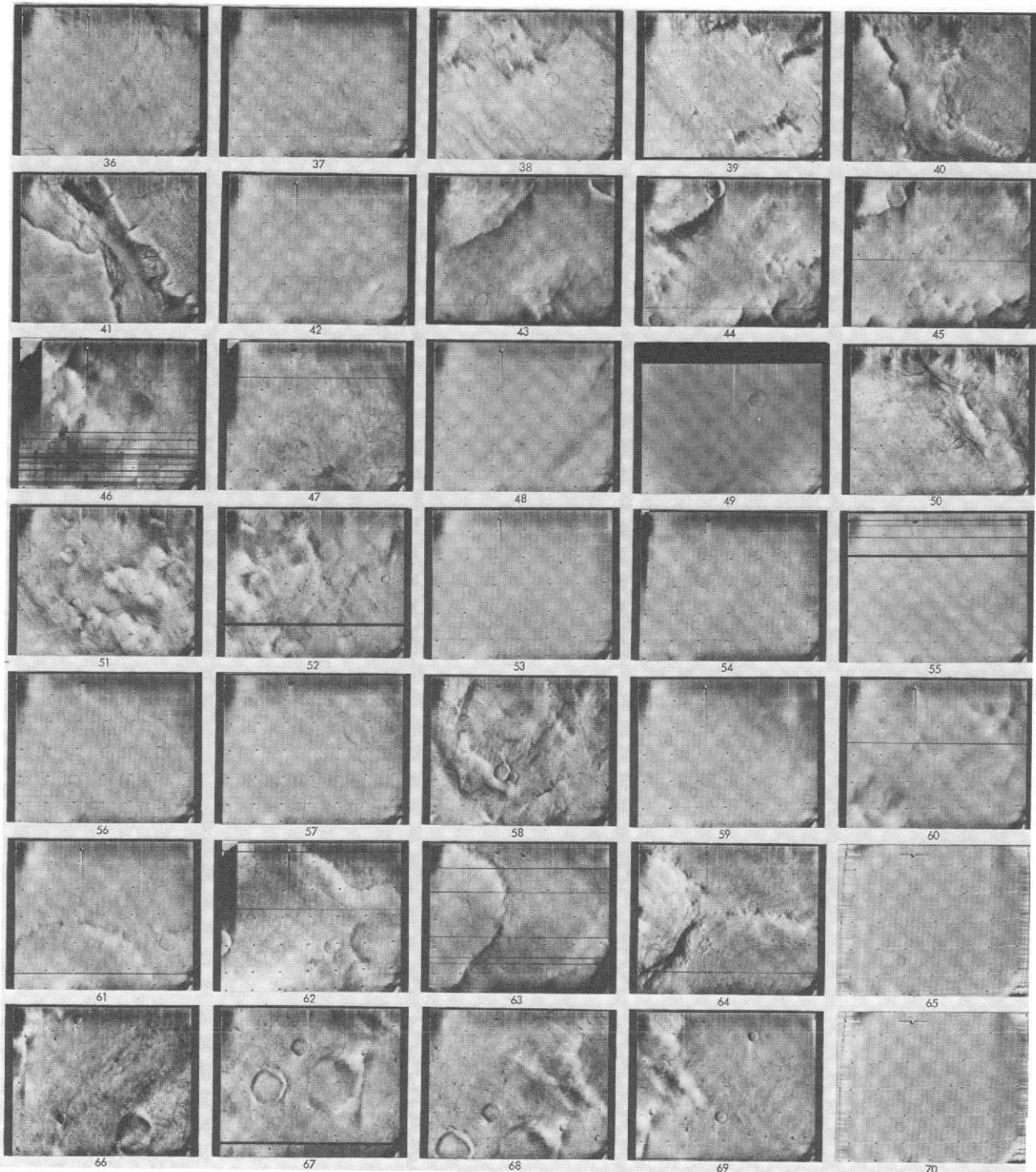


Fig. VII-7m. Narrow-angle frames in the Hellas quadrangle (contd).

17
C

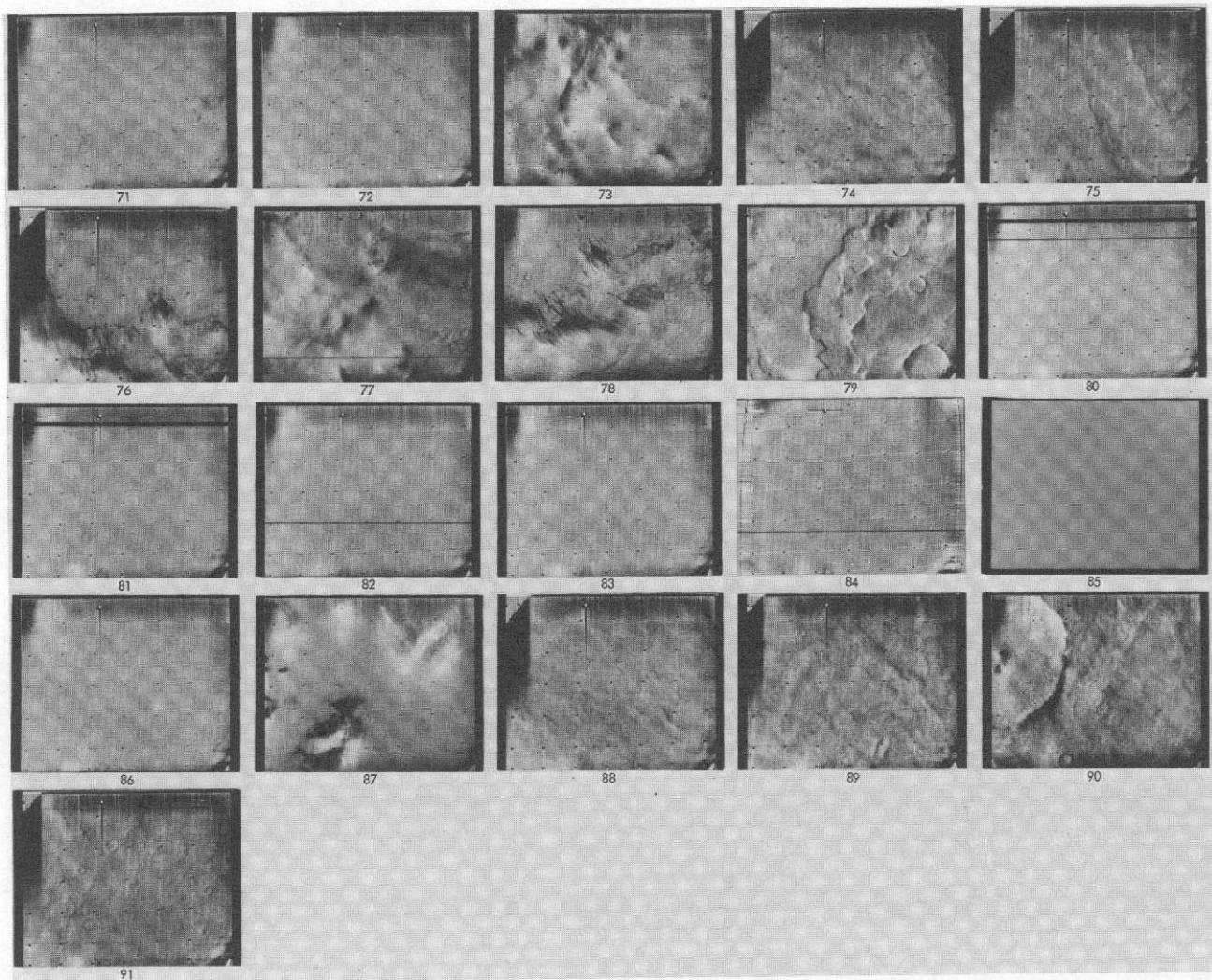


Fig. VII-7m. Narrow-angle frames in the Hellas quadrangle (contd). Images with little detail may have been underexposed (see histograms in original data and Section IV).

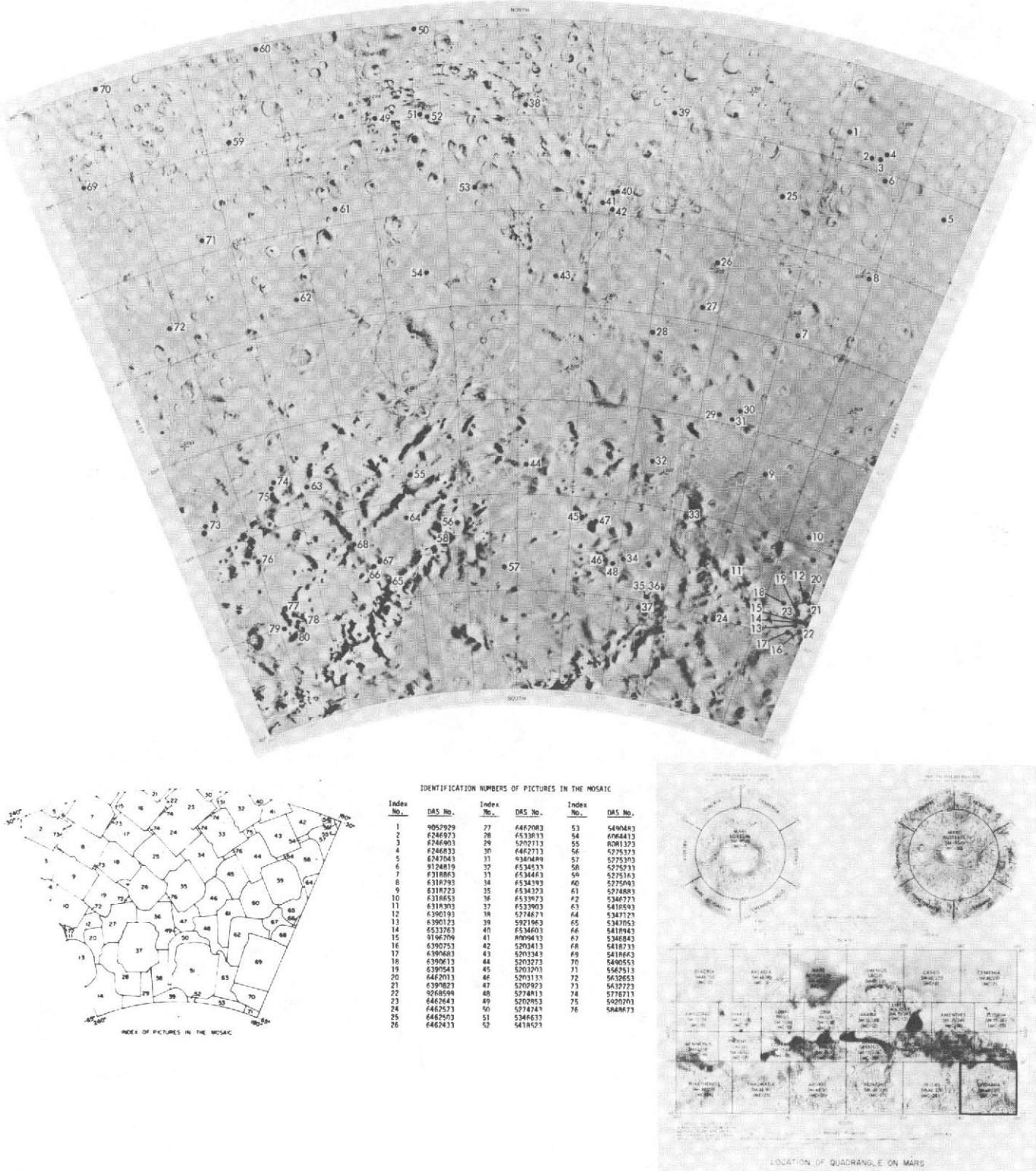


Fig. VII-7n. The Eridania quadrangle (MC-29). Photomosaic of wide-angle mapping frames in Lambert Projection serving as index map for locations of narrow-angle frames. Index numbers correspond to those for the accompanying narrow-angle frames and the picture data listings of Table VII-4n, and not to the charts and tables directly below the photomosaic.

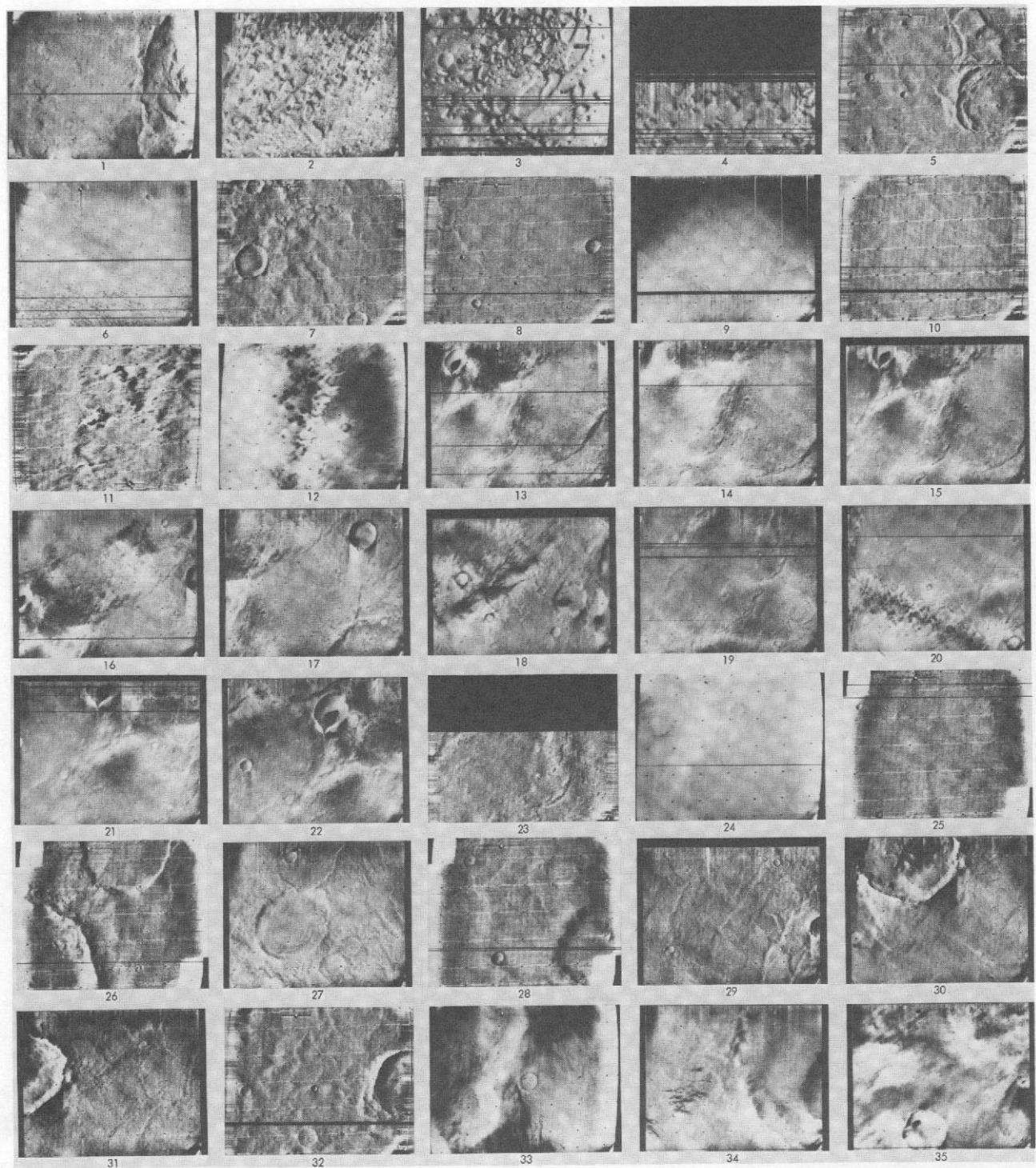


Fig. VII-7n. (contd). Narrow-angle frames (VAGC versions) that lie in the Eridania quadrangle: Revs 100–676; viewing angles less than 80° . Index numbers correspond to those on the photomosaic of this quadrangle and to Table VII-4n.

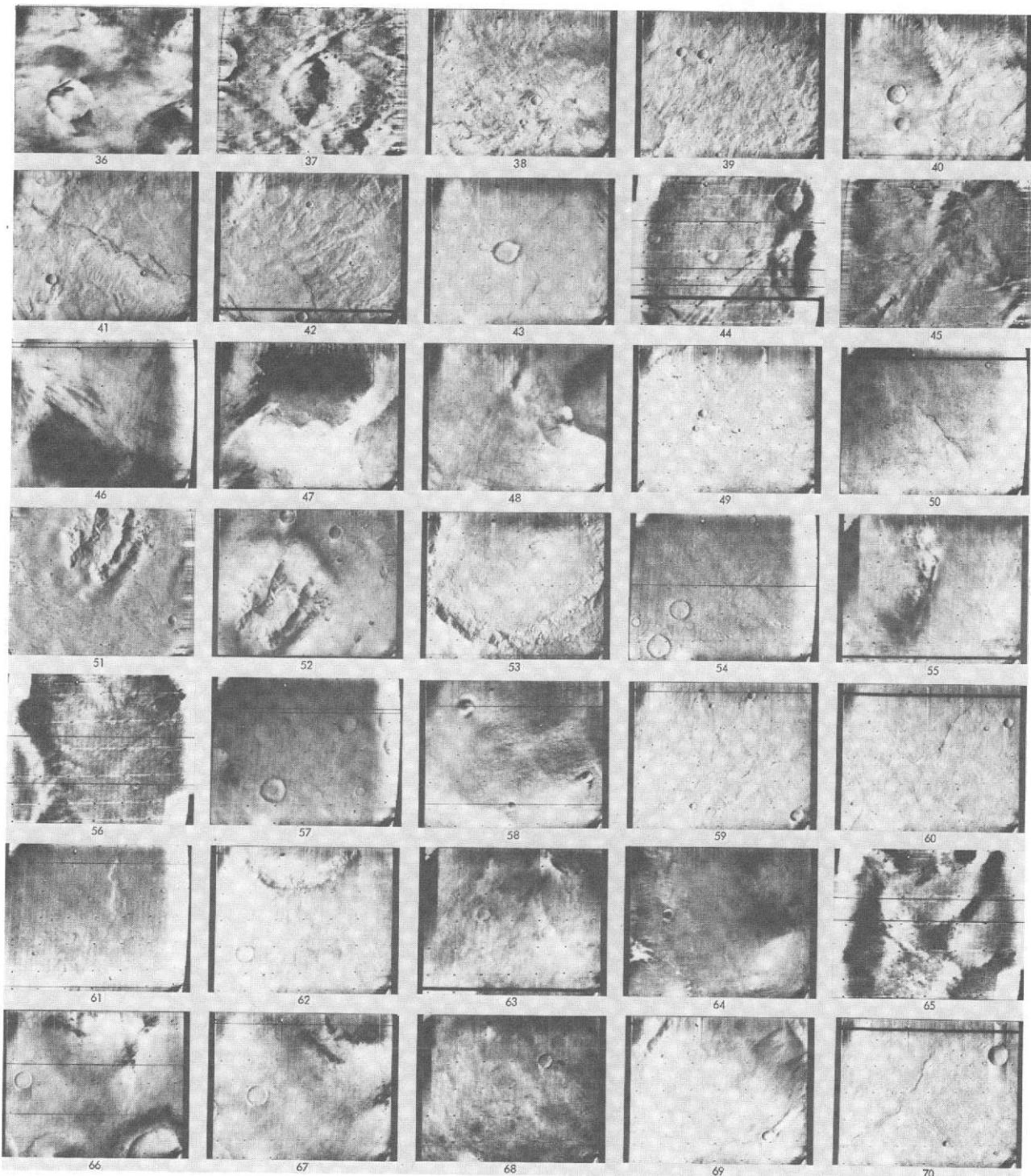


Fig. VII-7n. Narrow-angle frames in the Eridania quadrangle (contd.).

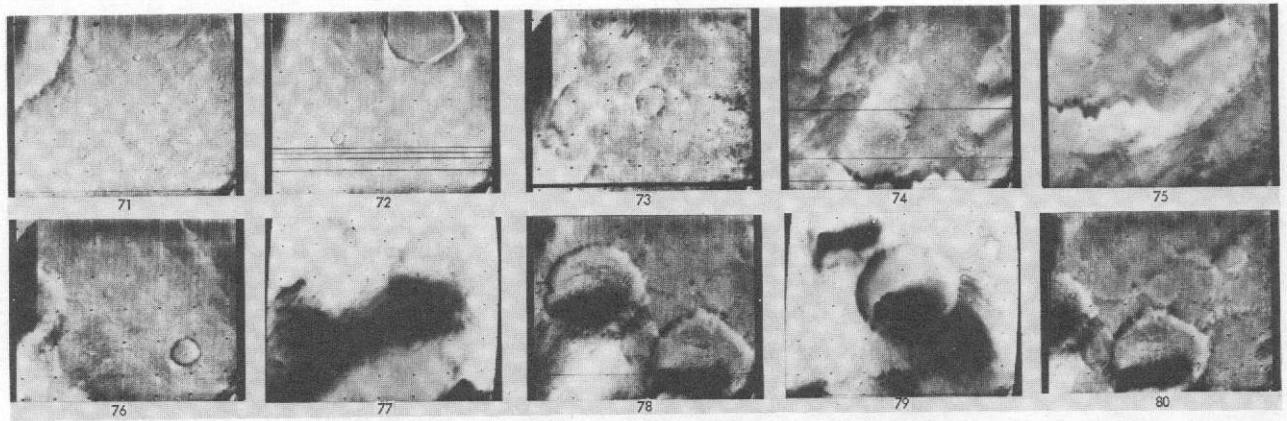


Fig. VII-7n. Narrow-angle frames in the Eridania quadrangle. (contd).

Table VII-3a. Listings for narrow-angle frames in the Diacria quadrangle (MC-2): Revs 100–676; viewing angles less than 80°. Index numbers correspond to those on the photomosaic of this quadrangle and to the accompanying narrow-angle frames (see Fig. VII-6a)

Index number	Rev	Frame number	Center of picture		Range (SRR-5), km	Lighting angle (SLAR-5), °	Viewing angle (VAR-5), °	North direction (NORAN) ^a	Sun direction (SUNAN) ^a	DAS time
			Latitude (LR-5), °	Longitude (LOR-5), °						
1	185	24	44.05	126.71	3,488	78.65	8.14	288	178	08227174
2	187	22	38.00	122.11	3,222	72.14	2.94	292	179	08298994
3	187	20	30.75	127.07	3,017	64.95	6.56	295	181	08298854
4	185	28	59.63	132.93	4,119	82.17	26.36	295	176	08227454
5	183	28	52.29	131.92	3,955	85.21	12.04	285	179	08155488
6	185	26	53.97	131.04	3,902	80.46	18.46	292	176	08227384
7	417	10	50.42	137.79	4,341	34.59	5.95	351	171	11481654
8	148	32	49.84	138.25	3,393	77.98	39.68	302	172	06895908
9	183	26	49.38	135.28	3,823	82.07	9.04	288	178	08155418
10	183	24	44.28	135.48	3,484	79.55	9.06	287	178	08155208
11	185	22	37.39	131.56	3,250	72.29	.79	292	179	08227034
12	222	15	38.34	139.41	3,002	62.06	16.53	291	174	09557804
13	185	20	30.58	136.20	3,052	65.53	8.01	295	181	08226894
14	181	28	53.88	149.84	3,870	81.19	19.21	292	176	08083458
15	181	26	44.78	144.78	3,463	80.20	10.87	287	178	08083248
16	183	22	37.91	140.72	3,244	73.07	1.99	292	179	08155068
17	222	13	37.90	140.46	2,878	60.66	24.73	283	168	09557664
18	183	20	30.75	145.19	3,042	66.32	7.26	294	181	08154928
19	450	14	60.44	152.86	5,151	42.51	8.05	350	178	12328436
20	179	28	59.60	159.16	4,119	84.30	25.54	293	177	08011638
21	181	30	59.25	151.13	4,079	83.00	26.40	294	176	08083528
22	179	24	44.74	153.99	3,505	80.96	9.19	287	178	08011358
23	142	32	38.40	155.41	3,039	81.21	13.17	290	177	06680028
24	179	22	37.84	159.37	3,263	74.26	1.39	291	179	08011218
25	181	24	38.16	150.25	3,216	73.50	3.45	291	179	08083108
26	218	16	35.61	155.23	3,089	64.29	11.25	294	180	09414024
27	218	18	36.01	155.51	3,284	64.75	6.63	296	182	09414164
28	181	22	30.90	155.16	3,012	66.38	6.92	294	180	08082968
29	144	32	59.95	162.83	3,857	81.86	55.62	317	173	06751988
30	179	26	56.15	162.86	3,976	80.87	23.64	296	176	08011568
31	140	32	45.23	165.64	3,199	83.86	24.83	291	177	06608138
32	450	12	49.91	160.65	4,674	31.89	4.59	1	176	12328156
33	216	19	44.28	163.32	3,533	70.43	7.96	292	178	09342414
34	216	17	37.69	168.27	3,296	63.71	.28	296	179	09342274
35	259	01	38.18	162.21	3,203	44.18	18.50	305	164	10615409
36	179	20	30.70	163.91	3,065	67.51	8.29	293	181	08011078
37	177	32	62.66	172.00	3,839	83.53	53.39	286	174	07939188
38	214	25	59.65	178.02	4,150	76.24	24.91	296	173	09270804
39	103	32	50.14	173.32	3,488	84.68	67.66	318	174	05276598
40	214	23	54.31	176.62	3,946	73.98	17.61	295	175	09270734
41	216	21	54.31	177.37	4,016	68.61	24.01	304	171	09342624
42	450	10	50.52	178.30	4,548	36.69	19.54	7	153	12328016
43	214	21	44.17	172.53	3,537	71.12	7.76	292	178	09270524
44	214	19	37.95	177.98	3,300	64.26	.46	296	179	09270384
45	216	15	31.04	173.12	3,096	56.58	7.98	299	182	09342134

^aTerms are defined in Fig. III-15.

Table VII-3b. Listings for narrow-angle frames in the Arcadia quadrangle (MC-3): Revs 100-676; viewing angles less than 80°. Index numbers correspond to those on the photomosaic of this quadrangle and to the accompanying narrow-angle frames (see Fig. VII-6b)

Index number	Rev	Frame number	Center of picture		Range (SRR-5), ^a km	Lighting angle (SLAR-5), ^a deg	Viewing angle (VAR-5), ^a deg	North direction (NORAN) ^a	Sun direction (SUNAN) ^a	DAS time
			Latitude (LR-5), ^a deg	Longitude (LOR-5), ^a deg						
1	162	32	56.66	65.90	3,566	82.78	44.53	292	174	07399908
2	431	10	58.49	62.30	5,100	42.39	5.10	342	177	11836021
3	164	32	51.74	62.42	3,442	76.92	37.63	299	171	07471868
4	431	08	49.44	64.82	4,635	33.06	4.88	352	184	11835741
5	667	06	49.06	63.83	4,087	65.39	6.78	103	182	13314430
6	199	22	44.31	61.20	3,524	76.56	9.63	288	178	08731174
7	199	20	37.91	66.86	3,280	69.72	2.09	293	180	08731034
8	201	14	30.69	62.80	3,074	61.79	7.71	297	182	08802854
9	197	21	54.49	74.61	3,864	78.95	19.43	291	176	08659354
10	528	11	49.38	70.25	12,081	73.23	16.81	259	182	12993017
11	195	22	44.66	79.90	3,510	77.35	10.00	288	178	08587184
12	197	19	44.78	70.14	3,466	77.22	12.81	287	178	08659144
13	197	17	38.18	75.85	3,210	70.30	4.82	292	179	08659004
14	158	32	31.62	79.13	3,093	77.15	6.33	290	181	07255988
15	199	18	30.76	71.93	3,078	62.46	7.73	297	182	08730894
16	193	26	48.33	85.66	4,249	82.64	2.16	286	179	08515644
17	234	12	48.56	83.27	3,345	65.82	26.96	287	169	09989914
18	234	14	48.23	86.61	3,390	63.99	21.83	293	169	09989984
19	431	06	49.00	80.16	4,441	33.02	12.38	357	161	11835601
20	193	20	44.85	89.21	3,482	77.66	11.15	288	178	08515154
21	195	20	38.00	85.44	3,264	70.52	1.84	293	179	08587044
22	197	15	30.88	80.96	2,957	62.96	4.62	296	181	08658864
23	193	24	59.64	94.68	4,091	81.33	25.96	293	176	08515434
24	193	22	54.17	93.16	3,881	79.53	18.49	291	176	08515364
25	423	12	48.73	92.77	4,531	35.14	13.31	351	198	11658570
26	191	24	44.71	98.78	3,547	77.91	7.85	289	178	08443194
27	193	18	38.29	94.73	3,232	70.89	3.26	292	179	08515014
28	156	32	30.06	92.51	3,064	73.58	11.10	291	181	07183958
29	193	16	30.91	99.45	3,024	63.81	5.96	295	181	08514874
30	195	18	30.96	90.41	3,061	63.38	7.11	296	182	08586904
31	119	32	45.02	106.38	3,346	74.52	64.55	317	166	05852488
32	187	28	49.44	108.15	3,930	86.69	11.93	282	179	08299414
33	154	32	44.34	101.78	3,147	79.49	24.37	291	175	07111928
34	187	26	41.19	109.86	3,813	83.33	11.51	286	180	08299344
35	189	24	44.54	108.06	3,513	78.12	8.58	288	178	08371164
36	191	22	37.97	104.15	3,310	71.17	.75	293	179	08443054
37	191	20	30.93	109.06	3,116	64.08	9.55	296	182	08442914
38	189	28	59.71	113.39	4,131	81.97	25.52	294	176	08371444
39	417	15	59.45	113.48	5,181	47.80	11.21	329	185	11482144
40	189	26	54.22	112.14	3,923	80.04	18.07	292	176	08371374
41	417	12	49.59	119.46	4,609	37.13	12.57	346	196	11481794
42	423	10	48.63	110.90	4,254	32.41	5.07	356	171	11658430
43	115	32	43.49	115.98	3,149	79.56	61.19	304	170	05708428
44	152	32	44.63	116.43	3,188	76.48	29.50	297	173	07039898
45	187	24	44.81	116.86	3,470	78.80	10.98	287	178	08299134
46	189	22	38.14	113.18	3,273	71.68	1.41	292	179	08371024
47	189	20	30.81	118.14	3,076	64.44	8.53	295	181	08370884

^aTerms are defined in Fig. III-15.

Table VII-3c. Listings for narrow-angle frames in the Mare Acidalium quadrangle (MC-4): Revs 100–676; viewing angles less than 80°. Index numbers correspond to those on the photomosaic of this quadrangle and to the accompanying narrow-angle frames (see Fig. VII-6c)

Index number	Rev	Frame number	Center of picture		Range (SRR-5), ^a km	Lighting angle (SLAR-5), ^a deg	Viewing angle (VAR-5), ^a deg	North direction (NORAN) ^a	Sun direction (SUNAN) ^a	DAS time
			Latitude (LR-5), ^a deg	Longitude (LOR-5), ^a deg						
1	211	21	56.33	9.40	3,928	76.35	22.20	292	174	09162864
2	445	13	58.86	8.22	5,105	41.18	11.46	354	167	12188827
3	445	11	48.73	8.73	4,622	31.36	8.43		168	12188547
4	211	19	44.70	5.91	3,488	72.64	11.30	290	177	09162654
5	213	17	38.16	2.55	3,247	64.65	2.69	296	179	09234404
6	213	15	30.73	7.50	3,043	57.11	6.94	299	181	09234264
7	176	32	55.13	14.80	3,665	71.77	49.22	311	165	07903208
8	172	32	45.10	14.96	3,163	77.04	24.49	288	174	07759428
9	174	32	49.94	15.09	3,364	73.26	36.52	299	169	07831318
10	211	17	38.08	11.43	3,238	65.63	3.28	295	179	09162514
11	211	15	30.78	16.50	3,031	58.12	6.10	298	181	09162374
12	207	22	46.65	26.31	3,903	74.50	2.34	292	179	09019154
13	445	09	48.16	23.01	4,495	34.96	20.75	4	149	12188407
14	675	04	46.51	26.61	3,914	63.75	9.79	99	181	13460593
15	168	32	42.20	28.61	3,109	80.67	20.15	283	177	07615648
16	170	32	40.47	29.82	3,088	72.03	18.22	293	174	07687538
17	207	21	44.63	24.55	3,484	73.97	11.44	289	178	09018874
18	209	20	38.27	21.05	3,230	66.21	3.69	295	179	09090624
19	209	18	31.06	25.90	3,020	58.93	5.29	298	181	09090484
20	437	11	60.14	31.12	5,181	43.89	7.19	341	180	12013019
21	205	22	59.81	39.18	4,109	79.00	25.48	294	175	08947264
22	205	20	53.99	38.02	3,896	76.68	17.45	292	176	08947194
23	437	09	50.76	33.47	4,714	34.31	6.58	353	188	12012739
24	242	10	48.62	33.80	3,512	71.48	34.91	278	174	10277824
25	135	32	43.94	30.60	3,298	69.97	64.56	312	161	06427818
26	205	18	44.45	33.61	3,503	74.75	10.65	289	178	08946984
27	205	16	38.15	39.15	3,256	67.97	3.20	294	179	08946844
28	207	19	38.04	30.08	3,233	67.04	3.52	294	179	09018734
29	207	17	30.87	35.14	3,025	59.65	5.68	298	181	09018594
30	203	22	44.12	43.29	3,542	75.08	8.21	290	179	08875094
31	203	20	37.78	48.47	3,304	68.54	1.79	294	180	08874954
32	205	14	30.88	44.26	3,049	60.55	6.43	297	182	08946704
33	166	32	55.09	52.92	3,539	78.26	44.20	300	171	07543758
34	201	22	59.63	57.69	4,121	79.91	24.70	293	175	08803414
35	201	20	54.00	56.29	3,913	77.90	16.89	292	176	08803344
36	437	07	51.76	51.12	4,504	35.24	10.81	359	164	12012599
37	201	18	44.29	52.31	3,519	75.80	9.49	289	178	08803134
38	201	16	37.75	57.63	3,276	69.11	2.29	293	180	08802994
39	203	18	30.76	53.50	3,105	61.31	8.54	297	183	08874814

^aTerms are defined in Fig. III-15.

Table VII-3d. Listings for narrow-angle frames in the Ismenius Lacus quadrangle (MC-5): Revs 100-676; viewing angles less than 80°. Index numbers correspond to those on the photomosaic of this quadrangle and to the accompanying narrow-angle frames (see Fig. VII-6d)

Index number	Rev	Frame number	Center of picture		Range (SRR-5), km	Lighting angle (SLAR-5), deg	Viewing angle (VAR-5), deg	North direction (NORAN) ^a	Sun direction (SUNAN) ^a	DAS time
			Latitude (LR-5), deg	Longitude (LOR-5), deg						
1	225	03	64.95	300.98	4,480	79.22	27.48	293	174	09666584
2	186	28	59.52	307.99	4,103	82.05	26.30	295	176	08263434
3	186	26	54.08	305.96	3,891	80.52	18.70	292	177	08263364
4	235	10	49.19	309.47	4,529	50.17	61.06	324	144	10026104
5	416	12	49.53	304.02	4,596	37.26	12.80	345	196	11445814
6	186	24	44.80	301.97	3,483	78.73	10.02	288	178	08263154
7	186	22	37.95	306.88	3,238	72.28	2.22	292	179	08263014
8	188	20	31.02	302.22	3,105	65.23	8.75	295	181	08334904
9	182	30	49.59	310.21	4,257	89.29	5.48	280	179	08119718
10	184	24	44.41	310.96	3,495	79.28	8.84	288	178	08191194
11	221	19	40.31	312.21	3,448	72.44	19.25	291	181	09522104
12	221	20	40.83	313.11	3,526	72.21	15.54	291	181	09522174
13	223	13	41.07	312.61	3,283	65.26	10.09	294	177	09593994
14	459	09	40.41	317.52	3,429	32.67	13.76	49	172	12537165
15	184	22	37.59	316.05	3,255	72.73	1.01	292	179	08191054
16	221	18	39.36	312.64	3,357	71.56	21.14	290	181	09522034
17	186	20	31.09	311.78	3,035	65.30	6.89	295	181	08262874
18	182	28	59.17	327.39	4,096	82.34	26.24	295	176	08119508
19	182	26	53.64	324.81	3,880	81.07	18.27	292	177	08119438
20	217	17	50.81	327.97	3,882	79.72	18.25	283	178	09378534
21	416	10	50.30	322.30	4,325	34.55	5.71	351	172	11445674
22	459	10	49.45	327.97	4,203	42.78	30.31	22	147	12537515
23	180	24	44.35	329.66	3,531	80.38	7.23	288	179	08047338
24	180	26	40.93	329.08	3,875	80.39	8.21	288	181	08047548
25	180	28	43.90	326.23	3,978	83.51	5.10	286	180	08047618
26	182	24	44.49	320.12	3,476	79.87	9.77	287	178	08119228
27	416	08	40.71	328.40	3,416	26.01	5.64	17	178	11445114
28	675	11	40.22	328.26	15,712	32.52	10.02	285	176	13471443
29	108	30	38.93	329.66	3,069	77.38	63.85	305	168	05456288
30	182	22	37.58	325.11	3,232	73.38	1.66	291	179	08119088
31	219	13	39.80	329.04	3,535	67.85	5.11	295	181	09450284
32	184	20	30.74	320.90	3,056	65.80	8.06	295	181	08190914
33	451	15	59.61	338.66	5,108	41.58	11.38	356	169	12364346
34	451	13	48.66	338.05	4,616	30.84	6.54	3	172	12364066
35	178	24	44.60	338.18	3,472	81.47	10.52	286	178	07975378
36	217	15	43.41	338.95	3,472	69.41	8.34	293	178	09378324
37	180	22	37.77	334.58	3,297	74.09	1.12	291	179	08047198
38	219	15	39.44	330.79	3,773	66.95	8.51	296	182	09450424
39	180	20	30.65	339.46	3,105	67.07	9.81	294	181	08047058
40	182	20	30.47	330.15	3,033	66.22	7.73	294	181	08118948
41	178	26	63.28	347.27	4,134	84.48	35.44	296	176	07975588
42	215	19	44.84	347.82	3,496	70.99	10.60	291	177	09306434
43	178	22	37.84	343.47	3,226	74.91	2.46	291	179	07975238
44	217	13	37.05	344.25	3,234	62.49	.78	297	179	09378184
45	260	12	36.32	344.91	2,825	38.08	40.58	282	129	10650899
46	260	13	35.74	345.16	2,844	37.60	36.48	290	136	10650969
47	178	20	30.70	348.50	3,023	67.81	6.81	294	181	07975098
48	260	14	34.86	345.23	2,879	36.94	32.66	296	142	10651039
49	451	08	57.53	356.18	3,685	45.11	60.42	140	253	12362876
50	139	32	43.99	350.68	3,150	83.37	23.86	291	177	06572158
51	213	19	44.67	356.97	3,494	71.70	10.56	291	177	09234544
52	215	17	38.35	353.33	3,250	63.97	2.97	296	178	09306294
53	215	15	31.09	358.12	3,044	56.59	6.48	299	181	09306154

^aTerms are defined in Fig. III-15.

Table VII-3e. Listings for narrow-angle frames in the Casius quadrangle (MC-6): Revs 100–676; viewing angles less than 80°. Index numbers correspond to those on the photomosaic of this quadrangle and to the accompanying narrow-angle frames (see Fig. VII-6e)

Index number	Rev	Frame number	Center of picture		Range (SRR-5), km	Lighting angle (SLAR-5), deg	Viewing angle (VAR-5), deg	North direction (NORAN) ^a	Sun direction (SUNAN) ^a	DAS time
			Latitude (LR-5), deg	Longitude (LOR-5), deg						
1	430	17	59.13	244.84	5,137	43.42	5.81	340	178	11800041
2	198	24	54.10	249.88	3,932	78.78	16.66	291	176	08695404
3	430	15	50.10	247.80	4,669	34.06	5.03	350	185	11799761
4	198	22	44.31	246.03	3,536	76.68	8.84	289	178	08695194
5	200	22	37.90	242.25	3,276	69.45	2.27	293	179	08767014
6	200	20	30.87	247.04	3,072	62.44	7.15	297	182	08766874
7	198	26	59.65	250.64	4,135	80.98	24.19	292	176	08695474
8	196	24	44.62	254.87	3,486	77.35	11.46	287	178	08623164
9	198	20	37.84	251.43	3,295	70.00	1.70	293	180	08695054
10	198	18	30.99	256.40	3,093	62.95	7.81	296	182	08694914
11	194	24	54.71	268.22	3,948	79.87	17.78	291	176	08551414
12	430	13	50.56	263.39	4,465	34.33	11.04	356	163	11799621
13	120	30	42.24	267.57	3,103	81.05	63.50	285	171	05888328
14	157	32	44.03	267.36	3,137	79.16	23.17	290	175	07219938
15	194	22	44.38	264.93	3,538	77.24	7.94	289	178	08551204
16	118	30	37.85	266.96	2,944	86.56	60.37	258	176	05816298
17	194	20	37.83	269.99	3,300	70.76	.67	293	179	08551064
18	196	22	38.18	260.53	3,235	70.53	3.64	292	179	08623024
19	196	20	30.99	265.58	3,026	63.28	5.57	296	181	08622884
20	194	26	60.20	270.31	4,160	81.41	25.50	294	176	08551484
21	231	11	60.33	270.07	3,939	76.51	34.74	282	172	09882184
22	422	15	61.88	273.34	5,142	48.38	13.15	332	182	11622940
23	422	12	49.22	275.75	4,569	36.25	14.40	349	199	11622590
24	192	24	44.34	273.62	3,512	77.89	9.09	288	178	08479174
25	192	22	38.19	279.10	3,270	71.30	1.72	292	179	08479034
26	153	32	34.26	279.24	3,042	81.27	3.96	287	179	07075948
27	194	18	31.02	274.60	3,100	64.02	8.08	296	182	08550924
28	190	28	59.75	288.53	4,102	81.87	26.16	293	176	08407424
29	190	26	54.20	286.80	3,889	80.18	18.49	291	176	08407354
30	190	24	44.88	283.14	3,486	78.18	10.62	288	178	08407144
31	190	22	38.10	288.18	3,238	71.67	2.68	292	179	08407004
32	192	20	31.13	283.88	3,067	64.32	7.04	296	181	08478894
33	416	15	58.87	298.49	5,163	47.36	10.69	329	185	11446164
34	422	10	49.46	294.24	4,281	33.26	4.23	355	173	11622450
35	188	24	44.31	292.28	3,537	78.57	7.47	288	178	08335184
36	188	22	38.23	297.56	3,302	72.15	.89	292	179	08335044
37	190	20	31.03	293.21	3,033	64.50	6.35	295	181	08406864

^aTerms are defined in Fig. III-15.

Table VII-3f. Listings for narrow-angle frames in the Cebrenia quadrangle (MC-7): Revs 100–676; viewing angles less than 80°. Index numbers correspond to those on the photomosaic of this quadrangle and to the accompanying narrow-angle frames (see Fig. VII-6f)

Index number	Rev	Frame number	Center of picture		Range (SRR-5), km	Lighting angle (SLAR-5), ^a deg	Viewing angle (VAR-5), ^a deg	North direction (NORAN) ^a	Sun direction (SUNAN) ^a	DAS time
			Latitude (LR-5), deg	Longitude (LOR-5), deg						
1	444	14	60.93	189.17	5,156	43.20	11.04	350	170	12152917
2	212	25	51.04	184.50	3,993	73.97	9.61	294	177	09198914
3	136	31	45.30	182.75	3,287	84.07	67.95	250	173	06463658
4	173	32	42.53	183.23	3,165	80.55	19.55	284	177	07795408
5	175	32	42.58	184.20	3,164	72.92	18.73	293	174	07867298
6	212	21	44.49	181.96	3,533	71.86	8.45	291	178	09198634
7	212	23	42.14	184.00	3,864	70.22	6.44	295	181	09198844
8	668	04	40.97	184.59	7,893	18.20	35.62	27	171	13352510
9	136	29	35.95	186.78	2,858	77.26	58.25	262	167	06463588
10	138	31	39.48	184.63	2,979	73.37	59.50	285	164	06535548
11	212	19	38.09	187.11	3,293	65.17	.91	296	179	09198494
12	138	29	32.09	186.24	2,696	68.28	52.76	283	161	06535478
13	214	17	31.17	183.00	3,102	56.96	8.45	299	182	09270244
14	210	23	54.41	194.95	3,930	75.36	17.82	294	175	09126954
15	444	12	49.79	191.40	4,666	32.20	6.44	359	172	12152637
16	210	21	44.64	190.39	3,529	73.18	9.82	290	178	09126744
17	210	19	37.96	195.87	3,284	66.21	1.87	295	179	09126604
18	212	17	30.96	191.96	3,094	57.87	8.12	299	182	09198354
19	208	21	53.86	203.63	3,917	76.03	16.62	293	175	09055064
20	444	10	50.56	205.80	4,522	36.12	18.45	3	153	12152497
21	206	19	44.33	209.23	3,536	74.30	8.92	290	178	08982964
22	208	19	44.49	200.13	3,524	73.53	9.35	290	178	09054854
23	208	17	38.01	205.36	3,282	66.83	1.88	295	179	09054714
24	210	17	31.10	200.94	3,080	58.93	7.12	298	182	09126464
25	676	04	31.61	209.84	3,531	74.63	13.36	106	176	13496293
26	206	23	59.54	214.16	4,134	78.83	24.14	294	175	08983244
27	436	17	59.99	215.40	5,170	43.91	7.23	341	180	11977039
28	206	21	54.32	212.88	3,935	76.87	17.08	292	176	08983174
29	436	15	50.71	217.84	4,703	34.41	6.89	352	189	11976759
30	204	24	44.53	218.23	3,477	75.04	11.81	288	178	08911004
31	206	17	37.79	214.47	3,255	67.60	1.92	294	180	08982824
32	206	15	30.87	219.67	3,094	60.25	8.02	298	182	08982684
33	208	15	31.02	210.19	3,078	59.69	7.10	298	182	09054574
34	676	05	31.89	211.04	3,657	75.22	15.23	105	176	13496363
35	128	30	43.70	228.26	3,171	80.87	65.12	277	171	06176098
36	202	22	43.97	227.47	3,529	75.58	8.96	289	178	08839114
37	204	22	38.05	223.81	3,226	68.17	4.10	293	179	08910864
38	165	32	33.38	222.10	3,020	79.18	9.43	288	180	07507778
39	167	32	33.36	223.25	3,097	70.52	10.43	293	179	07579738
40	204	20	30.89	228.69	3,015	60.98	5.07	297	182	08910724
41	245	01	63.14	237.32	4,921	66.09	35.17	322	166	10386534
42	202	26	59.75	233.44	4,135	79.59	24.76	294	175	08839394
43	436	13	51.53	235.30	4,488	34.97	10.25	359	165	11976619
44	200	24	44.16	235.84	3,518	76.08	9.36	289	178	08767154
45	202	20	37.65	233.01	3,288	68.81	2.12	294	180	08838974
46	202	18	30.91	238.27	3,086	61.54	7.76	297	182	08838834

^aTerms are defined in Fig. III-15.

Table VII-3g. Listings for narrow-angle frames in the Amazonis quadrangle (MC-8): Revs 100-676; viewing angles less than 80°. Index numbers correspond to those on the photomosaic of this quadrangle and to the accompanying narrow-angle frames (see Fig. VII-6g)

Index number	Rev	Frame number	Center of picture		Range (SRR-5), ^a km	Lighting angle (SLAR-5), ^a deg	Viewing angle (VAR-5), ^a deg	North direction (NORAN) ^a	Sun direction (SUNAN) ^a	DAS time
			Latitude (LR-5), ^a deg	Longitude (LOR-5), ^a deg						
1	668	03	26.66	139.21	8,765	29.74	79.33	46	250	13351950
2	107	30	17.96	135.63	2,535	83.00	58.07	245	172	05419958
3	107	32	18.76	135.38	2,301	85.63	14.25	285	179	05420448
4	146	29	16.58	138.76	2,857	70.17	24.49	291	187	06823738
5	220	15	16.37	139.48	2,960	58.62	68.87	153	91	05484934
6	222	12	16.52	136.15	2,646	55.13	29.46	310	199	09557454
7	148	23	9.10	135.35	2,184	59.98	10.72	290	184	06895278
8	148	19	.34	138.65	2,103	33.63	20.76	289	190	06895138
9	148	21	4.81	137.02	2,135	56.84	15.49	290	186	06895208
10	146	29	16.93	147.55	2,851	71.28	23.71	291	186	06751778
11	146	25	14.03	142.45	2,271	64.39	6.11	290	181	06823388
12	105	30	9.89	146.25	2,122	80.23	36.65	270	175	05348068
13	105	32	9.50	146.40	2,452	82.27	22.26	290	183	05348558
14	146	21	5.50	145.81	2,157	58.06	15.57	290	186	06823248
15	146	23	9.81	144.13	2,207	61.22	10.73	290	183	06823318
16	146	19	1.11	147.63	2,123	54.85	20.67	289	189	06823178
17	417	05	22.46	153.59	2,720	20.78	11.53	42	148	11480604
18	417	06	23.48	151.58	2,818	19.03	11.31	35	146	11480674
19	417	07	22.96	152.48	2,962	19.34	17.46	22	132	11480744
20	458	10	21.57	155.14	3,164	40.86	35.00	34	130	12500835
21	458	11	22.23	154.05	3,257	38.94	34.22	28	126	12500945
22	676	18	23.44	159.73	16,397	19.36	31.25	285	211	13508123
23	142	29	16.25	156.80	2,828	71.67	24.01	291	186	06679818
24	144	25	13.91	151.57	2,274	65.10	6.39	290	181	06751428
25	144	21	5.56	154.88	2,159	58.83	15.48	290	186	06751288
26	144	23	9.77	153.23	2,210	61.94	10.90	290	183	06751358
27	103	30	.53	159.80	1,895	74.15	16.37	284	179	05276108
28	144	19	1.22	156.74	2,124	55.59	20.52	289	189	06751218
29	185	18	1.35	156.39	1,979	32.58	24.57	276	170	08225914
30	220	14	1.37	157.18	2,044	38.01	38.21	197	114	09484754
31	458	06	3.97	152.08	1,924	45.37	13.58	125	192	12499955
32	458	07	4.59	151.51	1,959	44.30	8.52	120	188	12500065
33	458	08	3.45	152.37	2,130	44.90	16.62	103	172	12500245
34	140	29	18.11	164.42	2,849	74.62	21.67	290	185	06607928
35	140	25	14.48	169.90	2,291	66.93	6.26	290	181	06607578
36	142	25	13.39	161.05	2,253	65.31	6.14	290	181	06679468
37	142	21	5.06	164.50	2,139	58.92	15.29	289	185	06679328
38	142	23	9.26	162.80	2,189	62.07	10.69	290	183	06679398
39	417	01	6.84	163.58	2,026	35.38	33.98	144	216	11479764
40	417	02	5.81	164.55	1,979	36.29	25.96	145	212	11479834
41	142	19	.72	166.40	2,105	55.65	20.35	289	189	06679258
42	417	03	4.69	165.46	2,043	36.89	20.57	137	204	11479974
43	177	29	17.62	176.18	2,901	60.12	24.12	296	190	07938978
44	218	15	15.62	177.67	3,081	36.32	36.84	298	191	05413814
45	140	23	10.49	171.65	2,225	63.74	10.54	290	183	06607508
46	177	25	14.93	179.19	2,311	54.95	5.97	292	182	07938628
47	218	14	14.99	178.55	2,960	34.81	35.87	297	188	09413744
48	140	21	6.25	173.35	2,173	60.56	15.27	290	185	06607438
49	437	01	7.76	173.41	4,529	134.69	183.34	344	87	1194749
50	140	19	1.87	175.23	2,138	57.25	20.44	289	188	06607368

^aTerms are defined in Fig. III-15.

Table VII-3h. Listings for narrow-angle frames in the Tharsis quadrangle (MC-9): Revs 100-676; viewing angles less than 80°. Index numbers correspond to those on the photomosaic of this quadrangle and to the accompanying narrow-angle frames (see Fig. VII-6h)

Index number	Rev	Frame number	Center of picture		Range (SRR-5), km	Lighting angle (SLAR-5), deg	Viewing angle (VAR-5), deg	North direction (NORAN) ^a	Sun direction (SUNAN) ^a	DAS time
			Latitude (LR-5), deg	Longitude (LOR-5), deg						
1	236	12	24.20	97.59	2,651	34.26	25.82	296	159	10061454
2	236	13	24.37	96.92	2,743	35.05	25.44	298	164	10061524
3	156	29	16.06	96.17	2,906	44.66	27.52	292	189	07183748
4	156	23	10.01	99.34	2,217	57.93	11.39	291	184	07183328
5	156	25	14.13	97.67	2,281	61.11	6.92	291	182	07183398
6	197	13	13.56	90.73	2,145	43.57	39.26	238	135	08657884
7	158	21	7.11	91.37	2,198	55.29	15.49	291	187	07255288
8	158	19	2.76	93.18	2,161	52.08	20.56	291	190	07255218
9	154	29	15.04	105.26	2,884	64.75	28.22	292	189	07111718
10	113	32	11.46	104.67	2,428	85.18	24.42	291	181	05636468
11	154	25	13.15	106.75	2,256	61.22	7.11	291	182	07111368
12	199	16	10.79	104.25	2,477	22.84	53.05	277	127	08729914
13	232	13	12.30	104.38	2,973	39.30	32.77	307	205	09917604
14	676	12	10.38	107.45	13,846	47.88	57.20	327	233	13502943
15	676	16	13.29	108.25	16,590	68.00	40.64	278	195	13507913
16	154	23	9.11	108.49	2,193	58.02	11.46	291	184	07111298
17	156	21	5.78	100.55	2,166	54.86	16.00	291	187	07183258
18	528	16	9.62	103.89	14,941	65.42	49.34	262	199	12995257
19	676	10	9.79	108.30	11,755	36.80	71.24	10	254	13500493
20	676	14	9.56	105.73	15,590	60.86	49.84	300	210	13505463
21	156	19	1.39	102.72	2,132	51.72	21.05	290	191	07183188
22	258	01	25.38	112.12	4,830	153.13	184.28	138	133	10563119
23	258	03	24.39	112.47	4,590	154.05	183.57	137	131	10563329
24	152	25	12.66	115.91	2,233	61.42	6.62	290	182	07039338
25	152	29	14.18	114.21	2,863	45.03	28.70	292	190	07039688
26	152	23	8.43	117.61	2,172	58.20	11.33	290	184	07039268
27	111	31	.24	112.95	2,199	81.24	43.85	283	180	05563948
28	117	31	.13	112.75	1,954	53.50	27.82	281	169	05779968
29	152	21	4.13	119.25	2,124	55.12	16.08	290	187	07039198
30	154	19	.54	112.02	2,110	51.72	21.13	290	191	07111158
31	154	21	5.00	110.19	2,142	54.92	15.88	290	187	07111228
32	195	16	2.45	111.00	1,974	30.19	23.71	275	167	08585924
33	232	07	.21	112.81	1,955	23.65	37.10	199	113	09916554
34	232	09	4.01	111.50	2,008	25.79	38.43	202	110	09916624
35	232	10	.48	112.97	2,598	26.90	38.93	301	219	09917254
36	232	11	.56	112.64	2,769	27.58	42.97	301	221	09917324
37	232	12	.62	112.65	2,953	27.91	46.83	300	223	09917394
38	150	29	16.97	121.40	2,881	68.38	24.93	291	187	06967728
39	230	12	15.11	129.83	2,597	25.64	35.16	293	161	09845294
40	230	15	18.05	125.39	2,984	31.86	35.10	299	179	09845574
41	150	23	10.31	125.99	2,222	60.17	10.89	290	183	06967308
42	150	25	14.38	124.26	2,287	63.39	6.44	290	181	06967378
43	230	09	14.79	129.95	2,524	22.88	61.20	227	97	09846594
44	150	21	6.07	127.73	2,171	56.96	15.66	290	186	06967228
45	150	19	1.70	129.62	2,136	53.69	20.81	289	189	06967168
46	193	14	3.16	121.35	1,998	29.56	27.71	273	160	08513894
47	146	32	22.36	131.70	3,153	79.15	23.05	289	184	06823948
48	226	13	22.04	132.17	2,310	42.74	16.30	280	162	09701234
49	226	15	24.99	130.13	2,452	46.36	11.27	290	171	09701374
50	109	32	19.61	134.77	2,267	77.55	12.67	288	177	05492408
51	148	29	15.36	130.78	2,849	68.04	26.26	291	188	06895698
52	187	18	17.52	132.58	2,322	50.62	47.85	231	136	08297874
53	222	10	16.03	133.57	2,607	56.77	38.46	307	198	09557314
54	222	11	15.73	134.26	2,636	56.38	34.92	311	200	09557384
55	230	11	18.60	130.29	2,607	25.67	62.48	236	99	09846664
56	230	13	15.15	130.14	2,736	25.69	37.81	294	164	09845364
57	230	14	18.21	133.52	2,956	25.69	43.85	295	152	09845434
58	261	05	18.18	133.33	2,783	43.69	61.49	135	57	10686389
59	423	05	19.03	134.39	2,269	31.82	33.26	147	230	11656890
60	423	06	18.52	133.53	2,257	31.07	26.62	142	226	11656960
61	423	07	18.01	133.63	2,279	30.47	21.24	135	219	11657030
62	458	09	19.83	134.83	2,478	22.98	20.27	95	185	12500485
63	528	15	17.24	133.86	15,209	34.74	58.29	270	224	12995117
64	668	13	19.03	133.72	11,506	46.26	66.01	356	237	13354260
65	668	15	16.93	132.55	14,205	61.23	53.14	311	212	13357270
66	668	16	18.06	133.60	16,088	73.02	45.58	280	192	13360280
67	148	25	13.18	133.64	2,247	63.15	6.33	290	182	06895348

^a Terms are defined in Fig. III-15.

Table VII-3i. Listings for narrow-angle frames in the Lunae Palus quadrangle (MC-10): Revs 100–676; viewing angles less than 80°. Index numbers correspond to those on the photomosaic of this quadrangle and to the accompanying narrow-angle frames (see Fig. VII-6i)

Index number	Rev	Frame number	Center of picture		Range (SRR-5), km	Lighting angle (SLAR-5), deg	Viewing angle (VAR-5), deg	North direction (NORAN) ^a	Sun direction (SUNAN) ^a	DAS time
			Latitude (LR-5), deg	Longitude (LOR-5), deg						
1	166	29	17.42	49.74	2,862	62.35	24.25	294	188	07543548
2	168	21	5.38	45.56	2,146	50.46	15.34	291	188	07614948
3	159	01	.63	46.55	11,915	125.21	222.11	266	167	07283428
4	168	19	.99	47.84	2,112	47.26	20.49	290	192	07614878
5	164	29	18.15	58.00	2,906	64.37	24.11	294	188	07471658
6	166	23	10.35	53.44	2,210	54.79	10.17	291	184	07543128
7	166	25	14.45	51.71	2,276	58.02	5.68	291	182	07543158
8	166	21	6.14	55.10	2,157	51.67	14.77	291	187	07543058
9	131	31	2.73	52.70	2,122	45.02	40.30	281	158	06283548
10	166	19	1.77	56.56	2,121	48.47	19.89	290	191	07542968
11	123	32	28.44	61.72	2,489	84.57	30.98	277	177	05996408
12	125	30	25.49	63.54	2,686	71.74	61.99	254	161	06067878
13	125	32	22.70	64.28	2,369	72.01	17.44	289	174	06068368
14	160	32	22.26	64.80	3,085	77.84	23.82	293	184	07327878
15	205	12	24.46	61.51	2,594	40.75	57.74	250	123	08945724
16	238	07	21.42	66.19	2,661	50.07	20.81	307	194	10133484
17	238	09	23.58	62.06	2,816	54.68	25.96	308	194	10133554
18	242	07	23.70	62.08	2,607	38.18	10.39	299	175	10277404
19	242	09	24.86	61.24	2,706	39.72	10.91	301	177	10277474
20	437	05	23.58	61.04	2,523	24.32	4.80	90	190	12011339
21	478	03	22.31	64.95	2,413	48.65	41.70	142	214	12866063
22	478	04	23.91	61.00	2,402	44.56	36.82	134	214	12866133
23	478	05	24.38	61.19	2,416	44.38	32.62	133	212	12866203
24	162	29	17.20	67.09	2,886	64.79	24.82	293	189	07399658
25	164	25	15.46	60.67	2,313	59.53	6.00	291	181	07471308
26	164	23	11.31	62.37	2,247	56.29	10.58	291	184	07471238
27	164	21	7.16	64.04	2,193	53.15	15.13	291	187	07471168
28	164	19	2.86	65.50	2,154	49.92	20.13	291	191	07471058
29	203	16	21.35	70.57	2,413	39.42	49.86	255	128	06873834
30	667	03	22.47	73.18	3,048	78.23	18.21	109	176	13313730
31	667	04	21.60	72.16	3,198	77.90	22.47	108	175	13313800
32	160	29	17.75	75.67	2,874	66.15	23.56	293	187	07327738
33	160	25	14.73	79.29	2,293	60.33	6.34	291	182	07327388
34	162	23	10.43	71.86	2,227	56.37	11.11	291	184	07399278
35	162	25	14.59	70.22	2,292	59.54	6.56	291	182	07399348
36	162	21	6.16	73.50	2,176	53.25	15.87	291	187	07399208
37	162	19	1.77	75.40	2,142	50.00	21.07	291	191	07399138
38	667	02	20.51	84.53	2,582	89.82	6.72	116	179	13313450
39	158	25	15.47	88.02	2,318	61.65	6.22	291	182	07255428
40	158	29	18.96	83.52	2,886	68.38	21.82	293	187	07255778
41	158	23	11.34	89.71	2,252	58.43	10.77	291	184	07255358
42	160	23	10.66	81.03	2,227	57.10	10.80	291	184	07327318
43	160	21	6.46	82.70	2,175	53.96	15.44	291	187	07327248
44	667	01	8.56	89.54	2,383	100.44	19.03	115	181	13313240
45	160	19	2.02	84.48	2,139	50.79	20.61	290	191	07327178

^aTerms are defined in Fig. III-15.

Table VII-3j. Listings for narrow-angle frames in the Oxia Palus quadrangle (MC-11): Revs 100–676; viewing angles less than 80°. Index numbers correspond to those on the photomosaic of this quadrangle and to the accompanying narrow-angle frames (see Fig. VII-6j)

Index number	Rev	Frame number	Center of picture		Range (SRR-5), km	Lighting angle (SLAR-5), deg	Viewing angle (VAR-5), deg	North direction (NORAN) ^a	Sun direction (SUNAN) ^a	DAS time
			Latitude ^a (LR-5), deg	Longitude ^a (LOR-5), deg						
1	529	07	24.76	3.21	2,590	57.51	54.28	123	206	13021717
2	176	29	16.43	1.55	2,867	59.34	25.00	296	191	07902998
3	529	04	16.38	6.45	2,379	63.17	50.85	124	200	13021577
4	529	05	17.86	5.15	2,357	61.24	47.44	124	200	13021647
5	176	25	14.00	4.42	2,274	54.38	5.79	292	182	07902648
6	215	13	11.00	4.45	2,075	38.79	32.88	234	134	09305174
7	529	03	13.11	9.54	2,336	67.34	51.21	127	197	13021507
8	176	21	5.61	7.85	2,158	47.97	15.15	292	189	07902508
9	176	23	9.81	6.12	2,209	51.13	10.46	292	185	07902578
10	176	19	1.22	9.80	2,123	44.74	20.38	291	193	07902438
11	172	29	16.69	19.55	2,842	61.65	23.82	295	190	07759218
12	174	29	16.70	10.46	2,857	60.62	24.26	295	190	07831108
13	174	25	13.95	14.04	2,273	54.90	6.12	292	182	07830758
14	135	30	9.71	18.16	2,041	60.55	34.57	264	160	06427328
15	174	21	5.56	17.33	2,158	48.64	15.31	292	188	07830618
16	174	23	9.78	15.71	2,209	51.70	10.71	292	185	07830688
17	174	19	1.23	19.22	2,122	45.47	20.34	291	193	07830548
18	213	13	2.53	17.55	1,878	33.83	9.07	267	168	09233284
19	451	06	2.57	18.44	2,265	56.55	40.71	144	207	12362176
20	451	07	3.14	17.54	2,322	55.19	40.26	137	203	12362246
21	170	29	16.63	28.67	2,832	62.64	23.61	295	190	07687328
22	172	25	13.87	23.59	2,265	55.49	5.91	291	182	07758868
23	172	21	5.40	26.88	2,150	49.21	15.23	291	188	07758728
24	172	23	9.67	25.26	2,201	52.29	10.53	292	185	07758798
25	172	19	.97	28.74	2,116	46.05	20.46	291	192	07758658
26	248	13	22.11	36.61	2,565	33.23	14.74	298	170	10493074
27	445	04	17.85	34.88	2,254	38.96	31.75	142	218	12186797
28	445	05	18.84	33.28	2,269	37.03	27.10	137	216	12186867
29	445	06	18.38	34.00	2,369	37.11	21.33	123	204	12187007
30	675	02	17.80	30.95	3,398	77.20	33.36	109	172	13460103
31	170	25	13.49	32.90	2,259	56.20	6.16	291	182	07686978
32	170	21	5.16	36.35	2,145	49.85	15.36	291	188	07686838
33	170	23	9.36	34.60	2,196	53.01	10.68	292	185	07686908
34	209	14	8.87	33.54	2,012	39.52	28.78	241	141	09089504
35	170	19	.90	38.30	2,109	46.63	20.29	291	192	07686768
36	211	13	4.53	30.01	1,896	31.99	14.35	263	158	09161394
37	168	29	16.59	40.92	2,855	60.79	25.34	294	189	07615438
38	168	25	13.63	42.51	2,261	56.81	6.31	291	182	07615088
39	209	15	10.90	43.04	2,202	32.75	22.11	286	169	09089784
40	248	11	10.14	41.21	2,378	22.33	24.01	296	185	10492864
41	168	23	9.56	44.24	2,197	53.60	10.73	291	185	07615018
42	248	09	5.89	42.88	2,344	18.96	28.22	295	195	10492754
43	248	07	1.54	44.63	2,325	16.14	32.68	293	209	10492724

^aTerms are defined in Fig. III-15.

Table VII-3k. Listings for narrow-angle frames in the Arabia quadrangle (MC-12): Revs 100-676; viewing angles less than 80°. Index numbers correspond to those on the photomosaic of this quadrangle and to the accompanying narrow-angle frames (see Fig. VII-6k)

Index number	Rev	Frame number	Center of picture		Range (SRR-5), km	Lighting angle (SLAR-5), °	Viewing angle (VAR-5), °	North direction (NORAN)	Sun direction (SUNAN)	DAS time
			Latitude ^a (LR-5), deg	Longitude ^a (LOR-5), deg						
1	147	25	13.60	318.03	2,261	63.80	6.29	290	181	06659368
2	147	23	9.52	319.78	2,197	60.57	10.76	290	183	06659298
3	106	33	16.19	324.57	2,262	81.01	1.53	288	180	05384468
4	145	30	16.89	323.21	2,055	70.72	23.96	291	187	06787758
5	106	30	13.62	325.52	2,121	78.72	8.14	286	178	05384328
6	145	26	13.99	326.90	2,275	64.87	6.20	290	181	06787408
7	145	24	9.80	328.63	2,211	61.63	10.91	290	183	06787338
8	147	21	5.24	321.44	2,147	57.45	15.50	290	186	06859228
9	147	19	.81	323.34	2,114	54.17	20.75	289	189	06859158
10	141	31	19.22	339.55	2,869	74.88	20.54	290	184	06643908
11	143	20	16.59	331.57	2,843	71.67	23.93	291	186	06715798
12	143	16	13.67	336.27	2,266	65.24	6.41	290	181	06715448
13	143	14	5.34	339.75	2,153	58.82	15.65	290	186	06715308
14	145	22	5.52	330.39	2,162	58.39	15.81	290	186	06787268
15	145	20	1.14	332.28	2,128	55.12	20.94	289	189	06787198
16	217	11	29.97	348.62	3,036	55.31	7.93	300	182	09378044
17	139	29	17.12	349.62	2,823	74.10	22.43	290	185	06571948
18	141	27	15.36	344.74	2,315	67.42	5.68	290	181	06643558
19	141	25	11.34	346.52	2,248	64.17	10.10	290	183	06643488
20	219	10	10.06	347.63	2,394	37.95	18.76	300	195	09449444
21	219	11	10.76	346.26	2,513	39.20	22.18	302	197	09449514
22	219	12	10.63	347.08	2,672	38.72	27.97	302	200	09449584
23	141	23	7.10	348.29	2,194	60.92	14.95	290	185	06643418
24	143	12	.89	341.52	2,119	55.65	20.81	289	189	06715238
25	139	25	13.68	354.55	2,262	66.68	6.10	290	181	06571598
26	139	21	5.23	358.16	2,149	60.39	15.41	290	186	06571458
27	139	23	9.50	356.53	2,199	63.49	10.69	290	183	06571528
28	137	30	2.53	358.99	2,026	67.10	33.44	270	173	06499218
29	139	19	.78	359.56	2,115	57.17	20.61	289	189	06571388
30	141	21	2.68	350.14	2,158	57.62	20.19	289	188	06643348
31	178	18	2.59	358.45	1,978	44.19	36.42	232	140	07573908

^aTerms are defined in Fig. III-15.

Table VII-3I. Listings for narrow-angle frames in the Syrtis Major quadrangle (MC-13): Revs 100-676; viewing angles less than 80°. Index numbers correspond to those on the photomosaic of this quadrangle and to the accompanying narrow-angle frames (see Fig. VII-6I)

Index number	Rev	Frame number	Center of picture		Range (SRR-5), km	Lighting angle (SLAR-5), °	Viewing angle (VAR-5), °	North direction (NORAN) ^a	Sun direction (SUNAN) ^a	DAS time
			Latitude (LR-5), °	Longitude (LOR-5), °						
1	155	32	22.96	272.13	3,205	75.23	23.40	290	185	07147978
2	155	29	17.16	279.59	2,924	66.04	26.29	292	188	07147768
3	116	33	11.82	279.51	2,331	76.49	13.43	289	182	05744478
4	157	25	13.41	273.46	2,258	60.19	7.01	291	182	07219378
5	157	29	14.65	272.46	2,907	63.08	29.59	292	190	07219728
6	239	07	11.84	270.98	2,635	19.65	39.14	292	163	10169254
7	239	08	11.94	271.19	2,782	19.82	41.90	294	167	10169324
8	239	09	12.77	270.25	2,685	21.31	42.23	295	172	10169345
9	157	23	9.20	275.14	2,197	56.99	11.66	291	184	07219308
10	157	19	-.47	278.62	2,117	50.72	21.62	290	191	07219168
11	157	21	4.92	276.81	2,148	53.87	16.43	290	187	07219238
12	196	18	4.90	275.62	2,060	39.92	41.68	216	126	08621694
13	233	10	28.32	289.64	3,199	39.78	29.44	303	170	09533754
14	114	33	22.08	284.11	2,336	84.10	17.92	283	179	05672448
15	153	29	16.41	288.58	2,897	66.31	26.52	292	188	07075738
16	237	08	15.56	281.51	2,804	22.00	42.08	294	153	10097364
17	237	09	16.10	281.00	2,916	22.95	42.77	295	157	10097434
18	430	10	15.05	281.66	2,278	31.73	15.16	113	194	11798151
19	114	30	13.10	288.51	2,126	76.77	8.00	286	179	05672308
20	155	23	10.80	283.44	2,243	58.95	11.33	291	184	07147348
21	155	25	14.82	281.69	2,309	62.18	6.94	291	182	07147418
22	233	07	11.23	283.61	2,813	34.78	31.37	304	205	0953514
23	233	09	13.45	282.53	2,905	30.48	30.85	304	201	0953584
24	237	07	14.94	281.55	2,684	21.30	40.77	291	150	10097294
25	430	08	11.07	283.58	2,066	35.27	19.39	134	207	11797941
26	430	09	13.52	282.89	2,152	33.79	19.00	132	209	11798011
27	529	10	11.23	284.29	1,545	63.77	46.09	260	199	13032077
28	116	30	9.35	280.43	2,148	74.27	8.23	289	182	05744338
29	155	21	6.58	285.10	2,191	55.82	16.01	291	187	07147278
30	155	19	2.18	287.00	2,157	52.53	21.25	290	190	07147208
31	112	30	21.90	295.30	2,288	82.03	30.76	276	176	05600278
32	151	32	21.45	290.61	3,154	75.91	24.35	290	185	07003918
33	151	29	15.61	297.17	2,870	66.76	26.71	292	188	07003708
34	153	23	10.09	292.61	2,220	59.08	11.22	291	184	07075318
35	153	25	14.30	290.91	2,284	62.32	6.51	290	182	0707538
36	153	21	5.83	294.28	2,170	55.94	15.97	290	187	07075248
37	231	08	9.35	292.55	2,366	33.78	18.78	302	198	09881274
38	231	09	9.07	293.18	2,517	33.42	25.34	303	201	09881344
39	231	10	8.03	293.91	2,710	32.77	32.79	303	206	09881414
40	233	06	6.46	292.77	2,782	24.05	40.68	296	204	09953374
41	153	19	1.42	296.05	2,135	52.79	21.06	290	190	07075178
42	194	16	4.79	294.14	1,985	31.58	35.47	248	136	08549734
43	233	04	3.96	294.13	2,551	21.41	38.12	294	203	09953234
44	233	05	4.54	293.64	2,688	22.36	40.69	295	206	09953304
45	149	30	17.91	305.03	2,894	69.88	23.69	291	186	06931748
46	149	26	14.93	308.43	2,309	64.28	6.52	290	181	06931358
47	151	25	13.49	300.66	2,260	62.41	6.57	290	182	07003358
48	151	23	9.29	301.75	2,197	59.21	11.23	290	184	07003288
49	151	19	.56	305.34	2,117	52.80	21.32	290	190	07003148
50	151	21	4.99	303.43	2,149	56.06	16.06	290	187	07003218
51	147	29	15.97	314.93	2,856	68.96	25.51	291	187	06859718
52	149	24	10.79	310.11	2,244	61.09	11.08	291	184	06931328
53	149	22	6.60	311.79	2,192	57.94	15.72	290	186	06931258
54	149	20	2.24	313.72	2,156	54.61	20.91	290	189	06931188

^aTerms are defined in Fig. III-15.

Table VII-3m. Listings for narrow-angle frames in the Amethes quadrangle (MC-14): Revs 100–676; viewing angles less than 80°. Index numbers correspond to those on the photomosaic of this quadrangle and to the accompanying narrow-angle frames (see Fig. VII-6m)

Index number	Rev	Frame number	Center of picture		Range (SRR-5), ^a km	Lighting angle (SLAR-5), ^a deg	Viewing angle (VAR-5), ^a deg	North direction (NORAN) ^a	Sun direction (SUNAN) ^a	DAS time
			Latitude ^a (LR-5), deg	Longitude ^a (LOR-5), deg						
1	163	32	26.38	226.48	3,198	82.22	23.50	291	182	07435888
2	243	07	29.32	227.12	3,277	50.29	14.80	306	189	10313804
3	243	08	29.49	227.51	3,413	50.33	17.86	305	189	10313874
4	167	25	15.32	226.64	2,308	58.43	5.76	291	182	07579178
5	167	23	11.26	228.38	2,240	55.19	10.19	291	184	07579168
6	479	05	21.47	232.54	2,316	41.80	34.54	125	210	12902043
7	479	06	21.08	233.37	2,295	42.29	27.38	125	207	12902113
8	126	33	17.69	239.08	2,268	70.06	10.89	289	177	06104278
9	165	29	15.14	235.09	2,878	61.23	27.92	294	191	07507568
10	241	06	18.10	234.32	2,428	45.44	24.29	302	192	10241214
11	241	07	18.32	235.07	2,474	45.15	20.00	306	194	10241264
12	241	08	18.76	235.43	2,547	45.29	17.85	308	196	10241354
13	165	25	13.63	236.52	2,252	57.87	5.76	291	182	07507218
14	165	21	5.28	239.98	2,136	51.48	15.00	291	187	07507078
15	165	23	9.54	238.29	2,187	54.62	10.26	291	184	07507148
16	167	21	7.09	230.12	2,186	51.98	14.84	291	187	07579038
17	167	19	2.74	232.04	2,149	48.69	20.01	291	191	07578968
18	206	13	2.24	238.90	1,910	27.25	29.64	245	138	08981494
19	124	30	15.11	248.62	2,157	69.00	10.97	287	176	06032248
20	124	33	17.62	248.41	2,316	70.86	11.15	289	178	06032388
21	126	30	15.07	240.01	2,129	67.68	13.93	286	174	06104138
22	163	29	17.71	242.67	2,893	64.47	24.37	293	188	07435678
23	163	23	10.80	247.18	2,236	56.25	10.94	291	184	07435258
24	163	25	14.87	245.44	2,301	59.48	6.47	291	182	07435328
25	163	21	6.55	248.55	2,185	53.00	15.80	291	187	07435188
26	165	19	.81	241.80	2,103	48.33	20.26	290	191	075070C8
27	202	16	1.88	249.65	1,904	36.01	29.51	231	137	08837644
28	668	01	29.16	257.65	3,086	63.09	10.57	114	180	133497E0
29	436	C8	20.45	251.65	2,280	30.61	22.86	129	218	11975079
30	436	09	21.25	250.24	2,319	29.00	18.15	121	212	11975149
31	436	10	20.86	250.54	2,447	29.00	11.46	99	190	11975289
32	122	30	15.23	257.99	2,149	65.72	11.56	287	175	059602E8
33	122	33	17.78	257.43	2,303	71.73	10.63	289	178	05960428
34	159	30	18.16	259.84	2,683	66.99	23.12	293	187	07291758
35	161	30	17.46	251.43	2,878	65.42	24.16	293	188	07363718
36	161	24	10.56	256.41	2,225	56.77	10.76	291	184	07363298
37	161	26	14.62	254.66	2,290	60.01	6.29	291	182	073633E8
38	161	22	6.36	258.08	2,172	53.64	15.37	291	187	07363228
39	161	20	1.93	259.68	2,137	50.46	20.56	291	191	07363158
40	163	19	2.19	250.84	2,149	49.75	20.94	291	191	07435118
41	436	04	1.74	253.43	1,881	38.63	20.27	127	194	11974659
42	436	05	2.25	252.66	1,885	37.41	13.36	124	190	11974729
43	436	06	1.25	253.62	1,975	38.28	7.60	111	175	11974849
44	473	05	22.01	263.51	2,343	43.44	35.86	134	213	12686233
45	473	06	22.49	263.14	2,345	42.37	30.76	131	211	12686303
46	473	07	21.58	264.63	2,363	43.70	25.76	129	207	12686373
47	159	26	15.08	263.68	2,304	60.96	6.26	291	182	07291408
48	159	24	11.02	265.38	2,238	57.75	10.68	291	184	07291338
49	159	22	6.83	267.03	2,184	54.64	15.25	291	187	07291268
50	473	02	6.23	268.77	1,994	52.92	28.73	133	200	12685953
51	473	03	5.77	269.33	1,993	53.28	23.53	131	197	12686023
52	159	20	2.39	268.88	2,148	51.39	20.53	290	190	07291158
53	198	16	.48	269.94	1,849	35.31	23.91	241	145	08693724
54	200	18	1.78	260.29	1,895	35.37	29.13	233	137	08765684

^a Terms are defined in Fig. III-15.

Table VII-3n. Listings for narrow-angle frames in the Elysium quadrangle (MC-15): Revs 100-676; viewing angles less than 80°. Index numbers correspond to those on the photomosaic of this quadrangle and to the accompanying narrow-angle frames (see Fig. VII-6n)

Index number	Rev	Frame number	Center of picture		Range (SRR-5), km	Lighting angle (SLAR-5), deg	Viewing angle (VAR-5), deg	North direction (NORAN) ^a	Sun direction (SUNAN) ^a	DAS time
			Latitude (LR-5), deg	Longitude (LOR-5), deg						
1	175	29	18.13	184.59	2,894	61.56	23.07	296	189	07E670E8
2	175	25	15.00	188.67	2,315	55.65	6.24	292	182	07E665738
3	177	23	10.92	180.56	2,244	51.69	10.36	292	185	07938558
4	218	13	14.26	180.71	2,863	32.68	36.10	296	184	09413674
5	177	21	6.84	182.68	2,189	48.54	14.81	292	188	07938488
6	177	19	2.47	184.52	2,151	45.36	19.92	292	192	07938418
7	101	30	26.07	190.32	2,949	65.69	69.62	306	157	05204148
8	173	25	15.24	198.35	2,309	56.23	5.72	292	182	07794848
9	173	29	18.58	194.23	2,876	62.61	21.94	295	188	07795158
10	528	06	15.34	198.38	2,335	68.69	37.54	134	194	12985877
11	175	23	10.92	190.42	2,249	52.39	10.77	292	185	07866668
12	175	21	6.76	192.11	2,196	49.25	15.35	292	188	07866598
13	214	15	7.69	192.07	2,028	34.91	35.10	224	126	09269124
14	450	05	7.15	192.10	2,274	43.19	23.24	101	175	12326476
15	450	06	7.47	191.56	2,384	42.26	26.08	86	162	12326546
16	450	07	8.27	190.79	2,642	40.64	32.41	54	135	12326686
17	175	19	2.45	194.08	2,159	45.95	20.48	292	192	07866528
18	430	19	25.83	201.67	6,720	58.40	122.25	32	212	11801371
19	169	32	24.72	203.49	3,169	75.32	21.15	293	185	07651628
20	181	20	21.95	203.53	3,619	28.90	83.35	294	115	08081988
21	130	33	19.34	201.77	2,485	85.73	35.58	280	179	06248058
22	132	33	19.33	203.00	2,262	75.34	15.35	284	177	06319948
23	171	25	15.03	207.77	2,301	56.89	5.65	292	182	07722958
24	171	29	18.54	203.18	2,863	63.74	21.58	295	188	07723308
25	130	29	10.67	207.98	2,209	77.08	26.92	287	181	06247918
26	130	31	14.95	205.10	2,333	61.23	30.88	284	180	06247988
27	132	29	10.45	206.56	2,072	68.33	6.33	286	179	06319808
28	132	31	14.83	205.13	2,158	71.69	10.38	285	178	06319878
29	171	23	10.83	209.47	2,235	53.64	10.35	292	185	07722888
30	173	23	11.19	200.06	2,241	53.00	10.11	292	184	07794778
31	173	21	6.94	201.70	2,187	49.88	14.81	292	187	07794708
32	173	19	2.50	203.56	2,151	46.64	20.11	291	192	07794638
33	134	33	29.59	212.53	2,696	63.38	45.92	297	160	06391838
34	668	11	25.01	213.18	10,093	29.98	55.48	7	112	13353560
35	134	31	24.30	213.35	2,554	59.68	43.32	294	159	06391768
36	676	01	24.18	213.06	3,112	81.12	15.83	110	177	13496013
37	676	02	24.97	213.19	3,230	80.63	17.11	109	177	13496083
38	134	29	19.27	214.44	2,442	55.98	41.72	292	159	06391698
39	169	29	17.75	215.46	2,893	61.64	24.52	294	189	07651418
40	169	23	10.73	218.98	2,233	54.26	10.55	292	184	07650958
41	169	25	14.78	217.20	2,299	57.53	6.08	291	182	07651068
42	171	21	6.58	211.12	2,182	50.52	15.08	292	188	07722818
43	444	05	7.85	214.56	1,989	36.91	14.40	124	195	12150747
44	444	06	8.15	214.36	2,023	35.93	7.63	119	189	12150817
45	444	07	7.32	215.58	2,183	36.71	12.50	98	170	12150957
46	171	19	2.22	212.56	2,145	47.33	20.17	291	192	07722748
47	207	01	1.75	216.01	7,879	163.27	124.53	99	99	09011734
48	167	29	18.75	224.67	2,886	62.91	22.99	294	188	07579528
49	169	21	6.63	220.71	2,179	51.10	15.04	292	187	07650928
50	169	19	2.34	222.68	2,142	47.80	20.12	291	191	07650858

^aTerms are defined in Fig. III-15.

Table VII-4a. Listings for narrow-angle frames in the Memnonia quadrangle (MC-16): Revs 100–676; viewing angles less than 80°. Index numbers correspond to those on the photomosaic of this quadrangle and to the accompanying narrow-angle frames (see Fig. VII-7a)

Index number	Rev	Frame number	Center of picture		Range (SRR-5), km	Lighting angle (SLAR-5), deg	Viewing angle (VAR-5), deg	North direction (NORAN) ^a	Sun direction (SUNAN) ^a	DAS time
			Latitude ^a (LR-5), deg	Longitude ^a (LOR-5), deg						
1	148	10	-4.56	139.73	1,765	50.15	7.92	273	174	06894788
2	189	14	-12.95	137.67	1,828	28.96	31.53	216	138	08369344
3	150	10	-17.31	136.01	1,692	42.82	8.25	273	187	06966608
4	150	08	-21.92	138.53	1,696	40.73	13.74	271	193	06966538
5	228	06	-25.86	139.54	1,897	27.16	32.32	177	147	09772004
6	146	16	-3.62	148.32	1,778	51.52	8.21	274	174	06822828
7	146	17	-3.30	145.67	2,105	51.59	25.92	288	193	06823108
8	148	17	-4.21	140.85	2,088	50.44	26.22	288	194	06895068
9	222	04	-4.45	149.50	2,679	33.35	67.98	151	110	09556264
10	222	09	-1.30	149.18	2,078	35.36	43.83	178	104	09556614
11	148	14	-9.17	141.72	1,722	47.25	2.93	273	177	06894718
12	148	12	-13.95	143.58	1,694	44.84	2.49	272	182	06894648
13	187	14	-10.74	147.95	1,732	28.73	18.25	246	160	08297524
14	148	10	-18.73	145.66	1,683	42.72	8.03	271	187	06894578
15	423	02	-19.65	142.19	1,727	56.86	19.28	132	188	11656120
16	148	08	-23.37	148.28	1,691	40.67	13.70	270	193	06894508
17	189	11	-22.55	142.55	1,746	27.71	21.75	214	156	08369204
18	423	01	-20.59	142.67	1,783	58.04	25.44	131	189	11656050
19	423	03	-21.65	143.18	1,690	58.29	10.59	127	181	11656260
20	111	28	-29.62	161.21	1,716	47.93	12.63	249	168	05563248
21	191	C7	-26.20	140.41	2,045	24.65	38.54	195	153	08440954
22	191	C8	-25.13	140.27	1,954	24.06	35.07	202	157	08441024
23	228	C7	-25.95	140.25	1,776	27.25	23.26	183	154	09772074
24	228	08	-25.40	140.29	1,703	26.91	15.21	191	161	09772144
25	144	16	-3.55	157.34	1,780	52.32	8.34	274	174	06750868
26	144	17	-3.20	158.78	2,106	52.31	25.80	288	193	06751148
27	222	05	-4.41	150.00	2,487	33.18	62.62	157	108	09556334
28	222	07	-4.65	150.60	2,042	33.62	43.35	176	107	09556544
29	261	03	-4.91	150.48	1,970	23.35	37.39	158	96	10686039
30	261	04	-4.39	150.28	1,929	23.74	32.04	160	93	10686109
31	144	14	-8.20	159.26	1,734	49.39	3.24	274	177	06750798
32	146	14	-8.32	150.35	1,732	48.49	2.89	274	177	06822758
33	222	06	-5.30	150.18	2,287	33.39	55.70	163	107	09556444
34	224	07	-9.02	153.14	1,721	22.59	9.45	237	163	09628574
35	224	09	-5.55	150.42	1,756	24.87	10.60	240	158	09628644
36	224	10	-5.87	150.53	2,049	25.76	25.57	293	214	05628924
37	224	11	-5.52	150.92	2,182	26.06	31.49	296	218	09628994
38	458	03	-7.90	151.26	1,829	51.58	26.88	123	188	12499645
39	458	04	-7.22	150.56	1,794	50.69	19.91	123	185	12499715
40	458	05	-6.58	150.68	1,785	49.83	12.98	122	182	12499785
41	146	12	-13.05	152.27	1,702	45.92	2.47	273	181	06822668
42	185	14	-14.39	156.61	1,692	30.05	12.86	244	165	08225494
43	146	10	-17.80	154.25	1,689	43.75	7.82	272	186	06822618
44	146	08	-22.41	156.66	1,693	41.71	13.18	271	192	06822548
45	187	11	-20.18	152.32	1,690	26.92	14.98	243	180	08297364
46	142	16	-4.37	167.00	1,770	52.34	8.13	274	174	06678968
47	142	17	-3.82	168.43	2,089	52.38	25.84	288	193	06679188
48	183	18	-8.84	164.29	1,944	33.97	20.99	278	177	08153948
49	218	11	-2.26	165.07	2,091	41.02	28.40	312	214	09413114
50	220	12	-4.28	161.68	1,935	32.61	35.62	192	115	09484654
51	220	13	-3.12	160.99	1,909	33.62	31.33	203	122	09484724
52	142	14	-9.16	168.86	1,726	49.48	2.74	274	177	06678838
53	144	12	-12.82	161.37	1,703	46.60	2.04	274	181	06750728

^aTerms are defined in Fig. III-15.

Table VII-4a. (contd)

Index number	Rev	Frame number	Center of picture		Range (SRR-5), km	Lighting angle (SLAR-5), deg	Viewing angle (VAR-5), deg	North direction (NORAN) ^a	Sun direction (SUNAN) ^a	DAS time
			Latitude (LR-5), deg	Longitude (LOR-5), deg						
54	145	01	-13.16	163.84	9,834	153.19	112.08	71	251	06781038
55	183	14	-14.19	165.82	1,697	30.46	13.99	244	164	08153528
56	144	10	-17.53	163.59	1,690	44.12	7.60	273	186	06750658
57	144	08	-22.23	165.55	1,694	42.08	13.14	271	191	06750588
58	185	11	-23.53	161.40	1,672	28.79	10.96	241	184	08225354
59	105	27	-26.64	166.66	1,710	51.00	14.33	254	168	05347368
60	133	01	-5.55	170.42	5,866	108.70	130.72	159	159	06350468
61	140	16	-3.09	175.61	1,788	54.11	7.90	275	174	06607018
62	140	17	-2.60	177.21	2,120	53.97	25.77	288	192	06607298
63	140	14	-7.76	177.55	1,741	51.09	2.71	275	178	06606948
64	179	18	-6.01	174.55	1,930	42.96	17.58	291	197	08010098
65	140	12	-12.28	179.69	1,710	48.18	2.39	275	181	06606878
66	142	12	-13.83	170.87	1,698	46.83	2.49	273	181	06678768
67	181	16	-14.04	175.14	1,708	30.82	16.48	241	160	08081568
68	189	08	-14.92	171.20	3,009	11.62	71.19	223	250	08368854
69	142	10	-18.42	173.09	1,666	44.42	7.71	273	186	06678698
70	142	08	-23.05	175.47	1,691	42.40	13.08	271	192	06678628
71	181	13	-23.09	179.83	1,678	29.17	11.86	237	177	08081428
72	183	11	-23.34	170.68	1,675	28.92	11.46	240	182	08153388
73	103	27	-27.55	176.29	1,714	51.15	13.89	254	169	05275408

^aTerms are defined in Fig. III-15.

Table VII-4b. Listings for narrow-angle frames in the Phoenicis Lacus quadrangle (MC-17): Revs 100-676; viewing angles less than 80°. Index numbers correspond to those on the photomosaic of this quadrangle and to the accompanying narrow-angle frames (see Fig. VII-7b)

Index number	Rev	Frame number	Center of picture		Range (SRR-5), km	Lighting angle (SLAR-5), deg	Viewing angle (VAR-5), deg	North direction (NORAN) ^a	Sun direction (SUNAN) ^a	DAS time
			Latitude (LR-5), deg	Longitude (LOR-5), deg						
1	158	16	-1.74	93.54	1,799	48.70	8.01	274	173	07254868
2	158	17	-1.68	95.21	2,141	48.81	25.91	290	194	07255148
3	236	10	-1.93	98.15	2,192	21.48	29.37	294	214	10061034
4	115	30	-9.66	95.44	2,213	77.23	45.65	305	188	05707938
5	158	14	-6.51	95.89	1,748	45.73	2.56	273	177	07254758
6	158	12	-11.22	97.72	1,715	43.26	2.68	273	182	07254728
7	199	12	-13.97	93.73	1,688	26.49	11.97	241	168	08729454
8	158	10	-15.86	99.71	1,697	41.11	7.82	273	187	07254658
9	160	10	-16.86	91.04	1,691	40.17	8.04	271	188	07326618
10	160	08	-21.46	93.50	1,694	38.33	13.46	270	194	07226548
11	199	09	-23.31	98.49	1,671	26.59	11.52	238	190	08729354
12	121	28	-25.79	94.74	1,656	46.98	3.36	260	176	05923398
13	156	16	-3.61	103.68	1,776	48.13	6.65	273	174	07182838
14	156	17	-3.13	104.78	2,116	48.47	26.54	289	195	07183118
15	431	04	-1.02	102.48	1,872	43.93	15.80	133	195	11833711
16	444	16	-3.49	100.26	13,676	118.99	112.29	327	147	12159217
17	156	14	-8.14	105.52	1,731	45.40	1.95	273	178	07182768
18	234	11	-9.46	108.41	1,745	20.59	6.65	256	189	05988654
19	236	09	-8.03	104.15	1,781	15.15	18.79	246	183	10060614
20	156	12	-12.72	107.40	1,702	43.00	2.96	272	182	07182698
21	197	09	-13.97	103.00	1,705	26.57	16.98	232	158	08657464

^aTerms are defined in Fig. III-15.

Table VII-4b. (contd)

Index number	Rev	Frame number	Center of picture		Range (SRR-5), km	Lighting angle (SLAR-5), deg	Viewing angle (VAR-5), deg	North direction (NORAN) ^a	Sun direction (SUNAN) ^a	DAS time
			Latitude (LR-5), deg	Longitude (LOR-5), deg						
22	234	06	-14.68	109.00	2,402	20.30	57.73	163	121	09988024
23	234	07	-14.72	108.42	2,230	21.01	52.30	167	122	09988094
24	234	08	-13.94	107.98	2,103	21.14	47.58	172	123	09988164
25	236	07	-11.07	105.47	1,755	15.49	19.07	241	191	10060544
26	431	01	-11.16	105.38	1,737	52.54	16.48	134	192	11833431
27	431	02	-10.28	105.01	1,746	51.49	13.52	133	190	11833501
28	528	17	-10.00	105.58	16,371	75.49	67.58	245	193	12996097
29	113	30	-17.01	109.57	2,284	71.74	47.15	312	194	05635978
30	156	10	-17.43	109.49	1,689	40.89	8.35	272	188	07182628
31	158	08	-20.47	102.08	1,697	39.16	13.18	271	193	07254588
32	197	06	-23.03	107.64	1,673	26.46	11.86	230	179	08657324
33	201	01	-21.96	101.00	2,282	18.16	50.00	198	170	08800894
34	201	02	-23.00	100.31	2,105	19.45	43.59	204	177	08800964
35	119	25	-29.77	106.17	1,662	45.80	3.02	261	182	05851368
36	119	27	-25.16	103.62	1,653	47.70	2.34	263	178	05851438
37	154	16	-4.45	112.81	1,765	48.33	7.25	272	174	07110808
38	154	17	-4.06	114.04	2,098	48.53	26.73	289	195	07110888
39	154	14	-9.18	114.75	1,721	45.54	1.93	272	177	07110738
40	187	08	-9.24	119.46	3,914	53.66	90.16	136	136	08296894
41	191	18	-6.73	119.51	1,991	39.70	22.76	296	205	08441934
42	154	12	-13.86	116.71	1,694	43.13	3.30	271	182	07110668
43	195	12	-13.74	111.76	1,693	27.38	13.48	241	165	08585504
44	234	09	-12.73	110.01	1,717	20.46	7.94	251	194	09988564
45	154	10	-18.48	118.86	1,684	41.04	8.49	271	188	07110598
46	156	08	-22.12	111.95	1,694	39.04	13.99	270	194	07182558
47	195	09	-22.98	116.54	1,670	26.90	11.39	237	185	08585364
48	117	28	-26.61	113.27	1,657	47.62	2.52	261	177	05779408
49	152	17	-4.64	123.24	2,077	48.72	26.36	288	195	07039058
50	152	19	-.23	121.13	2,092	51.94	21.13	290	191	07039128
51	109	30	-9.71	124.02	2,144	77.41	42.14	303	187	05491918
52	141	01	-7.46	122.72	6,174	50.49	72.55	110	179	06640128
53	152	16	-5.44	121.85	1,755	48.62	7.16	271	174	07038778
54	189	18	-8.67	120.66	2,105	48.48	34.31	314	213	08369904
55	201	12	-9.49	122.91	4,090	12.27	90.15	267	267	08801944
56	226	11	-9.50	121.54	2,394	43.53	58.70	144	87	09700464
57	226	12	-8.79	121.11	2,352	44.21	56.28	141	75	09700534
58	228	09	-9.67	121.60	2,055	34.05	45.02	163	102	09772424
59	228	11	-6.97	120.39	2,066	35.14	44.49	165	98	09772494
60	152	12	-14.56	126.02	1,688	43.25	2.93	271	182	07038638
61	152	14	-10.02	123.86	1,714	45.81	2.16	271	177	07038708
62	154	06	-12.33	122.63	3,777	32.69	82.10	143	119	07109688
63	187	07	-11.64	120.14	3,983	52.67	90.04	136	136	08296824
64	191	14	-13.68	129.81	1,693	28.32	11.75	248	171	08441514
65	193	10	-13.74	120.50	1,700	27.96	15.62	237	160	08513474
66	226	10	-10.25	121.90	2,457	42.96	61.39	146	96	09700394
67	230	06	-11.14	120.55	2,629	24.68	65.28	153	113	09844034
68	230	07	-11.54	121.18	2,404	24.57	59.12	160	114	09844104
69	230	08	-10.90	121.66	2,239	24.02	53.72	166	115	09844174
70	152	10	-19.17	128.25	1,679	41.13	8.18	270	188	07038568
71	154	08	-23.08	121.37	1,690	39.23	13.92	269	194	07110528
72	193	07	-23.01	125.47	1,671	27.15	11.29	234	180	08513334
73	209	06	-28.89	124.35	3,869	63.58	69.29	155	205	09087754
74	150	16	-3.16	130.12	1,783	50.51	7.73	274	174	06966818
75	150	17	-2.79	131.61	2,119	50.46	26.18	288	193	06967098
76	150	14	-7.82	132.13	1,736	47.51	2.49	274	178	06966748
77	150	12	-12.57	134.02	1,706	44.99	2.88	273	182	06966678
78	152	08	-23.85	130.52	1,686	39.60	13.44	269	194	07038498
79	191	11	-22.90	134.38	1,677	27.59	12.75	244	190	08441374
80	193	04	-24.57	131.74	2,069	23.10	40.68	196	152	08512984
81	113	27	-28.62	131.60	1,708	47.97	12.79	250	168	05635278
82	193	03	-25.23	131.46	2,191	23.61	44.82	189	146	08512914

^aTerms are defined in Fig. III-15.

Table VII-4c. Listings for narrow-angle frames in the Coprates quadrangle (MC-18): Revs 100–676; viewing angles less than 80°. Index numbers correspond to those on the photomosaic of this quadrangle and to the accompanying narrow-angle frames (see Fig. VII-7c)

Index number	Rev	Frame number	Center of picture		Range (SRR-5), ^a km	Lighting angle (SLAR-5), ^a deg	Viewing angle (VAR-5), ^a deg	North direction (NORAN) ^a deg	Sun direction (SUNAN) ^a deg	DAS time
			Latitude (LR-5), deg	Longitude (LOR-5), deg						
1	133	31	-6.68	47.57	2,260	39.09	47.23	280	160	06355438
2	168	16	-3.99	48.28	1,773	44.31	8.29	269	172	07614528
3	168	17	-3.52	49.66	2,096	44.16	25.91	289	197	07614808
4	248	05	-2.92	46.49	2,323	14.27	37.40	291	226	10492654
5	207	15	-7.55	49.06	1,928	32.19	19.84	291	207	09017614
6	248	03	-7.57	48.53	2,341	13.97	42.38	288	243	10492584
7	190	02	-11.33	48.66	5,253	74.28	85.48	170	195	08403784
8	170	10	-18.15	45.07	1,685	36.88	7.67	267	188	07686208
9	170	08	-22.63	47.42	1,688	35.61	12.61	266	196	07686138
10	131	28	-27.20	48.60	1,663	44.06	3.32	255	176	06282968
11	445	01	-26.16	47.03	1,698	70.89	12.62	127	184	12185957
12	166	16	-3.21	57.63	1,780	45.21	8.41	270	172	07542638
13	166	17	-2.72	58.58	2,102	45.29	25.32	289	196	07542918
14	102	09	-9.01	55.01	5,349	8.78	88.10	94	263	05238098
15	166	14	-7.86	59.48	1,733	42.54	3.39	270	176	07542568
16	168	14	-8.64	50.40	1,727	41.47	2.95	269	176	07614458
17	102	07	-10.07	58.85	5,375	11.66	86.37	99	259	05238028
18	168	12	-13.27	52.55	1,698	39.06	2.40	268	182	07614388
19	190	01	-12.96	50.33	5,209	75.97	82.40	151	193	08403714
20	248	01	-12.45	50.87	2,385	15.53	47.72	284	256	10492514
21	168	10	-17.96	54.62	1,685	37.32	7.66	267	188	07614318
22	120	07	-20.34	55.87	5,586	50.49	90.15	179	179	05885878
23	168	08	-22.57	56.79	1,688	36.16	12.72	266	195	07614248
24	120	09	-27.35	51.70	5,139	84.87	84.19	171	186	05885948
25	129	27	-27.15	58.07	1,661	44.57	3.08	256	176	06211098
26	129	30	-25.27	52.21	2,423	51.97	54.24	287	211	06211658
27	127	30	-3.36	60.99	1,840	55.70	12.52	279	173	06139768
28	164	16	-1.87	66.46	1,798	46.73	8.23	272	173	07470748
29	164	17	-1.60	67.91	2,134	46.69	25.50	290	195	07471028
30	164	14	-6.58	68.24	1,748	44.00	3.13	272	177	07470678
31	114	07	-13.33	66.81	5,594	75.06	90.63	197	197	05669858
32	121	31	-11.61	69.86	2,224	73.81	44.93	310	192	05923958
33	166	12	-12.67	61.43	1,702	40.21	2.20	270	182	07542498
34	205	08	-13.95	66.39	1,696	24.61	14.03	235	165	08453034
35	478	01	-11.62	69.10	1,738	65.93	12.49	124	185	12865573
36	114	09	-15.42	65.84	5,467	73.43	90.67	199	199	05669928
37	166	10	-17.32	63.71	1,688	38.13	7.65	269	188	07542428
38	166	08	-21.84	66.06	1,689	36.62	12.72	268	195	07542358
39	127	27	-26.39	67.24	1,659	45.23	3.31	257	176	06139208
40	162	16	-2.91	76.16	1,784	46.67	7.46	272	173	07398768
41	162	17	-2.60	77.42	2,122	46.83	26.21	290	196	07399068
42	149	01	-8.47	72.07	15,375	125.23	224.72	297	190	06918168
43	162	14	-7.48	78.11	1,737	43.84	2.54	272	177	07398718
44	123	30	-11.74	70.07	1,988	64.11	29.99	299	194	05995918
45	161	01	-10.42	71.27	6,865	142.89	125.45	95	95	07357768
46	162	12	-12.13	79.59	1,706	41.47	2.58	271	182	07398648
47	164	12	-11.24	70.16	1,714	41.53	2.09	272	182	07470608
48	203	12	-14.22	75.53	1,688	25.51	10.68	243	173	08873414
49	164	10	-15.87	72.33	1,696	39.33	7.37	271	188	07470538
50	437	02	-18.38	76.31	1,704	57.46	15.70	128	184	12010219
51	437	03	-18.75	76.65	1,673	57.83	4.33	127	182	12010289
52	164	08	-20.49	74.66	1,695	37.59	12.74	270	194	07470468
53	205	05	-23.14	71.20	1,675	25.36	12.16	232	188	08945164

^aTerms are defined in Fig. III-15.

Table VII-4c. (contd)

Index number	Rev	Frame number	Center of picture		Range (SRR-5), ^a km	Lighting angle (SLAR-5); ^a deg	Viewing angle (VAR-5); ^a deg	North direction (NORAN) ^a	Sun direction (SUNAN) ^a	DAS time
			Latitude (LR-5), ^a deg	Longitude (LOR-5), ^a deg						
54	125	25	-29.79	78.27	1,663	44.74	2.32	259	182	06067248
55	125	27	-25.23	75.83	1,654	46.40	2.89	260	177	06067318
56	160	16	-2.81	85.25	1,784	47.41	7.55	272	173	07326828
57	160	17	-2.53	86.51	2,123	47.56	26.18	289	195	07327108
58	119	30	-5.76	83.07	2,011	71.64	30.70	297	187	05851998
59	160	14	-7.31	87.07	1,738	44.69	2.94	272	177	07326758
60	238	04	-7.27	87.04	2,111	23.35	29.94	299	227	10132924
61	238	05	-6.65	86.90	2,244	23.66	34.82	302	230	10132994
62	238	06	-6.23	86.13	2,388	24.64	39.13	304	232	10133044
63	240	01	-6.96	85.36	2,724	11.87	67.62	162	109	10203974
64	240	02	-6.92	86.53	2,524	11.17	42.76	173	113	10204044
65	240	03	-7.71	87.17	2,306	11.41	56.12	182	121	10204114
66	240	04	-7.41	85.64	1,774	14.19	19.29	238	174	10204534
67	240	05	-6.98	85.46	1,802	14.45	18.66	251	188	10204604
68	240	06	-6.59	85.23	1,858	14.80	20.91	264	200	10204674
69	240	07	-7.08	85.57	2,245	15.26	39.23	286	233	10204844
70	240	09	-5.14	84.78	2,321	15.99	39.69	289	228	10204954
71	242	04	-7.32	84.89	2,006	7.85	39.08	250	228	10276454
72	242	05	-6.96	84.48	2,054	7.89	39.74	258	232	10276564
73	242	06	-6.47	84.26	2,132	7.80	41.68	265	236	10276634
74	160	12	-12.02	88.52	1,706	42.30	2.26	272	182	07326688
75	201	08	-13.93	84.73	1,691	25.84	12.51	240	168	08801454
76	162	10	-16.80	81.95	1,690	39.54	7.70	271	188	07398578
77	162	08	-21.44	84.19	1,691	37.97	12.96	270	194	07398508
78	201	05	-23.14	89.43	1,672	26.14	11.68	236	189	08801314
79	203	09	-23.29	80.43	1,680	25.88	13.38	240	195	08873274
80	205	01	-24.59	83.00	2,209	20.60	46.16	197	186	08944744
81	205	02	-24.56	83.23	2,087	20.71	42.14	202	189	08944814
82	123	27	-26.00	85.58	1,656	46.48	3.02	259	177	05995358

^aTerms are defined in Fig. III-15.

Table VII-4d. Listings for narrow-angle frames in the Margaritifer Sinus quadrangle (MC-19): Revs 100–676; viewing angles less than 80°. Index numbers correspond to those on the photomosaic of this quadrangle and to the accompanying narrow-angle frames (see Fig. VII-7d)

Index number	Rev	Frame number	Center of picture		Range (SRR-5), ^a km	Lighting angle (SLAR-5); ^a deg	Viewing angle (VAR-5); ^a deg	North direction (NORAN) ^a	Sun direction (SUNAN) ^a	DAS time
			Latitude (LR-5), ^a deg	Longitude (LOR-5), ^a deg						
1	137	32	-4.03	.77	2,741	66.32	45.69	298	197	06499708
2	139	16	-4.22	.73	1,774	53.69	7.62	275	175	06571038
3	139	17	-3.64	2.02	2,098	53.87	25.86	288	192	06571318
4	139	14	-8.82	2.16	1,730	50.65	2.52	275	177	06570968
5	533	02	-5.92	.07	1,964	84.35	32.66	123	182	13165286
6	533	03	-5.11	.14	2,025	83.79	34.13	122	182	13165356
7	139	12	-13.37	4.81	1,701	47.90	2.48	274	181	06570898
8	451	02	-14.57	5.79	1,753	55.34	20.84	125	183	12361666
9	139	10	-17.86	6.62	1,687	45.58	7.16	273	185	06570828
10	451	03	-15.05	5.99	1,724	55.24	7.15	121	175	12361826
11	451	04	-15.63	6.35	1,782	55.59	14.53	115	170	12361856
12	139	08	-22.58	8.88	1,690	43.73	12.35	272	191	06570758
13	180	13	-23.32	4.29	1,679	29.84	12.13	248	188	08045518
14	184	10	-22.15	9.16	2,427	15.79	56.90	224	228	08189024
15	102	27	-27.95	1.12	1,723	51.22	14.77	253	168	05239428

^aTerms are defined in Fig. III-15.

Table VII-4d. (contd)

Index number	Rev	Frame number	Center of picture		Range (SRR-5), km	Lighting angle (SLAR-5), deg	Viewing angle (VAR-5), deg	North direction (NORAN) ^a	Sun direction (SUNAN) ^a	DAS time
			Latitude (LR-5), deg	Longitude (LOR-5), deg						
16	174	16	-3.71	19.75	1,780	42.46	8.19	268	171	07830198
17	176	16	-3.72	10.19	1,781	41.88	8.31	267	171	07902088
18	176	17	-3.28	11.77	2,106	41.72	25.75	290	198	07902368
19	176	14	-8.39	12.25	1,734	39.17	2.96	267	176	07902018
20	217	09	-5.28	10.30	2,024	20.45	29.35	277	200	09377064
21	529	01	-8.58	15.14	1,826	81.66	26.47	121	183	13021297
22	176	12	-13.03	14.34	1,704	36.95	2.33	267	182	07901948
23	176	10	-17.67	16.49	1,690	35.29	7.60	266	189	07901878
24	176	08	-22.34	18.62	1,693	34.42	12.79	265	197	07901808
25	178	09	-24.29	18.99	2,247	25.02	47.13	193	137	07973138
26	178	10	-23.10	19.54	2,140	24.12	44.15	201	141	07973208
27	178	13	-23.17	14.50	1,684	29.30	13.13	241	179	07973558
28	182	07	-24.93	19.60	2,608	18.44	57.07	203	213	08116848
29	182	08	-24.29	19.59	2,530	17.77	56.54	210	218	08116918
30	182	09	-24.68	18.71	2,406	18.08	54.00	216	218	08116988
31	184	07	-22.15	10.50	2,717	16.00	61.12	206	221	08188814
32	184	08	-20.59	11.14	2,693	14.53	62.30	215	229	08188884
33	184	09	-21.35	10.52	2,552	15.10	59.57	219	228	08188954
34	100	27	-29.87	11.72	1,736	50.62	14.41	252	168	05167468
35	176	06	-25.70	19.43	3,060	31.85	66.38	162	125	07900968
36	178	07	-25.61	19.69	2,533	24.99	54.19	181	132	07972998
37	178	08	-25.04	18.81	2,385	25.41	50.84	187	134	07973068
38	182	10	-25.21	18.46	2,313	18.59	52.22	221	222	08117058
39	172	16	-3.97	29.51	1,775	42.80	7.89	268	171	07758308
40	174	17	-3.28	21.27	2,106	42.36	25.83	290	198	07830478
41	174	14	-8.46	21.82	1,733	39.71	2.65	268	176	07830128
42	174	12	-13.07	23.88	1,703	37.48	2.53	267	182	07830058
43	174	10	-17.67	26.02	1,690	35.78	7.70	267	189	07829988
44	174	08	-22.27	28.21	1,692	34.77	12.75	266	196	07829918
45	217	07	-23.08	28.93	2,017	20.23	43.34	228	231	09376434
46	217	08	-22.54	28.57	2,041	19.66	45.00	236	237	09376504
47	135	27	-27.02	29.60	1,662	43.06	2.42	255	177	06426768
48	137	27	-26.93	20.25	1,662	42.43	2.48	253	176	06498658
49	174	06	-27.11	29.41	2,982	32.56	64.24	164	126	07829078
50	170	16	-3.91	38.58	1,774	43.49	8.68	268	171	07686418
51	172	17	-3.48	30.78	2,099	42.96	25.77	290	198	07758588
52	172	14	-8.55	31.15	1,730	40.49	3.41	268	176	07758238
53	172	12	-13.19	33.31	1,700	38.13	2.02	267	182	07758168
54	172	10	-17.81	35.47	1,686	36.38	7.23	267	188	07758098
55	172	08	-22.42	37.75	1,689	35.24	12.43	266	196	07758028
56	133	28	-27.00	39.11	1,662	43.52	3.20	254	176	06354878
57	215	06	-29.84	37.50	1,954	26.76	33.09	200	202	09304264
58	170	17	-3.46	40.36	2,090	43.53	25.43	289	197	07686698
59	170	14	-8.68	40.78	1,727	40.96	3.44	268	176	07686348
60	170	12	-13.48	42.75	1,698	38.75	2.22	268	182	07686278
61	445	02	-21.66	44.45	1,702	66.22	14.76	129	186	12186027
62	122	07	-28.94	43.21	5,047	66.07	79.80	158	185	05957838
63	213	05	-27.77	42.82	2,082	24.66	38.87	189	178	09232304
64	213	06	-27.25	42.45	1,979	24.24	34.95	194	183	09232374

^a Terms are defined in Fig. III-15.

Table VII-4e. Listings for narrow-angle frames in the Sinus Sabaeus quadrangle (MC-20): Revs 100–676; viewing angles less than 80°. Index numbers correspond to those on the photomosaic of this quadrangle and to the accompanying narrow-angle frames (see Fig. VII-7e)

Index number	Rev	Frame number	Center of picture		Range (SRR-5), km	Lighting angle (SLAR-5), deg	Viewing angle (VAR-5), deg	North direction (NORAN)	Sun direction (SUNAN) ^a	DAS time
			Latitude (LR-5), deg	Longitude (LOR-5), deg						
1	149	18	-2.21	315.69	2,137	51.38	26.22	289	195	06931118
2	149	15	-6.95	316.20	1,746	48.44	2.77	275	177	06930768
3	149	13	-11.55	318.24	1,713	45.68	2.43	274	182	06930698
4	190	13	-22.86	318.58	1,670	27.76	10.88	236	180	08405324
5	147	16	-4.10	323.56	1,772	50.90	7.95	273	174	06858808
6	147	17	-3.73	325.33	2,099	50.95	26.21	288	194	06859088
7	147	14	-8.78	325.87	1,727	48.02	2.78	273	177	06858738
8	188	18	-8.54	323.41	2,014	29.88	30.53	280	202	08333854
9	227	10	-6.77	329.16	1,905	12.31	31.85	251	182	09736584
10	227	11	-9.74	329.41	2,203	14.39	42.59	275	231	09736794
11	227	13	-8.83	329.55	2,515	14.04	51.13	279	239	09736934
12	422	08	-7.94	329.24	1,933	50.65	28.36	137	196	11620560
13	147	12	-13.49	327.81	1,698	45.49	2.48	273	181	06858668
14	147	10	-18.13	329.95	1,686	43.21	7.73	272	187	06858598
15	149	11	-16.21	320.40	1,697	43.24	7.80	273	186	06930628
16	149	09	-20.94	322.67	1,698	41.23	13.35	272	192	06930558
17	188	13	-22.97	327.72	1,676	28.18	12.22	244	188	08333364
18	110	27	-28.63	325.01	1,714	48.73	13.46	250	168	05527268
19	145	17	-3.61	332.73	1,780	52.02	8.08	274	174	06786848
20	145	18	-3.32	334.27	2,111	51.89	26.23	288	193	06787128
21	219	09	-4.90	337.03	2,183	42.46	48.22	163	89	09448744
22	145	15	-8.28	334.69	1,733	49.05	2.88	274	177	06786778
23	184	18	-8.23	334.94	1,783	37.11	7.26	277	188	08189754
24	186	18	-8.29	334.67	1,996	28.06	31.43	276	196	08261824
25	219	07	-7.57	338.78	2,139	40.53	47.60	163	94	09448674
26	227	08	-9.49	330.08	1,872	12.59	31.49	245	191	09736514
27	227	12	-9.49	330.01	2,369	14.04	47.81	278	237	09736864
28	145	13	-12.97	336.67	1,704	46.21	2.68	273	181	06786708
29	223	09	-12.59	339.58	1,717	22.41	7.65	253	189	09592554
30	422	04	-14.97	331.45	1,793	57.47	26.91	141	196	11620210
31	145	11	-17.51	339.06	1,690	43.79	7.78	272	186	06786638
32	422	03	-16.12	332.02	1,822	58.82	29.88	139	196	11620140
33	422	05	-17.34	332.56	1,827	59.05	27.46	135	191	11620350
34	147	08	-22.74	332.42	1,690	41.19	13.16	271	192	06858528
35	186	13	-23.10	336.72	1,672	28.46	10.98	238	180	08261334
36	143	09	-3.90	342.13	1,776	52.38	8.10	274	174	06714888
37	143	10	-3.67	343.53	2,105	52.38	26.32	288	193	06715168
38	223	10	-4.21	348.50	2,124	12.32	39.44	270	193	09592804
39	223	12	-2.95	346.12	2,133	14.91	36.63	274	192	09592874
40	143	07	-8.53	344.03	1,731	49.47	3.11	274	177	06714818
41	182	18	-5.86	340.44	1,778	41.05	16.51	255	164	08117758
42	260	10	-5.52	342.55	2,143	18.30	28.72	306	240	10650479
43	260	11	-5.87	342.64	2,305	19.03	35.46	309	244	10650549
44	143	05	-13.28	346.02	1,701	46.81	2.33	274	181	06714748
45	219	04	-11.57	346.23	2,749	31.59	68.38	151	115	09448184
46	219	05	-11.62	345.35	2,584	32.75	64.58	155	115	09448254
47	219	06	-10.33	345.26	2,461	32.90	61.40	158	113	09448324
48	223	08	-13.71	340.23	1,691	22.08	7.11	238	177	09592524
49	143	03	-17.98	348.22	1,689	44.39	7.83	273	186	06714678
50	223	07	-15.21	340.14	1,680	22.65	9.31	224	166	09592454
51	145	09	-22.14	341.28	1,692	41.88	12.91	272	192	06786568
52	184	13	-23.59	346.00	1,673	28.98	11.11	242	184	08189374
53	186	07	-23.19	343.45	2,622	21.89	57.71	179	130	08260774

^aTerms are defined in Fig. III-15.

Table VII-4e. (contd)

Index number	Rev	Frame number	Center of picture		Range (SRR-5), km	Lighting angle (SLAR-5), deg	Viewing angle (VAR-5), deg	North direction (NORAN) ^a	Sun direction (SUNAN) ^a	DAS time
			Latitude (LR-5), deg	Longitude (LOR-5), deg						
54	186	08	-22.65	343.19	2,467	21.86	54.41	185	133	08260844
55	186	09	-22.84	342.55	2,289	22.63	49.43	191	137	08260914
56	186	10	-23.26	342.76	2,116	23.01	43.25	199	145	08260984
57	223	05	-23.52	343.05	1,683	25.71	12.40	201	164	09592244
58	459	06	-23.33	343.67	1,771	74.32	24.11	123	183	12535485
59	459	07	-23.54	343.16	1,830	73.74	29.01	118	181	12535555
60	118	09	-29.66	345.64	4,248	21.72	63.81	140	222	05813918
61	260	05	-25.56	345.40	1,949	28.84	37.18	160	141	10649569
62	141	18	-2.03	350.58	1,802	54.43	8.27	276	174	06642998
63	141	19	-1.82	352.06	2,138	54.37	25.55	288	192	06643278
64	221	15	-3.89	356.01	1,940	13.47	35.64	244	148	09520634
65	221	17	-1.13	354.90	1,965	14.92	35.10	249	142	09520704
66	141	16	-6.60	352.50	1,752	51.39	3.35	276	177	06642928
67	180	18	-5.67	357.82	1,786	33.86	14.09	267	172	08045868
68	141	14	-11.15	354.44	1,718	48.62	1.54	276	181	06642858
69	260	07	-10.88	358.37	1,864	12.53	31.65	227	231	10649989
70	260	08	-10.39	358.81	1,913	12.06	33.56	239	244	10650059
71	260	09	-10.63	358.78	1,976	12.27	35.81	252	254	10650129
72	141	12	-15.82	356.47	1,699	46.11	6.82	275	185	06642788
73	416	03	-17.08	350.74	1,754	50.78	22.66	132	188	11443364
74	416	04	-15.96	350.11	1,717	49.36	16.64	132	186	11443434
75	416	05	-18.27	351.10	1,721	51.03	10.71	124	175	11443574
76	141	10	-20.59	358.67	1,698	43.93	12.41	274	190	06642718
77	143	01	-22.57	350.67	1,693	42.26	13.23	271	192	06714608
78	182	13	-23.32	355.27	1,676	29.09	11.41	240	180	08117408
79	104	11	-26.80	351.34	1,714	51.18	14.70	254	168	05311388

^a Terms are defined in Fig. III-15.

Table VII-4f. Listings for narrow-angle frames in the Iapygia quadrangle (MC-21): Revs 100–676; viewing angles less than 80°. Index numbers correspond to those on the photomosaic of this quadrangle and to the accompanying narrow-angle frames

Index number	Rev	Frame number	Center of picture		Range (SRR-5), km	Lighting angle (SLAR-5), deg	Viewing angle (VAR-5), deg	North direction (NORAN) ^a	Sun direction (SUNAN) ^a	DAS time
			Latitude (LR-5), deg	Longitude (LOR-5), deg						
1	107	06	-2.69	270.93	6,127	69.28	90.59	202	202	05417578
2	111	01	-1.17	273.19	13,647	129.25	220.62	296	187	05553378
3	157	16	-4.47	279.53	1,764	47.25	6.62	272	174	07218818
4	159	18	-2.13	270.65	2,130	48.18	25.99	290	195	07291128
5	159	15	-7.16	271.43	1,742	45.24	2.28	273	177	07290778
6	159	13	-11.75	273.48	1,710	42.63	2.86	273	182	07290708
7	159	11	-16.28	275.68	1,694	40.33	7.98	272	188	07290638
8	159	09	-20.95	277.82	1,694	38.71	13.17	271	194	07290568
9	200	13	-23.23	274.21	1,674	26.20	12.21	237	190	08765334
10	120	27	-25.27	279.05	1,655	47.44	3.76	261	176	05887418
11	122	27	-25.88	270.14	1,656	46.74	3.41	260	177	05959378
12	117	01	-1.21	280.79	9,404	144.87	120.62	91	91	05773388
13	155	16	-2.55	287.57	1,790	49.31	7.05	274	174	07146858
14	155	17	-2.35	288.57	2,140	49.31	26.70	289	195	07147138
15	157	17	-3.98	280.70	2,102	47.52	26.95	289	196	07219098
16	155	14	-7.21	289.45	1,743	46.45	1.93	274	178	07146768
17	157	14	-9.16	281.44	1,722	44.52	1.46	272	178	07218748
18	675	09	-9.59	288.88	15,563	71.66	109.52	26	206	13469623
19	157	12	-13.88	283.34	1,696	42.21	3.84	271	183	07218678
20	157	10	-18.58	285.42	1,686	40.28	9.15	270	189	07218608

^a Terms are defined in Fig. III-15.

Table VII-4f. (contd)

Index number	Rev	Frame number	Center of picture		Range (SRR-5), km	Lighting angle (SLAR-5), deg	Viewing angle (VAR-5), deg	North direction (NORAN) ^a	Sun direction (SUNAN) ^a	DAS time
			Latitude (LR-5), deg	Longitude (LOR-5), deg						
41	430	4	-17.49	288.26	1,739	55.25	21.27	130	187	11797241
22	430	5	-16.51	287.68	1,703	53.95	14.78	130	185	11797311
23	430	6	-18.69	288.67	1,723	55.48	12.48	122	176	11797451
24	157	8	-23.09	287.98	1,693	38.49	14.41	269	195	07218538
25	198	11	-23.02	283.09	1,674	26.53	12.31	240	191	08693374
26	118	27	-27.65	289.16	1,659	47.08	2.08	260	178	05815388
27	120	25	-29.81	281.64	1,663	45.52	1.49	260	181	05887348
28	153	16	-3.42	296.80	1,779	49.41	7.20	274	174	07074828
29	153	17	-2.95	298.17	2,117	49.49	26.31	289	194	07075108
30	237	6	-3.67	290.53	2,196	3.83	47.44	258	224	10096664
31	153	14	-8.00	298.89	1,734	46.38	2.13	273	178	07074758
32	237	4	-6.08	290.81	2,131	5.63	46.15	252	237	10096554
33	103	6	-13.31	298.93	5,651	74.56	82.74	172	197	05273728
34	105	6	-14.15	298.91	5,783	83.73	85.70	174	187	05345688
35	155	12	-11.88	291.38	1,712	43.91	3.26	274	183	07146718
36	155	10	-16.61	293.44	1,697	41.70	8.72	273	188	07146648
37	107	9	-24.10	297.86	5,494	88.18	90.55	182	182	05417928
38	155	8	-21.26	295.91	1,700	39.68	14.28	272	194	07146578
39	196	13	-23.20	292.05	1,669	26.83	10.95	233	182	08621344
40	116	27	-25.71	297.17	1,654	48.41	2.33	263	178	05743428
41	198	5	-29.81	290.86	2,219	26.50	42.41	182	155	08692814
42	198	6	-29.29	290.95	2,087	26.10	37.93	188	160	08692884
43	198	7	-29.37	290.54	1,954	26.43	31.82	194	166	08692954
44	198	8	-29.89	290.32	1,836	27.11	24.44	202	174	08693024
45	151	16	-4.21	305.83	1,770	49.72	7.88	273	174	07002798
46	151	17	-3.87	307.36	2,101	49.61	26.55	288	194	07003078
47	190	18	-1.59	306.34	1,824	36.78	23.03	243	148	08405674
48	151	14	-8.94	307.80	1,725	46.83	2.52	273	177	07002728
49	192	18	-6.26	303.64	1,776	29.53	14.61	263	171	08477704
50	229	7	-9.42	305.08	2,845	24.08	70.44	148	112	09807964
51	229	9	-8.47	304.94	2,693	24.27	67.34	152	111	09808054
52	151	12	-13.66	305.84	1,697	44.28	2.95	272	182	07002658
53	153	12	-12.56	300.56	1,704	43.75	3.14	273	182	07074688
54	231	6	-13.77	303.48	1,726	21.52	10.19	257	201	09880574
55	153	10	-17.17	302.58	1,690	41.62	8.08	272	187	07074618
56	231	4	-19.70	305.38	1,972	22.58	39.46	177	139	09880084
57	231	5	-18.93	305.45	1,864	22.13	33.29	184	143	09800154
58	235	7	-15.28	301.06	2,109	14.34	45.96	255	252	10024564
59	235	8	-15.85	300.15	2,192	15.04	48.27	261	255	10024634
60	235	9	-15.95	300.25	2,336	15.18	52.65	266	259	10024704
61	153	8	-21.88	305.12	1,692	39.96	13.34	271	193	07074548
62	192	13	-22.92	309.80	1,670	27.45	11.19	239	185	08477354
63	194	11	-22.97	300.77	1,672	27.31	11.71	243	190	08549384
64	231	3	-20.27	305.48	2,104	22.79	45.26	172	136	09880014
65	114	27	-29.69	308.00	1,715	47.03	12.52	248	168	05671258
66	149	17	-2.34	314.17	1,795	51.52	7.93	275	174	06930838
67	151	10	-18.32	312.09	1,685	42.01	8.35	271	187	07002588
68	151	8	-23.00	314.49	1,692	40.19	13.87	270	193	07002518

^aTerms are defined in Fig. III-15.

Table VII-4g. Listings for narrow-angle frames in the Mare Tyrrhenum quadrangle (MC-22): Revs 100–676; viewing angles less than 80°. Index numbers correspond to those on the photomosaic of this quadrangle and to the accompanying narrow-angle frames (see Fig. VII-7g)

Index number	Rev	Frame number	Center of picture		Range (SRR-5), km	Lighting angle (SLAR-5), deg	Viewing angle (VAR-5), deg	North direction (NORAN) ^a	Sun direction (SUNAN) ^a	DAS time
			Latitude (LR-5), deg	Longitude (LOR-5), deg						
1	169	14	-7.24	225.05	1,743	42.00	3.02	271	177	07650438
2	169	12	-11.81	227.21	1,710	39.44	2.26	270	182	07650368
3	444	02	-13.60	229.60	1,773	61.44	22.91	135	192	12150257
4	169	10	-16.32	229.35	1,693	37.43	7.21	269	188	07650298
5	167	16	-2.04	232.58	1,796	45.53	8.35	271	172	07578618
6	167	17	-1.71	233.99	2,128	45.54	25.33	290	195	07578858
7	208	13	-2.94	231.41	1,827	23.87	21.55	254	157	09053384
8	167	14	-6.66	234.41	1,747	42.80	3.41	271	176	07579548
9	121	01	-13.61	233.18	5,943	108.52	193.90	261	167	05918708
10	167	12	-11.46	236.33	1,713	40.40	2.11	271	182	07578478
11	444	01	-14.33	230.09	1,788	62.51	25.94	135	192	12150187
12	167	10	-16.19	238.43	1,696	38.36	7.63	270	188	075784C8
13	444	03	-15.00	230.56	1,872	62.37	28.43	126	186	12150397
14	169	08	-20.99	231.36	1,692	36.22	12.23	268	195	07650228
15	130	27	-25.58	232.71	1,658	44.75	3.33	258	176	06247078
16	165	16	-4.12	242.63	1,768	44.99	8.39	269	172	07506658
17	165	17	-3.73	243.86	2,087	45.17	25.78	289	196	07506938
18	165	14	-8.78	249.66	1,723	42.21	3.16	269	176	07506588
19	204	18	-7.37	245.62	1,763	29.93	4.75	269	183	08909604
20	103	09	-11.87	249.47	5,083	25.54	83.87	168	245	05274078
21	165	12	-13.45	246.66	1,694	39.91	2.10	269	182	07506518
22	165	10	-18.21	248.63	1,681	38.22	7.44	268	188	07506448
23	243	06	-19.76	240.55	2,274	27.82	53.57	155	122	10311914
24	167	08	-20.75	240.74	1,695	36.76	12.79	269	195	07578338
25	243	04	-21.21	240.78	2,387	28.43	56.59	154	124	10311844
26	479	03	-23.20	246.47	1,669	72.77	3.42	120	179	12901343
27	128	25	-29.86	244.65	1,665	43.67	2.27	257	181	06175118
28	128	27	-25.28	242.04	1,656	45.36	3.08	259	177	06175188
29	163	16	-2.48	251.16	1,790	46.83	7.98	272	173	07434768
30	163	17	-2.27	252.80	2,131	46.60	26.25	290	195	074345048
31	105	C9	-7.33	251.31	5,385	37.74	90.25	234	234	05346038
32	163	14	-7.11	253.09	1,742	46.00	2.92	272	177	07434698
33	163	12	-11.85	255.08	1,709	41.50	2.56	272	182	07434628
34	163	10	-16.57	257.26	1,694	39.35	8.13	271	188	07434558
35	163	08	-21.20	259.73	1,696	37.55	13.65	270	195	07434488
36	165	08	-22.88	250.56	1,686	36.88	12.83	267	195	07506378
37	204	13	-23.19	255.78	1,674	25.51	11.81	229	184	08909184
38	479	02	-22.06	254.07	1,779	80.55	25.14	124	183	12901203
39	126	27	-27.29	252.26	1,661	45.24	3.54	256	176	06103228
40	159	17	-24.46	269.52	1,790	48.10	7.53	273	173	07290848
41	161	17	-2.96	260.74	1,783	46.99	7.40	272	173	07362808
42	161	18	-2.61	261.90	2,120	47.24	26.09	290	195	073630F8
43	161	15	-7.61	262.74	1,736	46.09	2.21	272	177	07362738
44	161	13	-12.15	264.74	1,705	41.61	2.84	271	182	07362668
45	161	11	-16.78	266.63	1,690	39.72	7.71	271	188	07362558
46	115	09	-24.27	264.17	5,536	92.87	90.24	176	176	05705908
47	161	09	-21.53	268.70	1,691	38.29	13.04	270	194	07362528
48	202	11	-23.20	264.77	1,673	26.10	11.92	238	191	08837254
49	124	27	-25.53	260.70	1,655	46.44	3.39	259	176	06031338
50	436	03	-27.28	262.54	1,691	64.55	11.40	127	180	11974099

^a Terms are defined in Fig. III-15.

Table VII-4h. Listings for narrow-angle frames in the Aeolis quadrangle (MC-23): Revs 100–676; viewing angles less than 80°. Index numbers correspond to those on the photomosaic of this quadrangle and to the accompanying narrow-angle frames (see Fig. VII-7h)

Index number	Rev	Frame number	Center of picture		Range (SRR-5), km	Lighting angle (SLAR-5), deg	Viewing angle (VAR-5), deg	North direction (NORAN) ^a	Sun direction (SUNAN) ^a	DAS time
			Latitude (LR-5), deg	Longitude (LOR-5), deg						
1	177	16	-2.43	185.02	1,799	42.31	8.11	269	172	07938068
2	177	17	-2.01	186.54	2,131	42.21	25.35	291	197	07938348
3	189	07	-2.32	181.09	4,009	17.95	90.16	254	254	06368784
4	216	13	-1.33	186.02	1,810	29.21	10.24	254	161	09341014
5	177	14	-7.06	186.56	1,750	39.61	3.01	269	177	07937598
6	177	12	-11.58	189.10	1,716	37.19	2.09	269	182	07937928
7	179	14	-13.99	185.04	1,702	30.97	14.26	248	167	08009678
8	140	10	-16.78	181.66	1,694	45.63	7.36	274	185	06606808
9	140	08	-21.43	183.84	1,694	43.74	12.26	273	191	06606738
10	179	11	-23.13	189.68	1,683	29.29	13.11	245	185	08009538
11	218	10	-23.78	182.92	2,085	29.78	41.94	292	243	05412834
12	220	11	-23.24	188.99	1,867	20.91	32.51	212	202	09484234
13	224	06	-24.66	184.54	2,316	25.09	56.75	232	247	09628224
14	101	27	-29.03	186.36	1,726	50.98	14.15	253	168	05203448
15	183	07	-26.76	183.79	2,142	22.10	42.30	204	170	08152968
16	183	08	-25.84	184.14	2,073	21.28	40.89	212	178	08153038
17	218	08	-26.38	182.29	2,025	31.74	40.51	295	245	09412764
18	224	04	-26.31	182.92	2,159	26.19	48.88	218	235	09628084
19	224	05	-25.39	183.37	2,212	25.40	52.13	225	241	09628154
20	115	06	-2.06	196.31	6,168	34.94	90.32	55	235	05705558
21	175	16	-2.24	194.41	1,801	43.09	8.14	270	172	07866178
22	175	17	-1.97	196.08	2,139	42.83	25.75	291	197	07866458
23	450	01	-2.14	193.17	1,842	49.65	14.57	129	192	12326056
24	450	02	-1.45	192.69	1,876	48.62	12.24	125	188	12326126
25	450	03	-2.63	193.43	2,004	49.20	23.33	106	173	12326266
26	175	14	-6.90	196.40	1,751	40.30	2.89	270	176	07866108
27	175	12	-11.53	198.40	1,717	37.97	2.32	269	182	07866038
28	207	02	-14.29	193.84	4,364	130.63	134.87	133	133	09013274
29	177	10	-16.11	191.25	1,698	25.34	7.15	268	189	07937858
30	177	08	-20.80	193.25	1,696	34.37	12.22	267	196	07937788
31	138	25	-29.91	157.29	1,668	41.35	1.95	253	182	06534568
32	138	27	-25.42	194.68	1,659	42.73	3.16	255	176	06534638
33	218	05	-29.73	192.78	1,992	28.06	33.53	180	160	09412064
34	218	06	-29.11	192.78	1,883	27.56	27.81	186	165	09412134
35	218	07	-29.45	192.15	1,775	28.17	19.23	193	171	09412204
36	220	09	-25.76	190.29	1,882	23.24	32.00	206	202	09484164
37	173	16	-2.14	204.15	1,799	43.50	8.48	270	171	07794288
38	173	17	-2.00	205.54	2,132	43.51	25.54	290	197	07794568
39	197	01	-0.47	206.94	13,854	126.02	222.93	274	177	08647664
40	528	01	-2.25	203.23	2,041	81.72	41.39	129	185	12985387
41	528	02	-1.52	202.41	2,015	80.55	37.92	129	185	12985457
42	528	03	-3.57	204.53	2,089	82.49	37.37	124	183	12985557
43	676	19	-2.37	202.01	17,926	27.06	107.86	248	248	13511833
44	173	14	-6.76	206.01	1,749	40.82	3.52	270	176	07794218
45	212	15	-8.42	208.37	1,819	27.37	12.86	277	197	09197234
46	173	12	-11.47	207.89	1,715	38.56	1.72	269	182	07794148
47	173	10	-16.26	209.91	1,698	36.75	7.32	269	188	07794078
48	175	10	-16.08	200.40	1,699	36.20	7.22	268	188	07865968
49	175	08	-20.71	202.55	1,697	34.98	12.37	268	196	07665858
50	136	25	-29.99	206.82	1,668	41.79	2.89	255	182	06462678
51	136	27	-25.50	204.21	1,658	43.21	2.20	256	177	06462748
52	171	16	-2.34	213.16	1,794	44.01	8.52	270	171	07722398
53	171	17	-2.19	215.01	2,125	44.15	25.47	290	197	07722678

^aTerms are defined in Fig. III-15.

Table VII-4h. (contd)

Index number	Rev	Frame number	Center of picture		Range (SRR-5), a km	Lighting angle (SLAR-5), a deg	Viewing angle (VAR-5), a deg	North direction (NORAN) ^a	Sun direction (SUNAN) ^a	DAS time
			Latitude (LR-5), deg	Longitude (LOR-5), deg						
54	171	14	-7.02	215.53	1,745	41.41	3.52	270	176	07722328
55	210	15	-5.21	214.91	1,761	30.24	9.48	251	163	09125274
56	131	01	-10.97	211.61	7,170	134.93	123.71	96	96	06278438
57	171	12	-11.85	217.45	1,712	39.11	2.12	270	182	07722258
58	171	10	-16.53	219.69	1,696	37.07	7.65	269	188	07722168
59	173	08	-20.97	212.37	1,699	35.25	13.03	267	196	07794008
60	134	27	-25.68	213.64	1,658	43.81	2.28	257	177	06390858
61	173	07	-25.48	214.72	1,713	34.60	17.86	266	203	07793938
62	216	05	-27.40	215.68	2,121	24.79	42.30	199	210	09340174
63	216	06	-27.63	214.85	2,024	24.85	39.03	205	213	09340244
64	169	16	-2.52	223.15	1,792	44.74	8.26	270	172	07650508
65	169	17	-2.09	224.68	2,122	44.64	25.39	290	196	07650788
66	171	08	-20.96	222.01	1,694	35.60	12.48	268	195	07722118
67	132	27	-25.70	223.12	1,658	44.33	3.00	257	177	06318968

^aTerms are defined in Fig. III-15.

Table VII-4i. Listings for narrow-angle frames in the Phaethontis quadrangle (MC-24): Revs 100-676; viewing angles less than 80°. Index numbers correspond to those on the photomosaic of this quadrangle and to the accompanying narrow-angle frames (see Fig. VII-7i)

Index number	Rev	Frame number	Center of picture		Range (SRR-5), a km	Lighting angle (SLAR-5), a deg	Viewing angle (VAR-5), a deg	North direction (NORAN) ^a	Sun direction (SUNAN) ^a	DAS time
			Latitude (LR-5), deg	Longitude (LOR-5), deg						
1	115	25	-34.99	126.82	1,736	44.94	7.94	244	172	05707168
2	115	27	-30.59	123.93	1,726	46.51	13.08	246	167	05707238
3	209	07	-31.78	123.24	3,667	62.95	67.03	159	205	09087824
4	115	23	-39.37	129.99	1,761	43.88	2.62	242	177	05707098
5	117	20	-44.54	126.32	1,813	42.86	19.15	251	198	05779128
6	117	22	-40.19	122.14	1,746	43.46	13.51	255	193	05779198
7	119	16	-53.31	126.72	2,042	43.98	1.38	213	180	05850738
8	121	15	-56.57	123.72	2,137	45.19	3.77	204	183	05922628
9	123	12	-59.36	121.35	2,225	46.94	8.02	197	186	05994518
10	135	09	-64.98	124.23	3,174	66.70	18.70	119	184	06425298
11	113	25	-33.02	134.26	1,715	46.22	7.88	248	172	05635208
12	113	23	-37.27	137.35	1,736	44.75	2.91	247	177	05635138
13	152	06	-38.27	130.85	2,610	41.99	50.77	178	137	07037658
14	195	05	-35.24	136.96	1,984	30.04	33.18	207	210	08584944
15	195	06	-35.04	136.58	1,963	29.81	34.68	215	216	08585014
16	115	21	-43.61	133.78	1,803	43.19	2.89	239	182	05707028
17	115	19	-47.55	138.21	1,862	42.92	8.11	236	188	05706958
18	117	17	-53.86	137.84	2,075	43.75	.59	210	180	05778708
19	119	14	-56.49	132.91	2,119	45.06	5.81	207	185	05850668
20	121	13	-59.27	130.61	2,224	46.70	8.12	198	187	05922558
21	158	05	-57.02	136.91	2,265	47.88	3.81	176	178	07253468
22	160	05	-58.55	131.71	2,287	49.81	1.52	173	181	07325428
23	170	01	-56.55	136.37	3,367	69.30	13.98	113	185	07684318
24	170	03	-56.73	135.95	3,274	68.95	16.08	116	186	07684388
25	170	04	-57.01	135.45	3,186	68.61	18.49	118	187	07684458
26	135	07	-63.02	133.78	3,334	70.16	23.46	111	184	06425228
27	111	26	-33.93	144.05	1,725	46.09	7.72	247	172	05563178
28	166	03	-33.71	148.29	4,011	56.76	54.94	127	206	07540608
29	111	24	-38.19	147.22	1,748	44.67	2.71	246	177	05563108
30	150	06	-38.72	141.08	2,444	41.81	45.77	183	139	06965698

^aTerms are defined in Fig. III-15.

Table VII-4i. (contd)

Index number	Rev	Frame number	Center of picture		Range (SRR-5), km	Lighting angle (SLAR-5), deg	Viewing angle (VAR-5), deg	North direction (NORAN) ^a	Sun direction (SUNAN) ^a	DAS time
			Latitude (LR-5), deg	Longitude (LOR-5), deg						
31	166	01	-38.70	147.58	3,866	57.75	46.01	121	202	07540538
32	113	21	-41.45	140.88	1,772	43.70	2.20	244	182	0563068
33	113	19	-45.65	144.96	1,826	43.20	7.74	241	188	05634998
34	115	16	-54.83	147.46	2,099	44.37	1.06	210	180	05706678
35	117	15	-56.95	143.96	2,154	44.97	5.26	205	185	05778638
36	119	12	-59.14	140.44	2,212	46.37	10.73	201	189	05850598
37	127	06	-60.50	144.21	3,686	56.27	14.77	127	175	06137388
38	127	09	-60.47	144.16	3,094	55.60	7.97	137	184	06137738
39	107	27	-30.18	159.32	1,724	48.88	12.97	250	169	05419258
40	109	27	-30.79	151.04	1,732	47.73	13.25	247	168	05491218
41	123	09	-34.33	150.59	3,900	31.02	55.66	146	218	0593888
42	125	09	-33.17	150.74	3,916	37.66	57.12	148	221	06065848
43	166	04	-33.37	150.86	3,968	58.49	57.23	133	206	07540678
44	226	07	-32.20	150.79	2,377	31.73	47.98	162	143	09699694
45	226	09	-31.88	150.26	2,221	31.69	43.37	165	145	09699764
46	109	23	-39.51	156.81	1,768	44.96	3.26	244	176	05491078
47	109	25	-35.20	153.81	1,782	46.10	8.18	246	171	05491148
48	111	22	-42.37	150.80	1,787	43.72	2.55	243	182	05563038
49	111	20	-46.44	154.93	1,843	43.25	7.72	240	188	05562968
50	148	06	-45.49	158.30	2,198	41.84	28.74	190	152	06893668
51	113	16	-53.35	154.37	2,048	43.84	1.09	215	181	05634718
52	115	14	-57.82	153.93	2,180	45.51	5.43	204	185	05706608
53	117	13	-59.77	151.21	2,247	46.69	10.14	198	189	05778568
54	156	05	-59.73	151.05	2,1302	50.56	2.73	173	181	07181438
55	105	25	-31.17	169.31	1,709	48.80	9.07	253	172	05347298
56	107	25	-34.68	162.15	1,732	47.05	7.64	249	173	05419188
57	107	23	-39.07	165.33	1,757	45.63	2.33	247	177	05419118
58	107	21	-43.14	169.15	1,758	44.43	2.89	244	182	05419048
59	109	21	-43.62	160.65	1,809	43.96	2.02	241	182	05491008
60	458	01	-44.91	160.45	1,857	81.64	27.54	126	176	12499155
61	458	02	-44.47	160.78	1,877	81.37	31.51	123	175	12499225
62	109	19	-47.57	165.15	1,867	43.40	7.39	238	187	05490938
63	111	17	-54.07	163.98	2,072	44.21	.98	214	180	05562688
64	148	05	-51.26	168.79	2,547	42.72	30.80	176	156	06893388
65	113	12	-59.31	167.61	2,219	46.13	10.67	203	190	05634578
66	113	14	-56.48	160.39	2,126	44.76	5.76	210	185	05634648
67	152	05	-58.26	168.48	2,356	48.59	4.21	172	178	07037378
68	162	03	-58.52	169.47	3,200	65.56	12.10	120	185	07396758
69	162	04	-58.87	169.88	3,112	65.74	14.94	122	186	07396828
70	115	12	-60.41	161.58	2,274	47.04	10.23	197	189	05706538
71	154	05	-60.31	161.04	2,330	50.96	2.63	172	180	07109408
72	103	25	-32.04	178.97	1,715	48.99	8.72	253	172	05275338
73	185	07	-34.49	177.57	1,934	28.69	28.28	207	195	08224934
74	185	08	-34.32	177.14	1,885	28.67	27.58	215	201	08225004
75	105	21	-39.84	175.77	1,756	45.35	1.68	250	181	05347158
76	105	23	-35.51	172.38	1,725	46.84	3.88	252	176	05347228
77	105	19	-44.01	179.61	1,805	44.32	6.88	246	186	05347088
78	107	19	-47.10	173.51	1,855	43.75	8.10	241	188	05418978
79	109	16	-54.93	174.41	2,108	44.45	.82	212	180	05490658
80	111	13	-59.88	178.10	2,246	46.38	10.76	201	189	05562548
81	111	15	-57.16	170.38	2,151	45.08	5.60	208	185	05562618
82	150	05	-57.20	173.33	2,303	47.20	5.41	177	177	06965418
83	162	01	-59.05	171.05	3,293	66.68	9.22	117	183	07396688
84	193	02	-57.95	178.76	2,539	59.95	14.64	145	188	08512124
85	195	02	-58.76	179.93	2,982	65.61	11.37	126	183	08583894
86	230	04	-58.34	179.74	2,529	65.16	8.57	136	182	09843124
87	230	05	-59.21	179.50	2,433	65.55	7.07	138	183	09843194

^a Terms are defined in Fig. III-15.

Table VII-4j. Listings for narrow-angle frames in the Thaumasia quadrangle (MC-25): Revs 100-676; viewing angles less than 80°. Index numbers correspond to those on the photomosaic of this quadrangle and to the accompanying narrow-angle frames (see Fig. VII-7j)

Index number	Rev	Frame number	Center of picture		Range (SRR-5), km	Lighting angle (SLAR-5), deg	Viewing angle (VAR-5), deg	North direction (NORAN) ^a	Sun direction (SUNAN) ^a	DAS time
			Latitude (LR-5), deg	Longitude (LOR-5), deg						
1	127	25	-30.94	69.95	1,670	43.58	2.06	256	181	06139138
2	129	25	-31.61	60.83	1,674	43.01	2.09	254	181	06211028
3	129	23	-35.90	63.88	1,702	41.91	7.02	252	187	06210958
4	129	21	-60.22	67.17	1,747	41.48	12.00	249	193	06282088
5	131	20	-44.88	61.83	1,816	41.50	17.99	245	199	06282708
6	133	17	-54.73	64.75	2,088	44.46	2.10	202	182	06354178
7	170	06	-50.47	68.50	2,028	43.17	6.23	187	175	07685298
8	135	14	-57.76	61.59	2,166	46.53	7.30	196	186	06425998
9	174	05	-57.54	62.09	2,323	50.34	6.80	168	176	07828798
10	178	05	-57.85	61.96	2,620	55.18	11.05	149	184	07972368
11	178	06	-58.09	61.49	2,522	55.14	10.18	152	186	07972438
12	135	12	-60.28	69.24	2,263	48.73	11.96	189	190	06425928
13	127	21	-39.83	76.32	1,743	41.78	12.72	251	193	06138998
14	127	23	-35.45	72.96	1,698	42.41	7.49	254	187	06139068
15	129	19	-44.72	71.01	1,812	41.74	17.62	246	198	06210818
16	131	17	-54.84	74.64	2,093	44.42	2.26	203	182	06282288
17	211	06	-51.66	79.78	2,622	53.12	24.29	147	185	09159714
18	133	15	-57.74	71.23	2,171	46.35	6.88	196	186	06354108
19	133	13	-60.39	79.06	2,269	48.63	11.93	189	190	06354038
20	172	05	-61.24	70.31	2,335	53.68	8.33	168	174	07756908
21	123	25	-30.48	88.24	1,666	44.67	2.10	258	181	05995288
22	125	23	-34.21	81.22	1,688	43.30	7.39	257	187	06067178
23	164	06	-32.72	80.49	2,542	34.78	51.13	177	134	07469628
24	125	21	-38.56	84.61	1,730	42.28	12.65	254	192	06067108
25	125	19	-42.98	88.40	1,790	41.97	18.12	250	198	06067038
26	127	19	-44.10	80.22	1,805	41.68	17.90	247	198	06138928
27	207	07	-41.06	84.56	1,977	37.82	31.33	202	213	09016634
28	207	08	-40.87	83.68	1,979	37.43	34.78	210	219	09016704
29	129	16	-54.99	84.14	2,091	44.49	2.81	204	182	06210398
30	166	06	-50.54	81.21	2,037	44.30	13.15	189	166	07541518
31	168	06	-51.55	81.24	2,020	43.73	2.75	190	181	07613408
32	211	05	-50.98	80.66	2,769	53.00	28.46	144	185	09159544
33	131	15	-57.90	81.27	2,177	46.32	7.27	197	186	06282218
34	170	05	-57.90	83.04	2,331	50.33	5.22	168	177	07685018
35	131	13	-60.57	89.28	2,277	48.61	12.48	189	190	06282148
36	121	26	-30.31	97.44	1,666	45.07	1.97	259	181	05923328
37	123	23	-34.83	91.15	1,692	43.31	7.05	256	186	05995218
38	160	06	-33.83	90.73	2,729	41.64	57.28	173	133	07325708
39	123	21	-39.10	94.43	1,734	42.40	11.93	253	192	05995148
40	123	19	-43.50	98.27	1,795	42.09	17.42	250	198	05995078
41	203	05	-41.05	95.10	1,825	36.70	18.65	205	203	08872854
42	203	06	-40.36	95.50	1,845	36.01	25.64	214	212	08872924
43	242	01	-41.71	96.76	1,930	42.68	35.37	207	222	10275934
44	242	02	-41.06	96.34	1,999	41.89	41.40	219	233	10276004
45	242	03	-40.42	95.61	2,081	41.06	46.68	231	244	10276074
46	125	16	-52.69	98.60	2,044	43.59	1.46	209	178	06066618
47	127	16	-54.18	92.89	2,075	43.88	2.25	206	182	06138508
48	178	01	-53.10	99.11	3,341	70.66	23.07	114	188	07971948
49	178	02	-52.23	97.63	3,278	69.37	26.76	118	189	07972018
50	178	04	-52.79	97.62	3,200	69.32	28.89	121	190	07972088
51	127	14	-57.31	99.35	2,158	45.59	7.23	200	186	06138438
52	129	14	-57.93	90.70	2,175	46.22	7.52	198	186	06210328
53	129	12	-60.47	98.42	2,273	48.30	12.24	190	190	06210258

^aTerms are defined in Fig. III-15.

Table VII-4j. (contd)

Index number	Rev	Frame number	Center of picture		Range (SRR-5), ^a km	Lighting angle (SLAR-5), ^a deg	Viewing angle (VAR-5), ^a deg	North direction (NORAN) ^a	Sun direction (SUNAN) ^a	DAS time
			Latitude (LR-5), ^a deg	Longitude (LOR-5), ^a deg						
54	119	23	-34.26	108.98	1,689	44.31	8.17	259	187	05851298
55	121	24	-34.78	100.29	1,692	43.70	7.07	257	187	05923258
56	121	22	-39.28	103.44	1,735	42.91	12.37	254	192	05923188
57	158	06	-35.07	101.18	2,589	41.63	53.11	177	135	07253748
58	199	05	-37.29	109.59	1,809	33.05	14.76	199	187	08728934
59	199	06	-37.11	109.36	1,771	32.97	14.72	208	195	08729004
60	121	20	-43.76	107.29	1,798	42.56	18.01	251	198	05923118
61	217	01	-44.11	109.10	3,923	88.24	32.24	91	181	09374614
62	123	16	-53.12	108.58	2,063	43.71	1.92	208	177	05994658
63	125	14	-56.01	104.35	2,117	45.00	3.64	204	183	06066548
64	164	05	-57.54	109.17	2,269	49.07	3.38	174	178	07469348
65	106	07	-61.08	109.20	3,676	73.16	42.40	115	190	05381878
66	106	09	-61.96	107.74	3,606	72.32	44.25	120	192	05381948
67	127	12	-60.07	107.06	2,257	47.72	12.35	193	190	06138368
68	166	05	-61.09	107.73	2,315	53.49	6.97	168	183	07541238
69	117	26	-31.08	116.02	1,669	45.66	2.75	260	182	05779338
70	117	24	-35.62	118.87	1,698	44.31	7.99	258	187	05779268
71	119	21	-38.70	112.16	1,731	43.29	13.34	257	193	05851228
72	156	06	-36.41	111.53	2,597	41.55	52.08	177	136	07181718
73	197	02	-39.10	119.74	1,834	34.51	13.90	196	186	08656904
74	197	03	-38.63	119.58	1,792	34.11	13.99	205	193	08656974
75	119	19	-43.09	116.03	1,793	42.67	18.81	253	198	05851158
76	121	17	-53.50	117.85	2,062	44.03	1.47	209	178	05922698
77	123	14	-56.38	114.32	2,137	45.12	3.01	203	182	05994588
78	125	12	-59.02	111.22	2,205	46.83	8.56	198	187	06066478
79	162	05	-55.27	116.95	2,305	47.54	8.71	174	175	07397388
80	162	06	-56.61	117.11	2,077	47.87	20.98	198	198	07397668

^aTerms are defined in Fig. III-15.

Table VII-4k. Listings for narrow-angle frames in the Argyre quadrangle (MC-26): Revs 100–676; viewing angles less than 80°. Index numbers correspond to those on the photomosaic of this quadrangle and to the accompanying narrow-angle frames (see Fig. VII-7k)

Index number	Rev	Frame number	Center of picture		Range (SRR-5), ^a km	Lighting angle (SLAR-5), ^a deg	Viewing angle (VAR-5), ^a deg	North direction (NORAN) ^a	Sun direction (SUNAN) ^a	DAS time
			Latitude (LR-5), ^a deg	Longitude (LOR-5), ^a deg						
1	102	25	-32.46	3.79	1,724	49.09	9.58	252	171	05239358
2	102	23	-36.81	6.83	1,742	47.25	4.40	250	175	05239288
3	104	03	-44.28	4.34	1,809	44.49	6.77	246	186	05311108
4	104	05	-40.06	4.44	1,760	45.54	1.36	249	181	05311178
5	180	07	-42.26	7.91	1,927	39.42	18.79	189	159	08044958
6	180	08	-41.48	8.24	1,838	38.76	11.94	197	165	08045028
7	180	09	-41.36	7.97	1,777	38.91	6.39	206	173	08045098
8	180	10	-41.03	6.42	1,750	39.44	9.95	217	180	08045168
9	106	16	-54.57	7.88	2,086	44.29	1.85	216	182	05382718
10	108	14	-57.61	4.87	2,176	45.19	5.05	208	185	05456608
11	110	12	-59.58	1.46	2,227	46.17	11.02	204	190	05526568
12	163	01	-58.91	9.95	3,663	79.17	16.30	94	181	07432458
13	100	25	-34.30	14.57	1,742	48.53	9.21	250	171	05167398
14	100	23	-38.60	17.70	1,765	46.84	4.09	249	176	05167328
15	102	21	-40.98	10.23	1,775	45.79	.61	248	180	05239218
16	102	19	-45.05	14.15	1,825	44.75	5.72	245	185	05239148
17	106	14	-57.70	14.25	2,168	45.18	6.73	210	186	05382648
18	145	06	-59.47	14.43	2,319	49.02	5.85	179	174	06785448
19	163	03	-58.42	10.35	3,415	78.66	32.02	105	184	07432738
20	163	04	-58.87	10.22	3,368	78.43	35.61	109	185	07432808

^aTerms are defined in Fig. III-15.

Table VII-4k. (contd)

Index number	Rev	Frame number	Center of picture		Range (SRR-5), km	Lighting angle (SLAR-5), deg	Viewing angle (VAR-5), deg	North direction (NORAN) ^a	Sun direction (SUNAN) ^a	DAS time
			Latitude ^a (LR-5), deg	Longitude ^a (LOR-5), deg						
21	108	12	-60.19	12.62	2,270	46.38	10.01	201	189	05454538
22	137	25	-31.33	23.00	1,675	41.11	2.63	252	182	06498588
23	137	23	-35.74	25.94	1,703	40.42	7.65	250	188	06498518
24	100	21	-42.78	21.22	1,803	45.58	1.06	246	181	05167258
25	137	21	-40.30	29.23	1,750	40.45	13.17	247	195	06498448
26	100	19	-46.81	25.33	1,857	44.71	6.17	243	186	05167188
27	102	16	-53.06	23.64	2,050	44.29	.21	221	180	05238868
28	102	14	-56.16	29.88	2,127	46.55	5.01	215	185	05238798
29	106	12	-60.27	21.90	2,264	46.32	11.49	203	190	05382578
30	135	25	-31.54	32.25	1,675	41.79	2.79	253	182	06426698
31	190	04	-31.41	39.97	4,013	66.44	61.58	131	201	08403854
32	215	05	-30.17	38.04	2,034	27.14	35.84	193	198	09304194
33	135	23	-36.00	35.19	1,704	41.06	7.98	251	188	06426628
34	135	21	-40.43	38.53	1,751	40.89	13.24	248	194	06426558
35	137	19	-44.76	33.24	1,817	40.98	18.85	243	200	06498378
36	100	16	-54.41	35.66	2,096	44.34	.75	218	180	05166908
37	139	06	-53.62	30.23	2,027	45.07	4.89	204	178	06569198
38	186	04	-52.85	36.92	3,126	58.60	24.37	130	188	08259864
39	194	02	-50.81	39.86	3,420	82.46	44.32	114	185	08547914
40	221	13	-51.48	37.24	2,410	56.65	21.74	150	191	09519374
41	102	12	-58.82	37.05	2,217	45.24	9.75	209	189	05238728
42	141	07	-61.63	31.20	2,290	50.93	9.39	184	175	06641598
43	141	08	-61.37	31.00	2,167	50.80	30.62	216	205	06641878
44	122	09	-32.02	40.82	4,853	83.14	78.45	160	188	05957908
45	133	26	-31.54	41.94	1,675	42.05	2.32	253	182	06354808
46	133	24	-36.04	44.97	1,705	41.21	7.69	251	188	06354738
47	133	22	-40.34	48.26	1,750	40.95	12.62	248	193	06354668
48	135	19	-44.68	42.48	1,814	41.21	18.39	244	200	06426488
49	112	07	-49.78	40.66	3,422	49.50	28.13	139	199	05597828
50	112	09	-49.80	40.92	3,347	49.46	30.47	144	201	05597898
51	137	16	-54.69	45.76	2,083	44.57	2.56	200	182	06497958
52	100	14	-57.50	41.07	2,175	45.17	4.63	212	184	05166838
53	139	05	-57.61	40.69	2,346	46.78	9.59	181	172	06569638
54	147	03	-57.48	41.36	3,279	54.75	16.77	134	181	06856778
55	147	04	-56.85	40.42	3,169	53.80	16.59	136	183	06856848
56	155	01	-57.66	42.81	3,643	75.23	14.82	100	182	07144548
57	155	03	-56.69	43.31	3,397	74.67	31.42	112	187	07144828
58	155	04	-55.99	42.30	3,360	73.84	35.56	117	189	07144898
59	172	06	-56.42	46.78	2,132	51.25	24.06	187	162	07757188
60	186	01	-57.35	41.11	3,267	63.47	17.31	124	182	08259724
61	186	02	-56.96	41.82	3,147	63.43	15.85	125	184	08259794
62	221	11	-56.49	49.60	2,497	65.51	21.68	139	189	09519304
63	100	12	-60.10	48.75	2,268	45.96	9.55	205	189	05166768
64	131	26	-31.74	51.22	1,675	42.72	1.95	253	182	06282918
65	131	24	-36.23	54.22	1,705	41.02	7.26	251	187	06282848
66	131	22	-40.62	57.75	1,751	41.38	12.66	249	193	06282778
67	133	20	-44.53	52.07	1,811	41.23	17.48	244	199	06354598
68	135	16	-56.79	55.11	2,083	44.61	2.61	201	182	06426068
69	137	14	-57.69	52.29	2,166	46.59	7.38	194	186	06497888
70	176	05	-58.38	55.65	2,314	51.74	2.60	166	179	07900688
71	137	12	-60.03	59.90	2,261	48.70	11.82	187	189	06497818

^aTerms are defined in Fig. III-15.

Table VII-4I. Listings for narrow-angle frames in the Noachis quadrangle (MC-27): Revs 100–676; viewing angles less than 80°. Index numbers correspond to those on the photomosaic of this quadrangle and to the accompanying narrow-angle frames (see Fig. VII-7I)

Index number	Rev	Frame number	Center of picture		Range (SRR-5), ^a km	Lighting angle (SLAR-5), ^a deg	Viewing angle (VAR-5), ^a deg	North direction (NORAN) ^a	Sun direction (SUNAN) ^a	DAS time
			Latitude (LR-5), ^a deg	Longitude (LOR-5), ^a deg						
1	116	23	-34.65	302.77	1,692	44.74	8.03	259	187	05743288
2	116	21	-38.88	306.19	1,735	43.43	13.02	257	192	05743218
3	430	03	-35.11	302.95	1,746	76.76	18.31	123	181	11797031
4	116	19	-43.38	309.89	1,757	42.93	18.50	253	198	05743148
5	118	19	-45.11	302.66	1,822	42.57	18.87	249	198	05815108
6	140	04	-45.64	306.72	4,000	79.79	58.52	130	190	06605058
7	212	01	-45.01	308.78	3,815	83.78	29.69	95	183	09194924
8	214	01	-46.02	300.09	3,810	84.91	29.84	94	182	09266814
9	237	02	-45.69	305.68	2,113	47.48	19.56	162	187	10095544
10	120	16	-53.22	302.29	2,053	43.84	9.97	211	179	05886718
11	120	14	-56.40	308.36	2,129	45.00	4.43	205	183	05886648
12	122	12	-59.46	305.86	2,226	46.98	8.11	197	186	05958538
13	161	06	-59.64	307.36	2,291	51.03	2.55	172	180	07361408
14	112	27	-30.52	317.17	1,725	47.36	13.02	247	167	05599228
15	114	25	-34.10	310.81	1,724	45.36	7.43	246	172	05671188
16	114	23	-38.40	313.90	1,748	46.14	2.37	244	177	05671118
17	194	08	-36.39	314.46	1,809	31.58	21.46	214	203	08549034
18	114	21	-42.54	317.43	1,788	43.35	2.64	242	182	05671048
19	194	07	-40.15	318.86	1,872	34.84	24.48	210	208	08548964
20	153	06	-45.18	319.05	2,101	40.10	22.78	191	158	07073708
21	155	06	-48.19	313.55	2,002	41.49	10.82	196	169	07145738
22	196	07	-47.02	311.39	1,914	41.92	12.02	190	192	08620784
23	196	08	-46.19	311.30	1,892	41.07	17.68	198	200	08620854
24	196	09	-45.54	311.60	1,903	40.43	24.95	207	209	08620924
25	196	10	-45.32	312.47	1,961	40.22	33.70	217	219	08620994
26	210	01	-45.37	318.15	3,841	83.08	30.66	95	183	09123034
27	118	16	-54.34	313.74	2,095	46.03	.32	208	179	05814688
28	118	14	-57.40	319.96	2,174	45.34	4.55	203	184	05814618
29	120	12	-59.23	315.52	2,219	46.56	9.31	199	188	05886578
30	159	06	-56.42	311.20	2,286	47.37	6.96	175	176	07289448
31	159	07	-56.89	310.97	2,083	47.84	22.84	201	200	07289728
32	110	25	-33.03	327.81	1,719	46.78	8.39	249	172	05527198
33	112	25	-34.89	320.04	1,735	45.67	7.95	245	172	05599158
34	112	23	-39.22	323.26	1,760	44.43	2.67	243	176	05599088
35	190	09	-39.35	326.35	1,802	35.54	8.72	198	175	08404904
36	190	10	-35.22	323.08	1,779	33.15	13.17	199	168	08404974
37	112	21	-43.41	326.90	1,802	43.66	2.54	241	182	05599018
38	194	06	-43.68	324.03	1,956	38.50	28.28	205	211	08548894
39	114	19	-46.58	321.53	1,843	43.03	7.73	239	188	05670978
40	229	04	-47.44	328.93	2,532	45.96	37.45	157	163	09807354
41	229	05	-47.55	329.84	2,352	46.10	31.18	159	166	09807424
42	116	16	-53.62	320.89	2,053	44.04	1.33	213	180	05742728
43	116	14	-56.70	326.97	2,131	45.03	5.64	208	185	05742658
44	157	05	-57.69	325.22	2,329	48.58	4.37	172	179	07217418
45	157	06	-58.31	325.30	2,155	49.13	26.07	197	202	07217698
46	118	12	-60.33	327.52	2,269	47.25	9.86	196	188	05814548
47	165	03	-64.40	325.99	3,222	65.34	5.47	123	177	07504628
48	204	01	-62.98	322.13	3,226	71.54	9.33	117	179	08907574
49	204	02	-63.62	323.49	3,101	72.24	4.06	117	179	08907644
50	204	04	-64.12	321.10	2,992	71.44	2.06	120	179	08907714
51	241	01	-64.33	327.56	2,567	77.63	23.66	119	182	10239114
52	241	03	-63.70	323.41	2,498	75.59	25.54	124	182	10239184
53	108	25	-34.71	337.93	1,738	46.55	8.42	247	172	05455168

^aTerms are defined in Fig. III-15.

Table VII-41. (contd)

Index number	Rev	Frame number	Center of picture		Range (SRR-5), km	Lighting angle (SLAR-5), deg	Viewing angle (VAR-5), deg	North direction (NORAN) ^a	Sun direction (SUNAN) ^a	DAS time
			Latitude ^a (LR-5), deg	Longitude ^a (LOR-5), deg						
54	108	27	-30.29	335.16	1,729	48.29	13.47	249	168	05455238
55	188	07	-31.30	336.36	2,153	27.69	38.74	187	156	08332804
56	188	08	-31.20	335.99	2,017	27.88	33.17	193	161	08332874
57	188	09	-30.85	335.86	1,909	27.77	27.95	200	167	08332944
58	188	10	-30.53	335.40	1,822	27.83	22.79	208	174	08333014
59	422	02	-30.11	335.15	1,708	69.35	13.12	129	184	11620000
60	110	23	-37.30	330.88	1,740	45.24	3.39	247	176	05527128
61	192	07	-38.68	330.76	2,017	33.17	27.77	194	197	08676794
62	192	08	-37.94	331.19	1,984	32.42	29.57	202	205	08476864
63	192	09	-38.24	330.27	1,937	32.70	29.52	209	210	08476934
64	192	10	-37.81	330.72	1,959	32.26	34.45	217	218	08477004
65	110	21	-41.53	334.35	1,776	44.16	1.82	245	182	05527058
66	190	08	-43.30	330.04	1,839	38.34	5.19	195	181	08404834
67	110	19	-45.68	338.36	1,829	43.56	7.14	242	187	05526988
68	112	19	-47.36	331.12	1,859	43.31	7.55	238	188	05598948
69	190	07	-47.04	334.46	1,892	41.43	5.30	191	185	08404764
70	194	05	-46.91	330.11	2,060	42.54	32.63	199	213	08548824
71	229	06	-47.97	330.53	2,188	46.55	23.75	162	168	09807494
72	114	16	-54.05	331.30	2,074	43.93	1.12	212	180	05670698
73	114	14	-57.02	337.74	2,154	44.87	5.95	206	185	05670628
74	116	12	-59.33	334.15	2,222	46.34	10.16	201	189	05742588
75	155	05	-59.11	333.89	2,275	49.72	2.31	176	181	07145458
76	167	01	-59.06	336.01	3,589	72.41	5.37	105	181	07576308
77	202	03	-58.40	336.61	2,745	70.28	30.25	132	189	08836104
78	202	04	-58.50	335.15	2,704	69.48	33.90	137	191	08836174
79	130	06	-64.57	335.80	3,289	68.61	22.87	114	184	06245538
80	106	25	-34.62	347.04	1,730	47.01	6.98	250	173	05383208
81	106	27	-30.13	344.03	1,721	49.02	12.52	251	169	05383278
82	118	07	-30.02	346.04	4,357	22.43	63.52	136	220	05813848
83	108	23	-39.05	341.01	1,762	45.25	3.28	245	176	05455098
84	108	21	-43.27	344.63	1,802	44.31	1.99	243	181	05455028
85	108	19	-47.20	348.99	1,859	43.67	7.15	239	187	05454958
86	110	16	-53.35	348.10	2,054	43.81	.90	216	180	05526708
87	112	16	-54.50	341.10	2,096	44.03	.67	211	180	05598668
88	151	05	-54.89	343.69	2,380	45.18	16.24	176	169	07001398
89	112	14	-57.36	347.60	2,176	44.93	5.35	205	185	05598598
90	114	12	-59.59	345.30	2,249	46.23	10.81	199	190	05670558
91	149	05	-59.88	345.69	3,576	50.25	45.35	161	152	06928878
92	151	06	-55.05	344.15	2,049	45.41	12.49	199	191	07001678
93	153	05	-58.30	341.12	2,300	48.63	2.56	175	178	07073428
94	416	02	-56.15	343.27	2,300	77.31	50.35	146	169	11442944
95	110	07	-60.62	346.69	3,740	49.20	46.88	168	147	05525868
96	110	09	-60.43	346.54	3,566	49.15	44.57	170	148	05525938
97	149	02	-64.04	346.46	4,399	54.21	53.38	158	152	06928528
98	149	04	-61.05	347.65	3,714	51.28	46.28	160	152	06928808
99	153	03	-60.40	347.22	3,489	51.36	34.73	150	162	07072798
100	153	04	-61.40	346.76	3,316	52.24	31.23	152	163	07072868
101	194	03	-62.32	344.52	2,525	60.59	1.71	146	179	08548194
102	194	04	-61.77	343.54	2,435	59.79	3.11	149	180	08548264
103	227	06	-60.41	345.52	2,726	59.32	29.97	154	167	09735114
104	260	03	-60.77	344.72	2,726	62.64	46.89	164	159	10648869
105	260	04	-60.05	347.22	2,559	61.80	43.18	163	159	10648939
106	262	15	-64.67	341.77	2,428	66.49	41.21	173	172	10720969

^aTerms are defined in Fig. III-15.

Table VII-4I. (contd)

Index number	Rev	Frame number	Center of picture		Range (SRR-5), km	Lighting angle (SLAR-5), deg	Viewing angle (VAR-5), deg	North direction (NORAN) ^a	Sun direction (SUNAN) ^a	DAS time
			Latitude (LR-5), ^a deg	Longitude (LOR-5), ^a deg						
107	104	09	-31.30	353.97	1,713	48.99	9.56	253	172	05311318
108	104	07	-35.74	357.03	1,728	47.06	4.13	252	176	05311248
109	106	23	-38.95	350.42	1,755	45.40	1.61	248	178	05383138
110	161	04	-38.07	350.50	3,792	55.53	48.38	128	204	07360778
111	161	05	-37.85	350.37	3,725	55.11	50.12	134	206	07360848
112	106	21	-43.19	353.91	1,797	44.49	3.63	245	183	05383068
113	106	19	-47.26	357.89	1,855	44.05	8.57	242	188	05382998
114	145	07	-49.36	358.09	2,039	42.65	12.30	198	167	06785728
115	147	06	-49.86	356.90	2,029	40.90	6.91	199	179	06857688
116	108	16	-54.61	358.34	2,096	44.41	7.77	214	180	05454678
117	149	07	-54.52	358.67	2,096	44.42	24.22	205	204	06929718
118	110	14	-56.58	354.18	2,133	44.71	5.82	211	185	05526638
119	112	12	-59.98	355.03	2,270	46.41	10.09	198	189	05598528
120	147	05	-58.65	358.93	2,372	48.84	14.83	178	167	06857408
121	149	06	-59.41	359.24	2,276	49.31	2.16	179	180	06929438
122	153	01	-61.18	354.78	4,033	53.53	38.70	140	162	07072518

^aTerms are defined in Fig. III-15.

Table VII-4m. Listings for narrow-angle frames in the Hellas quadrangle (MC-28): Revs 100–676; viewing angles less than 80°. Index numbers correspond to those on the photomosaic of this quadrangle and to the accompanying narrow-angle frames (see Fig. VII-7m)

Index number	Rev	Frame number	Center of picture		Range (SRR-5), km	Lighting angle (SLAR-5), deg	Viewing angle (VAR-5), deg	North direction (NORAN) ^a	Sun direction (SUNAN) ^a	DAS time
			Latitude (LR-5), ^a deg	Longitude (LOR-5), ^a deg						
1	128	23	-34.33	247.51	1,690	42.46	7.46	255	187	06175048
2	130	21	-39.15	241.25	1,735	41.65	12.46	252	193	06246668
3	210	07	-35.92	248.75	1,999	32.98	34.51	203	215	09124504
4	210	08	-35.89	248.18	1,984	32.79	36.32	211	221	09124574
5	130	19	-43.49	245.20	1,796	41.51	17.90	248	199	06246798
6	132	16	-53.86	248.28	2,057	43.93	2.59	205	182	06318268
7	134	14	-56.76	244.83	2,132	45.65	7.37	199	186	06390088
8	136	12	-59.30	242.31	2,222	47.86	11.85	191	190	06461908
9	173	05	-56.44	244.59	2,289	48.96	8.03	170	175	07792888
10	175	05	-59.67	241.88	2,275	53.01	4.23	167	181	07864778
11	126	25	-31.77	255.07	1,674	43.58	1.78	255	181	06103158
12	126	23	-36.20	258.19	1,704	42.40	7.14	252	187	06103088
13	128	21	-38.72	250.74	1,732	41.74	12.60	253	193	06174978
14	128	19	-43.10	254.47	1,792	41.61	17.90	249	199	06174908
15	208	05	-41.06	257.65	2,699	38.04	43.20	158	177	09052054
16	208	06	-40.80	256.66	2,552	37.56	40.24	162	177	09052124
17	130	16	-53.83	257.54	2,057	43.92	2.16	206	182	06246378
18	169	06	-50.27	253.43	1,989	42.92	2.79	191	178	07649388
19	132	14	-56.99	254.51	2,138	45.73	7.39	199	186	06318198
20	134	12	-59.48	252.26	2,228	47.83	12.25	192	190	06390018
21	146	01	-62.27	257.28	3,361	70.48	15.13	109	182	06820728
22	146	03	-61.72	254.58	3,267	68.96	17.00	114	184	06820798
23	146	04	-61.93	254.81	3,200	68.97	21.24	117	185	06820868
24	124	23	-34.62	266.42	1,691	43.16	7.55	256	187	06031198
25	124	25	-30.11	263.38	1,665	44.60	2.05	258	181	06031268
26	124	21	-38.97	269.77	1,734	42.24	12.75	254	193	06031128
27	134	07	-39.64	269.92	3,699	32.80	49.88	144	199	06389388
28	134	09	-38.97	265.07	3,636	30.07	51.65	149	193	06389458
29	136	07	-39.60	269.38	3,632	38.07	47.67	143	208	06461278
30	136	09	-39.99	264.55	3,520	35.45	47.73	148	206	06461348
31	204	08	-39.72	269.71	1,856	35.47	17.41	189	186	08908694
32	204	09	-39.58	269.30	1,835	35.37	15.20	196	192	08908764
33	101	06	-40.05	269.09	4,076	41.22	40.56	132	206	05201768
34	101	09	-41.37	267.05	3,597	39.39	44.83	154	214	05202118
35	126	19	-44.80	265.42	1,812	41.90	17.32	246	198	06102948
36	126	21	-40.59	261.57	1,750	41.88	12.36	250	192	06103018

^aTerms are defined in Fig. III-15.

Table VII-4m. (contd)

Index number	Rev	Frame number	Center of picture		Range (SRR-5), km	Lighting angle (SLAR-5), deg	Viewing angle (VAR-5), deg	North direction (NORAN) ^a	Sun direction (SUNAN) ^a	DAS time
			Latitude ^a (LR-5), deg	Longitude ^a (LOR-5), deg						
37	138	09	-41.11	264.90	3,464	42.38	45.32	147	210	06533238
38	177	03	-44.57	265.60	3,527	56.07	38.35	125	197	07936038
39	177	04	-44.14	264.23	3,440	54.79	39.57	130	199	07936108
40	204	07	-40.47	269.57	1,970	36.22	20.14	182	180	0890824
41	204	10	-40.01	269.06	1,805	35.83	17.15	205	201	08908834
42	128	16	-53.76	266.77	2,049	43.90	2.67	208	182	06174488
43	167	06	-51.24	262.65	1,980	43.79	.81	193	179	07577498
44	171	05	-52.59	261.00	2,332	45.56	15.33	170	185	07720998
45	171	06	-52.91	260.79	2,128	45.67	26.67	194	205	07721278
46	130	14	-56.87	263.94	2,138	45.51	7.04	201	186	06246308
47	132	12	-59.72	261.97	2,234	47.88	12.26	192	190	06318128
48	122	23	-34.87	275.73	1,692	43.52	7.09	256	186	05959238
49	122	25	-30.43	272.80	1,666	44.91	1.91	258	181	05959308
50	202	06	-34.57	275.40	1,934	30.56	25.68	190	177	08836804
51	202	07	-34.33	274.85	1,845	30.50	20.65	197	182	08836874
52	202	08	-34.83	274.61	1,776	31.09	16.01	205	191	08836944
53	122	21	-39.26	279.03	1,736	42.62	12.30	253	192	05959168
54	134	06	-39.87	274.72	3,776	35.56	48.51	140	202	06389318
55	136	06	-38.61	274.54	3,763	40.95	48.25	138	210	06461208
56	138	06	-38.38	275.24	3,769	48.57	48.25	137	210	06533098
57	138	07	-39.80	270.28	3,616	45.42	46.86	142	210	06533168
58	202	05	-35.29	275.35	2,030	31.23	29.74	184	171	08836734
59	124	19	-43.32	273.51	1,795	41.97	17.98	250	199	06031058
60	126	16	-55.02	278.27	2,097	46.44	2.21	205	182	06102528
61	128	14	-56.81	273.09	2,130	45.39	7.46	202	186	06174418
62	130	12	-59.52	271.59	2,234	47.49	12.07	194	190	06246238
63	165	06	-55.16	274.89	2,033	47.10	7.26	192	182	07505538
64	169	05	-59.32	271.04	2,286	51.89	3.59	169	182	07649108
65	120	23	-34.38	284.50	1,689	44.06	6.92	258	186	05887278
66	200	07	-32.95	283.01	2,124	29.14	36.22	182	164	08764774
67	200	08	-32.25	282.95	2,010	28.57	31.94	188	168	08764844
68	200	09	-32.30	282.59	1,894	28.79	25.74	195	174	08764914
69	200	10	-32.80	282.49	1,798	29.39	18.96	202	182	08764984
70	120	21	-38.93	287.74	1,732	43.11	12.45	255	192	05887208
71	122	19	-43.58	282.86	1,796	42.24	17.56	250	198	05959098
72	124	16	-53.17	283.55	2,055	43.89	1.71	208	178	06030638
73	163	06	-54.07	281.76	1,996	46.24	7.87	196	182	07433648
74	124	14	-56.31	289.32	2,128	45.17	3.40	203	182	06030568
75	126	14	-57.98	285.15	2,181	46.04	7.30	199	186	06102458
76	128	12	-59.50	280.65	2,227	47.30	12.43	195	190	06174348
77	165	05	-56.20	282.66	2,360	47.80	12.08	170	173	07505258
78	167	05	-59.67	281.04	2,279	52.01	5.42	170	183	07577218
79	177	01	-57.20	283.05	3,609	71.68	9.89	107	182	07935758
80	116	25	-30.30	299.73	1,665	46.48	2.94	261	182	05743358
81	118	25	-32.09	291.82	1,674	45.34	2.90	258	182	05815318
82	118	23	-36.40	295.03	1,705	43.82	8.04	256	187	05815248
83	118	21	-40.74	298.60	1,754	42.87	13.38	253	193	05815178
84	120	19	-43.27	291.66	1,793	42.51	17.89	252	198	05887138
85	479	01	-44.95	290.33	2,332	117.49	43.49	95	169	12900643
86	122	16	-53.41	292.86	2,064	44.07	2.23	209	177	05958678
87	161	07	-51.43	292.52	1,992	43.32	1.79	195	181	07361688
88	122	14	-56.62	298.79	2,138	45.34	3.46	204	182	05958608
89	124	12	-59.14	296.21	2,216	46.84	7.99	197	186	06030498
90	163	05	-58.50	293.01	2,284	49.89	4.42	173	176	07433368
91	126	12	-60.48	293.28	2,281	48.01	12.43	191	190	06102388

^a Terms are defined in Fig. III-15.

Table VII-4n. Listings for narrow-angle frames in the Eridania quadrangle (MC-29): Revs 100–676; viewing angles less than 80°. Index numbers correspond to those on the photomosaic of this quadrangle and to the accompanying narrow-angle frames (see Fig. VII-7n)

Index number	Rev	Frame number	Center of picture		Range (SRR-5), a km	Lighting angle (SLAR-5), a deg	Viewing angle (VAR-5), a deg	North direction (NORAN) ^a	Sun direction (SUNAN) ^a	DAS time
			Latitude (LR-5), deg	Longitude (LOR-5), deg						
1	101	25	-33.42	189.31	1,731	+8.70	8.91	251	171	05203378
2	142	06	-34.63	187.69	2,498	33.78	46.58	187	138	06677788
3	181	09	-34.59	187.02	1,904	31.48	23.50	197	164	08081008
4	181	10	-34.00	186.78	1,819	31.23	18.15	205	170	08081078
5	103	23	-36.34	181.89	1,733	47.20	3.81	251	176	05275268
6	123	06	-35.20	186.37	4,264	59.96	48.06	124	203	05993538
7	103	19	-44.64	188.97	1,815	44.78	6.14	246	186	05279128
8	103	21	-40.49	185.14	1,767	45.79	.94	249	181	05279198
9	105	16	-52.06	188.54	2,017	43.93	.36	222	180	05346808
10	107	16	-54.64	183.03	2,088	44.41	1.47	215	181	05416698
11	107	14	-57.66	189.50	2,169	45.21	6.19	209	186	05418628
12	109	14	-57.74	181.28	2,188	45.14	5.13	206	184	05490588
13	117	07	-59.03	181.20	3,778	50.10	23.40	135	171	05777588
14	117	10	-58.93	181.23	3,113	49.52	11.50	146	181	05777938
15	154	01	-58.92	181.10	3,483	54.32	24.82	136	174	07108708
16	154	03	-59.32	180.52	3,337	54.36	22.02	138	174	07108778
17	154	04	-59.58	181.70	3,184	54.82	17.63	139	176	07108848
18	156	01	-58.04	183.07	3,354	58.03	16.11	129	180	07180738
19	156	03	-58.55	181.40	3,230	57.56	14.34	132	181	07180808
20	156	04	-57.73	180.97	3,121	56.71	14.17	134	183	07180878
21	193	01	-58.76	180.39	2,615	61.25	11.64	140	185	08512144
22	228	04	-58.84	180.11	2,587	62.23	13.76	141	178	09771094
23	230	03	-58.82	180.95	2,628	66.07	9.85	133	181	09843054
24	109	12	-60.07	189.32	2,284	46.21	10.11	199	189	05490518
25	101	23	-37.62	192.41	1,752	46.90	4.09	250	176	05203308
26	101	21	-41.81	195.88	1,788	45.54	1.21	247	181	05203238
27	140	06	-44.09	196.38	2,136	40.81	26.19	196	154	06605898
28	101	19	-45.98	199.86	1,861	44.67	6.41	244	186	05203168
29	158	01	-49.66	193.45	3,451	64.64	28.81	121	192	07252768
30	158	03	-49.13	191.85	3,386	63.29	31.70	125	194	07252838
31	158	04	-49.71	192.17	3,309	63.45	33.67	129	195	07252908
32	103	16	-52.71	198.14	2,035	44.34	.57	222	180	05274848
33	105	14	-55.23	194.41	2,092	44.24	5.16	217	185	05346738
34	144	05	-58.00	199.81	2,320	47.43	5.76	179	175	06749468
35	146	05	-59.86	196.74	2,316	49.52	3.01	177	182	06821428
36	146	06	-59.85	196.88	2,212	49.47	31.42	205	208	06821708
37	107	12	-60.30	197.13	2,265	46.44	11.05	202	190	05418558
38	136	23	-34.44	209.69	1,694	40.87	8.01	252	188	06462608
39	138	23	-34.34	200.17	1,692	40.48	7.07	252	188	06534498
40	138	21	-38.84	203.44	1,735	40.23	12.54	249	194	06534428
41	179	07	-39.58	204.32	1,845	33.57	18.58	212	197	08009118
42	179	08	-39.88	203.72	1,829	34.06	21.68	221	205	08009188
43	138	19	-43.36	207.26	1,797	40.64	18.27	245	200	06534358
44	101	16	-53.53	209.39	2,072	44.24	.18	219	179	05202888
45	103	14	-55.98	203.99	2,110	44.77	4.98	217	185	05274778
46	105	12	-58.09	201.36	2,180	45.01	10.06	210	190	05346668
47	142	05	-56.10	203.73	2,388	45.80	15.62	179	167	06677508
48	144	06	-58.24	200.53	2,125	47.70	23.91	206	201	06749748
49	134	23	-34.75	219.20	1,695	41.36	8.37	253	188	06390718
50	134	25	-30.25	216.28	1,668	42.32	3.06	255	182	06390788
51	214	07	-34.90	216.24	1,824	32.03	17.59	190	180	09268284
52	214	08	-34.98	215.89	1,758	32.21	12.10	197	186	09268354
53	136	21	-38.73	212.90	1,735	40.47	12.90	250	194	06462538

^aTerms are defined in Fig. III-15.

Table VII-4n. (contd)

Index number	Rev	Frame number	Center of picture		Range (SRR-5), ^a km	Lighting angle (SLAR-5), ^a deg	Viewing angle (VAR-5), ^a deg	North direction (NORAN) ^a	Sun direction (SUNAN) ^a	DAS time
			Latitude (LR-5), ^a deg	Longitude (LOR-5), ^a deg						
54	136	19	-43.10	216.67	1,795	40.69	18.21	247	200	06462468
55	138	16	-53.73	219.58	2,052	44.02	2.50	202	182	06533938
56	101	14	-56.55	215.70	2,149	44.55	4.80	214	184	05202818
57	103	12	-58.89	211.10	2,200	45.58	9.97	210	189	05274708
58	140	05	-57.41	216.24	2,309	46.64	7.48	182	173	06605618
59	132	23	-34.74	228.49	1,693	41.87	7.35	254	187	06318828
60	132	25	-30.24	225.68	1,668	42.85	2.19	256	182	06318898
61	134	21	-39.11	222.48	1,738	40.90	13.45	251	194	06390648
62	134	19	-43.42	226.27	1,799	41.03	18.62	248	200	06390578
63	136	16	-53.30	228.89	2,048	43.59	2.18	204	182	06462048
64	177	06	-54.06	220.27	2,005	46.93	10.96	190	188	07936948
65	101	12	-59.34	223.01	2,241	45.46	9.77	207	189	05202748
66	111	07	-57.95	224.18	3,653	53.98	10.51	127	180	05561568
67	111	10	-57.91	223.57	3,140	52.99	16.25	142	191	05561918
68	138	14	-56.75	225.73	2,132	45.92	7.07	197	186	06533868
69	130	23	-34.71	238.03	1,693	42.20	7.22	254	187	06246938
70	130	25	-30.13	235.34	1,667	43.13	2.00	256	181	06247008
71	132	21	-39.14	231.80	1,736	41.32	12.60	251	193	06318758
72	132	19	-43.44	235.71	1,797	41.27	17.91	247	199	06318688
73	134	16	-53.71	238.52	2,052	43.89	2.57	205	182	06390158
74	173	06	-52.63	231.51	1,990	45.87	6.60	190	175	07793168
75	175	06	-52.90	231.81	2,009	45.56	12.50	192	191	07865058
76	136	14	-56.39	234.97	2,127	45.45	6.75	198	186	06461978
77	138	12	-59.56	233.11	2,227	48.31	12.00	190	190	06533798
78	177	05	-59.99	232.99	2,281	53.69	4.91	166	181	07936668
79	179	05	-60.06	234.47	2,567	56.43	5.53	150	181	08008348
80	179	06	-60.13	233.09	2,472	56.07	4.19	154	182	08008418

^aTerms are defined in Fig. III-15.

RANGE, km	WIDE-ANGLE CAMERA		NARROW-ANGLE CAMERA	
	SCALE, km/pixel	APPROXIMATE PICTURE WIDTH, km	SCALE, km/pixel	APPROXIMATE PICTURE WIDTH, km
1000	0.30		0.030	
	0.40	300	0.040	30
	0.50	400	0.050	40
2000	0.60	500	0.060	50
	0.70	600	0.070	60
	0.80	700	0.080	70
3000	0.90		0.090	
	1.00	800	0.100	80
		900		90
4000				
	1.20	1000	0.120	100
	1.60		0.160	140
6000		1500	0.200	180
	2.00		0.250	200
8000	2.50	2000		
	3.00	2500	0.300	250
10,000			0.350	
	3.50	3000	0.400	300
12,000	4.00		0.450	350
14,000	4.50	3500	0.500	400
		4000		

Fig. VII-8. Nomogram for relating range to picture scale and width.

References

- VII-1. Sharp, R. P., "Mars: Fretted and Chaotic Terrains." *J. Geophys. Res.*, Vol. 78, p. 4073, 1973.
- VII-2. Masursky, H., Batson, R., Borgeson, W., Carr, M., McCauley, J., Milton, D., Wildey, R., Wilhelms, D., Murray, B., Horowitz, N., Leighton, R., Sharp, R., Thompson, W., Briggs, G., Chandeysson, P., Shipley, E., Sagan, C., Pollack, J., Lederberg, J., Levinthal, E., Hartmann, W., McCord, T., Smith, B., Davies, M., de Vaucouleurs, G., and Leovy, C., "Television Experiment for Mariner Mars 1971," *Icarus*, Vol. 12, p. 10, 1970.
- VII-3. Wu, S. S. C., Shafer, F. J., Nakata, G. M., Jordan, R., and Blasius, K. R., "Photogrammetric Evaluation of Mariner 9 Photography," *J. Geophys. Res.*, Vol. 78, p. 4405, 1973.
- VII-4. Blasius, K. R., "A Study of Martian Topography by Analytic Photogrammetry," *J. Geophys. Res.*, Vol. 78, p. 4411, 1973.
- VII-5. *Preliminary Viking Data Analysis Team Report*, Report M75-144-0, Langley Research Center, NASA, 1972.
- VII-6. Batson, R. M., "Cartographic Products From the Mariner 9 Mission," *J. Geophys. Res.*, Vol. 78, p. 4424, 1973.
- VII-7. *1:5,000,000-Scale Airbrushed Shaded Relief Maps of Mars*, U. S. Geological Survey, Center of Astrogeology, Flagstaff, Arizona, 1974.
- VII-8. *Mariner 9 Albedo Charts of Mars*, prepared by James Roth under the direction of Dr. Gerard de Vaucouleurs, Department of Astronomy, The University of Texas at Austin, 1973.
- VII-9. Wilhelms, D. E., "Comparison of Martian and Lunar Multiringed Circular Basins," *J. Geophys. Res.*, Vol. 78, p. 4804, 1973.
- VII-10. Carr, M. H., Masursky, H., and Saunders, R. S., "A Generalized Geologic Map of Mars," *J. Geophys. Res.*, Vol. 78, p. 4031, 1973.

VIII. Polar Studies

The pictures presented in this section were taken in order to map the regions poleward of the 65° parallels; to monitor the seasonal and diurnal behavior of frost deposits; and to examine frost deposits at high resolution. Because many pictures obtained in the polar regions serve more than one of these objectives, this section is devoted to all of these aspects of polar studies. More detailed descriptions of television data relating to variable surface features and cloud phenomena in the polar regions are given in Sections X and XI, respectively. Tables VIII-1 and VIII-2 are summaries of the polar photography presented in this section.

A. Fixed-Feature Observations

1. Wide-Angle Pictures

When Mariner 9 was inserted into Mars orbit, it was summertime in the southern hemisphere of Mars, and a substantial part of the region south of 65°S was continuously illuminated by the Sun. The equivalent part of the planet in the northern hemisphere was in continuous darkness. Obscuration by the great dust storm interfered with early attempts to photograph fixed features in the illuminated Mare Australe quadrangle (65°S to 90°S; see Section VII for quadrangle descriptions),

although frames that included the south polar cap were useful (see Section VIII-B).

The Mare Australe quadrangle was systematically mapped by means of wide-angle frames acquired on Revs 97-100 and on Rev 108, after surface detail had become distinctly visible through the dust cloud. An airbrushed rendition of the topographic features revealed by these pictures is reproduced in Fig. VIII-1; the frames used are identified and listed below the mosaic. This part of Mars, although clearer than other parts of the planet during this period, was still heavily obscured by dust, and the narrow-angle frames obtained, interspersed with the wide-angle mapping coverage, showed very little detail.

Because of the continued clearing of the south polar region, and the increased visibility of much of the fine structure of the surface, the process of remapping the Mare Australe quadrangle was started on Rev 125. As only one wide-angle frame every few revolutions was available for this task, the remainder of the mission up to Rev 262 was required to photograph the entire area under suitable lighting and viewing conditions. A mosaic of frames used in this second mapping phase appears in Fig. VIII-2. The frames are identified and listed below the mosaic, which uses rectified pictures transformed to Polar

Table VIII-1. Summary of coverage of the Mare Australis quadrangle^a

Revs	Science cycle	Orbital science links ^b		
		Zenith pass (even revolutions)	Nadir pass (odd revolutions)	
1-15	Post-orbital insertion mapping, calibration, and phase function			Mapping, calibration, and phase function sequences on Revs 1, 5, 7, 9, and 11 include the south polar cap. Multiple filters.
16-23	Interim sequence	Polar: 4A(O) (-30m) ^{c,d}	Polar:	4B (-30m) ^e
24-63	Recon I	Polar: 3BA (-34m) ^f	Polar:	3BA (-34m) ^f
64-99	Recon II	Sextad: 3BA (-33m32s) ^f	Sextad:	3BA (-33m32s) ^f
100-138	Mapping Cycle I	Pentad: 2AB, 1A (-33m) ^g	TLR:	1B (-37m54s)
			Tetrad:	2A, 1BA (-33m)
139-177	Mapping Cycle II	Tetrad 1: 1BA, 2B (-33m42s)	Single B No. 1: (-37m54s)	
			Triad:	1AB, 1B (-33m42s)
178-217	Mapping Cycle III	Tetrad 1: 2B, 1AB (-32m18s)	Tetrad 1:	2B, 1AB (-32m18s)
		Dyad 1: 2B (-23m54s)	Dyad 1:	2B (-23m54s)
218-262 ^h	Extended mission, Phase I	Triad 1: 3B (variable time) ⁱ	Triad 1:	3B (variable time) ⁱ
		Triad 2: 3B (variable time) ⁱ	Triad 2:	3B (variable time) ⁱ
		Triad 3: 1B, 1AB (variable time) ⁱ	Triad 3:	1B, 1AB (variable time) ⁱ
		Ground command: 1AB (variable time) ⁱ	Ground command:	1AB (variable time) ⁱ
416-676	Extended mission, Phases II, III, IV	One link: 1AB (-8m46s), Rev 416 only	One link	1A, 1B, 3A (-7m43s), Rev 459 only

^aIn addition to coverage presented here, long-range coverage of the south polar cap and surrounding polar region was obtained in the pre-orbital sequence and in many global sequences taken on almost all orbital passes between Revs 16 and 138.

^bThe concept of picture links is described in Section II.

^cTimes listed are nominal times from periapsis as listed in Volume II.

^dIncludes polar cap except for Rev 24.

^eVery little coverage of frost cap or polar region in spite of link designation.

^fMulticolor and polarization filters.

^gColor filter failed on Rev 116.

^hMapping sequence on Rev 262.

ⁱDuring each revolution, at least one of these links was used for polar observations.

Table VIII-2. Summary of coverage of the Mare Boreum quadrangle

Revs	Science cycle	Orbital science links ^a		
		Zenith pass (even revolutions)		Nadir pass (odd revolutions)
100-138 ^b	Mapping Cycle I	Tetrad:	1A, 1BA, 1A (-16m) ^c , ^d	Dyad 2: 1AB (18m48s) ^e
139-177	Mapping Cycle II	Dyad:	1AB (30m) ^f	Dyad: 1AB (30m) ^f
178-217	Mapping Cycle III	Tetrad 3:	2AB (30m) ^g	Tetrad 2: 2AB (39m48s) ^g
		Dyad 2:	1AB (43m24s) ^h	Dyad 4: 1AB (45m24s) ^h
218-262	Extended mission, Phase I	Triad 5:	1B, 1AB ^g	Triad 5: 1B, 1AB ^g
416-459	Extended mission, Phase II: Arcturus	Ground command:	1A, 1AB ^f	Ground command: 1A, 1AB ^f
473-533	Extended mission, Phase III: Canopus	North collar, etc.:	1A ⁱ 3B, Rev 458 only 5B, Rev 459 only	{ (2h20m to 3h4m)
		North collar, etc.:	2A, Revs 478, 479 3A, Rev 528 only 1A, Rev 529 only 3B, Rev 478 only 4B, Revs 479, 528 1B, Rev 529 only	{ (1h44m to 2h5m)
667-676	Extended mission, Phase IV: Vega	North pole targets:	1A, Revs 667, 668 5B, Revs 667, 668 4B, Revs 675, 676	{ (1h30m to 1h45m)

^aThe concept of picture links is described in Section II.

^bNo north polar coverage before Rev 100.

^cTimes listed are nominal times from periaxis as listed in Volume II.

^dCoverage only on Revs 100, 102, 118, 120.

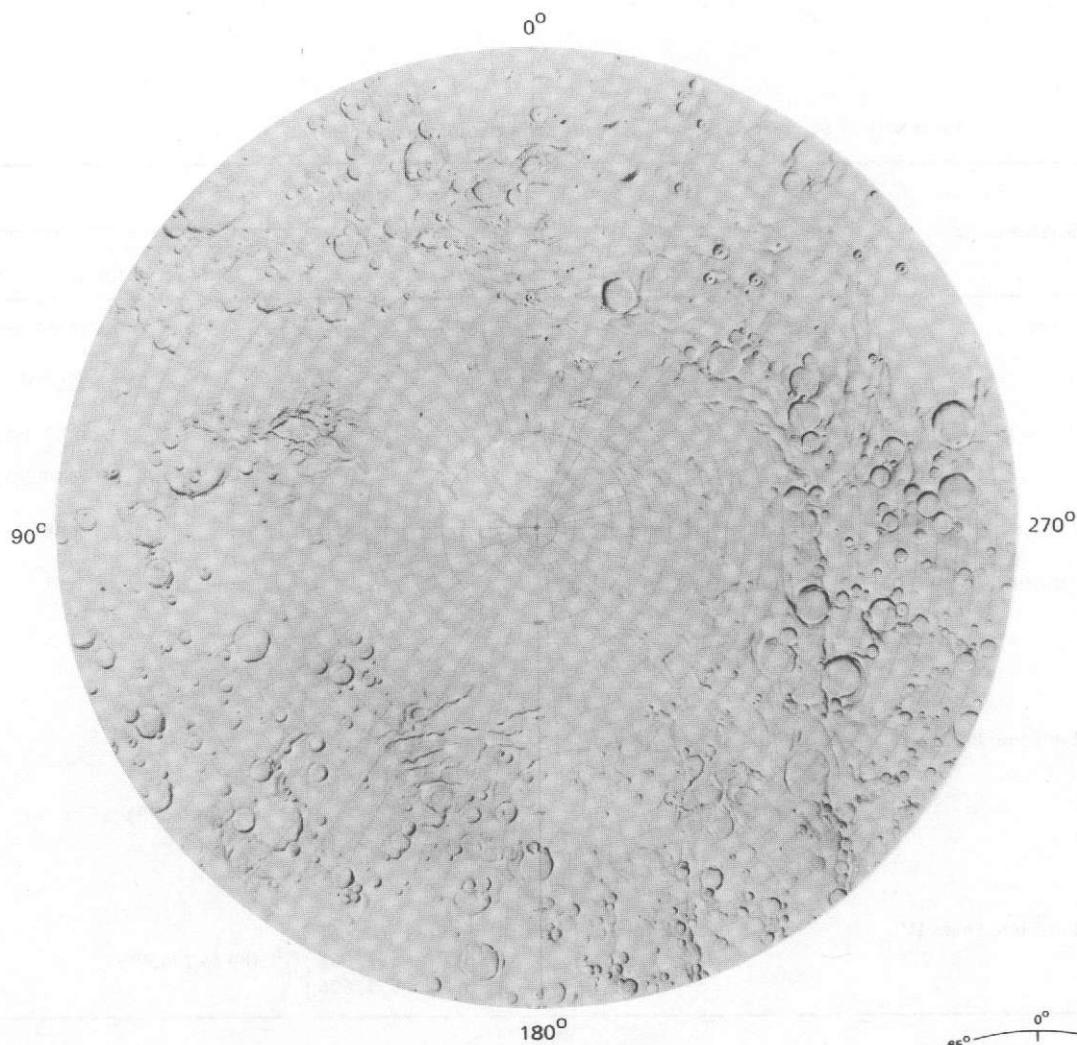
^eCoverage only on Revs 101 and 129.

^fTargeted north of 65°N.

^gSome frames north of 65°N.

^hOnly some of these frames received; most of them north of 65°N.

ⁱOn Revs 416, 417, 422, 423, 430, 431, 436, 437, 444, 445, 451, 458, 459.



IDENTIFICATION NUMBERS OF PICTURES IN MOSAIC

Index No.	Rev	DAS Time	Index No.	Rev	DAS Time
1	97	5058588	14	99	5130338
2	97	5058658	15	99	5130408
3	97	5058728	16	99	5130478
4	97	5058798	17	99	5130548
5	97	5058868	18	99	5130618
6	98	5094218	19	99	5130688
7	98	5094288	20	100	5166038
8	98	5094358	21	100	5166108
9	98	5094428	22	100	5166178
10	98	5094498	23	108	5453808
11	98	5094568	24	108	5453878
12	99	5130058	25	108	5453948
13	99	5130258			

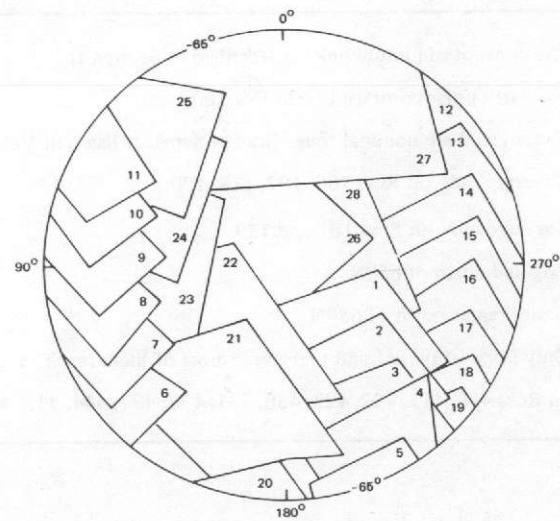
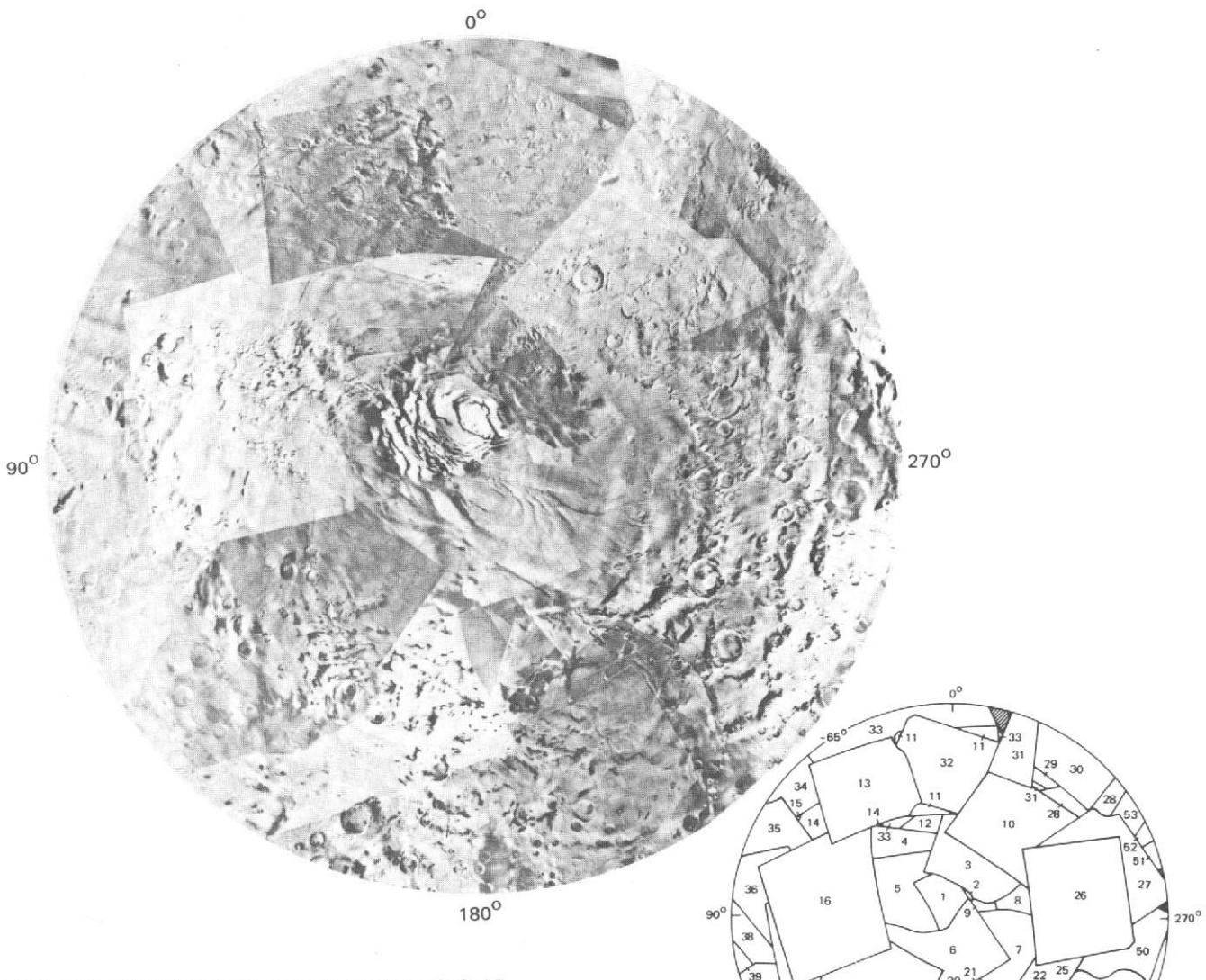


Fig. VIII-1. Airbrushed rendition of the Mare Australe quadrangle, based on wide-angle frames from Revs 97-100 and Rev 108. Persistent dust obscuration degraded most of the pictures used. The airbrush drawing was made by the U.S. Geological Survey, Flagstaff, Arizona.



IDENTIFICATION NUMBERS OF PICTURES IN MOSAIC

Index No.	Rev	DAS time	Index No.	Rev	DAS time	Index No.	Rev	DAS time
1	208	9051674	19	100	5166178	37	174	7828138
2	231	9878724	20	116	5741928	38	98	5094428
3	198	8691944	21	124	6029908	39	98	5094353
4	141	6640938	22	160	7324768	40	135	6425338
5	213	9231224	23	144	6748808	41	98	5094218
6	187	8295814	24	189	8367844	42	150	6964753
7	185	8223854	25	183	8151888	43	127	6136378
8	173	7792228	26	175	7864118	44	199	8727854
9	216	9339094	27	99	5130268	45	121	5921898
10	202	8835864	28	130	6245648	46	261	10684539
11	157	7216758	29	165	7504598	47	148	6892728
12	262	10720729	30	204	8907684	48	220	9483434
13	192	8475854	31	128	6173618	49	146	6820768
14	108	5453878	32	200	8763834	50	181	8079928
15	98	5094638	33	116	5740523	51	99	5130198
16	172	7756248	34	98	5094703	52	99	5130128
17	164	7468688	35	98	5094563	53	130	6245718
18	152	7036713	36	98	5094493			

Fig. VIII-2. Photomosaic of the Mare Australis quadrangle, based primarily on wide-angle frames obtained between Revs 116 and 262. Some earlier dust-obscured frames were used to fill small gaps in coverage between 65°S and 70°S. R&S pictures produced at the JPL Image Processing Laboratory (see Section VI) comprise the mosaic elements. The mosaic was assembled by the U.S. Geological Survey, Flagstaff, Arizona.

Stereographic Projection at the JPL Image Processing Laboratory (see Section VI).

Throughout the entire Mariner 9 mission, the Sun, as viewed from Mars, was moving north and changing the lighting conditions in the polar regions. On Rev 234, Mars reached the equinox, and the entire north polar region was brought into sunlight for all or part of the day. However, the northern parts of the planet were still obscured by haze on Rev 262, when television data acquisition was suspended (see Section I) because of the power reduction caused by the solar occultation of the spacecraft. Thus, wide-angle pictures of the Mare Boreum quadrangle (65°N to 90°N) acquired before this solar occultation period were not useful for mapping of fixed surface features; however, they did provide information regarding frost distribution (see Section VIII-B) and also revealed structure in the atmosphere (see Section XI).

When photography was resumed on Rev 416, the general north polar haze, or hood, was much less evident, although cloud phenomena still could be observed. Fixed surface features were observed clearly north of 65°N , and all of this area (Mare Boreum) was photographed by the wide-angle camera. However, these pictures were taken from much greater distances than were comparable frames of the Mare Australe quadrangle, and show much less surface detail. Furthermore, the rapidly receding ice cap resulted in contrast variation between adjacent pictures, which created many problems for the cartographer. Figure VIII-3 is a mosaic of wide-angle pictures taken between Revs 416 and 451, with the frames identified and listed below. The individual pictures were taken over a 3-wk period during which the mean latitude of the edge of the polar cap increased from 68°N to 71°N . The rectified pictures in the mosaic were computer-processed to display fine detail at the expense of albedo differences. The abrupt albedo change at the polar-cap edge, however, introduced an artifact (a dark band), ranging in latitude from 68°N to 71°N , which does not match in the contiguous mosaic elements taken at different times.

2. Narrow-Angle Pictures

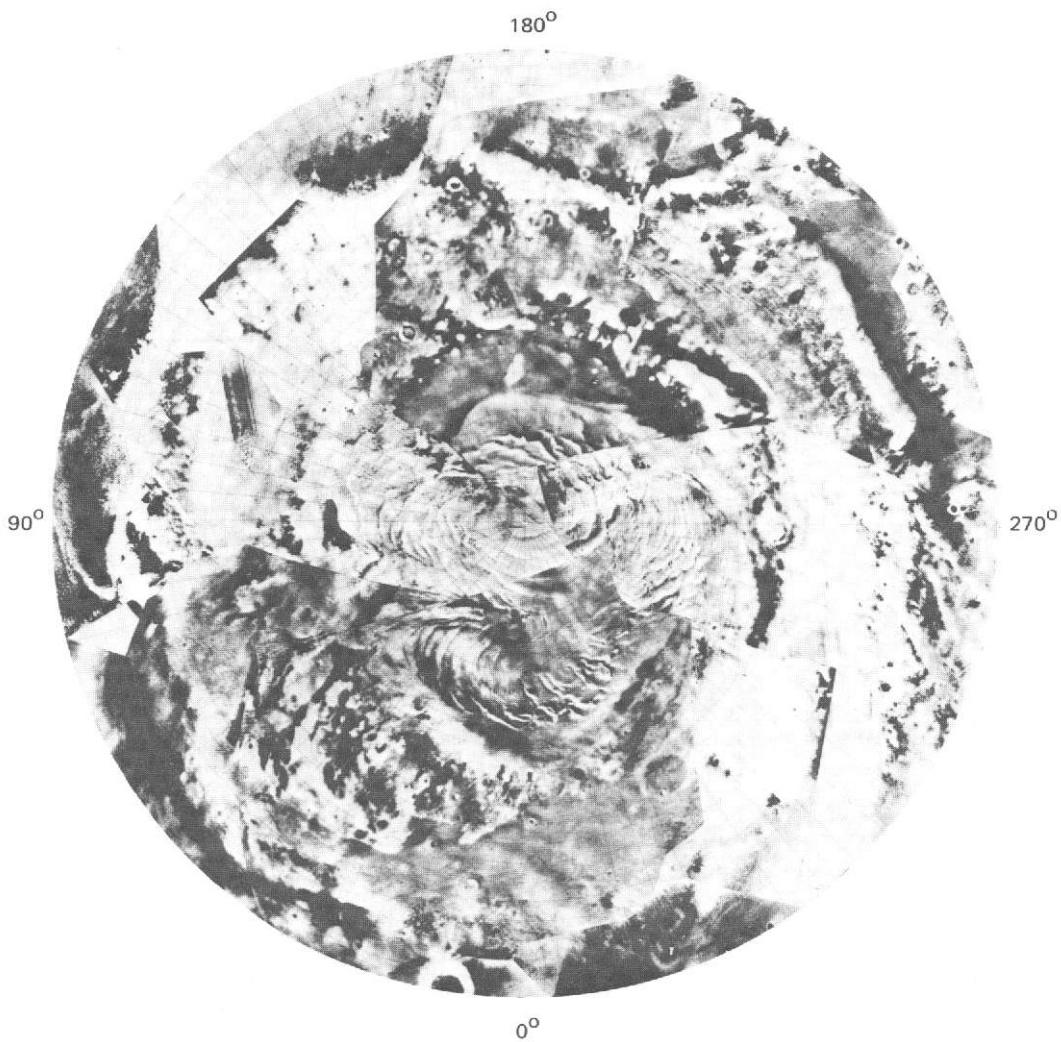
The high-resolution camera was used to explore geologic features in the polar regions of Mars in the greatest possible detail. In the case of the Mare Australe quadrangle, even the early exploratory pictures, which culminated in the polar mapping swaths of Revs 97-99, contained a considerable amount of narrow-angle coverage (Fig. VIII-4a). Pictures taken between Revs 100 and 262 generally show more detail (Fig. VIII-4b) than those taken before Rev 100. However, some pictures

acquired near the fall equinox (Rev 234) suffered from the effects of haze obscuration by the developing south polar hood. When photography was resumed on Rev 416, part of the Mare Australe quadrangle was not illuminated by the Sun, and the rest of the quadrangle was masked by the winter haze.

Observations of the Mare Boreum quadrangle followed a slightly different pattern. On early revolutions, the north polar region was either in darkness or masked by dust or haze. Some surface detail was visible in pictures taken just before the solar occultation period (Fig. VIII-5a). By Rev 416, most of the north polar region was clear, and the cap was receding rapidly. However, it was not possible to obtain pictures with acceptable viewing conditions from a distance of less than 5000 km. Thus, narrow-angle frames taken between Rev 416 and the end of the mission cover larger areas of the Mare Boreum quadrangle; consequently, they have less surface resolution than those taken in the Mare Australe quadrangle between Revs 100 and 262. In addition, it was not possible to acquire as many narrow-angle pictures under clear conditions as was possible in the Mare Australe quadrangle. Resolution differences are illustrated by a comparison of the size and number of picture footprints shown in Figs. VIII-4b and VIII-5b.

Dense and, in some cases, duplicate coverage in the polar regions was obtained in especially interesting areas identified from wide-angle frames. Contiguous coverage was obtained along contacts between different geologic units and perpendicular to these contacts wherever it appeared that important transitions might be observed. Coverage was especially dense on the laminated terrains (see Refs. VIII-1 and VIII-2). Repeated coverage of the same area was obtained for stereophotogrammetric determinations of topographic relief (see Section VII), studies of changes in frost cover (see Section VIII-B), and surveillance of variable features outside the frost zone (see Section X).

Differences in the number and average scale of narrow-angle pictures taken in the polar regions require some differences in the manner in which they are presented in this document. The narrow-angle pictures of the Mare Australe quadrangle taken between Revs 1 and 99 (Fig. VIII-4a), which show very little detail, are not reproduced. However, the 314 frames of the Mare Australe quadrangle with viewing angles less than 80° , obtained between Revs 100 and 262, are presented and are indexed in seven separate sectors of the area south of 65°S (see Fig. VIII-6). The narrow-angle frames are reproduced in arrays of 35 pictures (Fig. VIII-7); the frames in sector α , the circular area bounded by 80°S , appear first. The order in which the pictures appear is determined by longitude.



IDENTIFICATION NUMBERS OF PICTURES IN MOSAIC

Index No.	Rev	DAS time	Index No.	Rev	DAS time
1	445	12188937	13	444	12152887
2	442	11622765	14	450	12328401
3	436	11977144	15	417	11482109
4	444	12153097	16	423	11658885
5	417	11481969	17	431	11835981
6	423	11658745	18	437	12012984
7	430	11836121	19	445	12188797
8	437	12013124	20	451	12364311
9	451	12364451	21	416	11446129
10	416	11445989	22	422	11622905
11	430	11800141	23	430	11800001
12	436	11977004			

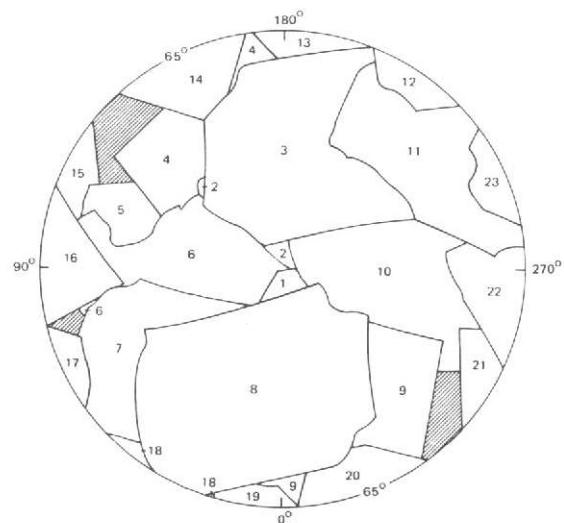


Fig. VIII-3. Photomosaic of the Mare Boreum quadrangle, based on wide-angle frames between Revs 416 and 451. Pictures used in the mosaic were obtained at much greater distances than those in Fig. VIII-2. Large-scale albedo markings are, in many cases, artifacts of the computer processing, which was coordinated at the JPL Image Processing Laboratory (see Section VI). The mosaic was assembled by the U.S. Geological Survey, Flagstaff, Arizona.

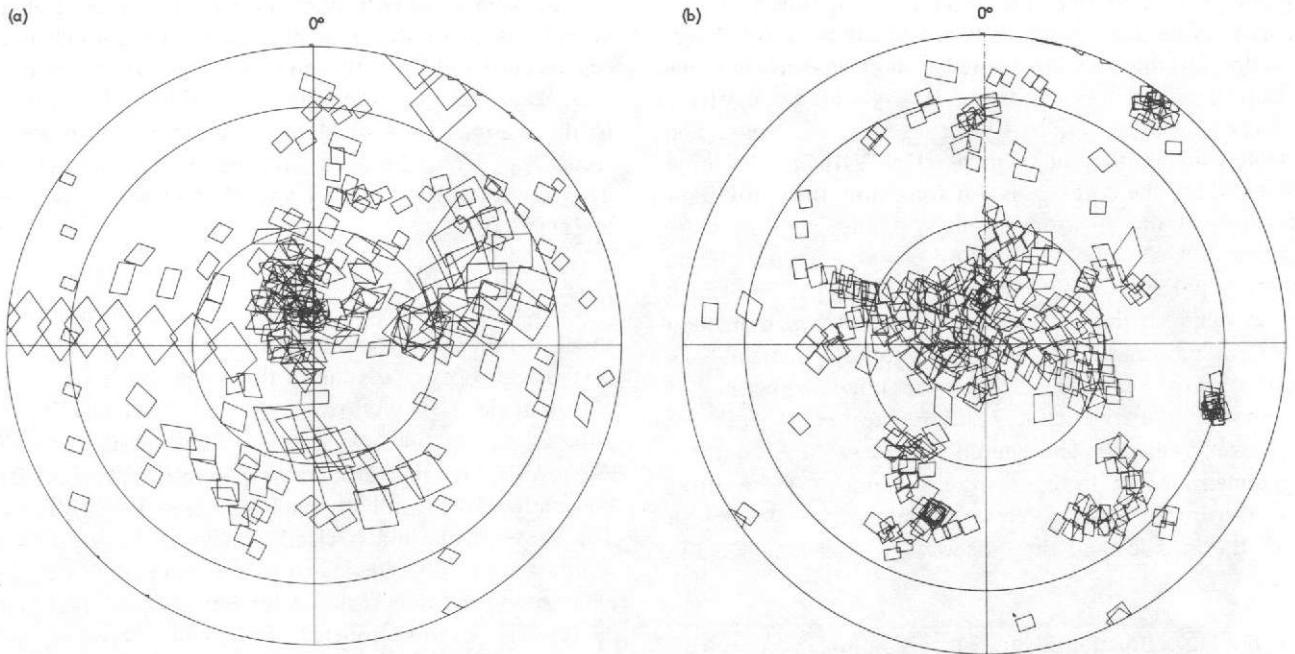


Fig. VIII-4. Narrow-angle footprint plots for the Mare Australis quadrangle; viewing angles less than 80° . (a) Revs 1-99.
(b) Revs 100-262.

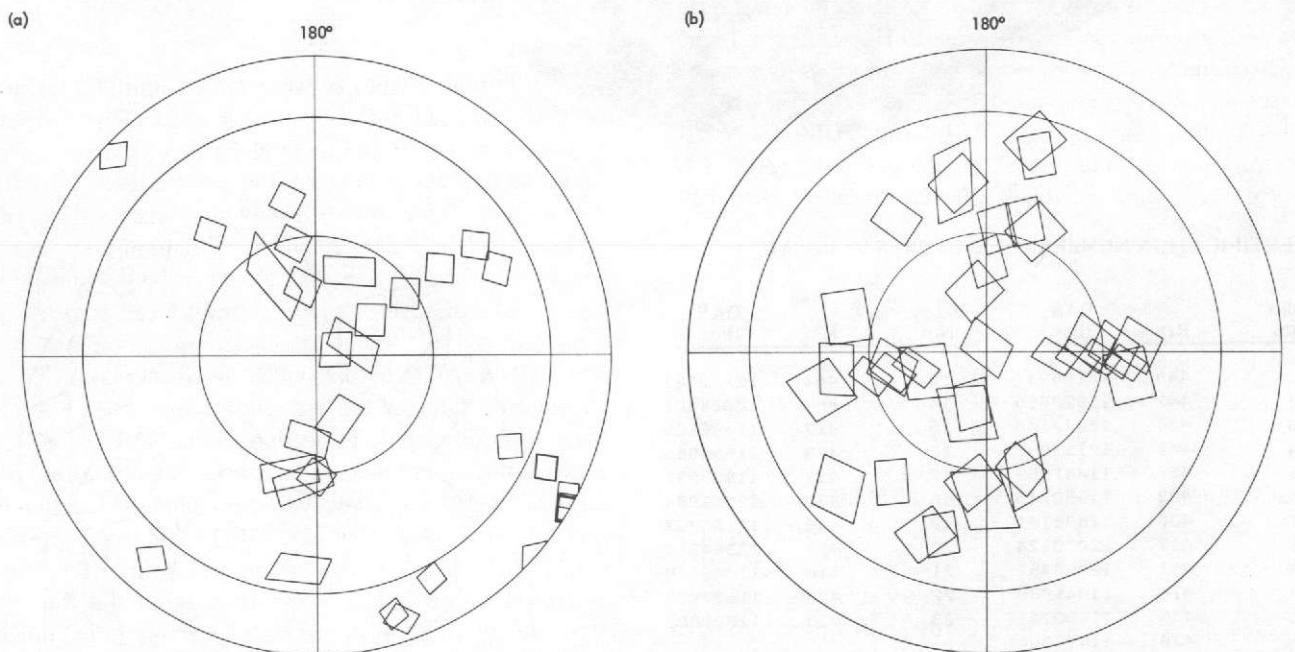


Fig. VIII-5. Narrow-angle footprint plots for the Mare Boreum quadrangle; viewing angles less than 80° . (a) Revs 100-262.
(b) Revs 416-676.

All frames with centers in the 0° to 10° longitude range are presented before proceeding westward to the next 10° longitude wedge. Lighting, viewing geometry, range, and scale information corresponding to each frame is given in Table VIII-3. The location of the center of each frame also appears in the table and in the index maps (Fig. VIII-7). In those cases for which the coverage is not too dense, the entire footprint corresponding to a narrow-angle picture appears in the index map. Where only the picture center is indicated, the orientation and approximate scale of the frame can be defined from the values of the north direction (NORAN, as defined in Fig. III-15) and range. It is important to note that the locations of footprints and picture centers are not exact because of camera-pointing inaccuracies. Pointing errors of $1/3^{\circ}$ are typical (see Volume II) and amount to about one-third of the linear dimensions of the narrow-angle frames. These errors can be recognized easily wherever prominent features appear in both the mosaics and the narrow-angle frames indexed in the map.

For the Mare Boreum quadrangle, all pictures with viewing angles (VAR-5 in Fig. III-15) less than 80° , taken between Rev 100 and the end of the mission, are reproduced. Pictures taken between Revs 100 and 262, which were significantly affected by haze, are indexed separately from those obtained after Rev 416. Because of the small number of frames and the larger areas covered by them, the entire Mare Boreum quadrangle is appropriate as an index map. However, the frames still are ordered into seven sectors for the purposes of presentation (see Fig. VIII-8) and tabulation (see Table VIII-4). All pictures in the arrays of Figs. VIII-7 and VIII-8 are VAGC versions of the real-time television pictures (see Section IV), with the exception of Revs 100-108 in which the HPF version is used.

B. Frost Studies

1. Mare Australe Quadrangle: Wide- and Narrow-Angle Frames

Preflight plans called for monitoring of the seasonal and diurnal variations in the frost cover in the Mare Australe quadrangle. When Mariner 9 arrived at Mars, the south polar cap was approaching its minimum size and filled only a part of a wide-angle picture acquired from the closest distance attainable. The wide-angle camera was used initially to observe the cap under different colors and polarizations. Much smaller areas within the polar cap were viewed with the narrow-angle camera through its single filter.

During the early stages of the mission, more photography than anticipated was devoted to the polar cap because other

regions were so heavily obscured by dust. This photography covered much of the summer season, during which the polar cap receded only slightly, and past equinox, when haze and frost again began to form. The relationship of the photography to the seasonal state of Mars can be visualized more readily from Fig. I-7. Detailed information on the relationship between revolution number and Martian season is presented in Table VIII-5.

In the period between Revs 24 and 91, which corresponds to all of the Recon I and most of the Recon II science cycles, sextad sequences consisting of three wide-angle (A) and three narrow-angle (B) pictures were used extensively in the photography of the polar cap (see Tables VIII-1 and VIII-2). Figure VIII-9 is a typical sextad sequence from Rev 36 showing the south polar cap in both shading-corrected and HPF versions. The frost distribution is clearly visible in these pictures, but the dust storm obscures much of the topographic detail in the area around the polar cap. After Rev 100, the rapid clearing of the dust storm permitted photography showing both the cap and the surrounding terrain. Figure VIII-10a is an example of a wide-angle image of the south polar cap in which the cap is close to the minimum size. Figure VIII-10b is a mosaic of narrow-angle frames covering the same area as Fig. VIII-10a, taken over an extended period of time but still with the cap near its minimum size.

All wide-angle frames between Revs 1 and 262 taken from distances less than 5000 km, which include the south polar cap, appear in Fig. VIII-11. In all of these frames, the cap is near the minimum size and covers an area less than $250,000 \text{ km}^2$. The pictures show the recession and stabilization of the boundaries of the polar cap and its obscuration by haze soon after the equinox. Most frames appear in the shading-corrected version. In some cases, where the polar cap is close to the terminator and the frame is slightly underexposed, the raw version (R) provides better picture detail for reasons discussed in Section IV. Four of the wide-angle frames from Fig. VIII-11 appear in stereographic projection in Fig. VIII-12. This form of presentation permits an accurate determination of the change in frost cover. Table VIII-6 presents the location of the center of each frame from Fig. VIII-11 and the viewing angle, lighting angle, and north direction measured at the center of the frame. Also listed is the latitude of the Sun, which determines the time of day at each point within the polar cap. Figure VIII-13 shows the way in which changes in the Sun's latitude and longitude caused great variations in lighting conditions at the residual south polar cap.

Narrow-angle pictures in the vicinity of the residual south polar cap, acquired between Revs 1 and 262, are shown in

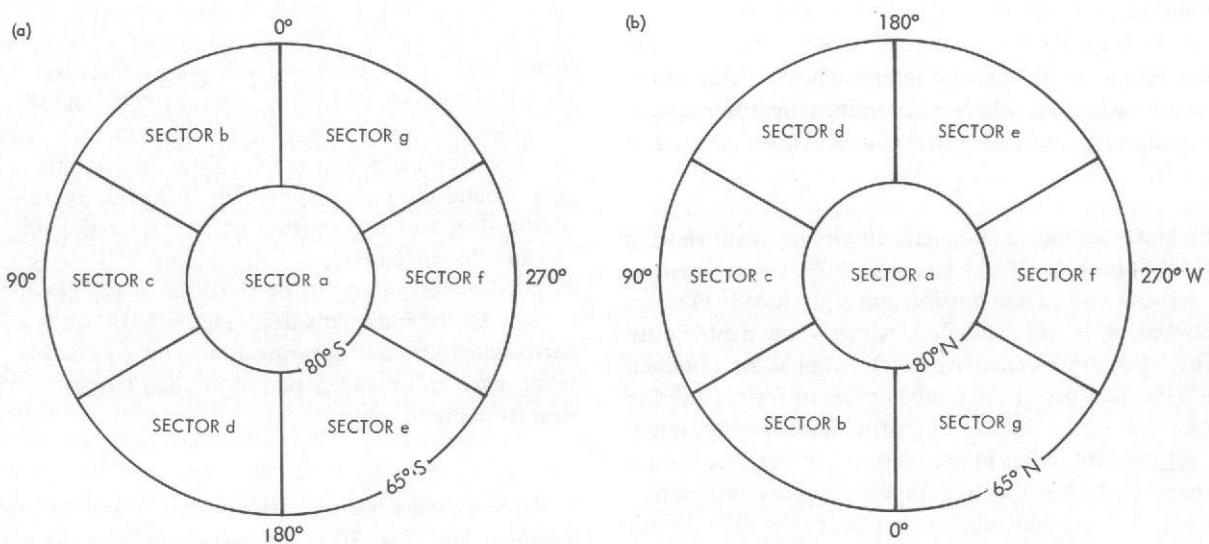


Fig. VIII-6. Index maps for the polar regions. (a) Mare Australis (MC-30). (b) Mare Borealis (MC-1).

Fig. VIII-14. The frames displayed have centers that fall in an area bounded by specific latitudes and longitudes (Fig. VIII-15). The viewing and lighting angles, range, and location for each are supplied in Table VIII-7. In Fig. VIII-15, the footprints of these frames are plotted and indexed to Fig. VIII-14 and Table VIII-8. All frames in Fig. VIII-14 are reproduced in the shading-corrected version, which is the most suitable to display albedo differences defining the boundaries of frost. All frames acquired after Rev 100 shown in Fig. VIII-4 are also displayed in Fig. VIII-7 in the VAGC version, which provides better topographic detail. Specially processed stereographic projections of four narrow-angle frames of the same area (Fig. VIII-16) show the seasonal change in frost cover.

Some observations of the Mare Australe quadrangle during the winter season were made after the period of solar occultation of the spacecraft had ended and the television cameras became reactivated. Wide- and narrow-angle frames that show possible frost formation between 70°S and 50°S appear in Fig. VIII-17. These frames also are affected by the presence of the south polar haze. Viewing and lighting angles and locations of these frames are given in Table VIII-8.

2 North Polar Cap and Haze Cover

At the time of Mariner 9 orbit insertion, orbital and camera-pointing constraints precluded viewing the illuminated part of the planet any farther north than 40°N . By Rev 100, however, the orbital plane had rotated sufficiently with respect to the Sun direction to permit areas as far north as 65°N to be viewed, although obliquely. At that time, the latitude of the Sun was near 15°S , and areas north of 75°N were in continuous darkness.

All wide-angle frames with centers north of 65°N that were taken between Rev 100 and the end of the mission are shown

in Fig. VIII-18. The shading-corrected version is used, and the pictures are arranged in chronological order. Viewing and lighting angles and locations are given in Table VIII-9.

Most wide-angle pictures of the Mare Boreum quadrangle taken shortly after Rev 100 are highly oblique and show the limb of Mars. As time passed, viewing conditions became more favorable, but a haze layer extended down to about 45°N , obscuring the surface (see Section XI) and margin of the frost deposits.

When Mariner 9 became operational after solar occultation on Rev 416, the haze had almost entirely disappeared. Pictures taken between then and the end of the mission (Fig. VIII-18, index numbers 50-67) show the springtime recession of the cap. The final picture in the Mare Boreum quadrangle was taken on Rev 676 immediately before summer solstice in the northern hemisphere. For comparison, the first picture of the south polar cap was taken in the southern summer several weeks after solstice.

Stereographic projections of some of the late north polar frames showing the springtime retreat of the south polar cap appear in Fig. VIII-19. Because of the large size of the cap in the spring, mosaics of pictures corrected for photometric effects of lighting angle differences are necessary to show the entire area of frost cover.

Some of the narrow-angle pictures in the Mare Boreum quadrangle also contain information about the frost deposits, although no repetitive monitoring of a single area was possible. VAGC versions of these narrow-angle pictures, which reveal the topographic detail, are presented in Fig. VIII-8. Shading-corrected versions of some of these pictures are displayed in Fig. VIII-20.

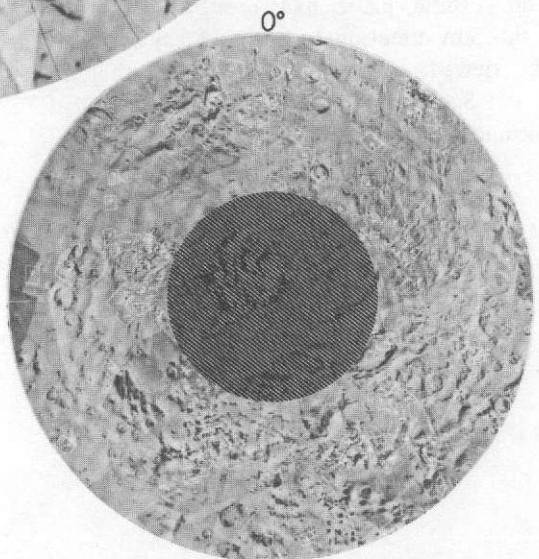
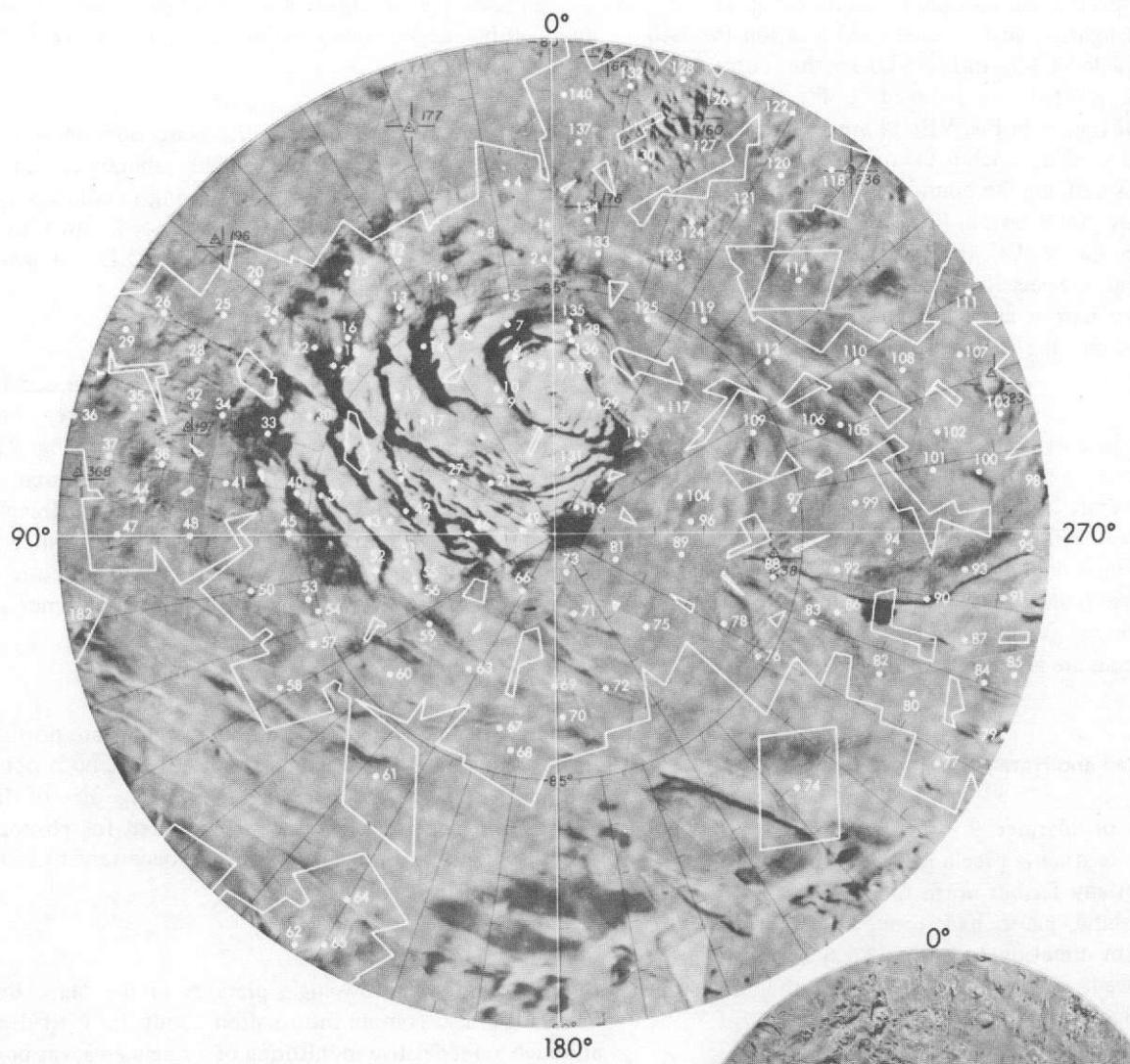


Fig. VIII-7a. VAGC versions of narrow-angle pictures in the Mare Australis quadrangle during Revs 100-262. Index map sector *a*: index numbers 1-140.



Fig. VIII-7b. Narrow-angle pictures located on index map sector a: index numbers 1-35. Images with little detail may have been underexposed (see histograms in original data and Section IV).

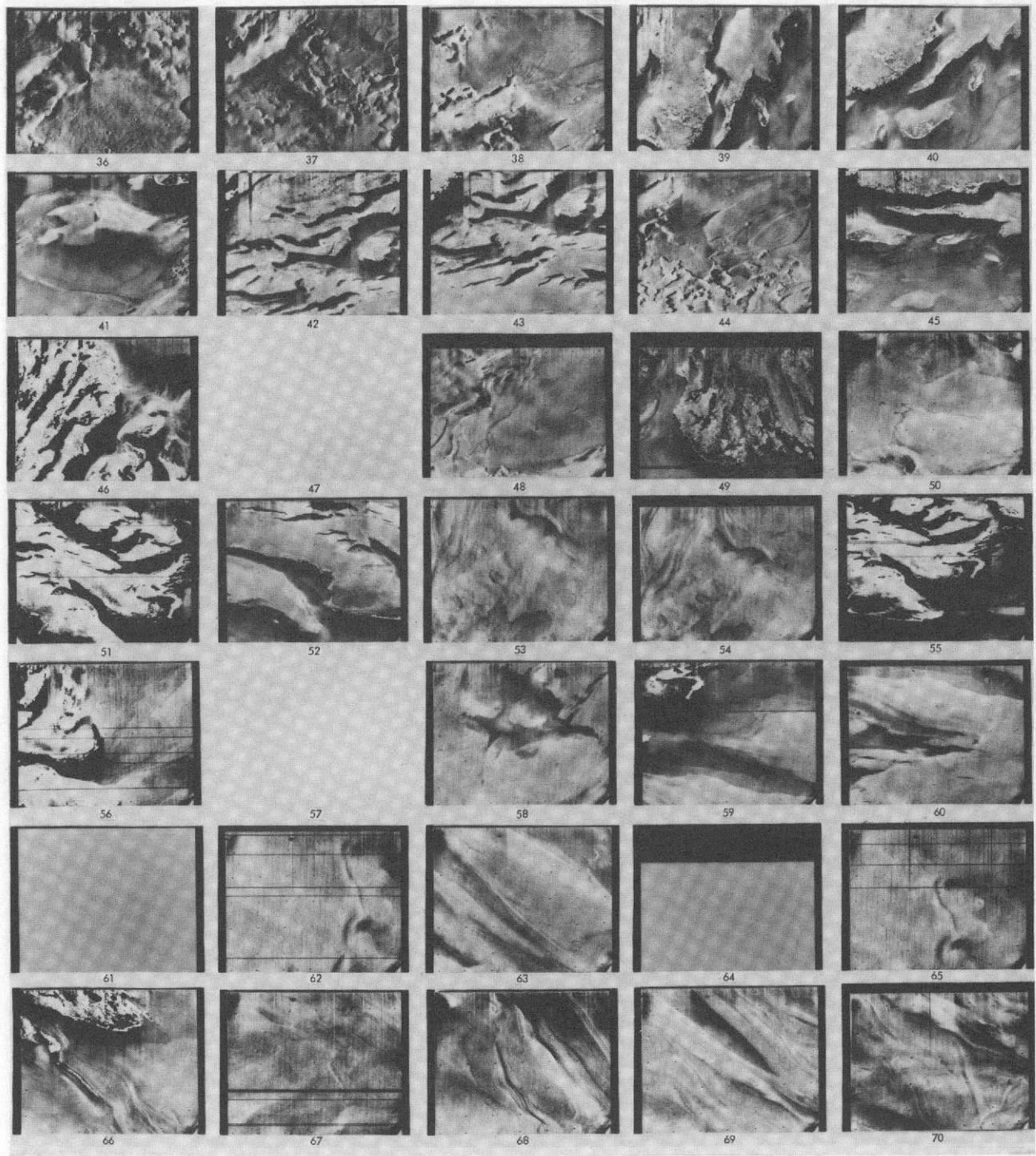


Fig. VIII-7c. Narrow-angle pictures located on index map sector *a*: index numbers 36-70. Images with little detail may have been underexposed (see histograms in original data and Section IV). Blanks denote pictures planned but not recovered.

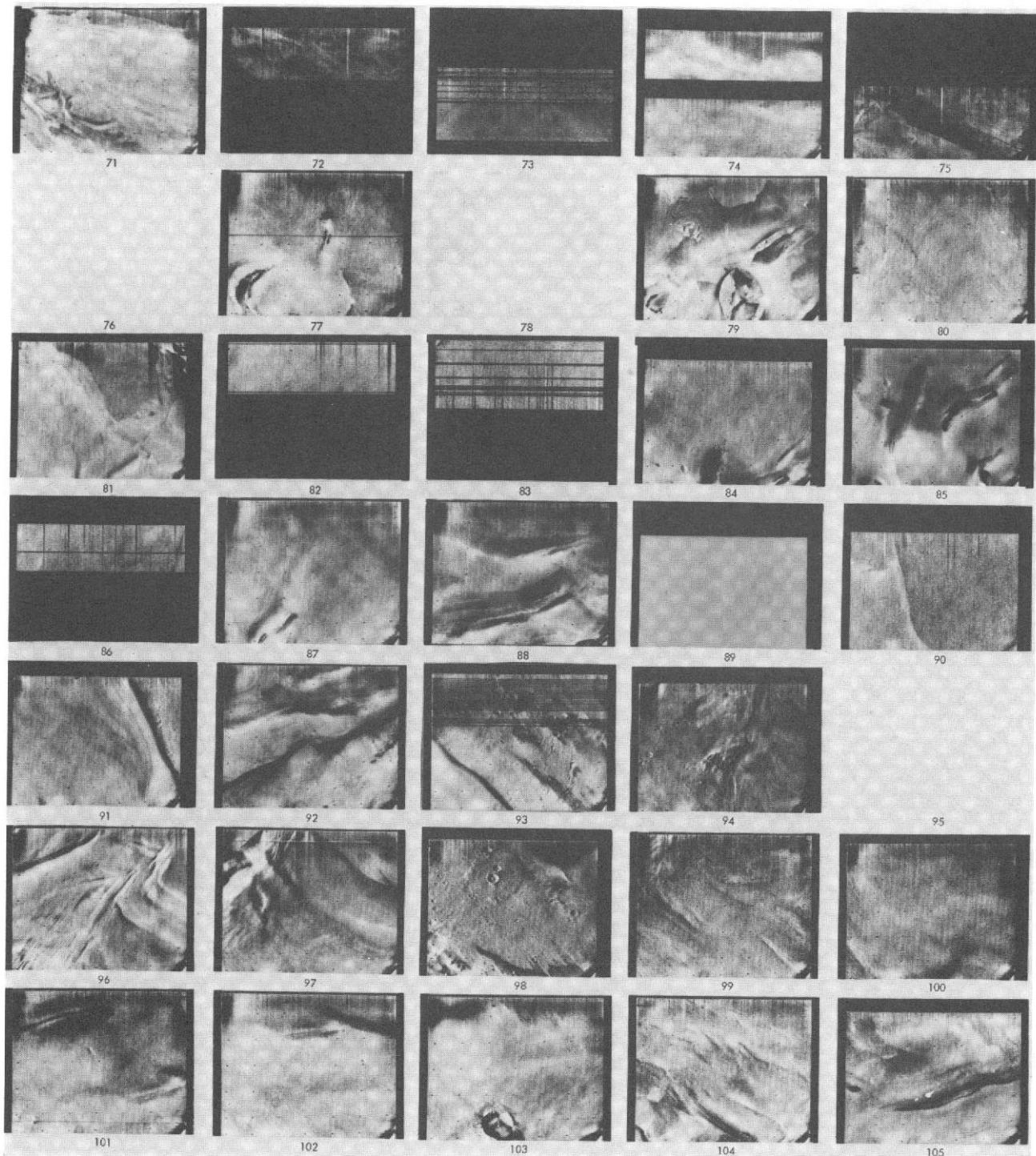


Fig. VIII-7d. Narrow-angle pictures located on index map sector a: index numbers 71-105. Images with little detail may have been underexposed (see histograms in original data and Section IV). Blanks denote pictures planned but not recovered.

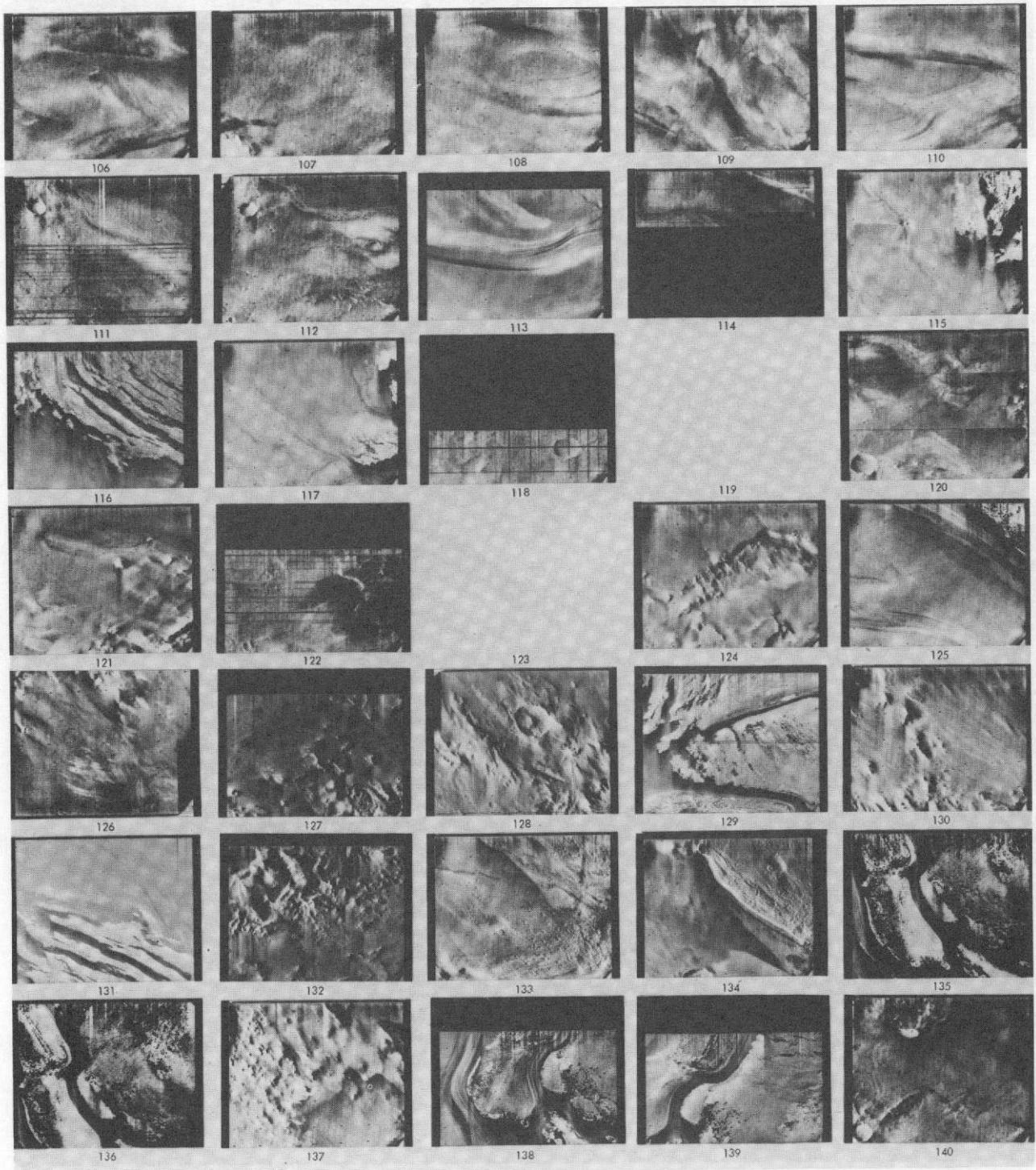


Fig. VIII-7e. Narrow-angle pictures located on index map sector *a*: index numbers 106-140. Images with little detail may have been underexposed (see histograms in original data and Section IV). Blanks denote pictures planned but not recovered.

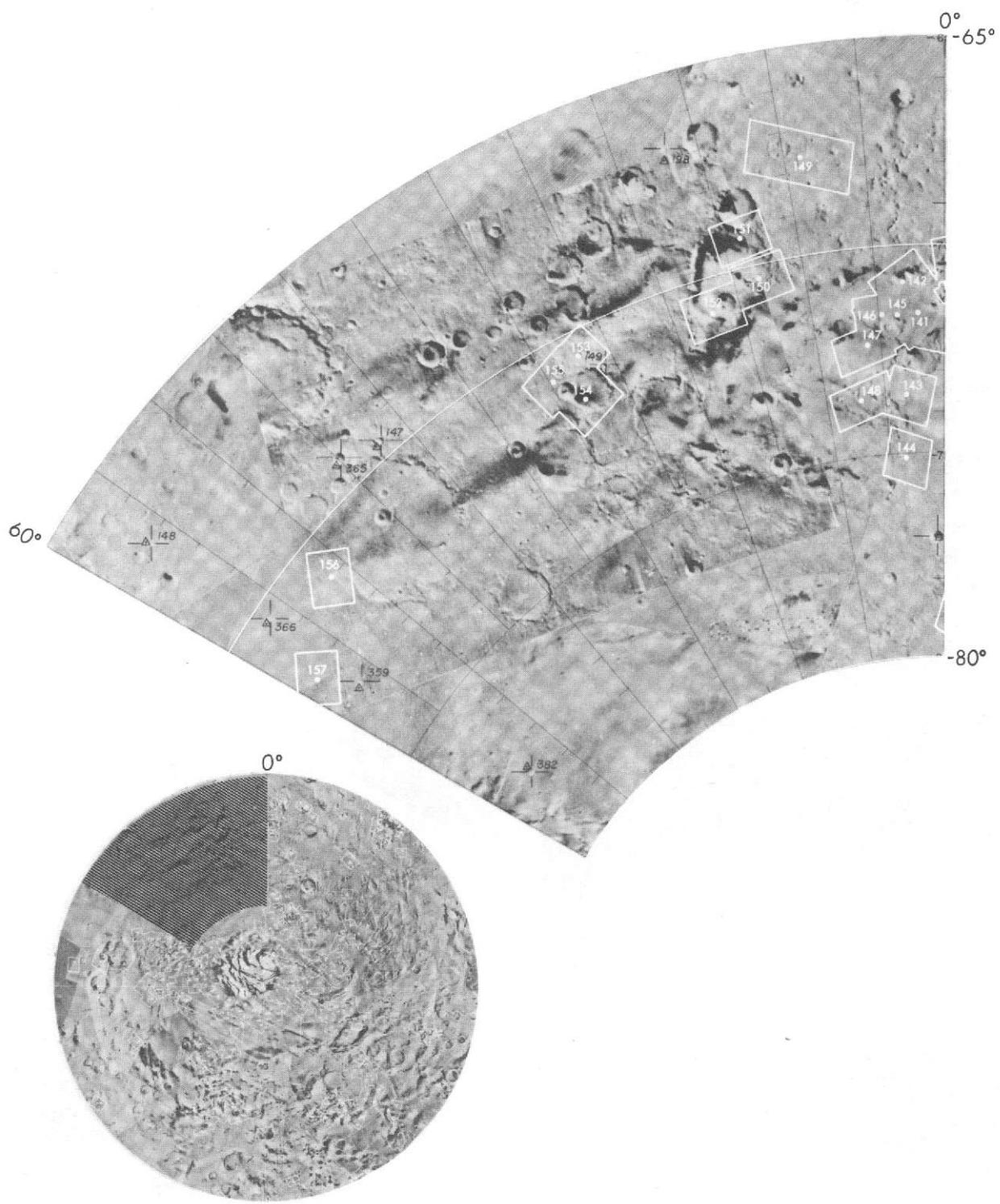


Fig. VIII-7f. VAGC versions of narrow-angle pictures in the Mare Australe quadrangle during Revs 100-262. Index map sector b: index numbers 141-157.

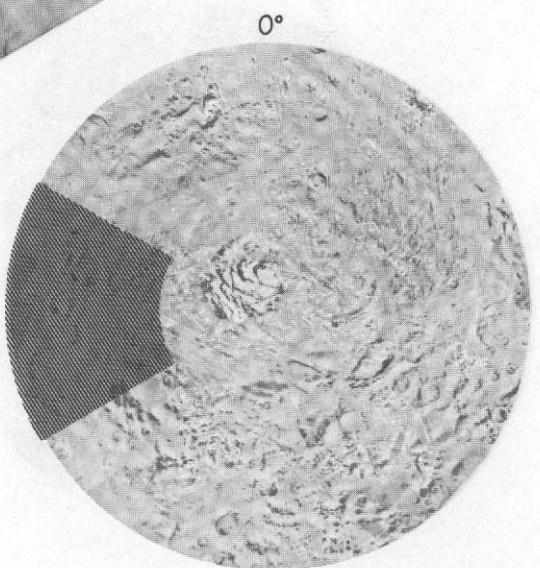


Fig. VIII-7g. VAGC versions of narrow-angle pictures in the Mare Australe quadrangle during Revs 100-262. Index map sector c: index numbers 158-184.

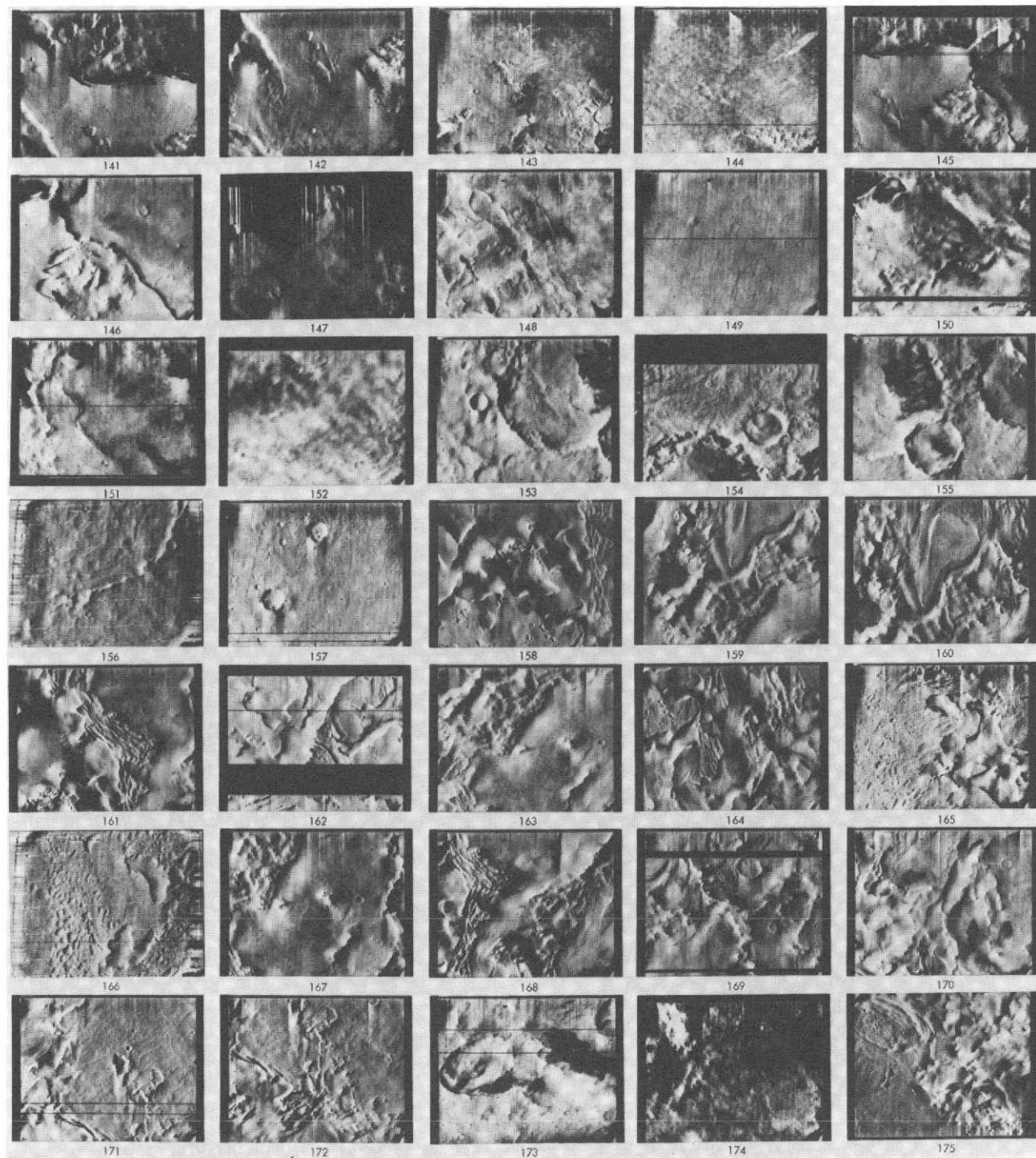


Fig. VIII-7h. Narrow-angle pictures located on index map sectors *b* and *c*: index numbers 141-175.

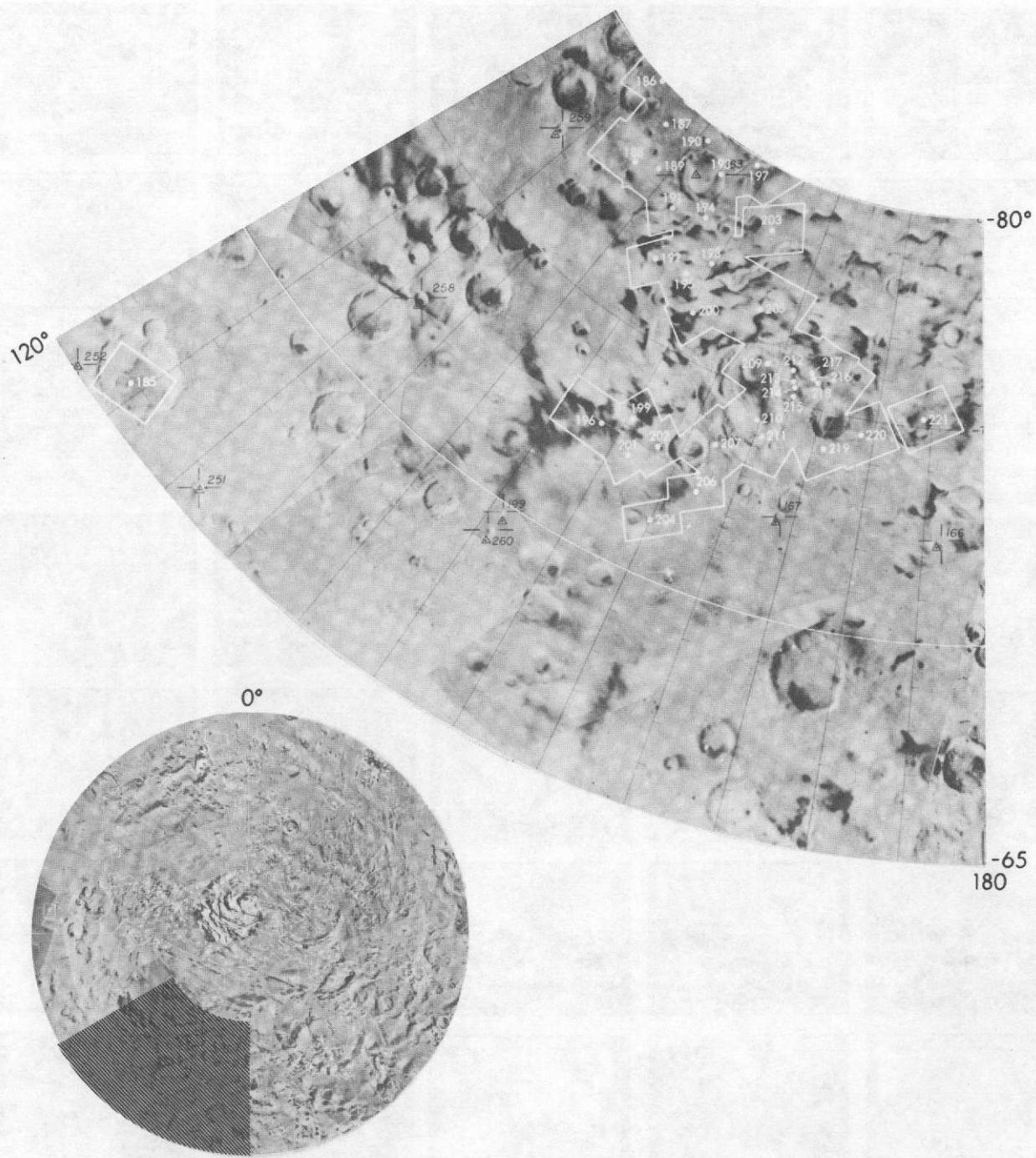


Fig. VIII-7i. VAGC versions of narrow-angle pictures in the Mare Australe quadrangle during Revs 100-262. Index map sector *d*: index numbers 185-221.



Fig. VIII-7j. Narrow-angle pictures located on index map sectors *c* and *d*: index numbers 176-210. Images with little detail may have been underexposed (see histograms in original data and Section IV).

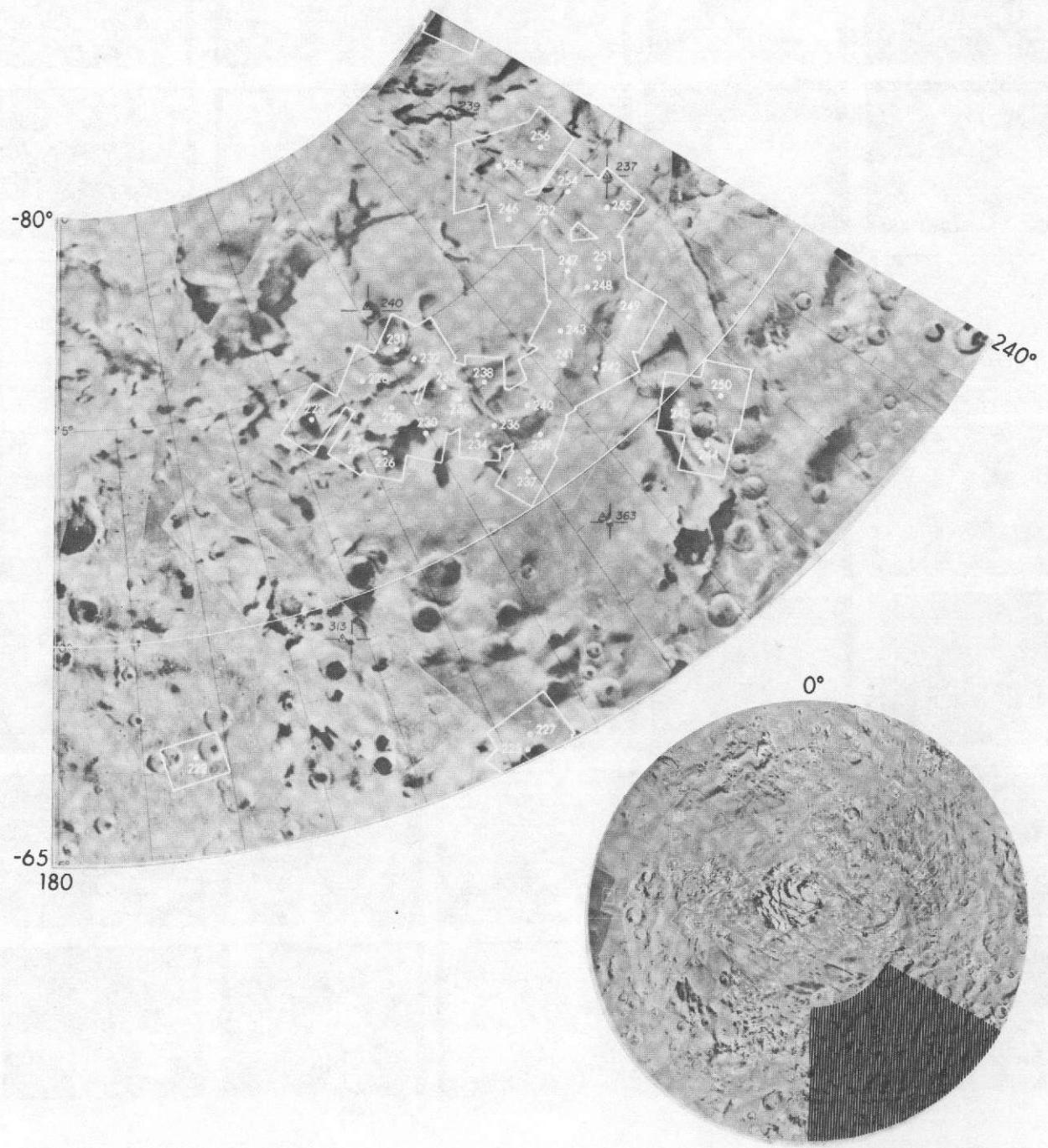


Fig. VIII-7k. VAGC versions of narrow-angle pictures in the Mare Australis quadrangle during Revs 100-262. Index map sector e: index numbers 222-256.



Fig. VIII-7I. Narrow-angle pictures located on index map sectors *d* and *e*: index numbers 211-245.

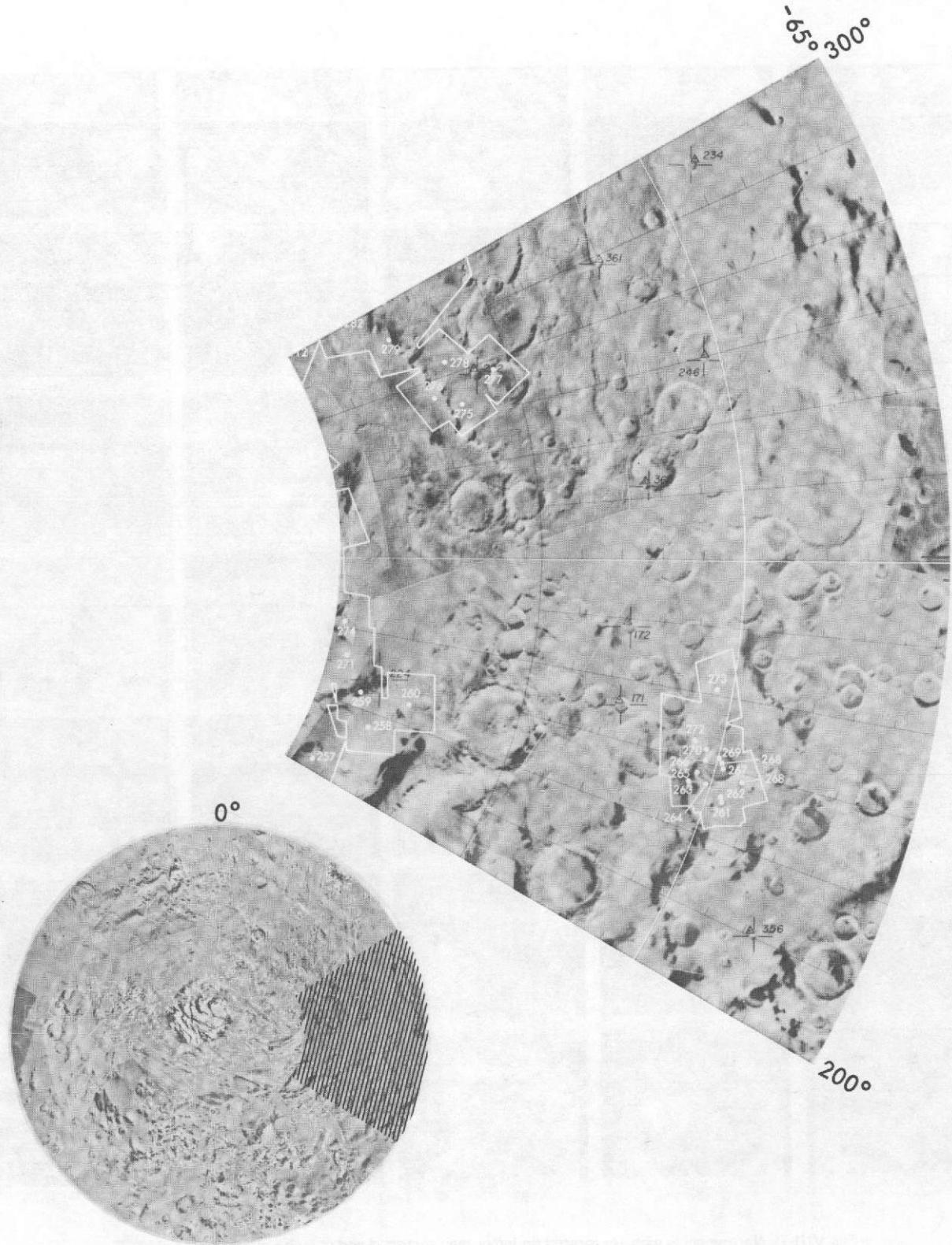


Fig. VIII-7m. VAGC versions of narrow-angle pictures in the Mare Australe quadrangle during Revs 100-262. Index map sector f: index numbers 257-279.

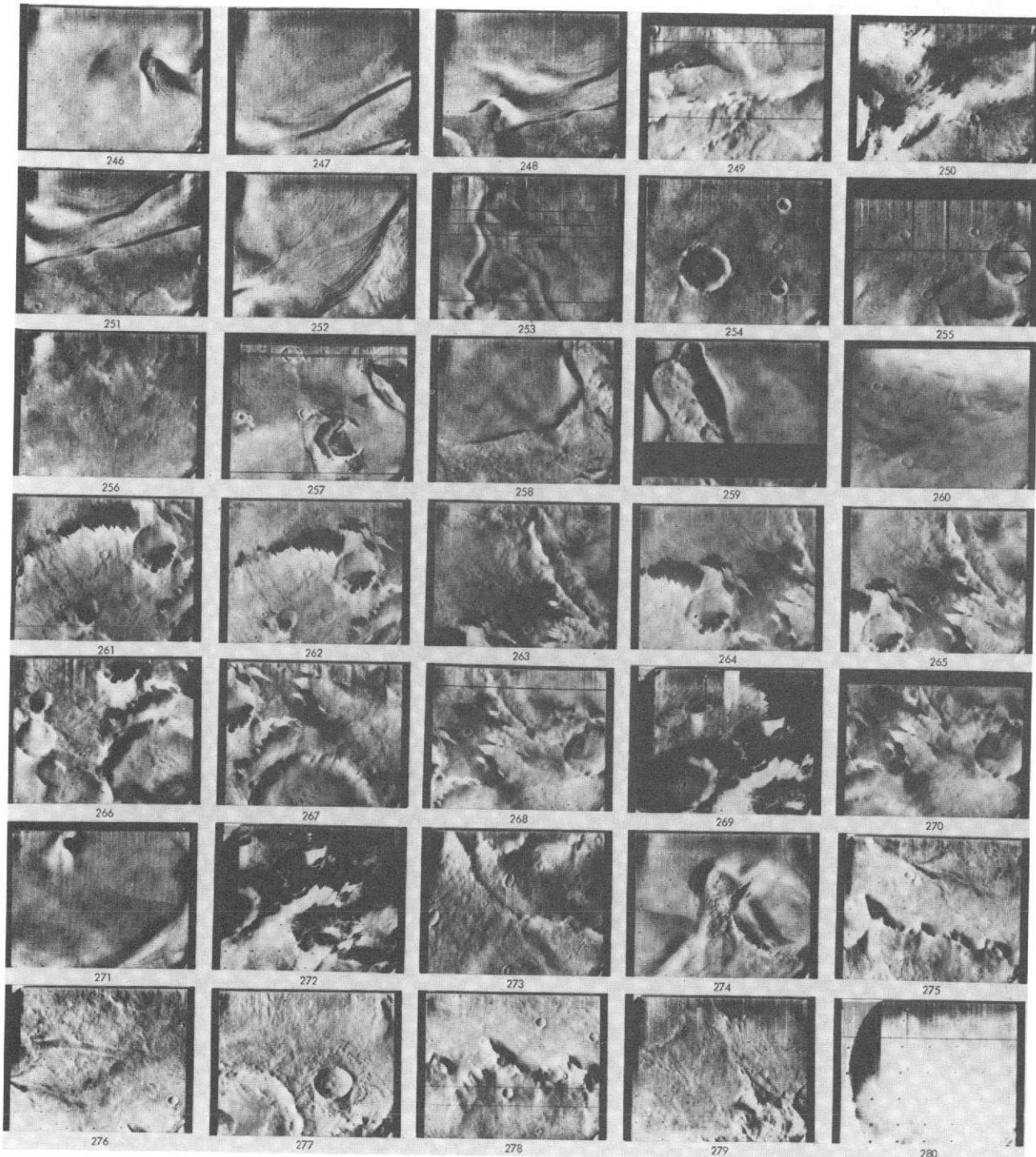


Fig. VIII-7n. Narrow-angle pictures located on index map sectors e and f: index numbers 246-280.

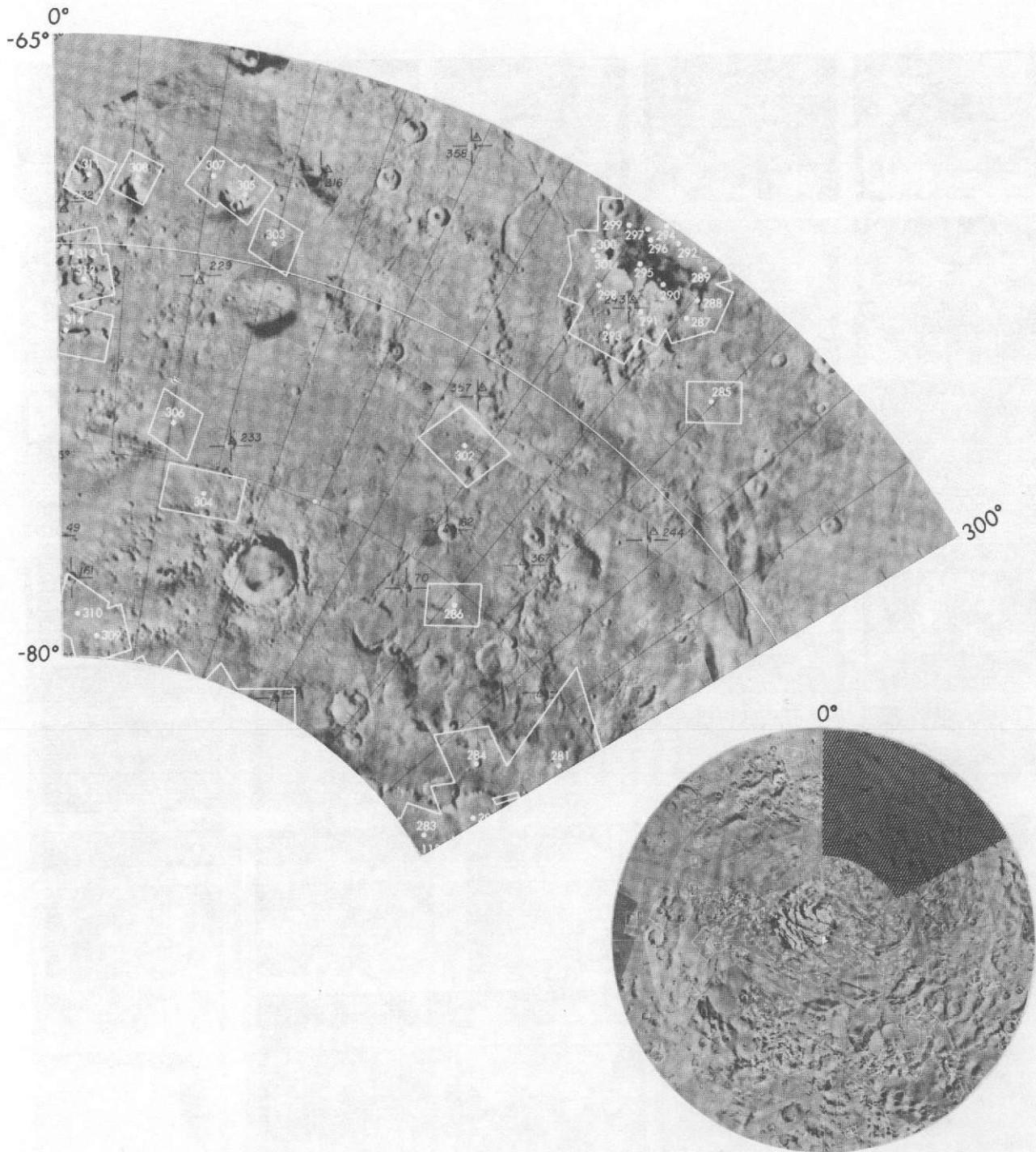


Fig. VIII-7o. VAGC versions of narrow-angle pictures in the Mare Australis quadrangle during Revs 100-262. Index map sector g: index numbers 280-314.



Fig. VIII-7p. Narrow-angle pictures located on index map sector g: index numbers 281-314.

Table VIII-3. Narrow-angle frames in the Mare Australis quadrangle; viewing angles less than 80°: Revs 100-262

Index number	Rev	Frame number	Center of picture		Range (SRR-5), km	Lighting angle (SLAR-5), deg	Viewing angle (VAR-5), deg	North direction (NORAN) ^a	Sun direction (SUNAN) ^a	DAS time
Sectors										
1	262	C7	-83.67	.88	2,999	85.85	50.87	166	186	10,720,689
2	162	C6	-84.41	2.47	3,104	77.92	50.16	183	170	8,118,288
3	116	09	-86.56	6.40	3,558	73.46	44.27	134	168	5,741,958
4	182	C5	-82.67	7.02	3,103	76.30	46.08	176	169	8,118,218
5	168	03	-85.13	10.59	4,009	80.43	54.15	218	171	7,612,498
6	206	01	-86.38	10.72	3,696	87.66	46.04	46	178	8,979,534
7	229	02	-85.67	11.63	3,566	85.58	43.14	130	177	9,808,724
8	156	01	-83.77	12.66	3,600	82.56	39.27	99	175	8,619,734
9	188	01	-87.15	20.30	3,671	81.75	45.32	137	174	8,331,754
10	116	C7	-86.89	20.57	3,678	74.18	44.51	114	168	5,741,888
11	168	04	-86.44	22.54	3,862	79.20	53.22	209	170	7,612,568
12	156	C2	-83.70	29.16	3,514	84.25	40.52	76	176	8,619,804
13	155	04	-84.49	34.11	3,629	80.65	42.76	68	173	7,288,818
14	159	05	-85.45	34.27	3,560	80.68	44.64	67	173	7,288,888
15	227	C2	-83.34	37.31	3,627	85.51	38.75	111	177	9,734,624
16	109	09	-84.29	46.09	4,056	80.65	58.13	299	170	5,689,888
17	145	C2	-86.62	48.28	4,228	76.71	45.92	137	169	6,784,538
18	105	C6	-84.31	48.32	4,077	80.40	58.46	307	170	5,489,538
19	159	02	-85.84	48.88	4,163	81.87	45.29	52	173	7,288,538
20	260	01	-82.16	49.43	3,057	87.60	39.83	112	178	10,648,519
21	145	05	-88.36	49.82	3,668	78.13	47.02	128	170	6,848,888
22	196	04	-83.93	51.33	3,501	86.55	44.79	54	177	8,619,874
23	184	04	-84.45	52.25	3,391	79.98	40.92	116	173	8,187,904
24	227	05	-82.92	52.71	3,730	87.00	40.99	81	177	9,734,904
25	227	04	-82.07	56.12	3,289	87.38	38.63	80	178	9,734,834
26	227	C3	-81.04	60.00	3,354	87.93	36.40	78	179	9,734,764
27	262	05	-87.77	62.15	3,205	91.47	54.62	79	190	10,720,619
28	180	C1	-82.08	63.75	3,484	77.27	36.74	129	172	8,043,908
29	180	C5	-80.50	63.75	2,923	75.88	40.73	121	173	8,044,328
30	184	01	-84.54	64.07	3,606	81.02	40.49	104	173	8,187,764
31	168	C1	-86.78	69.62	1,945	78.75	48.03	180	171	7,612,428
32	180	07	-82.34	70.26	3,374	78.04	36.86	119	172	8,043,978
33	180	04	-83.94	70.33	3,334	79.08	40.23	116	173	8,044,048
34	227	C1	-82.96	71.30	3,751	89.36	39.13	70	179	9,734,554
35	180	06	-81.19	73.30	2,950	77.40	46.41	110	175	8,044,398
36	219	03	-80.09	75.75	3,191	83.14	33.41	103	176	9,446,924
37	219	02	-81.01	79.42	3,320	84.10	34.55	101	176	9,231,254
38	219	C4	-82.00	79.46	3,332	80.44	37.67	136	173	7,000,768
39	151	C3	-85.22	80.46	3,736	80.52	44.45	59	173	8,187,634
40	184	C2	-84.75	80.67	3,525	82.52	41.93	81	175	9,159,294
41	215	04	-83.31	81.03	3,357	82.63	38.99	122	175	9,303,144
42	176	C4	-86.94	91.32	3,610	80.36	44.74	130	172	7,900,128
43	176	C3	-86.65	84.50	3,705	80.27	44.12	128	173	7,900,058
44	213	C2	-81.72	84.86	3,244	80.77	36.76	131	174	9,231,184
45	211	04	-84.68	89.46	3,430	82.30	41.84	136	174	9,159,364
46	145	04	-88.25	89.56	3,782	79.02	46.97	75	171	6,784,818
47	219	C1	-81.22	89.77	3,441	85.74	35.08	90	177	9,446,854
48	213	C1	-82.66	90.14	3,564	81.97	38.07	127	175	9,231,114
49	226	01	-89.41	91.55	3,888	87.80	50.19	224	178	9,698,644
50	211	C2	-83.81	100.66	3,493	82.50	39.64	125	175	9,159,294
51	133	10	-86.96	101.59	3,620	75.51	44.66	138	169	6,353,408
52	207	06	-86.28	101.66	3,501	82.84	44.70	146	174	9,015,584
53	151	04	-84.85	105.05	3,718	82.62	48.17	41	174	7,000,838
54	151	01	-85.01	108.40	4,282	82.91	47.16	33	174	7,000,488
55	133	07	-86.95	110.41	4,244	75.80	46.01	132	168	6,353,058
56	141	C6	-87.01	110.89	3,588	78.34	46.08	74	171	6,641,038
57	211	01	-84.66	115.22	3,629	84.21	40.64	108	176	9,159,224
58	215	02	-83.66	119.27	3,495	86.77	40.24	75	178	9,303,074
59	207	04	-86.89	126.87	3,011	84.30	44.57	115	175	9,015,514
60	207	03	-85.66	130.85	3,674	83.90	42.40	113	176	9,015,444
61	262	C3	-83.95	143.96	3,660	97.60	59.30	28	196	10,720,549
62	137	09	-80.19	147.44	3,551	79.20	42.23	70	174	6,497,188
63	236	06	-86.74	148.21	3,111	86.54	56.74	118	176	10,059,284
64	215	01	-81.53	150.31	3,653	91.15	42.20	47	181	9,303,004
65	137	06	-80.46	150.42	4,070	79.95	39.51	60	173	6,496,838
66	236	04	-88.64	151.22	3,267	88.09	54.55	123	173	10,059,144
67	133	C8	-85.80	164.57	3,744	78.25	45.02	62	171	6,353,338
68	187	04	-85.49	168.38	3,155	87.95	54.91	78	177	10,059,214
69	236	05	-86.86	178.84	3,531	88.08	43.75	95	178	10,058,794
70	236	C3	-86.16	183.04	3,531	88.08	43.75	95	178	10,058,724
71	236	02	-88.29	193.48	3,697	88.97	46.97	82	179	10,058,654
72	236	01	-86.64	197.62	3,742	89.09	44.25	80	179	9,698,714
73	226	02	-89.12	199.33	3,721	87.42	48.42	138	178	9,698,724
74	237	01	-82.91	223.41	3,805	85.77	57.56	213	176	10,094,844
75	226	C3	-87.29	224.69	3,534	87.06	45.68	100	177	9,698,784
76	226	05	-85.18	237.49	3,226	87.23	46.55	76	178	9,698,994
77	187	C2	-80.93	238.47	3,414	80.94	34.87	94	175	8,295,774
78	226	04	-86.08	240.04	3,327	87.58	46.26	75	178	9,698,924
79	140	01	-80.06	244.91	4,016	70.11	38.19	142	166	6,604,708
80	185	04	-82.03	245.29	3,323	80.65	37.50	94	174	8,223,884

^a Terms are defined in Fig. III-15.

Table VIII-3. (contd)

Index number	Rev	Frame number	Center of picture		Range (SRR-5), ^a km	(SLAR-5), ^a deg	Viewing angle (VAR-5), ^a deg	North direction (NORAN), ^a deg	Sun direction (SUNAN), ^a deg	DAS time
			Latitude ^a (LR-5), deg	Longitude ^a (LOR-5), deg						
Sector # (contd)										
81	224	02	-88.69	246.34	3.670	87.63	47.69	84	178	9,626,754
82	222	03	-82.80	246.64	3.333	85.27	38.18	97	177	9,554,864
83	226	C6	-84.46	250.07	3.195	88.28	49.47	64	178	9,699,064
84	218	03	-80.82	250.28	2.909	81.69	43.66	105	175	9,411,364
85	218	02	-80.29	251.94	2.929	81.64	39.94	107	175	9,411,294
86	222	02	-84.38	253.52	3.485	86.40	40.08	90	178	9,554,794
87	185	02	-81.40	254.75	3.417	81.81	36.69	85	175	8,223,814
88	212	C8	-85.50	257.97	3.167	82.71	46.86	137	174	9,195,554
89	224	01	-87.36	259.12	3.730	88.01	45.60	70	178	9,626,684
90	222	01	-82.33	259.75	3.536	86.91	37.14	84	178	9,554,724
91	218	C1	-80.83	261.41	3.022	83.31	39.50	97	176	9,411,224
92	212	07	-84.25	261.93	3.183	81.88	43.10	135	174	9,195,484
93	185	01	-81.69	264.40	3.552	83.31	37.79	74	175	8,223,744
94	216	01	-83.17	266.53	3.513	83.73	38.17	112	176	9,338,984
95	183	C1	-80.56	269.71	3.515	82.33	35.49	80	175	8,151,778
96	214	03	-87.18	273.40	3.665	85.30	44.97	116	176	9,267,094
97	214	04	-85.12	275.23	3.473	84.32	41.73	111	176	9,267,164
98	216	02	-80.07	275.25	3.301	83.59	32.65	99	176	9,339,054
99	214	C6	-83.90	275.54	3.328	83.70	40.16	108	175	9,267,234
100	216	04	-81.41	277.70	3.254	84.34	36.29	94	176	9,339,124
101	212	C6	-82.26	278.99	3.273	81.92	37.18	117	174	9,195,344
102	210	06	-82.00	294.51	3.275	81.06	36.81	122	174	9,123,554
103	210	04	-80.71	294.68	3.340	80.27	34.39	124	174	9,123,384
104	176	C1	-87.39	285.28	4.086	83.91	53.31	280	175	7,899,988
105	212	03	-83.85	290.28	3.538	83.97	39.24	106	176	9,195,204
106	212	04	-84.35	290.70	3.450	84.19	40.37	103	175	9,195,274
107	210	03	-81.08	293.61	3.454	81.67	34.55	116	175	9,123,314
108	208	04	-87.26	295.06	3.109	80.99	39.18	117	174	9,051,704
109	206	04	-85.51	296.18	3.401	82.49	43.28	132	174	8,979,674
110	208	02	-83.00	298.94	3.218	81.88	39.30	114	174	9,051,634
111	239	06	-80.38	299.92	2,835	80.62	45.07	145	173	10,167,224
112	243	02	-80.06	300.71	3.303	82.99	35.07	133	175	10,310,654
113	208	01	-84.47	308.77	3.367	83.60	41.14	102	175	9,051,564
114	239	04	-82.91	315.85	2,962	83.99	46.34	124	175	10,167,154
115	206	05	-87.53	316.92	3,216	84.67	52.75	88	175	8,979,954
116	224	03	-89.28	317.45	3,625	88.47	50.21	18	178	9,626,824
117	206	06	-86.70	319.20	3,158	84.34	54.27	85	175	8,980,024
118	243	C1	-80.88	322.63	3,398	86.51	34.19	108	177	10,310,584
119	234	01	-84.75	324.08	4,325	93.56	54.42	344	182	9,986,484
120	239	02	-81.48	327.39	3,381	84.35	36.29	125	176	10,166,734
121	239	03	-82.50	329.47	3,302	85.15	37.90	121	176	10,166,804
122	239	01	-80.22	329.50	3,456	84.01	34.38	124	176	10,166,664
123	299	01	-84.05	334.11	3,748	62.57	45.86	165	174	9,806,654
124	204	06	-83.16	335.78	3,008	83.16	48.60	86	175	8,908,064
125	206	02	-85.77	335.90	3,497	85.10	42.59	81	176	8,979,604
126	152	C6	-80.48	337.29	2,885	75.10	42.67	157	170	8,476,234
127	233	C2	-61.67	340.92	3,397	82.24	38.50	141	175	9,950,784
128	152	05	-80.51	343.98	2,931	75.43	40.10	149	170	8,476,164
129	173	C1	-87.31	344.30	4,204	83.25	40.96	49	175	7,791,978
130	196	C5	-82.36	345.79	3,012	78.96	42.31	122	173	8,620,154
131	188	04	-88.73	349.05	3,544	82.75	49.11	169	173	8,331,894
132	233	C1	-80.81	349.83	3,465	82.58	36.33	132	175	9,950,714
133	204	05	-84.19	350.13	3,181	84.98	48.94	72	176	8,907,994
134	229	03	-83.60	353.33	3,421	82.91	41.76	148	175	9,806,794
135	124	09	-85.75	355.03	3,538	74.85	43.36	99	170	6,029,868
136	124	07	-86.36	355.40	3,652	75.07	43.35	98	169	6,029,798
137	156	06	-82.12	355.84	2,977	79.71	45.29	108	174	8,620,224
138	231	C1	-85.93	355.86	3,666	85.65	43.99	138	176	9,878,684
139	188	C2	-86.59	357.94	3,569	80.72	45.78	160	173	8,331,824
140	233	C3	-81.09	358.10	3,227	83.69	35.45	119	176	9,950,854
Sector b										
141	157	C4	-71.71	2.15	3,169	68.11	16.44	125	174	7,216,858
142	157	C3	-70.95	3.05	3,271	67.93	15.66	123	174	7,216,788
143	184	C5	-73.64	3.09	2,836	67.24	34.02	167	165	8,188,184
144	184	C6	-75.16	3.59	2,770	68.76	35.86	168	166	8,188,254
145	157	C1	-71.65	3.83	3,811	68.92	24.11	122	171	7,216,508
146	200	02	-71.67	4.64	3,171	82.01	22.51	93	178	8,763,794
147	235	C4	-72.41	6.47	2,765	83.46	35.08	100	179	10,023,164
148	235	C6	-73.68	7.02	2,789	83.90	41.27	98	179	10,023,234
149	132	C6	-67.59	9.06	3,846	85.91	50.64	79	180	6,317,428
150	235	02	-70.37	13.23	3,141	85.71	15.29	96	178	10,022,744
151	235	C3	-69.32	13.93	3,042	85.67	16.22	95	179	10,022,814
152	235	01	-70.88	17.14	3,258	87.17	16.30	92	179	10,022,674
153	152	C4	-70.64	27.57	3,018	76.02	17.18	109	178	8,475,884
154	192	C1	-71.65	28.28	3,227	76.83	16.64	107	176	8,475,744
155	192	C2	-70.69	29.72	3,118	76.87	16.44	106	177	8,475,814
156	108	C9	-70.99	51.81	3,166	60.23	15.14	136	175	5,453,908
157	182	C4	-72.13	58.60	3,059	71.18	17.42	125	174	5,453,938

^a Terms are defined in Fig. III-15.

Table VIII-3. (contd)

Index number	Rev	Frame number	Center of picture		Range (SRR-5), km	Lighting angle (SLAR-5), deg	Viewing angle (VAR-5), deg	North direction (NORAN) ^a	Sun direction (SUNAN) ^a	DAS time
			Latitude ^a (LR-5), deg	Longitude ^a (LOR-5), deg	(SRR-5), km	(SLAR-5), deg	(VAR-5), deg			
Sector c										
158	223	C3	-77.15	64.56	2,950	83.93	34.95	93	177	9,591,054
159	221	C7	-79.35	65.67	3,224	83.04	31.56	106	176	9,518,884
160	221	I0	-79.47	66.13	2,946	83.03	39.42	98	176	9,519,164
161	223	C2	-78.00	66.39	3,135	84.62	33.86	91	177	9,590,984
162	182	C1	-75.11	66.56	3,355	75.31	24.79	116	173	8,115,798
163	221	C6	-78.74	67.23	3,109	83.13	30.10	106	176	9,518,814
164	223	C4	-76.70	67.89	2,925	84.47	39.04	90	178	9,591,124
165	141	O3	-74.90	66.32	3,813	66.85	29.51	133	167	6,640,688
166	108	C7	-73.42	68.34	3,351	65.60	22.93	116	175	5,453,838
167	221	O9	-78.74	68.51	2,976	83.12	35.61	98	176	9,519,094
168	221	C5	-77.60	68.86	3,389	83.09	28.08	106	176	9,518,744
169	221	C8	-79.65	70.04	3,070	83.78	35.08	96	176	9,519,024
170	182	O2	-77.12	73.25	3,278	77.25	27.25	107	174	8,115,868
171	217	O6	-79.29	76.85	3,230	81.19	31.45	116	175	9,375,034
172	217	O4	-78.92	79.41	3,327	81.46	30.62	115	175	9,374,964
173	131	O7	-70.19	81.68	4,218	58.24	44.75	159	157	6,281,168
174	147	C1	-67.08	83.69	3,732	76.61	17.37	90	177	6,856,498
175	217	O3	-78.32	84.56	3,420	82.14	29.53	110	176	9,374,894
176	174	O4	-77.20	86.41	3,310	71.97	29.14	136	170	7,828,238
177	172	C4	-75.94	87.05	3,323	69.55	30.03	145	168	7,756,348
178	172	O3	-75.17	80.89	3,423	69.36	29.33	141	169	7,756,278
179	174	O3	-77.72	91.57	3,421	73.13	29.61	131	170	7,828,168
180	139	C1	-77.42	91.78	3,911	70.71	30.82	119	169	6,568,728
181	172	O1	-75.89	96.09	3,546	70.72	29.99	137	169	7,756,208
182	244	O1	-79.94	99.15	3,341	81.21	38.59	149	174	10,346,634
183	241	O4	-78.28	101.69	4,140	101.04	90.34	37	217	10,239,534
184	174	O1	-73.21	112.63	3,402	74.62	19.85	109	174	7,828,098
Sector d										
185	135	C6	-65.96	124.60	3,656	67.88	8.77	109	177	6,424,948
186	209	O5	-79.93	131.76	3,265	82.97	33.17	96	176	9,087,674
187	209	O3	-79.28	135.97	3,350	83.57	31.71	93	176	9,087,046
188	100	O9	-78.16	136.49	3,540	72.89	40.76	90	177	5,166,138
189	203	O4	-78.40	138.95	2,811	77.59	40.58	116	175	8,872,154
190	269	C2	-79.66	141.55	3,475	84.70	32.53	87	177	9,087,334
191	199	O4	-77.88	143.25	2,768	74.79	37.20	135	173	8,728,234
192	199	C3	-76.58	144.88	2,777	73.93	31.96	134	173	8,728,164
193	203	C3	-79.17	145.46	2,490	79.11	39.63	109	175	8,872,084
194	164	O3	-78.07	146.63	3,349	72.94	29.03	124	171	7,468,718
195	195	O4	-76.74	148.05	2,747	72.05	35.23	151	170	8,584,244
196	100	O7	-72.73	148.55	3,716	75.86	43.40	88	180	5,166,068
197	137	O7	-79.79	149.71	3,536	79.51	40.95	67	174	6,497,118
198	164	O1	-77.22	150.05	3,441	72.96	27.71	121	172	7,468,648
199	232	O6	-73.17	150.73	2,555	72.96	33.29	148	171	9,915,294
200	165	O3	-76.04	150.90	2,788	71.61	31.77	149	170	8,584,174
201	232	C5	-72.42	151.64	2,591	72.41	29.53	148	171	9,915,224
202	237	O4	-72.86	153.42	2,672	73.07	28.61	147	171	9,915,154
203	164	O4	-78.61	154.21	3,256	74.40	30.10	114	173	7,468,788
204	238	O3	-71.27	155.33	2,577	78.38	36.92	116	178	10,131,314
205	113	C6	-76.79	156.59	4,182	63.57	46.05	171	158	5,633,598
206	238	C2	-72.27	157.46	2,619	79.57	34.05	112	178	10,131,244
207	191	O1	-73.48	157.67	3,513	68.02	38.92	158	166	8,439,764
208	262	O1	-77.25	158.04	3,786	104.55	65.23	25	203	10,720,479
209	152	O4	-75.63	159.23	3,523	65.85	38.57	165	163	7,036,818
210	191	O2	-74.40	160.11	3,343	69.04	36.07	157	167	8,439,834
211	150	O4	-74.02	161.90	3,488	64.28	40.39	169	161	6,964,858
212	152	C3	-75.72	161.80	3,651	65.93	39.23	163	163	7,036,748
213	150	O3	-75.50	162.25	3,629	65.66	41.61	169	162	6,964,788
214	230	O1	-75.41	162.33	3,334	75.30	35.83	150	171	9,842,774
215	191	O4	-75.16	162.64	3,191	69.90	33.73	156	168	8,439,904
216	113	O9	-75.50	162.65	3,353	62.06	35.14	172	161	5,633,948
217	150	O1	-75.76	163.20	3,775	65.87	42.90	168	162	6,964,718
218	152	C1	-75.64	165.17	3,774	65.90	39.56	159	163	7,036,678
219	234	O5	-74.14	166.22	3,396	78.34	24.63	128	175	9,986,834
220	234	C4	-74.64	169.30	3,217	79.37	25.63	125	175	9,986,764
221	234	O3	-75.19	174.60	3,334	80.89	26.20	121	175	9,986,694
Sector e										
222	199	O2	-67.19	188.17	3,056	80.56	22.13	99	179	8,727,884
223	191	O6	-74.15	202.12	2,744	74.54	37.28	120	179	8,440,254
224	191	O5	-73.29	205.08	2,768	74.81	33.05	117	179	8,440,184
225	121	O10	-65.16	206.29	3,339	70.08	33.10	116	187	5,921,928
226	185	O6	-72.77	206.54	2,626	68.40	25.82	143	174	8,224,234
227	121	O7	-65.53	206.79	3,698	71.36	18.24	99	179	5,921,578
228	189	C6	-74.49	207.37	2,732	73.67	34.72	123	178	8,368,224
229	187	O6	-73.62	208.66	2,689	71.27	28.67	131	176	8,296,194
230	185	O5	-72.74	209.95	2,692	68.94	23.26	139	174	8,224,164
231	189	O5	-74.74	211.42	2,792	74.73	32.46	117	177	8,368,154
232	232	O1	-74.38	212.54	3,327	87.48	23.05	89	179	9,914,664
233	187	C5	-73.14	213.14	2,751	72.05	25.99	126	176	8,296,124
234	183	C5	-72.17	213.34	2,686	67.21	21.93	146	173	8,152,198
235	232	O2	-73.22	213.71	3,208	87.63	22.19	88	179	9,914,734

^a Terms are defined in Fig. III-15.

Table VIII-3. (contd)

Index number	Re.	Frame number	Center of picture		Range (SRR-5), ^a km	Lighting angle (SLAR-5), ^a deg	Viewing angle (VAR-5), ^a deg	North direction (NORAN) ^a	Sun direction (SUNAN) ^a	DAS time
			Latitude ^a (LR-5), deg	Longitude ^a (LOR-5), deg						
Sector e (contd)										
236	232	C3	-72.04	214.61	3.114	.87.74	23.41	87	179	9,914,804
237	189	04	-70.74	214.69	3.000	73.64	15.20	116	176	8,367,874
238	183	06	-73.00	216.05	2.637	68.37	26.12	143	174	8,152,268
239	261	01	-71.3	217.03	2.744	80.19	18.90	124	177	10,684,499
240	160	03	-71.93	217.74	3.499	83.05	36.05	77	178	7,324,798
241	160	C4	-72.25	221.59	3.486	84.07	40.82	76	178	7,324,868
242	160	01	-71.66	223.1	3.624	84.88	36.64	71	178	7,324,728
243	189	02	-72.82	223.2	3.147	77.07	19.93	105	176	8,367,804
244	148	C3	-68.60	224.97	3.256	65.18	10.97	124	174	6,892,758
245	148	04	-69.65	225.75	3.155	65.98	12.20	124	175	6,892,828
246	181	08	-75.52	226.79	2.725	70.48	30.69	140	173	8,080,308
247	144	04	-73.69	227.17	3.214	64.99	22.65	140	169	6,748,908
248	144	01	-73.07	227.29	3.467	64.56	25.28	139	168	6,748,768
249	189	01	-71.90	227.62	3.241	78.13	18.41	102	177	8,367,734
250	148	01	-69.14	227.98	3.377	66.46	12.87	121	174	6,892,688
251	144	03	-73.19	228.66	3.326	64.86	22.88	138	169	6,748,838
252	181	C7	-74.83	229.05	2.770	70.22	26.91	138	173	8,080,238
253	125	06	-76.53	229.81	4.133	83.42	44.54	49	175	6,065,498
254	228	02	-74.88	232.14	3.211	87.13	25.84	86	178	9,770,744
255	228	01	-73.92	233.16	3.288	87.44	23.29	87	179	9,770,674
256	228	03	-76.05	233.88	3.162	87.55	29.96	83	179	9,770,814
Sector f										
257	187	C1	-79.37	241.65	3.476	81.07	32.12	92	175	8,295,704
258	220	C3	-78.42	248.54	3.213	82.15	29.68	109	176	9,482,904
259	183	C4	-78.94	251.95	3.229	78.75	31.87	100	174	8,151,918
260	220	C2	-77.65	252.82	3.297	82.76	28.02	105	176	9,482,834
261	220	05	-69.63	252.86	2.800	79.44	21.77	108	179	9,483,114
262	181	04	-69.70	252.94	3.146	72.24	12.20	116	176	8,079,888
263	220	06	-70.57	253.60	2.771	79.91	27.72	107	179	9,483,184
264	179	04	-70.13	253.73	2.997	69.59	13.07	125	175	8,008,068
265	181	C6	-70.40	254.14	3.054	72.85	14.47	115	176	8,079,958
266	179	02	-69.38	254.37	3.097	69.37	12.19	124	175	8,007,998
267	220	04	-69.83	255.20	2.877	80.38	19.35	105	179	9,483,044
268	181	C3	-70.30	255.76	3.265	73.33	13.84	113	176	8,079,818
269	126	09	-70.20	255.46	3.795	61.79	50.52	181	155	6,101,758
270	179	C1	-70.35	255.93	3.224	70.48	15.06	122	174	8,007,928
271	220	C1	-79.47	256.37	3.463	84.09	31.51	102	176	9,482,764
272	126	07	-70.67	256.49	3.940	61.87	51.48	180	155	6,101,688
273	220	C7	-70.36	256.42	2.840	81.68	47.18	110	182	9,483,394
274	183	C2	-79.72	260.63	3.366	80.59	33.49	90	174	8,151,848
275	175	C4	-76.44	286.77	3.206	75.84	26.40	108	174	7,864,218
276	175	C3	-77.05	288.12	3.324	76.47	27.07	106	174	7,864,148
277	173	C3	-75.46	288.94	3.286	73.56	23.75	117	173	7,792,258
278	173	C4	-76.52	291.35	3.206	74.57	25.97	114	173	7,792,328
279	142	04	-77.55	296.06	3.484	78.58	37.80	78	175	6,676,948
Sector g										
280	115	05	-76.58	300.41	4.150	89.00	33.65	30	179	5,849,968
281	119	C6	-76.05	300.67	4.586	89.67	59.03	19	179	5,849,618
282	142	03	-78.46	300.88	3.611	79.64	38.47	71	174	6,676,878
283	243	03	-79.68	302.18	3.175	82.87	33.99	130	175	10,310,724
284	142	C1	-77.65	305.62	3.722	80.77	38.31	66	175	6,676,808
285	130	09	-67.63	315.04	2.997	62.48	14.66	132	182	6,245,678
286	202	02	-75.38	319.40	2.977	74.87	25.03	128	174	8,835,894
287	198	03	-66.57	319.63	2.569	63.57	13.47	148	173	8,692,184
288	171	04	-66.07	319.92	3.153	75.56	20.74	105	181	7,720,438
289	200	C5	-65.38	320.71	2.557	65.02	7.30	141	178	8,764,144
290	198	04	-66.28	322.05	2.470	63.67	12.37	147	175	8,692,254
291	171	C3	-67.13	322.12	3.244	76.78	19.04	100	179	7,720,368
292	165	C4	-65.31	322.81	3.105	72.30	15.13	111	181	7,648,548
293	171	01	-67.85	323.10	3.638	77.79	13.10	95	177	7,720,088
294	165	04	-65.14	323.82	3.111	64.93	4.22	126	177	7,504,698
295	165	03	-66.22	323.85	3.194	73.14	12.56	108	179	7,648,478
296	128	09	-65.62	324.18	3.060	60.74	9.54	132	182	6,173,718
297	200	C6	-65.43	324.56	2.955	65.97	13.83	140	181	8,764,214
298	165	01	-67.16	325.15	3.025	74.43	10.59	103	177	7,648,198
299	165	01	-65.58	325.44	3.160	66.30	19.42	121	173	7,504,348
300	130	C7	-66.45	325.86	3.135	65.42	18.52	123	183	6,245,608
301	128	07	-66.57	326.16	3.163	62.11	8.62	127	180	6,173,648
302	175	01	-72.12	326.67	3.803	86.19	28.85	69	178	7,863,868
303	262	13	-69.37	345.16	2.529	71.21	42.33	173	175	10,720,899
304	132	09	-75.66	345.97	3.394	77.24	42.02	90	179	6,317,568
305	150	C6	-68.43	347.65	2.583	63.17	20.81	157	170	8,404,204
306	262	11	-74.12	349.81	2.652	76.09	44.14	172	179	10,720,829
307	190	05	-68.15	349.43	2.572	63.14	20.19	154	170	8,404,134
308	188	C6	-68.39	354.77	2.536	62.71	21.58	159	169	8,332,244
309	198	01	-79.48	354.93	3.182	79.74	32.39	107	174	8,691,904
310	262	09	-78.96	357.61	2.798	81.20	46.64	167	182	10,720,759
311	188	05	-68.40	357.79	2.617	62.98	20.36	156	169	8,332,174
312	200	C4	-70.89	357.98	3.046	79.65	20.62	100	178	8,763,864
313	200	C1	-70.26	358.84	3.214	79.98	15.79	100	178	8,763,724
314	132	C7	-72.10	359.34	3.603	81.33	46.01	83	180	8,317,498

^a Terms are defined in Fig. III-15.



Fig. VIII-8a. Index map for narrow-angle pictures in the Mare Boreum quadrangle during Revs 100-262. Index numbers 1-32.

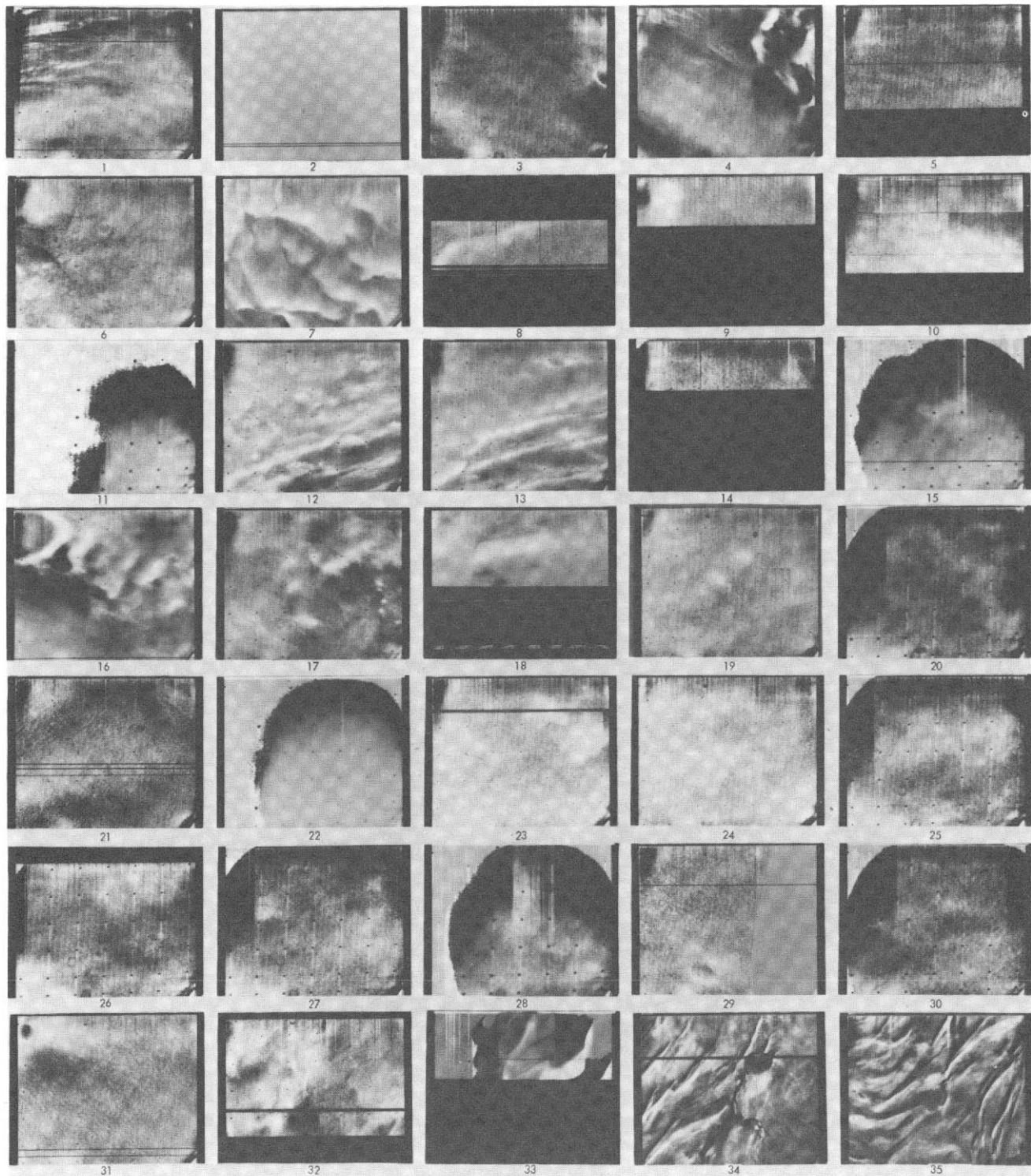


Fig. VIII-8b. VAGC versions of narrow-angle pictures located on Fig. VIII-8a. index numbers 1-32. Index numbers 33-35 are located on Fig. VIII-8c. Images with little detail may have been underexposed (see histograms in original data and Section IV).



Fig. VIII-8c. Index map for narrow-angle pictures in the Mare Boreum quadrangle during Revs 416-676: index numbers 36-69.

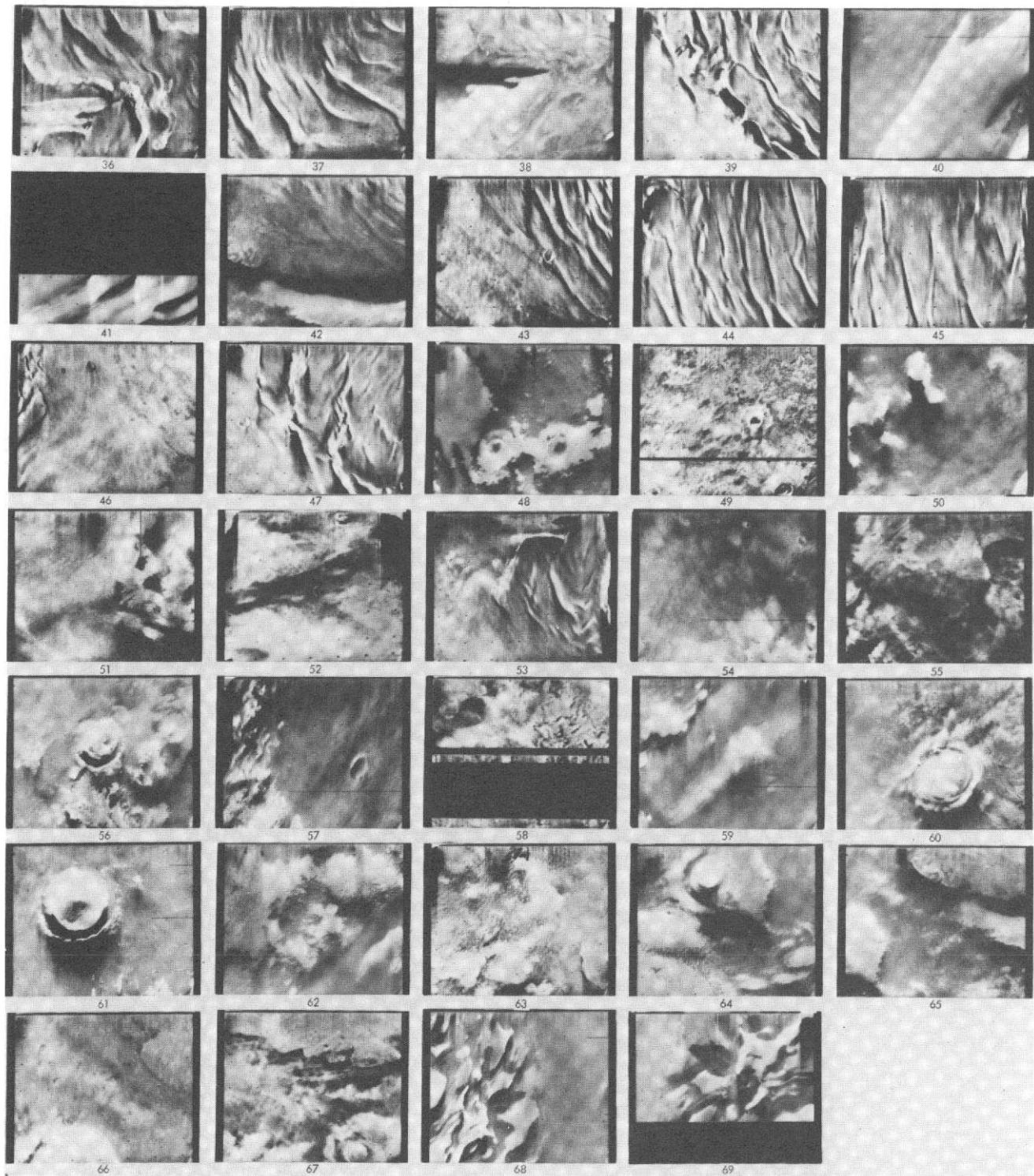


Fig. VIII-8d. VAGC versions of narrow-angle pictures located on Fig. VIII-8c: index numbers 36-69.

Table VIII-4. Narrow-angle frames in the Mare Boreum quadrangle; viewing angles less than 80°: Revs 100-676

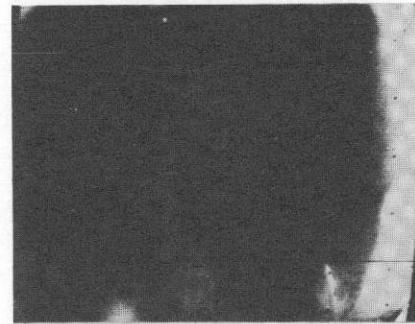
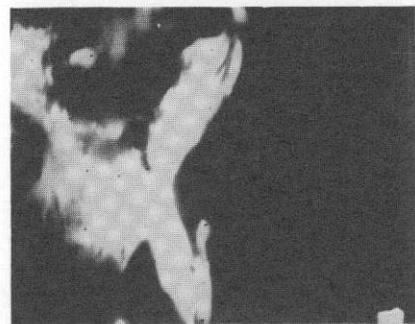
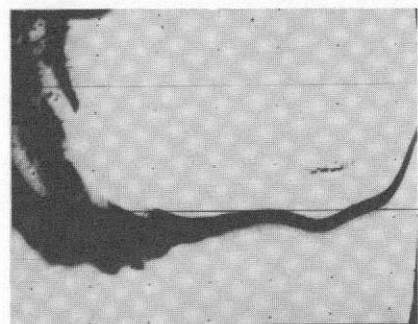
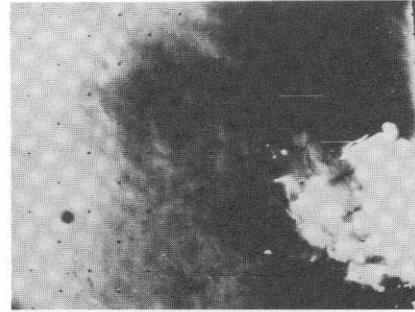
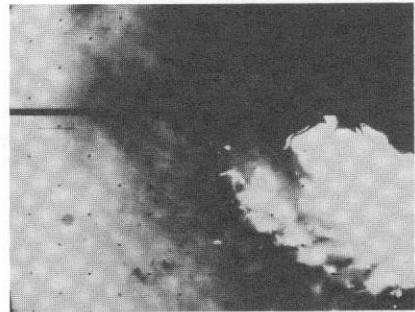
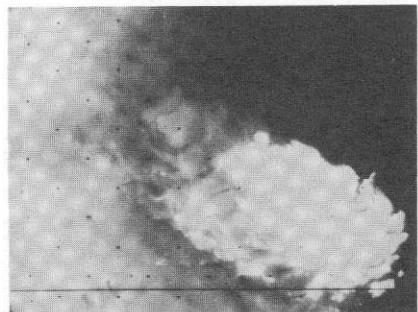
Index number	Rev	Frame number	Center of picture		Range (SRR-5), km	Lighting angle (SLAR-5), °	Viewing angle (VAR-5), °	North direction (NORAN) ^a	Sun direction (SUNAN) ^a	DAS time		
Revs 100 - 262												
Sector a												
1	186	30	82.80	5.43	5,412	89.03	61.24	355	178	8,263,644		
2	180	30	82.94	151.29	5,928	99.16	71.50	123	188	8,047,628		
3	259	05	80.30	168.46	5,636	79.81	42.82	330	172	10,616,599		
4	259	07	84.09	166.60	5,830	83.19	45.35	332	174	10,616,669		
5	189	30	82.35	201.12	5,628	88.85	65.45	9	179	8,371,654		
6	245	09	80.49	235.46	5,702	81.88	42.43	329	174	10,386,884		
7	245	11	84.36	237.30	5,895	84.98	44.94	333	176	10,386,954		
8	245	13	88.18	252.36	6,106	88.16	47.89	348	178	10,387,024		
9	183	30	86.76	252.59	5,621	94.25	66.12	24	183	8,155,698		
10	239	10	84.35	336.57	6,028	86.47	56.63	22	176	10,171,004		
Sector b												
11	188	26	71.99	4.29	5,256	77.99	67.78	350	168	8,335,394		
12	194	28	79.31	5.20	5,753	86.21	67.58	9	176	8,551,694		
13	192	30	79.83	11.99	5,706	86.63	67.31	8	176	8,479,664		
14	248	15	67.93	39.61	5,079	70.56	34.86	321	168	10,494,474		
Sector d												
15	191	26	66.02	138.33	4,563	75.41	48.74	326	169	8,443,404		
16	185	30	76.21	138.89	4,908	38.85	46.10	308	179	8,227,664		
17	259	03	76.64	169.55	5,461	76.40	40.81	329	170	10,616,529		
Sector e												
18	245	07	77.03	235.29	5,522	78.71	40.21	327	172	10,386,814		
19	245	05	73.46	235.80	5,357	75.53	38.43	326	170	10,386,744		
Sector f												
20	206	25	72.85	244.81	4,992	79.23	47.27	330	172	8,983,454		
21	190	30	71.78	295.02	4,732	85.87	40.03	305	177	8,407,634		
22	225	05	68.32	295.87	4,654	82.67	30.68	288	176	9,666,654		
23	225	09	68.28	295.88	4,824	82.88	26.79	289	176	9,666,794		
24	225	11	65.66	298.96	4,863	80.80	21.45	293	176	9,666,864		
Sector g												
25	225	07	65.19	300.79	4,664	79.65	24.14	294	175	9,666,724		
26	225	01	65.13	301.30	4,403	79.06	29.93	292	174	9,666,514		
27	225	13	65.15	301.45	4,965	79.77	20.24	296	176	9,666,934		
28	192	26	65.00	312.10	4,551	73.84	49.83	327	167	8,479,384		
29	178	30	68.89	332.45	4,576	92.55	33.78	281	181	7,975,868		
30	184	26	66.82	341.94	4,488	78.18	48.30	323	171	8,191,604		
31	178	28	67.40	343.26	4,327	87.91	38.84	292	178	7,975,658		
32	219	16	79.70	359.95	5,550	83.85	45.06	331	175	9,451,124		
Revs 416 - 676												
Sector a												
33	667	08	85.38	15.15	8,300	60.87	30.06	26	190	13,316,880		
34	528	08	84.53	18.38	10,513	71.46	36.94	207	168	12,991,267		
35	528	10	84.58	72.21	10,553	66.84	31.83	255	167	12,991,407		
36	458	14	81.83	77.85	6,156	65.46	37.85	303	176	12,502,585		
37	458	13	83.82	77.98	6,129	66.84	41.28	302	175	12,502,515		
38	676	07	81.90	81.41	8,407	61.07	35.57	326	198	13,499,093		
39	479	08	84.75	169.01	9,269	66.15	29.69	304	167	12,906,593		
40	668	06	82.33	180.61	8,213	57.71	26.44	16	191	13,352,860		
41	676	08	89.57	182.16	8,509	65.15	35.50	65	191	13,499,163		
42	675	07	81.06	265.58	8,468	60.77	35.57	324	198	13,463,183		
43	459	14	80.20	273.03	6,048	62.31	33.80	325	174	12,538,565		
44	459	13	82.09	274.01	6,021	63.95	37.57	326	174	12,538,495		
45	459	12	84.07	274.20	6,007	65.77	41.55	326	174	12,538,425		
Sector b												
46	528	07	77.61	1.29	10,584	78.50	42.22	199	172	12,991,197		
47	478	07	78.87	5.69	9,126	60.53	24.12	316	166	12,870,613		
48	667	09	74.19	14.21	8,153	49.97	14.74	22	187	13,316,950		
49	478	08	73.82	18.66	9,229	54.71	24.53	326	163	12,870,683		
50	667	10	76.41	36.39	8,310	54.41	19.27	42	181	13,317,020		
51	676	06	73.12	47.82	8,721	66.23	49.15	310	203	13,499,023		
Sector c												
52	478	06	75.76	76.86	9,484	60.00	42.43	13	157	12,870,543		
53	458	15	79.93	78.37	6,191	64.11	34.46	305	177	12,502,655		
54	667	11	77.22	83.27	8,668	63.94	32.72	81	176	13,317,090		
55	528	09	77.75	104.12	10,265	59.81	22.16	293	167	12,991,337		
Sector d												
56	676	09	76.50	145.66	8,273	52.11	18.37	19	190	13,499,233		
57	667	07	75.66	168.86	8,875	79.39	52.64	169	185	13,316,810		
58	479	11	75.65	170.39	9,370	59.52	19.80	304	168	12,906,803		
Sector e												
59	668	07	79.58	185.29	8,243	55.07	22.36	19	189	13,352,930		
60	479	10	71.92	193.15	5,350	52.97	24.25	324	163	12,906,733		
61	668	09	73.03	194.79	8,322	49.29	12.84	24	183	13,353,070		
62	668	08	78.55	197.08	8,316	54.66	20.54	29	185	13,353,000		
63	479	09	79.03	202.50	9,354	59.22	29.19	335	163	12,906,663		
Sector f												
64	675	05	77.06	267.92	8,296	58.27	36.94	332	202	13,463,043		
65	675	06	79.05	269.41	8,362	59.11	35.48	330	200	13,463,113		
66	459	15	77.96	274.51	6,071	60.17	29.36	327	174	12,538,635		
67	529	08	77.49	279.17	10,301	59.62	21.92	293	167	13,027,317		
Sector g												
68	668	05	79.46	341.45	8,692	75.57	48.02	169	187	13,352,790		
69	675	08	79.62	343.34	8,284	55.81	21.94	32	187	13,463,253		

^a Terms are defined in Fig. III-15.

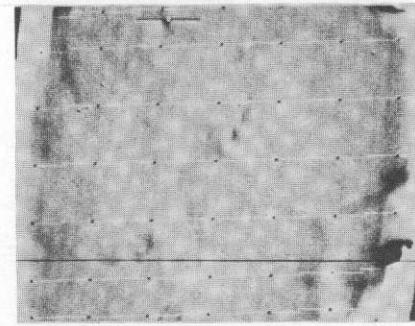
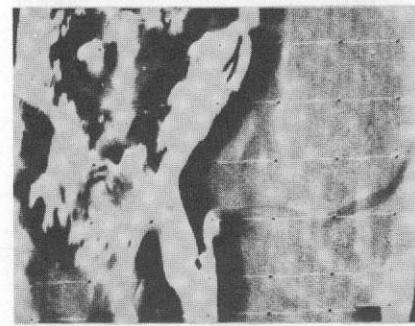
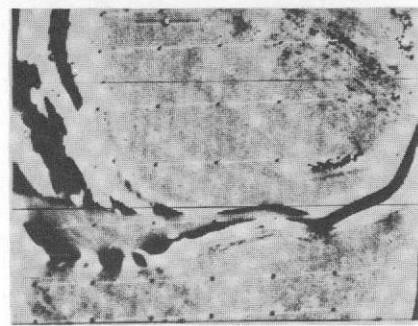
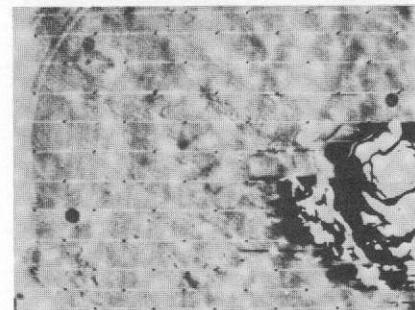
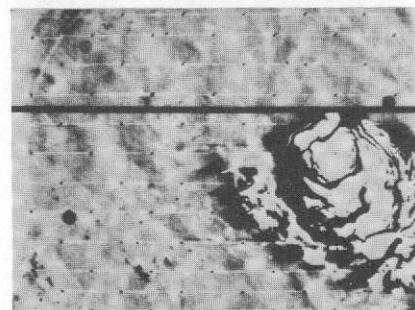
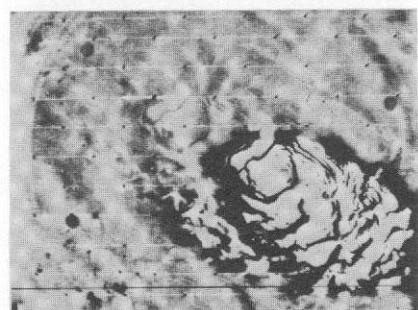
Note: There were no narrow-angle frames in sector e during Revs 100 - 262.

Table VIII-5. Areocentric longitude and equivalent Mars date during the mission

Rev	Julian date	Calendar date			Range, km X 10 ⁶	Areocentric longitude of the Sun, deg	Subsolar latitude, deg
		Year	Month	Day			
-	2441260.5	71	11	05	210.09	-73.09	-23.63
4	2441270.5	71	11	15	211.32	-66.99	-22.68
24	2441280.5	71	11	25	212.71	-60.96	-21.48
44	2441290.5	71	12	05	214.23	-55.01	-21.48
64	2441300.5	71	12	15	215.87	-49.14	-18.47
84	2441310.5	71	12	25	217.61	-43.37	-16.72
104	2441320.5	72	01	04	219.43	-37.70	-14.84
124	2441330.5	72	01	14	221.31	-32.11	-12.87
144	2441340.5	72	01	24	223.23	-26.63	-10.82
164	2441350.5	72	02	03	225.18	-21.23	-8.74
184	2441360.5	72	02	13	227.14	-15.93	-6.60
204	2441370.5	72	02	23	229.08	-10.73	-4.48
224	2441380.5	72	03	04	231.00	-5.60	-2.34
244	2441390.5	72	03	14	232.88	-0.56	-2.38
264	2441400.5	72	03	24	234.70	4.39	1.84
284	2441410.5	72	04	03	236.46	9.27	3.87
304	2441420.5	72	04	13	238.14	14.08	5.85
324	2441430.5	72	04	23	239.73	18.83	7.77
344	2441440.5	72	05	03	241.22	23.52	9.63
364	2441450.5	72	05	13	242.60	28.15	11.40
384	2441460.5	72	05	23	243.87	32.73	13.10
404	2441470.5	72	06	02	245.01	37.27	14.70
424	2441480.5	72	06	12	246.03	41.77	16.21
444	2441490.5	72	06	22	246.91	46.23	17.61
464	2441500.5	72	07	02	247.65	50.66	18.91
484	2441510.5	72	07	12	248.26	55.07	20.09
504	2441520.5	72	07	22	248.72	59.46	21.15
524	2441530.5	72	08	01	249.03	63.84	22.09
544	2441540.5	72	08	11	249.19	68.20	22.90
564	2441550.5	72	08	21	249.21	72.57	23.56
584	2441560.5	72	08	31	249.08	76.93	24.09
604	2441570.5	72	09	10	248.80	81.31	24.47
624	2441580.5	72	09	20	248.37	85.69	24.70
644	2441590.5	72	09	30	247.79	90.10	24.77
664	2441600.5	72	10	10	247.08	94.53	24.69
684	2441610.5	72	10	20	246.23	98.98	24.45
-	2441620.5	72	10	30	245.24	103.47	24.05



(a) SHADING-CORRECTED



(b) HPF

Fig. VIII-9. Sextad obtained on Rev 36. (a) Taken through orange, green, and blue filters. This version shows the appearance of the cap in different colors and can be combined to form color reproductions. (b) This version shows fine detail, in this case structure within the frost, atmospheric dust clouds, and surface markings and relief.

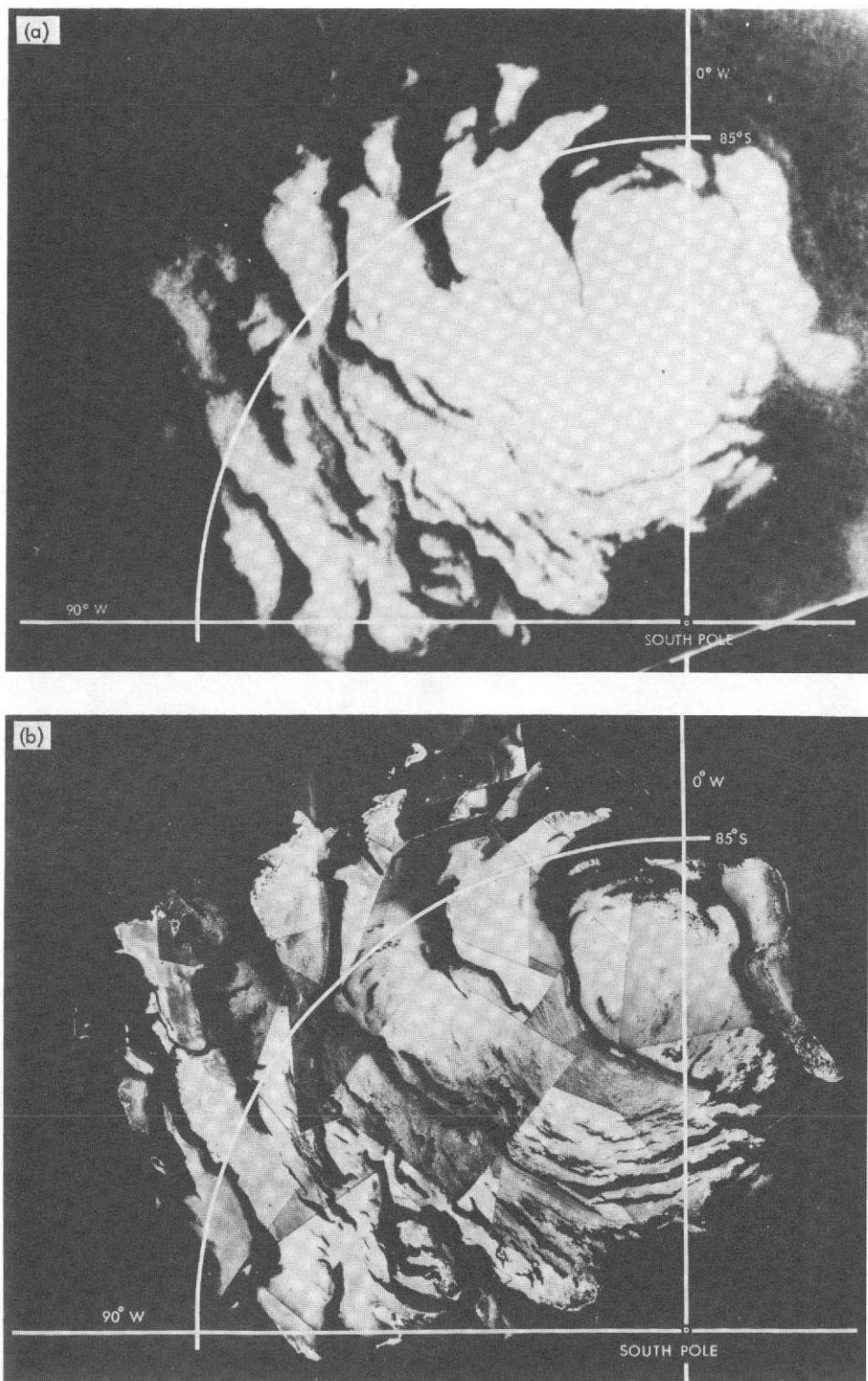


Fig. VIII-10. Stereographic projections. (a) Wide-angle frame of south polar cap. (b) Mosaic of narrow-angle frames showing the same area.

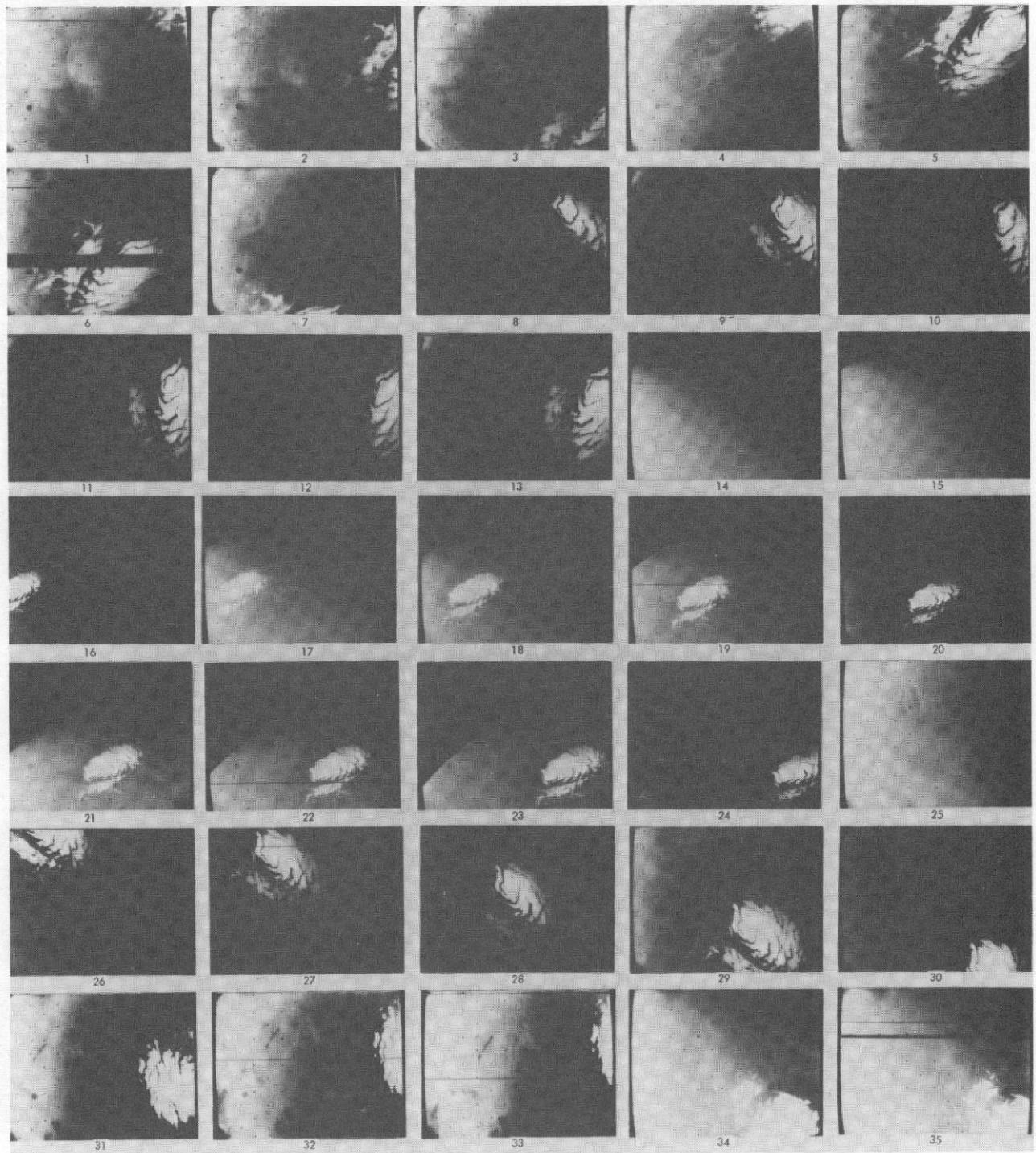


Fig. VIII-11a. Shading-corrected wide-angle frames showing the residual south polar cap (southern summer to early fall); distance less than 5000 km: index numbers 1-35.

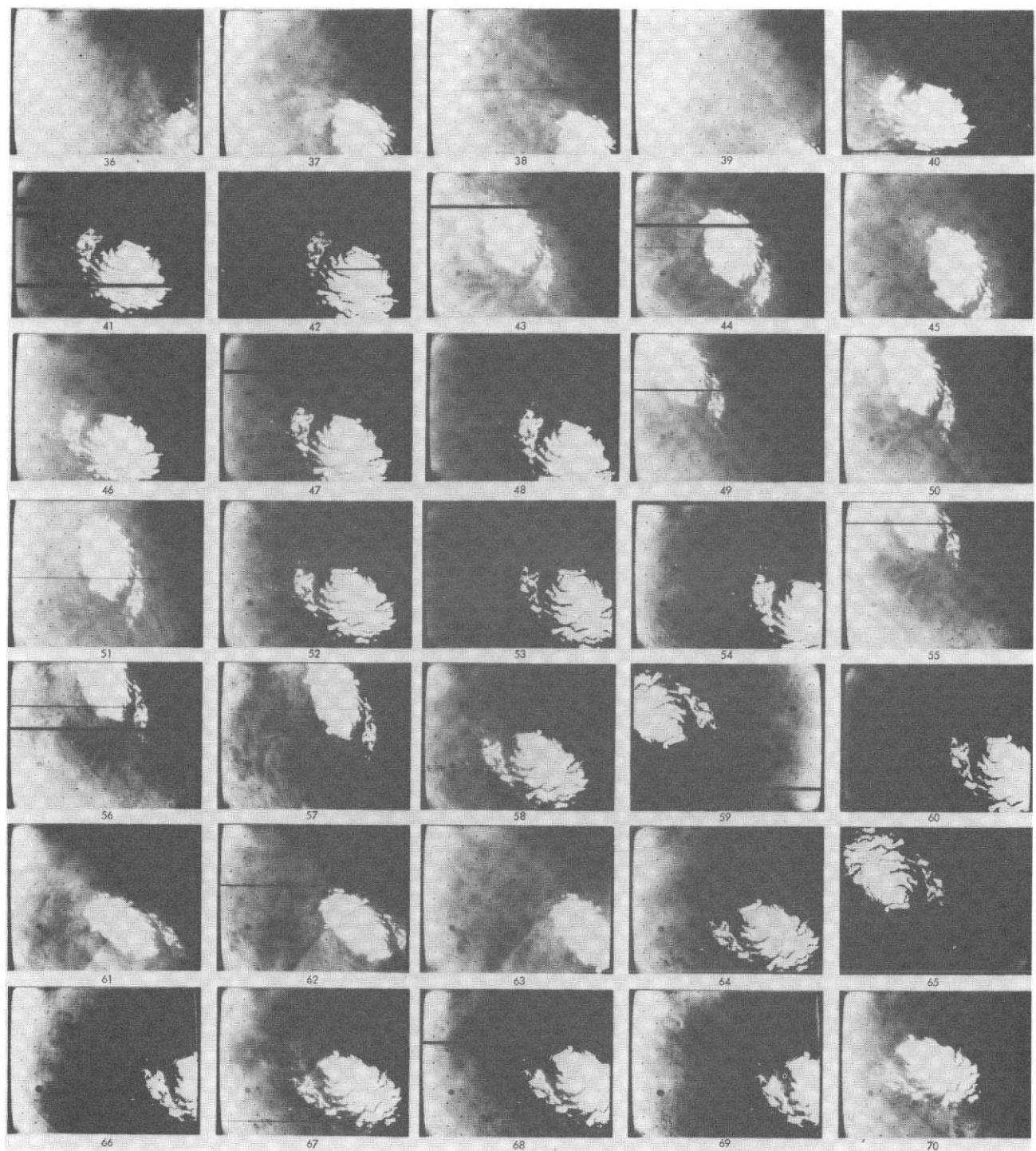


Fig. VIII-11b. Shading-corrected wide-angle frames showing the residual south polar cap (southern summer to early fall); distance less than 5000 km: index numbers 36-70.

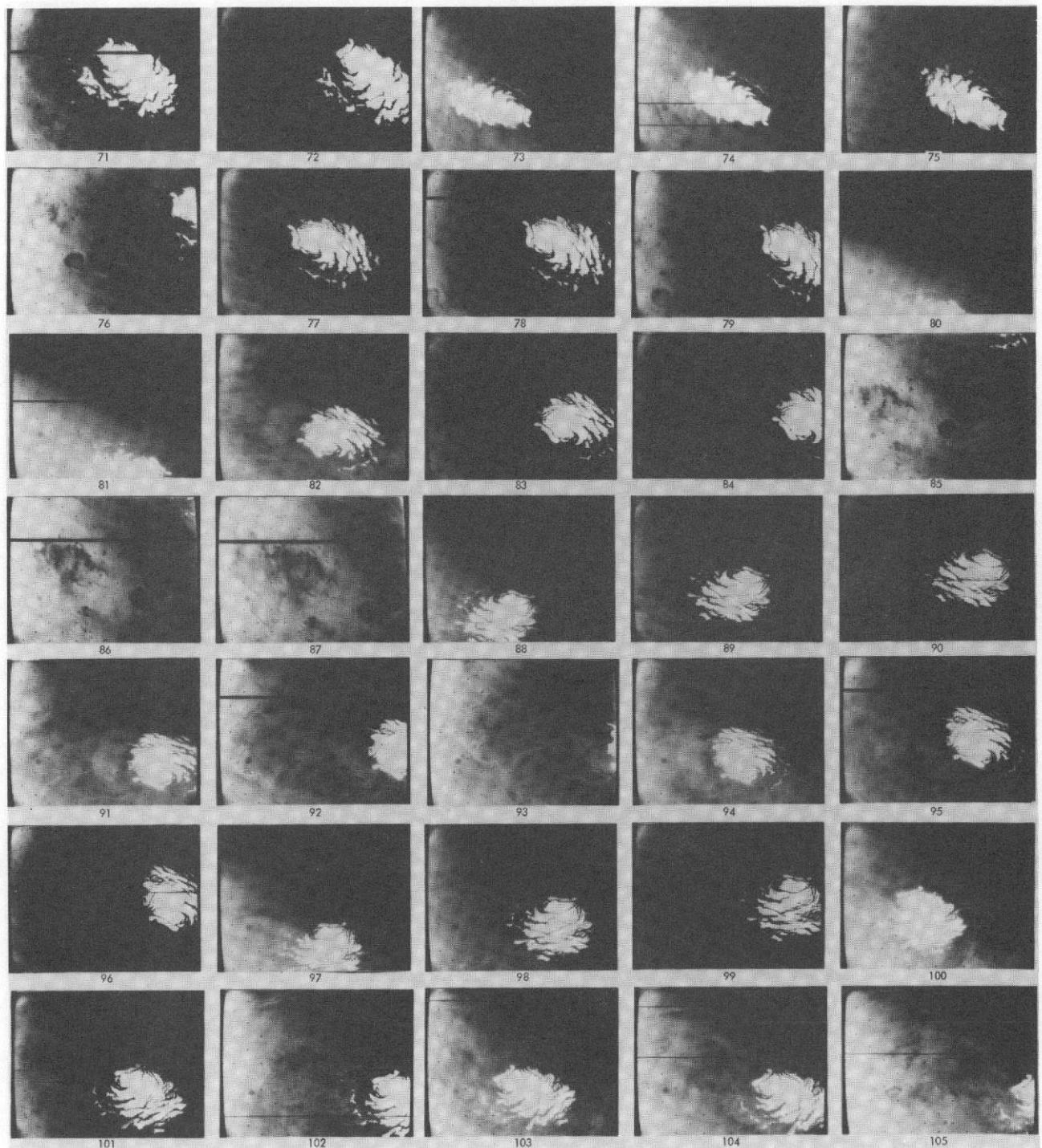


Fig. VIII-11c. Shading-corrected wide-angle frames showing the residual south polar cap (southern summer to early fall); distance less than 5000 km: index numbers 71-105.

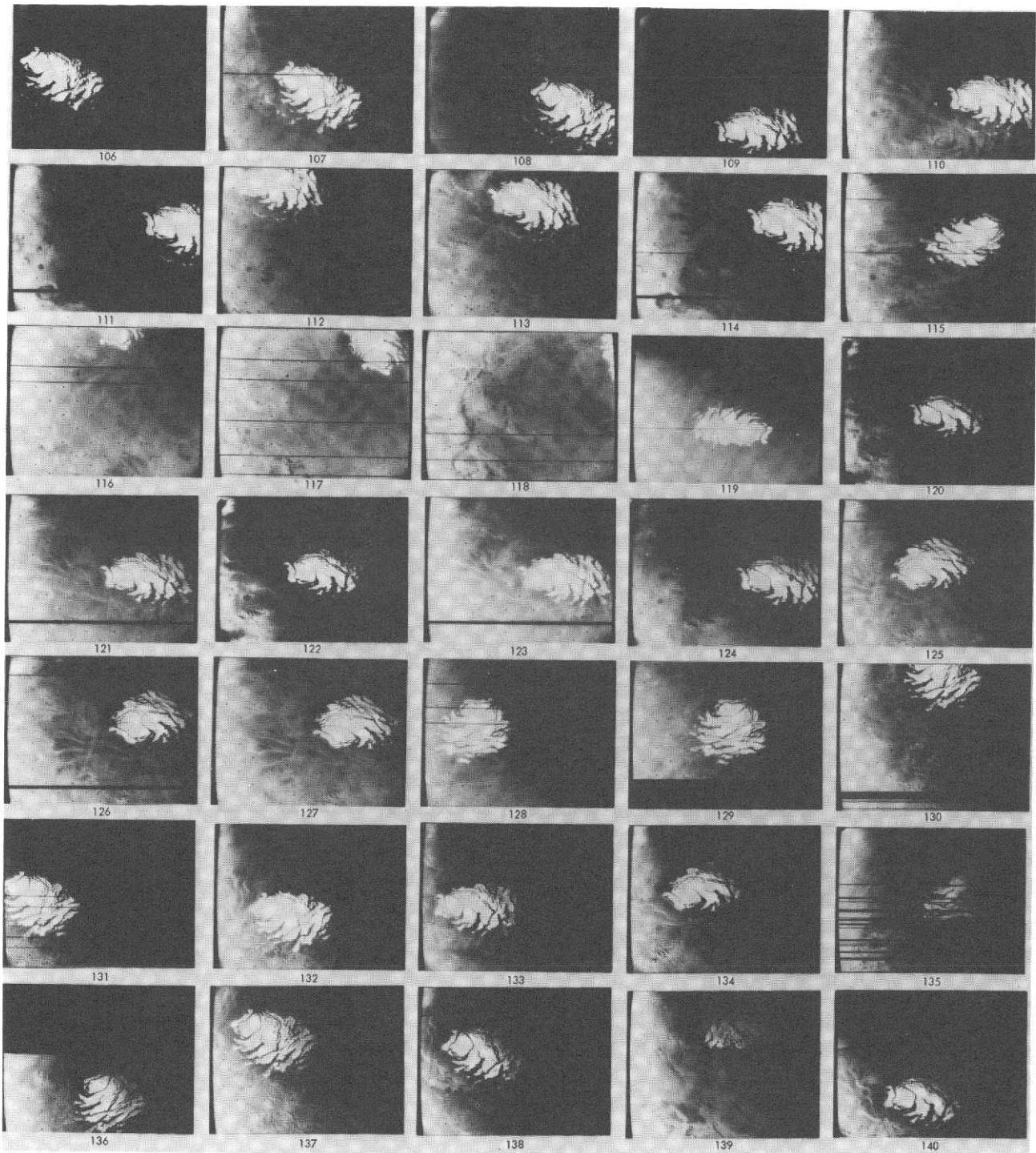


Fig. VIII-11d. Shading-corrected wide-angle frames showing the residual south polar cap (southern summer to early fall); distance less than 5000 km: index numbers 106-140.

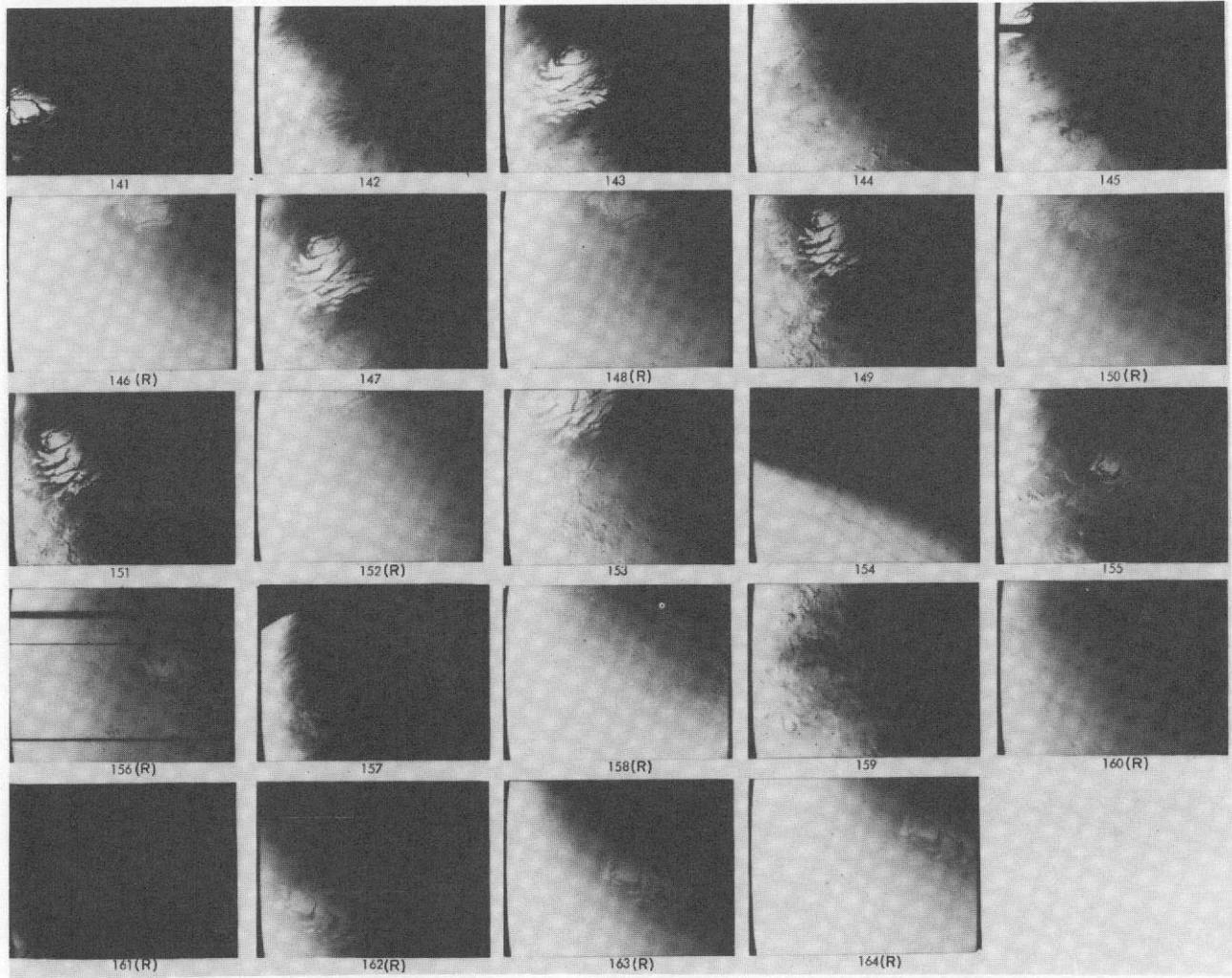
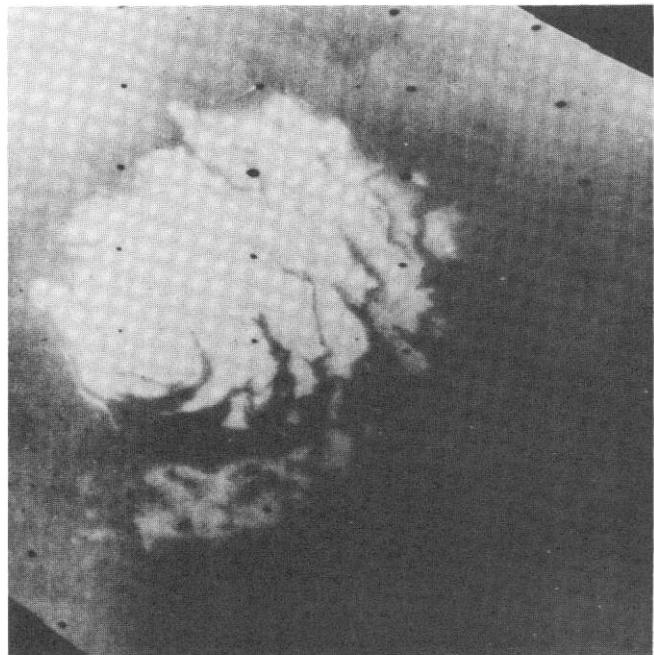
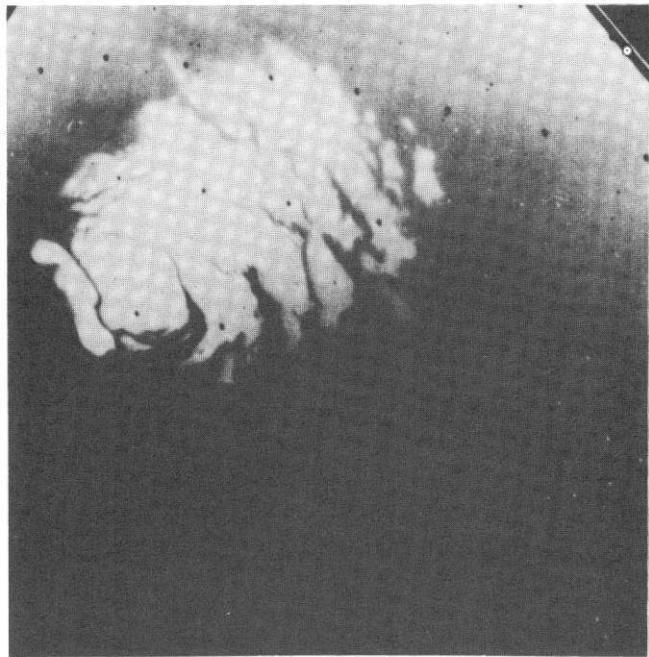


Fig. VIII-11e. Wide-angle frames showing the residual south polar cap (southern summer to early fall); distance less than 5000 km: index numbers 141-164. Most frames appear in the shading-corrected version. The raw version (R) is used where the cap is near the terminator and underexposed.



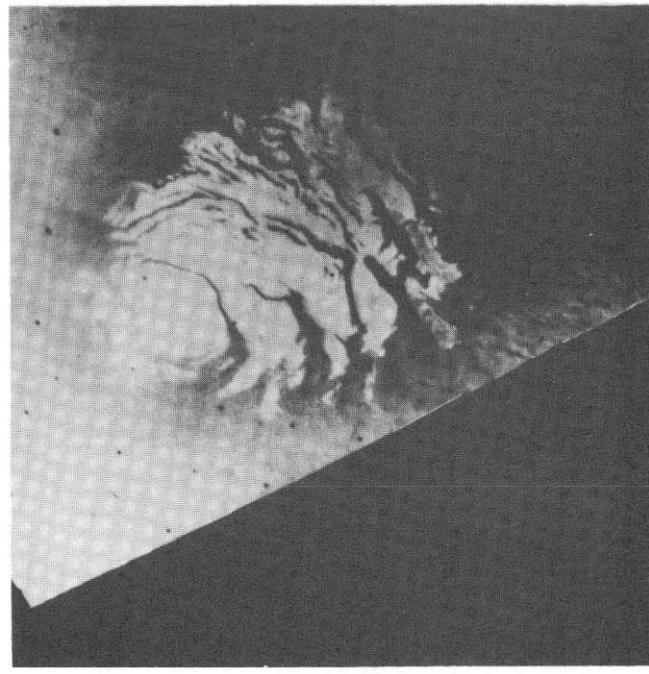
REV 28



REV 42



REV 72



REV 188

Fig. VIII-12. Stereographic projections of four wide-angle frames that show the retreat and stabilization of the south polar cap.

Table VIII-6. Wide-angle frames including the residual south polar cap during summer and early fall; distance less than 5000 km: Revs 1-262

Index number	Rev	Frame number	Center of picture			Lighting angle (SLAR-5), ^a deg	Viewing angle (VAR-5), ^a deg	North direction (NORAN) ^a	Sun direction (SUNAN) ^a	Subsolar latitude, deg	Subsolar longitude, deg	Filter	DAS time
			Latitude (LR-5), ^a deg	Longitude (LOR-5), ^a deg	Range (SRR-5), ^a km								
1	1	08	-76.01	48.58	3,080	55.69	52.19	161	184	-22.73	16.35	2	1,673,021
2	1	10	-78.52	22.01	2,828	55.84	46.84	176	181	-22.73	16.69	2	1,673,091
3	1	12	-78.15	353.69	2,618	56.48	42.26	201	177	-22.73	17.03	2	1,673,161
4	5	02	-78.43	78.89	3,311	61.74	56.33	144	183	-22.51	20.95	2	1,779,225
5	5	04	-82.62	49.07	3,064	61.01	51.26	159	180	-22.51	21.29	2	1,779,295
6	5	06	-83.07	2.67	2,826	60.96	47.15	199	178	-22.51	21.63	2	1,779,365
7	5	08	-80.13	331.10	2,638	61.50	43.66	242	175	-22.51	21.98	2	1,779,435
8	7	11	-80.08	4.30	3,589	57.71	34.09	166	140	-22.39	8.28	3	1,850,625
9	7	12	-79.84	4.01	3,445	57.48	32.90	152	146	-22.39	8.62	3	1,850,695
10	7	13	-79.66	7.28	3,190	57.27	32.14	162	159	-22.39	9.30	5	1,850,835
11	7	14	-79.50	9.44	3,081	57.11	32.73	165	165	-22.39	9.64	5	1,850,905
12	7	15	-79.80	10.16	2,998	57.40	34.73	169	170	-22.39	9.98	7	1,850,975
13	7	16	-80.04	12.02	2,933	57.65	37.53	172	174	-22.39	10.33	7	1,851,045
14	9	12	-71.10	87.90	6,704	71.21	52.71	4	131	-22.28	350.85	4	1,921,045
15	9	14	-73.21	87.83	6,598	70.60	53.23	3	129	-22.28	351.19	6	1,921,115
16	9	16	-76.21	89.09	6,525	70.16	54.65	128	-22.28	351.53	8	1,921,185	
17	9	18	-79.33	92.19	6,467	70.00	56.48	355	126	-22.28	351.87	2	1,921,255
18	9	20	-82.44	99.08	6,421	70.00	58.59	349	125	-22.28	352.21	4	1,921,325
19	9	22	-85.32	118.33	6,394	70.49	61.11	337	125	-22.28	352.55	6	1,921,395
20	9	24	-86.43	170.61	6,388	71.27	64.05	307	125	-22.28	352.89	8	1,921,465
21	9	26	-84.70	207.92	6,367	72.09	66.54	253	125	-22.28	353.23	2	1,921,535
22	9	28	-81.20	222.82	6,389	73.59	69.90	214	125	-22.28	353.57	4	1,921,605
23	9	30	-77.04	228.78	6,436	75.51	73.66	195	127	-22.28	353.91	6	1,921,675
24	9	32	-70.64	230.29	6,615	79.25	79.75	179	132	-22.28	354.25	8	1,921,745
25	11	02	-75.64	66.95	4,217	66.23	46.27	68	153	-22.16	346.35	2	1,994,125
26	11	04	-79.38	61.43	4,064	65.43	45.36	70	151	-22.16	346.69	4	1,994,195
27	11	06	-82.95	49.20	3,913	64.69	44.48	76	149	-22.16	347.03	6	1,994,265
28	11	08	-85.81	20.09	3,779	64.33	44.19	102	146	-22.16	347.37	8	1,994,335
29	11	10	-86.21	321.18	3,664	64.45	44.65	178	144	-22.16	347.71	2	1,994,405
30	11	12	-83.81	284.28	3,575	65.21	46.06	209	141	-22.16	348.05	4	1,994,475
31	16	12	-81.09	98.96	3,069	61.79	38.40	209	154	-21.86	142.18	2	2,174,165
32	18	11	-79.37	108.49	2,888	58.55	33.02	191	161	-21.73	131.56	2	2,245,985
33	20	10	-78.80	106.77	2,794	57.57	33.18	185	167	-21.60	120.95	2	2,317,805
34	24	22	-80.78	1.00	3,808	50.00	54.41	209	130	-21.34	97.68	2	2,461,025
35	24	24	-79.26	12.57	3,593	68.19	51.52	206	131	-21.34	98.02	4	2,461,095
36	24	26	-77.67	19.13	3,399	66.87	49.02	207	133	-21.34	98.36	6	2,461,165
37	25	19	-86.31	156.89	3,712	70.33	52.87	243	142	-21.28	272.37	2	2,496,935
38	25	21	-85.12	178.91	3,532	69.12	51.04	233	144	-21.28	272.71	4	2,497,005
39	25	23	-82.96	181.02	3,411	69.13	51.11	235	146	-21.28	273.05	6	2,497,075
40	26	22	-86.44	340.32	3,915	69.80	52.59	221	133	-21.21	86.39	2	2,532,705
41	26	24	-85.22	16.07	3,672	67.27	48.65	202	135	-21.21	5.73	4	2,532,775
42	26	26	-83.30	20.86	3,501	66.22	46.93	203	137	-21.21	87.07	6	2,532,845
43	27	19	-85.99	28.42	3,897	71.31	53.08	27	146	-21.14	261.08	2	2,568.615
44	27	21	-87.60	32.28	3,761	70.42	52.16	28	148	-21.14	261.42	4	2,568.685
45	27	23	-88.83	93.89	3,606	66.99	51.89	311	150	-21.14	261.76	6	2,568.755
46	28	22	-85.68	338.63	3,839	69.51	52.14	214	133	-21.07	75.78	2	2,604.525
47	28	24	-84.38	357.74	3,638	67.89	49.59	207	134	-21.07	76.12	4	2,604.595
48	28	26	-82.74	5.21	3,461	66.75	47.66	206	136	-21.07	76.46	6	2,604.664
49	29	17	-82.18	13.27	4,054	73.39	55.39	34	148	-21.01	250.13	2	2,640.365
50	29	19	-84.45	3.65	3,843	71.25	52.81	44	150	-21.01	250.47	4	2,640.435
51	29	21	-86.99	3.14	3,681	70.15	51.68	48	152	-21.01	250.82	6	2,640.505
52	30	22	-84.53	9.18	3,665	66.07	46.89	187	132	-20.94	65.17	2	2,676.345
53	30	24	-82.74	13.53	3,480	64.70	44.51	188	134	-20.94	65.51	4	2,676.415
54	30	26	-82.11	27.45	3,267	62.97	40.56	186	141	-20.94	65.85	6	2,676.485
55	31	19	-83.38	329.22	3,843	69.23	48.75	54	147	-20.87	239.53	2	2,712.185
56	31	21	-84.84	315.09	3,675	67.89	47.25	68	150	-20.87	239.87	4	2,712.255
57	31	23	-86.24	294.35	3,525	66.96	46.30	88	152	-20.87	240.21	6	2,712.325
58	32	22	-85.80	359.41	3,695	66.84	47.55	188	133	-20.80	54.57	2	2,748.165
59	32	24	-83.45	9.77	3,479	64.66	44.00	183	135	-20.80	54.91	4	2,748.235
60	32	26	-81.80	8.66	3,316	63.70	42.23	188	137	-20.80	55.25	6	2,748.305
61	33	19	-84.93	77.18	4,015	73.76	57.39	267	135	-20.73	229.27	2	2,784.075
62	33	21	-86.21	116.22	3,752	70.81	53.26	231	136	-20.73	229.61	4	2,784.145
63	33	23	-84.87	146.26	3,541	68.79	50.36	216	138	-20.73	229.95	6	2,784.215
64	34	22	-84.71	343.96	3,766	66.77	48.29	185	130	-20.65	43.97	2	2,819.985
65	34	24	-82.27	358.79	3,525	64.03	43.81	178	131	-20.65	44.31	4	2,820.055
66	34	26	-79.97	.20	3,337	62.37	40.99	180	133	-20.65	44.65	6	2,820.125
67	36	22	-85.08	353.56	3,653	65.76	45.64	174	132	-20.51	33.71	2	2,891.075
68	36	24	-82.40	.38	3,427	63.22	41.43	171	134	-20.51	34.05	4	2,891.945
69	36	26	-80.58	357.60	3,260	62.06	39.37	178	136	-20.51	34.39	6	2,892.015
70	38	22	-86.77	42.95	3,744	68.59	45.06	107	135	-20.36	23.11	2	2,963.695
71	38	24	-84.39	22.01	3,524	64.02	41.12	139	137	-20.36	23.45	6	2,963.765
72	38	26	-82.55	13.82	3,346	62.39	38.57	155	139	-20.36	23.79	6	2,963.835
73	41	18	-82.49	18.50	4,158	77.23	61.18	297	137	-20.14	187.92	2	3,071.570
74	41	20	-85.04	39.95	3,888	74.09	57.21	263	136	-20.14	188.26	4	3,071.640
75	41	22	-85.68	74.85	3,655	71.64	53.98	232	137	-20.14	188.60	6	3,071.710
76	44	22	-79.31	340.10	3,464	59.65	35.45	145	132	-19.91	352.37	2	3,179.370
77	46	22	-86.77	14.28	3,610	67.51	45.01	94	139	-19.76	342.12	2	3,251.260
78	46	24	-84.84	348.01	3,403	65.10	41.48	133	140	-19.76	342.46	2	3,251.330
79	46	26	-83.22	335.05	3,232	63.52	39.20	152	142	-19.76	342.81	2	3,251.400
80	49	19	-74.73	352.85	4,408	84.25	71.13	252	139	-19.53	146.58	2	3,359.060
81	49	21	-78.23	8.78	4,035	79.38	65.43	234	135	-19.53	146.92	2	3,359.130
82	52	22	-88.88	126.37	3,871	71.82	51.62	319	134	-19.29	310.03	2	3,466.650
83	52	24	-87.38	293.4									

Table VIII-6. (contd)

Center of picture												Filter	DAS time
Index number	Rev	Frame number	Latitude (LR-5), deg	Longitude (LOR-5), deg	Range (SRR-5), km	Lighting angle (SLAR-5), deg	Viewing angle (VAR-5), deg	North direction (NORAN), deg	Sun direction (SUNAN), deg	Subsolar latitude, deg	Subsolar longitude, deg		
91	56	22	-87.31	178.30	3,842	71.97	52.71	217	132	-18.97	288.53	2	3,610,220
92	56	24	-85.72	236.33	3,575	68.46	47.78	182	132	-18.97	288.87	4	3,610,290
93	56	26	-83.20	247.80	3,359	66.00	44.17	177	134	-18.97	289.21	6	3,610,360
94	58	22	-87.05	93.19	3,899	74.12	54.10	322	136	-18.80	277.61	2	3,681,970
95	58	24	-89.11	274.35	3,610	70.30	48.62	141	136	-18.80	277.95	4	3,682,040
96	58	26	-86.15	265.13	3,380	67.44	44.48	154	137	-18.80	278.29	6	3,682,110
97	59	18	-82.70	329.50	4,148	75.29	59.39	219	131	-18.72	91.98	2	3,717,810
98	59	20	-84.11	10.10	3,793	70.58	52.61	192	129	-18.72	92.32	4	3,717,880
99	59	22	-82.55	37.84	3,516	67.10	47.27	178	129	-18.72	92.66	6	3,717,950
100	65	19	-89.17	357.89	3,856	71.38	50.10	182	132	-18.22	59.58	2	3,933,130
101	65	21	-85.27	346.20	3,764	70.51	51.33	187	130	-18.22	59.92	4	3,933,200
102	65	23	-81.29	343.37	3,690	70.01	53.09	186	128	-18.22	60.26	6	3,933,270
103	69	19	-88.10	318.81	3,888	71.78	51.19	192	132	-17.88	38.45	2	4,076,770
104	69	21	-84.20	323.89	3,793	70.70	52.28	185	130	-17.88	38.79	2	4,076,840
105	69	23	-80.22	321.66	3,728	70.26	54.32	184	128	-17.87	39.13	2	4,076,910
106	71	19	-86.02	114.24	3,707	72.06	47.26	35	138	-17.70	28.22	8	4,148,660
107	71	21	-88.16	39.15	3,579	70.48	47.19	121	135	-17.70	28.56	2	4,148,730
108	71	23	-85.39	341.17	3,467	69.23	47.66	177	133	-17.70	28.91	4	4,148,800
109	79	19	-87.15	216.61	3,964	74.85	54.41	239	134	-18.99	347.01	8	4,436,150
110	79	21	-86.43	323.94	3,612	69.73	46.69	155	133	-16.99	347.35	2	4,436,220
111	79	23	-82.85	337.24	3,344	65.98	40.67	145	133	-16.99	347.69	4	4,436,290
112	81	19	-80.79	42.39	3,512	69.58	38.82	61	141	-16.81	336.80	2	4,508,040
113	81	21	-82.73	17.33	3,381	67.70	38.43	87	139	-16.81	337.14	2	4,508,110
114	81	23	-82.89	346.79	3,264	66.13	38.70	127	136	-16.81	337.48	2	4,508,180
115	88	02	-85.09	73.70	3,652	70.48	48.82	169	131	-16.17	120.22	2	4,759,480
116	97	10	-81.49	310.02	3,386	70.07	39.56	77	145	-15.33	253.78	2	5,058,373
117	97	12	-82.26	279.13	3,242	67.68	37.88	110	143	-15.33	254.12	2	5,058,443
118	97	14	-80.91	250.92	3,114	65.60	36.79	145	140	-15.33	254.46	2	5,058,513
119	109	07	-85.30	49.02	4,176	79.64	56.41	268	139	-14.17	192.98	8	5,489,783
120	109	08	-84.34	46.21	4,108	80.59	57.91	270	140	-14.17	193.32	2	5,489,853
121	109	10	-83.50	69.21	4,015	79.65	58.67	231	139	-14.17	193.66	4	5,489,923
122	116	06	-86.89	18.16	3,734	74.10	44.42	88	137	-13.47	339.55	2	5,741,853
123	116	08	-86.70	336.67	3,643	73.22	45.38	140	137	-13.47	339.89	2	5,741,923
124	116	10	-85.75	330.36	3,514	72.34	44.77	147	137	-13.47	340.23	2	5,741,993
125	124	06	-85.86	22.40	3,743	76.77	44.67	39	140	-12.67	300.56	5	6,029,763
126	124	08	-86.26	319.94	3,634	73.79	43.70	115	138	-12.67	300.99	5	6,029,833
127	124	10	-86.49	324.91	3,505	76.12	44.31	108	139	-12.67	301.24	5	6,029,903
128	133	09	-87.49	136.97	3,702	77.05	45.62	59	140	-11.76	75.31	5	6,353,373
129	133	11	-88.14	64.69	3,587	74.45	45.60	148	137	-11.76	75.65	5	6,353,443
130	141	04	-80.57	66.84	3,492	71.13	34.01	103	138	-10.93	346.67	5	6,640,933
131	141	05	-86.03	139.20	3,673	80.05	47.17	21	143	-10.93	35.01	5	6,641,003
132	145	03	-88.29	100.76	3,849	79.36	47.26	33	141	-10.52	14.70	5	6,784,782
133	151	02	-85.33	87.77	3,812	81.11	45.15	22	143	-9.89	345.61	5	7,000,733
134	159	03	-84.64	35.44	3,687	80.79	42.80	37	143	-9.05	307.40	5	7,288,783
135	168	02	-84.81	51.85	3,923	77.44	49.69	160	139	-8.10	82.62	5	7,612,463
136	176	02	-85.82	316.89	4,068	82.41	54.61	203	143	-7.25	42.09	5	7,900,023
137	180	03	-86.24	85.25	3,402	80.53	40.81	67	143	-6.83	22.85	5	8,046,013
138	184	03	-85.12	73.60	3,479	81.99	42.37	58	144	-6.40	2.96	5	8,187,869
139	187	03	-87.41	174.76	3,633	81.34	47.11	137	143	-6.08	168.28	5	8,295,809
140	188	03	-89.01	148.84	3,651	84.97	50.89	337	145	-5.97	343.73	5	8,331,859
141	196	03	-82.80	69.90	3,613	88.98	46.98	10	148	-5.12	305.29	5	8,619,839
142	206	03	-86.72	321.39	3,493	84.56	44.79	68	145	-4.05	256.40	5	8,979,639
143	207	05	-87.70	130.61	3,592	84.88	46.04	78	145	-3.95	71.18	5	9,015,549
144	208	03	-82.80	308.55	3,179	82.75	39.99	70	145	-3.84	246.97	5	9,051,669
145	209	04	-80.06	143.21	3,343	84.96	36.49	53	147	-3.74	74.6	5	9,087,439
146	210	05	-82.79	295.15	3,349	82.78	37.77	78	145	-3.63	236.18	5	9,123,419
147	211	03	-85.96	108.35	3,516	84.30	43.12	83	145	-3.52	50.95	5	9,159,329
148	212	05	-82.98	293.22	3,351	83.88	38.32	69	145	-3.42	226.05	5	9,195,309
149	213	03	-83.35	90.05	3,413	82.36	38.95	94	144	-3.31	40.84	5	9,231,219
150	214	05	-84.38	295.25	3,410	85.76	41.41	53	147	-3.20	215.95	5	9,267,199
151	215	03	-84.36	98.08	3,443	84.74	40.44	70	146	-3.10	30.73	5	9,303,109
152	216	03	-81.62	288.79	3,330	86.00	37.37	51	147	-2.99	205.84	5	9,339,089
153	217	05	-79.99	86.68	3,303	83.10	32.50	74	146	-2.89	20.62	5	9,374,999
154	218	04	-85.22	65.17	3,672	91.48	79.99	228	154	-2.78	199.48	5	9,411,749
155	223	01	-85.64	21.85	3,635	84.01	44.24	119	145	-2.25	350.64	5	9,590,739
156	231	02	-85.25	327.41	3,657	84.01	45.88	134	145	-1.40	312.26	5	9,878,719
157	234	02	-85.18	354.24	4,330	91.50	56.27	284	151	-1.09	116.94	5	9,986,519
158	239	05	-82.04	310.69	2,909	82.87	46.16	101	144	-0.56	276.29	5	10,167,189
159	241	02	-64.34	328.90	2,572	78.09	27.91	89	152	-3.35	266.53	5	10,239,149
160	260	02	-81.15	33.79	2,996	85.18	39.38	102	146	1.61	350.45	5	10,648,554
161	262	02	-80.73	155.71	3,638	101.06	62.81	353	170	1.82	340.70	5	10,720,514
162	262	04	-86.89	132.73	3,349	94.55	57.57	2	163	1.82	341.04	5	10,720,584
163	262	06	-86.45	9.47	3,118	88.69	53.38	127	158	1.82	341.38	5	10,720,654
164	262	08	-81.57	1.55	2,897	83.89	48.82	134	154	1.82	341.72	5	10,720,724

^a Terms are defined in Fig. III-15.

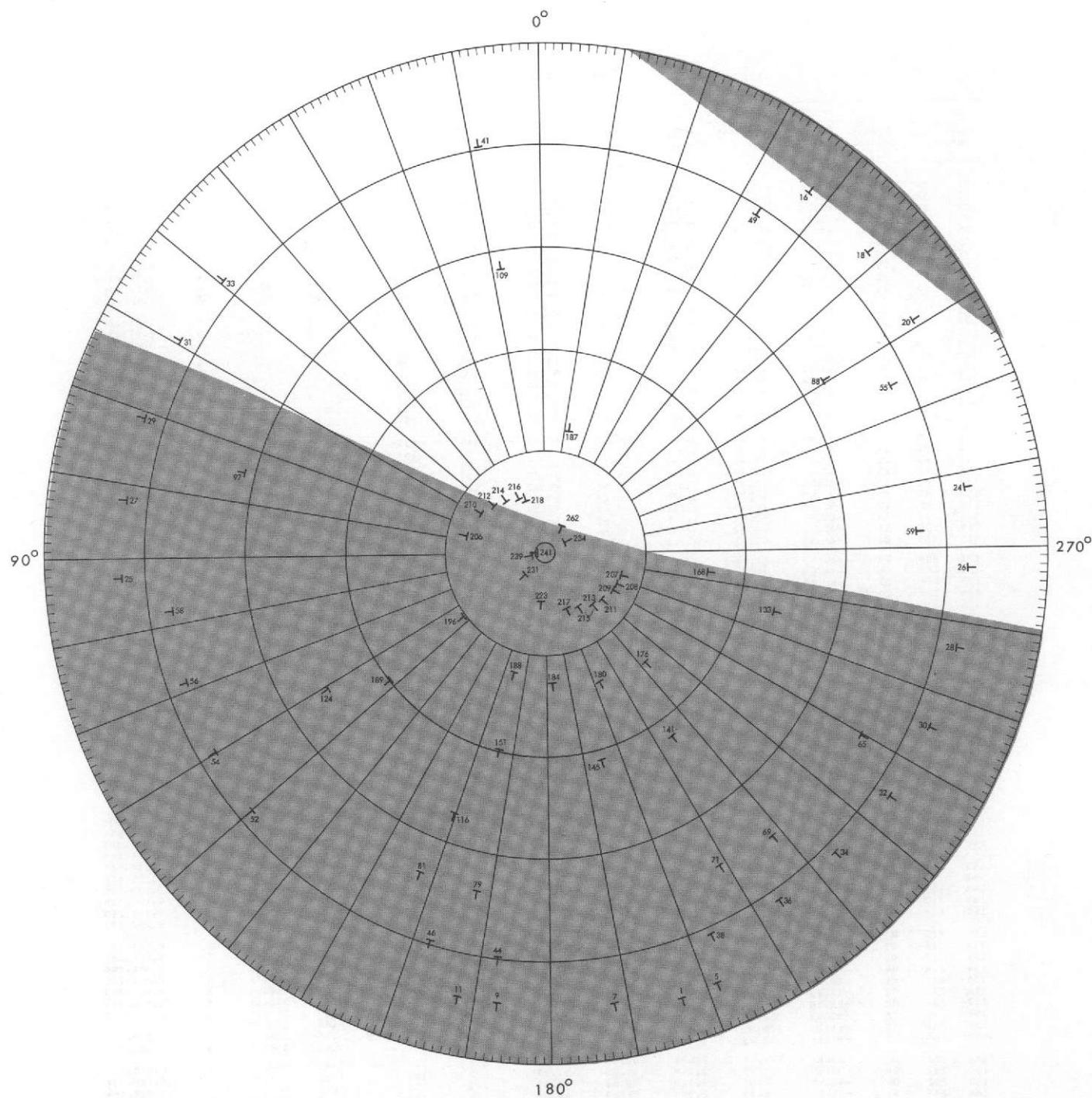


Fig. VIII-13. Variations in lighting conditions of the south polar cap for pictures taken during Revs 1-262. The junction of morning and evening terminators is plotted for the time at which the first polar cap picture was taken on a specific revolution. Locations are shown by the symbol T. The crossing of the T is aligned with the terminator, and the stem appears on the night side. The entire terminator is drawn for Revs 16 and 262.

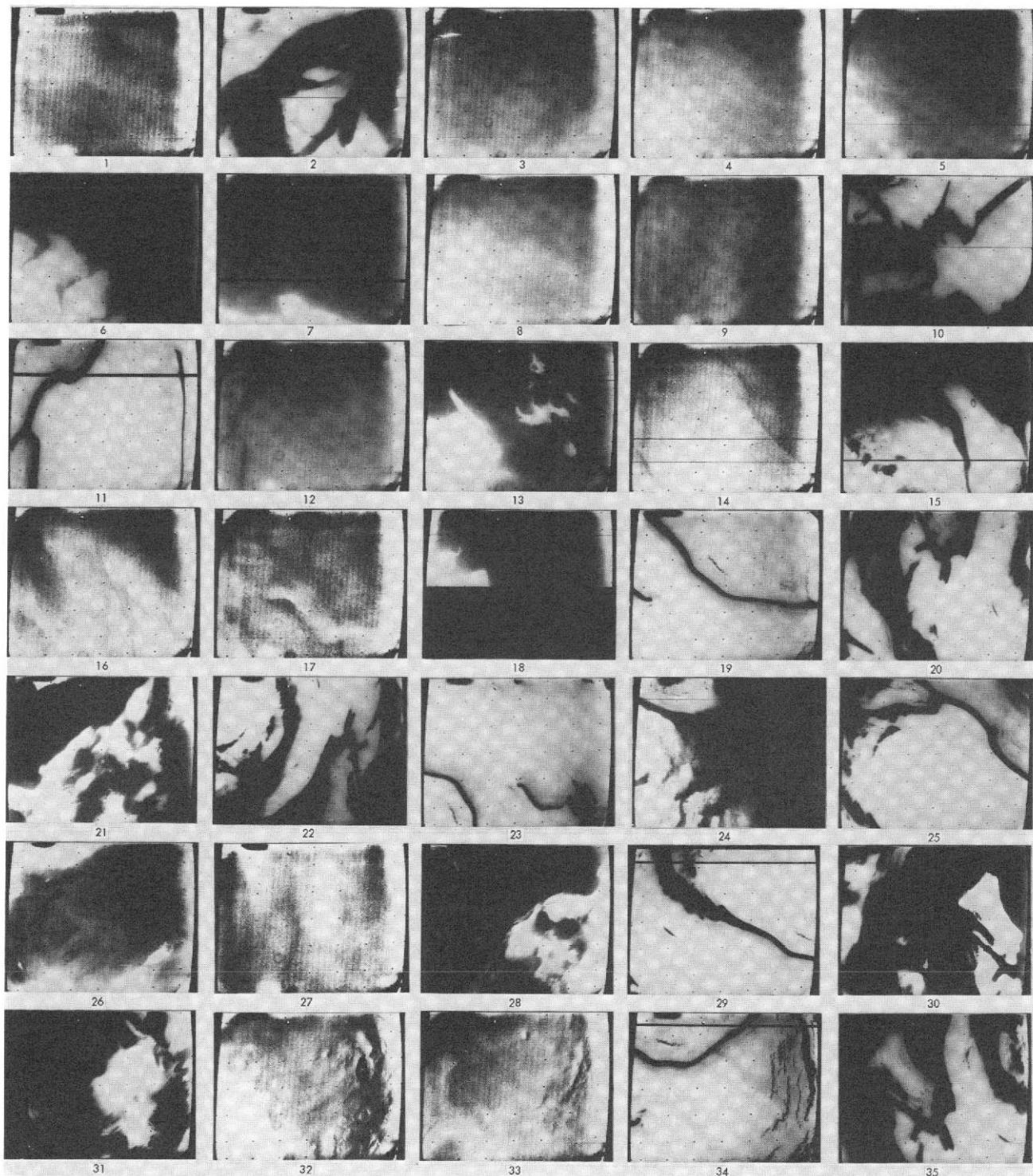


Fig. VIII-14a. Shading-corrected narrow-angle pictures of the residual south polar cap during Revs 1-262: index numbers 1-35.

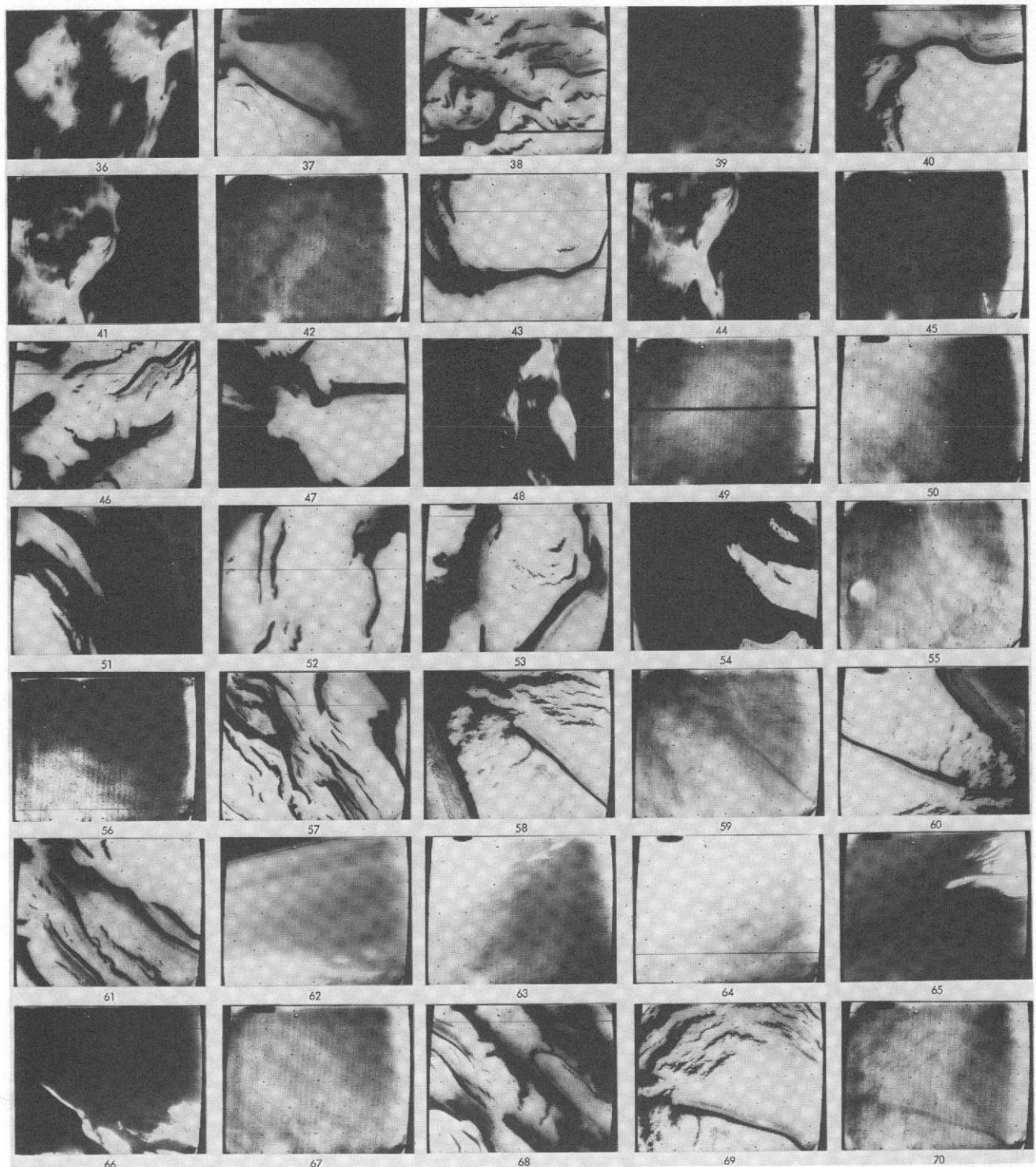


Fig. VIII-14b. Shading-corrected narrow-angle pictures of the residual south polar cap during Revs 1-262: index numbers 36-70.

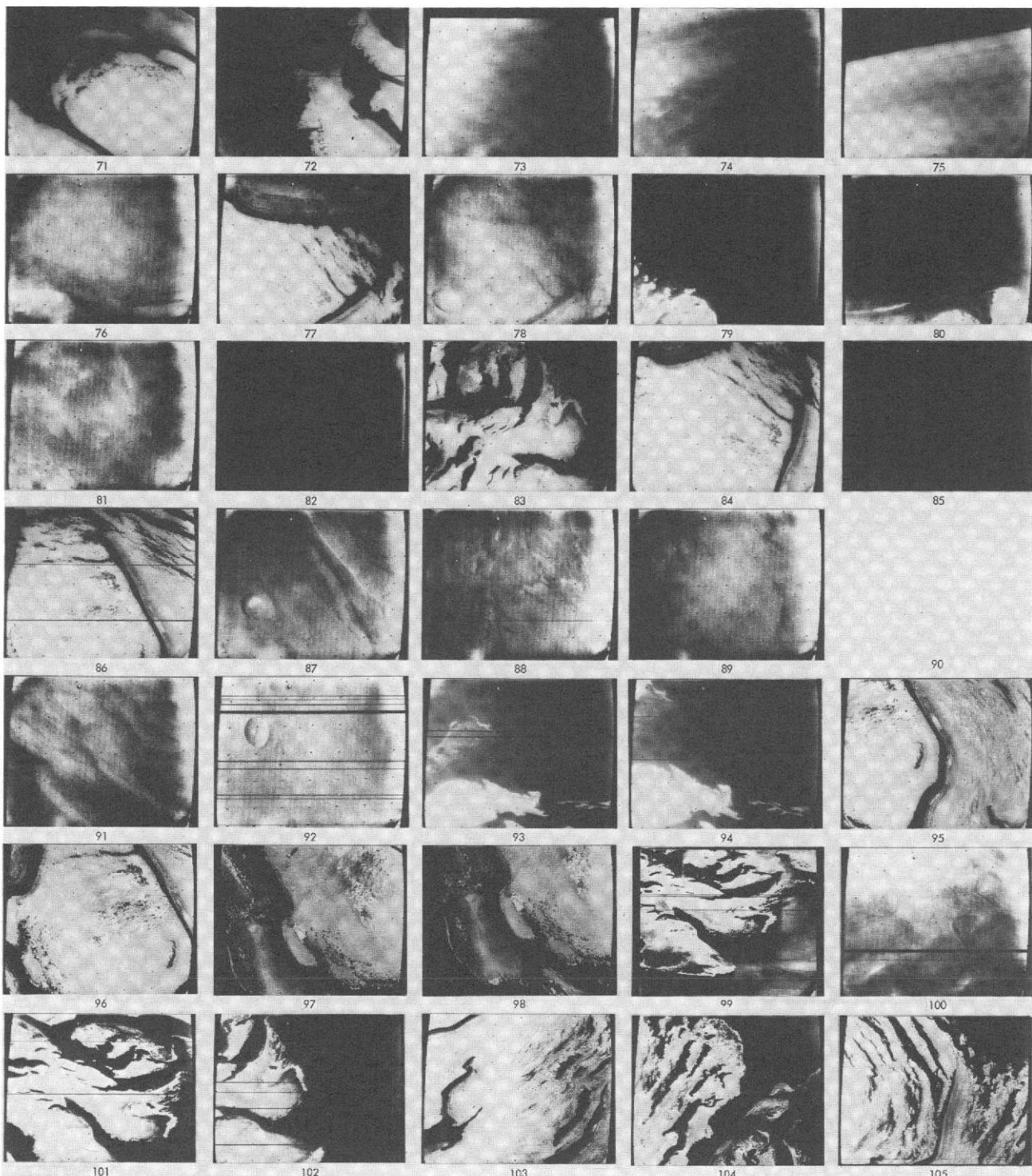


Fig. VIII-14c. Shading-corrected narrow-angle pictures of the residual south polar cap during Revs 1-262: index numbers 71-105. Blanks denote pictures planned but not recovered.

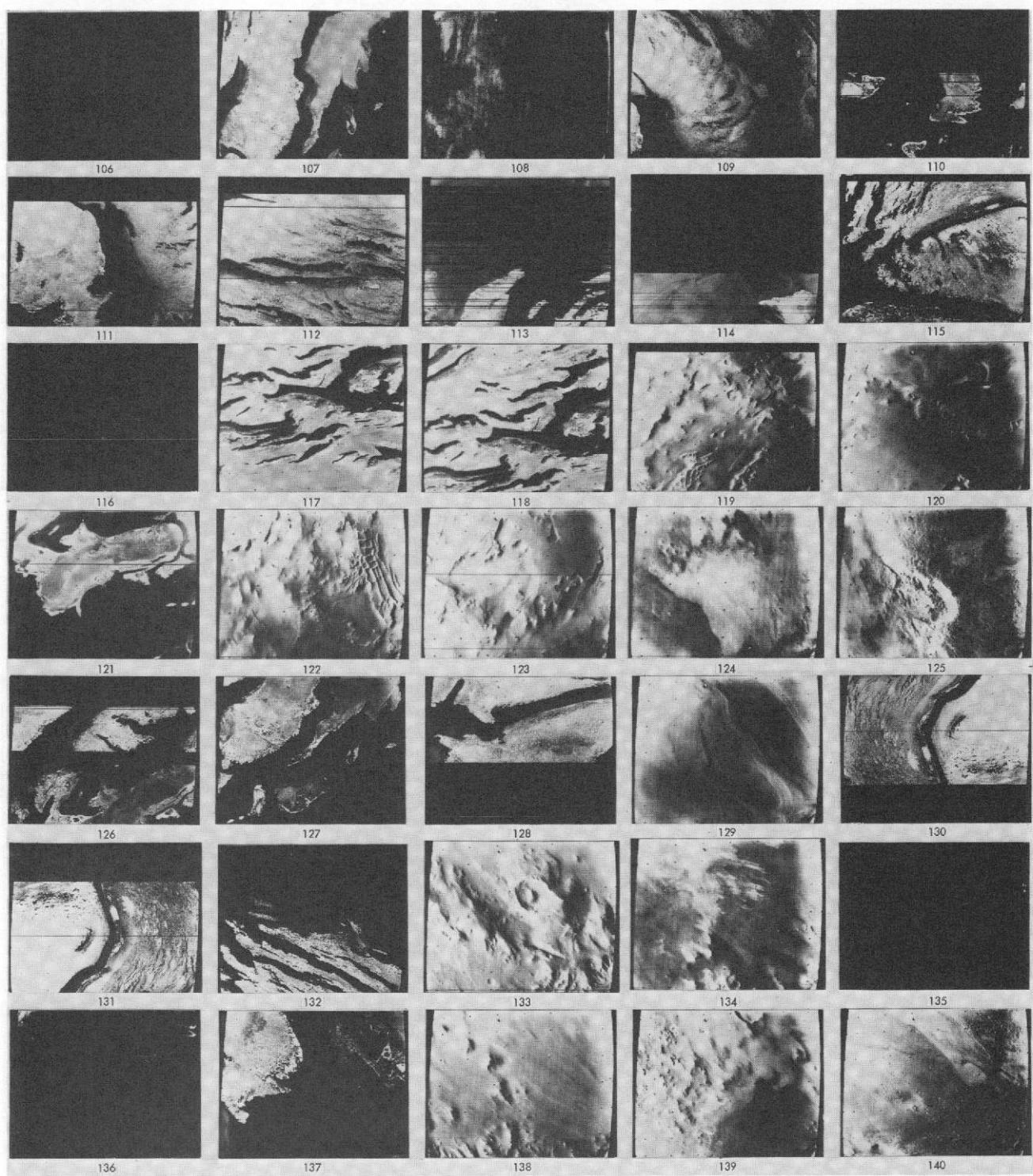


Fig. VIII-14d. Shading-corrected narrow-angle pictures of the residual south polar cap during Revs 1-262: index numbers 106-140. Images with little detail may have been underexposed (see histograms in original data and Section IV).

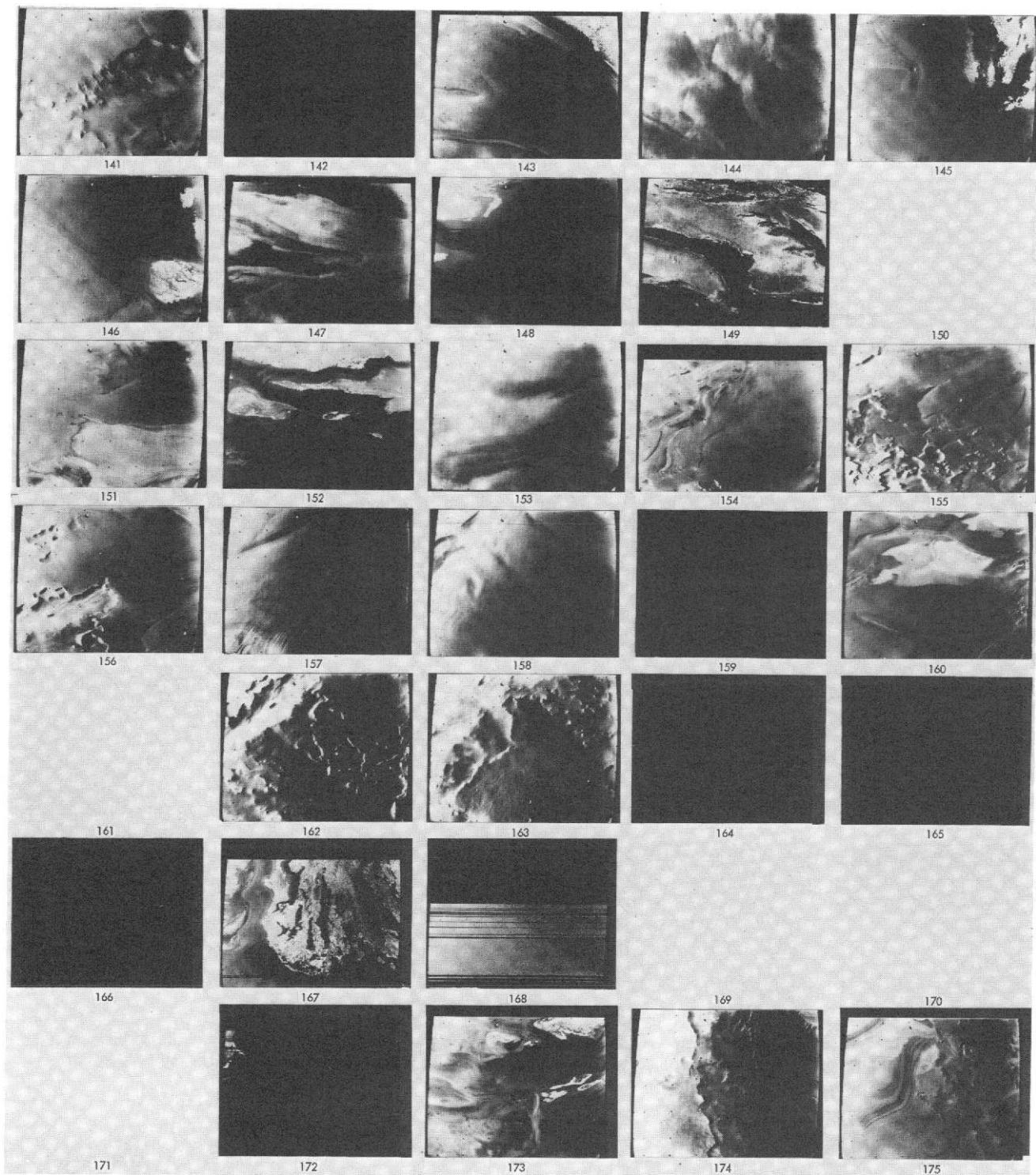


Fig. VIII-14e. Shading-corrected narrow-angle pictures of the residual south polar cap during Revs 1-262: index numbers 141-175. Images with little detail may have been underexposed (see histograms in original data and Section IV). Blanks denote pictures planned but not recovered.

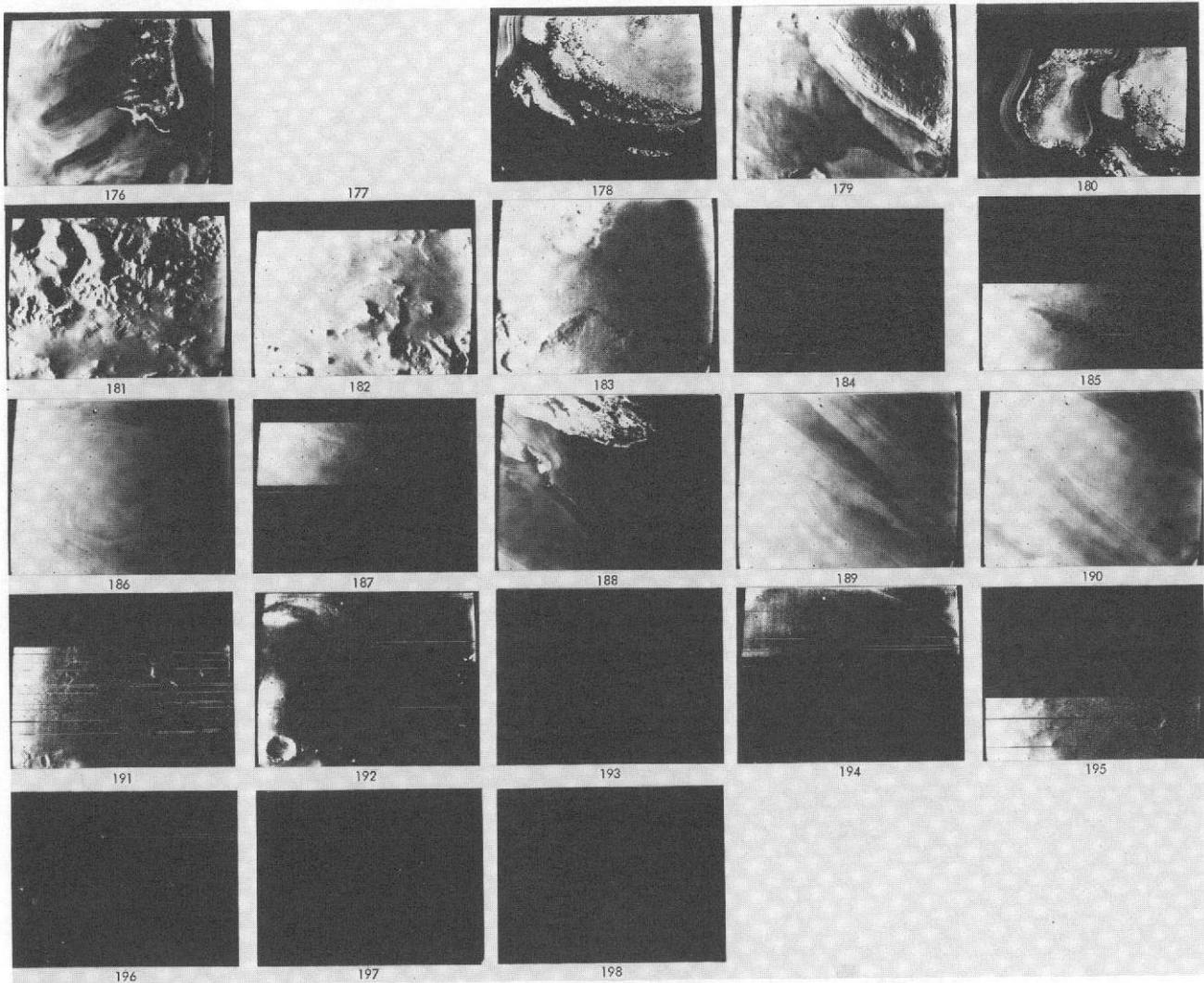
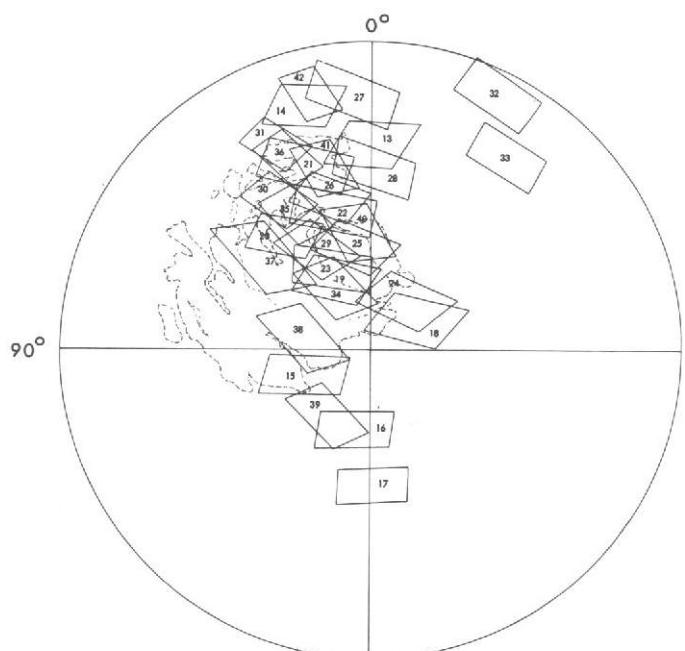
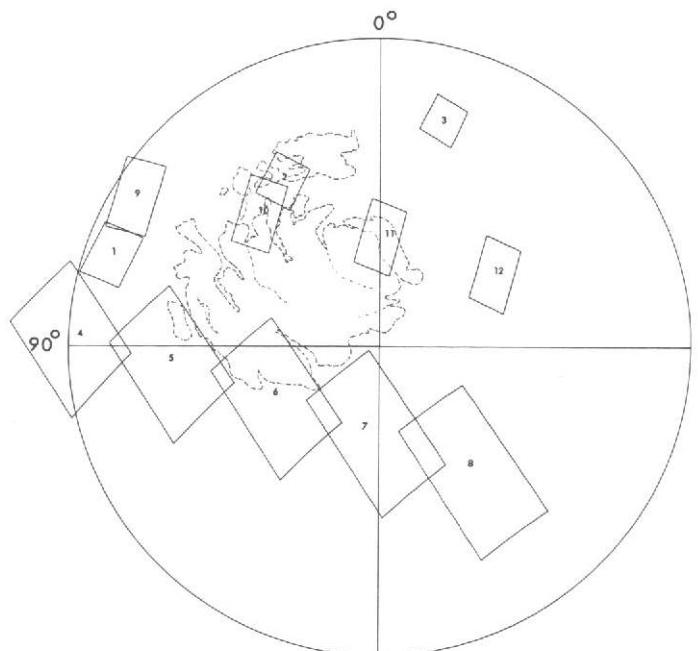
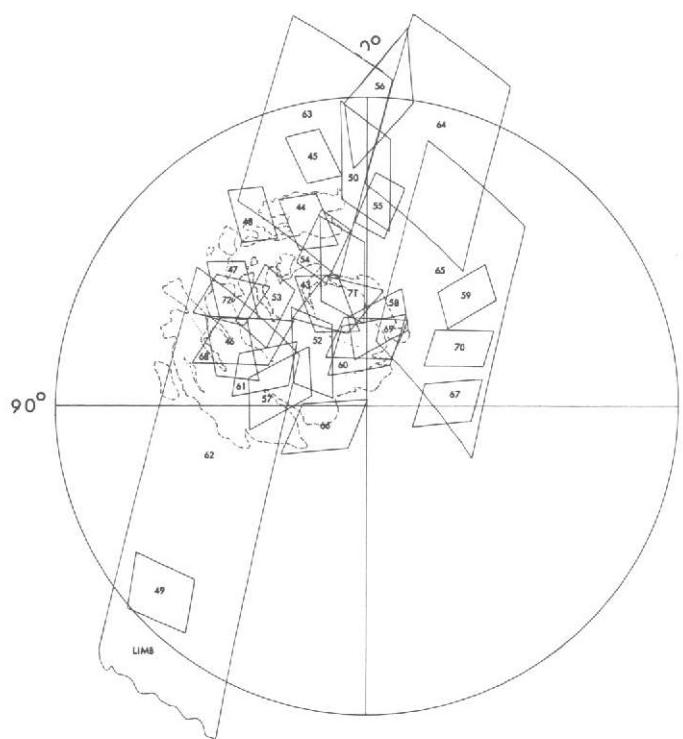


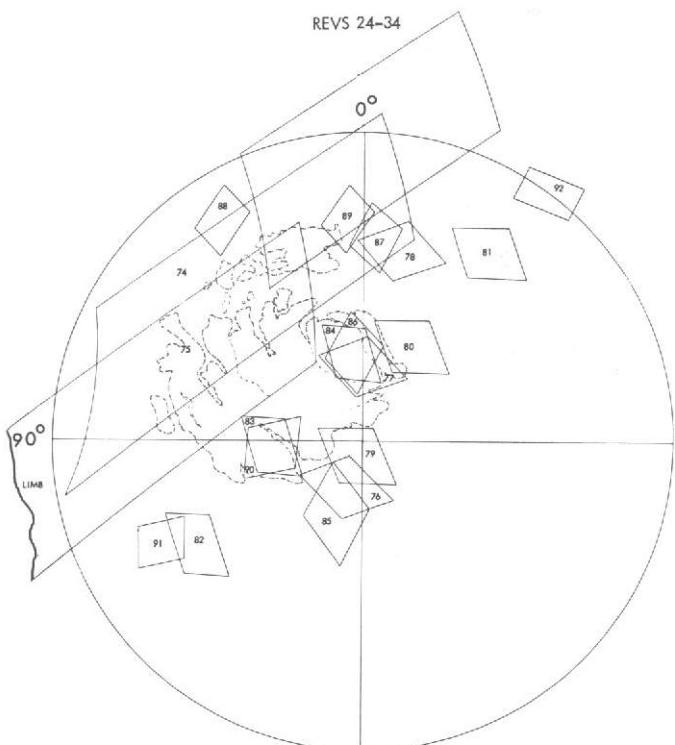
Fig. VIII-14f. Shading-corrected narrow-angle pictures of the residual south polar cap during Revs 1-262: index numbers 176-200. Images with little detail may have been underexposed (see histograms in original data and Section IV). Blanks denote pictures planned but not recovered.



REVS 1-23

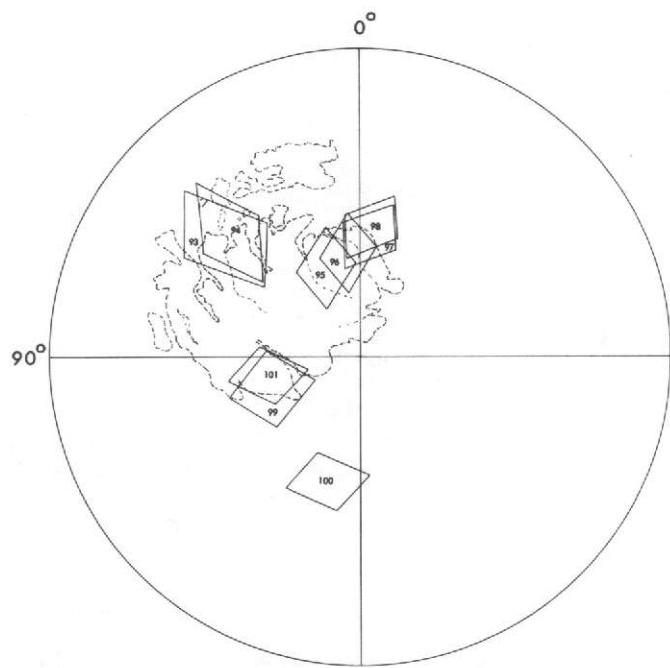


REVS 35-63

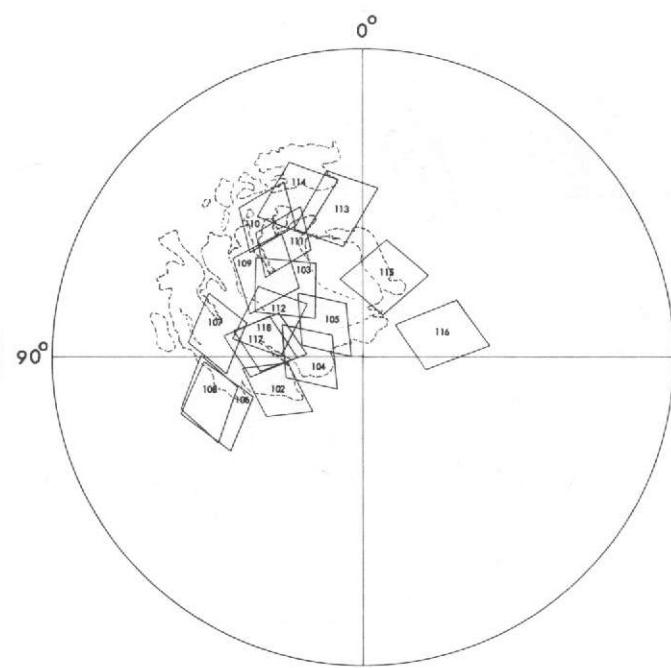


REVS 64-99

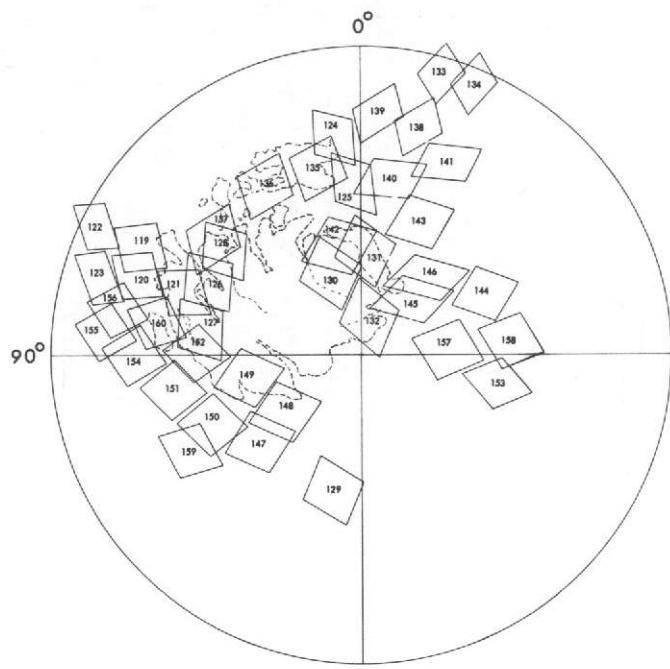
Fig. VIII-15. Footprint plots of narrow-angle pictures in the vicinity of the south polar cap corresponding to pictures in Fig. VIII-14. Frames with centers that fall in the area 85°S to 90°S, 0°W to 360°W and 80°S to 85°S, 315°W to 135°W are displayed. Observations are divided into eight periods for easy identification of the same areas taken on different dates, e.g., Revs 1-23, etc.



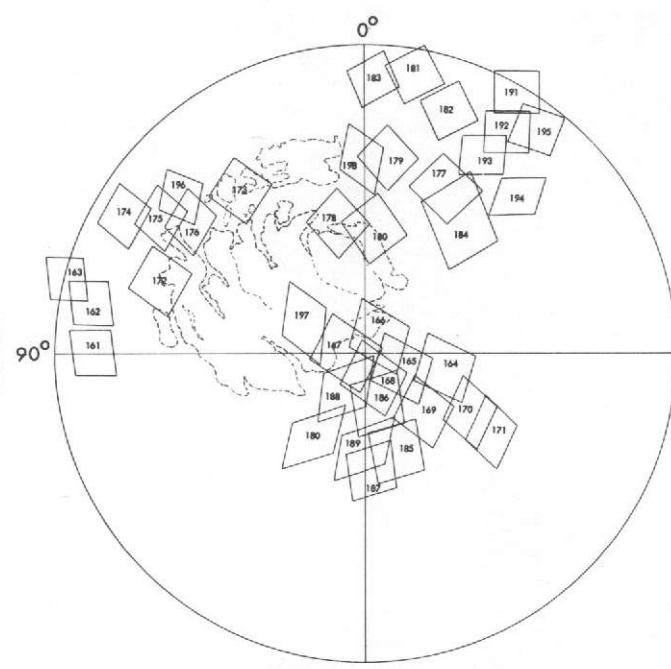
REVS 100-138



REVS 139-178



REVS 179-217



REVS 218-262

Fig. VIII-15. (contd.).

Table VIII-7. Narrow-angle frames in the vicinity of the south polar cap: Revs 1-262 (See Fig. VIII-14)

Index number	Rev	Frame number	Center of picture		Range (SRR-5), km	Lighting angle (SLAR-5), deg	Viewing angle (VAR-5), deg	North direction (NORAN) ^a	Sun direction (SUNAN) ^a	DAS time
Revs 1 - 23										
1	5	C3	-80° 29'	70° 40'	3,202	61.80	54.73	177	212	1,779,260
2	5	05	-83° 78'	30° 16'	2,957	61.35	50.15	202	209	1,779,330
3	5	C7	-82° 37'	34° 30'	2,750	61.52	46.27	253	206	1,779,400
4	9	15	-80° 04'	48° 09'	6,374	69.10	55.71	28	156	1,921,290
5	9	21	-83° 24'	34° 03'	6,326	69.22	57.89	22	155	1,921,360
6	9	23	-82° 26'	114° 58'	6,304	69.71	60.49	8	154	1,921,430
7	9	25	-87° 31'	176° 07'	6,261	70.39	63.07	331	154	1,921,500
8	9	27	-85° 14'	216° 54'	6,261	71.27	65.65	261	153	1,921,570
9	11	C5	-80° 77'	59° 15'	3,992	65.16	45.09	101	180	1,994,230
10	11	C7	-84° 20'	41° 92'	3,848	64.57	44.41	112	178	1,994,300
11	11	09	-86° 43'	359° 59'	3,718	64.35	44.30	158	175	1,994,370
12	11	11	-85° 59'	332° 37'	3,615	64.78	45.18	226	173	1,994,440
Revs 24 - 34										
13	24	21	-83° 35'	1° 38'	3,933	69.62	53.17	242	161	2,460,990
14	24	23	-81° 79'	15° 60'	3,620	67.77	50.28	237	162	2,461,060
15	25	18	-87° 77'	111° 70'	3,786	70.81	53.22	322	173	2,496,900
16	25	20	-87° 37'	169° 84'	3,597	69.31	51.13	270	175	2,496,970
17	25	22	-85° 59'	181° 51'	3,457	68.88	50.58	267	177	2,497,040
18	26	21	-88° 30'	303° 54'	3,973	70.12	52.40	287	165	2,532,670
19	26	23	-87° 46'	27° 00'	3,730	67.51	48.46	227	166	2,532,740
20	26	25	-85° 35'	37° 47'	3,533	65.81	45.73	222	168	2,532,810
21	27	18	-83° 71'	19° 22'	3,978	71.92	53.63	66	177	2,568,580
22	27	20	-85° 38'	14° 68'	3,811	70.74	52.37	73	179	2,568,650
23	27	22	-87° 14'	24° 82'	3,685	70.43	52.41	70	181	2,568,720
24	28	21	-88° 09'	325° 42'	3,885	69.58	51.52	256	164	2,604,490
25	28	23	-86° 62'	9° 31'	3,673	67.61	48.56	231	165	2,604,560
26	28	25	-86° 88'	15° 53'	3,500	66.49	46.76	231	167	2,604,630
27	29	18	-81° 74'	3° 39'	3,955	72.47	54.35	76	181	2,640,400
28	29	20	-84° 13'	358° 81'	3,774	70.91	52.06	83	183	2,640,470
29	30	21	-86° 30'	28° 71'	3,708	66.09	46.15	203	163	2,676,310
30	30	23	-84° 30'	31° 78'	3,509	65.34	43.17	204	165	2,676,380
31	30	25	-82° 65'	25° 01'	3,356	63.57	41.88	214	168	2,676,450
32	31	18	-80° 81'	333° 61'	3,932	70.08	49.63	83	179	2,712,150
Revs 35 - 63										
33	31	20	-82° 40'	324° E9'	3,764	66.68	48.18	93	181	2,712,220
34	32	21	-87° 68'	30° 46'	3,746	67.08	47.08	193	164	2,748,130
35	32	23	-84° 98'	29° 24'	3,524	64.68	43.29	197	166	2,748,200
36	32	25	-83° 22'	23° 54'	3,355	63.47	41.26	206	168	2,748,270
37	33	18	-85° 51'	48° 79'	4,056	73.75	56.70	346	166	2,784,040
38	33	20	-87° 85'	80° 63'	3,811	71.10	53.09	298	167	2,784,110
39	33	22	-87° 44'	148° 01'	3,593	68.92	50.01	247	169	2,784,180
40	34	21	-86° 17'	6° 90'	3,785	66.29	46.65	199	161	2,819,950
41	34	23	-83° 91'	14° 62'	3,565	64.07	42.89	196	162	2,820,020
42	34	25	-81° 47'	13° 46'	3,367	62.10	39.59	200	164	2,820,090
Revs 35 - 63										
43	36	21	-86° 41'	21° 49'	3,700	65.98	45.03	179	164	2,891,840
44	36	23	-83° 72'	17° 77'	3,777	63.47	40.93	185	165	2,891,910
45	36	25	-81° 72'	12° 17'	3,297	61.85	38.20	194	167	2,891,980
46	38	21	-85° 24'	66° 47'	3,770	66.22	43.60	107	166	2,963,660
47	38	23	-84° 24'	98° 97'	3,581	64.46	40.90	133	168	2,963,730
48	38	25	-82° 77'	30° 76'	3,393	62.46	37.89	161	171	2,963,800
49	39	16	-81° 03'	132° 72'	4,033	66.13	51.40	204	153	2,999,575
50	41	17	-82° 37'	1° 14'	4,704	77.41	60.63	359	167	3,071,535
51	41	19	-85° 60'	1J° 18'	3,974	74.24	56.68	344	167	3,071,605
52	41	21	-87° 59'	46° 23'	3,703	71.75	53.48	291	168	3,071,675
53	46	21	-85° 38'	44° 90'	3,678	68.19	45.20	92	170	3,251,225
54	46	23	-84° 62'	14° 07'	3,670	65.74	41.75	128	172	3,251,295
55	46	25	-83° 47'	356° 34'	3,292	63.90	39.19	155	174	3,251,365
56	49	20	-80° 21'	357° 85'	4,040	78.91	63.88	282	164	3,359,095
57	52	21	-87° 14'	77° 41'	3,932	72.45	51.50	35	165	3,466,615
58	52	23	-87° 28'	351° 81'	3,651	68.68	46.00	108	166	3,466,685
59	52	25	-85° 18'	317° 76'	3,430	65.93	42.05	158	168	3,466,755
60	55	18	-88° 06'	1° 85'	3,811	71.71	52.00	252	162	3,574,345
61	55	20	-86° 48'	70° 01'	3,549	68.42	47.20	207	163	3,574,415
62	56	17	-84° 45'	112° 26'	6,530	76.35	77.13	341	165	3,607,665
63	56	18	-81° 06'	10° 31'	6,758	71.86	63.86	37	162	3,607,735
64	56	19	-80° 79'	345° 45'	6,579	67.91	62.41	88	159	3,607,805
65	56	20	-85° 00'	326° 68'	6,684	67.83	67.25	125	158	3,607,875
66	56	21	-86° 53'	115° 99'	3,891	72.48	52.21	332	163	3,610,185
67	56	23	-87° 36'	272° 52'	3,601	68.49	46.42	182	163	3,610,255
68	58	21	-85° 54'	61° 65'	3,955	74.82	53.92	25	167	3,681,935
69	58	23	-87° 79'	359° 03'	3,668	70.87	48.43	71	167	3,682,005
70	58	25	-86° 46'	301° 90'	3,437	67.96	44.31	135	169	3,682,075
71	59	19	-86° 57'	16° 67'	3,806	70.44	50.91	220	160	3,717,845
72	59	21	-84° 41'	52° 01'	3,539	67.07	45.74	200	161	3,717,915
Revs 64 - 99										
73	64	01	-80° 05'	355° 66'	4,532	77.59	68.56	9	168	3,894,455
74	64	02	-83° 46'	24° 34'	9,676	77.50	73.63	355	167	3,894,525
75	64	03	-82° 86'	32° 28'	9,914	77.88	80.19	341	167	3,894,595
76	65	18	-88° 40'	159° 90'	3,904	72.07	49.56	46	163	3,933,095
77	65	20	-87° 59'	1° 17'	3,781	70.53	49.72	210	161	3,933,165
78	65	22	-83° 74'	349° 15'	3,697	69.84	51.19	214	159	3,933,235
79	69	18	-89° 48'	155° 37'	3,927	72.35	50.32	33	163	4,076,735
80	69	20	-86° 57'	333° 70'	3,804	70.69	50.51	211	160	4,076,805

^aTerms are defined in Fig. III-15.

Note: No frames taken between Revs 12-23.

Table VIII-7. (contd)

Index number	Rev	Frame number	Center of picture		Range (SRR-5), km	Lighting angle (SLAR-5), deg	Viewing angle (VAR-5), deg	North direction (NORAN) ^a	Sun direction (SUNAN) ^a	DAS time
			Latitude ^a , deg	Longitude ^a , deg						
Revs 64 - 99 (contd)										
81	69	22	-82° 70'	326° 79'	3,727	70.02	52.21	213	159	4,076,875
82	71	18	-83° 70'	122° 19'	3,705	72.85	47.05	61	169	4,148,625
83	71	20	-87° 06'	92.06	3,626	71.05	46.59	82	167	4,148,695
84	71	22	-87° 12'	7.99	3,504	69.60	46.70	187	164	4,148,765
85	79	18	-87° 55'	160° 08'	3,994	75.42	53.31	352	165	4,436,115
86	79	20	-87° 09'	5.82	3,666	70.25	45.58	140	164	4,436,185
87	79	22	-83° 38'	356° 73'	3,381	66.47	39.55	153	164	4,436,255
88	81	20	-81° 52'	32.55	3,436	68.53	38.16	100	170	4,508,075
89	81	22	-82° 77'	4.13	3,310	66.77	37.97	133	168	4,508,145
90	88	C1	-87° 07'	95.03	3,685	71.17	47.70	185	163	4,759,445
91	88	03	-82° 73'	117.24	3,375	66.56	40.06	166	163	4,759,515
92	97	09	-80° 00'	323.47	3,465	71.45	40.65	97	176	5,058,338
Revs 100 - 138										
93	109	06	-84° 31'	48.52	4,677	80.40	58.46	307	170	5,489,538
94	109	09	-84° 29'	46.09	4,056	80.65	58.13	299	170	5,489,888
95	116	07	-86° 89'	20.57	3,678	74.18	44.51	114	168	5,741,888
96	116	09	-86° 58'	6.40	3,556	73.46	44.27	134	168	5,741,958
97	124	C7	-86° 06'	355.40	3,652	75.07	43.35	98	169	6,029,798
98	124	09	-85° 75'	355.03	3,538	74.85	43.36	99	170	6,029,868
99	133	C7	-86° 95'	110.41	4,244	75.80	46.01	132	168	6,353,058
100	133	C8	-85° 80'	164.97	3,744	78.25	45.02	62	171	6,353,338
101	133	10	-86° 96'	101.59	3,620	75.51	44.66	138	169	6,353,408
Revs 139 - 178										
102	141	C6	-87° 01'	110.89	3,588	78.34	46.08	74	171	6,641,038
103	145	02	-86° 62'	48.28	4,228	76.71	45.92	137	169	6,784,538
104	145	04	-88° 25'	89.56	3,782	79.02	46.97	75	171	6,784,818
105	145	C5	-88° 36'	49.42	3,668	78.13	47.02	128	170	6,784,888
106	151	01	-85° 01'	108.40	4,282	82.91	47.16	33	174	7,000,488
107	151	C3	-85° 22'	80.46	3,736	80.52	44.45	59	173	7,000,768
108	151	04	-84° 85'	105.05	3,718	82.62	48.17	41	174	7,000,838
109	155	02	-85° 84'	48.88	4,163	81.87	45.29	52	173	7,288,538
110	155	04	-84° 49'	34.11	3,629	80.65	42.76	68	173	7,288,818
111	156	05	-85° 45'	34.27	3,560	80.68	44.64	67	173	7,288,888
112	168	C1	-86° 78'	69.62	3,945	78.75	48.03	180	171	7,612,428
113	168	C3	-85° 13'	10.59	4,009	80.43	54.15	218	171	7,612,498
114	168	C4	-84° 44'	22.54	3,862	79.20	53.22	209	170	7,612,568
115	173	C1	-87° 31'	344.30	4,204	83.26	46.96	49	175	7,791,978
116	176	01	-87° 39'	285.28	4,086	83.91	53.31	280	175	7,899,988
117	176	C3	-86° 65'	84.50	3,709	80.27	44.12	128	173	7,900,058
118	176	C4	-86° 94'	81.32	3,610	80.36	44.74	130	172	7,900,128
Revs 179 - 217										
119	180	01	-82° 08'	63.75	3,484	77.27	36.74	129	172	8,043,908
120	180	02	-82° 34'	70.26	3,374	78.04	36.84	119	172	8,043,978
121	180	04	-83° 94'	71.30	3,334	79.08	40.23	116	173	8,044,048
122	182	C5	-80.50	63.75	2,923	75.88	40.73	121	173	8,044,328
123	180	06	-81.19'	73.30	2,950	77.40	46.41	110	175	8,044,398
124	182	C5	-82.87'	7.02	3,103	76.30	46.08	176	169	8,116,218
125	182	C6	-84.41'	2.47	3,104	77.92	50.16	183	170	8,116,288
126	184	C1	-84.54'	64.07	3,006	81.02	40.49	104	173	8,187,764
127	184	C2	-84.75'	80.67	3,525	82.52	41.93	81	175	8,187,834
128	184	C4	-84.45'	52.25	3,391	79.98	40.92	116	173	8,187,904
129	187	C4	-85.49'	168.38	3,545	79.41	45.93	171	171	8,295,844
130	188	C1	-87.15'	20.30	3,671	81.75	45.32	137	174	8,331,754
131	188	C2	-86.59'	357.94	3,569	80.72	45.78	160	173	8,331,824
132	188	C4	-86.73'	349.05	3,544	82.75	49.11	169	173	8,331,894
133	192	C5	-80.51'	343.98	2,931	75.43	40.10	149	170	8,476,164
134	192	C6	-80.48'	337.29	2,885	75.10	42.67	157	170	8,476,234
135	196	C1	-83.77'	12.66	3,500	82.56	39.27	99	175	8,619,734
136	196	C2	-83.70'	29.16	3,514	84.25	40.52	76	176	8,619,804
137	196	C4	-83.93'	51.33	3,501	86.55	44.79	54	177	8,619,874
138	196	C5	-82.36'	345.79	3,012	78.96	42.31	122	173	8,620,154
139	196	C6	-82.12'	355.84	2,977	79.71	45.29	108	174	8,620,224
140	204	05	-84.19'	350.13	3,181	84.98	48.94	72	176	8,907,994
141	204	C6	-83.16'	335.78	3,068	83.16	48.60	86	175	8,908,064
142	206	01	-86.38'	11.72	3,696	87.46	46.04	46	178	8,979,534
143	206	02	-85.27'	335.90	3,497	85.10	42.55	81	176	8,979,604
144	206	04	-85.51'	296.18	3,401	82.49	43.28	132	174	8,979,674
145	206	05	-87.53'	316.52	3,216	84.67	52.75	88	175	8,979,954
146	206	C6	-86.70'	319.20	3,158	84.34	54.27	85	175	8,980,024
147	207	03	-85.66'	130.85	3,674	83.90	42.40	113	176	9,015,444
148	207	04	-86.89'	126.87	3,611	84.30	44.57	115	175	9,015,514
149	207	C7	-86.28'	131.60	3,501	82.84	44.70	146	174	9,015,584
150	211	01	-84.66'	115.22	3,629	84.21	40.64	108	176	9,159,224
151	211	02	-83.81'	100.66	3,493	82.50	39.64	125	175	9,159,294
152	211	04	-84.68'	89.46	3,430	82.30	41.84	136	174	9,159,364
153	212	08	-85.50'	257.97	3,167	82.71	46.86	137	174	9,195,554
154	213	C1	-82.66'	90.14	3,564	81.97	38.07	127	175	9,231,114
155	213	C2	-81.72'	88.66	3,424	80.77	36.76	131	174	9,231,184
156	213	C4	-82.00'	79.46	3,332	80.44	37.67	136	173	9,231,254
157	214	03	-87.18'	273.40	3,665	85.30	44.97	116	176	9,267,094
158	214	04	-85.12'	275.23	3,473	84.32	41.73	111	176	9,267,164
159	215	02	-83.66'	119.27	3,495	86.77	40.24	75	178	9,303,074
160	215	04	-83.31'	81.03	3,357	82.63	38.99	122	175	9,303,144

^a Terms are defined in Fig. III-15.

Table VIII-7. (contd)

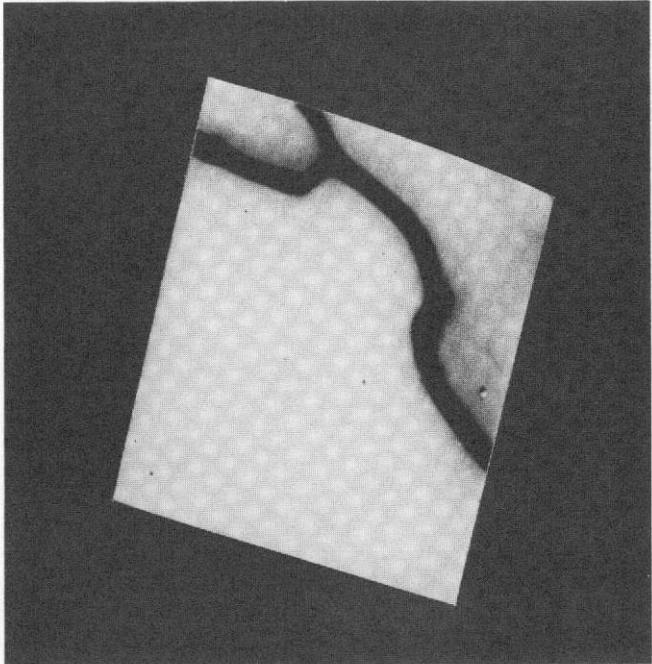
Index number	Rev	Frame number	Center of picture		Range (SRR-5), km	Lighting angle (SLAR-5), deg	Viewing angle (VAR-5), deg	North direction (NORAN) ^a	Sun direction (SUNAN) ^a	DAS time
			Latitude _(LR-5) , deg	Longitude _(LOR-5) , deg						
Revs 218-262										
161	219	C1	-81.22	89.77	3,441	85.74	35.08	90	177	9,446,854
162	219	02	-81.01	79.42	1,320	84.10	34.55	101	176	9,446,924
163	219	03	-80.99	75.75	3,151	83.14	33.41	103	176	9,446,994
164	224	C1	-87.36	259.12	3,730	88.01	45.60	70	178	9,626,684
165	224	02	-88.69	246.34	3,670	87.63	47.69	84	178	9,626,754
166	224	03	-89.28	317.45	3,625	88.47	50.21	18	178	9,626,824
167	226	01	-90.41	31.55	3,088	87.80	50.19	224	178	9,698,644
168	226	02	-89.12	199.33	3,721	87.42	48.42	138	178	9,698,714
169	226	03	-87.29	224.69	3,534	87.06	45.68	100	177	9,698,784
170	226	04	-86.08	241.04	3,127	87.58	46.26	75	178	9,698,924
171	226	05	-85.18	237.49	3,226	87.23	46.55	76	178	9,698,994
172	227	C1	-82.96	70.30	3,751	89.36	39.13	70	179	9,734,554
173	227	02	-83.34	37.31	3,627	85.51	38.75	111	177	9,734,624
174	227	03	-81.04	60.00	3,354	87.93	36.40	78	179	9,734,764
175	227	04	-82.07	50.12	3,289	87.38	38.63	80	178	9,734,834
176	227	05	-82.94	52.71	3,230	97.30	40.99	81	177	9,734,904
177	229	C1	-84.05	330.11	3,748	82.57	45.86	165	174	9,806,654
178	229	02	-85.67	11.63	3,566	85.58	43.14	130	177	9,806,724
179	229	03	-83.60	353.33	3,421	82.91	41.76	148	175	9,806,794
180	231	C1	-85.93	355.86	3,066	85.05	43.99	138	176	9,878,684
181	233	C1	-80.81	349.83	3,465	82.58	36.33	132	175	9,950,714
182	233	C2	-81.67	340.92	3,397	82.24	38.50	141	175	9,950,784
183	233	C3	-81.09	358.16	3,227	83.69	35.45	119	176	9,950,854
184	234	U1	-84.75	324.05	4,329	93.56	56.42	344	182	9,986,484
185	236	C1	-86.64	197.62	3,742	89.09	46.25	80	179	10,058,654
186	236	02	-88.29	193.43	3,597	88.97	46.97	82	179	10,058,724
187	236	03	-86.16	133.04	3,501	88.08	43.75	95	178	10,058,794
188	236	C4	-88.64	151.22	3,257	88.09	54.55	123	178	10,059,144
189	236	05	-86.86	178.84	3,155	67.95	54.91	78	177	10,059,214
190	236	06	-86.76	148.21	3,111	86.54	56.74	118	176	10,059,284
191	239	01	-80.22	329.90	3,456	84.01	34.38	124	176	10,166,664
192	239	02	-81.48	327.39	3,391	84.35	36.29	125	176	10,166,734
193	239	03	-82.50	324.47	3,302	85.15	37.90	121	176	10,166,804
194	239	04	-82.91	315.85	2,762	83.99	46.34	124	175	10,167,154
195	243	01	-80.88	322.63	3,398	86.51	34.19	108	177	10,310,584
196	260	C1	-82.16	49.43	3,157	87.60	39.83	112	178	10,648,519
197	262	05	-87.77	52.15	3,205	91.47	54.62	79	190	10,720,619
198	262	07	-83.67	.88	2,994	85.85	50.87	166	186	10,720,689

^aTerms are defined in Fig. III-15.

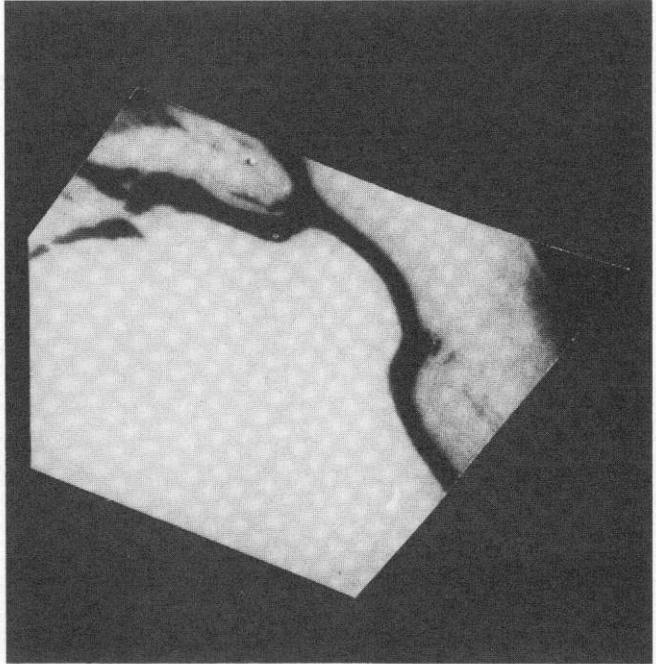
Table VIII-8. Wide- and narrow-angle frames showing frost and haze in the Mare Australis quadrangle: after Rev 416

Index number	Rev	Frame number	Center of picture		Range (SRR-5), km	Lighting angle (SLAR-5), deg	Viewing angle (VAR-5), deg	North direction (NORAN) ^a	Sun direction (SUNAN) ^a	Subsolar latitude, deg	Subsolar longitude, deg	Filter	DAS time
			Latitude _(LR-5) , deg	Longitude _(LOR-5) , deg									
1	416	01	-59.26	342.83	2,386	79.83	52.89	119	141	15.74	309.23	5	11,442,909
2	459	01	-73.29	268.48	3,793	92.24	91.62	151	151	18.70	278.63	5	12,535,030
3	459	03	-68.04	289.43	3,437	87.08	82.68	145	146	18.70	278.97	5	12,535,100
4	459	04	-54.89	324.50	2,367	83.01	56.33	114	143	18.70	279.31	5	12,535,170
5	459	05	-49.78	316.96	2,428	76.02	59.35	117	137	18.70	279.65	5	12,535,240
6	416	02	-56.15	343.27	2,300	77.31	50.35	146	169	15.74	309.40	5	11,442,944
7	459	02	-71.20	267.69	3,857	90.23	90.15	180	180	18.70	278.80	5	12,535,065

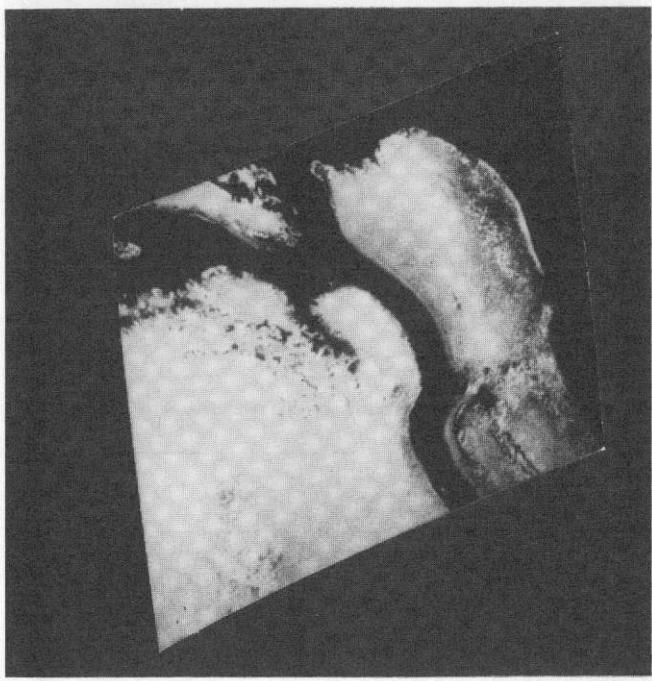
^aTerms are defined in Fig. III-15.



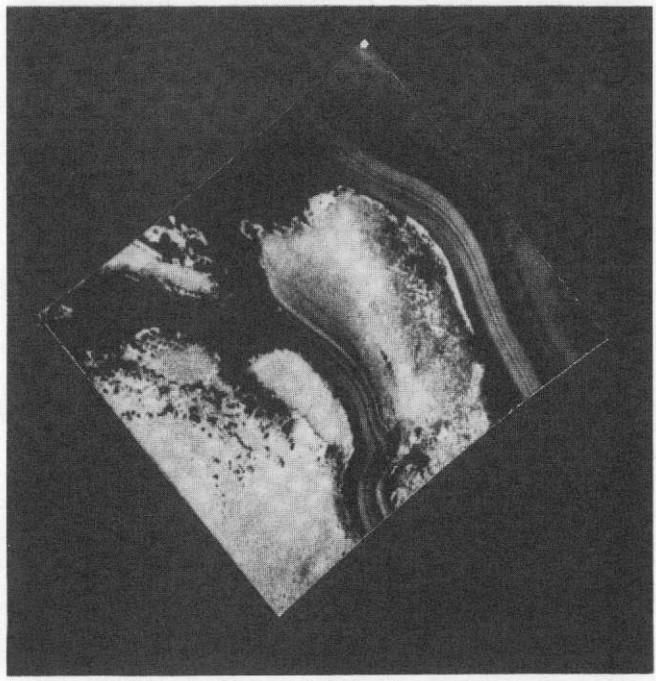
REV 11



REV 28



REV 124



REV 231

Fig. VIII-16. Narrow-angle pictures showing changes in frost cover in the area of the south polar cap known as the "fork". These projections were produced by the JPL Image Processing Laboratory.

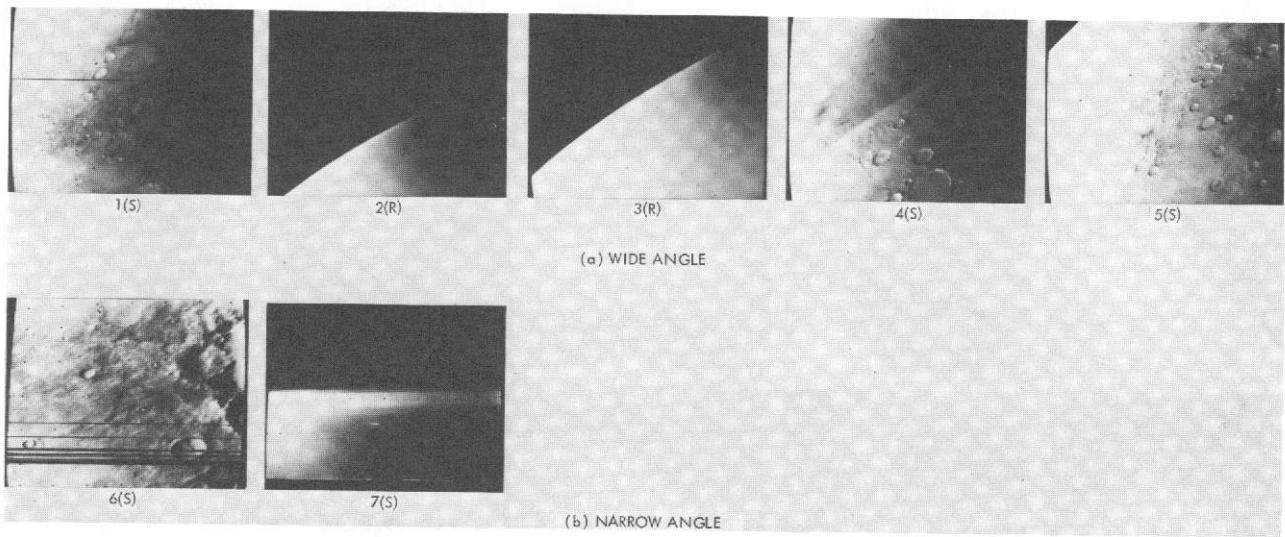


Fig. VIII-17. Shading-corrected (S) and raw (R) frames showing haze and frost developments in the Mare Australe quadrangle after Rev 416 (fall in the southern hemisphere).

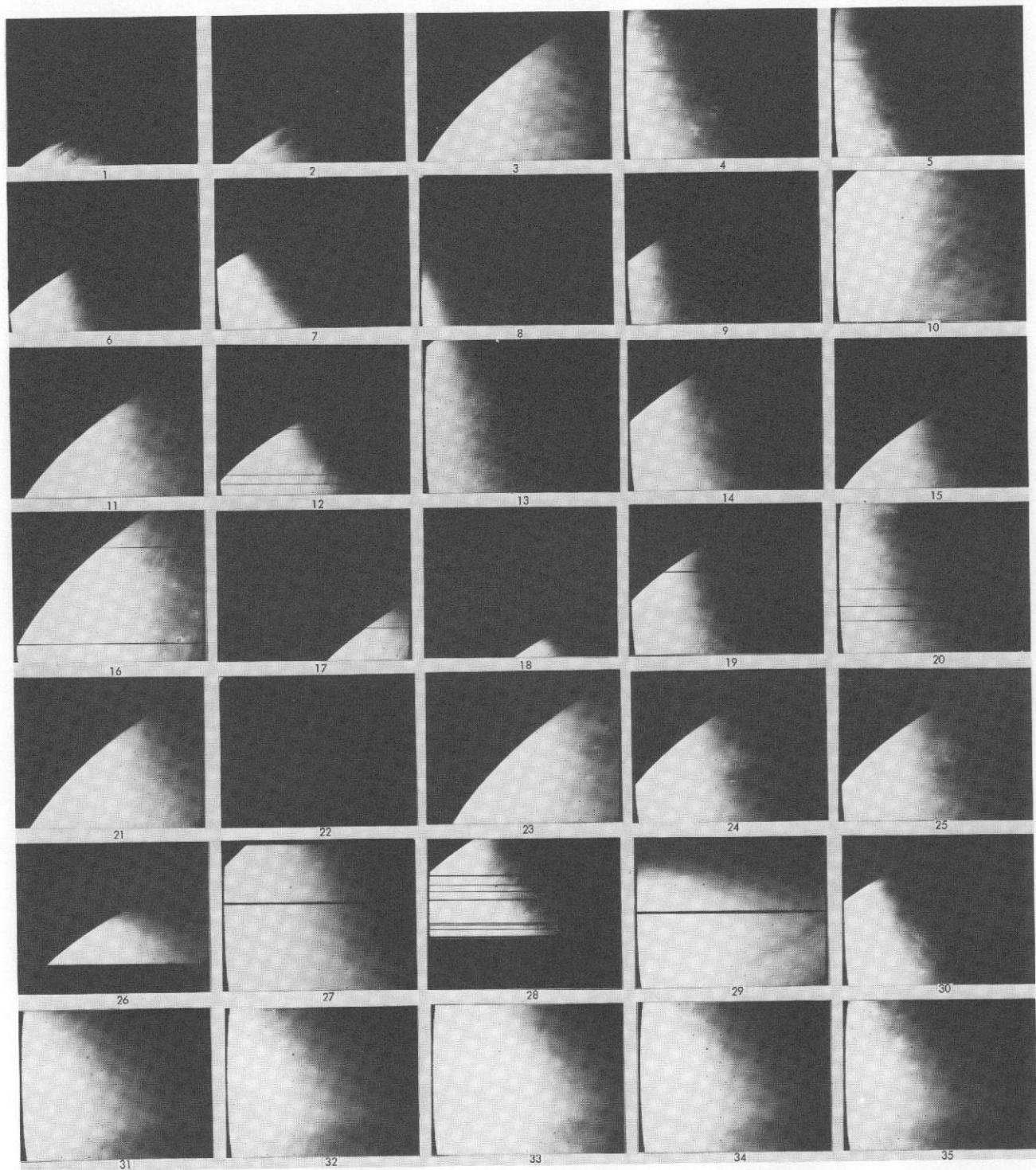


Fig. VIII-18a. Shading-corrected wide-angle frames during Revs 100-262, with centers north of 65°N : index numbers 1-35.

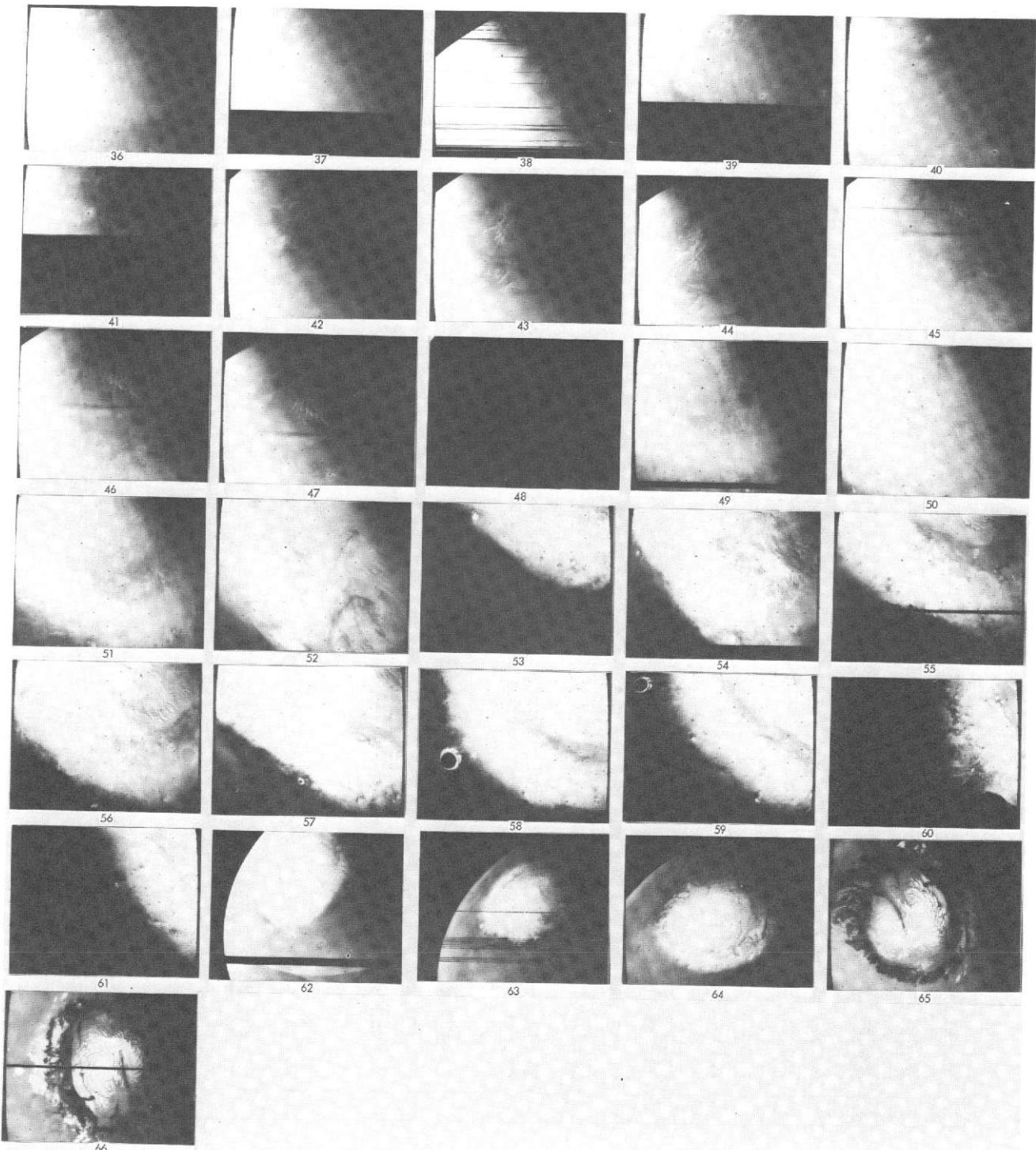
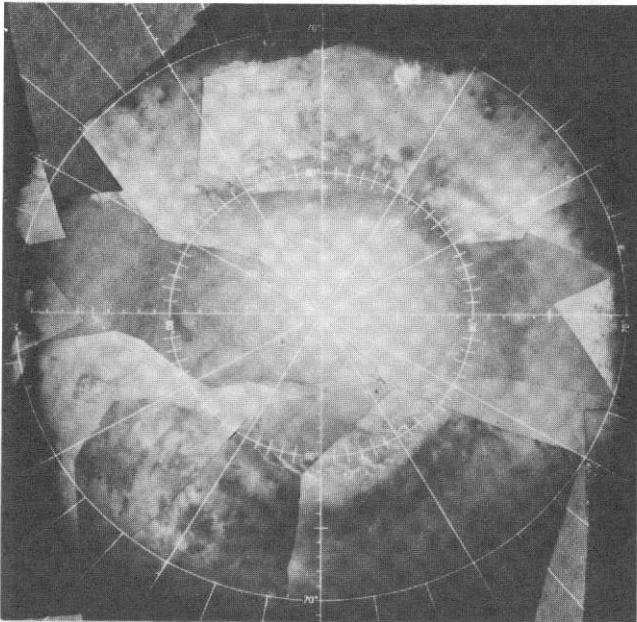


Fig. VIII-18b. Shading-corrected wide-angle frames with centers north of 65°N . Index numbers 36-49 were taken between Revs 100 and 262; index numbers 50-66 were taken between Revs 416 and 676.

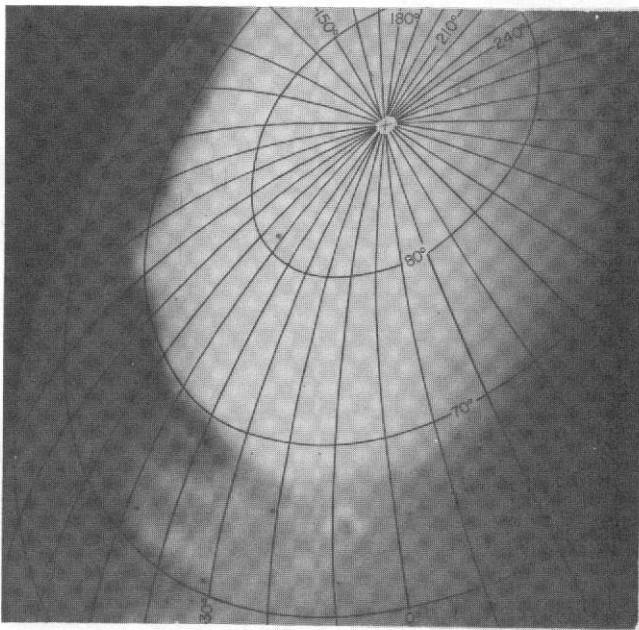
Table VIII-9. Wide-angle frames with centers north of 65° N: Revs 100-676

Index number	Rev	Frame number	Center of picture			Lighting angle (SLAR-5), ^a deg	Viewing angle (VAR-5), ^a deg	North direction (NORAN) ^a	Sun direction (SUNAN) ^a	Subsolar latitude, deg	Subsolar longitude, deg	Filter	DAS time
			Latitude (LR-5), ^a deg	Longitude (LOR-5), ^a deg	Range (SRR-5), ^a km								
1	100	32	65.27	3.68	4,363	94.30	91.58	334	154	-15.03	70.24	2	5,168,623
2	102	32	66.41	2.17	4,437	91.78	91.43	331	151	-14.84	60.39	7	5,240,583
3	147	31	67.37	355.81	4,577	79.65	75.40	312	139	-10.30	20.22	5	6,859,893
4	178	27	65.90	346.22	4,251	86.14	38.13	265	147	-7.03	50.01	5	7,975,623
5	178	29	67.76	335.90	4,502	90.97	33.07	254	149	-7.03	51.03	5	7,975,833
6	179	29	72.91	308.88	6,429	94.49	83.26	358	154	-6.92	226.14	5	8,011,813
7	180	29	86.14	135.23	5,729	97.07	68.58	49	156	-6.82	41.24	5	8,047,793
8	180	31	75.11	305.78	4,922	98.08	42.57	228	155	-6.82	41.58	5	8,047,863
9	183	29	85.94	218.62	5,502	92.53	64.83	337	151	-6.50	206.22	5	8,155,663
10	184	25	65.18	343.46	4,433	76.46	48.52	293	139	-6.39	19.99	5	8,191,369
11	184	27	71.21	61.19	5,921	82.14	81.20	328	141	-6.39	20.33	5	8,191,439
12	184	29	73.83	93.38	6,306	91.23	81.16	349	150	-6.39	21.36	5	8,191,649
13	185	29	74.67	142.27	4,835	87.24	45.62	281	147	-6.28	196.46	5	8,227,629
14	186	29	80.98	.34	5,323	87.34	60.60	321	147	-6.18	11.57	5	8,263,609
15	187	29	65.10	259.88	6,759	88.57	90.10	328	148	-6.07	186.68	5	8,299,589
16	188	25	70.25	1.24	5,174	76.22	67.36	317	136	-5.96	.76	5	8,335,359
17	188	27	68.24	51.99	6,169	82.18	94.77	321	141	-5.96	1.10	5	8,335,429
18	188	29	69.05	78.24	6,585	90.67	94.35	330	150	-5.96	2.13	5	8,335,639
19	189	29	81.27	187.24	5,507	87.26	64.08	331	147	-5.86	177.23	5	8,371,619
20	190	29	70.35	297.93	4,664	84.24	39.75	278	145	-5.75	352.34	5	8,407.599
21	191	27	69.01	205.72	5,956	79.32	80.63	326	139	-5.64	166.77	5	8,443,439
22	191	29	73.82	260.11	6,357	96.07	97.69	335	155	-5.64	167.79	5	8,443,649
23	192	27	67.34	20.92	5,986	77.96	82.05	323	137	-5.54	341.88	5	8,479,419
24	192	29	78.98	3.49	5,613	85.22	66.63	333	145	-5.54	342.90	5	8,479,629
25	194	27	78.42	356.12	5,654	84.63	66.75	333	144	-5.32	333.46	5	8,551,659
26	199	23	70.01	202.73	6,316	89.36	90.03	329	149	-4.79	127.99	5	8,731,349
27	206	24	71.31	246.58	4,939	77.60	47.57	300	140	-4.04	274.80	5	8,983,419
28	219	17	82.12	9.67	5,702	85.34	48.05	310	146	-2.66	31.29	5	9,451,159
29	222	16	66.77	134.30	4,073	79.77	56.26	237	140	-2.35	191.19	5	9,557,979
30	222	18	85.65	279.03	6,128	91.76	58.32	32	151	-2.34	196.64	5	9,559,099
31	225	02	67.53	299.61	4,513	80.89	32.66	260	144	-2.03	359.61	5	9,666,549
32	225	04	67.24	299.46	4,583	80.92	30.08	261	145	-2.03	359.95	5	9,666,619
33	225	06	67.35	299.54	4,671	81.06	28.31	262	145	-2.03	.29	5	9,666,689
34	225	08	67.29	299.41	4,759	81.19	26.42	263	145	-2.03	.63	5	9,666,759
35	225	10	67.05	299.29	4,846	81.24	24.42	263	146	-2.03	.97	5	9,666,829
36	225	12	67.25	300.00	4,950	81.20	23.45	264	146	-2.03	1.31	5	9,666,899
37	225	14	67.12	300.24	5,049	81.18	22.12	265	146	-2.03	1.65	5	9,666,969
38	239	11	84.55	307.20	6,007	85.22	50.93	333	145	-1.55	295.37	5	10,171,109
39	245	02	65.20	238.71	5,015	67.65	36.69	294	136	.07	264.05	5	10,386,569
40	245	04	72.11	238.45	5,310	73.94	38.94	297	139	.07	264.73	5	10,386,709
41	245	06	75.70	238.80	5,474	77.13	40.66	299	141	.07	265.07	5	10,386,779
42	245	08	79.34	239.75	5,649	80.33	42.68	302	143	.07	265.41	5	10,386,849
43	245	10	83.00	243.30	5,839	83.46	45.09	307	145	.07	265.75	5	10,386,919
44	245	12	86.61	257.35	6,044	86.57	47.83	320	147	.07	266.09	5	10,386,989
45	259	04	78.91	173.19	5,583	78.17	43.10	303	141	1.52	194.74	5	10,616,564
46	259	06	82.65	175.35	5,773	81.56	45.47	307	143	1.52	195.09	5	10,616,634
47	259	08	86.44	183.93	5,976	84.99	48.13	317	145	1.52	195.43	5	10,616,704
48	260	15	70.65	124.33	6,701	96.64	98.83	337	157	1.62	8.85	5	10,652,334
49	416	13	78.27	257.24	5,603	69.97	49.23	253	150	15.75	324.22	5	11,445,989
50	417	13	78.10	76.50	5,576	69.05	47.89	256	150	15.82	139.35	5	11,481,969
51	422	13	78.30	255.69	5,397	64.92	43.80	276	148	16.19	294.97	5	11,622,765
52	423	13	77.78	78.11	5,329	63.50	42.42	284	147	16.26	110.10	5	11,658,745
53	430	18	67.52	232.05	5,419	53.51	19.46	296	150	16.77	258.39	5	11,800,146
54	431	11	72.80	39.61	5,535	59.22	29.10	287	149	16.84	73.52	5	11,836,126
55	436	18	74.07	199.21	5,600	59.29	29.24	290	148	17.19	229.49	5	11,977,144
56	437	12	74.29	15.19	5,612	59.28	29.26	290	148	17.26	44.61	5	12,013,124
57	444	15	75.47	172.04	5,674	58.50	28.91	302	145	17.73	189.81	5	12,153,092
58	445	14	71.80	359.40	5,437	54.07	25.10	316	142	17.80	4.26	5	12,188,932
59	451	16	70.70	338.40	5,433	52.57	24.65	325	139	18.20	333.99	5	12,364,451
60	458	12	67.22	136.60	5,358	49.84	24.64	336	134	18.64	119.18	5	12,502,270
61	459	11	66.91	313.04	5,351	49.70	24.88	337	133	18.71	294.30	5	12,538,250
62	478	10	71.27	351.24	13,663	62.61	31.49	255	137	19.86	54.01	5	12,874,568
63	528	12	84.95	177.19	14,032	62.70	47.46	316	128	22.34	166.22	5	12,994,242
64	529	09	88.30	331.43	11,671	65.91	39.32	313	132	22.38	331.12	5	13,028,122
65	667	12	89.63	200.53	9,403	65.70	36.33	173	153	24.64	4.78	5	13,317,545
66	668	10	89.72	157.04	9,074	65.10	35.47	311	156	24.63	178.86	5	13,353,315

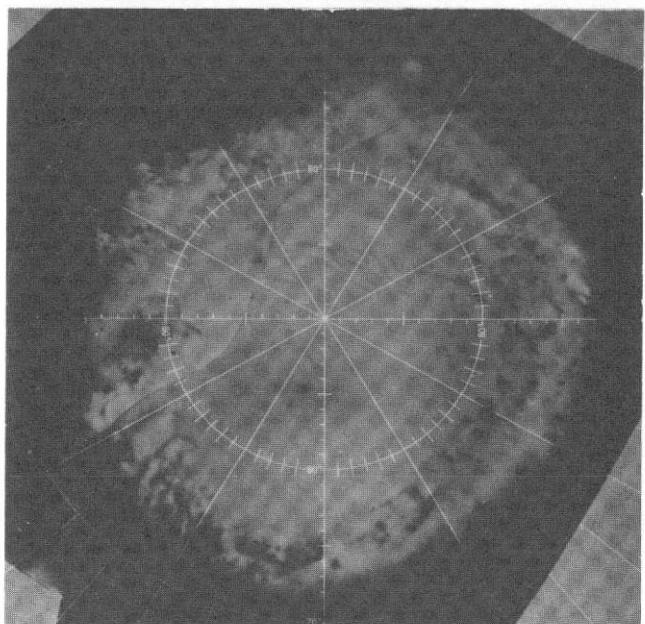
^aTerms are defined in Fig. III-15.



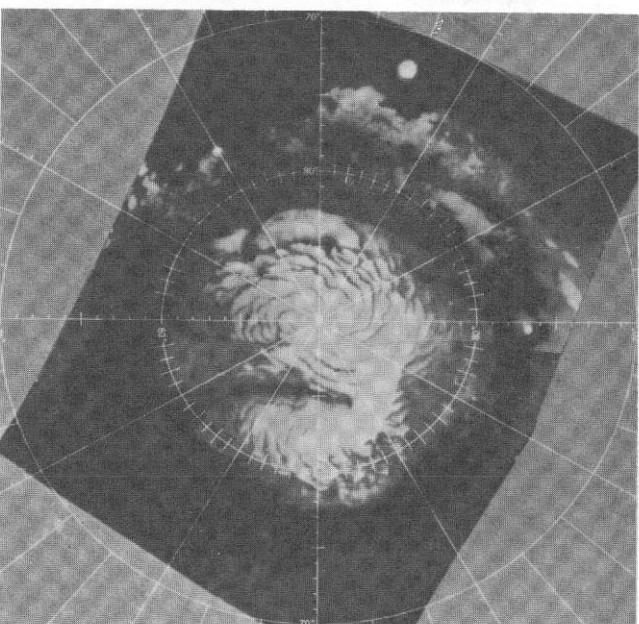
REVS 416-451



REV 478



REVS 528-529



REVS 667-668

Fig. VIII-19. Single frames and mosaics of wide-angle pictures of the north polar cap. Component frames are specially processed versions of frames in Fig. VIII-18 (condensed from Figs. 1-4 of Ref. VIII-2).

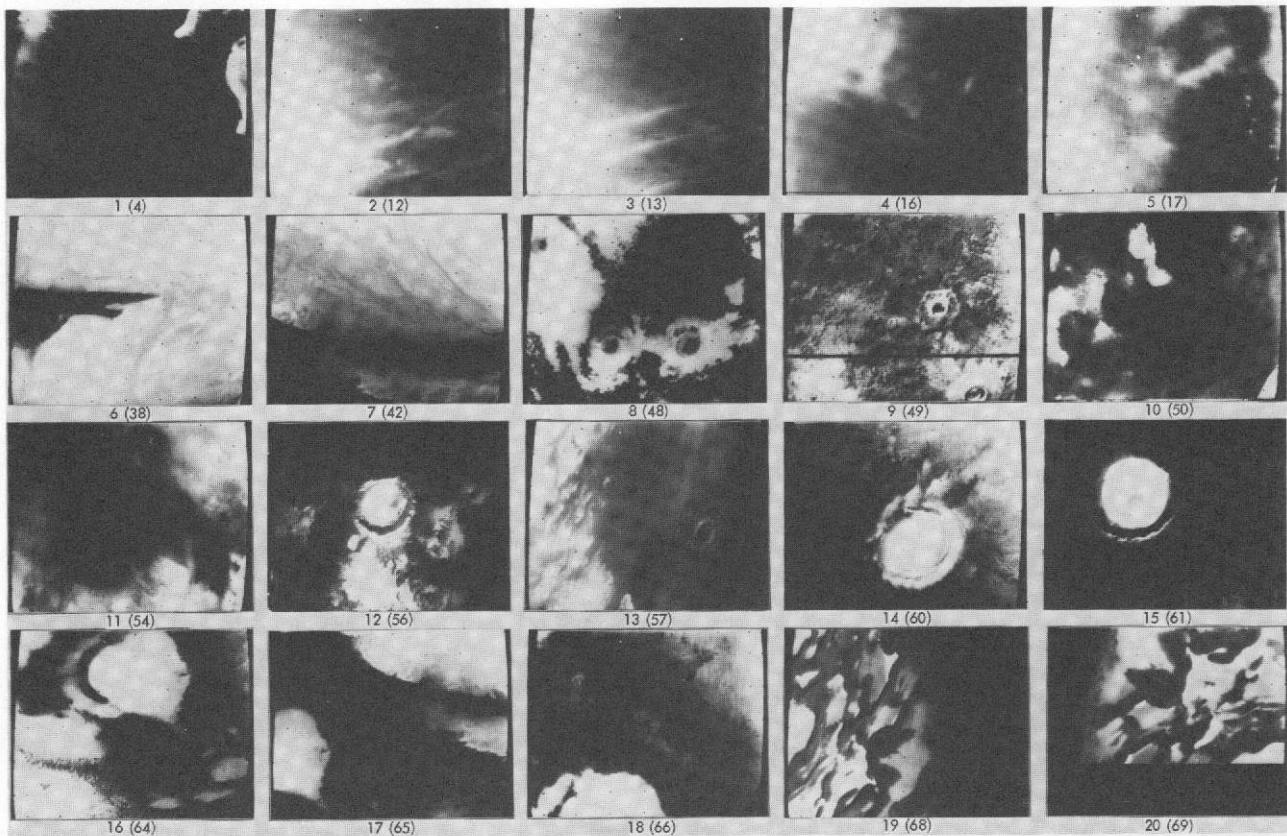


Fig. VIII-20. Shading-corrected narrow-angle frames of the north polar cap. This is a subset of frames shown in Fig. VIII-8 in the VAGC version. The first five pictures were taken between Revs 100 and 262; parenthetical numbers correspond to numbers in Fig. VIII-8a. The other 15 pictures were taken between Revs 416 and 676; parenthetical numbers correspond to numbers in Fig. VIII-8b.

References

- VIII-1. Murray, B. C., Soderblom, L. A., Cutts, J. A., Sharp, R. P., Milton, D. J., and Leighton, R. B., "Geological Framework of the South Polar Region of Mars," *Icarus*, Vol. 17, p. 328, 1972.
- VIII-2. Soderblom, L. A., Malin, M. C., Cutts, J. A., and Murray, B. C., "Mariner 9 Observations of the Surface of Mars in the North Polar Region," *J. Geophys. Res.*, Vol. 78, p. 4197, 1973.

IX. Geodesy

Astronomers have long studied the surface markings of Mars and have used them to establish coordinate systems of the planet's surface (Ref. IX-1). The Mariner 6 and 7 missions in 1969 offered an opportunity to improve the precision of the Earth-based coordinate systems. Far- and near-encounter pictures from Mariners 6 and 7 were used to determine the areocentric coordinates of 115 surface features (control points) that were clearly identifiable on two or more pictures (see Ref. IX-2). Some of these features were surface markings without discernible topographic expression, as were the features used in Earth-based coordinate systems. However, topographic features, craters in particular, were used on some far-encounter pictures and in areas covered by the moderate-resolution near-encounter pictures that encompassed about 10% of the planet's surface.

The 115 control points provided a network that could be used to refine positional information on areas of the Martian surface between control points. The various inadequacies in the network (Ref. IX-2) pointed to the need for a comprehensive geodetic experiment using pictures from the Mariner 9 mission to Mars.

A major objective of the Mariner 9 mission was to make accurate geodetic measurements of the surface features using television data. To accomplish this objective, a plan was developed to use the technique of multiphotograph stereophotogrammetry (Ref. IX-3), involving picture groups of well defined topographic features on the planet in several different viewing geometries. Overlapping pictures taken at different times, and hence from different positions in the same orbit, provided one set of viewing conditions. The 9° precession of the ground track (see Section VII), which occurred every other revolution, permitted the same features to be viewed on several successive revolutions with progressively changing viewing conditions. It was anticipated that the areographic coordinates (latitude, longitude, and elevation) of a large number of surface features could be determined, providing a control network spanning the entire southern hemisphere and part of the northern hemisphere. A significant refinement was expected in the shape of the planet and the direction of the rotation axis.

A. Mariner 9 Geodesy Data

The Mariner 9 mission plan called for far-encounter pictures to be taken of the northern hemisphere before insertion into orbit. In order to establish a preliminary control net of that part of the planet, pictures of the southern hemisphere were to be taken on the morning side of the planet in two distinct geometries: close to the terminator with near-vertical viewing (Fig. IX-1a) and farther from the terminator looking east (Fig. IX-1b). The dust storm that enveloped Mars at the time of arrival in November 1971 caused a complete change in the plan. It was impossible to acquire useful data on features outside the south polar region until after Rev 100.

By January 1972, the dust storm had subsided sufficiently to enable systematic mapping to begin; at that time, sequences of morning terminator pictures were acquired for geodesy. Since November the terminator had moved east relative to the spacecraft's orbit, so it was necessary to take the geodesy sequence farther south than was originally planned. On each revolution, only one group of five wide-angle pictures was obtained; these pictures were used to satisfy the needs of atmospheric reconnaissance (see Section XI) as well as geodesy. These "global" pictures provided usable overlapping coverage from about 70° S to about 25° S latitude during Mapping Cycle I (see Fig. IX-2), but the convergent stereophotogrammetric coverage typified by Fig. IX-1 was not obtained. The longitudinal coverage was good except for two gaps at about 90° and 270° , principally caused by the

loss of data during a snowstorm at the Goldstone 64-m antenna.

Several geodesy pictures also were taken in a latitude band from 0° to 25° N during Mapping Cycle II (Revs 139–178) at a range of about 3000 km near the evening terminator, with viewing angles of between 10° and 40° . In the sequence design summaries (see Volume II), each link is described as a tetrad on nadir passes and as tetrad 2 on zenith passes. Both consist of three wide- and one narrow-angle pictures and were taken with almost identical geometry (Fig. IX-3).

Footprint plots of coverage during Mapping Cycle I and II geodesy sequences are presented in the Mercator Projection of Fig. IX-4, which shows the high degree of east–west overlap that was achieved with the long-range global coverage in the southern hemisphere. As overlap occurred among pictures taken on different revolutions with ground tracks 9° or 18° apart, the different viewing conditions necessary for stereophotogrammetry were provided in that part of the planet.

The overlap in the 0° to 25° N band occurred among targeted tetrad frames taken during Mapping Cycle II, which are reproduced in Fig. IX-4, and mapping sequence frames, which are not shown in Fig. IX-4 but appear in Fig. VII-3a. In these cases, stereo was provided by slewing the cameras to view back along the ground track at the same area between 0° and 25° N latitude.

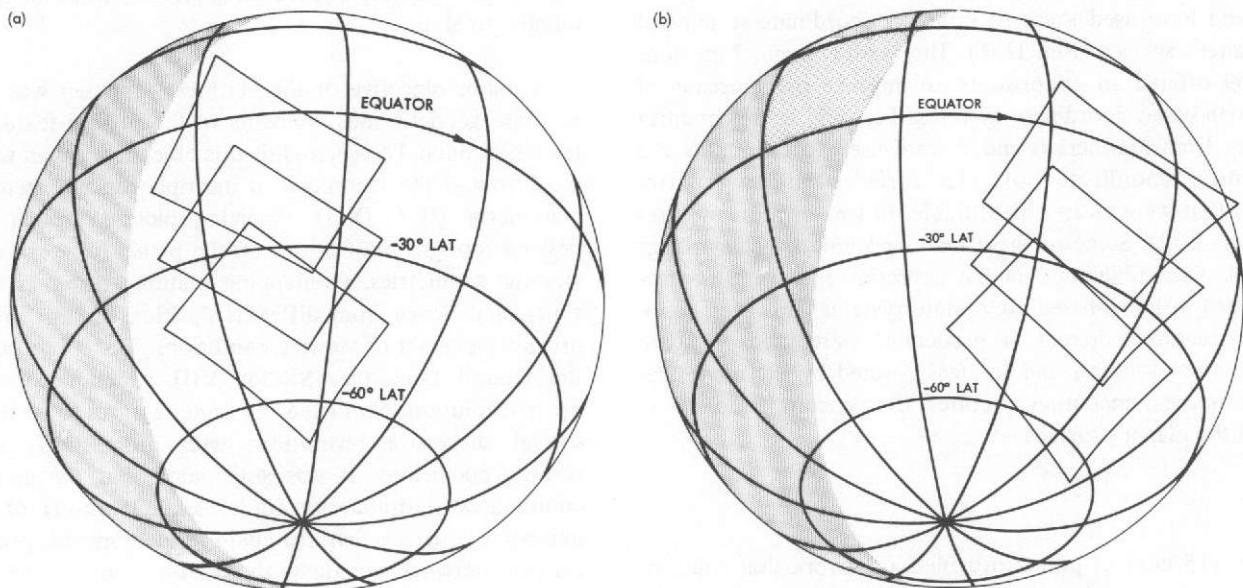
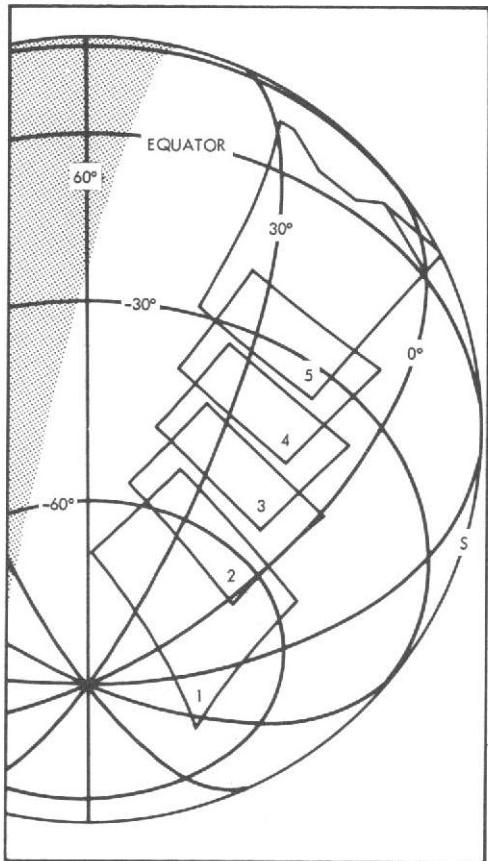
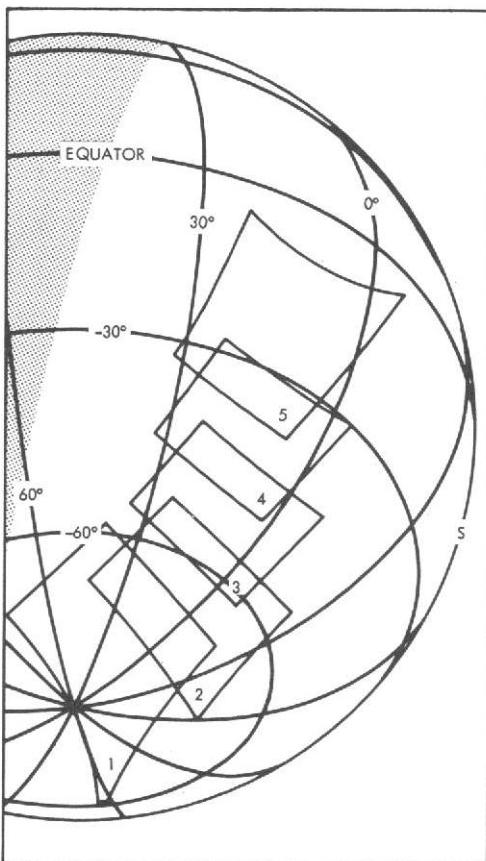


Fig. IX-1. Typical geodesy sequence planned for Mariner 9 before the global dust storm. (a) View near vertical. (b) Looking east.



(a) REV 118



(b) REV 120

Fig. IX-2. Geodesy sequence acquired during Mapping Cycle I (Revs 100–138). Contrary to the original plan for geodesy coverage, the viewing angle variation was limited to that provided by the field of view of the television camera. Coverage from successive zenith revolutions (a) and (b) indicates the degree of overlap typical of these sequences.

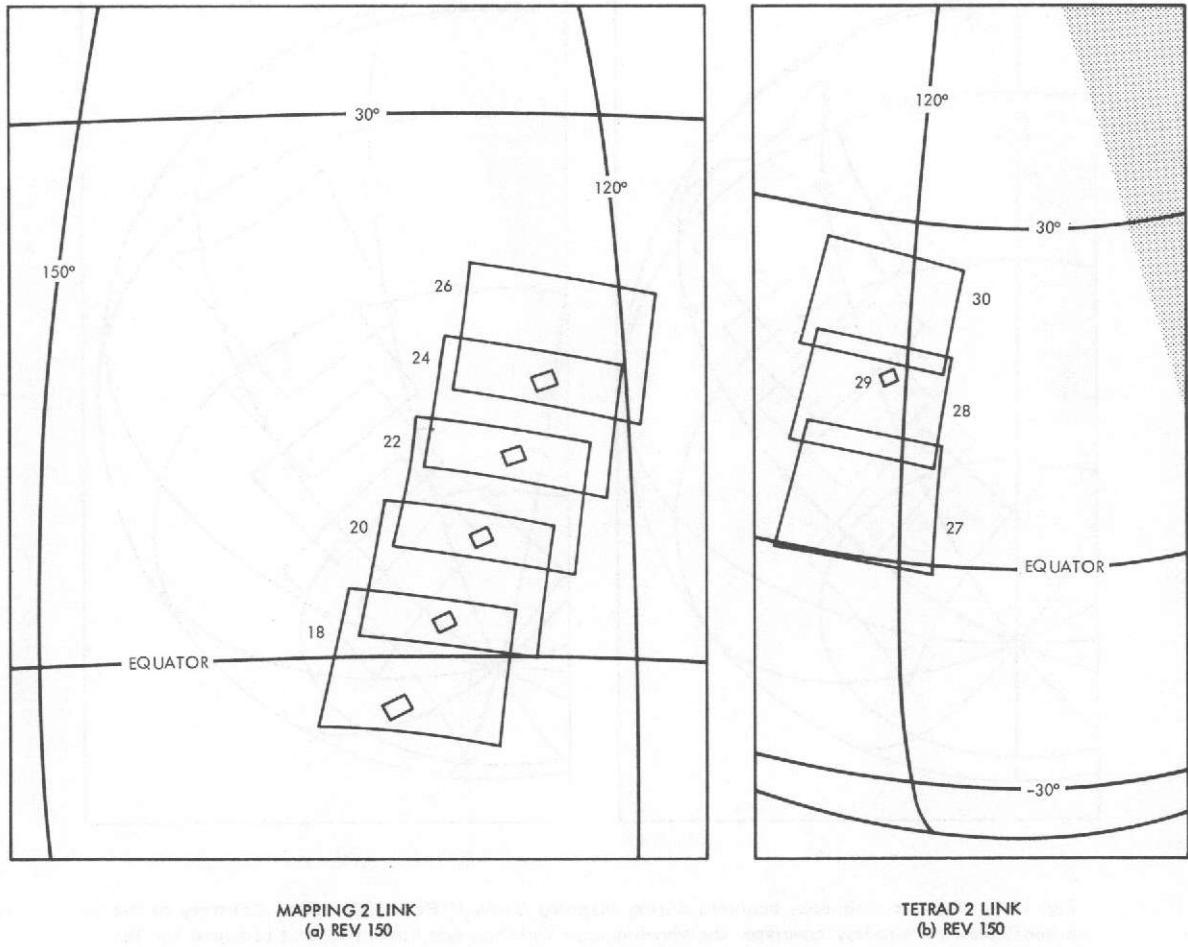


Fig. IX-3. Geodesy sequence acquired during Mapping Cycle II (Revs 139–178). (a) View near vertical. (b) Same area looking south along the ground track.

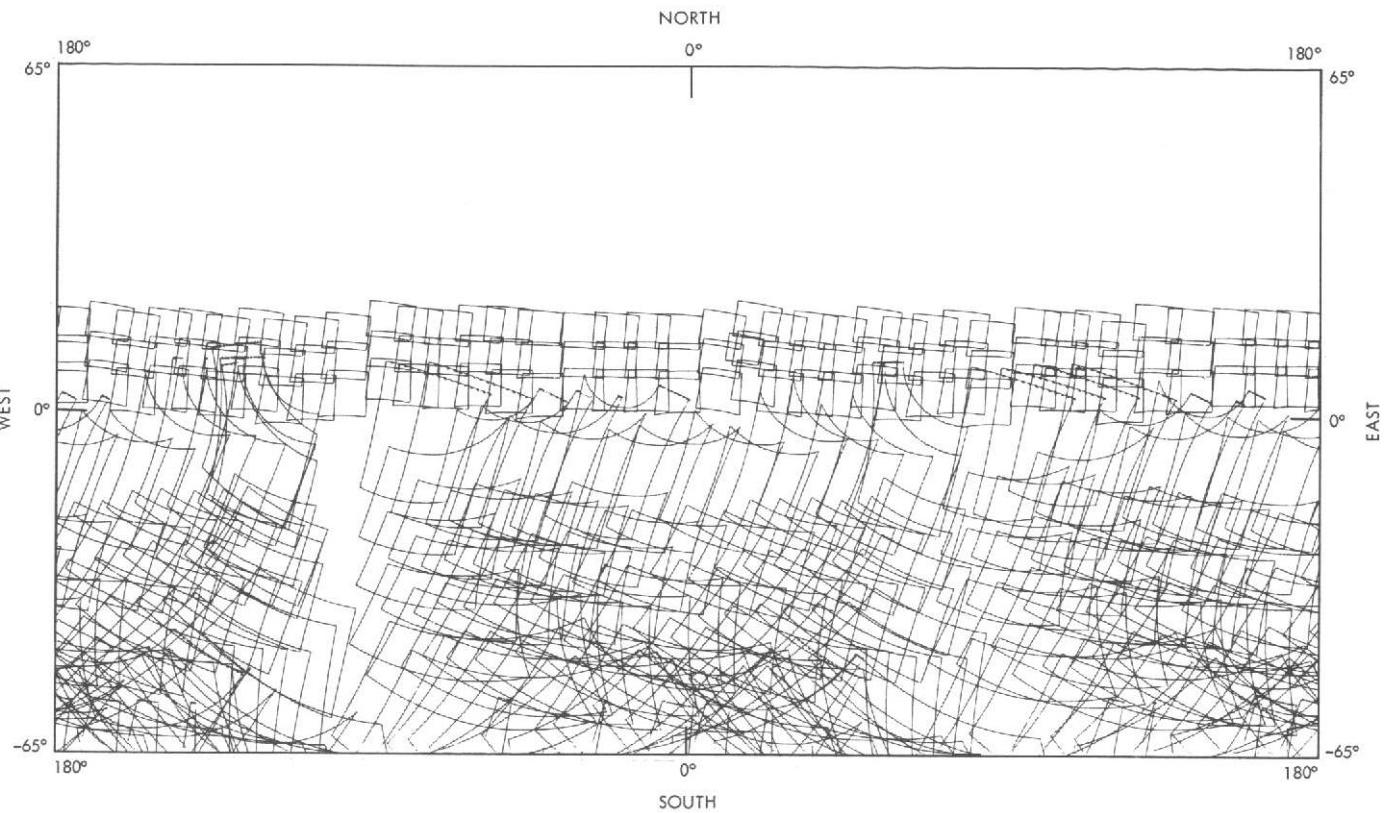


Fig. IX-4. Coverage obtained by geodesy links during Mapping Cycles I and II (Revs 100–178) provides a high degree of overlap in the southern hemisphere. The mapping links that overlap with geodesy links between 0° and 25°N are not shown.

Various types of pictures were used to provide geodetic coverage in the remaining three major latitude bands (Table IX-1). The south polar region presented few problems because duplicate coverage, with variation in viewing angle and quality suitable for geodesy, was acquired from mapping pictures (see Section VIII). The equatorial gap presented most problems because only mapping frames could be used, each covering only small areas and with little mutual overlap. In the northern part of the planet, however, routine mapping pictures, which were taken from higher altitudes, had sufficient overlap to be suitable for geodetic work. Coverage and overlap were sufficient to devise a primary control net in which latitude and longitude were well determined, but the lack of great variety in wide-angle stereoscopic pictures showing the same features from widely different viewing angles precluded accurate determinations of planetary radius.

B. Control Net

The control net was formed by selecting a few topographic features, two to ten, located on two or more frames (Ref. IX-4). The most common feature chosen was a crater,

with the center defined as the control point. The positions of these points on the frames were measured in picture element (pixel) units (row and column; see Section IV) accomplished by using special "map-gridded" pictures in which lines were inserted digitally every 25 pixels (see Fig. IX-5). The picture data were derived from the Experiment Data Record (EDR), which consists of digital data uncorrected for geometric distortion (see Section IV), and were processed to emphasize topographic detail. The pixel measurements were corrected for optical and electronic distortions and transferred into millimeter coordinates, referred to the focal plane of the camera. The geometric distortion transformations applied to the control point measurements were the same as those used in making the geometric corrections for the Reduced Data Record (RDR).

Primary and secondary control nets devised from the Mariner 9 data are described in detail in Refs. IX-4 through IX-6. The distribution of control points over Mars is shown in Fig. IX-6, and their distribution on a sample map chart in Fig. IX-7. Figure IX-8 shows secondary control points in the equatorial region.

Table IX-1. Geodesy pictures obtained by Mariner 9

Revs	Science cycle	Orbital science links		Comments
		Zenith pass (even revolutions)	Nadir pass (odd revolutions)	
1-15	Post-orbital insertion mapping calibration and phase function	—	—	
16-23	Interim sequence	3A(O) P - 1 h, 30 min	3A(O) P - 1 h, 30 min	No useful surface detail visible
24-63	Recon I	—	—	
64-99	Recon II	—	—	
100-138	Mapping Cycle I	Global (5A) P - 59 min, 36 s Used primarily for geodesy despite the global designation	Global (5A) P - 59 min, 36 s Used primarily for geodesy despite the global designation	70°S to 25°S Excellent overlap Range 5000 to 6200 km
139-177	Mapping Cycle II	TV mapping P + 13 min, 54 s	TV mapping P + 13 min, 54 s	0° to 20°N Regular mapping sequence, 2000 to 2400 km
139-177	Mapping Cycle II	Tetrad 2 (1A, 1AB, 1A) P + 24 min, 24 s	Tetrad (1A, 1AB, 1A) P + 24 min, 24 s	Overlaps mapping sequence looking back along the ground track 2800 to 3000 km
178-217	Mapping Cycle III	TV mapping 2 (3AB) P + 30 min	TV mapping 2 (3AB) P + 30 min	20°N to 45°N Large sidelap 3000 to 3600 km
218-262	Extended mission, Phase I	Triad 5 (1B, 1AB) P + 37 min to P + 55 min	Triad 5 (1B, 1AB) P + 11 min to P + 31 min	Some geodesy gaps filled
416-459	Extended mission, Phase 2: Arcturus	North collar mapping (3AB) P + 45 min to P + 55 min North polar mapping (A) P + 52 min to P + 59 min	North collar mapping (3AB) P + 45 min to P + 55 min North polar mapping (A) P + 52 min to P + 59 min	45°N to 70°N 70°N to 90°N Large overlap 4000 to 6000 km
473-533	Extended mission, Phase 3: Canopus	—	Rev 533 (2AB) P + 6 min, 40 s	Landmark for zero meridian (2AB) images
667-676		—	—	

Note: Geodesy coverage in the equatorial band between 25°S and the equator was extremely poor, and only minimally overlapping mapping frames from Mapping Cycles II and III were available to cover this zone.

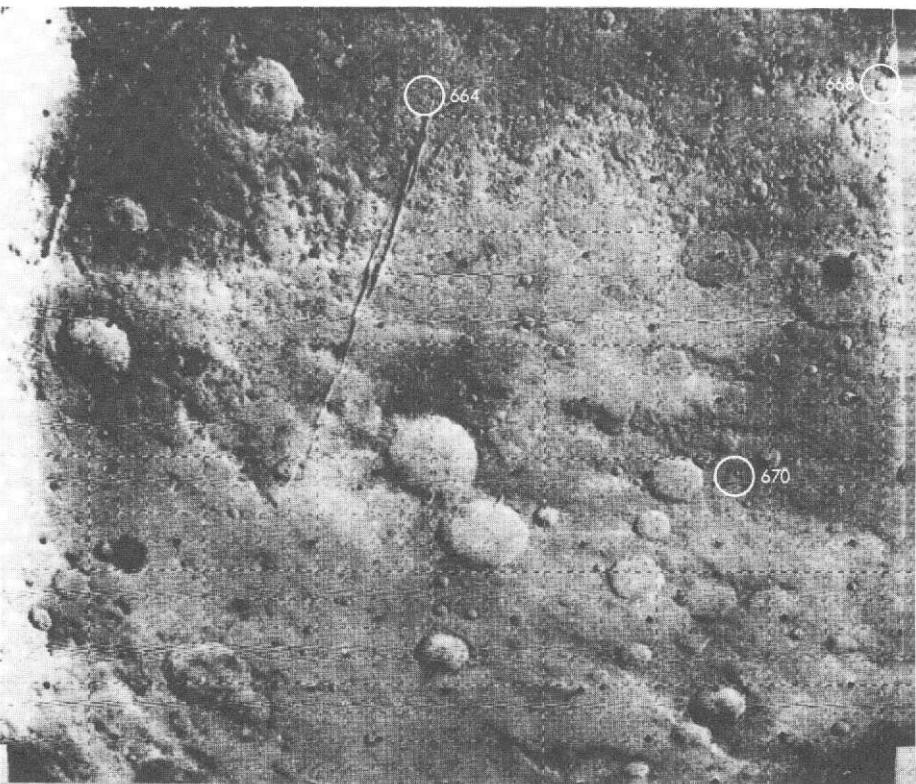
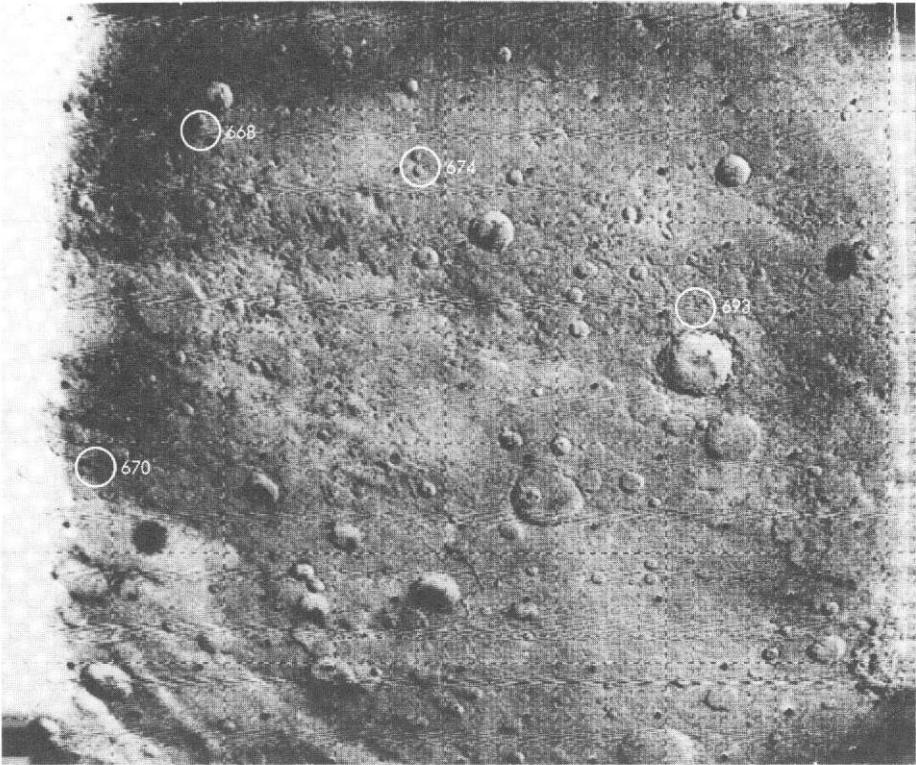
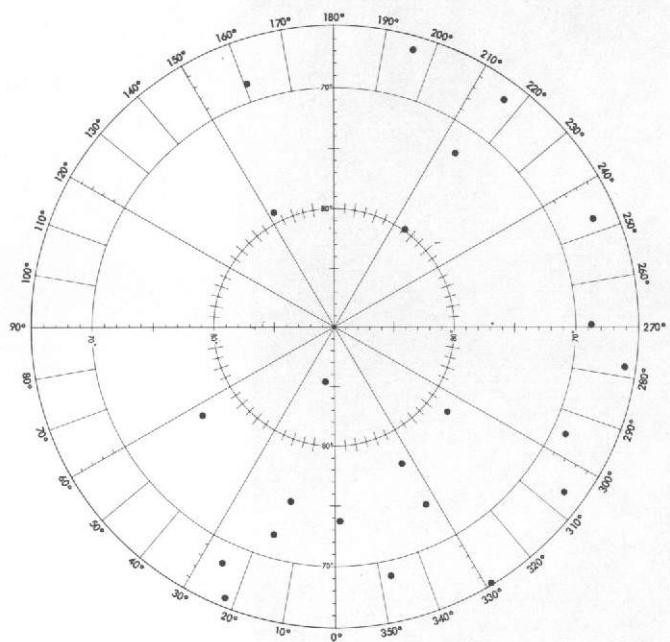
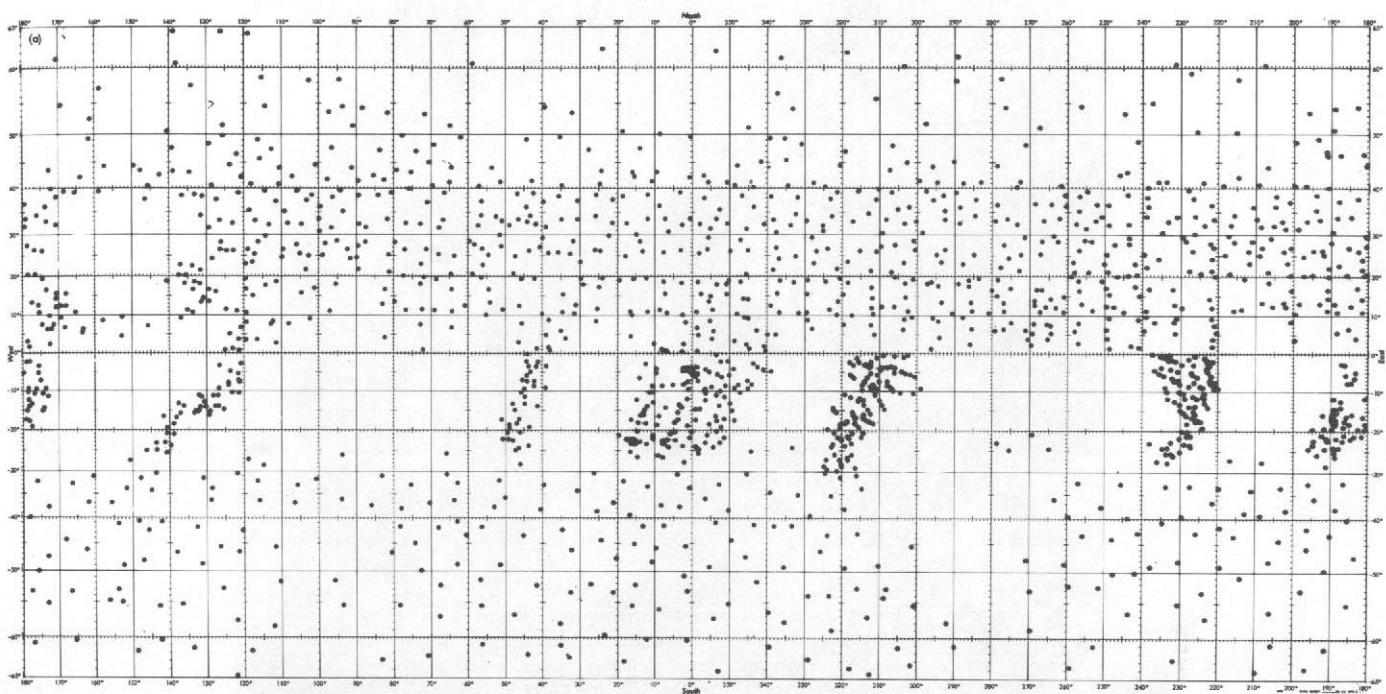
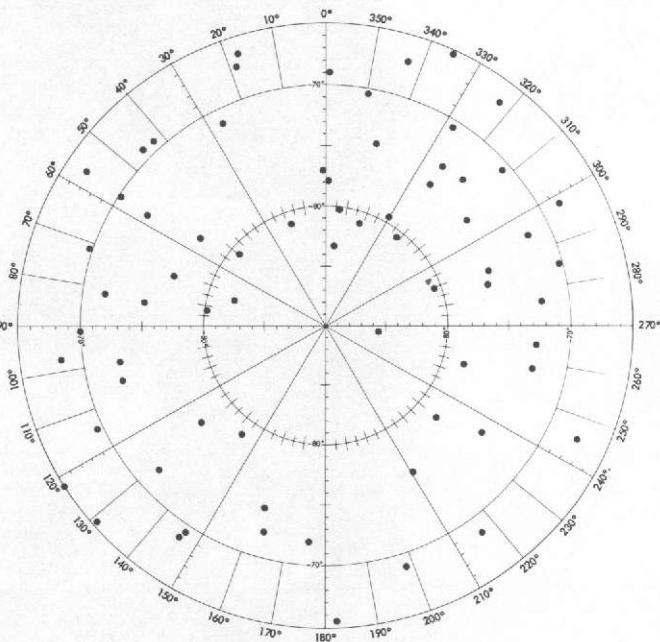


Fig. IX-5. Two pictures that overlap, thus showing the same control points. The "map grid" was introduced digitally by image processing techniques and was a help in making pixel measurements of feature locations.



NORTH POLAR REGION



SOUTH POLAR REGION

Fig. IX-6. Points of the June 1973 control net plotted on a chart of the central latitudes (Mercator Projection) and charts of each pole (Stereographic Projection).

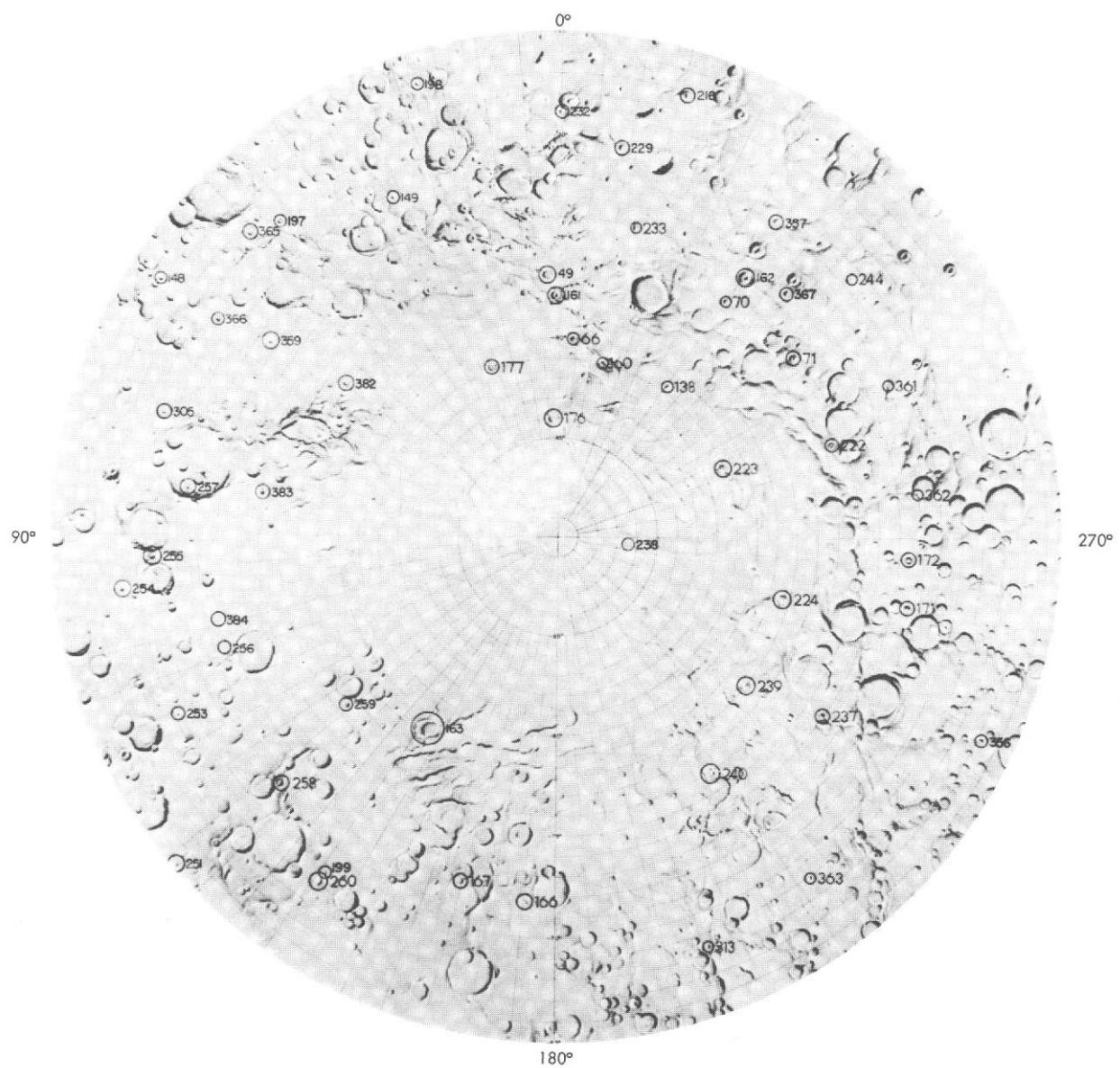


Fig. IX-7. Primary control points identified on the Mare Australe quadrangle (MC-30).

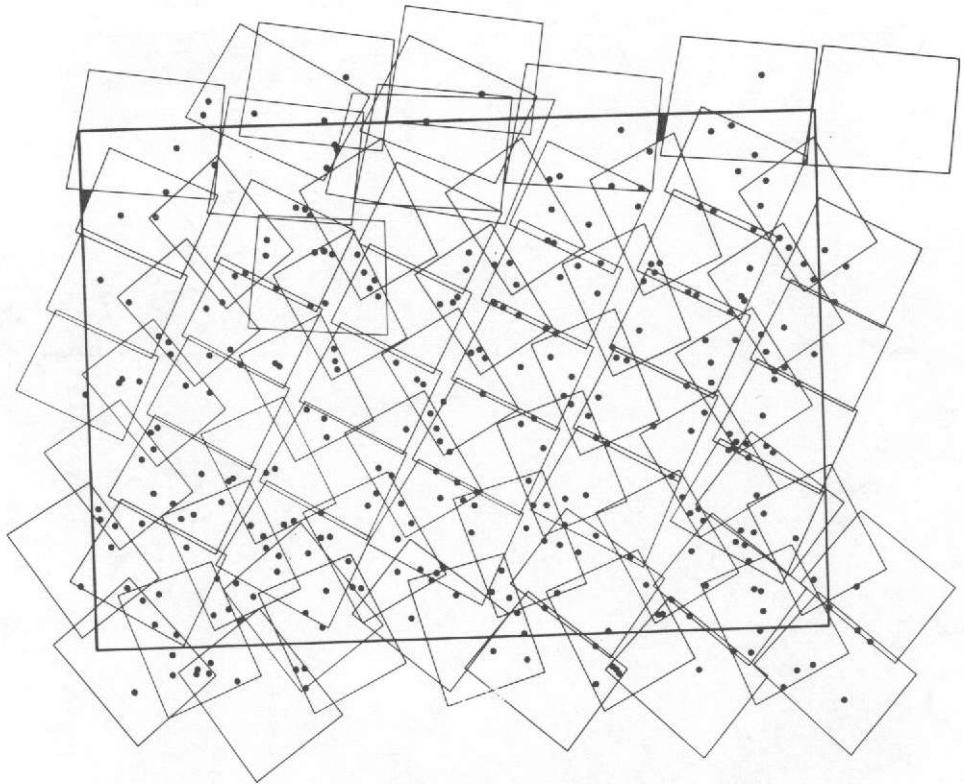


Fig. IX-8. Sample layout of secondary control net for a sample Mars quadrangle (Phoenicis Lacus, MC-17).

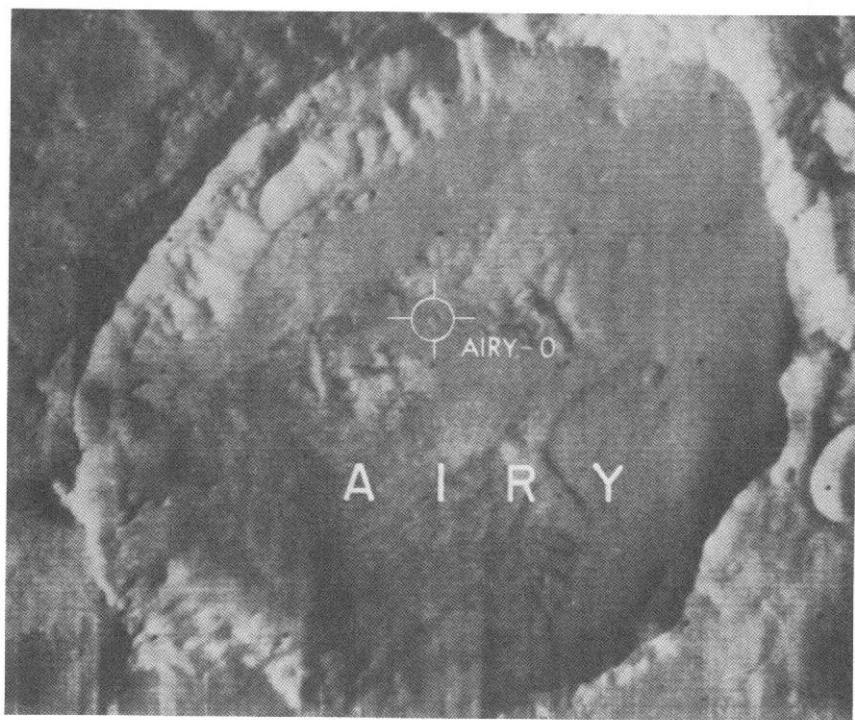
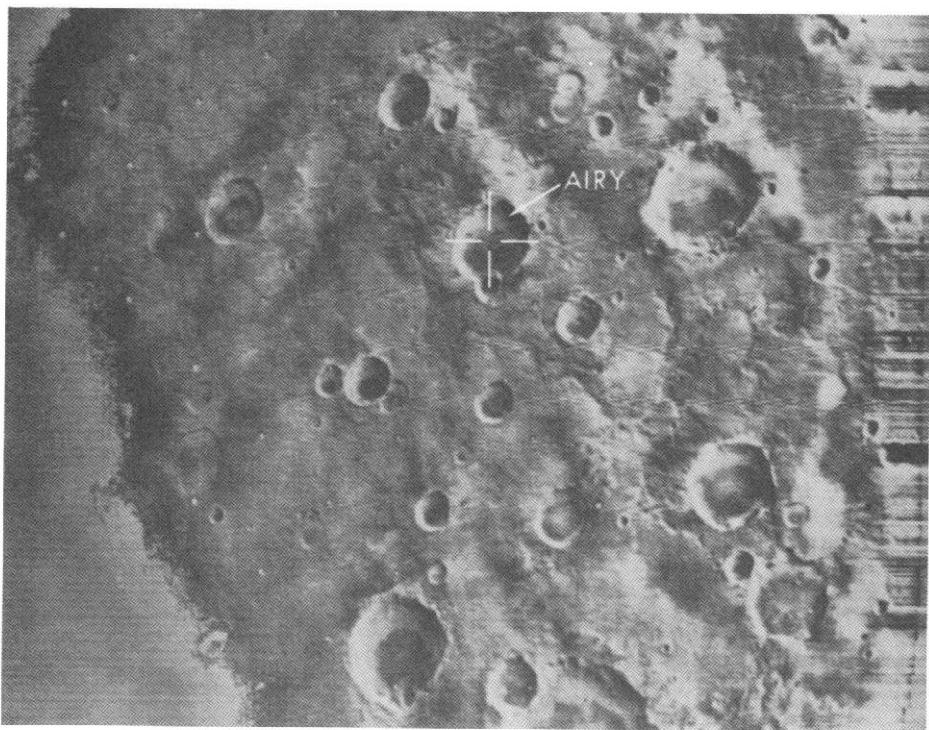


Fig. IX-9. The prime meridian passes through the center of the small crater Airy-0 shown in the narrow-angle picture. Airy-0 lies within the large crater Airy, which is shown in the wide-angle picture above.

C. Central Meridian

A photographic sequence was taken during Rev 533 under favorable viewing conditions in the region of the equator and central meridian of Mars. The small crater Airy-0, visible only in a narrow-angle frame (Rev 533, frame 03), was chosen

to define the central meridian of Mars (Fig. IX-9). This crater is too small to be resolved in the wide-angle frame that covers the same area (Rev 533, frame 01; see Fig. IX-9). To measure the position of Airy-0 in this frame, the larger crater Airy was registered in both narrow- and wide-angle frames visually and by using a computer registration technique at the Image Processing Laboratory of JPL.

References

- IX-1. de Vaucouleurs, G., "Charting the Martian Surface," *Sky and Telescope*, Vol. 30, p. 196, 1965; also "A Mars Chart for the Mariner Flights," *Sky and Telescope*, Vol. 41, p. 283, 1971.
- IX-2. Davies, M. E., "Coordinates of Features on the Mariner 6 and 7 Pictures of Mars," *Icarus*, Vol. 17, p. 116, 1972.
- IX-3. Masursky, H., Batson, R., Borgeson, W., Carr, M., McCauley, J., Milton, D., Wildey, R., Wilhelms, D., Murray, B., Horowitz, N., Leighton, R., Sharp, R., Thompson, W., Briggs, G., Chandeysson, P., Shipley, E., Sagan, C., Pollack, J., Lederberg, J., Levinthal, E., Hartmann, W., McCord, T., Smith, B., Davies, M., de Vaucouleurs, G., and Leovy, C., "Television Experiment for Mariner Mars 1971," *Icarus*, Vol. 12, p. 10, 1970.
- IX-4. Davies, M. E., and Arthur, D. W. G., "Martian Surface Coordinates," *J. Geophys. Res.*, Vol. 78, p. 4355, 1973.
- IX-5. de Vaucouleurs, G., Davies, M. E., and Sturms, F. M., Jr., "Mariner 9 Areographic Coordinate System," *J. Geophys. Res.*, Vol. 78, p. 4395, 1973.
- IX-6. Davies, M.E., *Mariner 9 Control Net of Mars: June 1973*, Rand Corporation R-1309-JPL, 1973.

X. Variable Surface Features

The existence of time variations in the albedo markings of the Martian surface has been known for more than a century from visual reports and has since been documented with photographic and photometric evidence. Some details of these changes, including their spatial and temporal development, have been controversial. A progressive contrast change, proceeding in the spring hemisphere from the vaporizing polar cap toward and across the equator, has been reported. This effect has been named "the wave of darkening" by de Vaucouleurs (Ref. X-1). In addition to seasonal changes, there also are many reports of "secular" changes involving unpredictable variations in the contrasts and configurations of surface markings which persist for many years. During a Martian year, because of the changing positions of terrestrial observing stations, relative to both Mars and the Sun, the resolution and the conditions of lighting and viewing of telescope images of Mars change drastically, making the isolation of true seasonal changes from observational effects extremely difficult. Observations from a spacecraft in the vicinity of Mars offer a better opportunity to characterize the gross temporal behavior of variable surface features. Spacecraft observations also are necessary to establish the fine structure of surface changes, providing a better indication of their true nature.

The Mariner 9 mission provided a better opportunity to study these variable surface features than did earlier flyby missions, making it possible to observe the surface of Mars for a longer time and at a higher resolution than ever before. Photometric calibration of the television cameras was performed to provide the capability of detecting subtle changes and to accurately determine their magnitude. Many surface areas that were known or suspected to undergo variations were identified for monitoring during the mission.

A. Observational Strategy

Before the loss of Mariner 8 at launch (see Section I), the orbit of the second spacecraft was optimized to investigate variable surface features. To avoid misinterpretation of brightness variations caused by changing lighting conditions as intrinsic albedo changes, this spacecraft was to arrive over the same area of Mars with all three photometric angles close to constant every several days, the time scale for seasonal changes reported by Earth-based observers (Ref. X-2). With the failure of Mariner 8, this strategy was necessarily abandoned, and Mariner 9 was placed into an orbit representing a compromise among various competing uses of the science systems.

With the post-trim orbital period just under 12 h, the Mariner 9 ground track drifted only about 9° /day. Accordingly, the same region was viewed on successive days with lighting, viewing, and phase angles varying by less than 10° , a value within acceptable limits. An even closer repetition of lighting and viewing conditions occurred after 39 revolutions when the ground track of a zenith pass was close to that of a nadir pass occurring $19\frac{1}{2}$ days earlier, and vice versa. Such picture pairs reproduced the lighting and viewing angles within 2° to 3° , and the phase angle within 5° to 10° . This reproducibility of the three photometric angles was required because the magnitude of albedo variations was expected to be small, and there was the definite possibility of confusing changes in albedo with changing positions and intensities of shadows. Most of the albedo changes discovered were so striking that they would have been observed even without careful control of photometric angles.

Through the end of data acquisition on Rev 676, 28 variable-feature target areas were systematically observed (see Ref. X-2), as indicated in Fig. X-1. These areas represent a wide range of albedos, positions, topographies, and elevations. They include regions reported in the classical literature to be highly time-variable and regions reported to be stable. Until the failure of the filter wheel during Rev 118, some of these regions were observed in three colors and in three polarizations, with the polarization vector stepped in 60° increments. After Rev 118, all wide-angle-camera observations were made with an orange polarization filter. All high-resolution narrow-angle pictures were obtained using a yellow filter. In addition to areas specifically designated as variable-feature targets, certain other areas not previously recognized as susceptible to variation were monitored. These areas included the four major volcanic structures of the Tharsis region.

Coverage of the variable-feature sites was not limited to pictures specifically designated as variable-feature pictures. Mapping, geology, geodesy, atmosphere, and polar frames are potentially useful in the study of variable features. Overlapping mapping frames are particularly useful and provide information on changes taking place during a $19\frac{1}{2}$ -day period.

The variety of pictures of possible significance to variable-feature studies and the lack of any strict definition of the size of a given variable-feature site have made it impractical to provide an exhaustive catalog of variable-feature coverage comparable to that presented for the polar caps in Section VIII. Fig-

ure X-2a shows, for example, footprints of the 26 wide-angle frames, taken between Revs 100 and 262, that intersected a 10° square area (0 to 10° W, 110 to 120° W) which included the caldera of Middle Spot. A single pair of these pictures used as the basis for a digital differenced picture appears in Fig. X-2b. Mariner 9 pictures whose centers fall within 10° square areas centered on two of the variable-feature sites of Table X-1 are identified in Table X-2; lighting and viewing data are tabulated.

Some variable-feature sites sustained obvious changes during the time they were observed by Mariner 9 (see Refs. X-3 and X-4). At least three types of changes were identified:

- (1) An essentially uniform contrast increase caused by the abatement of the dust storm.
- (2) Appearance of splotches, irregular dark markings at least partially related to topography.
- (3) Development of dark linear streaks generally emanating from craters.

The loci of these features appear in some cases to correspond well to Earth-based albedo markings. The integrated time variation of splotches and streaks has been suggested as the cause of the classical "seasonal" and secular albedo changes on Mars (see Ref. X-3).

B. Data Reduction

Only the greater changes in Martian albedo features can be determined by visual inspection of the Mariner 9 pictures. More subtle changes can be detected after geometric projection and registration of the images so that features appear at the same scale and in the same location. Digital subtraction of the registered data can be used to produce pictures showing the actual changes. This type of processing of variable-feature data has been performed at both the Image Processing Laboratory of JPL and at the Artificial Intelligence Laboratory of Stanford University (see Refs. X-5 and X-6); some of the results appear in Figs. X-3 through X-12.

Spatial distribution and directional properties of splotches and streaks have proved to be of as much interest as their time variations. In Fig. X-13 the splotches and streaks in the Mare Tyrrhenum-Hesperia quadrangle (MC-22) have been schematically mapped.

Table X-1. Variable-feature sites

Symbol	Classical name	Location		Symbol	Classical name	Location	
		Latitude	Longitude			Latitude	Longitude
VF1	Thyles Mons	75°S	160°W	VF17	Novissima Thyle	65°S	324°W
VF2	Hellespontica Depressio	60°S	345°W	VF18	Tiphys Fretum	60°N	225°W
VF3	Mare Chronium	60°S	180°W	VF19	Meridiani Sinus	7°S	347°W
VF4	Mare Hadriacum	40°S	270°W	VF20	Hesperia	23°S	241°W
VF5	Mare Sirenum	33°S	152°W	VF21	Bosporos	35°S	62°W
VF6	Argyre	50°S	40°W	VF22	Sinus Sabaeus	11°S	345°W
VF7	Pandora Fretum	20°S	345°W	VF23	Oxia Palus	12°N	17°W
VF8	Syrtis Major/Moeris Lacus	10°N	280°W	VF24	Mare Cimmerium	25°S	191°W
VF9	Cerberus Elysium	10°N	210°W	VF25	Arcadia	53°N	145°W
VF10	Coprates	11°S	70°W	VF26	Tharsis	10°S	107°W
VF11	Lunae Palus	20°N	65°W	VF27	Margaritifer Sinus	20°S	19°W
VF12	Arabia	15°N	315°W	VF28	Iapygia	15°S	301°W
VF13	Ismenius Lacus	40°N	330°W	VF29 ^a	Nix Olympica	18°N	134°W
VF14	Achilles Pons	40°N	30°W	VF30 ^a	North Spot	11°N	104°W
VF15	Propontis	40°N	185°W	VF31 ^a	Middle Spot	0°N	113°W
VF16	Promethei Sinus	70°S	255°W	VF32 ^a	South Spot	9°S	120°W

^aSupplementary site.

Table X-2. Coverage in 10° square areas centered on variable-feature sites

Index number	Rev	Frame number	Center of picture		Range (SRR-5) ^a , km	Lighting angle (SLAR-5) ^a , deg	Viewing angle (VAR-5) ^a , deg	North direction (NORAN) ^a	Sun direction (SUNAN) ^a	Das time
			Latitude (LR-5) ^a , deg	Longitude (LOR-5) ^a , deg						
VF7: Pandora Fretum										
1	30	31	-21.24	348.86	1,399	77.53	2.86	287	17°	2,677,990
2	30	32	-18.69	347.81	1,402	79.42	3.35	257	14°	2,678,025
3	32	30	-23.98	340.95	1,402	74.25	6.16	255	14°	2,749,775
4	48	11	-15.93	347.99	9,687	31.08	56.00	55	183	3,319,790
5	50	11	-17.11	340.12	9,566	33.42	53.37	55	178	3,391,610
6	58	08	-21.02	345.26	8,853	78.59	7.64	45	150	3,678,470
7	143	02	-20.08	349.48	1,687	43.20	10.12	242	158	6,714,643
8	143	03	-17.98	348.22	1,689	44.39	7.83	273	186	6,714,678
9	143	04	-15.45	347.11	1,692	45.55	4.63	243	153	6,714,713
10	145	08	-24.33	342.33	1,697	41.19	15.00	241	164	6,786,533
11	145	09	-22.14	341.28	1,692	41.88	12.91	272	192	6,786,568
12	145	10	-19.59	340.25	1,687	42.67	9.91	242	158	6,786,603
13	184	13	-23.59	346.00	1,673	28.98	11.11	242	184	8,189,374
14	184	14	-21.12	344.62	1,672	29.01	10.57	212	140	8,189,409
15	184	15	-16.52	342.14	1,682	29.80	11.56	214	139	8,189,479
16	186	77	-23.19	343.45	2,622	21.89	57.71	170	130	8,260,774
17	186	08	-22.65	343.19	2,467	21.86	54.41	185	133	8,260,844
18	186	09	-22.84	342.55	2,289	22.63	49.43	191	137	8,260,914
19	186	10	-23.26	342.76	2,116	23.01	43.25	190	145	8,260,984
20	223	05	-23.52	343.05	1,683	25.71	12.40	201	164	9,592,244
21	223	06	-21.00	341.56	1,696	24.74	15.73	171	128	9,592,279
22	223	07	-15.21	340.14	1,680	22.65	9.31	224	166	9,592,454
23	260	06	-23.06	343.82	1,986	27.20	40.25	120	106	10,649,604
24	416	06	-16.13	349.96	1,726	48.71	8.50	94	146	11,443,609
25	459	06	-23.33	343.67	1,771	74.32	24.11	123	183	12,535,485
26	459	07	-23.54	343.16	1,830	73.74	29.01	110	181	12,535,555
27	459	08	-23.23	341.92	1,843	72.46	28.46	86	140	12,535,590
VF8: Syrtis Major/Moeris Lacus										
28	35	05	9.61	282.14	10,160	86.35	44.02	84	182	2,852,010
29	35	06	11.72	280.73	10,160	85.53	46.37	84	181	2,852,080
30	35	07	11.83	276.84	10,070	81.75	47.09	83	186	2,852,150
31	35	08	8.96	276.89	9,875	80.36	44.27	82	186	2,852,220
32	41	02	10.13	280.71	9,665	115.63	118.80	129	120	3,674,265
33	41	03	10.18	279.55	9,500	114.23	116.31	132	132	3,067,335
34	116	29	8.99	280.78	2,106	73.67	6.46	258	151	5,744,303
35	116	30	9.35	280.43	2,148	74.21	8.23	289	182	5,744,338
36	116	31	11.75	279.61	2,181	75.91	6.32	258	151	5,744,373
37	116	32	10.16	280.44	2,296	74.98	14.56	259	153	5,744,443
38	116	33	11.82	279.51	2,331	76.49	13.43	289	182	5,744,478
39	155	22	8.96	284.44	2,214	57.30	13.27	260	155	7,147,313
40	155	23	10.80	283.44	2,243	58.95	11.33	291	184	7,147,348
41	155	24	13.06	282.73	2,273	60.49	8.80	261	152	7,147,383
42	155	25	14.82	281.69	2,309	62.18	6.94	291	182	7,147,418
43	155	27	6.90	281.24	3,005	61.40	40.40	261	166	7,147,663
44	157	22	7.32	276.11	2,169	55.36	13.66	260	155	7,219,273
45	157	23	9.20	275.14	2,197	56.99	11.66	201	184	7,219,308
46	233	07	11.23	283.61	2,813	34.78	31.37	304	203	9,953,514
47	233	08	11.73	284.15	2,887	34.61	32.91	274	173	9,953,549
48	233	09	13.45	282.93	2,905	36.48	30.85	304	201	9,953,584
49	237	07	14.94	281.55	2,664	21.30	40.77	201	150	10,097,294
50	430	08	11.07	283.58	2,086	35.27	19.39	134	207	11,797,941
51	430	09	13.52	282.89	2,152	33.79	19.00	132	209	11,798,011
52	529	10	11.23	284.29	15,445	63.77	46.09	260	199	13,032,077

^aThese terms are defined in Fig. III-15.

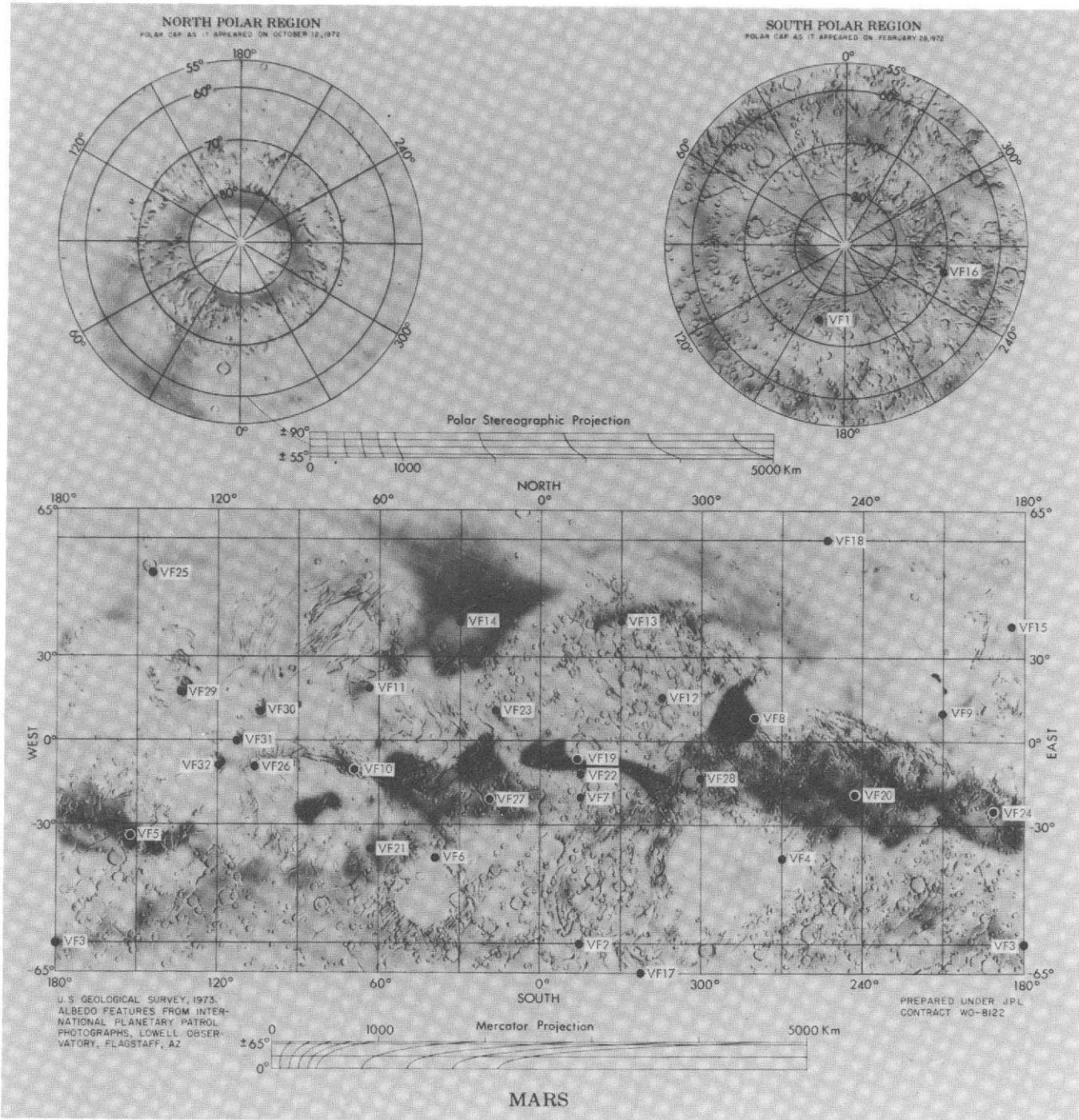


Fig. X-1. Variable-feature sites.

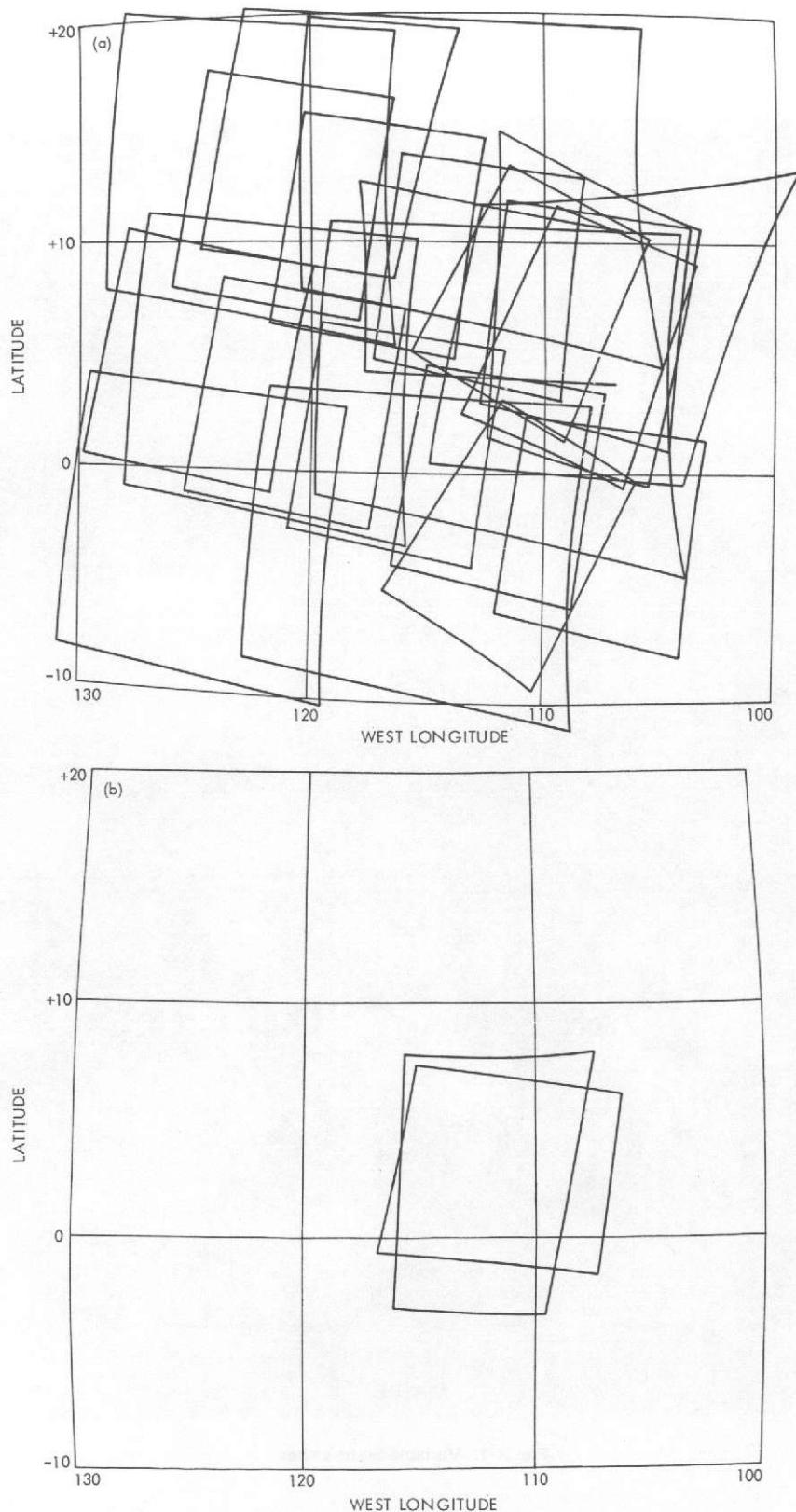


Fig. X-2. (a) Footprints of 26 wide-angle frames taken between Revs 100 and 262.
 (b) Pair of pictures with overlap appropriate for digital differencing.

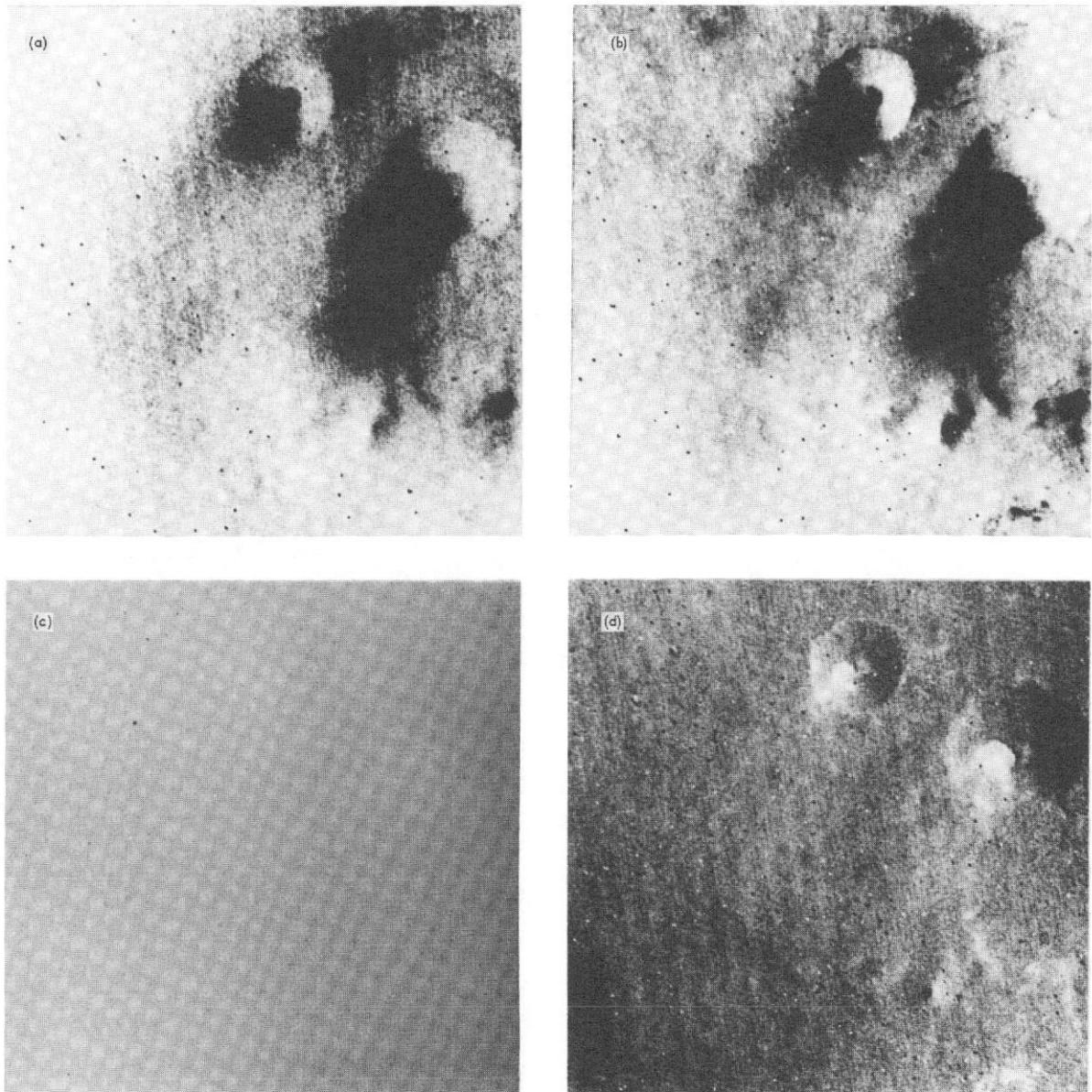


Fig. X-3. Surface variations in region of Hellespontica Depressio. (a) Rev 75, frame 20. (b) Rev 110, frame 07. (c) Differenced picture of a and b. (d) Enhanced differenced picture. Differenced pictures were generated at the IPL. These are not the frames shown in Fig. X-2b.

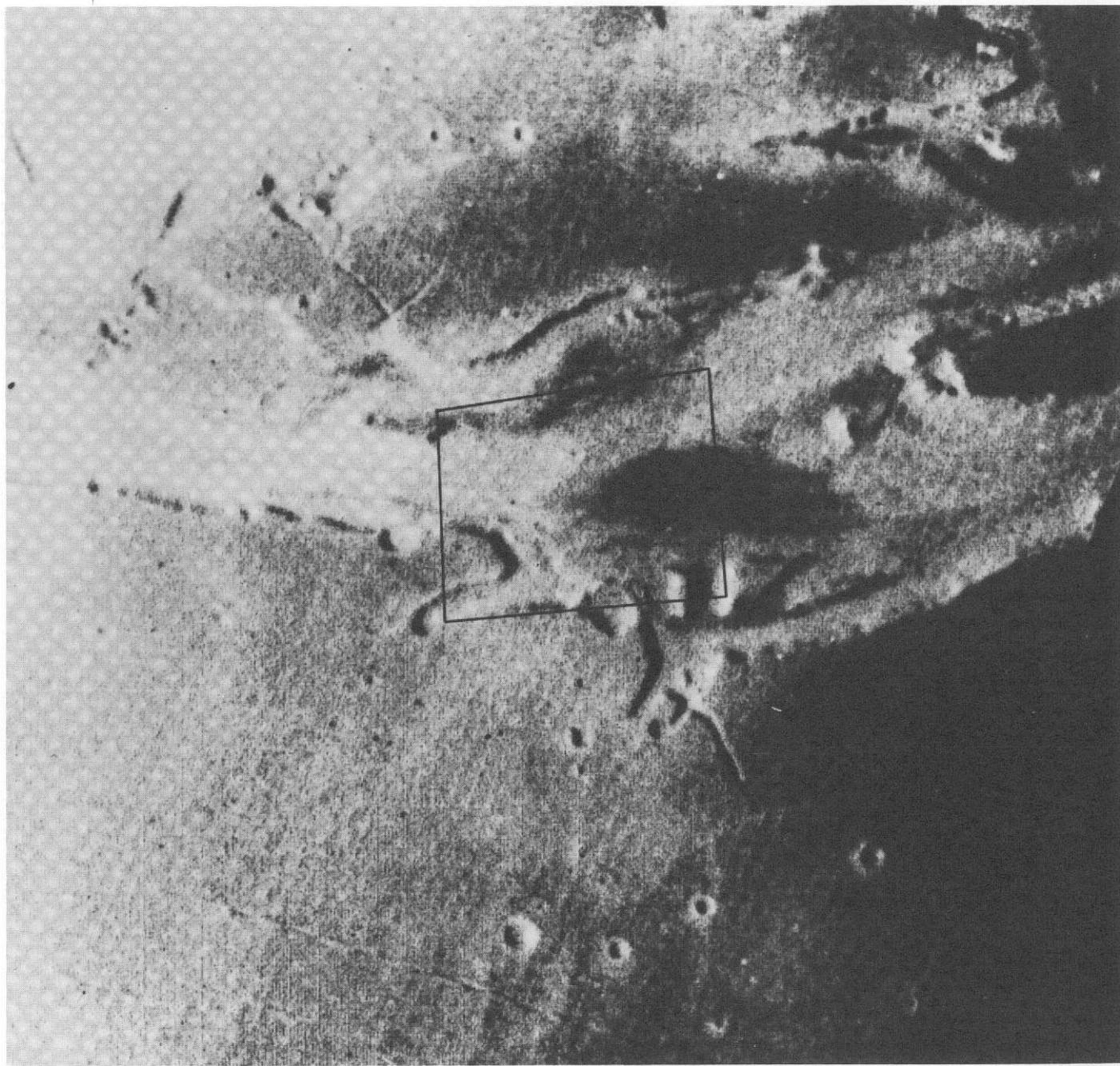


Fig. X-4. Wide-angle-camera view of VF11, Lunae Palus, centered at about 21° N, 63° W. The picture is about 300 km across. (IPL Roll 1329, 181918)

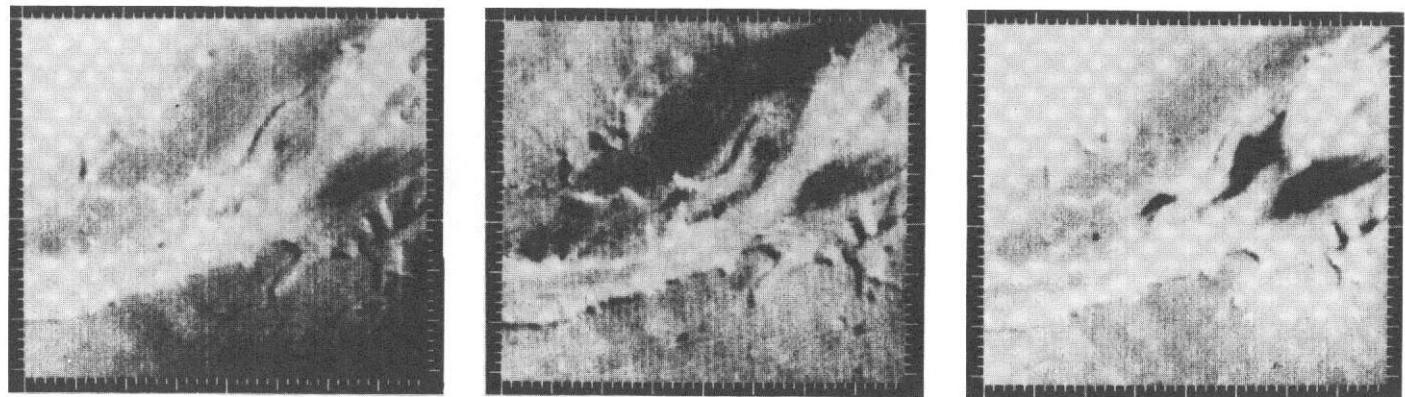


Fig. X-5. Changes within the Lunae Palus channel at the resolution of the wide-angle camera. Left to right: Revs 125, 160, and 238. Note the pronounced darkening within the channel during the 39-day interval between Revs 160 and 238. Center: 23° N, 66° W; $X = 260$ km. (Stanford AIL Picture Products STN 0166, 042911, 042912)

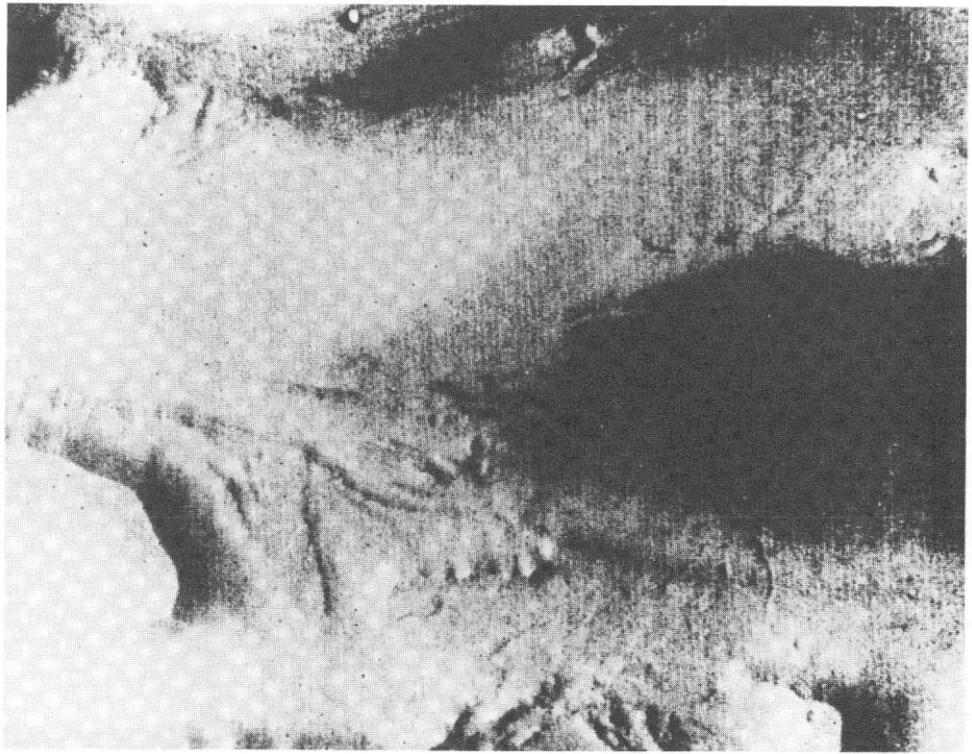


Fig. X-6. Narrow-angle view of the region outlined in Fig. X-4: Rev 160. The picture is about 75 km across and is centered at 22° N, 65° W. (IPL Roll 1329, 185802)

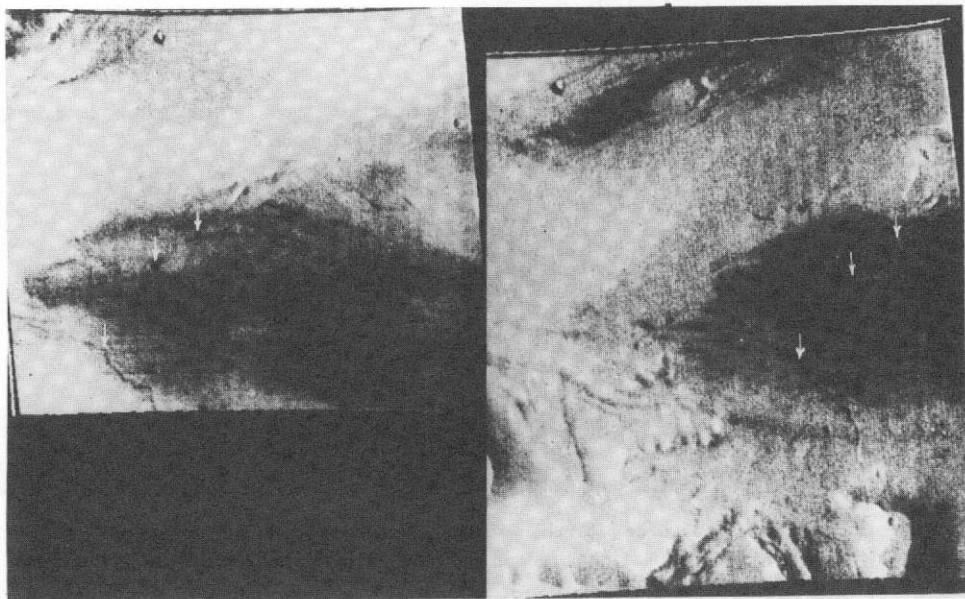


Fig. X-7. Right: Rev. 160. Same area as in Fig. X-6, but shown in orthographic projection. Left: same region observed on Rev 125. These two views do not overlap exactly and are not aligned with respect to each other. In each view, the upper two arrows point to a pair of dark spots; the bottom arrow points to a characteristic bend in the small channel. (IPL Roll 1329, 124209)

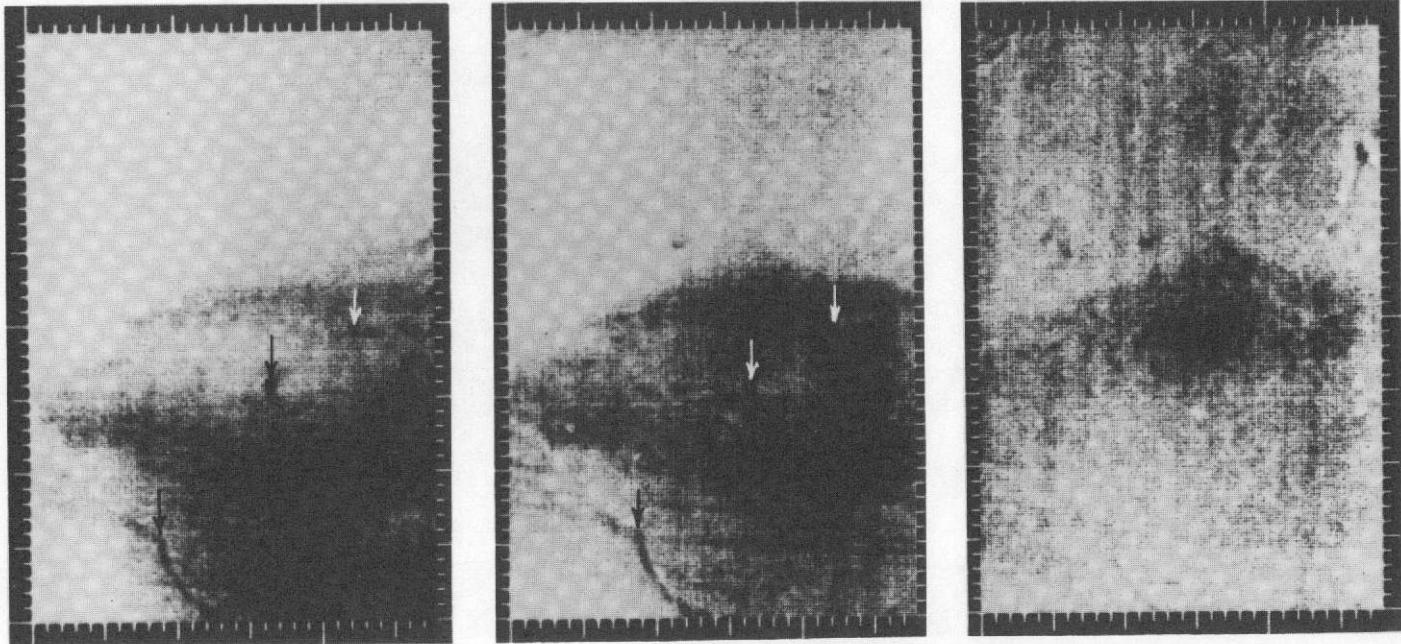


Fig. X-8. Region of the two dark spots and the small channel shown in Fig. X-7. Left: Rev 125. Middle: Rev 160. The two views, similarly scaled and projected, were aligned relative to each other and differenced picture element by picture element to give the picture difference at right. Note the darkening in the vicinity of the two dark spots. Center: 22.6° N, 64.5° W; $X = 30$ km. (Stanford AIL Picture Product STN 0166, 042904)

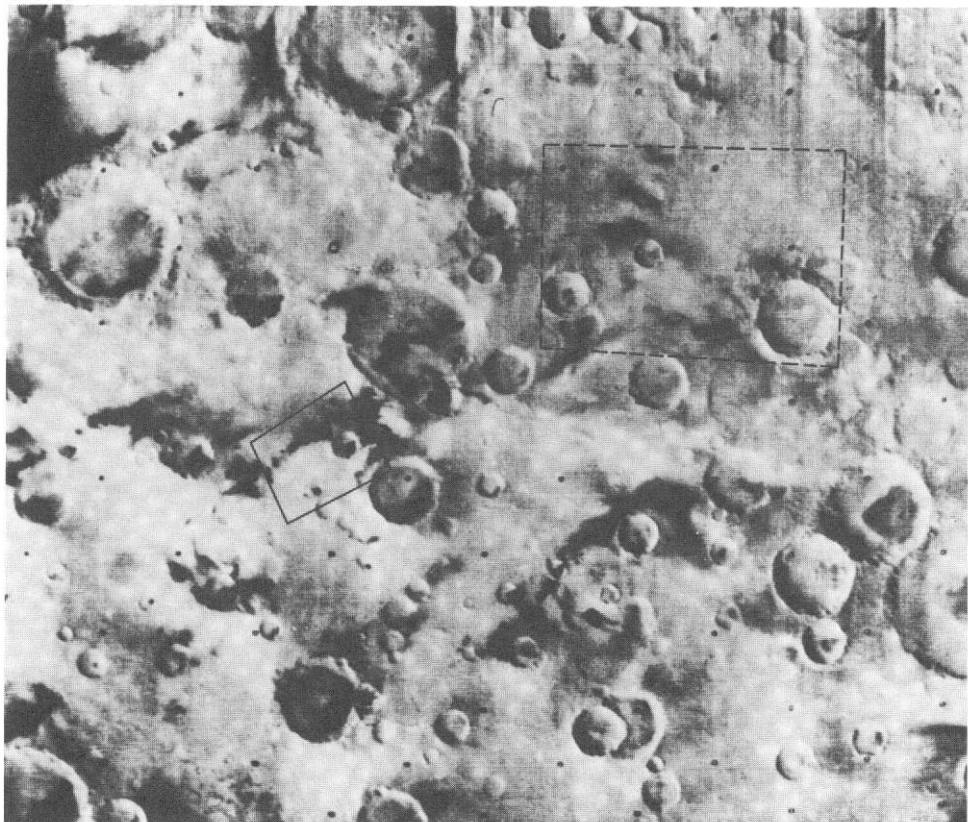


Fig. X-9. Wide-angle view of VF26, Promethei Sinus, centered at 71°S , 269°W . The picture is about 750 km across. The solid outline shows the area of Fig. X-10. The dashed line identifies another time variable zone. (MTVS 4211-09, DAS 08008038)

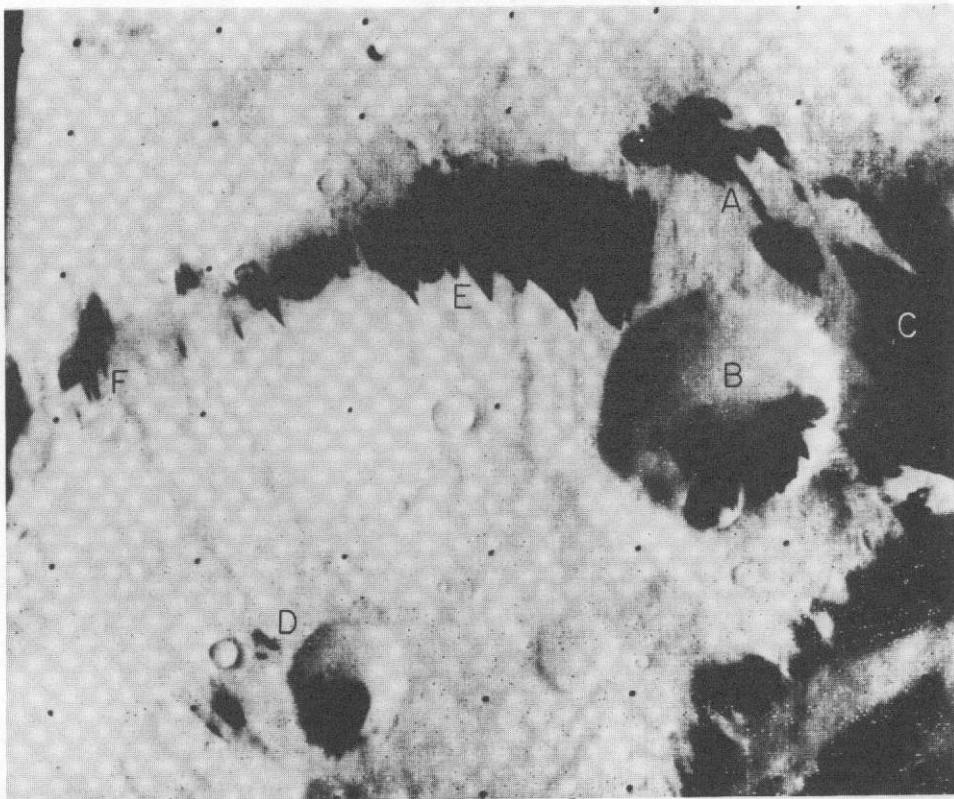


Fig. X-10. Narrow-angle view of region outlined in Fig. X-9. The picture is about 80 km across and is centered at 69.6° S, 253.1° W. Regions of special interest are indicated by letters. (MTVS 4213-12, DAS 08079893)

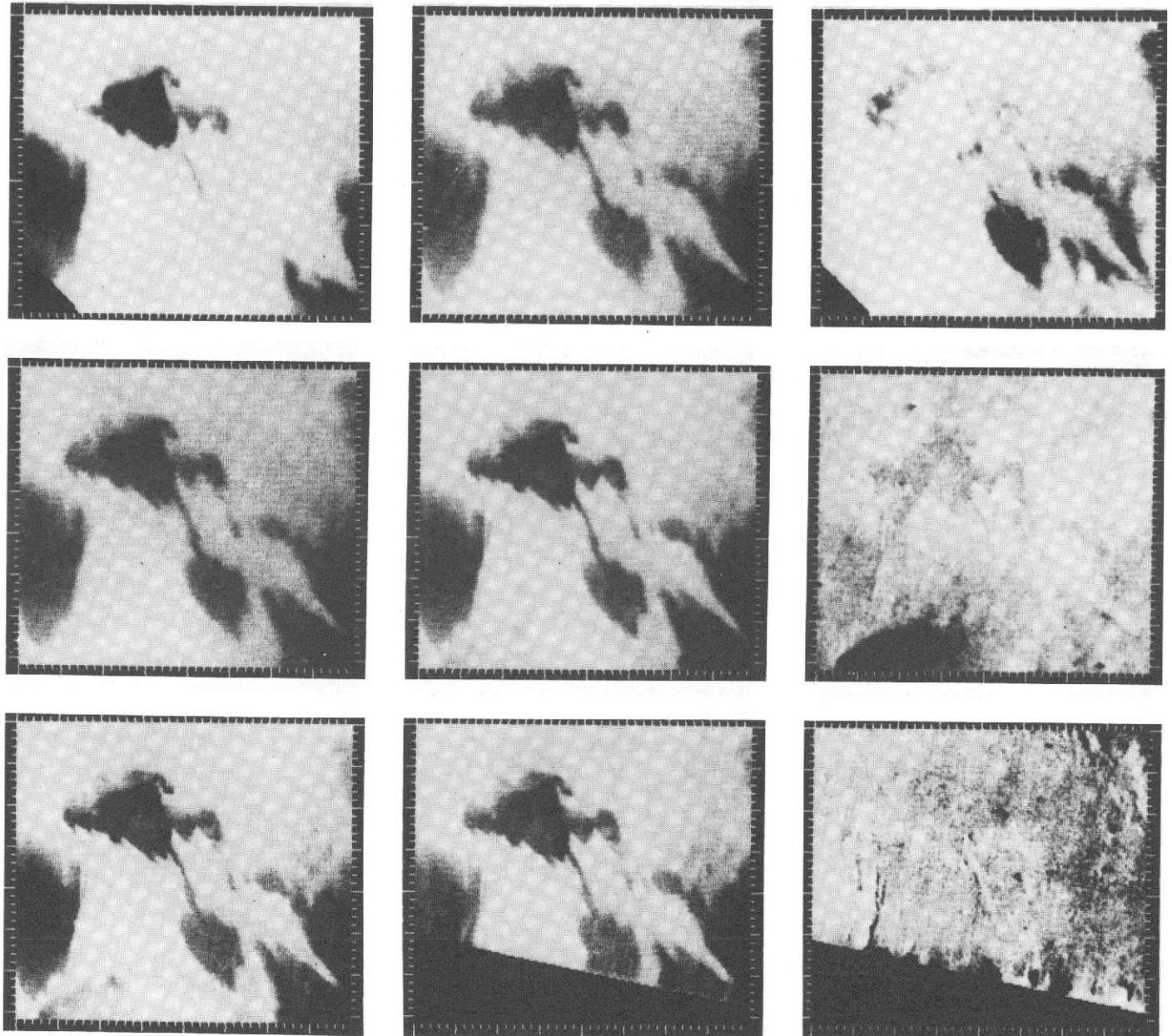


Fig. X-11. Changes in region A. Top row (left to right): Rev 99, Rev 126, Revs 126 to 99. Middle row: Rev 126, Rev 179, Revs 179 to 126. Bottom row: Rev 181, Rev 220, Revs 220 to 181. The window is about 20 km across and is centered at 70.1° S, 253.3° W. (Stanford AIL Picture Products STN 0167, 050609, 050610, 050611)

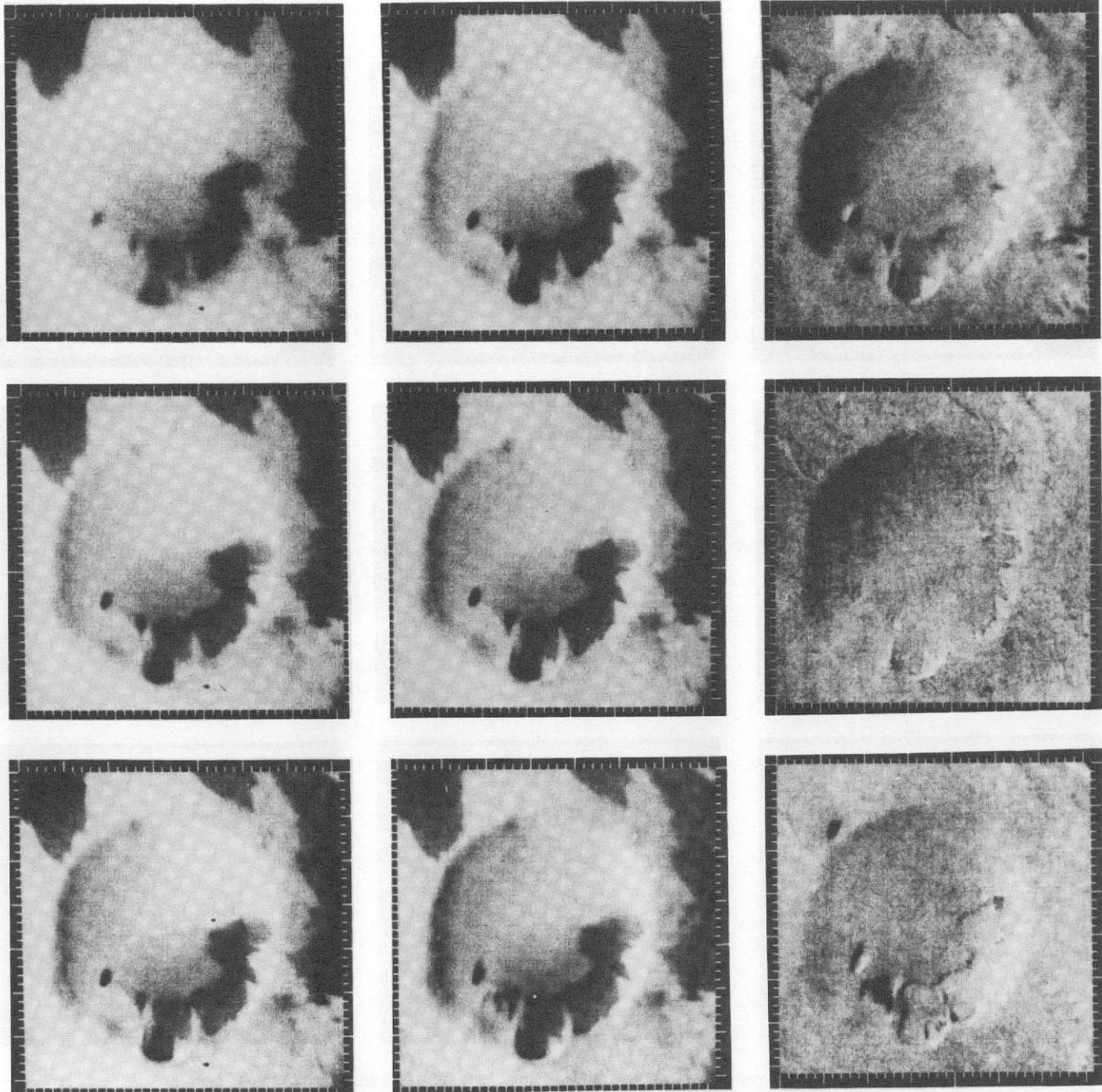


Fig. X-12. Changes in region B. Top row (left to right): Rev 126, Rev 179, Revs 179 to 126. Middle row: Rev 179, Rev 181, Revs 181 to 179. Bottom row: Rev 181, Rev 220, Revs 220 to 181. The window is about 20 km across and is centered at 69.9°S , 253.7°W . (Stanford AIL Picture Products STN 0173, 061109, 061110, and 061111)

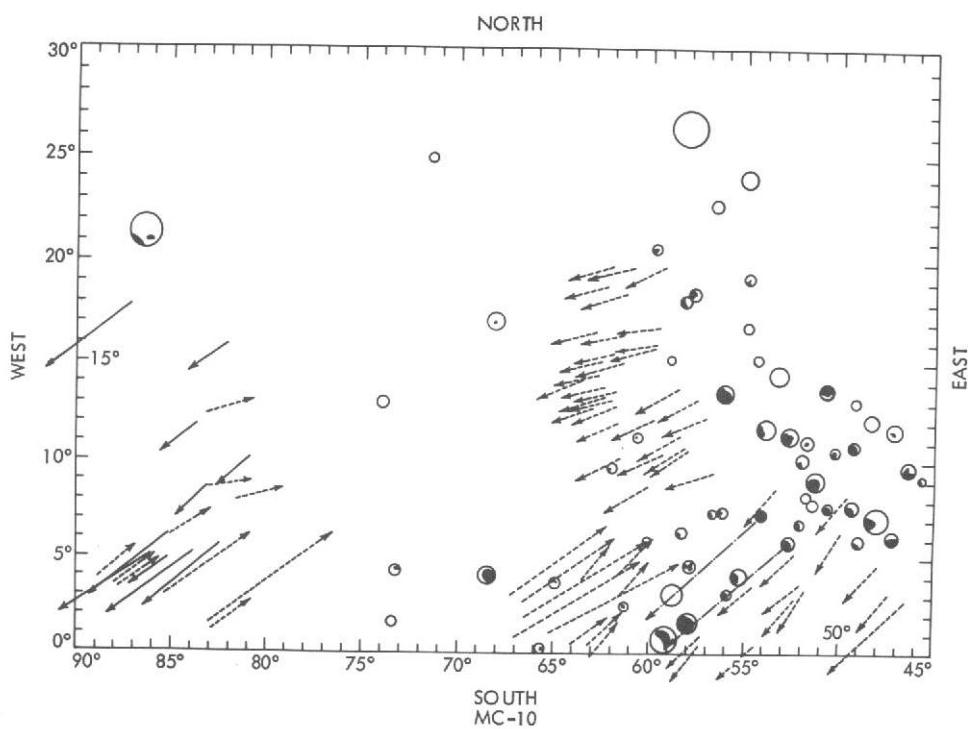


Fig. X-13. Splotch/streak map of the MC-10 region. This is the area surrounding Lunae Palus. Shown are all craters larger than about 50 km in diameter and all dark crater splotches. Solid arrows indicate the directions of dark crater tails, and dashed arrows those of bright crater tails. The arrow length is approximately four times the length of the tail. The shortest arrows shown are 2° (of latitude) and represent crater tails < 30 km in length.

References

- X-1. de Vaucouleurs, G., *Physics of the Planet Mars*, Faber and Faber, London, 1954.
- X-2. Masursky, H., Batson, R., Borgeson, W., Carr, M., McCauley, J., Milton, D., Wildey, R., Wilhelms, D., Murray, B., Horowitz, N., Leighton, R., Sharp, R., Thompson, W., Briggs, G., Chandeysson, P., Shipley, E., Sagan, C., Pollack, J., Lederberg, J., Levinthal, E., Hartmann, W., McCord, T., Smith, B., Davies, M., de Vaucouleurs, G., and Leovy, G., "Television Experiment for Mariner Mars 1971," *Icarus*, Vol. 12, p. 10, 1970.
- X-3. Sagan, C., Veverka, J., Fox, P., Dubisch, R., Lederberg, J., Levinthal, E., Quam, L., Tucker, R., Pollack, J. B., and Smith, B. A., "Variable Features on Mars: Preliminary Mariner 9 Television Results," *Icarus*, Vol. 17, p. 348, 1972.
- X-4. Sagan, C., Veverka, J., Fox, P., Dubisch, R., French, R., Gerasch, P., Quam, L., Lederberg, J., Levinthal, E., Tucker, R., Eross, B., and Pollack, J. B., "Variable Features on Mars, 2, Mariner 9 Global Results," *J. Geophys. Res.*, Vol. 78, p. 4163, 1973.
- X-5. Quam, L., *Computer Comparison of Pictures*, Ph.D Thesis, Stanford University, June 1971.
- X-6. Levinthal, E. C., Green, W. B., Cutts, J. A., Jahelka, E. D., Johansen, R. A., Sander, M. A., Seidman, J. B., Young, A. T., and Soderblom, L. A., "Mariner 9 - Image Processing and Products," *Icarus*, Vol. 18, p. 75, 1973.

XI. Atmospheric Photography

Clouds and haze in the Martian atmosphere were known to occur from Earth-based observations and from the brief 1969 flyby reconnaissance of Mariner 6 and 7. A major goal of the atmospheric studies conducted by the Mariner 9 television cameras was to observe, and thus to achieve a better understanding of, these phenomena. Earth-based observations had indicated that discrete white clouds were a recurrent phenomenon in the regions of Tharsis and Nix Olympica, where Mariner 9 subsequently revealed huge volcanic structures. These white clouds appeared to be composed of either water or carbon dioxide ice. Yellow clouds, presumably dust clouds, also had been recognized by Earth-based observers and were of interest to Mariner 9 experimenters.

Diffuse hazes, including those observed from Earth over the north polar region, were also study objectives. Limb pictures acquired by Mariner 7 revealed that haze in the atmosphere extended to a few tens of kilometers above the Martian surface and exhibited spatial variations in intensity and altitude. These pictures established the feasibility of examining the vertical structure of the atmosphere using television cameras. Horizontal scattering layers were observed that were so thin optically that they appeared as bright bands detached from the surface of the planet. Such scatterings would make a negligible contribution to the light forming an image of the surface obtained with near-vertical viewing con-

ditions, unless the image were obtained near or beyond the terminator where the surface was extremely dark.

Preflight plans for the Mariner 9 television experiment included provision for several different types of atmospheric photography (see Section II). Groups of long-range wide-angle pictures, which included a major part of the illuminated planetary disk, were intended for primary reconnaissance and study of the gross horizontal distribution of cloud phenomena. In some cases, these global frames included part of the limb of the planet and are useful in studies of the horizontal and vertical structures of clouds and haze. For viewing a particular area at significantly higher resolution, groups of wide- and narrow-angle pictures that could be targeted at the particular site were needed. Study of the vertical structure of the atmosphere was conducted by means of limb pictures designed to include part of the illuminated horizon of Mars. Images of the terminator (day/night boundary) also were scheduled because clouds are enhanced in brightness relative to the surface when the Sun is low in the sky, and cloud formation was expected to accompany the rapid temperature changes of Martian dawn and dusk.

In this section, atmospheric photography is organized into four categories: global, targeted, limb, and terminator. This

classification is not rigid. A specific pair of wide-angle (A) and narrow-angle (B) frames targeted at an interesting cloud feature may provide coverage similar to that in many frames designated "global" and, if the horizon is also included, becomes a limb frame. Many pictures planned for study of geology, polar frost phenomena, or variable surface features also revealed atmospheric phenomena. Many photographic sequences, notably those of the volcanic features of the Tharsis ridge, were recognized as being dual purpose in the planning phase because they were likely to show details of geologic and meteorologic interest. The classification into which such dual- or multi-purpose images are placed in this document was strongly influenced by the intent of those who originally planned the photography.

A. Global Pictures

In mid-September 1971, Earth-based telescopes first showed the existence of a dust storm in the southern hemisphere of Mars. Within 1 week it expanded to global proportions, and almost all of the typical Martian features were obscured. This condition remained through October and November as Mariner 9 approached the planet, and the first global pictures of Mars (acquired before the spacecraft was inserted into orbit) showed almost no detail in the illuminated Martian crescent. These pictures precluded any lingering hopes that it might be possible to observe white cloud activity in the Tharsis region and hazes near the morning terminator. However, they soon established that important scientific observations of the almost totally obscuring dust storm could be made by using the television cameras.

During three pre-orbital science sequences (POS-1, POS-2, and POS-3), 75 long-range pictures of Mars were obtained, and some pictures were directed at the Martian satellites (see Section XII). In the earliest narrow-angle frames of Mars, taken during POS-1, Mars appeared in the gibbous phase and occupied only a small part of the field of view of the camera. Pictures were taken on 1-h, 1½-min centers, so that the planet rotated 15° during the interval between each frame. During POS-3 the planet more than filled the field of view of the narrow-angle camera, and pictures were taken in mosaickable groups with a longer time interval between groups. Photography continued until less than 8 h before firing of the spacecraft's injection motor.

Examples of frames taken during the POS-1, POS-2, and POS-3 sequences appear in Fig. XI-1. A POS-1 frame taken from more than 670,000 km appears in both raw and contoured versions in Figs. XI-1a and XI-1b. The planet was almost featureless at that range except for four dark spots, subsequently identified with four shield volcanos in the

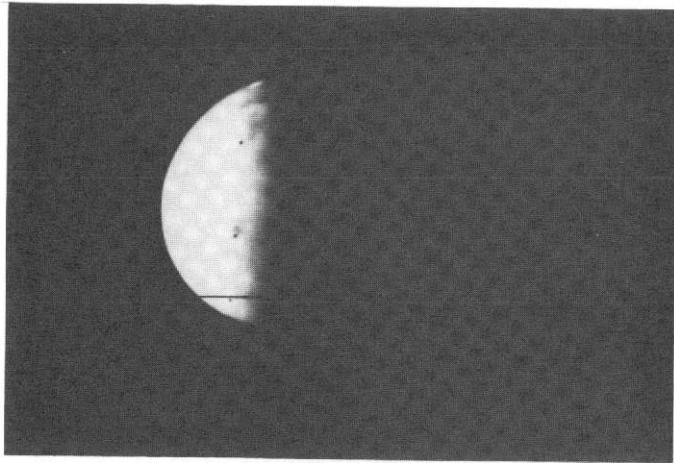
Tharsis region north of the equator near 120° longitude, and the small bright southern polar cap. These five features can be seen most readily in Fig. XI-1b as small circular or oval features imposed on the otherwise regular contour lines. A POS-2 narrow-angle picture taken significantly closer (178,000 km) shows the south polar cap more clearly (Figs. XI-1c and XI-1d). In all of these POS pictures, the northern part of Mars is near the bottom of the frame.

In a POS-3 narrow-angle picture (Fig. XI-1e), taken from 104,000 km, the planet more than fills the frame. Severe computer enhancements revealed a complex "wake" in the dusty atmosphere trailing from one of the four dark spots. All four spots and other complex atmospheric structures appear in a mosaic (Fig. XI-2) of this frame and three other frames that have been processed to exhibit maximum detail. Five wide-angle frames taken through different color filters (e.g., Fig. XI-1e) completed the pre-orbital photographic coverage of Mars.

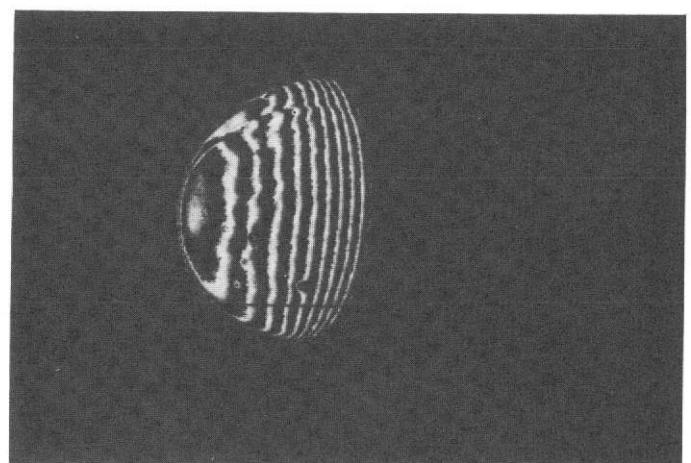
In the sequences of global photography after orbit insertion, the surface was almost completely obscured, but certain parts of the planet showed visible atmospheric activity. The coverage of this period is summarized in Table XI-1; more detailed information is given in Volume II of this document. One notable difference, apparent when these frames are compared with pre-orbital frames, is that north is at the top rather than at the bottom of the frame. A change of almost 180° in scan platform clock angle, which was necessary to bring the planet into the field of view after orbit insertion, was responsible for this.

Typical mosaics of global pictures acquired up to Rev 138 appear in Figs. XI-3 through XI-5. The routine (real-time) processing had not been upgraded when most of these early pictures were taken (see Section IV), and few of them have been subjected to special computer processing. They contain intrinsically less scene detail than global pictures acquired toward the end of the mission. However, it may be possible to extract important information concerning dust storm activity and atmospheric circulation from these rather unpromising data.

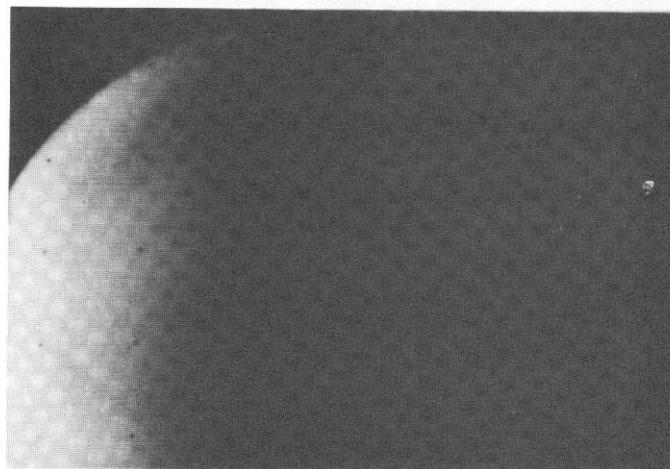
As the mission progressed, the time when the planet first moved into the field of view of the wide-angle camera shifted closer to periapsis, temporarily preventing the acquisition of additional global pictures. This shift was caused by mechanical constraints on instrument platform pointing and by the changing relationship of the spacecraft's orbit to the Sun direction, which determined the spacecraft's orientation in space. For the same reasons, the northern hemisphere could be viewed for a steadily increasing period after periapsis. However, in the period between Revs 139 and 262, the atmo-



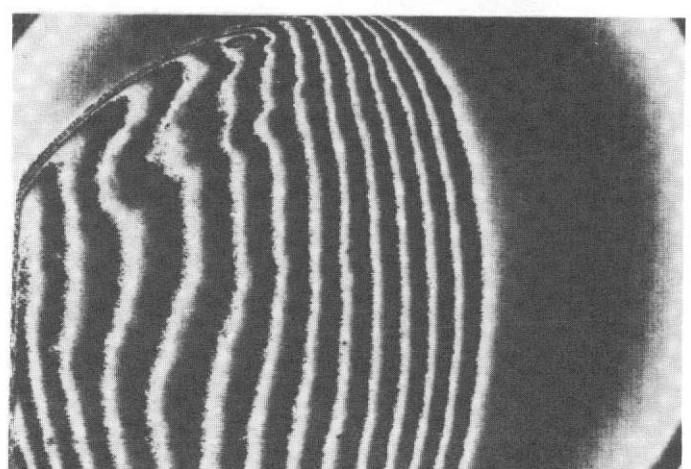
(a) POS-1: RAW



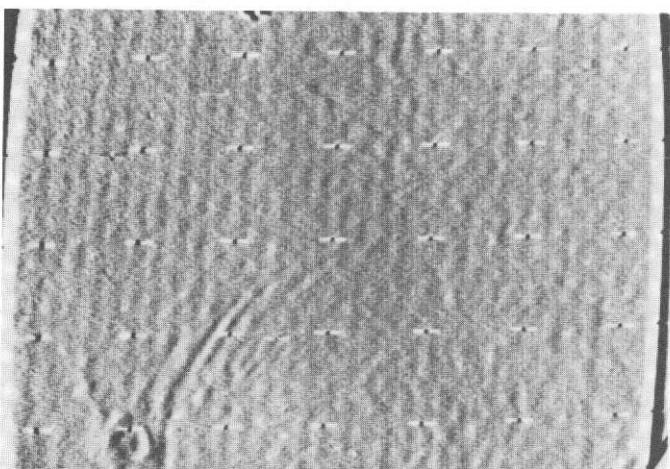
(b) POS-1: CONTOURED



(c) POS-2: RAW



(d) POS-2: CONTOURED



(e) POS-3: HPF



(f) POS-3: HPF

Fig. XI-1. Pre-orbital global coverage. South is at the top. (a-e) Narrow-angle frames. (f) Wide-angle frame.

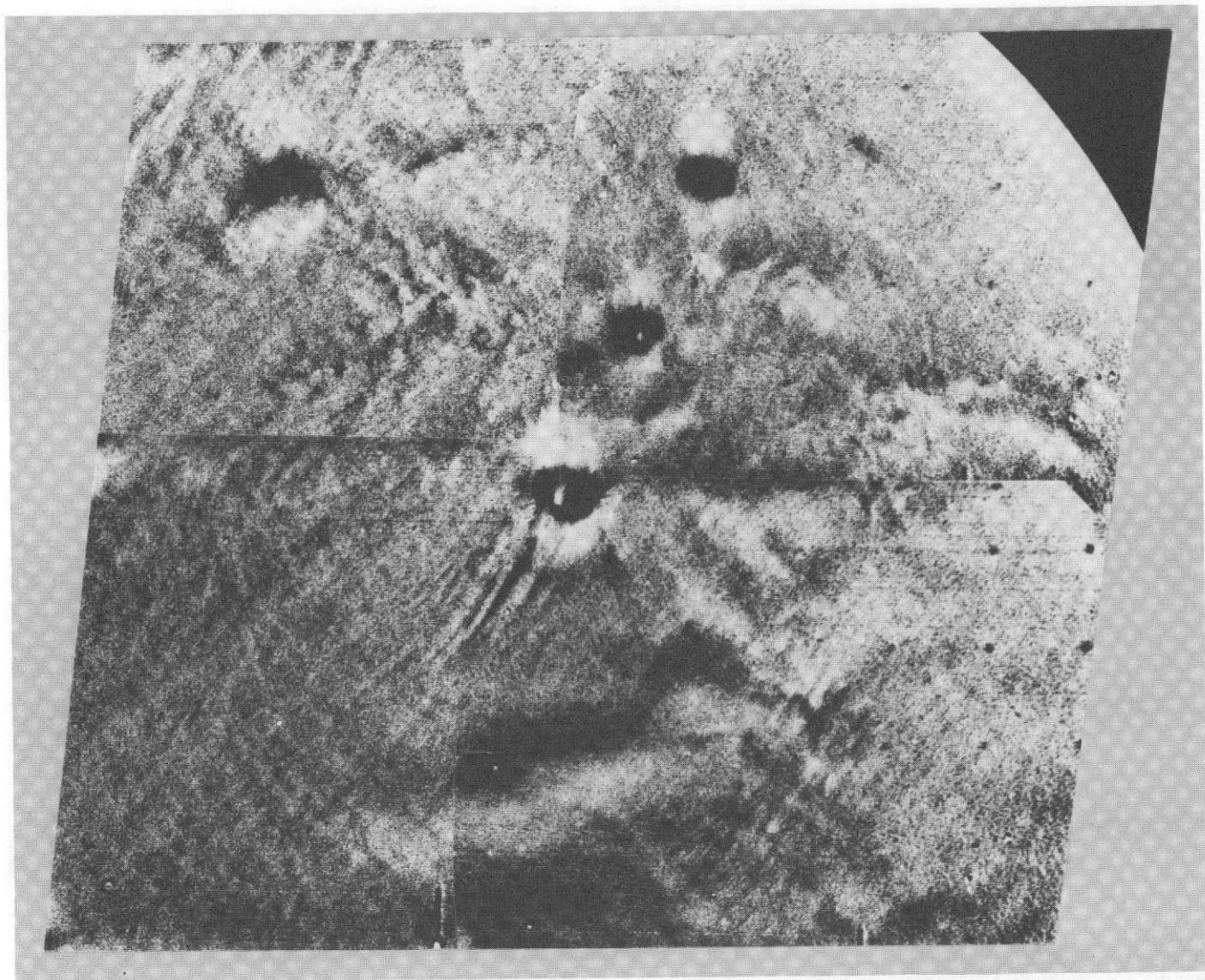


Fig. XI-2. Mosaic of pre-orbital (POS 3) narrow-angle frames showing the four dark spots.

spheric photography acquired within ± 1 h of periapsis was limited to single frames, doublets, or triplets. No attempt was made to cover the major part of the lighted disk. This coverage, therefore, is included in Section XI-B.

When the spacecraft resumed operation after solar occultation, Revs 416 through 459 were used to complete medium-resolution mapping coverage of the north polar collar (50° N to 65° N) and the Mare Boreum quadrangle (65° N to 90° N). These sequences were performed when the spacecraft was locked onto the star Arcturus; after their completion, Canopus was reacquired and again global pictures were acquired. Global frames were obtained during Revs 478 and 479 (Fig. XI-6), and a spectacular set of three frames was obtained during Rev 528. This revolution was selected carefully so that

the coverage of the major cloud phenomena and other physiographic features would be optimal. Figure XI-7 is a mosaic made from three specially processed frames.

When the spacecraft acquired Vega on Rev 667, it was possible to observe Mars from another viewpoint. During this period, wide-angle frames were targeted on cloud phenomena of Nix Olympica and North Spot; they are presented in Section XI-B. However, two single global pictures were obtained from close to the maximum range of the orbiting spacecraft (apoapsis). These pictures provide spectacular views of Syrtis Major and Meridiani Sinus, two of the most conspicuous surface markings on Mars known to planetary astronomers (Fig. XI-8).

Table XI-1. Summary of global photography

Revs	Science cycle	Orbital science links ^a	
		Zenith pass (even revolutions)	Nadir pass (odd revolutions)
1-15	Post-orbital insertion mapping, calibration, and phase function	—	—
16-23	Interim sequence	Atmospheric: 3A(V), 1A(O) (-2 ^h) ^b	Atmospheric: 4A(V), 1A(O) (-2 ^h)
24-63	Recon I	Global TV: 5A(V) (-1 ^h 44 ^m) 5A(O) (-1 ^h 33 ^m)	Global TV: 5A (1 ^h 45 ^m) ^c
64-99	Recon II	Global TV: 1B, 8A, 1B (-1 ^h 21 ^m 36 ^s) ^d	Global TV: 8A (-1 ^h 20 ^m 54 ^s) ^e
100-138	Mapping Cycle I	Global TV: 5A (-59 ^m 36 ^s) ^f	Global TV: 5A (-59 ^m 36 ^s) ^f
139-177	Mapping Cycle II	—	—
178-217	Mapping Cycle III	—	—
218-262	Extended mission, Phase I	—	—
416-459	Extended mission, Phase II: Arcturus	—	—
473-533	Extended mission, Phase II: Canopus	Global TV: 2A (3 ^h 3m39 ^s), Rev 478 only 3A (3 ^h 2m42 ^s), Rev 528 only	Global TV: 2A (2 ^h 54m19 ^s), Rev 479 only
667-676	Extended mission, Phase IV: Vega	—	Global TV: 1A (5 ^h 29m54 ^s), Rev 667 only 1A (4 ^h 13m27 ^s), Rev 675 only

^aThe concept of picture links is described in Section II.

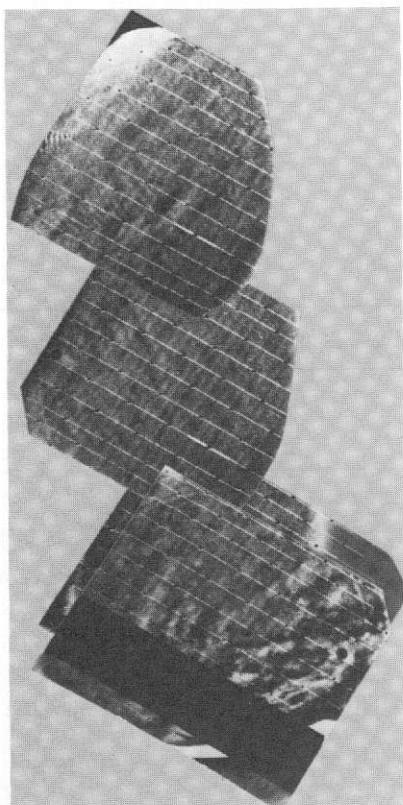
^bTimes listed are nominal times from periaxis as listed in Volume II.

^cOrange (O) and violet (V) on alternate revolutions.

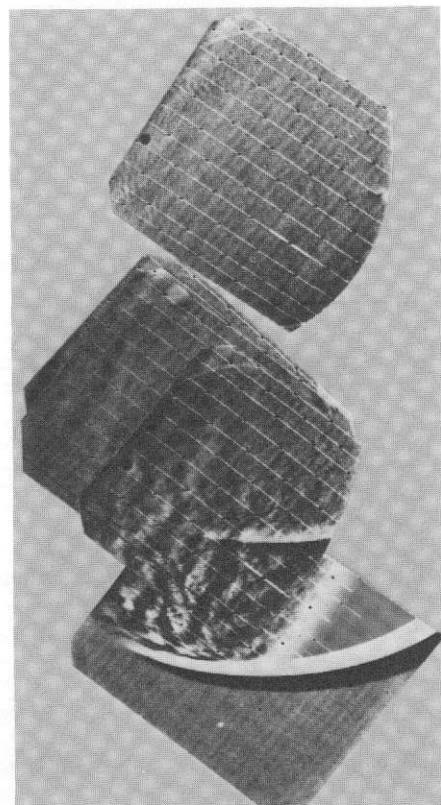
^dPrimarily mosaic of lighted disk; some calibration.

^eMosaic of lighted disk; various filters.

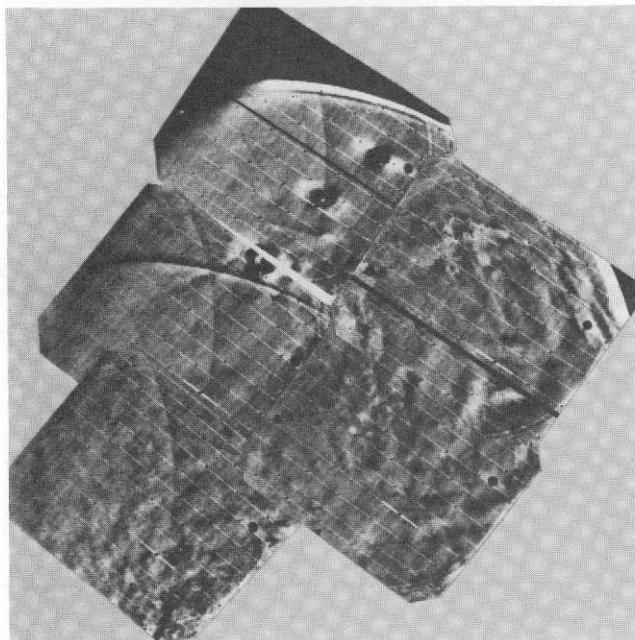
^fMosaic of lighted disk; some special targeting.



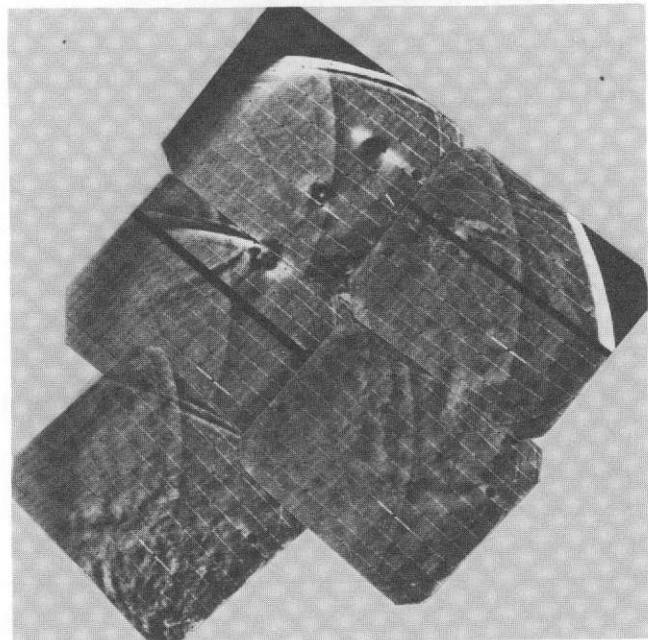
(a) INTERIM: REV 18



(b) INTERIM: REV 23

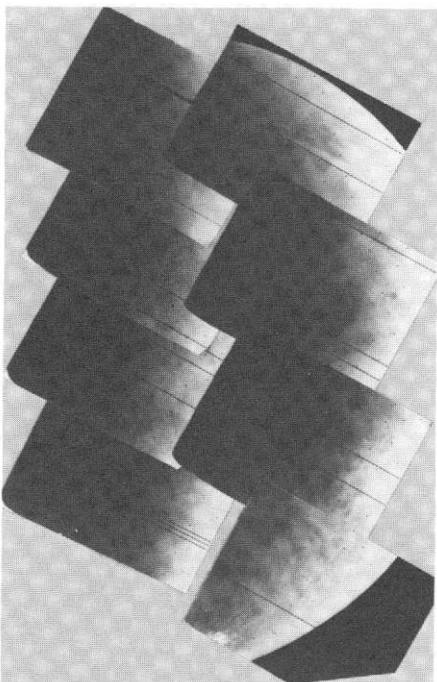


(c) RECON I: REV 30

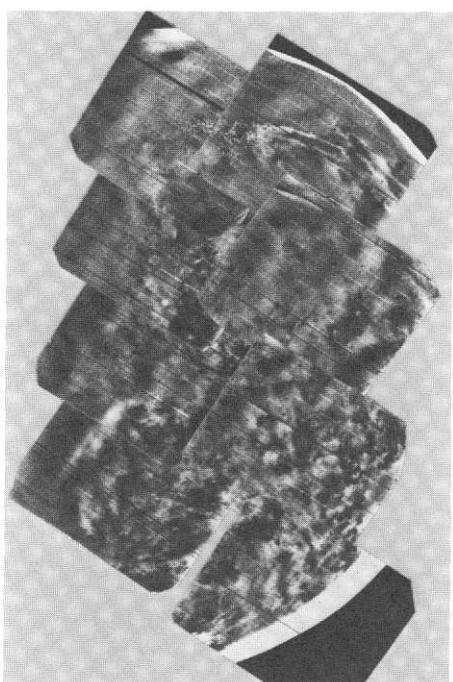


(d) RECON I: REV 30

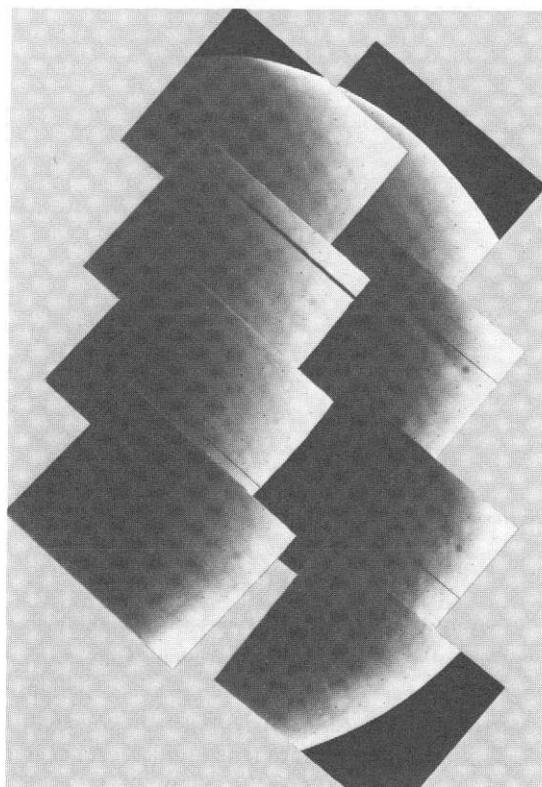
Fig. XI-3. Mosaics of global pictures typical of the interim and Recon I sequences: HPF versions. (a) Zenith pass: three violet frames, one orange frame. (b) Nadir pass: four violet frames, one orange frame. (c) Zenith pass: five orange frames. (d) Zenith pass: five violet frames. In Figs. XI-3a and XI-3b, the single orange frame is almost registered with one of the violet frames.



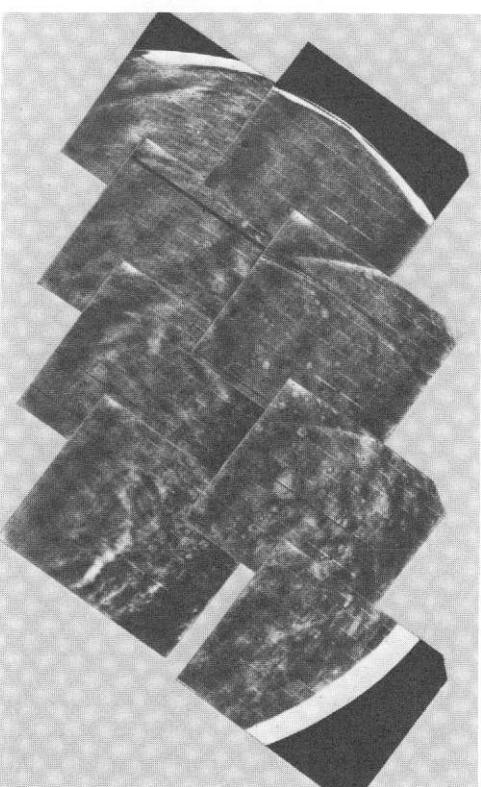
(a) REV 69: SHADING-CORRECTED



(b) REV 69: HPF

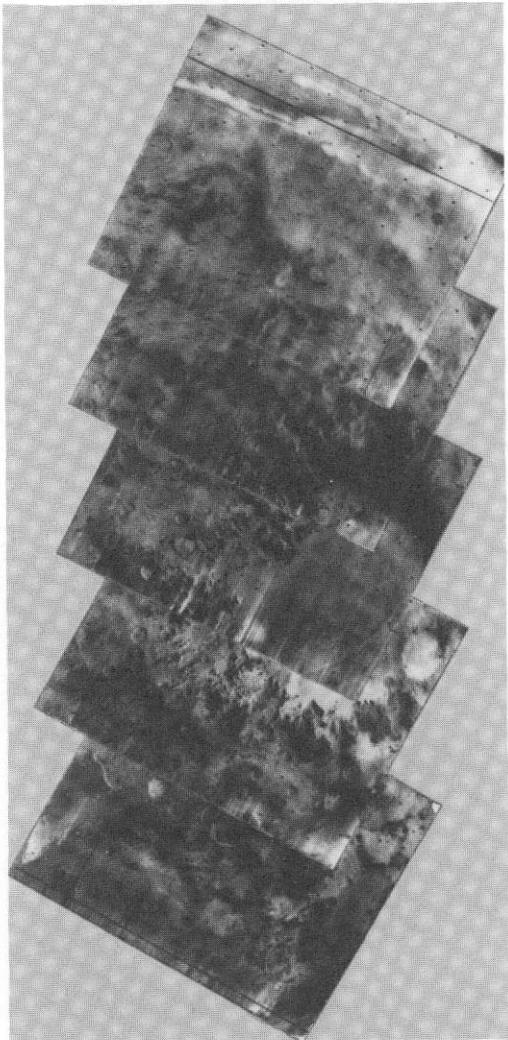


(c) REV 78: SHADING-CORRECTED

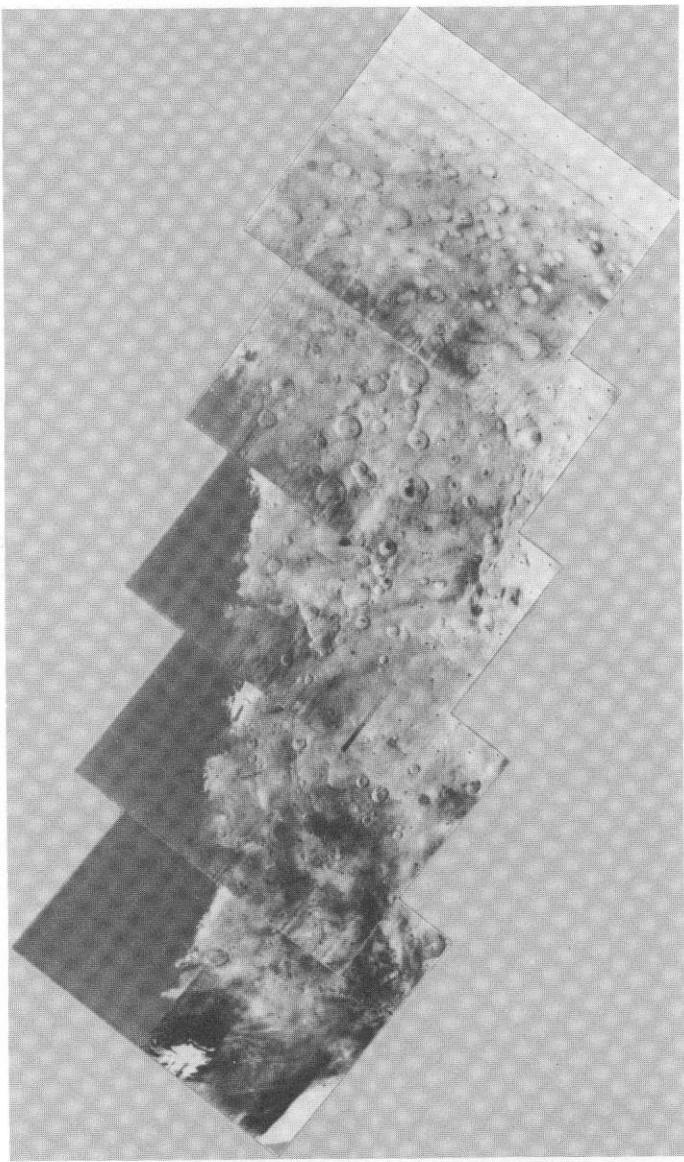


(d) REV 78: HPF

Fig. XI-4. Mosaics of global pictures typical of the Recon II sequences. (a, b) Orange frames. (c, d) Violet frames.



(a) REV 112



(b) REV 132

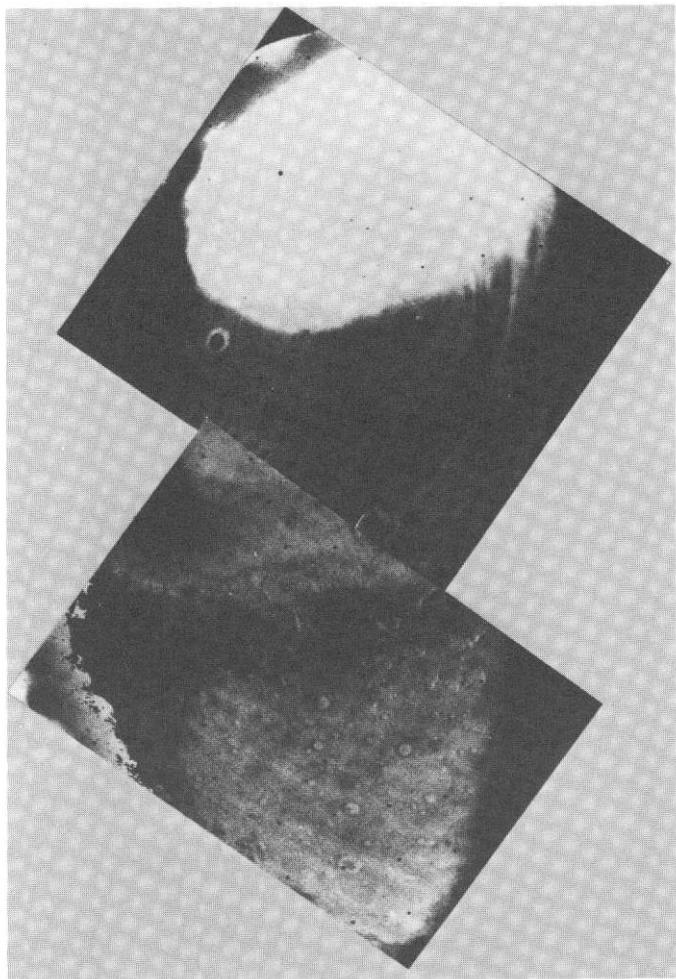
Fig. XI-5. Mosaics of global pictures acquired during Mapping Cycle I using a polarizing filter: VAGC versions.

B. Targeted Pictures

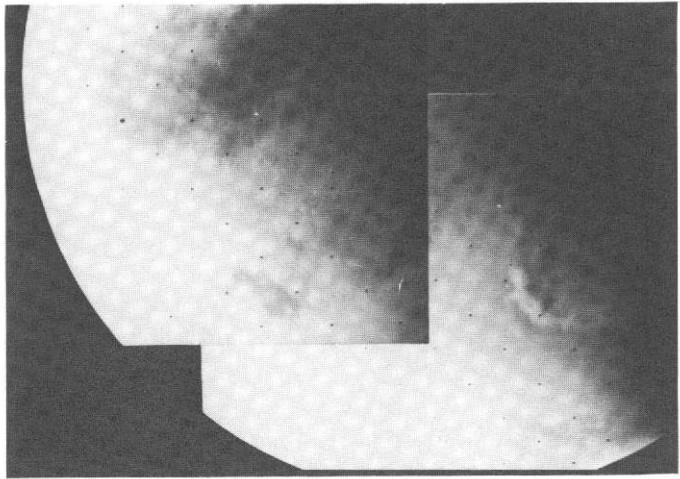
Before the Mariner 9 mission, it was anticipated that targeted links (see Section II) would be used primarily to observe areas on Mars in which Earth-based observations had revealed cloud activity, and to obtain better resolution of clouds that were first detected in global pictures. Because of the dust storm, targeted sequences served an additional function of systematically probing the dust-covered atmosphere for any indications of improving transparency. This targeted imagery for atmospheric studies included single narrow-angle

frames; mosaickable sets of two, three, or four narrow-angle frames; and nested wide- and narrow-angle frames. Single or multiple narrow-angle frames taken closer to periapsis than 30 min and frames taken after Rev 100 generally were intended for geologic rather than atmospheric studies. An accompanying wide-angle frame was usually required to establish an appropriate context for atmospheric detail visible at higher resolution.

Targeted photography acquired during the mission is summarized in Table XI-2. Up to Rev 262, picture sequences



(a) REV 478



(b) REV 479

Fig. XI-6. Mosaics of global pictures obtained during Phase III of the extended mission. In Fig. XI-6a, the frames have been digitally processed to suppress the large brightness differences due to variations in solar zenith angle, permitting the enhancement of detail near the edge of the north polar cap and in the eastern part of the frames (see Volume II Addendum for details of the parts of the planet covered).

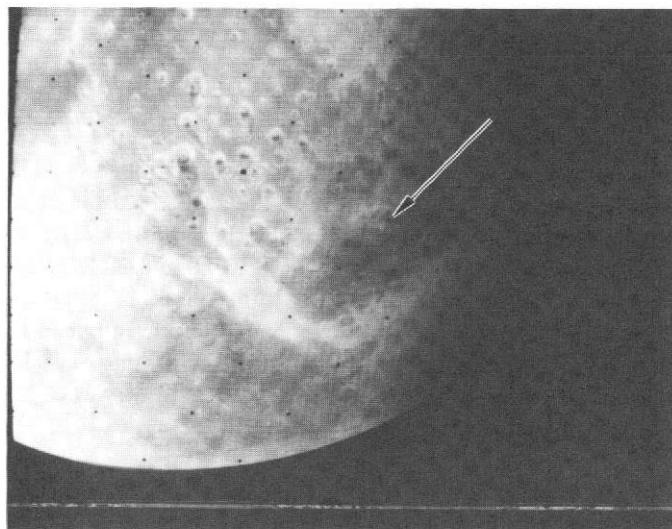
(links) were extremely rigid and fixed for the duration of each cycle. For example, on zenith passes of Recon II, between Revs 64 and 98, a tetrad picture sequence consisted of four narrow-angle frames that were taken at a fixed time with respect to periapsis; only the pointing of the camera could be adjusted and only within specific limits (see Section II). During the extended mission, greater flexibility was introduced when the time at which each link was taken was allowed to change. However, the links still had to occur in the same sequence, and a 5-min "time pad" had to separate them. In Phase II of the extended mission (Revs 416 through 459), it was possible to design entirely different picture sequences each revolution, partly because data were obtained on only two revolutions per week. For that reason, the picture sequences lost their identity as dyads, tetrads, etc., and the type and number of frames were explicitly tailored to each target.

Examples of mosaics and single frames of targeted photography from the standard mission are shown in Figs. XI-9 through XI-11. In Fig. XI-12, the location of each targeted link between 65°N and 65°S is plotted in Mercator Projection against the background of an airbrushed map of Martian surface features. These links are identified by symbols and by revolution number so that it is possible to identify them unambiguously by referring to the footprint plots given in Volume II. Links primarily intended for geology and variable features also are included. Very few links were directed north of 65°N until Rev 262; however, many were directed south of 65°S and included the polar cap, some variable features, and the limb of the planet.

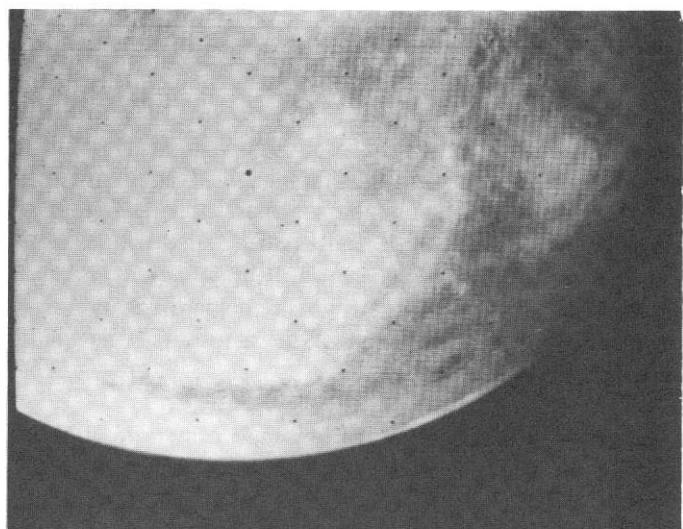
These simple plots of target locations are convenient for showing the distribution of the targeted frame in space and in



Fig. XI-7. Mosaic of global pictures obtained during Phase III of the extended mission (Rev 528). The mosaic covers almost all of the illuminated disk of Mars. At the top is the north polar cap. At the bottom are the four major shield volcanos that appeared as four dark spots in earlier pictures of the dust-covered planet.



(a) REV 667: MERIDIANI SINUS



(b) REV 676: SYRTIS MAJOR

Fig. XI-8. Global pictures obtained during Phase IV of the extended mission. These pictures show well known classical Martian surface features. (a) Dawes Forked Bay (arrow) was used as the Martian central meridian for more than 200 yr, until Mariner 9 provided a more precise reference (see Section IX). (b) Syrtis Major, the dark area north of the large circular crater near the lower right, is one of the most active Martian variable features.

time; however, they do not show the area covered by each picture group (see Volume II). Figure XI-13 is a footprint plot that shows coverage for the targeted frames taken during Recon I. There is insufficient space here to reproduce more of these plots, and the large amount of data presented on a single plot presents labeling problems. However, a complete set will be obtainable from the National Space Science Data Center (NSSDC) as part of the Mariner 9 data set (see Volume I Addendum).

Only isolated examples of frames for the early targeted sequences of the mission are included in this document (Figs. XI-9 through XI-11). However, during Mapping Cycle III, the final tetrad on both zenith and nadir passes included two wide-angle frames that regularly exhibited atmospheric structure. The last one or two frames in the mapping sequences, immediately preceding the targeted tetrads, also exhibited atmospheric structure, specifically at the north polar hood. These targeted and mapping frames were combined into the "hybrid" mosaics that appear in Fig. XI-14 (see Ref. XI-1).

In the final phases of the extended mission, pictures were no longer taken each revolution and, as already noted, different patterns of data acquisition were used on each data-taking revolution. Plots of all targeted locations between Revs 415 and 676 (Phases II, III, and IV) are not as meaningful as plots for the earlier revolutions. Most targeted pictures of atmospheric phenomena are reproduced in Fig. XI-15.

Figures XI-15a, XI-15b, and XI-15c are targeted wide-angle frames of Nix Olympica and the south polar region taken during Phase II of the extended mission. A wide-angle picture of the south polar region was commanded during Rev 436, but was not transmitted.

Figures XI-15d and XI-15e are two targeted frames acquired during Phase III of the extended mission. Another frame, a wide-angle frame targeted at Tempe during Rev 578, was not recovered. During Phase IV of the extended mission, 16 frames were targeted at atmospheric features; frames from Rev 668 (Figs. XI-15f and XI-15g) covered Elysium and Nix Olympica, and those from Rev 676 included North Spot and the Tharsis region. Interpretations of many of these pictures are presented in Refs. XI-2 and XI-3.

C. Limb Pictures

The limb, or horizon, appears in many wide- and narrow-angle pictures of Mars (see Table XI-3). Although all narrow-angle pictures that include the limb were targeted deliberately, some narrow-angle frames missed the limb, showing either black space or a part of the planet at extremely high viewing angles. Inclusion of the limb in wide-angle frames was usually incidental to another photographic objective, most often global coverage (see Figs. XI-1 through XI-11). However, wide-angle frames targeted at the limb were commonly associated with one or two narrow-angle frames as a dyad or triad.

Wide-angle limb frames in most cases revealed detached layers of thin haze (Fig. XI-16a), several tens of kilometers above the planetary surface, which extend horizontally over the surface of Mars for hundreds of kilometers. Horizontal changes do occur; the layers are observed to change in elevation, merge with other layers, and to fade gradually or terminate abruptly in the lateral or horizontal plane. Numerical profiles across the limb reveal levels and gradients in brightness in a quantitative fashion that can not be achieved visually (Fig. XI-16c). These profiles are a basic tool in the determination of distribution with height of the aerosol particles that compose the observed haze layers.

By careful pointing of the narrow-angle camera to include the limb, the structure of the limb haze layers was revealed in greater detail (Figs. XI-16b and XI-16d). The ultraviolet spectrometer (UVS) and infrared interferometer spectrometer provided complementary data on the vertical structure of the atmosphere in the same part of the planet.

A single limb picture supplies information on the vertical structure of the atmosphere above, or symmetrically about, a line segment on the planetary surface. This segment can be defined as the trace on the planet of the tangent line from the spacecraft to the solid surface of the planet. It can be computed for the idealized shape of the planet using tracking data. Only the part of this trace that appears in the field of view of the camera is of interest. Figures XI-16e and XI-16f show the traces of the limb for the pictures in Figs. XI-16a and XI-16b.

Figures XI-17 and XI-18 are other examples of limb pictures, and show some of the diversity in the visible vertical structure in the Martian atmosphere. These pictures are raw versions of the real-time data and provide a better display of the detached layers of haze than the other real-time enhancements (see Section IV).

Most Mariner 9 pictures that show the Martian limb have been computer-processed by the IPL to generate additional

enhancements and numerical photometric profiles. Each limb picture, in two processed versions, was reproduced on a microfiche card along with a number of profiles perpendicular to the limb. Data on five limb frames occupy a single microfiche card (Fig. XI-19), and 166 microfiche cards comprise the set of limb microfiche which will be available through NSSDC (see Section III). A presentation of the spatial and temporal distributions of the limb observations appears in the Mercator and Polar Stereographic plots of Figs. XI-20 and XI-21. Supporting numerical information for the plots is given in Tables XI-4 and XI-5. The figures and tables are intended to complement the pictures and numerical profiles in the Microfiche Catalog.

D. Terminator Pictures

Very few frames were specifically intended for observation of atmospheric phenomena at the day/night boundary except for frames targeted at the intersection of limb and terminator. However, many frames from global and targeted sequences and mapping polar and geodesy photography included part of the terminator. Observations across morning and evening terminators were obtained by the UVS and the infrared radiometer (Refs. XI-2 and XI-3). Because analysis of television observations of the terminator can add to the existing knowledge of atmospheric characteristics, a brief presentation of the terminator coverage is given here.

The locus of the morning and evening terminators in each frame is shown in Fig. XI-22. As the frames are not identified in the plots, anyone wishing to analyze these data must consult other documents. In Volume II, for example, the terminator is identified in all plotted frames. Sun elevation overlays also are available for Mariner 9 frames that contain this information. Analysis of the SEDR with an appropriate computer program could be used to select and label frames that contain the terminator. An example of a cloud formation near the terminator is shown in Fig. XI-23.

Table XI-2. Summary of targeted photography

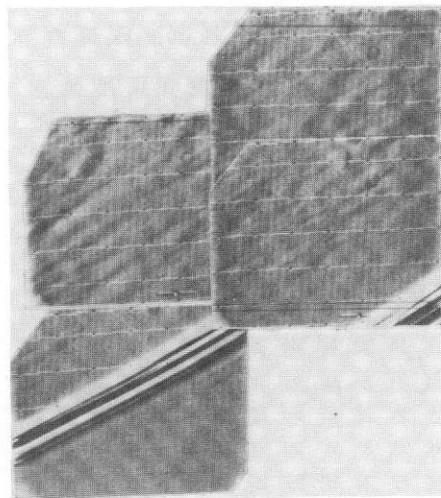
Revs	Science cycle	Zenith pass (even revolutions)	Nadir pass (odd revolutions)
1-15	Post-orbital insertion mapping, calibration, and phase function	—	—
16-23	Interim sequence	Atmospheric: 1B, 1A(V) (-40m) ^a	Atmospheric: 1A(V) (-1h16m) ^a
24-63	Recon I	Tetrad 1: 4B (-1h52m) ^a Tetrad 2: 4B (-1h24m) ^b	Tetrad 1: 4B (-1h52m) ^a Tetrad 2: 4B (-1h35m) ^b
64-99	Recon II	Tetrad 1: 4B (-1h30m) ^a Tetrad 2: 4B (-1h6m12s) ^b	Tetrad: 4B (-1h31m24s) ^a Tetrad: 3B (-1h5m44s) ^b
100-138	Mapping Cycle I	Pentad: 2AB, 1A (-33m) ^a Tetrad: 1A, 1BA, 1A (16m)	Dyad: 2B (-57m20s) TLR: 1B (-37m54s) Tetrad: 2A, 1BA (-33m) Dyad: 1AB (9m) Dyad 2: 1AB (18m48s)
139-177	Mapping Cycle II	Tetrad 1: 1BA, 2B (-33m42s) Tetrad 2: 1A, 1BA, 1A (24m24s) Dyad: 1AB (30m)	Triad: 1AB, 1B (-33m42s) Tetrad: 1A, 1AB, 1A (24m24s) Dyad: 1AB (30m48s)
178-217	Mapping Cycle III	Tetrad 1: 2B, 1AB (-32m18s) Tetrad 3: 2AB (-39m48s) ^b Dyad 2: 1AB (45m24s)	Tetrad 1: 2B, 1AB (32m18s) Dyad 3: 1AB (10m24s) ^b Tetrad 2: 2AB (39m48s)
218-262	Extended mission, Phase I	Triad 3: 1B, 1AB ^b Triad 5: 1B, 1AB ^b	Dyad 4: 1AB (45m24s) Triad 3: 1B, 1AB Triad 5: 1B, 1AB
416-459	Extended mission, Phase II: Arcturus	Atmospheric: 1A (-8m48s), ^c Rev 430 only South polar: 1A (-8m26s), ^c Rev 436 only	Atmospheric: 1A (-13m39s), Rev 451 only South polar (in dark): 1A, 1B, 3A (-7m43s), Rev 459 only
473-533	Extended mission, Phase III: Canopus	Tempe: 1B (2h38m12s), Rev 528 only Nix Olympica: 2B (3h20m12s), Rev 528 only	Geology: 1B (28m), Rev 529 only
667-676	Extended mission, Phase IV: Vega	Elysium: 1BA (1h46m25s), ^d Rev 668 only Elysium: 1BA (2h0m25s), Rev 668 only Nix Olympica: 1B (3h0m37s), Rev 668 only Hougeria: 1BA (4h0m49s), Rev 668 only	North Spot: 1BA (2h0m20s), Rev 676 only North Spot: 1BA (2h49m20s), Rev 676 only North Spot: 1BA (3h39m44s), Rev 676 only North Spot: 1BA (4h28m44s), Rev 676 only

^aAlmost exclusively used for limb frames.

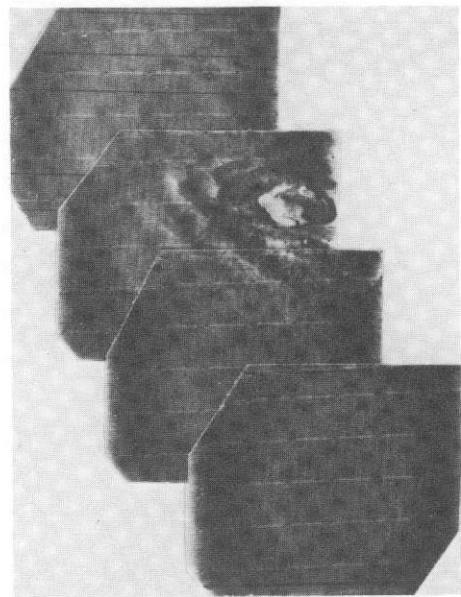
^bOther numbered dyads, triads, or tetrads consist entirely of narrow-angle frames and are devoted to geology.

^cNot transmitted.

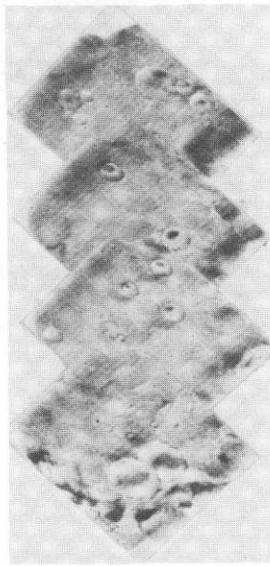
^dNix Olympica on the limb, 25,313.



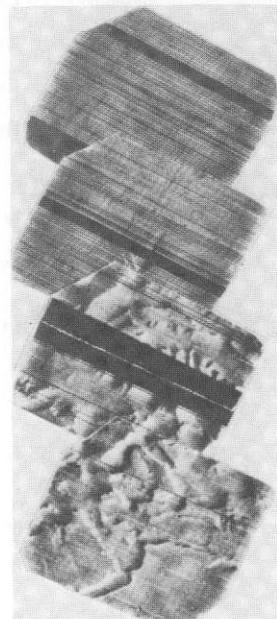
(a) RECON I: TETRAD 2; REV 56



(b) RECON I: TETRAD 1; REV 59

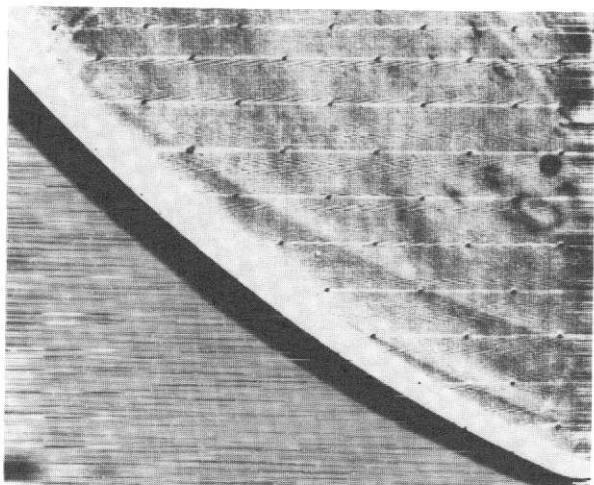


(c) RECON II: TETRAD 1; REV 86

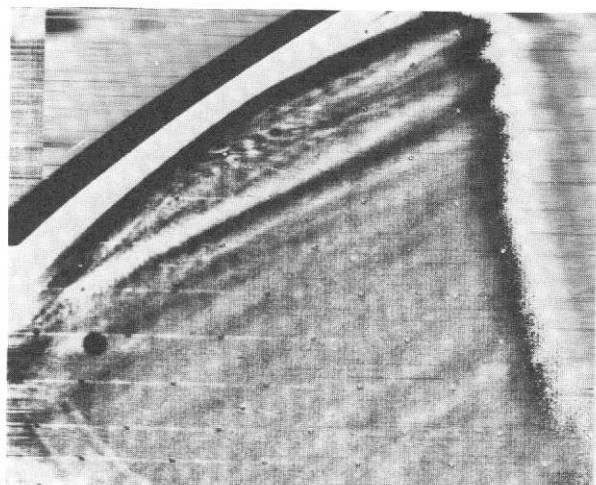


(d) RECON II: TETRAD 1; REV 69

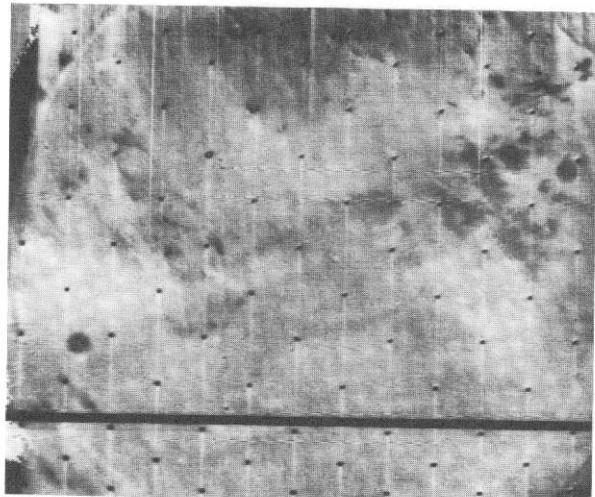
Fig. XI-9. Mosaics of narrow-angle targeted pictures typical of Recon I and II sequences: HPF versions.



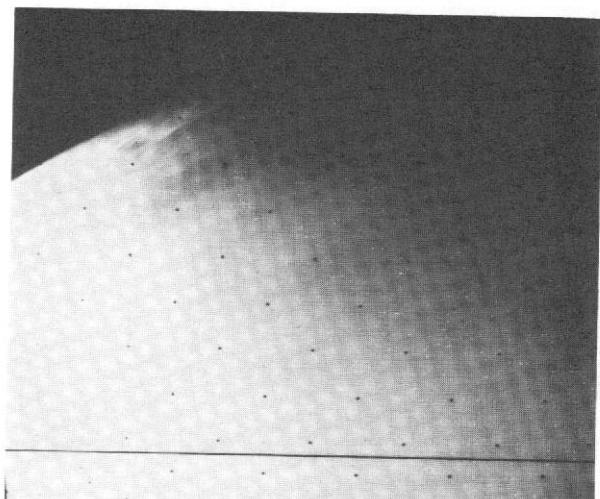
(a) MAPPING CYCLE I: TETRAD; REV 103



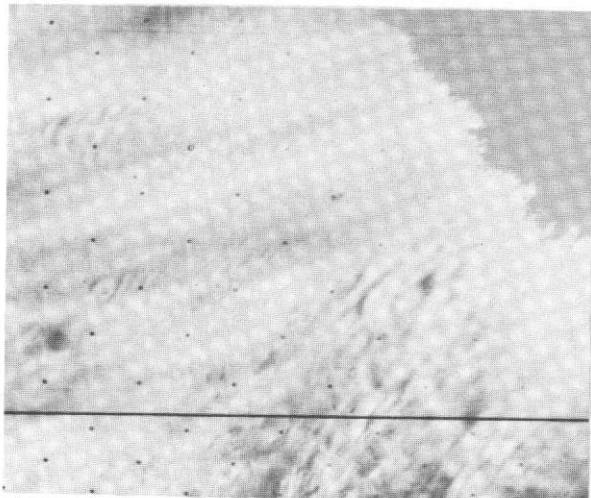
(b) MAPPING CYCLE I: DYAD 2; REV 103



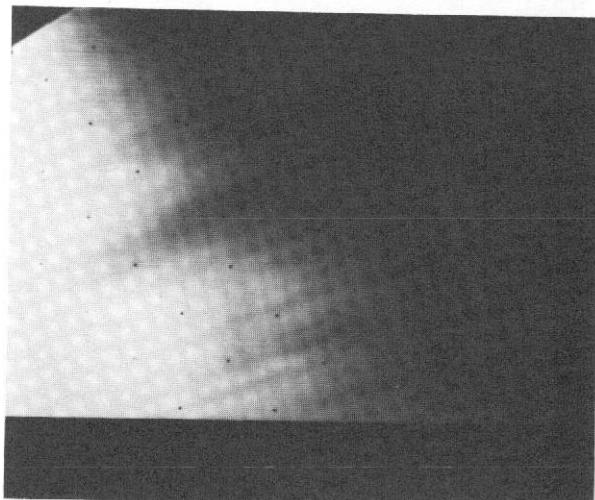
(c) MAPPING CYCLE I: PENTAD; REV 136



(d) MAPPING CYCLE I: TETRAD; REV 136

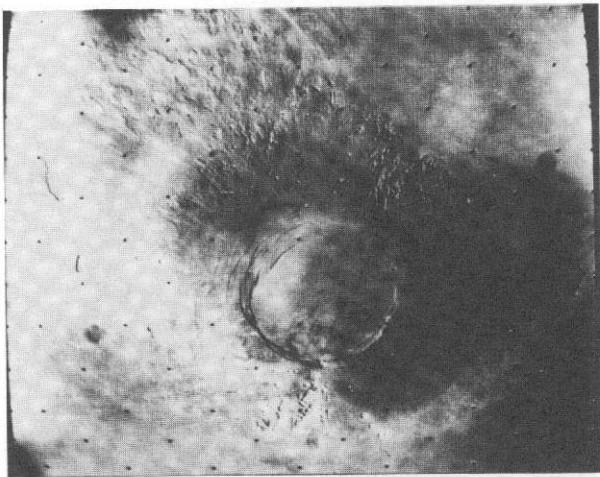


(e) MAPPING CYCLE II: DYAD; REV 162

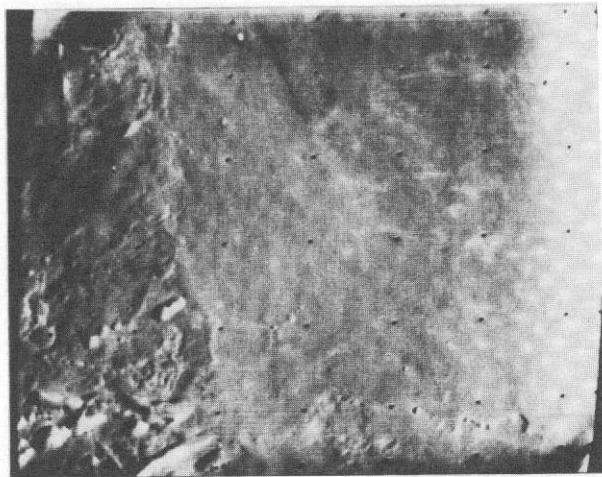


(f) MAPPING CYCLE II: DYAD; REV 161

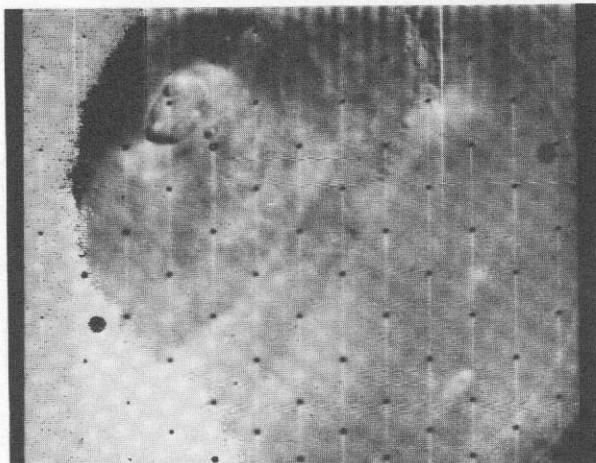
Fig. XI-10. Wide-angle targeted pictures typical of Mapping Cycles I and II. (a, b) HPF versions. (c, e) VAGC versions. (d, f) Shading-corrected versions.



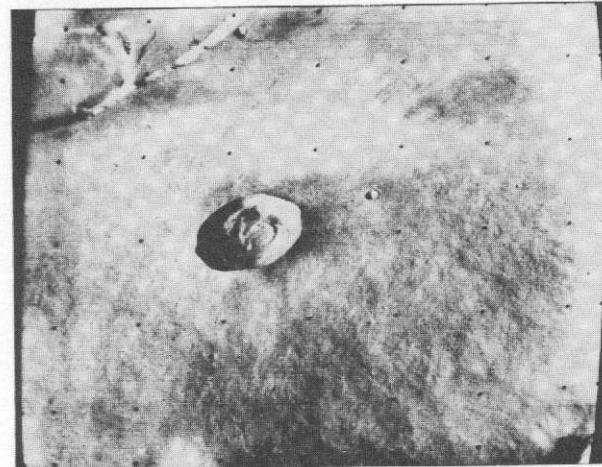
(a) MAPPING CYCLE III: DYAD 3; REV 191



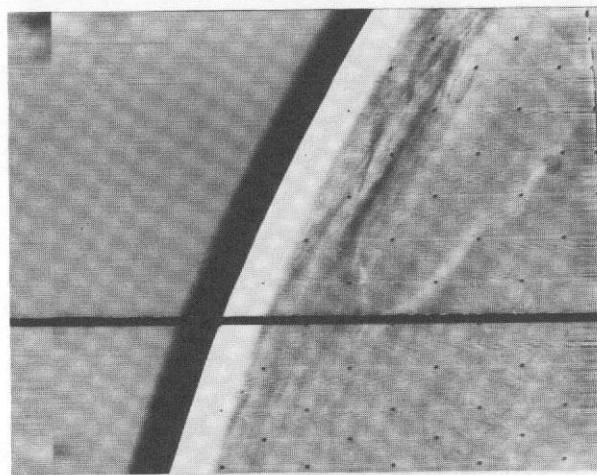
(b) MAPPING CYCLE III: DYAD 3; REV 191



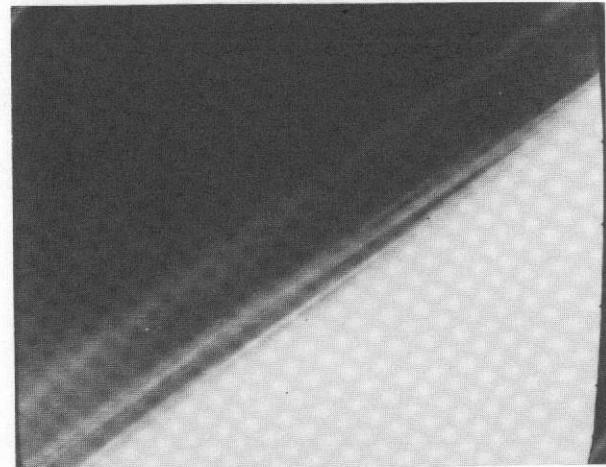
(c) MAPPING CYCLE III: DYAD 3; REV 187



(d) MAPPING CYCLE III: DYAD 3; REV 187

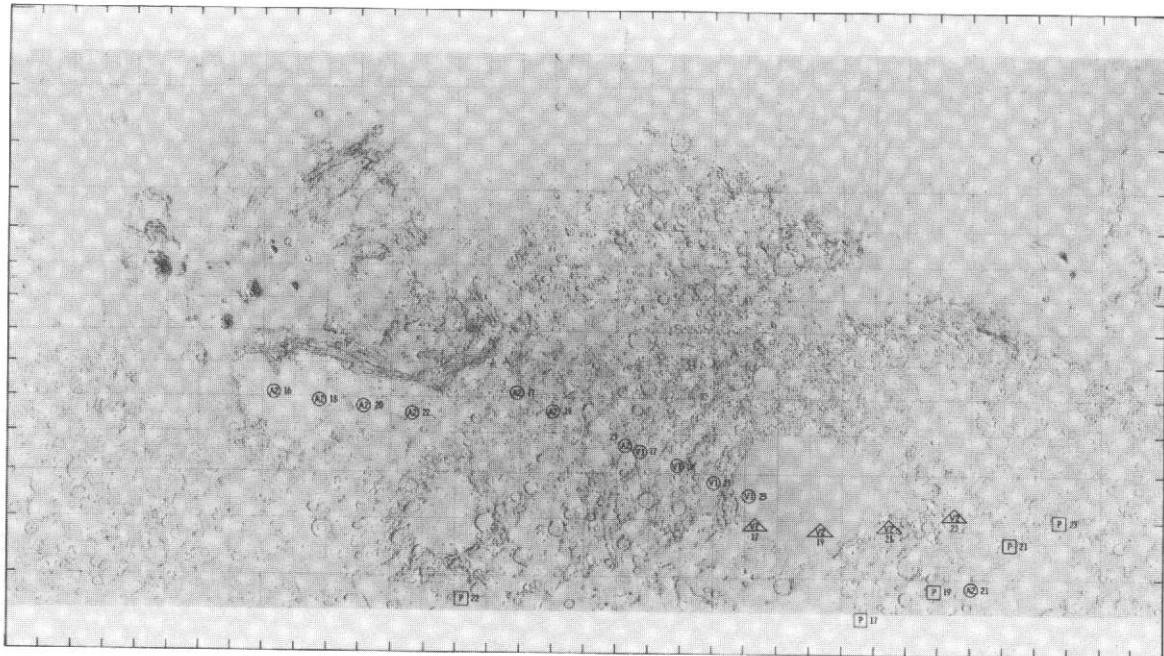


(e) EXTENDED MISSION, PHASE I: TRIAD 5; REV 222



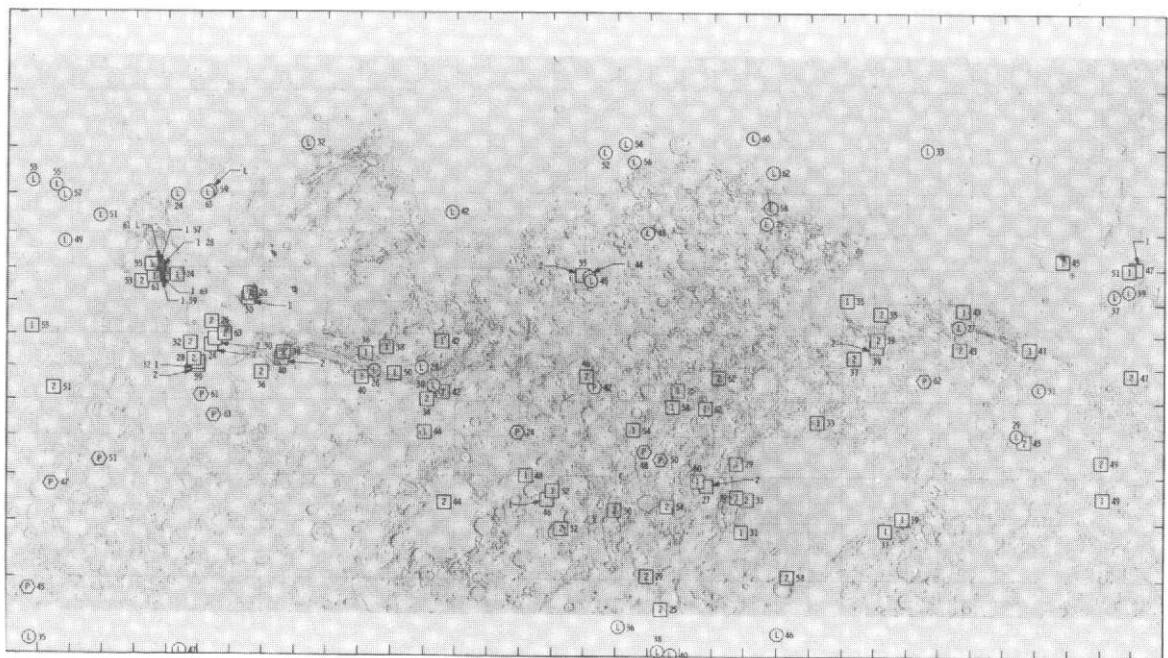
(f) EXTENDED MISSION, PHASE I: TRIAD 5; REV 222

Fig. XI-11. Targeted pictures typical of Mapping Cycle III and Phase I of the extended mission. (a) Wide-angle picture of South Spot: VAGC version. (b) Narrow-angle picture of South Spot: VAGC version. (c) Wide-angle picture of Nix Olympica: VAGC version. (d) Narrow-angle picture of Nix Olympica: VAGC version. (e) Wide-angle picture of Nix Olympica: VAGC version. (f) Narrow-angle picture of Nix Olympica: raw version.



(a) INTERIM SEQUENCE

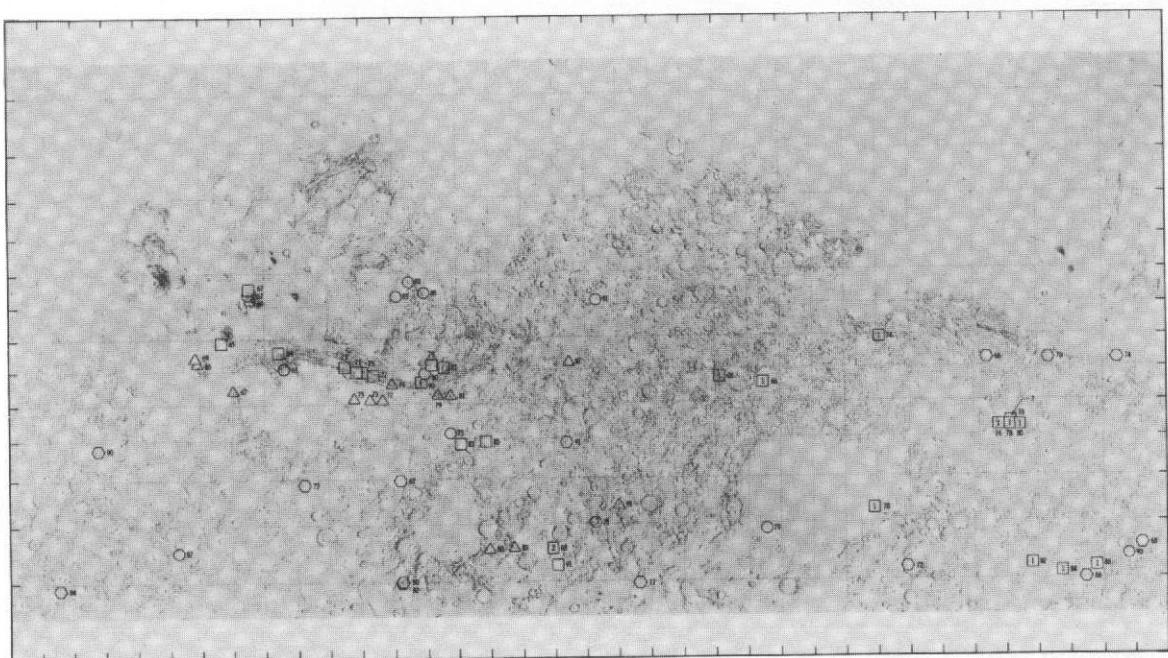
SEQUENCE	SYMBOL
ATMOSPHERIC 2	(A) 16
POLAR	(P) 17
VARIABLE SURFACE FEATURES	(V) 23
VARIABLE SURFACE FEATURES	(▲) 25



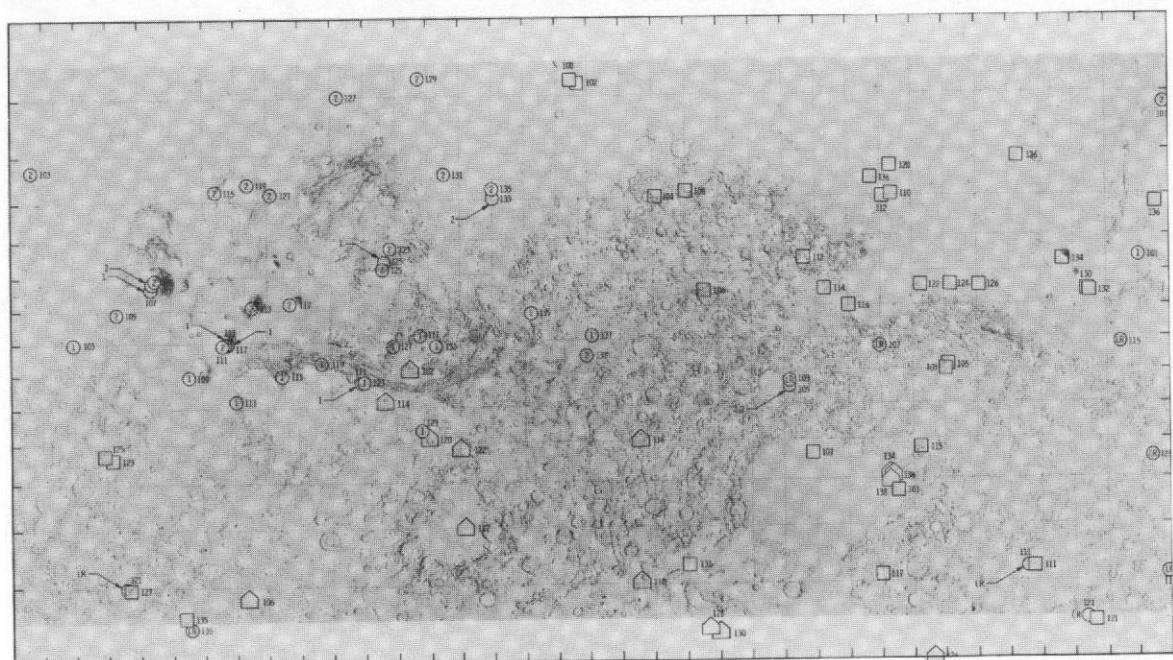
(b) RECON I

SEQUENCE	SYMBOL
LIMB	(L) 24
TETRAD 1	(I) 24
TETRAD 2	(?) 63
POLAR	(P) 63

Fig. XI-12. Targeted pictures from the standard mission (Revs 1-262). Each symbol represents the mean of the locations of centers of frames comprising a mosaickable group of links, e.g., tetrad, dyad, etc. Numerals outside the symbols represent the revolution number.



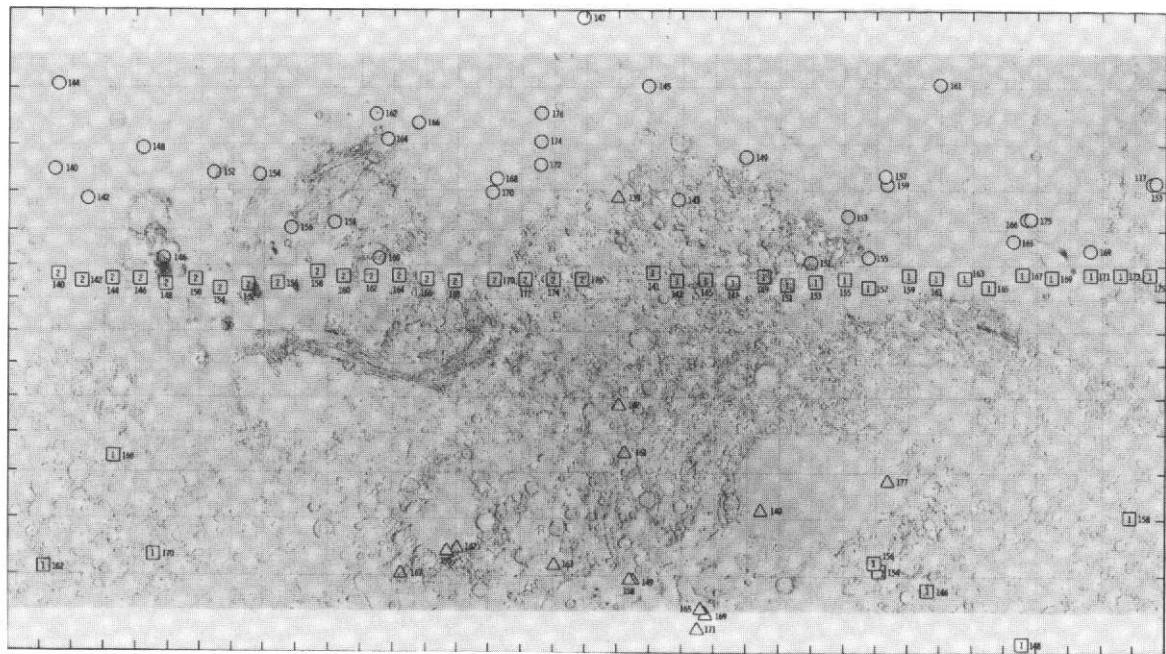
(c) RECON II



(d) MAPPING CYCLE I

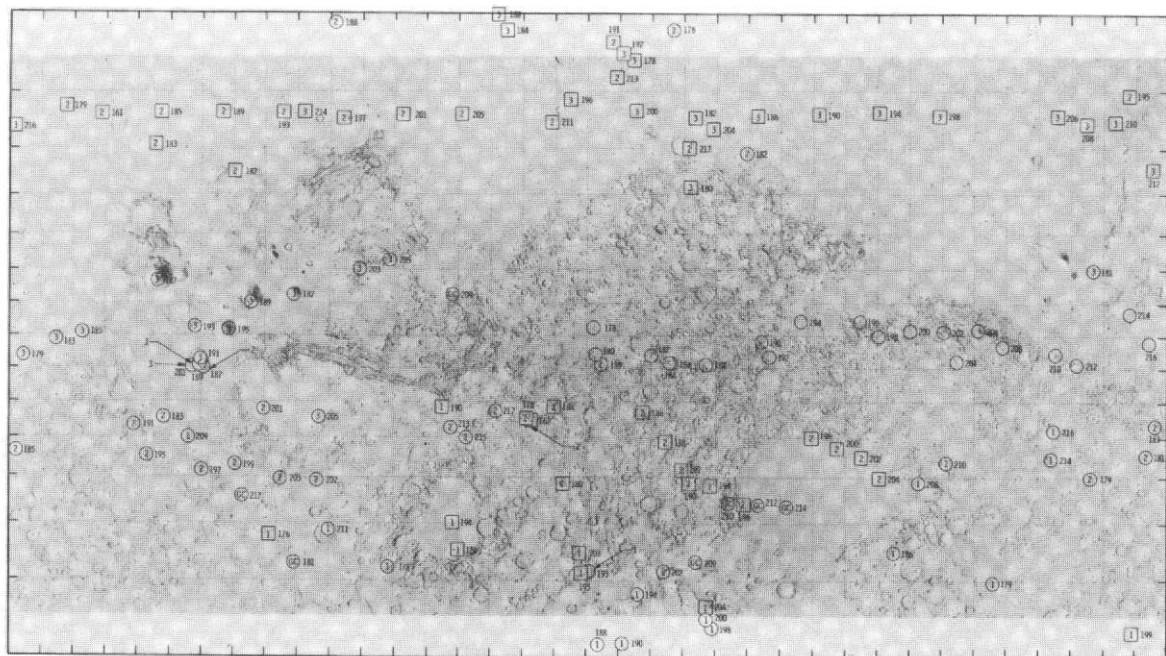
SEQUENCE	SYMBOL
BITRAD	□
PENTAD	○
DYAD	①
DYAD	②
BLR	③

Fig. XI-12. (contd).



(e) MAPPING CYCLE II

SEQUENCE	SYMBOL
ODD AND EVEN REVS	○ 177
EVEN REVS ONLY	□ 168
ODD REVS ONLY	□ 166
TRIAD	△ 155
TETRAD	□ 155



(f) MAPPING CYCLE III

SEQUENCE	SYMBOL
TETRAD 1	□ 178
TETRAD 2	□ 178
TETRAD 3	□ 178
DYAD 1	○ 179
DYAD 2	○ 179
DYAD 3	○ 179
GROUND STATE	○ 211
COMPLEMENT	○ 212

Fig. XI-12. (contd.).

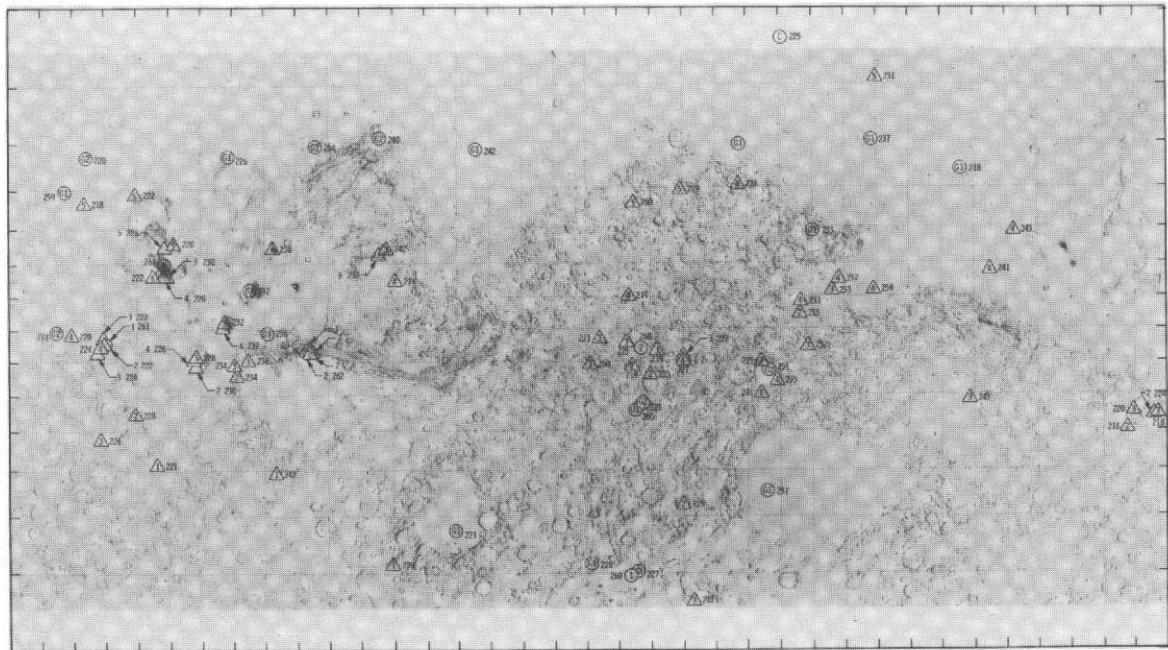


Fig. XI-12. (contd).

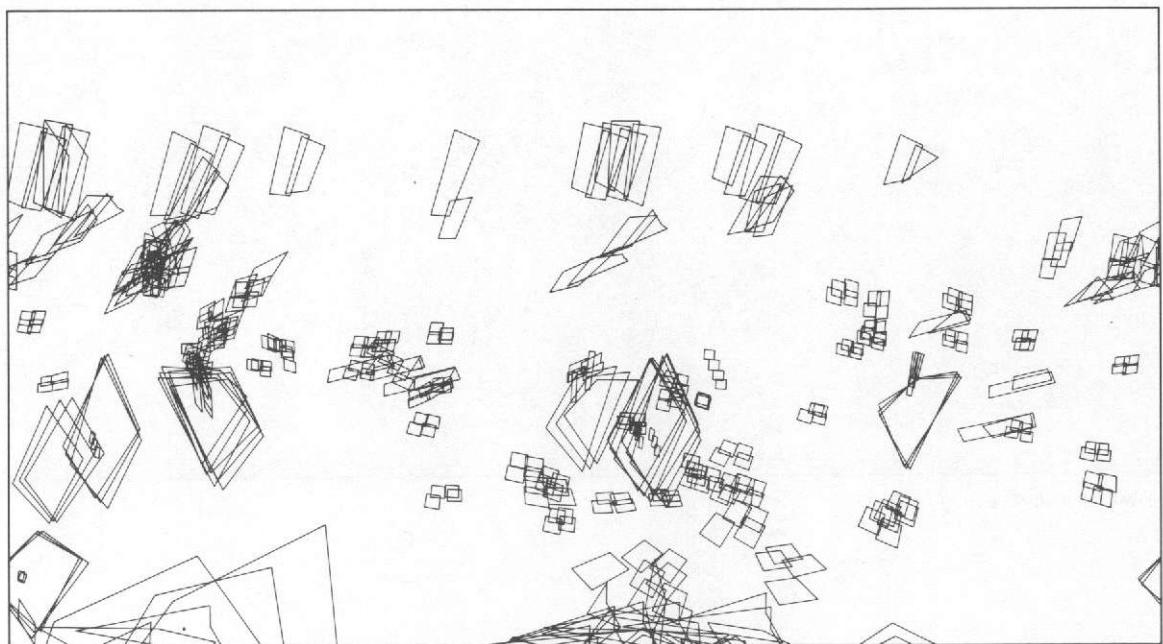
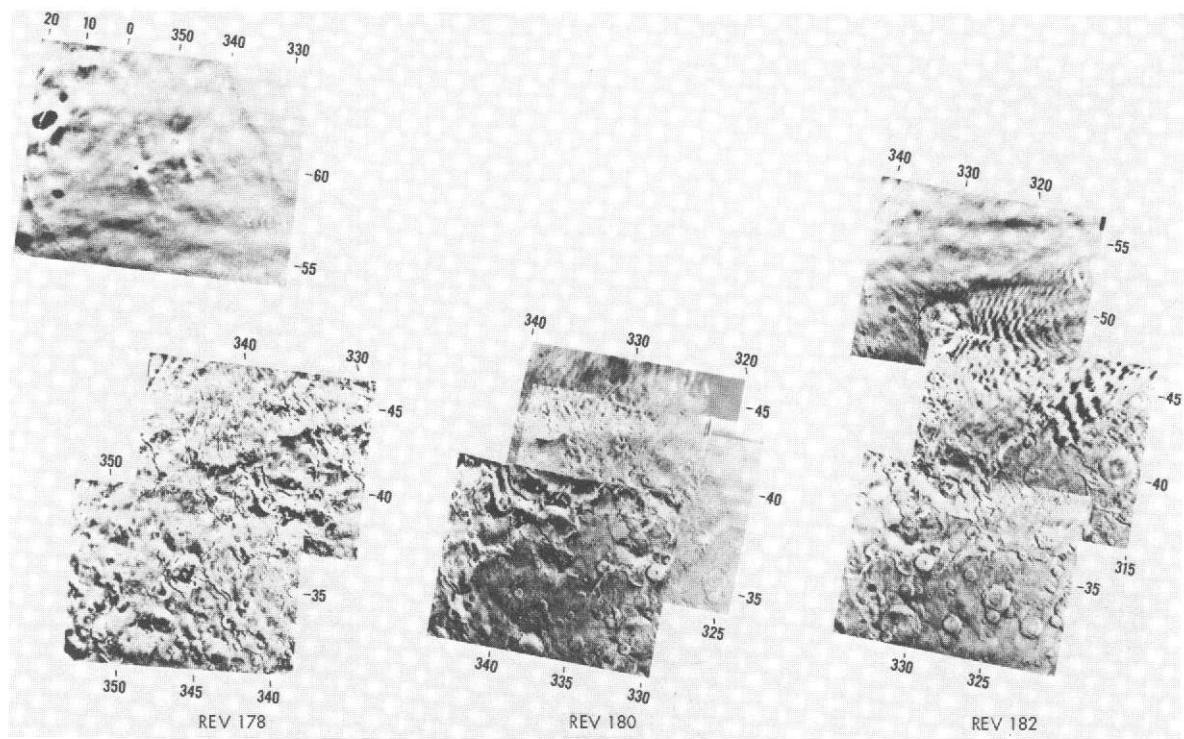
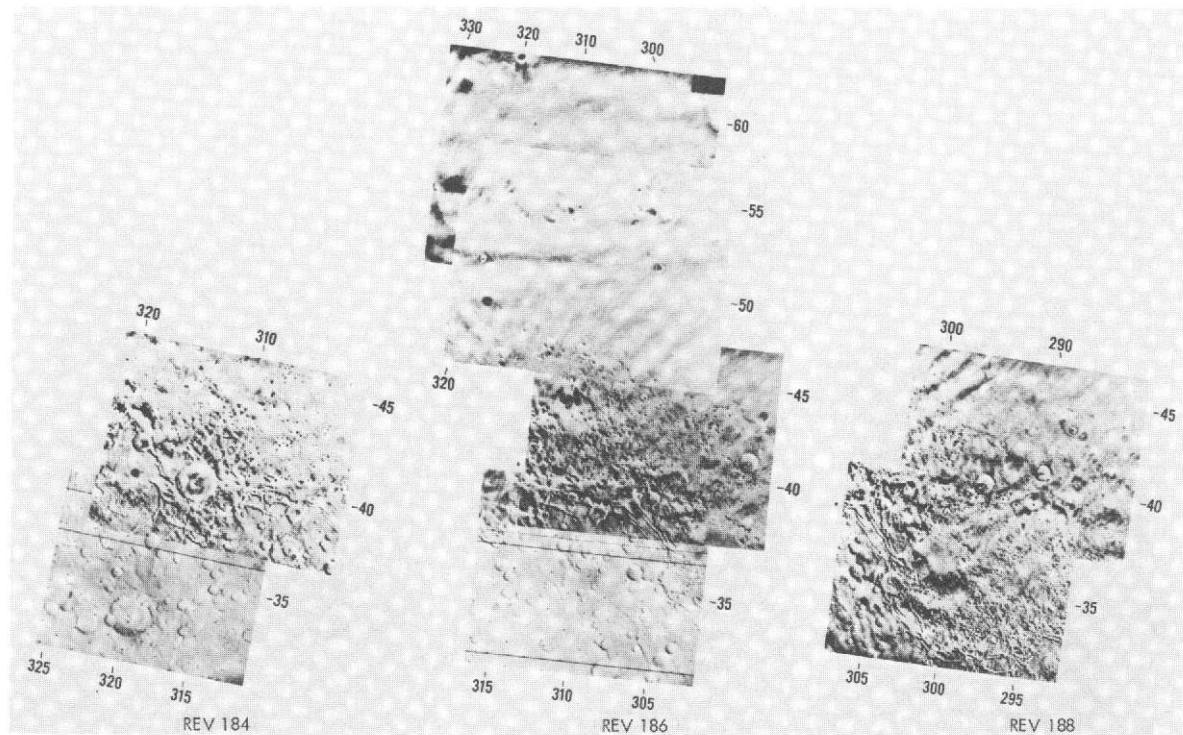


Fig. XI-13. Footprint plot showing actual coverage provided by targeted frames acquired during Recon I. The locations of the mean of the center coordinates of each group of frames comprising a targetable link are shown in Fig. XI-12b.

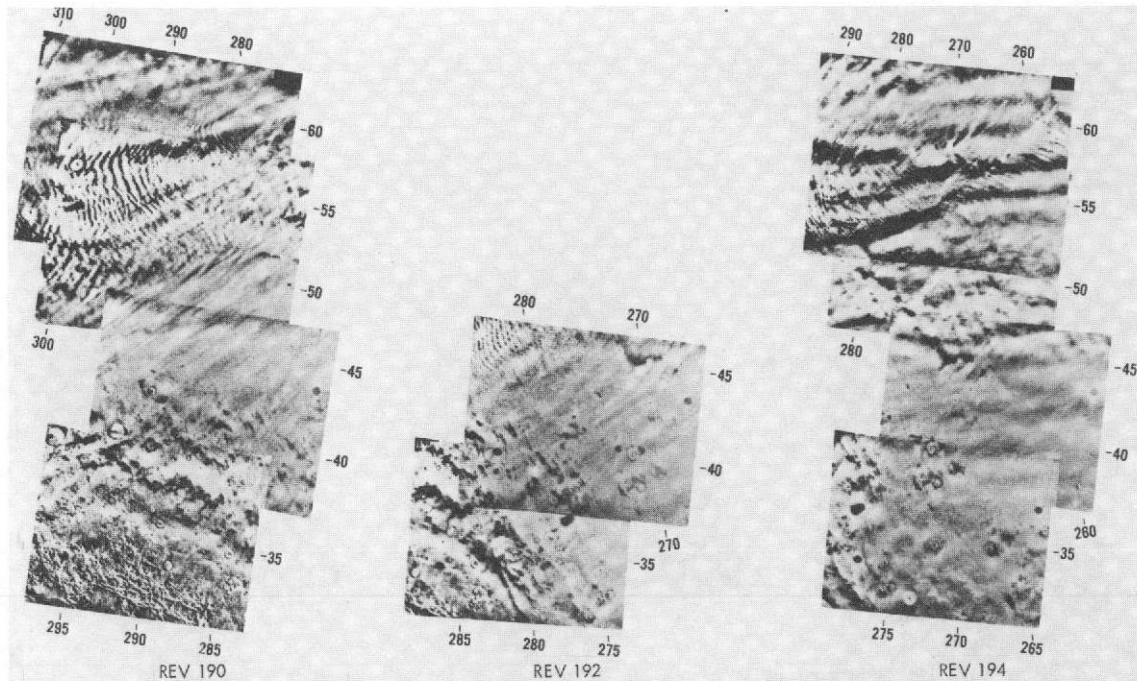


(a) REV 178, 180, 182

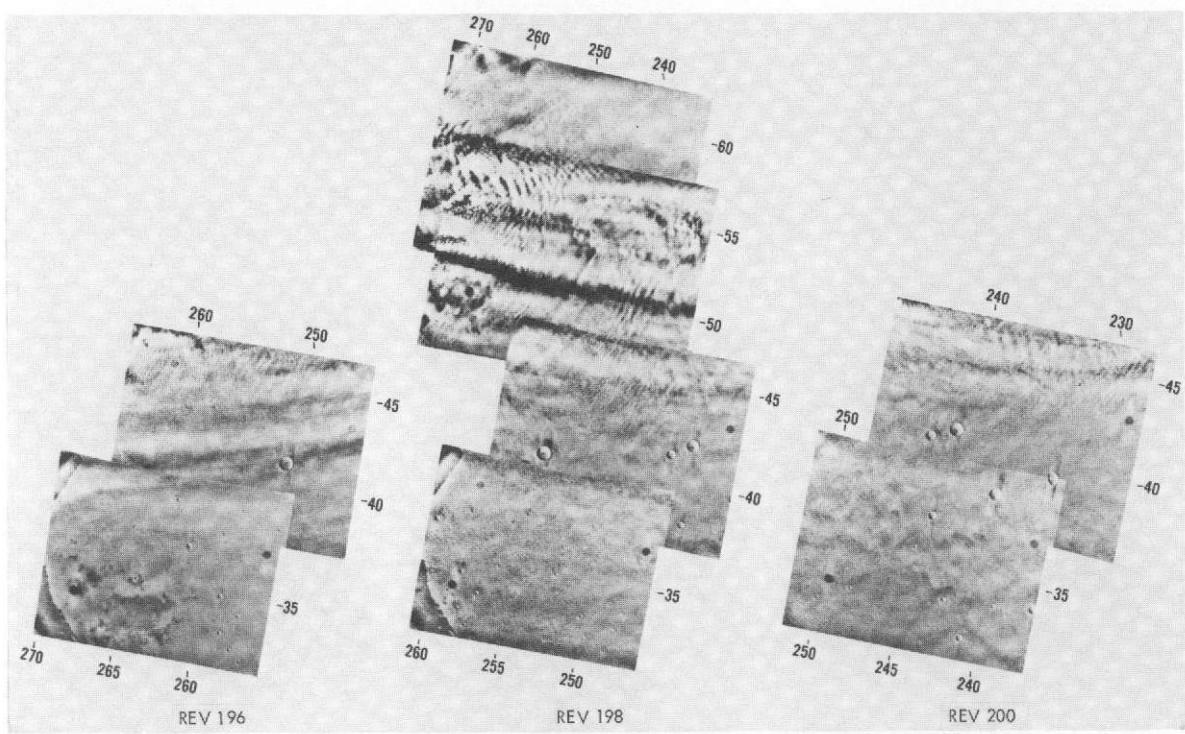


(b) REV 184, 186, 188

Fig. XI-14. Hybrid mosaics of targeted and mapping frames acquired during Mapping Cycle III. (a-g) Zenith revolutions.
(h-o) Nadir revolutions.

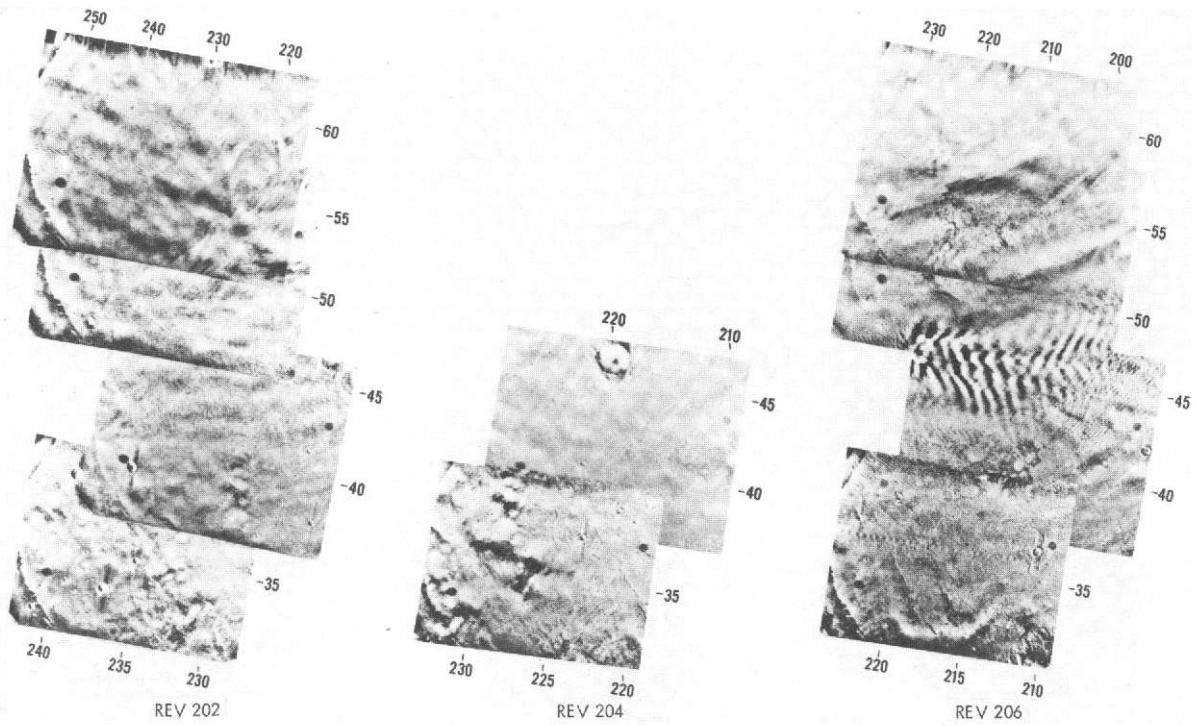


(c) REVS 190, 192, 194

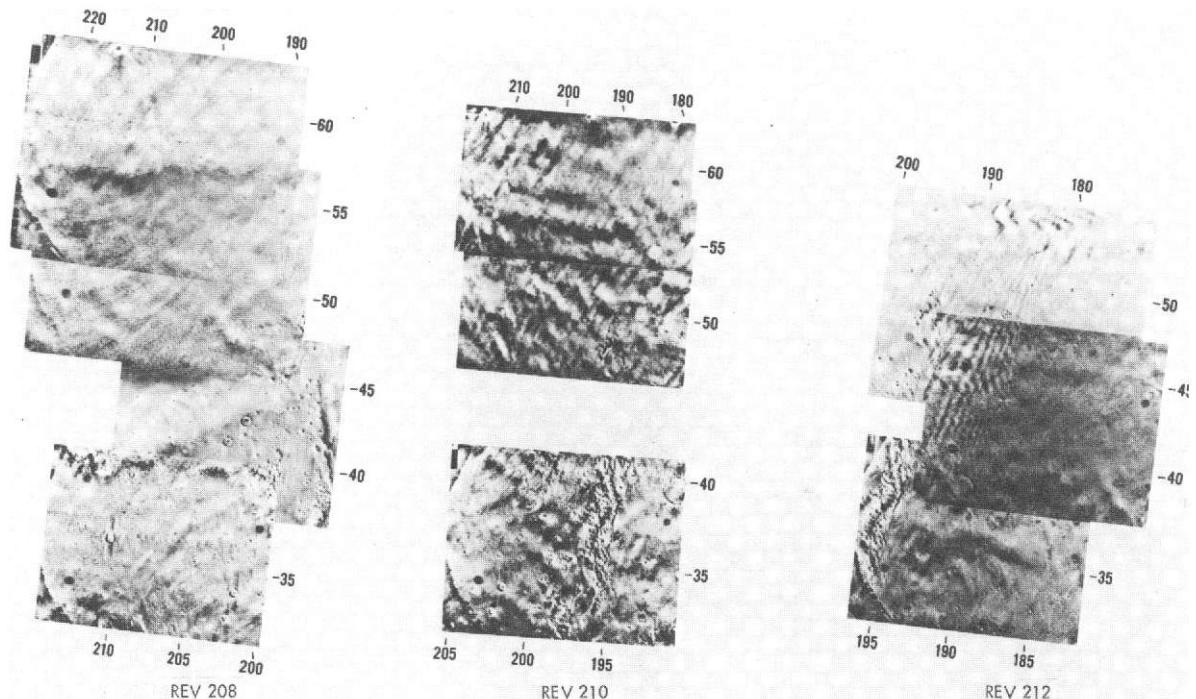


(d) REVS 196, 198, 200

Fig. XI-14. (contd).

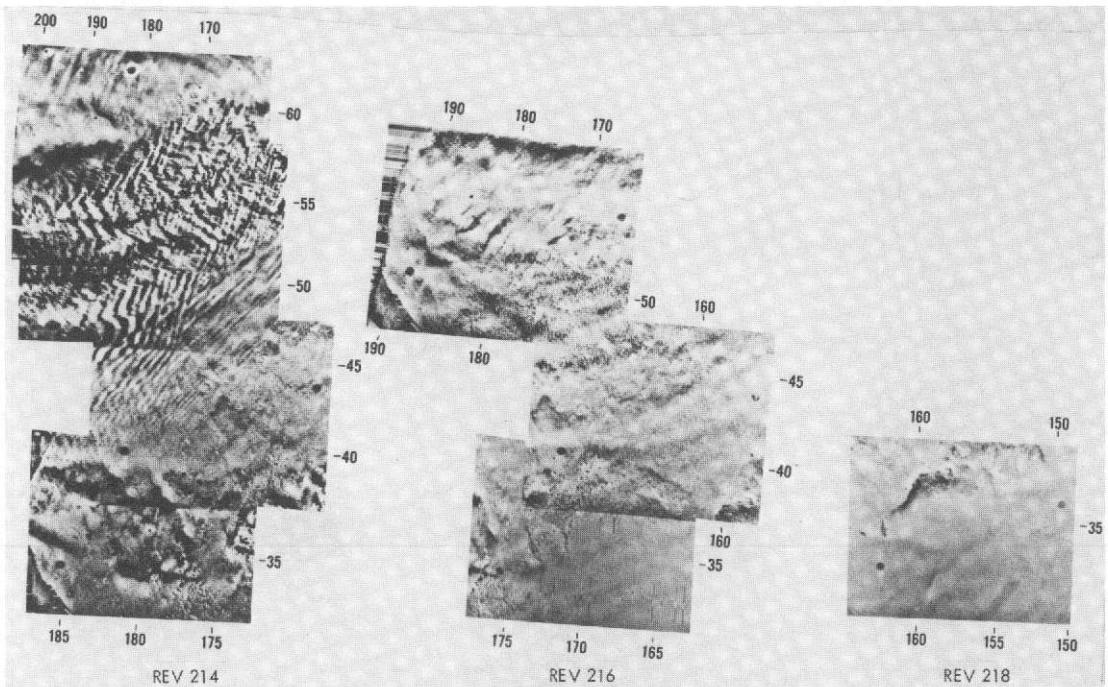


(e) REVS 202, 204, 206

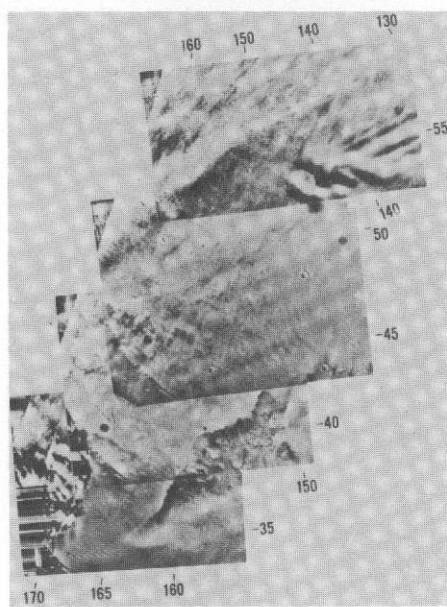


(f) REVS 208, 210, 212

Fig. XI-14. (contd).

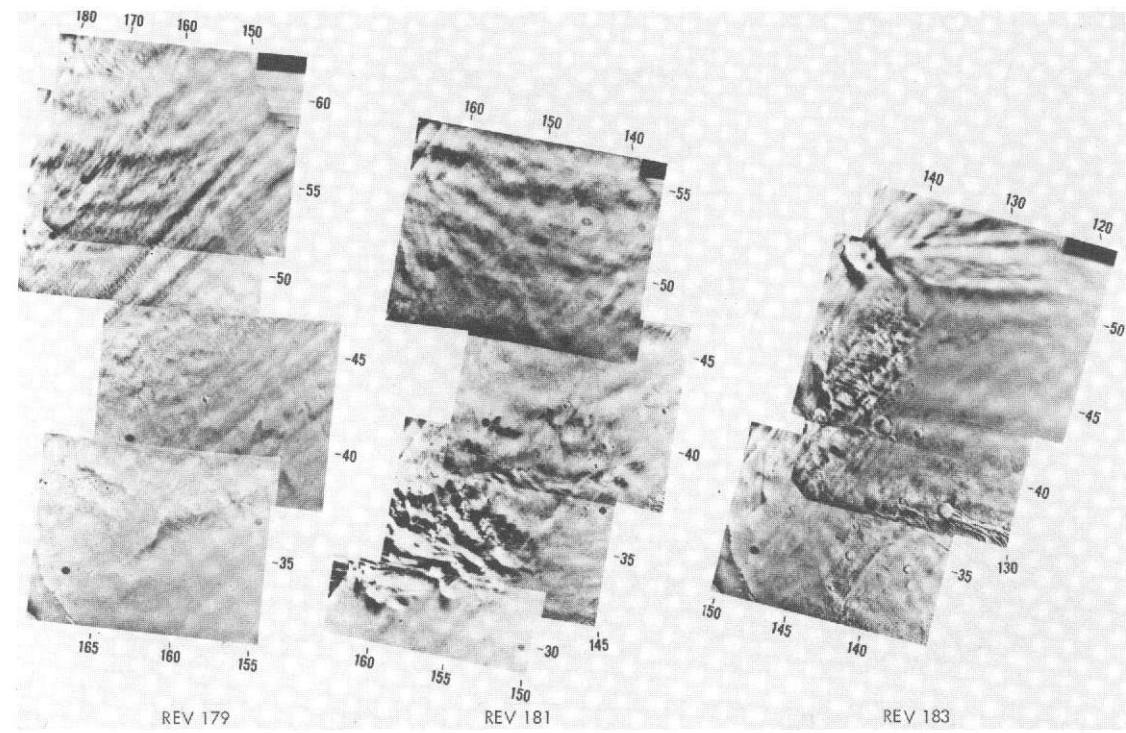


(g) REVS 214, 216, 218

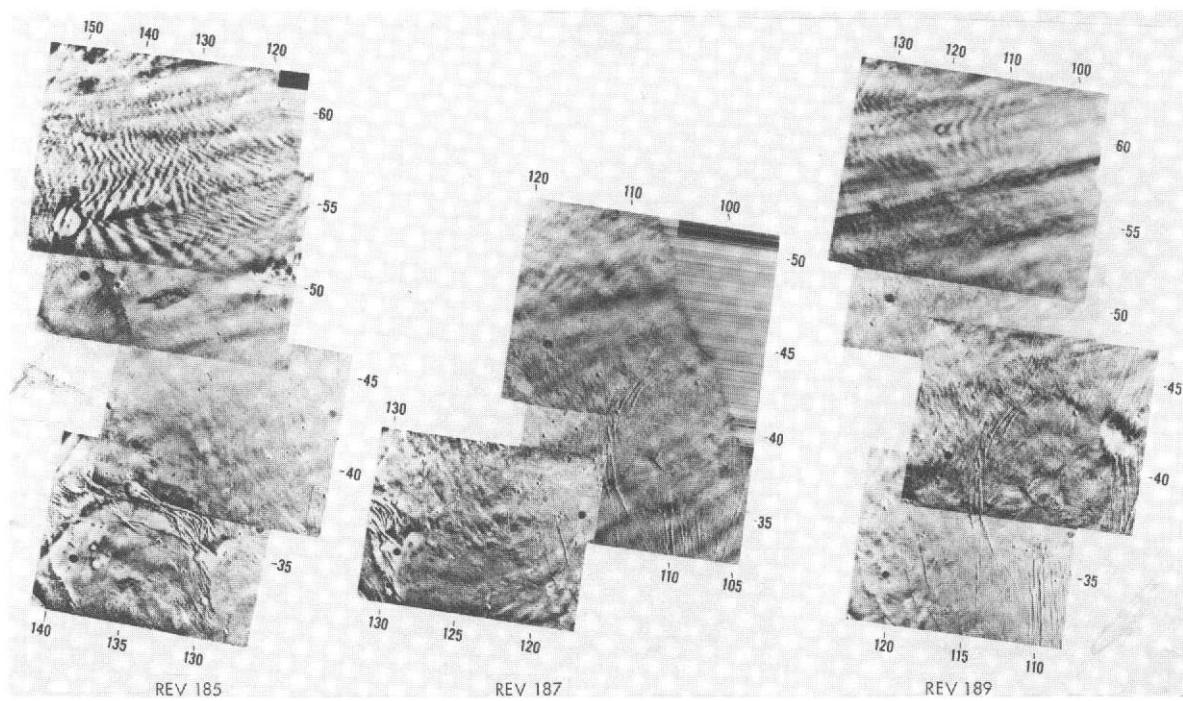


(h) REV 220

Fig. XI-14. (contd).

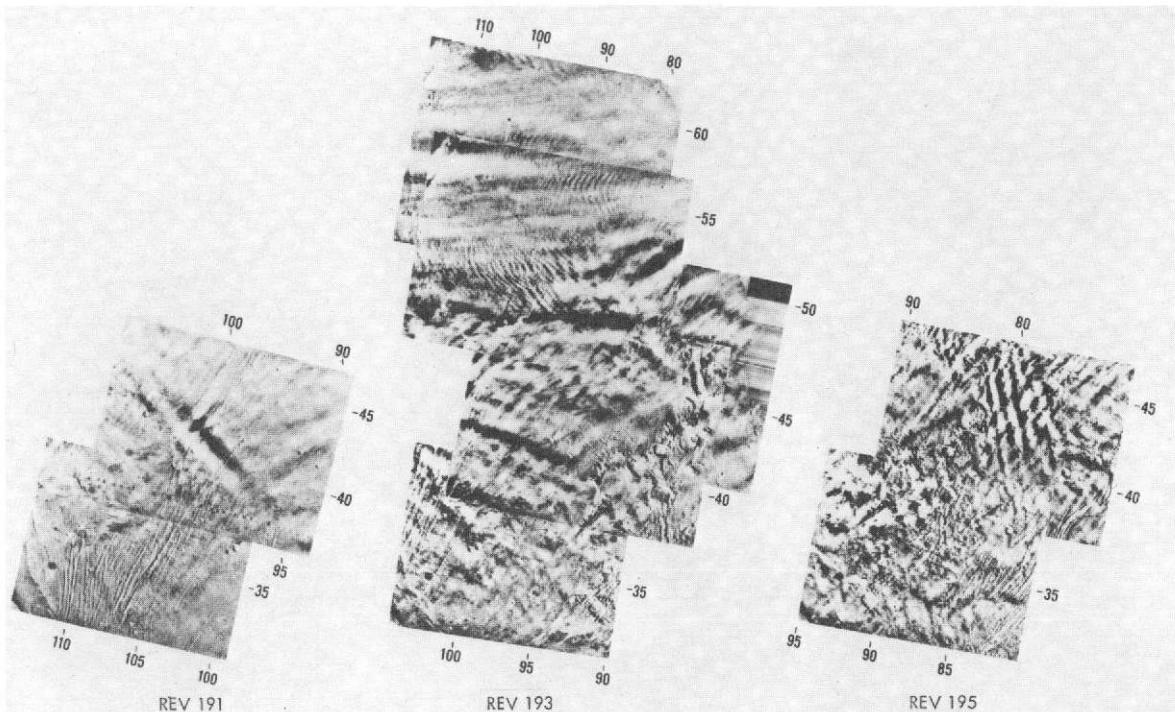


(i) REVS 179, 181, 183

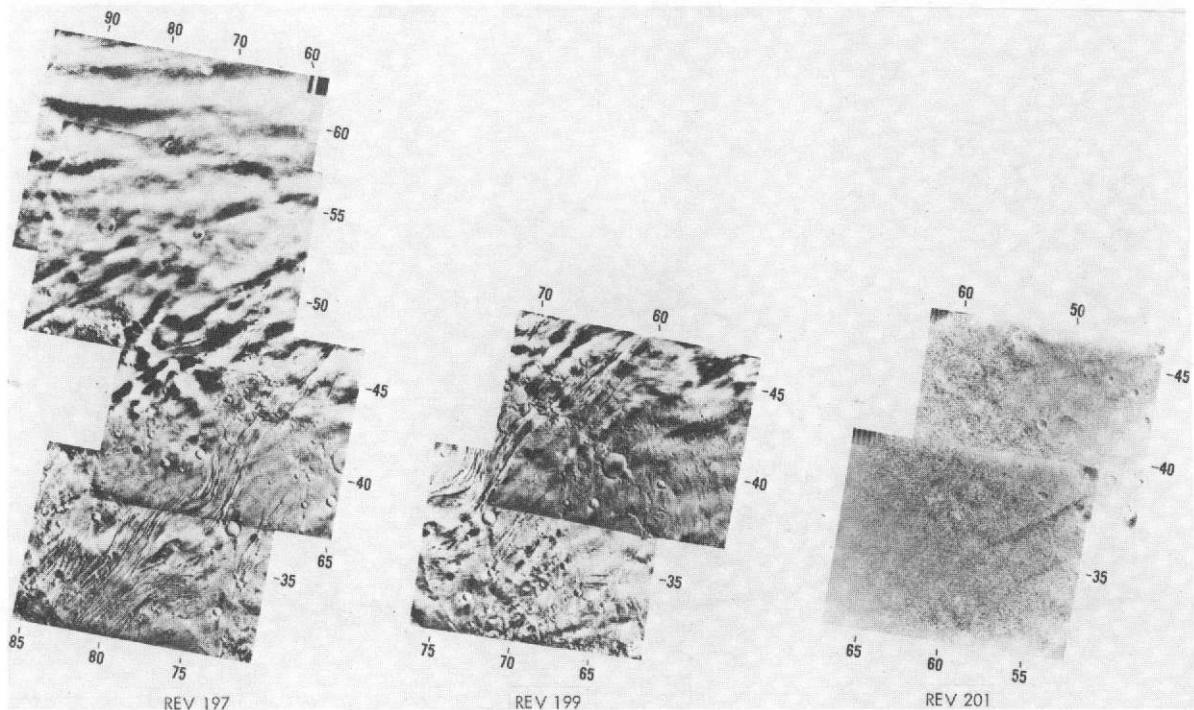


(j) REVS 185, 187, 189

Fig. XI-14. (contd.).

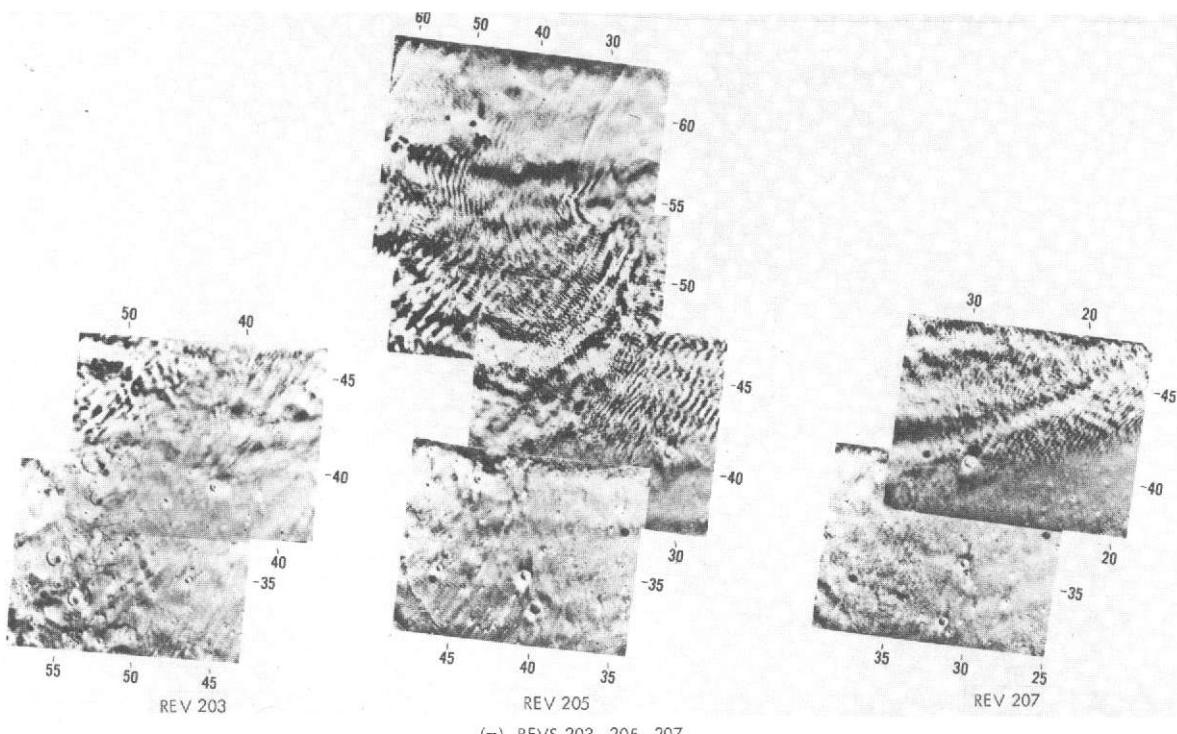


(k) REVS 191, 193, 195

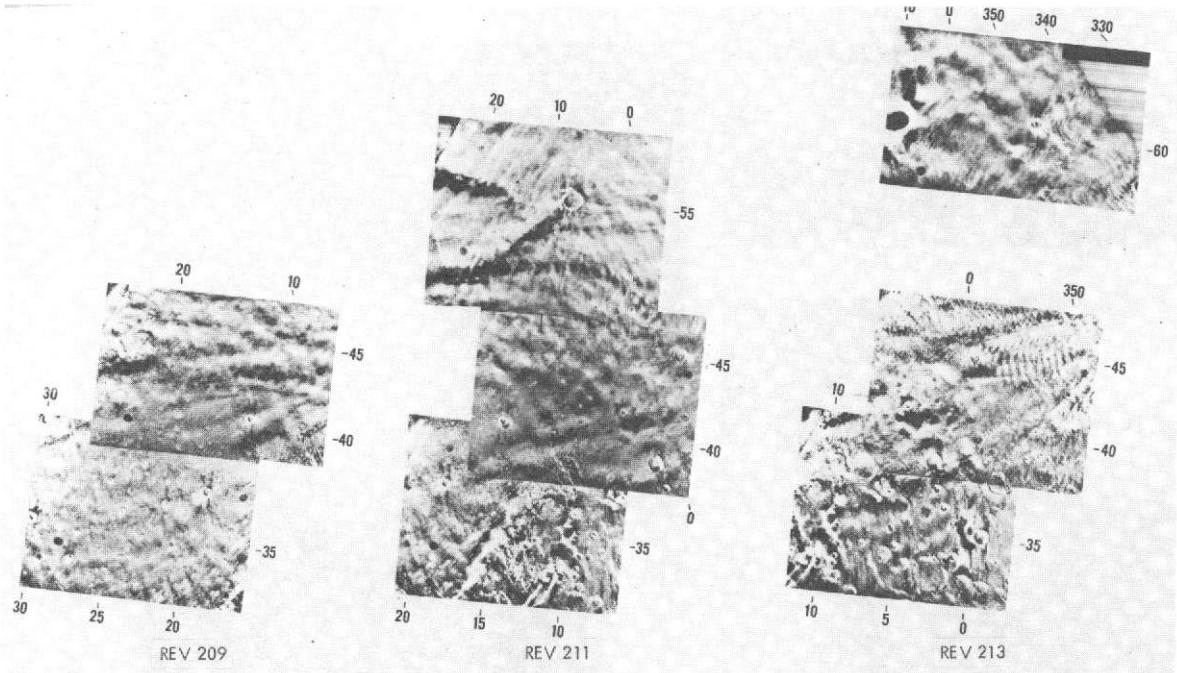


(l) REVS 197, 199, 201

Fig. XI-14. (contd.).

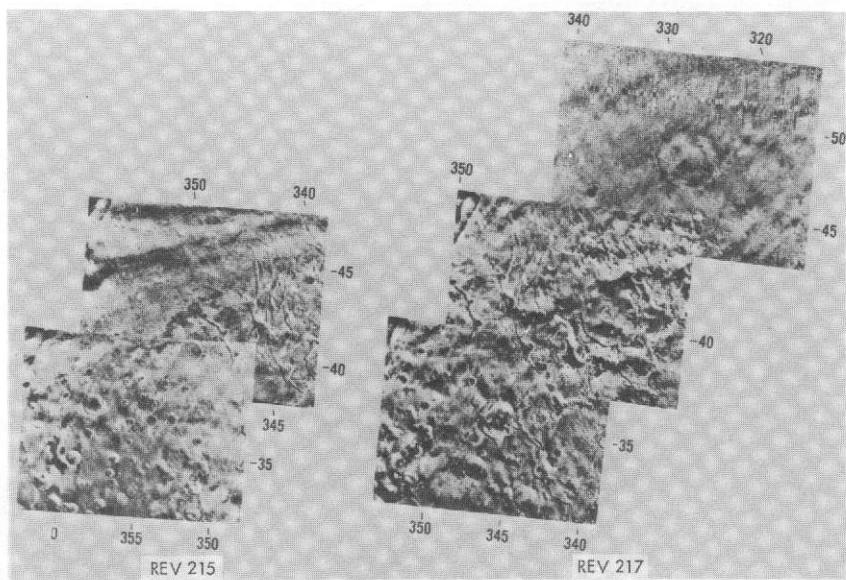


(m) REVS 203, 205, 207



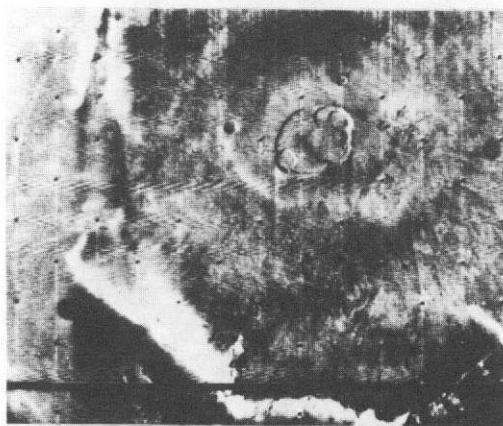
(n) REVS 209, 211, 213

Fig. XI-14. (contd.).

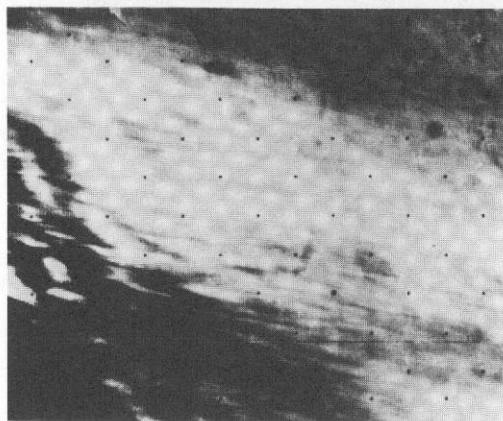


(o) REVS 215, 217

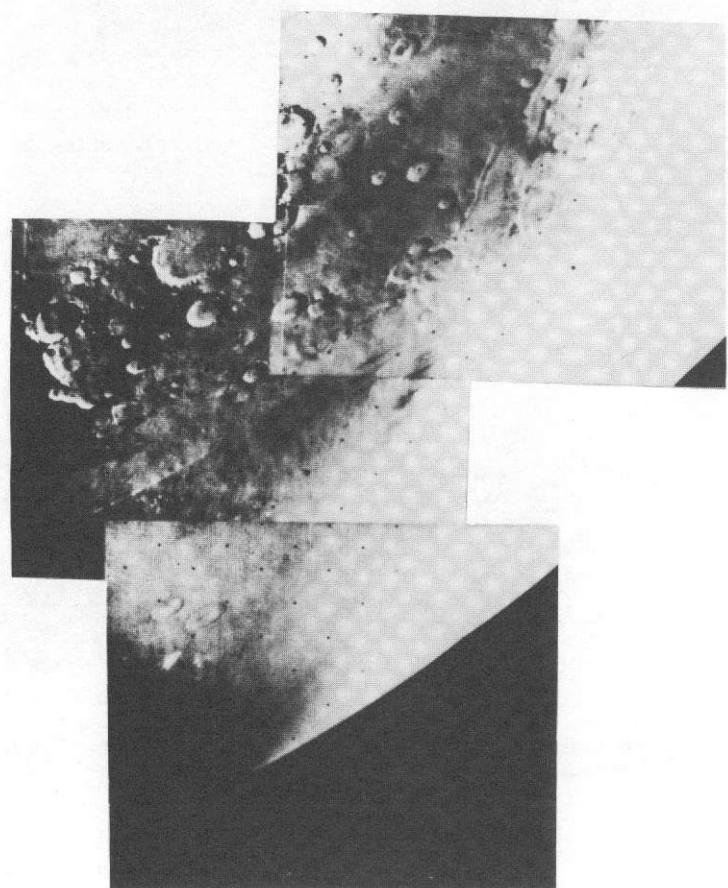
Fig. XI-14. (contd).



(a) NIX OLYMPICA: REV 423

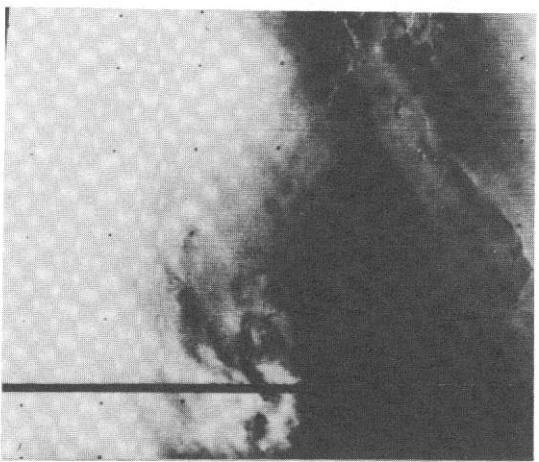


(b) HELLAS: REV 430

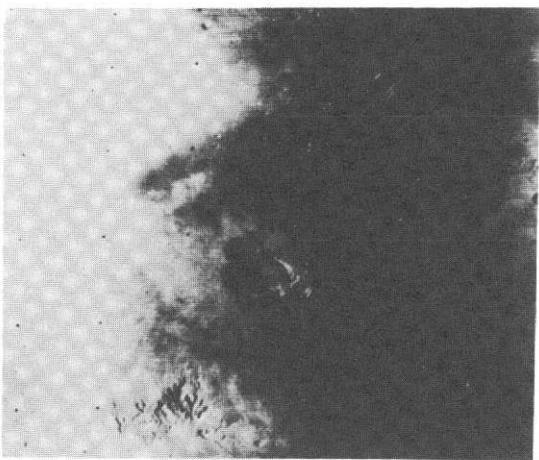


(c) SOUTH POLAR REGION: REV 459

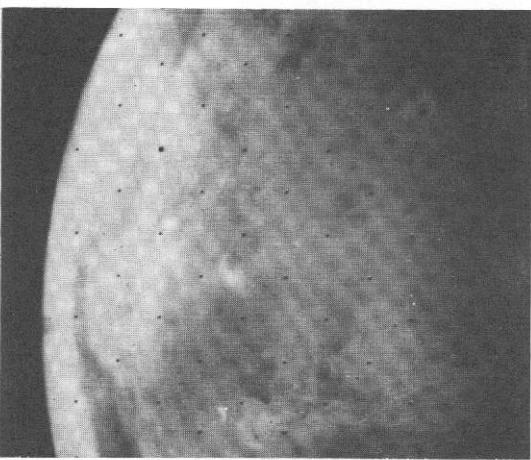
Fig. XI-15. Targeted frames of atmospheric features viewed during Phases II, III, and IV of the extended mission (Revs 416-676).



(d) NIX OLYMPICA: REV 528



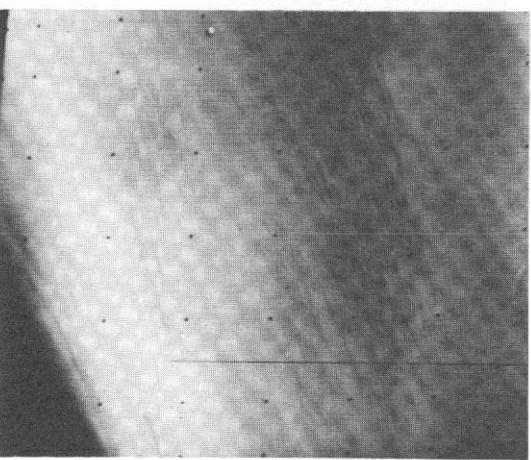
(e) NORTH SPOT: REV 528



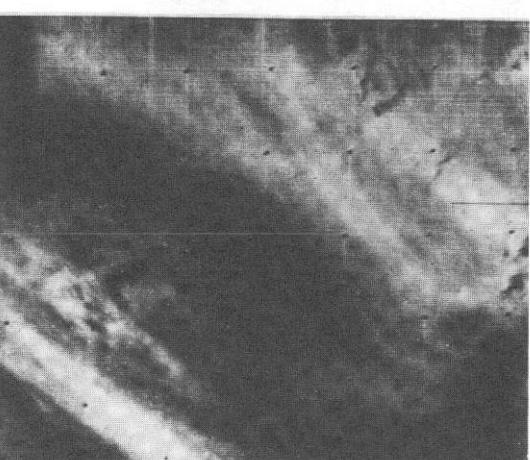
(f) ELYSIUM: REV 668



(g) ELYSIUM: REV 668

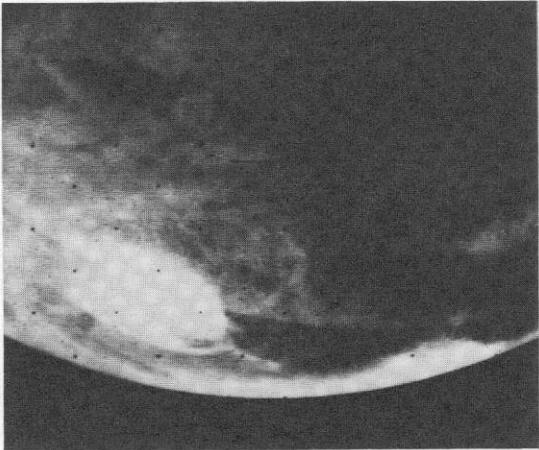


(h) NIX OLYMPICA NEAR LIMB: REV 668

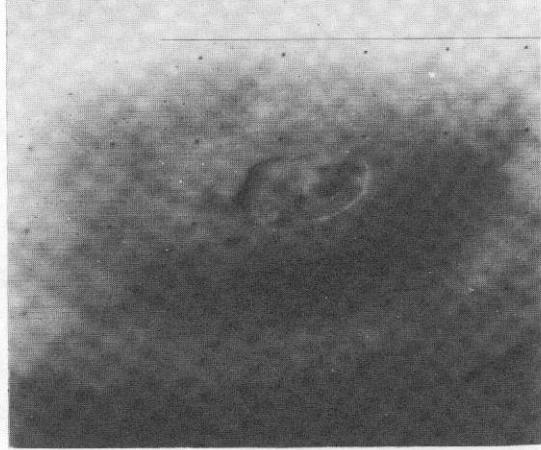


(i) NIX OLYMPICA: REV 668

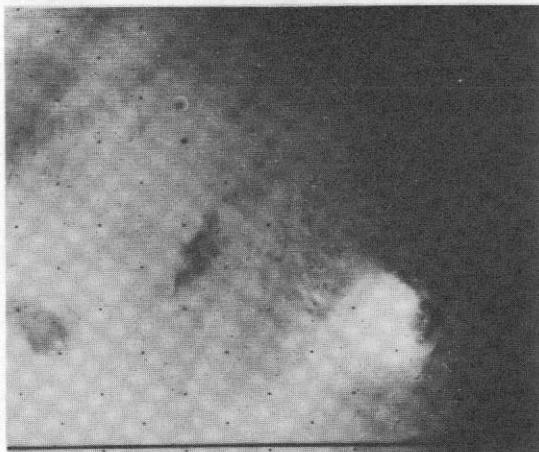
Fig. XI-15. (contd.).



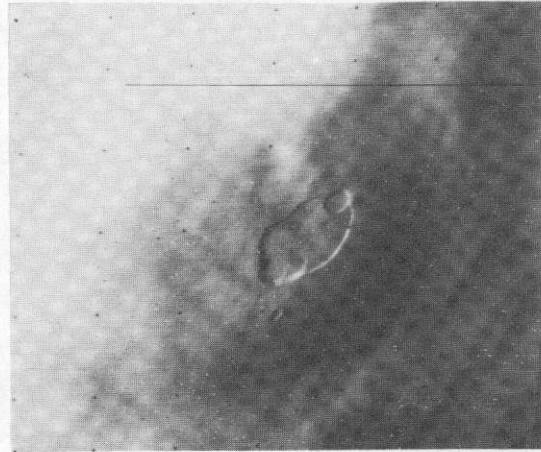
(j) NIX OLYMPICA REGION: REV 668



(k) NIX OLYMPICA SHIELD: REV 668



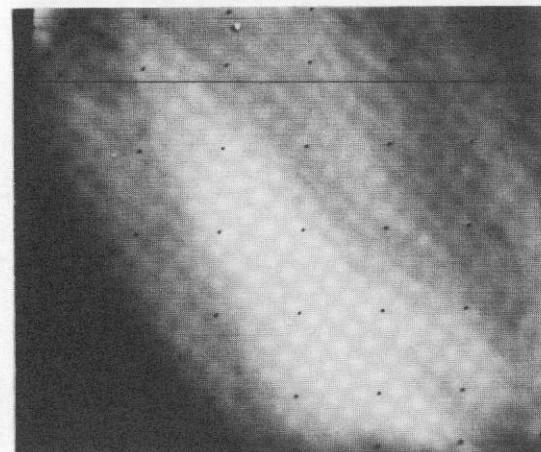
(l) NIX OLYMPICA: REV 668



(m) NIX OLYMPICA SHIELD: REV 668

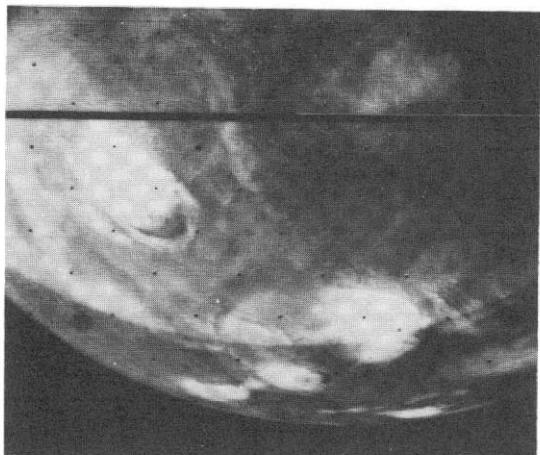


(n) THARSIS REGION: REV 676

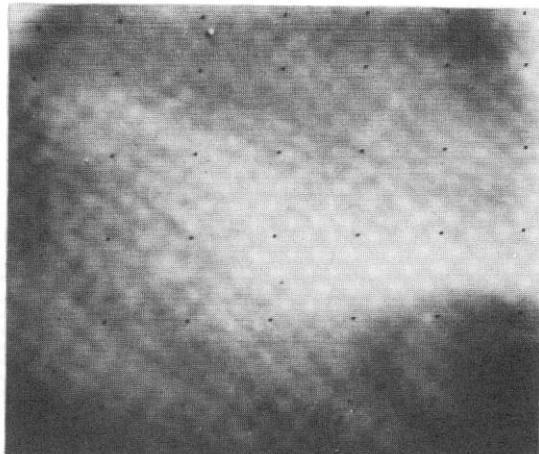


(o) NORTH SPOT: REV 676

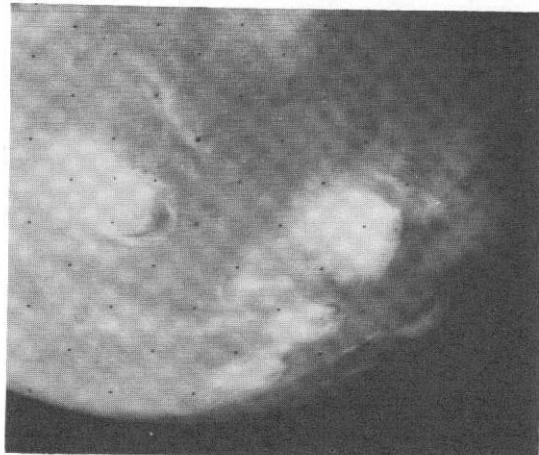
Fig. XI-15. (contd).



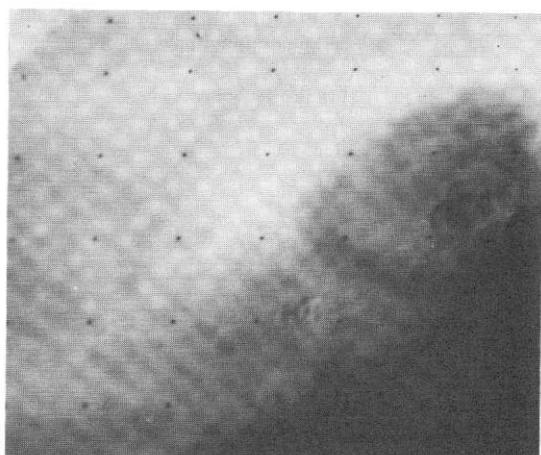
(p) THARSIS REGION: REV 676



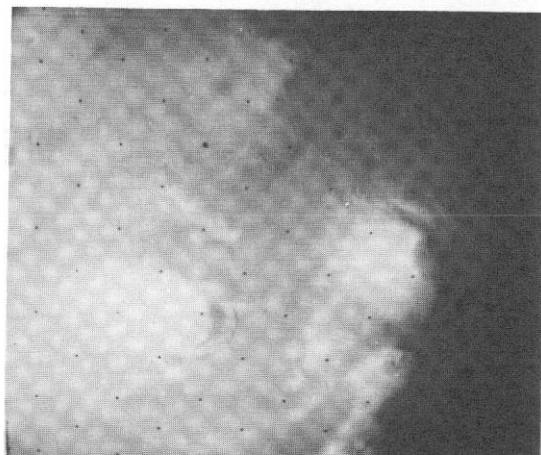
(q) NORTH SPOT: REV 676



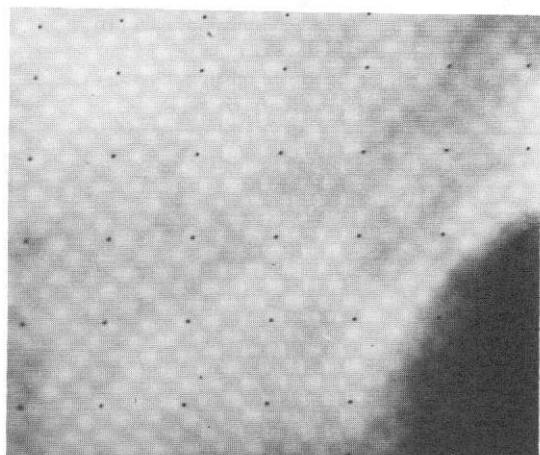
(r) THARSIS REGION: REV 676



(s) NORTH SPOT: REV 676



(t) THARSIS REGION: REV 676

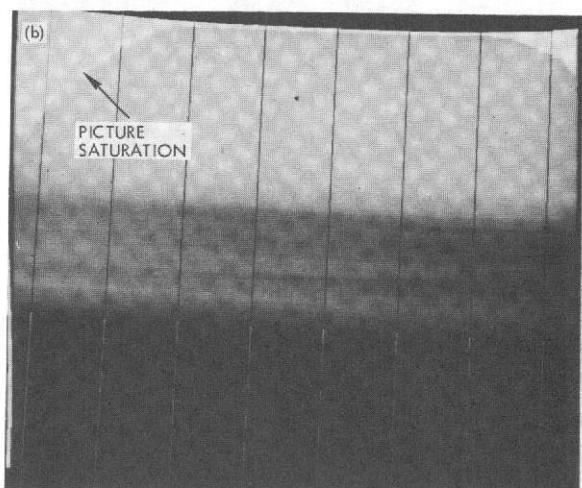
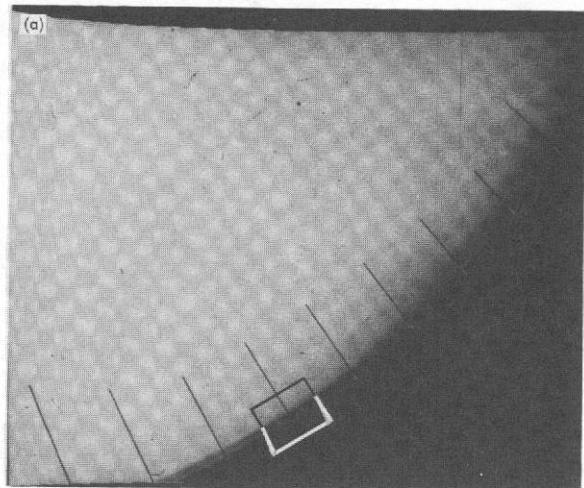


(u) NORTH SPOT: REV 676

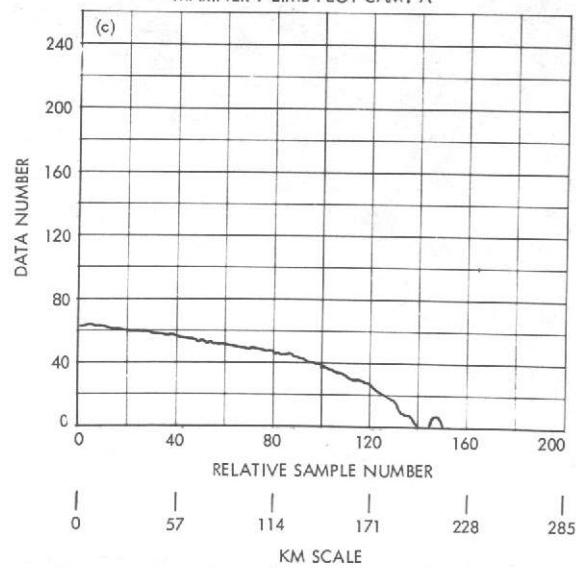
Fig. XI-15. (contd).

Table XI-3. Limb observations by Mariner 9

Revs	Phase	Number of pictures	
		Wide-angle camera (A)	Narrow-angle camera (B)
1-15	Post-orbital insertion mapping, calibration, and phase function	47	3
16-23	Interim sequence	22	1
24-63	Recon I	226	94
64-99	Recon II	115	36
100-138	Mapping Cycle I	125	23
139-177	Mapping Cycle II	10	3
178-217	Mapping Cycle III	31	20
218-262	Extended mission, Phase I	18	2
416-459	Extended mission, Phase II	7	0
473-533	Extended mission, Phase III	9	0
667-676	Extended mission, Phase IV	11	2



MARINER 9 LIMB PLOT CAM. A



MARINER 9 LIMB PLOT CAM. B

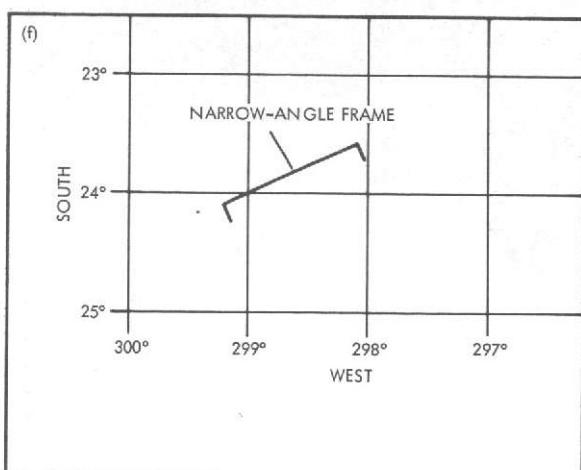
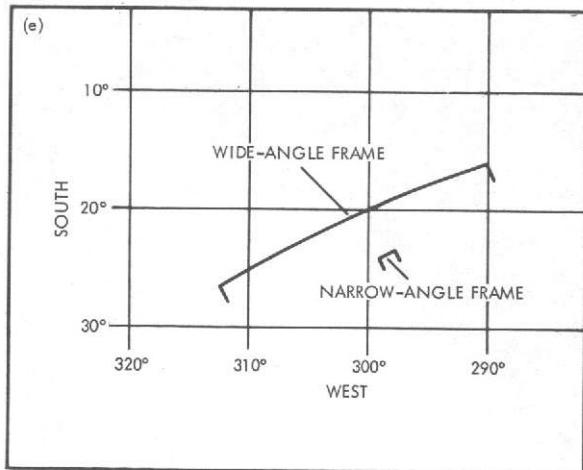
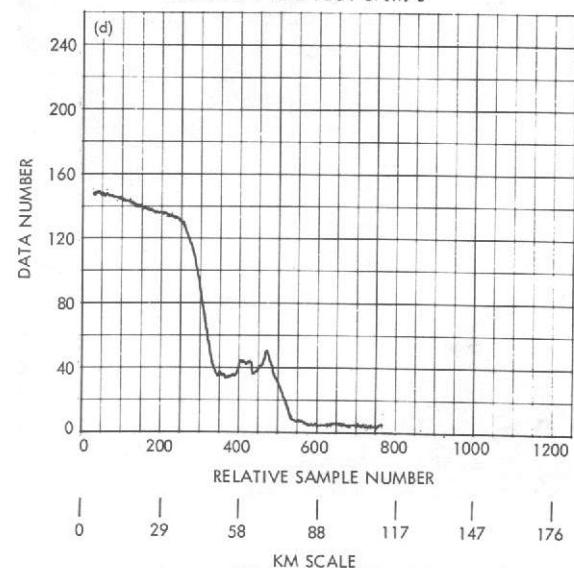
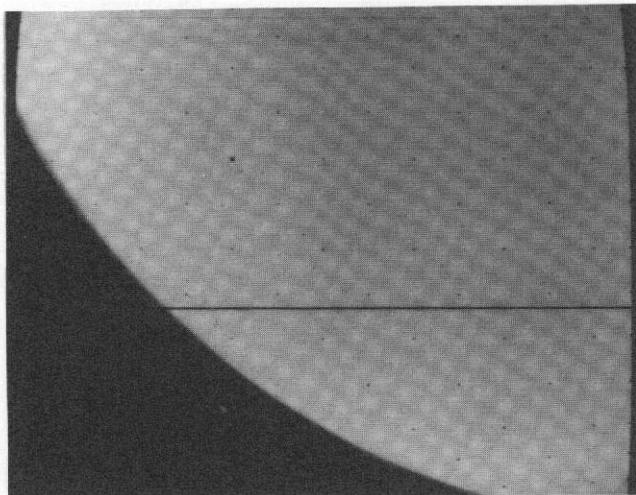
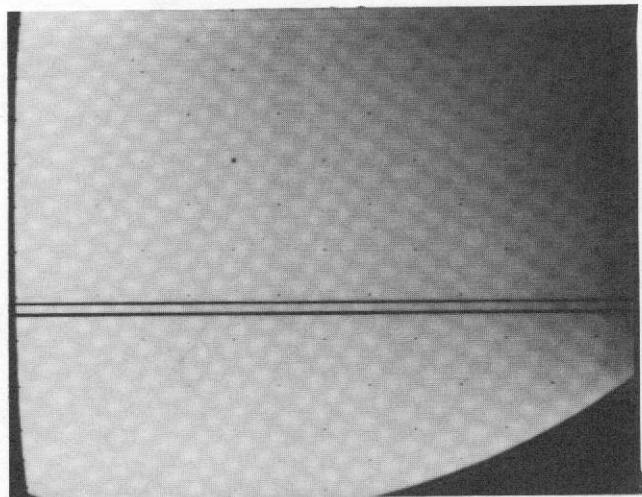


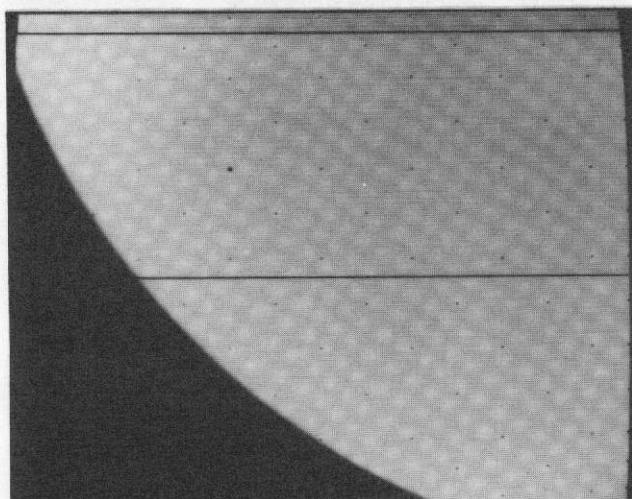
Fig. XI-16. Limb frames and data derived from them. (a, b) Limb picture and sample limb trace. The location of the narrow-angle frame (b) is identified in Fig. XI-16a. (c, d) Numerical photometric limb traces. (e, f) Mercator projections of limb traces.



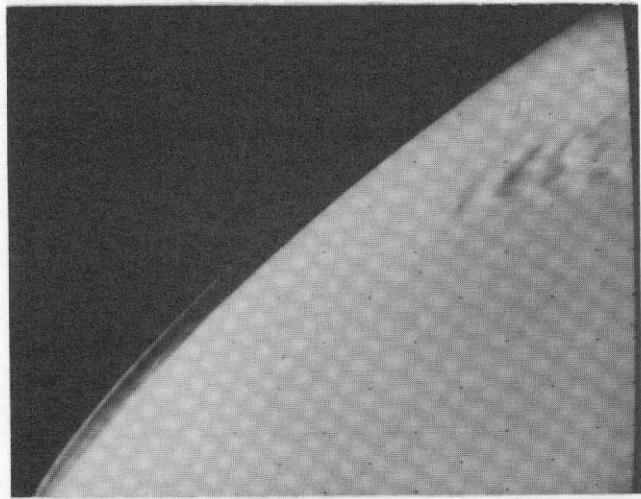
(a) REV 43



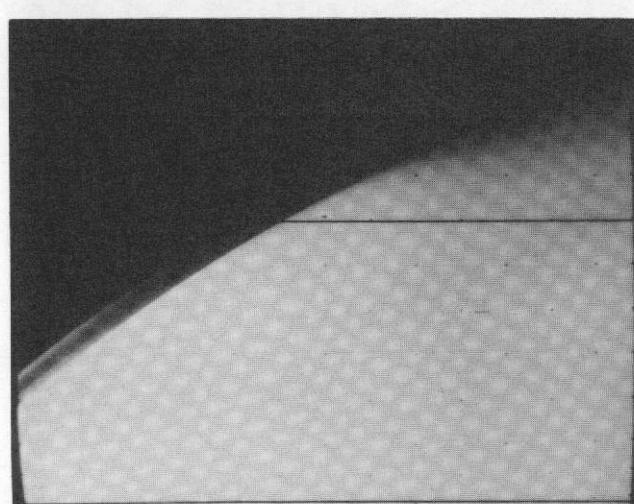
(b) REV 47



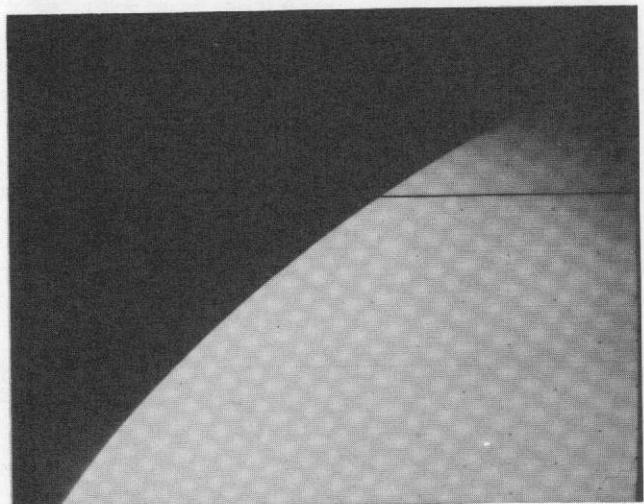
(c) REV 48



(d) REV 127

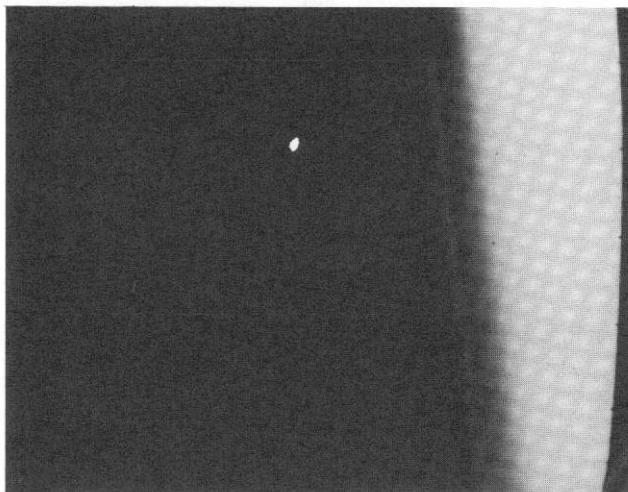


(e) REV 128

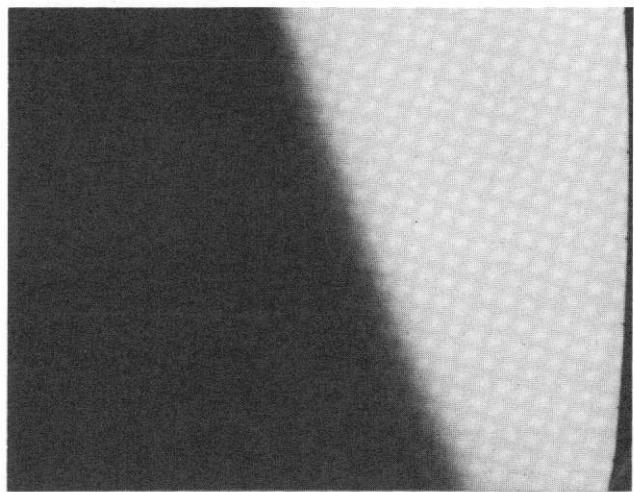


(f) REV 184

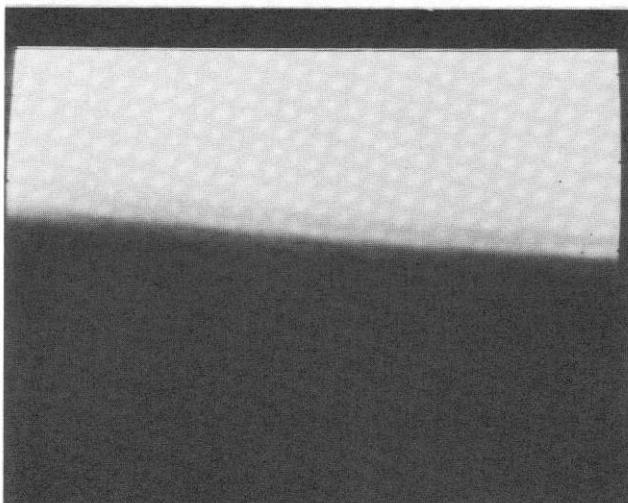
Fig. XI-17. Diverse limb haze structures visible in wide-angle frames.



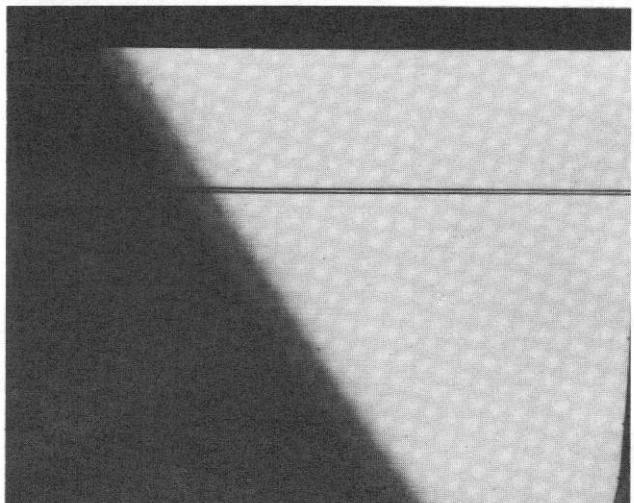
(a) REV 28



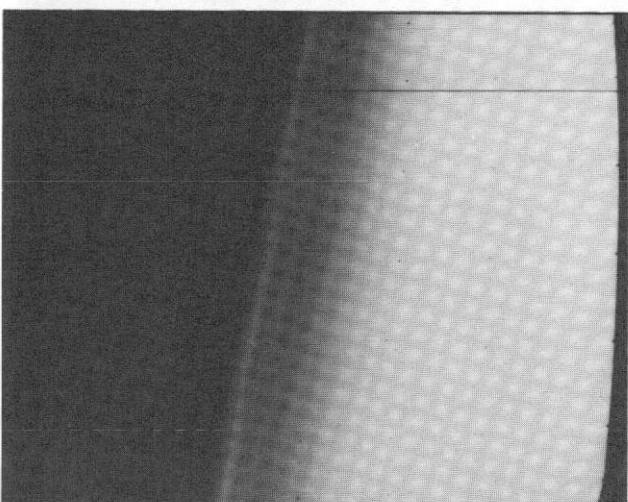
(b) REV 29



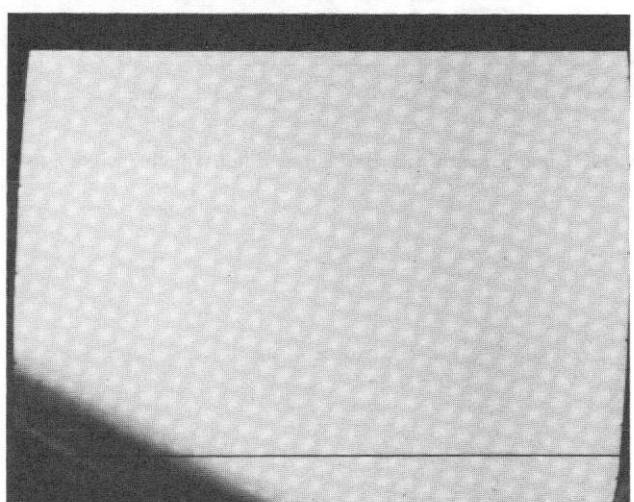
(c) REV 33



(d) REV 37



(e) REV 42



(f) REV 48

Fig. XI-18. Diverse limb haze structures visible in narrow-angle frames.

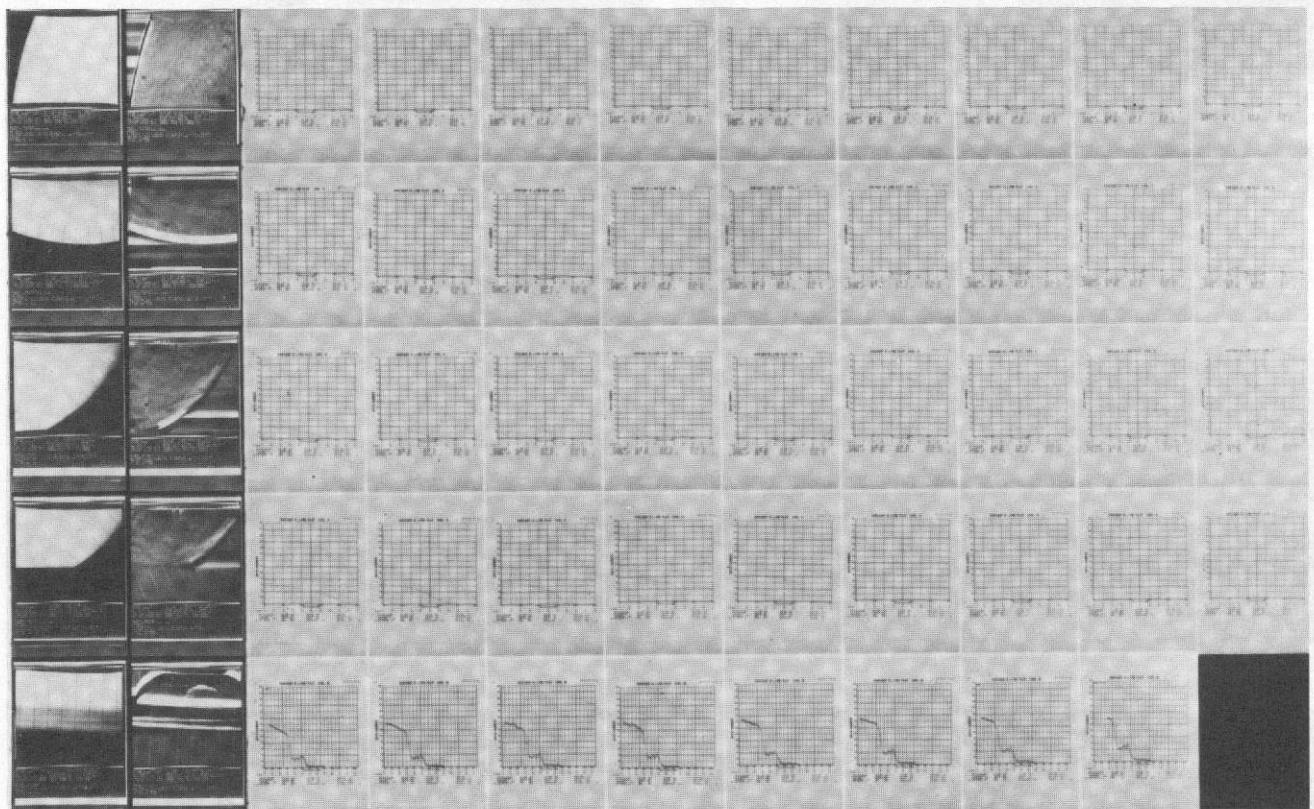
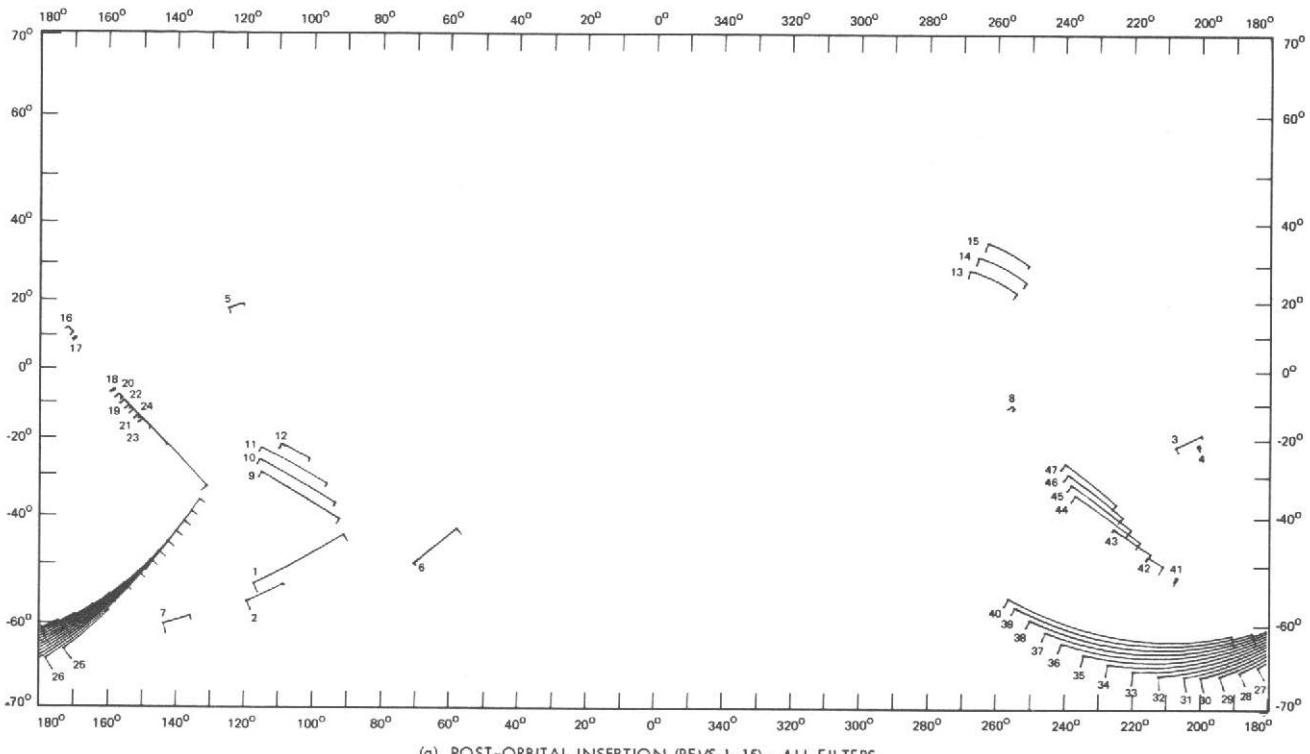


Fig. XI-19. Sample microfiche of Martian limb, which includes the two frames shown in Fig. XI-16. This figure is not shown actual size.



(a) POST-ORBITAL INSERTION (REVS 1-15): ALL FILTERS

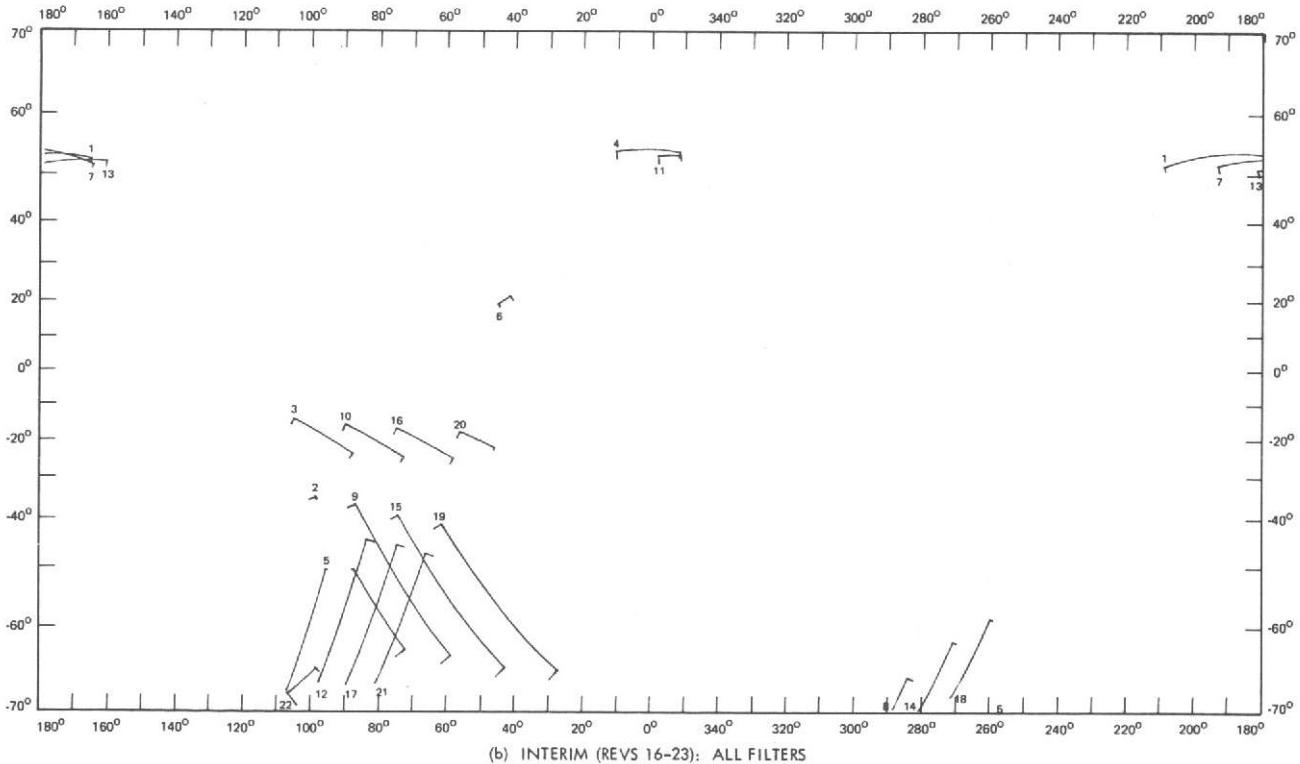


Fig. XI-20. Limb traces for wide-angle frames: 70°N to 70°S (see Table XI-4). Full lines separated by dashed lines indicate two separate sectors of the limb appearing in a picture.

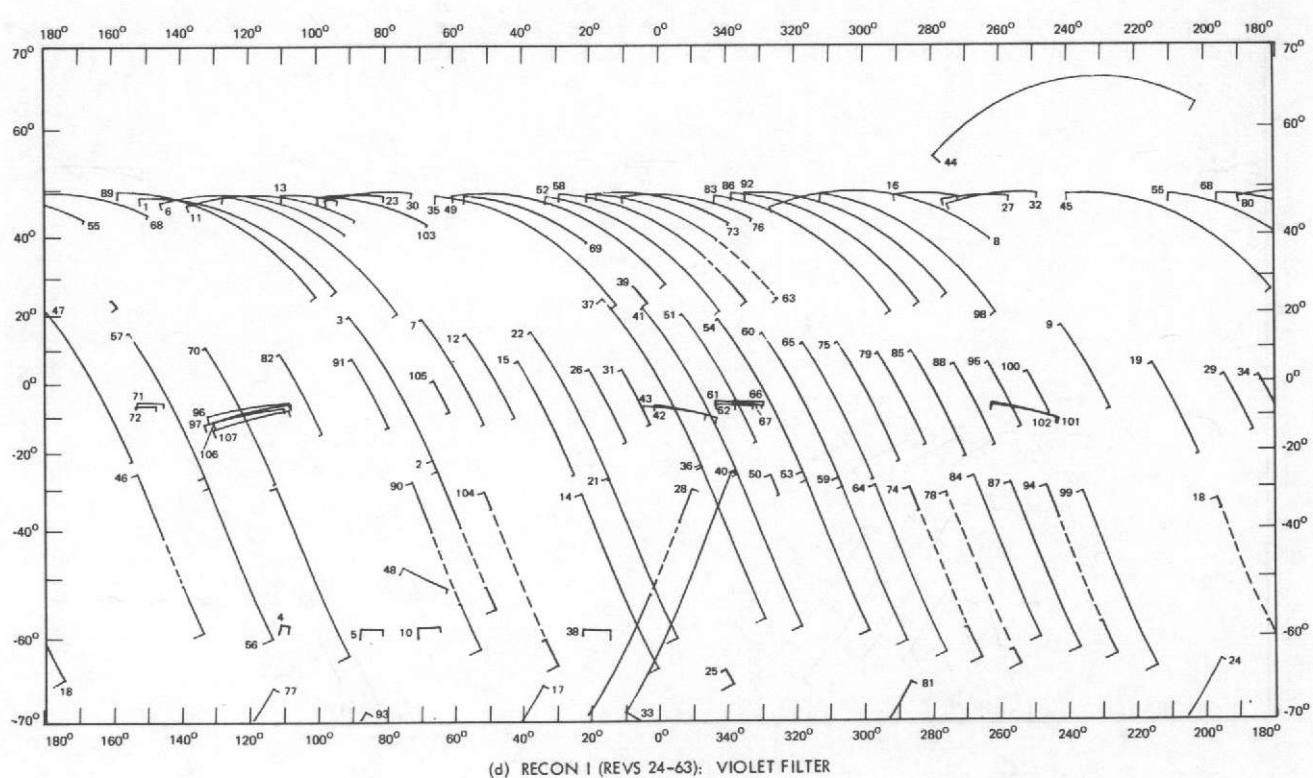
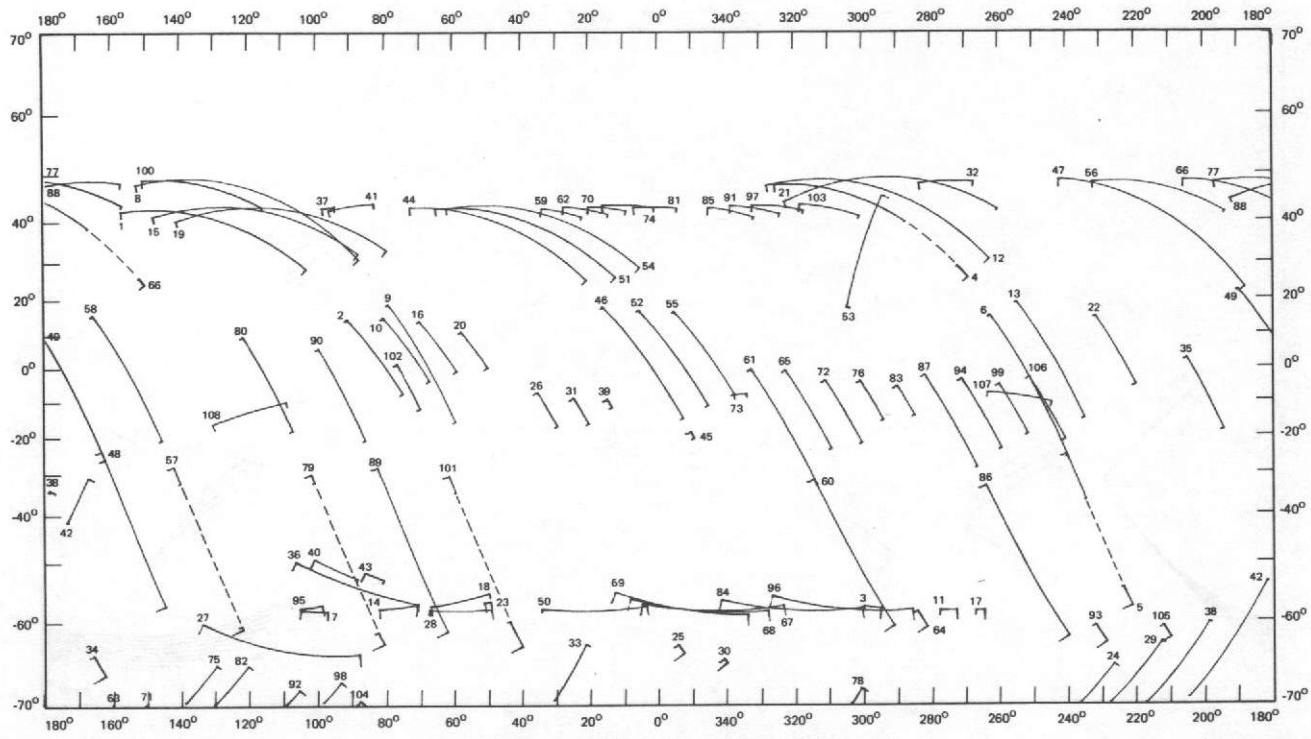


Fig. XI-20. (contd.)

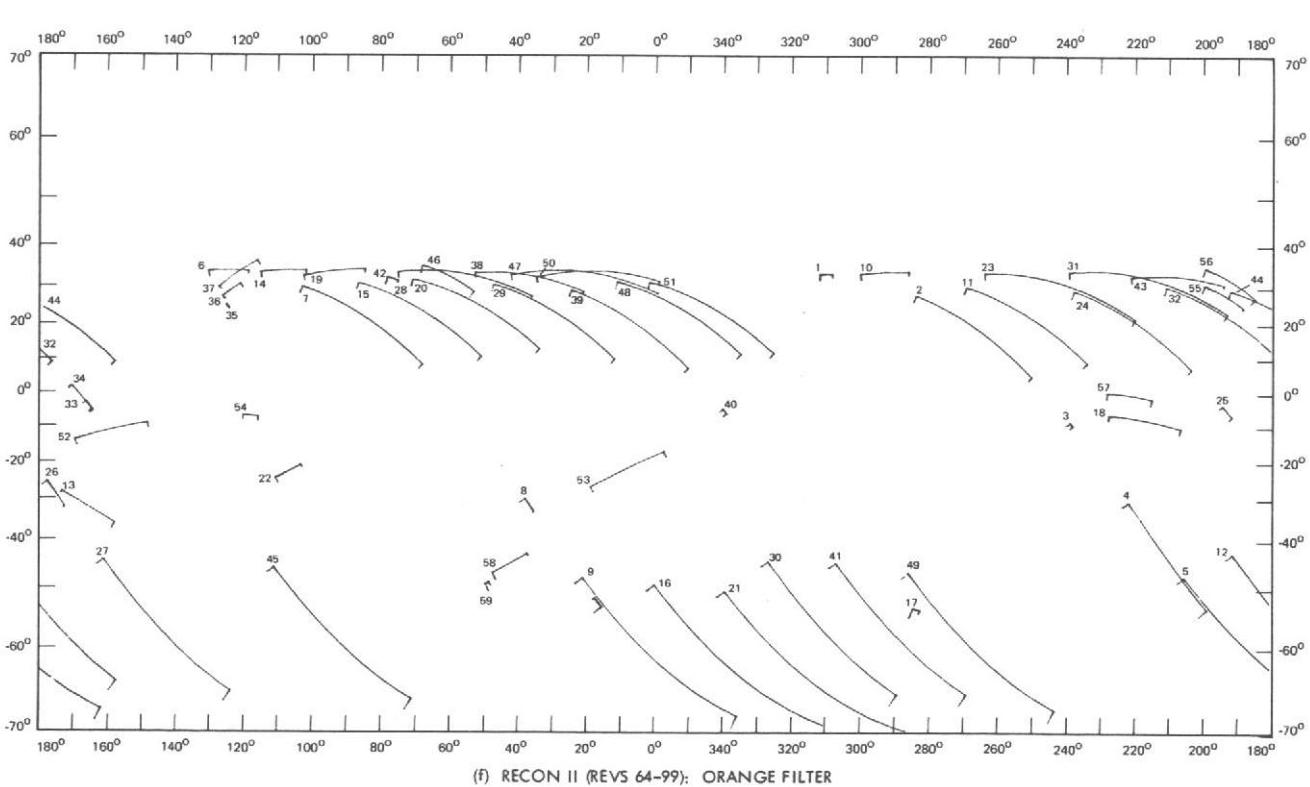
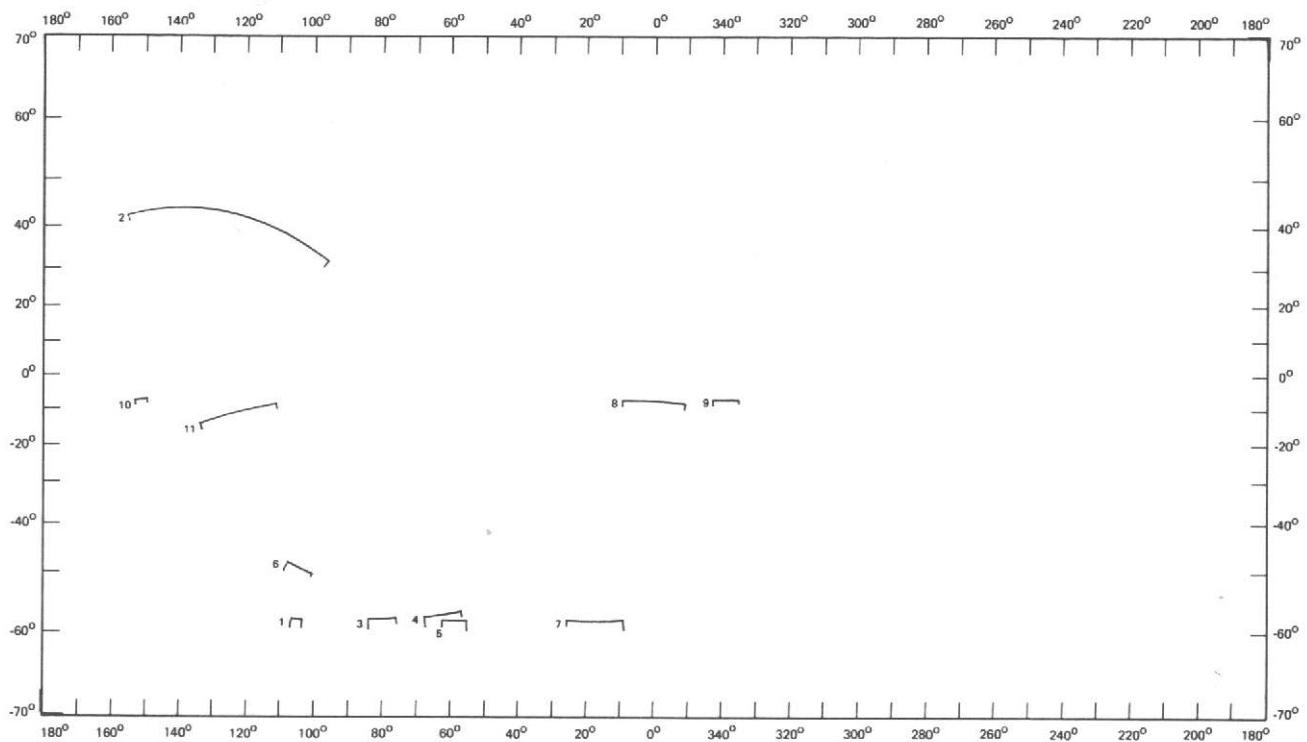


Fig. XI-20. (contd).

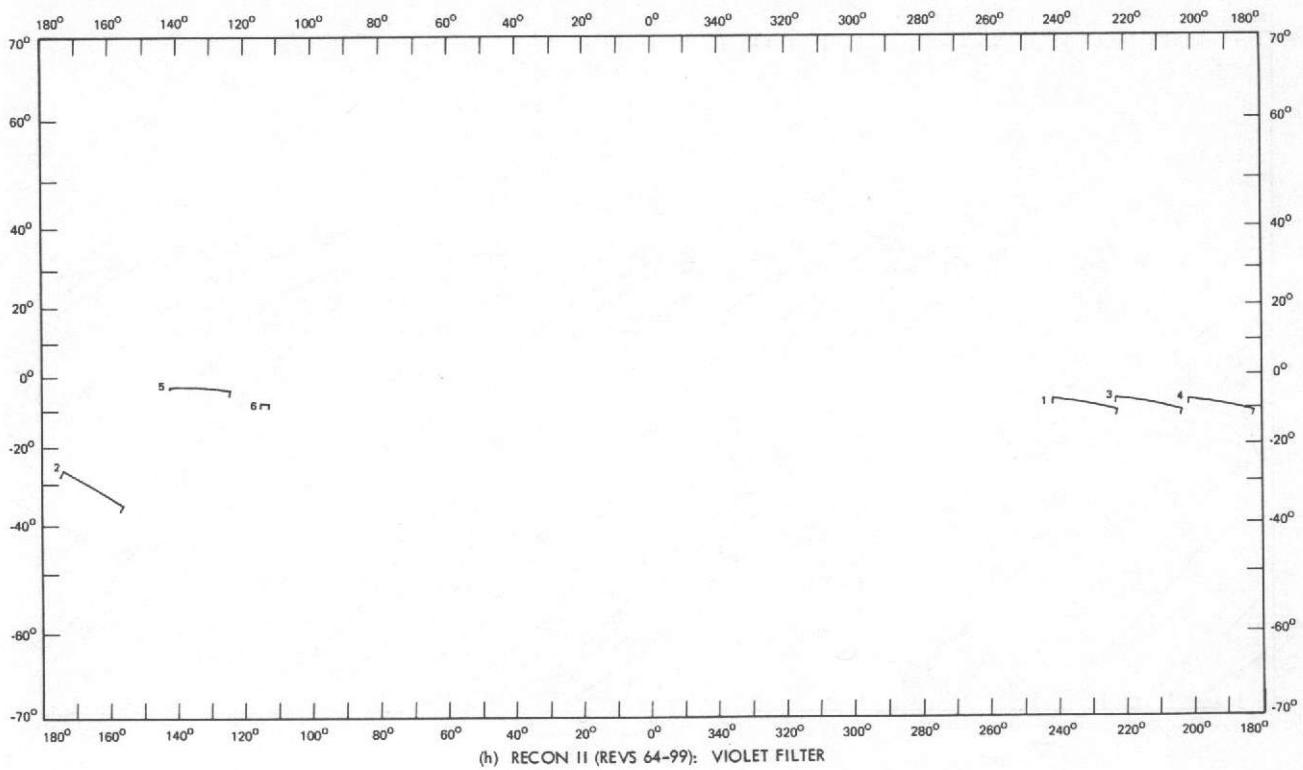
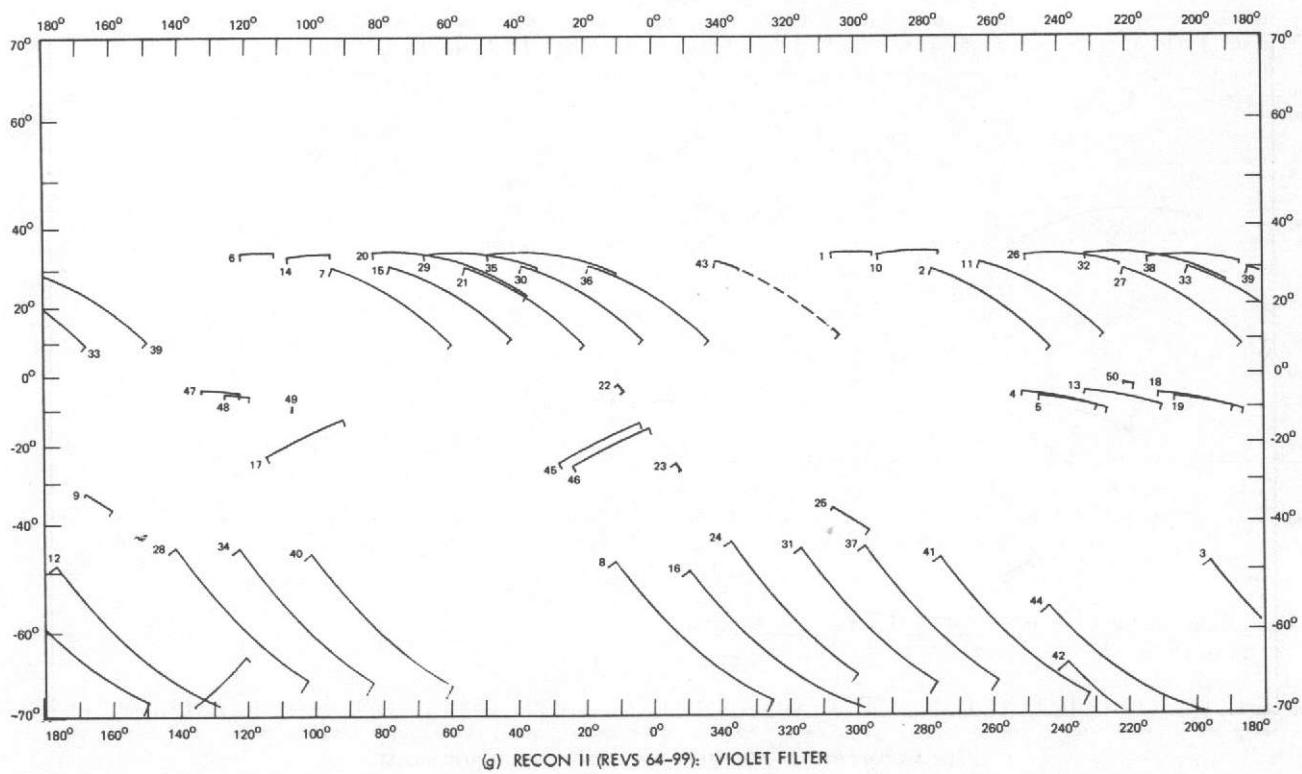
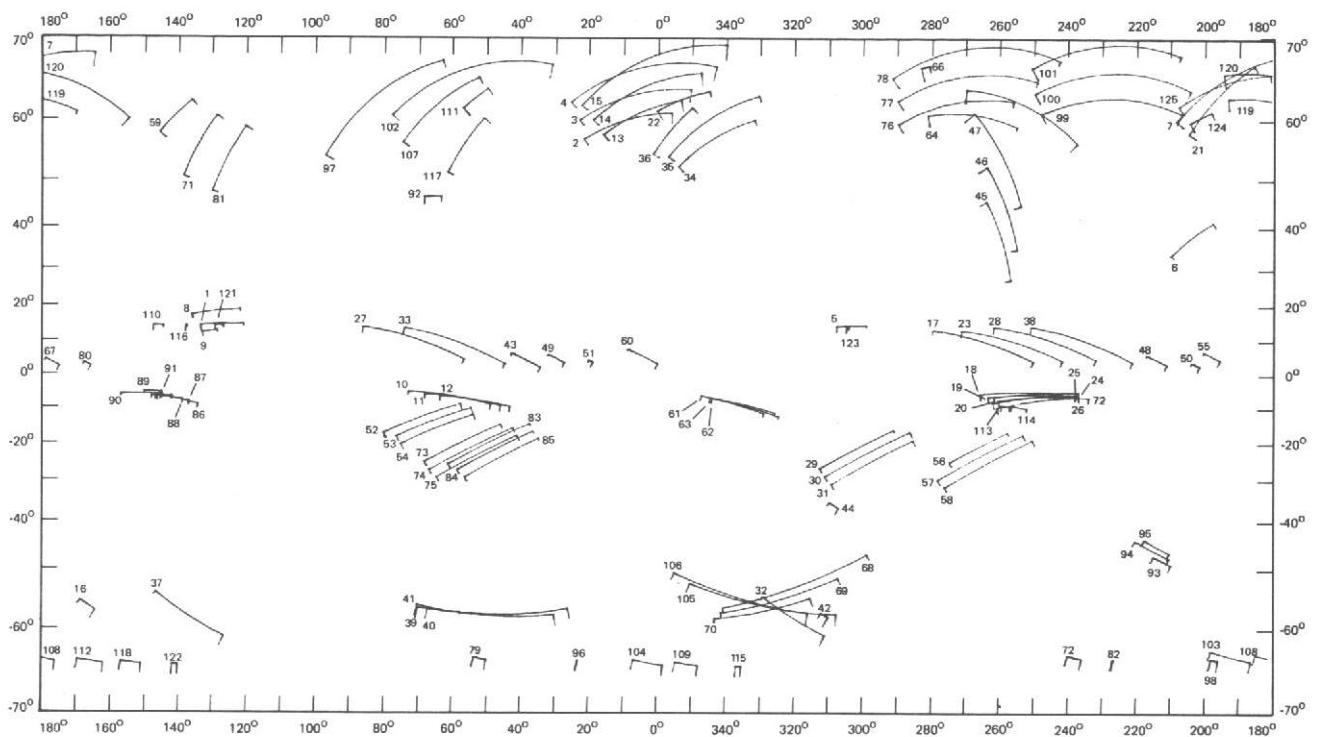
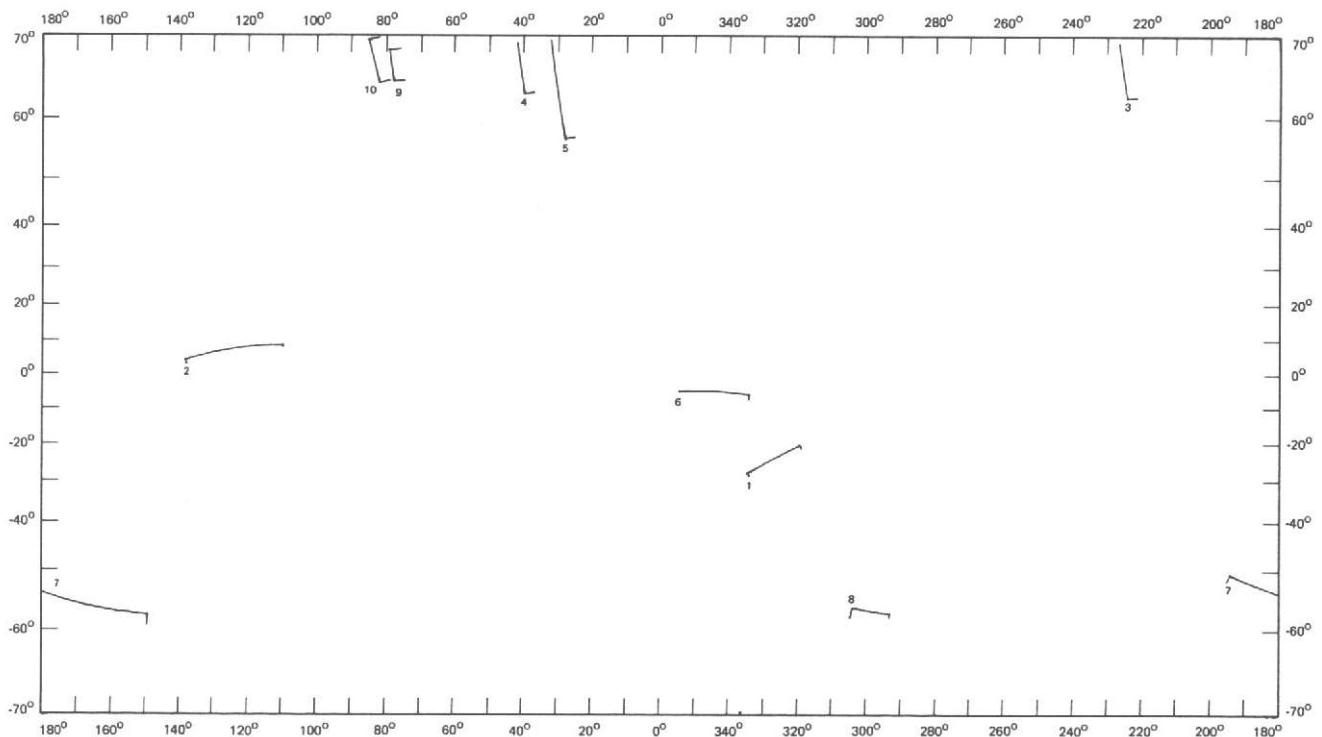


Fig. XI-20. (contd).



(i) MAPPING CYCLE I (REVS 100-138): POLARIZING FILTERS



(j) MAPPING CYCLE II (REVS 139-177): POLARIZING FILTERS

Fig. XI-20. (contd).

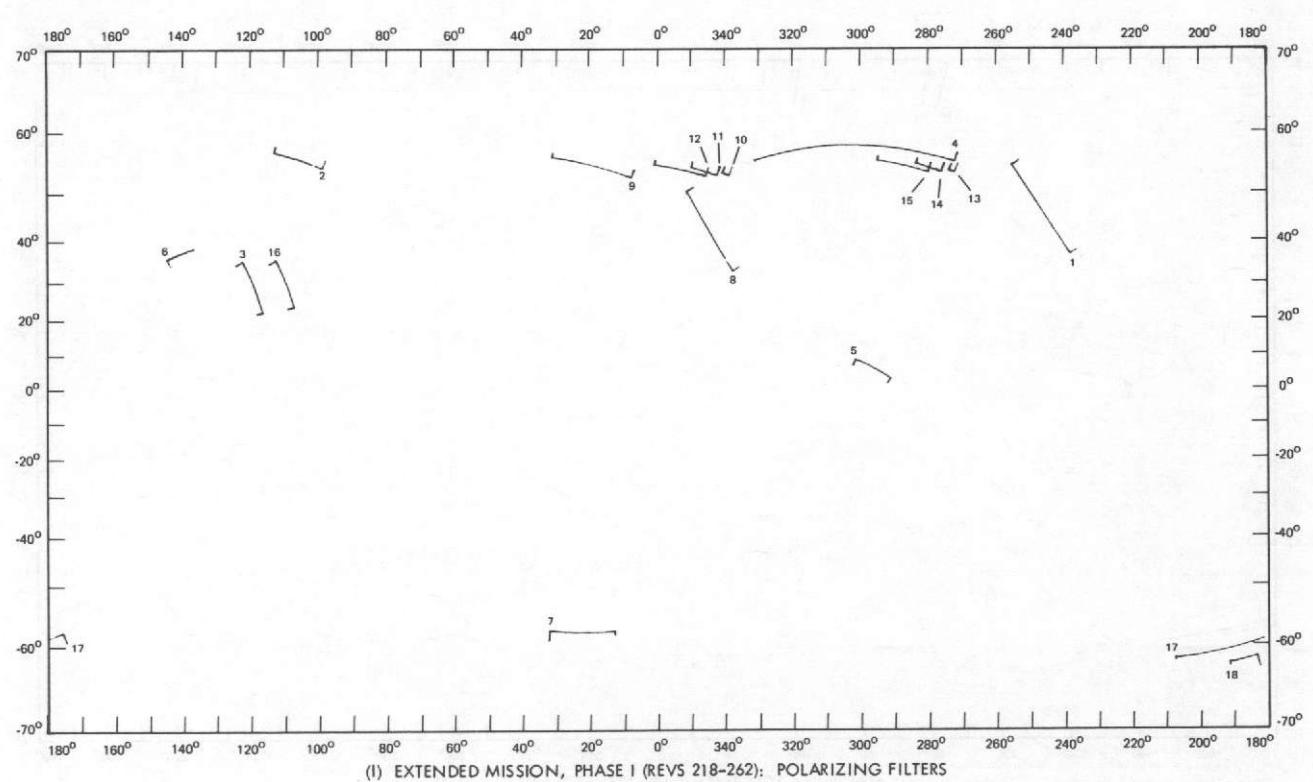
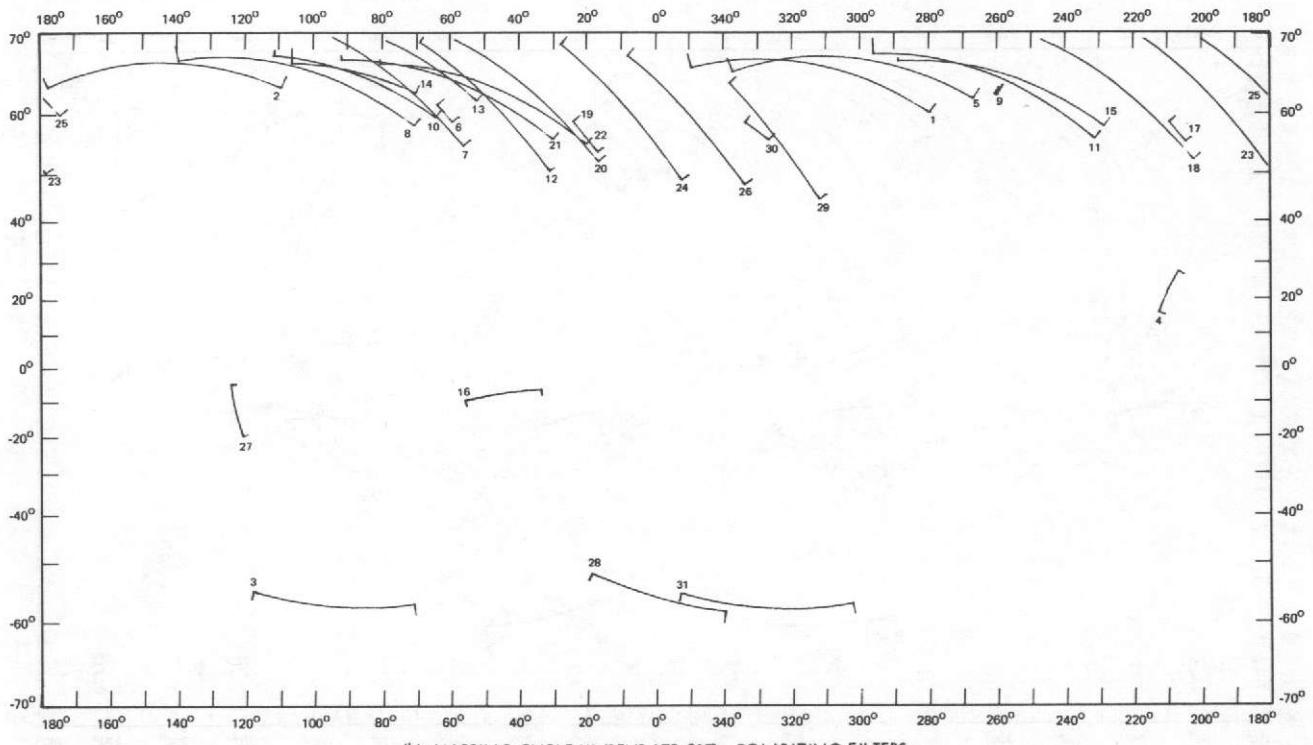
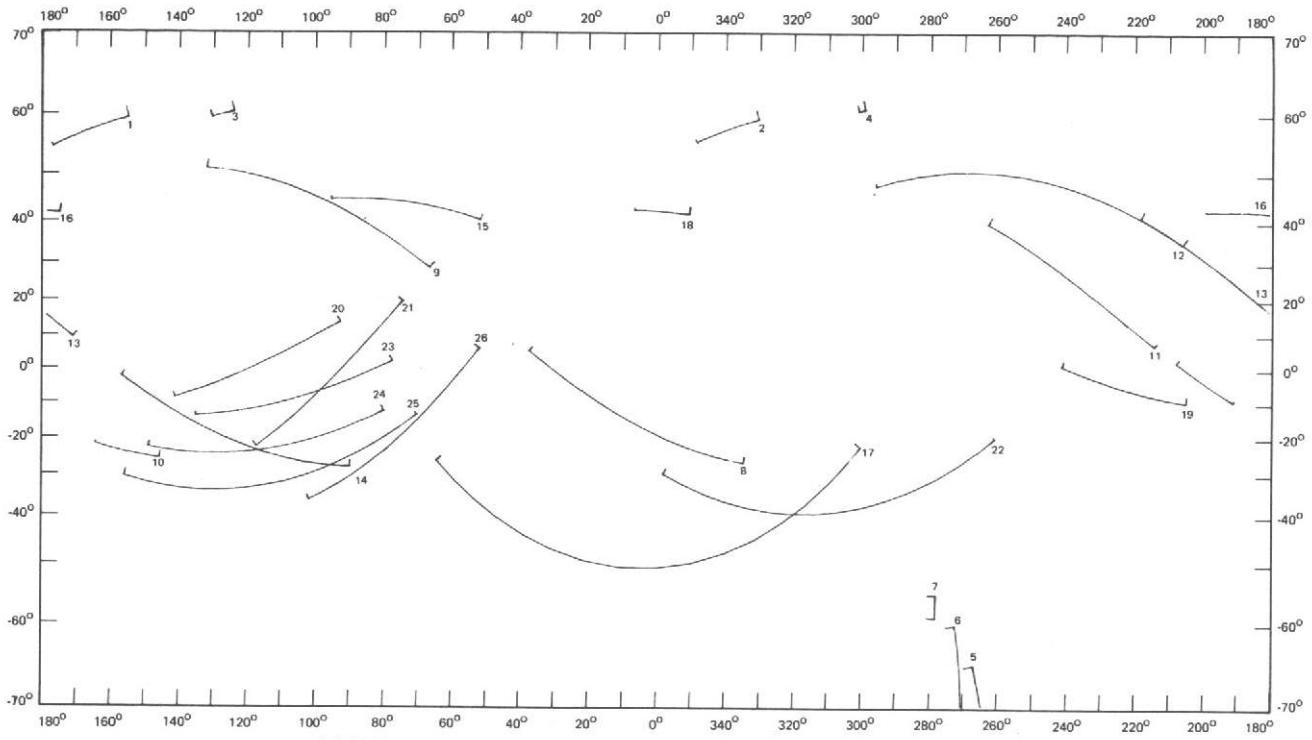


Fig. XI-20. (contd).



(m) EXTENDED MISSION, PHASES II, III, IV (REVS 416-676): POLARIZING FILTERS

Fig. XI-20. (contd.).

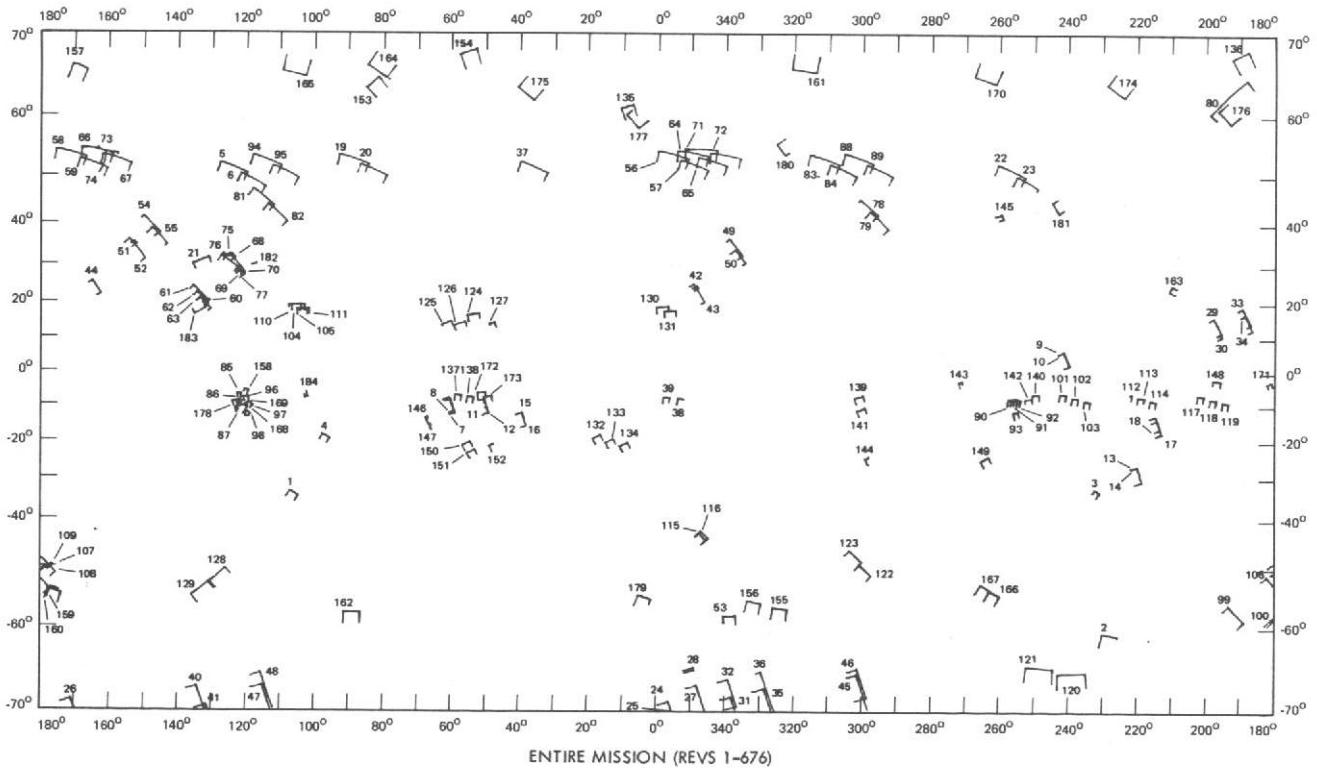


Fig. XI-21. Limb traces for narrow-angle frames: 70°N to 70°S (see Table XI-5).

Table XI-4a. Limb traces for wide-angle frames: 70°N to 70°S (see Fig. XI-20a)

Index number	Rev	Frame number	Limb profile								Filter	DAS time	Microfiche ID			
			Left margin		Right margin		Center of limb									
			Latitude, deg	Longitude, deg	Latitude, deg	Longitude, deg	Range, km	Lighting angle, deg	Hour angle, h	Phase angle, deg						
1	1	2	90.9	-43.0	117.3	-52.7	4981.6	71.8	6.2	49.4	2	1672891	22-4			
2	1	4	108.5	-52.8	119.3	-55.7	4849.3	76.0	5.5	46.7	2	1672951	22-5			
3	2	2	109.9	-17.7	207.4	-21.0	4534.7	4.6	11.8	85.6	2	1710821	23-1			
4	2	4	200.5	-20.3	201.0	-20.6	4413.1	2.2	12.0	87.9	2	1710891	23-2			
5	2	32	120.4	19.7	125.0	18.5	3388.5	90.8	17.5	81.9	2	1711871	151-4			
6	3	2	57.8	-41.7	70.2	-48.9	4349.9	39.4	9.4	78.9	2	1748621	151-5			
7	5	2	135.8	-58.1	143.6	-59.3	4637.1	84.5	4.1	37.9	2	1779225	23-3			
8	5	32	254.7	-10.3	255.5	-9.3	3428.0	122.1	20.7	32.1	2	1780275				
9	6	2	92.0	-39.7	115.1	-28.3	5424.4	78.0	18.0	41.3	2	1814855	115-3			
10	6	4	93.2	-36.0	115.6	-24.9	5154.6	79.2	18.0	41.3	2	1814895	23-4			
11	6	6	95.7	-31.3	115.1	-21.8	4890.7	80.4	18.0	41.8	2	1815135	23-5			
12	6	8	100.8	-24.8	109.1	-20.8	4634.2	82.7	18.1	41.7	2	1815275	24-1			
13	7	26	254.2	23.0	268.0	29.0	3401.2	122.8	19.8	59.8	1	1852515				
14	7	28	251.5	25.8	265.5	32.4	3430.8	126.0	20.0	61.8	1	1852585	47-3			
15	7	30	250.8	30.3	262.9	35.8	3472.8	128.0	20.1	65.0	1	1852555	47-4			
16	8	2	170.3	11.2	171.9	12.9	9959.9	34.4	12.1	65.0	4	1884295				
17	8	4	169.4	9.7	160.7	10.1	9842.5	32.4	12.2	66.1	8	1884765	26-4			
18	8	20	158.0	-5.4	158.3	-5.1	8866.1	23.7	13.1	66.4	8	1884295	26-5			
19	8	22	155.9	-7.8	156.9	-6.7	8739.6	23.8	13.3	66.2	8	1884925	27-1			
20	8	24	153.3	-10.5	155.4	-8.4	8613.0	24.3	13.4	66.0	2	1885655	27-2			
21	8	26	150.6	-13.3	154.0	-9.8	8485.0	25.2	13.6	65.8	4	1885135	27-3			
22	8	28	147.5	-16.4	152.7	-11.1	8356.7	26.5	13.8	65.4	8	1885205	27-4			
23	8	30	142.7	-21.0	151.3	-12.5	8227.1	26.7	14.0	64.9	8	1885275	27-5			
24	8	32	130.9	-31.9	140.9	-13.7	8097.2	33.7	14.4	63.6		1885745	28-1			
25	9	2	133.0	-35.2	148.7	-50.2	9141.7	109.7	1.0	31.2	0	1920676	28-2			
25	9	2	159.6	-57.3	172.6	-63.0	9141.7	97.4	.2	38.9	8	1920635	28-3			
25	9	4	135.4	-37.9	170.0	-64.2	916.0	104.0	1.2	34.0	8	1920765	28-4			
27	9	6	137.6	-40.2	183.0	-65.0	8892.8	102.8	1.0	34.0	7	1920835	28-4			
28	9	8	139.9	-42.4	188.4	-65.6	8766.4	101.5	.8	34.0	8	1920995	28-5			
29	9	10	142.4	-44.6	194.6	-66.1	8639.8	100.3	.6	34.0	2	1920975	29-1			
30	9	12	144.9	-46.6	190.8	-66.3	8511.9	99.2	.3	34.0	4	1921045	29-2			
31	9	14	147.3	-48.3	204.6	-66.2	8383.7	98.3	.1	33.8	8	1921115	29-3			
32	9	16	151.0	-50.5	212.2	-66.1	8254.1	96.8	23.8	34.1	8	1921185	29-4			
33	9	18	155.0	-52.7	219.8	-65.5	8124.2	95.3	23.4	34.4	2	1921255				
34	9	20	159.4	-54.6	227.1	-64.7	7993.0	93.8	22.9	34.7	4	1921325	29-1			
35	9	22	164.2	-56.4	234.1	-63.5	7861.4	92.4	22.5	35.0	8	1921395	76-2			
36	9	24	169.5	-57.9	240.7	-61.9	7729.5	90.9	22.0	35.4	8	1921465	76-3			
37	9	26	174.2	-58.9	245.4	-60.3	7596.1	89.9	21.6	35.6	2	1921535	76-4			
38	9	28	179.4	-59.8	250.1	-58.5	7462.3	88.8	21.2	35.8	4	1921605	76-5			
39	9	30	184.7	-60.4	254.4	-56.6	7327.0	87.7	20.8	36.0	8	1921675	77-1			
40	9	32	190.8	-60.8	256.4	-55.1	7192.4	86.9	20.6	36.0	8	1921745	77-2			
41	11	20	206.7	-51.4	207.0	-51.3	4904.1	99.5	21.5	11.0	4	1994755	77-4			
42	11	22	210.9	-49.2	215.5	-47.4	4774.7	99.5	21.1	13.0	8	1994825	77-5			
43	11	24	214.6	-46.9	225.5	-41.5	4646.6	99.4	20.7	15.1	6	1994895	78-1			
44	11	26	217.7	-44.4	236.9	-33.7	4522.2	98.8	20.2	18.3	2	1994665	78-2			
45	11	28	220.4	-41.7	238.1	-31.1	4401.7	99.5	18.9	20.1	4	1995035	78-3			
46	11	30	222.6	-38.9	239.1	-28.4	4283.8	100.3	19.5	20.0	8	1995115	78-11			
47	11	32	224.8	-36.0	240.0	-25.6	4171.6	101.2	20.3	19.9	8	1995175	78-1			

Note: Double entries correspond to two separate sectors of the limb appearing in a single picture.

Table XI-4b. Limb traces for wide-angle frames: 70°N to 70°S (see Fig. XI-20b)

Index number	Rev	Frame Number	Limb profile								Filter	DAS time	Microfiche ID			
			Left margin		Right margin		Center of limb									
			Latitude, deg	Longitude, deg	Latitude, deg	Longitude, deg	Range, km	Lighting angle, deg	Hour angle, h	Phase angle, deg						
1	16	3	51.2	164.8	51.7	209.6	12781.9	94.9	7.6	60.0	8	2169645	80-3			
2	16	7	-34.9	98.4	-34.4	98.7	10499.2	28.7	14.0	70.7	2	2171225	70-3			
2	16	7	-62.7	72.1	-49.9	87.3	10499.2	48.8	15.1	66.3	2	2171225	70-3			
3	16	9	-23.4	87.8	-13.8	105.2	6161.4	40.3	14.9	64.0	8	2173605	70-4			
4	17	1	53.8	352.1	54.1	11.0	12842.9	95.1	7.5	60.6	8	2205525	93-4			
5	17	3	-49.9	95.6	-69.8	257.2	12652.5	80.3	23.4	64.3	8	2205665	80-1			
6	17	11	21.5	41.9	19.3	45.4	9523.6	104.8	5.4	40.6	8	2207695	21-4			
7	18	3	52.3	165.4	51.9	193.5	12615.2	95.7	7.4	59.9	8	2241575	22-1			
8	18	4	-66.0	284.2	-79.3	35.3	12224.5	78.9	22.5	63.6	2	2241855	22-2			
9	18	7	-63.5	58.5	-36.1	87.0	10301.5	43.2	14.8	67.9	2	2243115	22-3			
10	18	9	-24.4	72.8	-15.5	90.0	5923.0	44.5	15.2	63.0	8	2245425	131-2			
11	19	1	53.4	351.8	53.3	358.6	12671.1	96.5	7.3	60.3	8	2277415	47-5			
12	19	3	-44.0	83.7	-71.3	243.5	12478.5	84.2	23.8	63.3	8	2277555	48-1			
13	20	3	51.8	161.0	51.1	181.8	12433.9	96.3	7.2	59.8	8	2313465	48-3			
14	20	4	-61.4	271.1	-77.6	34.3	12037.6	80.6	22.7	63.2	2	2313745	48-4			
15	20	7	-65.0	42.8	-38.6	74.4	10085.5	46.1	15.0	67.4	2	2315005	48-5			
16	20	9	-74.7	8.1	-16.5	75.0	5667.0	48.6	15.5	61.9	2	2317395	49-1			
17	21	3	-45.1	74.7	-71.9	230.6	12292.9	84.5	23.6	63.3	8	2349415	49-2			
18	22	4	-58.0	260.1	-73.2	35.0	11741.2	80.5	22.3	62.9	2	2345705	49-4			
19	22	7	-65.3	27.0	-40.6	61.5	9743.1	88.9	15.3	66.5	2	2346065				
20	22	9	-21.7	46.3	-17.4	56.4	5272.9	53.7	15.8	60.7	8	2349345	93-5			
21	23	3	-45.8	66.1	-74.1	213.5	12106.1	85.3	23.6	63.2	8	2421335	40-5			
22	23	6	-65.1	08.4	-68.0	106.7	10049.6	91.6	23.2	52.3	2	2422665	50-2			

Note: Double entries correspond to two separate sectors of the limb appearing in a single picture.

Table XI-4c. Limb traces for wide-angle frames: 70°N to 70°S (see Fig. XI-20c)

Index number	Rev	Frame number	Limb profile								Filter	DAS time	Microfiche ID			
			Left margin		Right margin		Center of limb									
			Latitude, deg	Longitude, deg	Latitude, deg	Longitude, deg	Range, km	Lighting angle, deg	Hour angle, h	Phase angle, deg						
1	24	12	28.1	103.0	42.0	157.2	10908.3	73.5	9.1	63.0	2	245A015	11-3			
2	24	16	-7.4	74.7	14.4	91.0	10461.4	25.3	12.1	73.9	2	245A295	11-4			
3	24	22	-57.5	294.6	-57.1	299.7	5431.5	99.7	22.7	13.9	2	2461025	11-5			
4	25	9	39.8	287.5	47.8	325.7	11720.4	81.0	8.7	63.9	2	2493365	12-1			
4	25	9	25.9	269.1	28.9	272.1	11720.4	51.0	11.0	72.3	2	2493365	12-1			
5	25	12	-36.0	234.5	-24.3	240.2	11406.8	19.0	13.2	77.0	2	2493575	12-2			
5	25	12	-57.1	220.9	-54.0	223.5	11406.8	42.5	14.3	73.4	2	2493575	12-2			
6	25	13	-25.1	239.8	15.6	262.8	11300.3	18.2	12.4	76.9	2	2493645	12-3			
7	25	19	-58.1	96.8	-57.8	104.9	5380.7	100.4	23.4	11.4	2	2496935	12-4			
8	26	7	30.6	87.5	47.7	152.9	11891.0	78.7	9.0	65.6	2	2529135	1-3			
9	26	11	-15.6	59.3	18.6	79.2	11476.6	23.4	12.1	77.1	2	2529415	1-4			
10	26	16	-3.6	66.9	14.9	80.7	10606.3	27.1	12.0	74.6	2	2529075	14-3			
11	26	22	-57.7	272.5	-57.8	277.5	5606.3	100.7	23.4	13.8	2	2532705	1-5			
12	27	9	30.7	262.8	47.6	328.1	11865.0	79.0	8.9	65.8	2	2565045	59-2			
13	27	13	-14.4	234.9	19.3	254.9	11449.5	24.2	12.1	77.3	2	2565325	59-3			
14	27	19	-56.8	70.9	-57.6	81.9	5571.2	101.5	.3	11.8	2	2568615	59-4			
15	28	12	32.0	87.7	40.9	147.8	10997.2	80.6	8.4	62.5	2	2601515	6-5			
16	28	16	-.8	58.9	13.9	70.1	10552.8	27.9	11.9	75.1	2	2601725	7-1			
17	28	22	-57.8	264.4	-57.8	267.0	5540.6	100.7	23.3	13.8	2	2604525	7-2			
18	29	17	-55.0	49.7	-57.1	66.8	5658.8	102.1	.8	12.2	2	2604365	8-2			
19	30	12	32.9	79.5	40.0	141.1	10976.3	82.8	8.1	62.4	2	2673335	74-1			
20	30	16	-.3	49.8	10.9	57.7	10530.7	26.7	11.9	75.9	2	2673615	12-5			
21	31	7	42.5	260.4	44.2	323.0	11926.4	92.9	7.4	63.3	2	2704615	13-2			
22	31	11	-4.7	219.8	15.4	231.8	11513.1	26.5	11.9	78.6	2	2708895	13-3			
23	31	19	-56.4	49.2	-56.6	51.0	5650.7	102.2	.6	12.6	2	2712185	13-4			
24	32	14	-65.3	226.4	-74.5	256.7	10767.9	88.0	22.8	60.5	2	2745275	15-1			
25	32	15	-63.9	352.3	-62.8	354.2	10655.7	53.2	15.2	71.3	2	2745365	15-2			
26	32	16	-16.8	29.4	-6.9	35.4	10543.3	12.4	12.6	78.2	2	2745435	15-3			
27	33	17	-64.0	87.5	-59.8	133.5	7731.7	80.8	19.5	50.2	2	2782055	3-2			
28	33	19	-57.6	48.8	-57.8	67.0	5547.8	101.1	23.4	14.5	2	2784075	3-3			
29	34	14	-62.3	212.4	-73.2	241.3	10701.6	90.5	23.1	60.0	2	2817185	4-5			
30	34	15	-65.2	339.7	-64.6	340.7	10590.6	55.1	15.4	71.3	2	2817255	5-1			
31	34	16	-16.1	20.2	-8.6	24.7	10477.1	11.7	12.6	78.7	2	2817225	5-2			
32	35	9	48.2	267.5	48.0	283.5	11804.7	95.2	7.1	63.6	2	2852395	152-1			
33	35	11	-62.8	21.2	-74.1	42.2	11597.5	90.6	23.5	64.2	2	2852535	15-5			
34	35	12	-66.6	161.8	-64.2	165.2	11492.3	51.5	14.6	75.2	2	2852605	16-1			
35	35	13	-17.7	194.3	3.3	205.1	11386.9	13.9	12.2	81.0	2	2852675	16-2			
36	35	19	-56.8	70.4	-49.4	106.3	5483.3	93.9	20.6	26.8	2	2855065	151-2			
37	36	12	43.0	94.7	42.7	98.2	10997.2	95.1	6.8	60.5	2	2888865	61-4			
38	36	14	-33.7	178.3	-34.0	178.4	10777.3	122.0	1.4	49.7	2	2889005	61-5			
39	36	14	-59.6	198.6	-71.2	221.8	10777.3	93.5	23.5	60.0	2	2889005	61-5			
39	36	16	-11.4	13.4	-8.9	14.8	10552.6	12.0	12.4	79.5	2	2889145	62-1			
40	37	17	-52.5	88.1	-48.9	100.8	5587.0	98.2	19.6	34.6	2	2927785	75-1			
41	38	12	43.8	83.2	42.3	96.4	11090.3	97.9	6.6	60.7	2	2960635	152-3			
42	38	14	-30.5	166.9	-41.0	173.0	10871.0	121.0	1.3	51.5	2	2960825	62-5			
42	38	14	-52.9	181.8	-69.1	204.6	10871.6	98.3	23.9	59.5	2	2960825	62-5			
43	39	17	-52.7	80.6	-51.3	86.1	5703.1	88.0	19.6	35.8	2	2999610	63-5			
44	40	12	25.2	20.8	42.9	72.7	10965.8	71.8	9.0	69.7	2	3032650	153-2			
45	40	15	-20.1	349.2	-18.3	350.3	10633.6	9.3	12.7	81.2	2	3032860	153-1			
46	40	16	-14.5	352.5	17.9	16.0	10520.2	22.9	11.8	79.8	2	3032930	160-4			
47	41	8	23.2	198.0	48.7	242.3	11861.9	70.5	9.4	73.6	2	3068000	160-5			
48	41	11	-57.1	144.2	-23.5	163.0	11550.7	24.7	13.1	82.4	2	3068210	130-4			
49	41	12	-25.8	161.9	22.8	190.2	11445.4	19.8	11.8	82.7	2	3068200	140-2			
50	41	18	-57.0	3.3	-57.6	33.9	5566.0	101.5	23.3	16.7	2	3071570	14A-3			
51	42	12	25.9	12.3	42.8	65.1	10953.3	73.3	8.9	69.9	2	3104540	72-2			
52	42	16	-10.8	345.2	16.9	5.6	10507.6	24.2	11.7	80.2	2	3104820	72-3			
53	43	2	45.5	294.4	17.9	304.6	15825.6	155.8	1.6	71.8	2	3136600	10-1			
54	44	12	28.5	5.2	42.8	62.0	11032.8	77.7	8.5	69.5	2	3176360	88-2			
55	44	16	-7.4	337.5	16.6	355.3	10589.5	25.8	11.6	80.9	2	3176440	44-4			
56	45	7	41.9	193.9	48.2	232.5	11805.8	87.0	7.9	70.0	2	3211790	149-1			
57	45	10	-31.9	139.9	-27.6	141.9	11493.3	13.5	12.7	84.8	2	3211990	149-2			
57	45	10	-60.6	121.5	-60.1	122.0	11493.3	45.6	14.0	80.1	2	3211990	149-2			
58	45	11	-20.5	145.2	15.6	165.5	11388.0	18.1	11.8	84.1	2	3212060	149-3			
59	46	12	40.7	22.1	42.7	33.9	10976.3	83.1	8.0	68.3	2	3248250	155-2			
60	46	15	-60.1	270.8	-30.9	314.3	10643.1	52.5	13.6	80.7	2	3248460	45-4			
61	46	16	-32.2	313.3	-.1	332.7	10530.7	6.9	12.4	83.2	2	3248530	45-5			
62	48	12	41.3	14.3	43.1	27.6	10995.1	85.5	7.7	68.4	2	3320070	47-1			
63	48	14	-69.8	159.7	-75.7	190.1	10774.2	84.4	21.7	67.8	2	3320210	47-2			
64	48	15	-60.3	281.1	-57.9	284.0	10663.0	46.9	14.4	78.5	2	3320280	25-4			
65	48	16	-22.9	309.1	-.3	322.7	10550.7	8.5	12.2	83.9	2	3320350	25-5			

Note: Double entries correspond to two separate sectors of the limb appearing in a single picture.

Table XI-4c. (contd)

Index number	Rev	Frame number	Limb profile								Filter	DAS time	Microfiche ID			
			Left margin		Right margin		Center of limb									
			Latitude, deg	Longitude, deg	Latitude, deg	Longitude, deg	Range, km	Lighting angle, deg	Hour angle, h	Phase angle, deg						
66	49	7	38.3	166.8	48.7	206.1	11840.1	82.3	8.3	73.1	2	3355420	98-3			
66	49	7	24.1	150.2	25.9	151.8	11840.1	49.5	10.5	81.8	2	3355420	98-3			
67	49	17	-56.9	323.3	-56.8	4.5	5530.2	101.2	22.8	19.9	2	3358090	98-5			
68	49	19	-57.8	327.7	-56.0	8.1	5393.7	100.5	22.6	18.9	2	3358090	98-5			
69	49	21	-58.5	333.6	-54.8	12.6	5258.6	99.7	22.2	18.3	2	3359130	99-1			
70	50	12	42.1	9.2	43.1	20.2	10978.4	88.3	7.4	68.1	2	3391890	86-3			
71	50	14	-69.6	149.5	-73.9	166.6	10758.4	86.4	22.0	67.8	2	3392030	86-4			
72	50	16	-21.3	300.2	-3.3	311.0	10533.9	7.5	12.1	84.6	2	3392170	86-5			
73	50	26	-7.3	333.9	-7.6	337.5	5242.0	18.2	11.1	76.9	2	3395040	87-3			
74	52	12	42.8	1.0	43.4	16.0	11040.1	91.6	7.1	68.1	2	3463640	155-3			
75	52	14	-65.4	129.4	-73.2	151.4	10821.3	89.7	22.5	67.8	2	3463780	155-4			
76	52	16	-14.9	293.9	-3.5	300.8	10597.9	10.2	12.0	85.3	2	3463920	155-1			
77	53	7	43.3	156.8	48.3	197.1	11852.6	90.8	7.4	72.2	2	3498990				
78	53	9	-68.1	300.5	-76.3	322.9	11646.5	87.2	22.6	72.4	2	3499130				
79	53	10	-31.8	100.6	-29.6	101.7	11542.3	13.2	12.5	87.9	2	3499200				
79	53	10	-62.7	80.4	-61.0	82.1	11542.3	46.6	13.8	83.0	2	3499200	86-5			
80	53	11	-18.0	107.0	9.5	121.6	11437.0	16.0	11.7	87.4	2	3499270	87-1			
81	54	12	42.7	354.3	42.9	7.0	10966.9	93.1	6.9	68.1	2	3535600	80-1			
82	54	14	-65.5	120.2	-71.1	134.2	10746.9	91.1	22.6	67.7	2	3535600	80-2			
83	54	16	-13.6	284.7	-5.0	290.0	10522.3	9.9	11.9	85.0	2	3535740	89-3			
84	55	17	-57.3	300.3	-56.1	341.4	5582.9	99.9	22.2	24.7	2	3574410	34-1			
85	56	12	40.7	331.9	42.9	345.0	10985.7	85.1	7.7	71.6	2	3607210	84-2			
86	56	15	-61.6	239.5	-32.4	263.9	10653.6	33.0	13.4	84.3	2	3607420	114-5			
87	56	16	-27.8	266.4	-1.8	281.9	10541.2	4.5	12.1	86.9	2	3607420	85-2			
88	57	7	47.0	157.2	44.8	192.3	11784.9	103.6	6.0	69.7	2	3642560	150-3			
89	57	9	-61.0	61.7	-27.9	82.3	11472.5	27.9	12.9	87.7	2	3642770				
90	57	10	-20.7	85.6	6.0	99.5	11367.1	12.7	11.7	89.0	2	3642840	85-4			
91	58	12	41.4	324.2	43.3	338.6	10996.2	97.8	7.4	71.5	2	3678960	64-5			
92	58	14	-68.3	105.3	-75.1	133.2	10776.3	86.4	21.8	71.1	2	3679100	65-1			
93	58	15	-62.5	228.4	-60.0	231.8	10665.1	48.6	14.3	81.8	2	3679170	65-2			
94	58	16	-22.8	259.3	-2.9	271.1	10552.8	6.1	12.0	87.6	2	3679240	65-3			
95	58	22	-56.9	98.5	-57.4	105.1	5539.0	103.9	23.7	18.7	2	3681070	65-4			
96	59	18	-57.6	285.4	-55.4	326.5	5613.3	98.5	21.7	28.3	2	3717810	67-2			
97	60	12	42.2	317.3	43.5	332.3	11009.8	99.7	7.2	71.4	2	3750710	31-1			
98	60	14	-67.4	93.0	-73.8	114.2	10789.9	88.2	22.0	71.3	2	3750850	31-2			
99	60	16	-18.8	251.5	-4.4	260.0	10566.4	7.4	11.8	80.3	2	3750900	31-3			
100	61	7	42.8	115.6	48.6	151.0	11813.0	89.8	7.5	75.5	2	3786060	31-4			
101	61	10	-34.3	59.2	-30.0	61.2	11500.6	14.3	12.3	90.7	2	3786270	32-1			
102	61	11	-63.0	39.7	-59.5	43.4	11500.6	45.8	13.6	86.1	2	3786270	32-1			
103	62	12	41.0	300.9	43.6	318.4	11037.0	47.6	7.4	73.4	2	3822460	54-2			
104	62	14	-69.5	87.4	-75.1	111.6	10817.1	85.8	21.6	73.0	2	3822600	54-3			
105	62	15	-61.8	209.7	-60.1	212.0	10706.0	47.9	14.1	83.6	2	3822670	54-4			
106	62	16	-20.4	240.5	-2.4	251.2	10593.7	7.8	11.8	89.1	2	3822740	54-5			
107	62	26	-9.8	244.6	-7.0	263.6	5318.0	10.7	12.2	79.3	2	3825610	56-2			
108	63	28	-9.6	108.9	-16.1	130.5	5274.1	47.1	8.8	67.9	2	3861520	51-3			

Note: Double entries correspond to two separate sectors of the limb appearing in a single picture.

Table XI-4d. Limb traces for wide-angle frames: 70°N to 70°S (see Fig. XI-20d)

Index number	Rev	Frame number	Limb profile								Filter	DAS time	Microfiche ID			
			Left margin		Right margin		Center of limb									
			Latitude, deg	Longitude, deg	Latitude, deg	Longitude, deg	Range, km	Lighting angle, deg	Hour angle, h	Phase angle, deg						
1	24	7	26.3	94.2	48.0	151.7	11760.0	72.2	9.5	66.4	8	2457455	04-2			
2	24	10	-38.9	58.1	-21.9	66.4	11446.4	19.3	13.3	76.7	8	2457665	04-3			
2	24	10	-55.0	47.9	-51.2	50.7	11446.4	40.1	14.1	73.6	8	2457665	04-3			
3	24	11	-24.9	64.9	19.4	90.7	11341.0	20.1	12.3	76.4	8	2457735	80-2			
4	25	23	-57.8	108.3	-57.5	110.6	5111.7	99.9	22.9	10.3	8	2497075	131-4			
5	27	23	-58.3	81.1	-58.2	87.4	5299.0	100.6	23.8	10.6	8	2568755	2-1			
6	28	7	40.3	91.7	47.0	145.7	11843.2	96.5	8.1	63.8	8	2600955	73-4			
7	28	11	-11.8	51.2	18.7	69.5	11426.6	25.0	12.0	77.5	8	2601235	6-4			
8	29	7	39.0	263.3	45.9	327.6	11931.6	87.9	8.0	64.1	8	2636725	7-5			
9	29	11	-7.6	228.2	16.8	242.6	11516.3	25.9	12.0	77.9	8	2637075	8-1			
10	29	21	-57.8	64.4	-58.0	71.0	5386.6	101.0	.2	11.0	8	2640505	8-4			
11	30	7	43.3	88.8	46.4	138.0	11823.4	90.1	7.7	63.4	8	2672775	73-4			
12	30	11	-10.0	42.3	14.5	56.5	11406.8	23.5	12.0	78.3	8	2673055	73-5			
13	32	7	47.4	93.9	48.6	110.4	11834.9	90.1	7.7	64.2	8	2784505	14-2			
14	32	10	-63.9	.3	-30.8	22.7	11523.6	33.1	12.6	78.0	8	2784805	14-4			
15	32	11	-25.9	24.9	6.6	41.5	11418.2	12.7	12.4	80.1	8	2784875	14-5			
16	33	7	48.0	272.5	48.4	291.3	11851.5	93.1	7.3	63.7	8	2780505	2-4			
17	33	9	-66.0	34.3	-75.7	57.2	11644.4	87.9	23.3	64.5	8	2780645	16-3			
18	33	10	-34.7	196.0	-32.2	197.2	11540.2	19.3	13.1	80.2	8	2780715	2-5			
18	33	10	-65.2	173.9	-57.2	182.3	11540.2	47.1	14.3	75.7	8	2780715	2-5			
19	33	11	-20.5	202.6	5.7	216.0	11434.9	14.2	12.3	80.4	8	2780745	7-1			
20	34	7	42.3	67.8	48.2	99.7	11775.6	84.1	8.3	66.6	8	2816485	4-2			
21	34	10	-59.7	354.7	-26.7	14.9	11462.6	28.9	13.4	79.2	8	2816695	4-3			
22	34	11	-27.1	14.6	15.0	37.7	11356.7	15.5	12.2	80.4	8	2816765	4-4			
23	36	7	48.2	80.5	48.1	100.0	11844.2	95.3	7.1	64.2	8	2888305	60-5			
24	36	9	-62.8	196.1	-74.3	217.4	11637.1	90.5	23.5	64.8	8	2888445	61-1			
25	36	10	-65.9	338.5	-64.0	340.9	11532.9	50.8	14.5	75.9	8	2888455	61-2			
26	36	11	-17.0	9.8	4.2	20.7	11427.6	14.5	12.2	81.4	8	2888545	61-3			
27	37	7	45.0	257.7	47.4	277.3	11781.5	96.4	6.9	63.9	8	2924285	74-3			
28	37	9	-29.7	350.6	-37.7	354.4	11573.6	122.8	1.3	54.6	8	2924425	74-4			
28	37	9	-52.5	2.9	-72.7	29.0	11573.6	96.6	24.0	63.0	8	2924425	74-4			
29	37	11	-13.9	186.6	2.5	195.2	11363.0	15.0	12.1	81.5	8	2924565	74-5			
30	38	7	48.9	72.4	47.5	97.7	11931.6	98.7	6.7	64.2	8	2960125	62-3			
31	38	11	-12.1	2.5	4.1	10.9	11517.5	16.5	12.0	82.1	8	2960405	62-4			
32	39	7	48.6	249.4	46.5	275.8	11686.2	100.0	6.5	63.9	8	2996110	75-2			
33	39	9	-25.2	339.0	-69.0	10.1	11662.1	111.5	.8	50.4	8	2996250	63-3			
34	39	11	-8.6	179.6	2.2	185.2	11452.7	17.2	12.0	82.3	8	2996300	63-4			
35	40	7	22.5	12.5	48.3	65.5	11815.1	69.3	0.5	73.4	8	3032000	17-5			
36	40	10	-56.7	329.0	-23.2	347.8	11502.7	24.6	13.1	81.9	8	3032000	17-3			
37	40	11	-24.0	347.5	24.2	16.6	11397.4	21.6	11.8	82.0	8	3032370	153-1			
38	41	22	-58.5	14.5	-58.3	22.4	5283.6	101.0	23.3	13.0	8	3107170	148-5			
39	42	7	38.3	21.1	48.3	57.0	11803.7	90.4	8.6	70.9	8	3107300	153-4			
39	42	7	23.0	3.4	27.5	7.5	11803.7	49.2	10.7	79.1	8	3103900	153-4			
40	42	10	-57.9	318.4	-24.7	337.6	11491.2	25.8	13.1	82.5	8	3104130	71-5			
41	42	11	-25.8	337.0	21.7	4.9	11385.9	10.1	11.8	83.0	8	3104260	72-1			
42	42	22	-10.1	343.1	-6.3	1.2	5478.6	16.1	12.7	75.8	8	3107550	0-2			
43	42	24	-9.1	346.4	-6.6	4.6	5341.7	14.7	12.5	76.5	8	3107620	9-3			
44	43	4	63.3	203.2	55.4	279.9	15033.2	112.0	5.4	75.5	8	3137370	10-2			
45	43	11	26.5	181.5	48.5	240.8	11845.3	75.2	9.0	72.9	8	3139800	10-3			
46	43	14	-41.2	144.9	-25.4	152.5	11534.0	17.3	12.8	83.9	8	3140100	10-5			
46	43	14	-58.8	133.1	-50.8	139.2	11534.0	39.6	13.7	80.7	8	3140100	10-5			
47	43	15	-22.1	154.1	20.8	179.0	11427.6	20.4	11.8	83.3	8	3140170	11-1			
48	43	21	-51.5	62.1	-47.4	75.1	5532.6	86.4	19.3	37.3	8	3143450	9-5			
49	44	7	28.1	358.0	48.4	60.4	11878.6	77.7	8.8	72.7	8	3175000	144-5			
50	44	10	-31.2	325.1	-26.0	327.5	11567.3	12.4	12.6	84.7	8	3176010	97-5			
51	44	11	-17.0	331.6	20.0	353.4	11462.0	22.6	11.7	83.5	8	3176040	89-1			
52	46	7	20.7	342.2	48.1	33.1	11824.5	67.8	0.5	76.0	8	3247690	44-5			
53	46	10	-58.6	298.7	-25.2	318.2	11512.1	25.9	13.1	83.9	8	3247900	45-1			
54	46	11	-27.5	317.1	18.6	342.8	11406.8	16.3	11.8	84.7	8	3247970	45-2			
55	47	7	40.0	179.6	48.4	211.0	11839.0	81.9	72.5	8	3283600	140-5				
55	47	7	22.0	158.3	24.0	160.0	11839.0	46.8	10.7	81.6	8	3283600	140-5			
56	47	10	-59.6	113.0	-26.3	132.9	11527.7	26.9	13.1	84.2	8	3283810	141-2			
57	47	11	-29.1	131.5	14.9	155.1	11422.4	13.3	11.9	85.3	8	3283880	94-4			
58	48	7	34.6	346.2	48.6	29.0	11842.2	78.8	8.6	73.8	8	3319510	46-2			
58	48	7	23.3	334.4	30.4	341.1	11842.2	51.8	10.4	80.9	8	3319510	46-2			
59	48	10	-60.1	287.7	-26.8	307.7	11530.9	27.3	13.0	84.5	8	3319720	46-4			
60	48	11	-29.2	306.5	14.7	330.0	11425.5	13.1	11.9	85.7	8	3319790	46-5			
61	48	22	-6.5	330.0	-5.2	343.6	5531.4	14.9	11.6	76.6	8	3323080	26-1			
62	48	24	-6.7	332.6	-6.1	343.3	5394.9	14.6	11.6	77.0	8	3323150	26-2			
63	50	7	38.8	343.0	48.6	21.1	11826.6	82.9	8.2	73.3	8	3391330	85-4			

Note: Double entries correspond to two separate sectors of the limb appearing in a single picture.

Table XI-4d. (contd)

Index number	Rev	Frame number	Limb profile								Filter	DAS time	Microfiche ID			
			Left margin		Right margin		Center of limb									
			Latitude, deg	Longitude, deg	Latitude, deg	Longitude, deg	Range, km	Lighting angle, deg	Hour angle, h	Phase angle, deg						
63	50	7	24.0	325.3	24.5	325.7	11826.6	48.7	10.5	R2.3	8	3391530	A5-4			
64	50	10	-61.7	276.1	-28.6	297.1	11515.2	29.0	13.1	R5.0	8	3391540	A6-1			
65	50	11	-27.1	297.7	11.9	318.3	11409.9	12.6	11.8	R6.5	8	3391610	B6-2			
66	50	22	-5.5	329.6	-5.2	338.6	5512.6	19.1	11.1	76.1	8	3394000	B7-1			
67	50	24	-6.3	331.5	-6.4	337.8	5377.2	18.5	11.1	76.5	8	3394070	B7-2			
68	51	7	43.4	168.0	48.5	197.1	11808.9	87.5	7.8	72.2	8	3427240	41-2			
69	51	10	-62.1	90.6	-29.1	111.8	11497.5	29.5	13.1	85.2	8	3427450	41-4			
70	51	11	-28.0	112.2	10.8	132.6	11391.1	11.4	11.9	86.8	8	3427520	41-5			
71	51	17	-5.6	144.8	-5.4	152.5	5490.3	18.8	11.1	76.3	8	3430110	42-1			
72	51	19	-6.4	147.0	-6.6	153.0	5354.7	18.8	11.1	76.6	8	3430180	42-2			
73	52	7	42.5	339.5	48.8	18.2	11884.8	88.6	7.7	72.6	8	3463090	142-5			
74	52	10	-35.1	284.1	-29.2	286.9	11574.6	14.8	12.5	R7.5	8	3463220	05-2			
75	52	10	-62.5	255.7	-58.1	270.1	11574.6	44.9	13.7	R3.1	8	3463220	05-2			
76	54	7	-22.3	240.0	12.0	308.1	11469.3	15.2	11.7	R7.2	8	3463360				
77	54	9	-66.2	113.1	-75.7	135.5	11609.0	88.7	22.7	72.2	8	3535040	38-3			
78	54	10	-31.5	275.7	-30.4	276.2	11503.8	13.5	12.5	R8.1	8	3535110	38-4			
79	54	10	-63.4	254.3	-61.4	256.6	11503.8	47.3	13.8	R3.1	8	3535110	38-4			
80	55	7	44.4	149.3	47.9	191.0	11876.5	03.5	7.1	72.4	8	3535400	40-2			
81	55	9	-65.6	286.6	-74.4	304.5	11670.4	90.0	22.9	72.5	8	3570090	40-3			
82	55	11	-14.5	98.6	8.9	111.1	11461.1	17.7	11.6	R8.0	8	3571020	40-4			
83	56	7	20.7	292.5	48.3	343.5	11832.6	69.1	0.3	79.6	8	3606650				
84	56	10	-59.6	248.4	-26.2	268.2	11521.5	26.1	12.8	R7.7	8	3606860	35-1			
85	56	11	-21.0	270.6	9.5	286.6	11416.2	14.6	11.6	R8.6	8	3616090	34-1			
86	56	7	23.0	284.1	48.8	338.9	11842.2	72.6	0.0	79.4	8	3678400	64-1			
87	58	10	-61.2	236.9	-27.9	257.3	11531.9	27.8	12.8	R8.2	8	3678610	64-3			
88	58	11	-17.9	261.4	5.7	274.1	11426.8	14.2	11.6	R8.4	8	3678640	64-4			
89	59	8	24.9	100.3	49.2	158.3	11897.3	75.4	8.8	79.2	8	3714200	66-3			
90	59	11	-39.9	66.6	-27.7	72.4	11588.2	16.0	12.4	R9.1	8	3714450	66-5			
91	59	11	-61.3	52.2	-54.1	58.3	11588.2	41.7	13.3	R6.5	8	3714450	66-5			
92	60	7	25.4	276.0	48.9	334.8	11855.7	76.4	8.7	79.2	8	3750150	30-2			
93	60	9	-68.9	86.2	-76.7	109.4	11649.0	86.8	22.3	75.3	8	3750200	30-3			
94	60	10	-36.7	243.1	-28.8	246.9	11544.9	14.9	12.4	R9.4	8	3750460	30-4			
95	60	10	-62.1	226.1	-57.2	230.7	11544.4	43.9	13.5	R6.3	8	3750470	30-4			
96	61	17	-5.5	106.2	-9.4	132.1	5499.7	39.5	0.4	71.3	8	3789630	32-3			
97	61	19	-7.0	109.7	-11.9	132.9	5364.2	39.6	9.4	71.2	8	3789700	32-4			
98	62	7	20.3	261.6	48.6	312.6	11880.6	69.6	9.2	R1.9	8	3821000	53-4			
99	62	10	-63.7	214.5	-30.3	236.1	11570.5	30.3	12.8	R9.5	8	3822110	54-1			
100	62	11	-9.0	246.0	3.5	252.5	11465.2	18.2	11.4	R9.9	8	3750490	30-5			
101	62	22	-10.6	243.2	-5.9	262.8	5589.9	11.0	12.2	R9.0	8	3825470	55-5			
102	62	24	-10.2	243.7	-6.4	263.1	5453.9	10.9	12.2	R9.1	8	3825540	55-6			
103	63	14	20.2	76.6	48.5	127.2	11847.4	69.5	0.1	R2.2	8	3857810	55-5			
104	63	17	-34.6	49.2	-30.3	51.2	11536.1	14.5	12.3	R1.6	8	3858020	57-2			
104	63	17	-63.5	29.6	-59.8	33.4	11536.1	46.0	13.5	R7.0	8	3858020	57-2			
105	63	16	-8.2	61.4	1.0	66.2	11430.8	17.4	11.4	R1.0	8	3858020	57-3			
106	63	24	-5.9	107.8	-11.0	130.4	5545.5	48.4	R8.8	67.6	8	3861380	51-1			
107	63	26	-7.6	108.2	-13.4	130.3	5409.1	47.6	R8.8	67.8	8	3861450	51-2			

Note: Double entries correspond to two separate sectors of the limb appearing in a single picture.

Table XI-4e. Limb traces for wide-angle frames: 70°N to 70°S (see Fig. XI-20e)

Index number	Rev	Frame number	Limb profile								Filter	DAS time	Microfiche ID			
			Left margin		Right margin		Center of limb									
			Latitude, deg	Longitude, deg	Latitude, deg	Longitude, deg	Range, km	Lighting angle, deg	Hour angle, h	Phase angle, deg						
1	25	21	-58.1	102.9	-57.8	106.1	5245.5	100.2	23.2	10.7	4	2497005	131-1			
2	26	12	31.2	95.8	41.8	155.0	11048.5	78.8	R6	62.5	4	2529695	145-2			
3	27	21	-57.4	75.3	-57.9	83.5	5435.6	101.0	*1	11.1	4	2568695	59-5			
4	29	19	-56.6	56.4	-57.5	67.0	5522.0	101.5	*6	11.5	4	2640475	8-1			
5	33	21	-58.1	54.8	-58.0	61.8	5411.4	100.9	23.4	12.9	4	2784145	3-4			
6	35	21	-50.3	100.1	-48.0	107.1	5347.0	90.0	19.7	31.1	4	2856075	151-3			
7	41	26	-57.9	8.7	-58.0	25.3	5419.7	101.4	23.4	14.6	4	3071640	148-4			
8	42	26	-8.3	350.9	-7.4	9.3	5207.4	13.0	12.2	77.2	7	3176900	9-4			
9	48	26	-7.1	335.1	-7.1	342.7	5259.6	14.1	11.6	77.4	7	3323220	26-3			
10	51	21	-7.5	149.0	-7.8	152.7	5219.3	18.3	11.0	77.0	7	3430050	42-3			
11	61	21	-8.7	110.6	-14.4	133.4	5228.9	19.4	9.3	71.3	7	3789770	73-3			

Table XI-4f. Limb traces for wide-angle frames: 70°N to 70°S (see Fig. XI-20f)

Index number	Rev	Frame number	Limb profile								Filter	DAS time	Microfiche ID			
			Left margin		Right margin		Center of limb									
			Latitude, deg	Longitude, deg	Latitude, deg	Longitude, deg	Range, km	Lighting angle, deg	Hour angle, h	Phase angle, deg						
1	64	9	33.3	308.4	33.3	312.0	9599.0	88.6	7.0	67.1	2	3895120	75-5			
2	64	10	5.3	250.3	28.0	284.1	9478.0	47.3	10.0	80.5	2	3895190	76-1			
3	64	11	-8.9	238.4	-7.9	239.2	9356.8	10.5	11.8	86.5	2	3895260	52-2			
4	64	12	-53.0	199.2	-29.9	222.1	9234.5	30.8	13.6	83.5	2	3895330	52-3			
5	64	13	-67.5	161.6	-46.9	205.8	9110.8	52.6	15.1	77.8	2	3895400	52-4			
6	65	8	33.8	118.7	34.0	130.4	9695.4	88.8	7.0	67.9	2	3930960	84-4			
7	65	9	8.5	68.1	30.0	103.1	9575.6	51.7	9.7	80.0	2	3931030	53-1			
8	65	11	-32.5	35.4	-29.1	38.0	9333.4	17.5	12.9	86.2	2	3931170	53-2			
8	65	11	-52.8	15.4	-51.1	17.6	9333.4	42.8	14.2	81.6	2	3931170	53-2			
9	65	12	-68.2	335.8	-47.2	21.2	9211.0	52.6	15.1	78.5	2	3931240	53-3			
10	68	9	33.9	286.1	33.5	300.2	9682.7	92.1	6.7	67.8	2	4038690	85-1			
11	68	10	9.4	234.3	30.3	269.5	9562.9	53.4	9.6	80.5	2	4038760	85-2			
12	68	13	-64.2	157.2	-42.1	191.7	9197.2	45.5	14.4	81.5	2	4038970	85-3			
13	68	22	-35.5	157.7	-27.6	173.2	5470.3	54.2	15.9	65.2	2	4040930	123-1			
14	69	8	34.1	101.9	33.7	115.2	9698.6	92.6	6.6	68.0	2	4074600	123-3			
15	69	9	10.9	50.9	31.0	86.8	9577.8	55.6	9.4	80.3	2	4074670	123-4			
16	69	12	-69.1	310.8	-48.6	*1	9213.1	54.1	15.1	79.4	2	4074880	123-5			
17	69	23	-53.3	282.7	-52.8	284.6	5351.2	90.1	19.7	37.5	2	4076910	124-1			
18	70	22	-9.6	206.9	-5.7	227.8	5510.3	11.2	11.8	80.3	2	4112750	125-2			
19	73	11	34.3	84.9	32.8	102.7	9717.7	97.1	6.2	67.9	2	4218310	118-4			
20	73	12	13.1	34.0	31.9	71.0	9597.9	59.5	9.1	80.6	2	4218380	118-5			
21	73	15	-69.8	286.4	-49.8	339.6	9233.4	55.4	15.2	80.4	2	4218590	119-1			
22	73	24	-20.4	103.3	-23.9	110.7	5506.8	82.6	6.1	46.7	2	4220550	119-3			
23	74	9	21.8	220.2	33.7	264.1	9646.7	73.9	8.1	76.4	2	4254290	119-4			
24	74	10	7.7	203.8	29.3	238.2	9526.8	52.1	9.6	82.8	2	4254360	119-5			
25	74	11	-6.2	191.9	-2.7	194.8	9405.8	16.6	11.3	89.5	2	4254430	120-1			
26	74	12	-31.6	172.3	-25.1	177.4	9283.4	13.3	12.6	89.5	2	4254500	120-2			
27	74	13	-65.3	123.7	-43.7	161.0	9159.9	47.2	14.5	82.9	2	4254570	120-3			
28	77	8	27.6	36.2	33.8	75.3	9695.4	82.2	7.5	74.7	2	4362090	144-2			
29	77	9	10.2	11.9	30.6	47.5	9575.6	56.2	9.3	82.8	2	4362160	144-3			
30	77	12	-65.6	289.3	-43.8	326.9	9210.0	47.0	14.4	84.1	2	4362370	144-4			
31	80	9	23.3	193.4	34.1	239.7	9725.1	78.2	7.8	77.3	2	4469940	158-4			
32	80	10	9.0	176.2	30.3	211.1	9605.3	55.0	9.3	84.3	2	4469960	158-5			
33	80	11	-5.1	164.1	-2.4	166.3	9485.4	18.6	11.1	91.5	2	4470130	159-1			
34	80	12	-4.8	164.6	2.1	170.5	9363.2	21.7	11.0	90.8	2	4470100	159-2			
35	80	27	25.3	125.2	25.3	125.3	3415.3	61.3	15.0	86.8	2	4473950	5-3			
36	80	29	30.7	121.3	27.6	126.4	3453.2	64.9	15.2	86.6	2	4474020	159-3			
37	80	31	36.4	116.2	29.9	127.4	3502.1	69.0	15.3	86.1	2	4474090	159-4			
38	81	8	28.8	21.1	33.6	52.8	9642.4	83.3	7.3	75.5	2	4505470	5-4			
39	81	9	7.7	350.5	29.2	24.7	9521.5	53.4	9.4	84.8	2	4505490	5-5			
40	81	10	-5.5	339.1	-4.1	340.3	9400.4	17.3	11.1	91.8	2	4506010	6-1			
41	81	12	-65.6	269.2	-44.1	307.1	9155.6	47.2	14.3	85.2	2	4506150	6-2			
42	82	31	31.5	75.2	32.4	78.3	3429.4	93.8	17.6	53.9	2	4545400	154-1			
43	84	9	30.9	194.4	32.9	221.5	9588.4	88.5	6.9	76.4	2	4613670	68-5			
44	84	10	9.2	157.7	29.5	192.5	9467.4	56.0	9.2	84.9	2	4613740	69-1			
45	84	13	-66.2	71.0	-45.2	111.1	9099.1	48.6	14.4	85.6	2	4613950	69-2			
46	84	31	28.7	53.2	35.2	68.1	3460.2	99.1	18.0	49.3	2	4617730	69-3			
47	85	8	28.4	359.5	33.2	42.3	9708.1	87.2	7.0	75.9	2	4649510	69-4			
48	85	9	11.8	335.0	31.3	11.3	9587.3	60.0	9.0	84.6	2	4649590	69-5			
49	85	12	-67.4	243.4	-46.2	286.0	9222.7	49.5	14.4	86.2	2	4649790	70-1			
50	87	7	31.4	358.9	32.6	34.9	9684.8	92.8	6.5	74.5	2	4721330	71-1			
51	87	8	11.9	325.4	31.2	1.8	9564.0	60.7	8.9	85.0	2	4721400	71-2			
52	90	2	-8.4	148.3	-13.4	169.5	5226.5	47.9	8.7	71.3	2	4831370	149-5			
53	91	23	-16.4	357.4	-26.1	18.9	5310.9	78.7	6.4	52.1	2	4867210	90-2			
54	92	8	-6.8	115.8	-6.4	120.3	5389.0	21.0	10.7	82.1	2	4903050	91-1			
55	93	30	25.0	188.8	30.8	200.0	3432.2	95.6	17.9	44.8	2	4940710	19-3			
56	93	32	27.4	185.4	35.0	199.9	3472.8	98.5	18.0	45.5	2	4940780	91-4			
57	95	32	-1.1	215.3	.8	228.4	4133.6	48.3	15.1	68.3	2	4987323	92-1			
58	97	2	-42.2	37.5	-46.3	47.6	5901.1	114.4	2.0	24.6	2	5058093	115-4			
59	97	4	-48.1	48.6	-48.5	49.6	5773.9	113.0	1.6	23.0	2	5058163	115-5			

Note: Double entries correspond to two separate sectors of the limb appearing in a single picture.

Table XI-4g. Limb traces for wide-angle frames: 70°N to 70°S (see Fig. XI-20g)

Index number	Rev	Frame number	Limb profile									Filter	DAS time	Microfiche ID			
			Left margin		Right margin		Center of limb										
			Latitude, deg	Longitude, deg	Latitude, deg	Longitude, deg	Range, km	Lighting angle, deg	Hour angle, h	Phase angle, deg							
1	66	5	33.8	205.1	33.8	307.3	9682.7	90.2	6.8	67.7	8	3966870	97-1				
2	66	10	8.2	242.9	29.8	277.7	9562.9	51.5	9.7	80.4	8	3966940	97-2				
3	66	13	-68.4	148.9	-47.7	195.7	9197.2	53.2	15.1	78.6	8	3967150	97-3				
4	66	20	-8.9	229.2	-4.8	251.1	5607.5	13.1	11.6	79.4	8	3969040	98-1				
5	66	22	-9.7	226.1	-6.0	246.3	5471.5	10.8	11.9	79.7	8	3969110	98-4				
6	67	8	33.9	111.2	33.8	121.4	9678.5	90.4	6.8	68.0	8	4002790	99-2				
7	67	9	9.3	59.0	30.2	94.2	9558.7	53.0	9.6	80.3	8	4002850	99-3				
8	67	12	-68.3	324.6	-47.5	10.9	9192.9	52.9	15.1	79.0	8	4003060					
9	68	20	-36.2	159.4	-32.1	167.3	5606.3	55.7	16.0	64.8	8	4040860	157-5				
10	70	9	34.2	275.6	33.4	293.5	9719.8	93.6	6.5	68.1	8	4110510	124-2				
11	70	10	12.0	227.1	31.5	263.5	9600.0	57.3	9.3	80.2	8	4110590	124-3				
12	70	13	-68.9	127.9	-48.1	176.0	9234.5	53.3	15.0	80.1	8	4110790	154-1				
13	70	20	-8.8	210.0	-4.4	232.8	5647.2	14.2	11.5	79.9	8	4112840	125-1				
14	71	8	33.7	94.7	32.9	107.6	9632.9	94.5	6.4	67.7	8	4146890	125-5				
15	71	9	10.8	41.5	30.5	77.1	9513.0	55.8	9.4	80.7	8	4146960	125-4				
16	71	12	-69.2	297.8	-49.4	349.1	9146.0	55.2	15.2	79.5	8	4146770	126-1				
17	73	22	-12.4	91.2	-22.7	113.8	5643.7	80.2	6.3	49.7	8	4220480	119-2				
18	74	20	-9.3	189.0	-5.1	211.0	5561.9	12.8	11.5	80.7	8	4256460	121-2				
19	74	22	-10.0	185.8	-6.3	206.1	5425.6	10.1	11.8	80.9	8	4256730	121-3				
20	75	8	22.9	36.6	34.1	82.2	9702.6	76.2	7.9	76.1	8	4290200	121-5				
21	75	9	8.9	20.1	30.2	55.1	9583.1	54.1	9.4	82.8	8	4290270	122-1				
22	75	10	-4.6	8.4	-2.5	10.1	9462.1	18.0	11.2	89.9	8	4290340	122-2				
23	75	11	-26.6	351.6	-24.7	353.0	9340.9	9.8	12.4	80.2	8	4290410	122-3				
24	75	12	-65.4	294.8	-43.5	336.8	9218.5	46.7	14.4	85.6	8	4290480	122-4				
25	75	19	-41.0	296.2	-35.0	306.9	5626.2	61.5	16.4	63.3	8	4292770	57-4				
26	78	9	30.9	222.3	33.3	250.2	9629.7	46.9	7.0	73.0	8	4398070	58-2				
27	78	10	9.1	186.3	29.7	221.1	9508.8	58.7	9.3	83.4	8	4398140	58-3				
28	78	13	-66.0	101.8	-44.7	140.9	9141.7	48.2	14.5	83.9	8	4398150	58-4				
29	79	8	30.2	33.7	33.5	66.9	9679.5	86.3	7.1	73.9	8	4433980	58-5				
30	79	9	10.4	2.7	30.6	38.3	9559.7	56.8	9.2	83.3	8	4434050	143-3				
31	79	12	-66.4	276.6	-44.9	316.2	9194.0	48.3	14.5	84.4	8	4434260	59-1				
32	82	9	26.8	190.9	33.5	232.6	9674.2	93.0	7.3	76.1	8	4541780	163-1				
33	82	10	9.2	167.1	30.1	202.1	9554.4	55.7	9.2	84.6	8	4541850	144-5				
34	82	13	-66.3	82.4	-44.8	121.8	9186.6	48.0	14.4	85.5	8	4542060	145-1				
35	83	6	28.8	10.4	33.6	48.3	9693.3	85.7	7.1	75.6	8	4577690	67-5				
36	83	9	10.2	343.1	30.6	18.6	9573.5	57.3	9.1	84.6	8	4577760	68-3				
37	83	12	-66.1	258.6	-44.5	297.4	9207.8	47.4	14.3	86.0	8	4577970	68-1				
38	86	9	31.4	186.8	32.6	214.2	9583.1	91.0	6.7	74.2	8	4685490	70-3				
39	86	10	10.2	194.9	29.9	184.3	9462.1	57.9	9.0	85.1	8	4685560	70-4				
40	86	13	-66.7	59.1	-45.9	100.5	9093.7	49.4	14.5	86.1	8	4685770	70-5				
41	87	11	-67.7	231.8	-46.7	275.4	9199.3	50.1	14.5	86.7	8	4721610	71-3				
42	91	5	-63.1	120.2	-63.9	238.0	10017.9	75.9	18.3	83.5	8	4864600	17-1				
43	91	8	29.8	334.1	31.8	341.1	9662.6	77.5	7.7	81.3	8	4864900	17-2				
43	91	6	11.8	304.7	13.5	306.6	9662.6	42.9	9.8	91.7	8	4864900	17-2				
44	91	12	-70.4	168.8	-55.7	243.6	9176.9	63.3	15.9	83.0	8	4865180	49-4				
45	91	19	-13.6	3.6	-24.6	27.8	5582.9	86.9	5.9	48.2	8	4867070	144-1				
46	91	21	-15.1	1.0	-25.4	23.6	5445.6	83.0	6.1	49.9	8	4867140	49-1				
47	92	4	-4.8	121.6	-3.9	133.0	5562.3	30.9	10.1	80.1	8	4902910	49-4				
48	92	6	-5.8	118.7	-5.2	126.1	5525.5	25.7	10.4	81.2	8	4902980	49-5				
49	92	12	-8.8	106.0	-8.8	106.1	4987.7	9.3	11.6	83.3	8	4903260	49-3				
50	95	30	-2.8	218.2	-2.1	221.2	4214.7	49.0	15.2	67.4	8	4987253	91-5				

Note: Double entries correspond to two separate sectors of the limb appearing in a single picture.

Table XI-4h. Limb traces for wide-angle frames: 70°N to 70°S (see Fig. XI-20h)

Index number	Rev	Frame number	Limb profile									Filter	DAS time	Microfiche ID			
			Left margin		Right margin		Center of limb										
			Latitude, deg	Longitude, deg	Latitude, deg	Longitude, deg	Range, km	Lighting angle, deg	Hour angle, h	Phase angle, deg							
1	60	24	222.9	-10.3	-7.0	241.9	5335.8	10.2	12.2	70.9	7	3969180	98-5				
2	60	24	156.0	-34.8	-25.9	173.7	5334.6	55.0	16.0	64.4	4	4041800	123-2				
3	70	24	203.4	-10.3	-6.8	223.3	5374.8	9.7	12.0	80.4	4	4112820	142-3				
4	74	24	112.7	-10.6	-7.3	201.7	5289.5	9.0	12.1	81.0	7	4256600	121-4				
5	92	2	124.2	-3.7	-2.6	142.1	5800.5	37.2	9.6	78.5	4	4902840	49-3				
6	92	10	112.7	-7.6	-7.4	115.1	5253.9	16.7	11.0	82.6	4	4903120	91-2				

Table XI-4i. Limb traces for wide-angle frames: 70°N to 70°S (see Fig. XI-20i)

Index number	Rev	Frame number	Limb profile								Filter	DAS time	Microfiche ID			
			Left margin		Right margin		Center of limb									
			Latitude, deg	Longitude, deg	Latitude, deg	Longitude, deg	Range, km	Lighting angle, deg	Hour angle, h	Phase angle, deg						
1	100	5	14.7	120.8	14.5	133.3	7654.1	79.5	7.0	70.6	2	5164083	116-1			
2	100	29	60.9	355.7	56.9	21.3	4271.0	89.0	16.0	74.4	8	5168483	116-2			
3	100	31	64.0	350.2	59.8	22.6	4362.5	91.6	16.1	75.0	8	5168553	116-1			
4	100	32	66.8	342.7	62.4	25.1	4458.4	94.1	16.3	75.9	2	5168623	116-2			
5	101	5	14.4	298.7	14.2	307.4	7611.4	80.2	7.0	70.3	2	5200963	116-4			
6	101	29	41.0	197.7	33.4	209.8	3925.9	63.8	14.6	81.9	2	5204113	116-5			
7	101	31	68.3	164.3	59.8	208.5	4492.2	90.6	15.6	79.0	8	5204603	117-1			
8	102	1	19.0	121.8	17.5	135.7	8077.6	92.3	6.2	68.5	8	5236663	117-3			
9	102	5	13.1	128.5	12.4	132.8	7573.1	91.4	6.1	65.0	2	5236943	117-4			
10	102	6	-8.8	48.4	-4.8	72.5	5647.2	15.1	11.2	83.3	8	5237993	117-5			
11	102	8	-5.2	45.6	-5.6	67.7	5522.0	11.5	11.4	83.4	8	5238063	118-1			
12	102	10	-9.4	42.8	-6.3	63.4	5398.5	8.7	11.7	83.3	2	5238133	118-2			
13	102	29	62.7	353.0	57.6	15.6	4328.3	87.1	15.6	76.8	8	5240443	A1-3			
14	102	31	66.1	347.1	59.9	18.7	4423.2	89.4	15.7	77.6	8	5240513	A1-4			
15	102	32	69.3	339.7	61.9	22.0	4525.3	91.7	15.7	78.5	7	5240583	A1-5			
16	103	1	-56.8	165.9	-55.1	168.3	8049.4	56.1	15.3	83.5	2	5272643	B2-1			
17	103	5	-4.0	249.9	13.1	279.4	7549.6	52.1	8.9	82.2	2	5272993	B2-2			
18	103	7	-5.4	241.7	-5.4	265.4	5619.2	31.8	10.0	79.4	8	5273773	B2-3			
19	103	8	-6.2	237.5	-6.5	263.1	5493.8	28.2	10.2	79.9	8	5274443	B2-4			
20	103	10	-6.7	233.7	-7.3	260.0	5371.3	24.4	10.4	80.5	2	5274113	B2-5			
21	103	31	67.0	175.8	57.8	204.7	4546.0	83.2	14.6	85.0	8	5276563	93-2			
22	104	13	63.8	314.8	61.1	-1.1	4363.8	P0.1	15.8	75.3	8	5312403	83-3			
23	105	5	4.2	241.4	12.9	270.8	7512.6	53.2	8.8	82.3	2	5344993	104-4			
24	105	7	-5.2	236.7	-6.5	261.4	5586.4	36.7	9.6	77.0	2	5345933	160-3			
25	105	6	-5.7	237.6	-8.1	261.7	5462.1	36.6	9.6	77.3	8	5346003	105-5			
26	105	10	-6.4	236.7	-9.5	260.5	5339.3	35.1	9.7	77.3	7	5346073	20-1			
27	106	5	4.5	56.3	14.0	86.0	7637.7	53.7	8.8	83.1	2	5380793	105-5			
28	107	5	4.5	231.6	14.0	261.4	7643.2	54.0	8.8	83.3	2	5416773	92-2			
29	107	7	-16.1	290.8	-26.5	312.4	5715.9	92.7	5.4	45.9	8	5417823	92-3			
30	107	8	-16.6	285.9	-28.6	310.9	5589.9	99.2	5.7	47.0	8	5417893	92-4			
31	107	10	-18.9	285.1	-30.5	309.0	5465.6	87.1	5.8	47.1	7	5417963	93-1			
32	108	1	-60.6	310.7	-54.5	328.5	8163.2	57.8	15.4	85.1	2	5452473	93-2			
33	108	5	3.1	44.4	13.7	73.9	7659.5	51.3	8.9	84.7	2	5452753	93-3			
34	108	29	59.8	331.6	52.2	353.8	4264.6	40.5	15.0	77.5	8	5456253	102-2			
35	108	31	63.2	330.2	54.0	356.7	4356.2	92.1	15.0	78.9	2	5456323	102-3			
36	108	32	61.6	349.9	54.4	1.2	4453.3	77.7	14.3	84.8	4	5456703	102-4			
37	109	1	-60.7	126.4	-53.7	146.4	8183.8	56.9	15.3	85.9	2	5488453	102-5			
38	109	5	3.8	221.0	14.1	250.6	7681.4	52.9	8.8	84.5	2	5488733	103-1			
39	109	7	-57.1	57.4	-56.3	70.0	5753.0	97.6	20.6	42.9	8	5489793	103-2			
40	109	6	-56.4	25.8	-56.4	66.9	5626.2	103.4	21.8	35.2	2	5489953	103-3			
41	109	10	-57.4	29.8	-55.8	70.1	5500.9	102.1	21.6	34.0	4	5489923	103-4			
42	110	1	-57.9	309.7	-57.2	311.7	8090.7	57.9	15.4	85.3	2	5524503	109-2			
43	110	5	2.1	34.0	6.3	42.5	7586.2	39.2	9.7	88.7	2	5524783	109-3			
44	110	6	-36.5	306.7	-35.1	309.5	5532.6	58.1	16.0	68.4	2	5525003	109-4			
45	110	29	26.8	256.6	45.4	263.8	4316.9	123.4	20.1	40.0	8	5528283				
46	110	31	34.5	254.8	52.1	263.7	4411.8	123.3	20.2	44.9	8	5528553				
47	110	32	44.3	253.6	60.8	267.4	4511.0	120.6	20.2	51.4	8	5528823				
48	111	6	3.0	211.0	6.0	216.8	7620.2	39.8	9.6	89.0	2	5560763	109-5			
49	112	5	3.5	27.0	5.9	31.8	7662.8	40.2	9.6	89.4	2	5596743	110-1			
50	113	5	2.6	201.5	3.8	203.8	7575.7	37.5	9.7	90.0	2	5632793	110-2			
51	114	5	3.7	18.7	4.3	20.0	7624.6	39.3	9.6	90.0	2	5668773	110-3			
52	114	6	-8.5	57.4	-16.7	80.0	5694.9	77.3	6.7	58.8	8	566923	110-4			
53	114	6	-9.7	54.3	-17.7	76.2	5568.9	73.5	6.9	60.1	8	5669493	95-5			
54	114	10	-11.6	53.7	-19.9	74.9	5444.4	71.8	7.0	59.9	2	5669963	96-1			
55	115	5	4.4	195.4	6.8	200.3	7669.4	43.1	9.4	89.5	2	5704753	96-3			
56	115	7	-16.7	257.5	-24.9	274.4	5739.1	95.9	5.2	45.8	8	5705003	127-2			
57	115	8	-17.3	253.0	-29.5	277.9	5613.3	94.4	5.3	45.1	8	5705473	127-3			
58	115	10	-18.8	250.2	-31.4	275.8	5488.0	91.4	5.5	45.6	2	5705943	127-4			
59	115	31	62.5	135.9	57.9	145.3	4443.3	79.2	14.4	80.5	8	5708393	96-2			
60	118	5	3.2	359.7	7.4	8.4	7662.8	43.4	9.4	90.3	2	5812763	19-1			
61	118	6	-11.4	328.7	-6.2	347.0	5733.3	9.2	11.5	87.5	8	5813813	19-2			
62	118	8	-12.3	324.3	-6.9	343.4	5606.3	5.6	11.7	87.1	8	5813883	156-1			
63	118	14	-11.2	325.4	-6.8	344.4	5482.1	6.4	11.7	86.4	7	5813953	156-2			
64	118	29	58.7	254.9	60.5	280.9	4259.5	94.0	16.9	61.5	2	5816263	161-3			
65	118	31	56.1	237.2	64.0	269.7	4351.1	102.1	18.1	57.5	2	5816333	161-4			
66	118	32	66.9	280.6	66.7	283.0	4447.1	91.3	16.0	69.8	2	5816403	156-3			
67	119	5	2.4	174.4	4.6	178.7	7566.5	39.9	9.6	91.1	5	5848813	156-4			
68	119	7	-46.6	298.4	-56.3	340.5	5637.8	114.1	.5	27.4	5	5849863	156-5			
69	119	8	-51.1	306.9	-57.1	341.1	5512.6	112.1	.2	26.2	5	5849933	157-1			
70	119	10	-54.6	314.9	-58.0	342.9	5387.8	110.0	23.8	24.9	5	585003	161-5			

Table XI-4i. (contd)

Index number	Rev	Frame number	Limb profile								Filter	DAS time	Microfiche ID			
			Left margin		Right margin		Center of limb									
			Latitude, deg	Longitude, deg	Latitude, deg	Longitude, deg	Range, km	Lighting angle, deg	Hour angle, h	Phase angle, deg						
71	119	31	60.4	128.7	50.4	138.2	4523.5	71.5	13.6	86.4	5	5852453	157-2			
72	120	1	-63.8	235.5	-63.3	239.6	8092.8	72.2	17.1	83.0	5	5884513	20-2			
73	120	6	-14.4	45.8	-24.7	68.0	5657.7	91.8	5.6	49.2	5	5885A43	21-3			
74	120	8	-15.5	42.1	-26.9	66.6	5532.6	88.8	5.8	49.7	5	5885913	20-4			
75	120	10	-17.6	40.9	-28.7	64.4	5407.9	86.5	5.9	49.8	5	5885933	20-5			
76	120	29	62.4	255.9	59.2	289.6	4313.1	87.8	15.9	67.8	5	5888293	21-1			
77	120	31	65.0	248.9	62.5	289.7	4406.6	91.0	16.1	68.0	5	5888363	21-2			
78	120	32	67.5	242.3	65.4	291.4	4506.0	93.5	16.3	68.8	5	5888433	21-3			
79	121	2	-64.0	49.8	-63.6	53.4	8109.1	72.7	17.1	83.2	5	5920493	127-5			
80	121	6	2.5	165.4	3.5	167.3	7603.6	39.3	9.6	92.0	5	5920773	128-1			
81	121	32	58.7	120.2	47.5	129.9	4493.5	68.9	13.5	86.8	5	5924413	128-2			
82	122	1	-63.9	226.3	-63.8	226.5	8111.2	73.0	17.2	83.5	5	5956473	128-3			
83	122	6	-14.2	37.1	-25.4	61.0	5676.3	93.7	5.4	48.5	5	5957803	106-4			
84	122	8	-16.4	36.1	-26.9	58.4	5551.3	91.2	5.6	48.5	5	5957873	106-5			
85	122	10	-18.4	34.6	-28.7	56.2	5426.8	88.8	5.7	48.7	5	5957943	107-1			
86	123	7	-8.7	134.0	-6.2	145.0	5675.1	14.8	11.1	87.5	5	5993793	107-2			
87	123	8	-7.8	136.5	-6.1	146.5	5550.2	16.5	11.0	86.5	5	5993853				
88	123	10	-7.3	138.5	-6.4	145.9	5425.6	16.9	11.9	85.8	5	5993923	107-3			
89	125	7	-5.1	144.6	-4.7	149.8	5640.2	32.1	0.9	83.6	5	6065743	107-4			
90	125	8	-5.6	144.4	-5.6	156.7	5515.0	34.8	9.7	81.8	5	6065813	107-5			
91	125	10	-6.2	141.6	-6.1	147.8	5390.2	28.7	10.1	83.1	5	6065993	108-1			
92	125	29	46.3	63.0	46.4	68.0	3939.1	79.9	16.0	58.5	5	6067943	108-2			
93	126	6	-48.7	209.6	-47.0	214.8	5733.3	72.9	17.2	64.9	5	6101653	108-3			
94	126	8	-47.5	210.2	-43.7	220.2	5607.5	71.0	17.0	66.8	5	6101723	108-4			
95	126	16	-46.4	210.1	-43.5	217.5	5482.1	72.2	17.1	62.6	5	6101723	108-5			
96	127	1	-64.0	23.0	-64.0	23.1	8128.6	72.8	17.1	85.3	5	6136303	143-1			
97	127	31	67.0	52.6	54.1	96.9	4478.4	79.2	14.2	76.2	5	6140223	109-1			
98	128	1	-64.0	195.8	-63.8	197.8	8079.8	73.4	17.2	85.1	5	6172293	104-1			
99	128	29	60.7	206.9	60.7	247.8	4322.0	90.1	16.3	62.3	5	6176063	104-2			
100	128	31	63.8	204.2	63.6	249.7	4416.9	91.8	16.4	63.8	5	6176133	104-3			
101	128	32	68.0	207.2	66.7	250.6	4517.2	92.5	16.2	66.2	5	6176203	104-4			
102	129	31	67.0	30.5	60.5	77.5	4459.6	86.7	16.4	63.8	5	6212113	165-4			
103	130	1	-64.0	186.3	-62.7	197.9	8093.9	71.1	16.8	86.8	5	6244173	105-1			
104	131	2	-64.6	358.0	-63.9	6.8	8155.7	73.3	17.1	86.7	5	6280093	105-2			
105	131	9	-57.4	307.4	-52.2	350.2	5598.1	93.7	19.7	49.8	5	6281483	105-3			
106	131	11	-57.2	315.7	-50.2	354.8	5473.0	91.1	19.3	40.8	5	6281553	105-4			
107	131	32	65.6	52.2	56.3	74.4	4457.1	77.9	14.2	74.9	5	6284003	106-3			
108	132	1	-64.1	175.7	-63.2	184.9	8090.7	72.1	16.0	87.0	5	6316063	106-2			
109	133	2	-64.6	347.7	-64.1	354.4	8145.9	74.0	17.2	87.0	5	6351973	99-4			
110	133	6	14.2	144.0	14.5	147.1	7642.1	79.4	7.0	81.1	5	6352253	99-5			
111	133	32	64.1	49.5	61.5	56.7	4465.9	79.2	14.3	73.1	5	6355093	102-1			
112	134	1	-64.4	161.6	-63.9	169.1	8079.6	74.4	17.2	86.7	5	6387953	100-1			
113	134	8	-9.3	256.7	-8.8	259.0	5399.6	7.5	11.5	89.0	5	6389423	100-2			
114	134	10	-9.9	251.9	-8.9	256.3	5277.7	3.8	11.8	88.4	5	6389493	100-3			
115	135	1	-64.7	335.1	-64.7	336.6	8136.2	76.4	17.5	86.6	5	6423053	100-4			
116	135	5	14.4	137.1	14.4	137.6	7632.2	81.2	6.8	80.9	5	6424143	100-5			
117	135	31	60.0	50.7	51.1	61.1	4474.7	69.5	13.4	79.7	5	6427783	165-5			
118	136	1	-64.4	150.6	-64.1	156.5	8073.3	75.3	17.3	87.0	5	6459843	101-1			
119	136	30	60.8	169.4	62.9	193.3	4329.6	91.7	16.7	57.1	5	6463623	100-2			
120	136	32	59.8	154.4	66.0	194.6	4425.7	96.3	17.4	56.0	5	6463693	101-1			
121	137	5	14.3	126.6	14.5	128.0	7631.1	81.7	6.8	81.3	5	6496033				
122	138	1	-64.5	139.8	-64.5	141.3	8079.8	76.7	17.5	87.1	5	6531733	101-4			
123	138	5	14.0	303.9	14.0	304.5	7575.3	82.8	6.7	80.7	5	6532013	101-5			
124	138	30	61.1	198.2	59.5	204.4	4325.6	78.4	14.7	67.7	5	6535513	110-5			
125	138	32	66.0	180.9	61.9	207.7	4420.6	83.6	15.1	66.1	5	6535583	111-1			

Table XI-4j. Limb traces for wide-angle frames: 70°N to 70°S (see Fig. XI-20j)

Index number	Rev	Frame number	Limb profile								Filter	DAS time	Microfiche ID			
			Left margin		Right margin		Center of limb									
			Latitude, deg	Longitude, deg	Latitude, deg	Longitude, deg	Range, km	Lighting angle, deg	Hour angle, h	Phase angle, deg						
1	140	3	-19.8	319.6	-27.2	334.9	5552.5	01.1	4.8	45.6	5	6605023	111-2			
2	141	2	8.9	110.2	4.7	134.6	7052.9	95.1	5.8	71.0	5	6640163	111-3			
3	144	31	74.5	228.9	62.8	224.5	5381.9	79.7	11.2	86.0	5	6751953	163-3			
4	145	32	74.1	44.3	63.3	40.2	5383.1	79.7	11.2	85.7	5	6787933	111-4			
5	147	31	82.6	36.4	56.8	28.2	5363.0	80.4	11.2	84.2	5	6859993	111-5			
6	161	3	-5.5	334.4	-4.4	354.8	5670.5	46.8	8.9	86.4	5	7360743	112-3			
7	167	2	-57.2	149.5	-50.1	194.3	5644.8	85.9	18.3	65.9	5	7576553	129-5			
8	176	2	-56.9	293.3	-55.9	304.2	5700.7	91.2	18.9	65.9	5	7900023				
9	176	31	68.6	79.6	64.9	78.3	5383.1	75.6	10.6	76.5	5	7903173	42-4			
10	176	33	69.7	85.7	64.7	82.5	5506.8	76.8	10.3	77.7	5	7903243	154-3			

Table XI-4k. Limb traces for wide-angle frames: 70°N to 70°S (see Fig. XI-20k)

Index number	Rev	Frame number	Limb profile								Filter	DAS time	Microfiche ID			
			Left margin		Right margin		Center of limb									
			Latitude, deg	Longitude, deg	Latitude, deg	Longitude, deg	Range, km	Lighting angle, deg	Hour angle, h	Phase angle, deg						
1	179	29	66.1	349.7	60.2	280.1	6814.7	94.5	6.3	84.3	5	A011A13	42-5			
2	180	29	63.6	178.2	63.6	109.8	6854.9	101.3	5.1	81.1	5	A047703	43-2			
3	181	2	-56.6	70.7	-54.7	117.8	5986.2	90.5	18.8	72.2	5	A01649	43-4			
4	181	19	28.0	207.3	16.9	212.9	3960.1	29.5	11.8	75.4	5	A01953	43-5			
5	183	29	65.7	337.7	62.3	267.4	6791.3	97.6	5.7	81.1	5	A15663	163-4			
6	184	25	61.3	64.1	58.7	59.6	6288.9	74.1	9.2	86.9	5	A191369	129-2			
7	184	27	72.0	116.3	54.9	56.3	6418.1	83.2	8.2	83.7	5	A191470	129-3			
8	184	29	66.9	139.9	58.2	70.8	6805.6	91.4	6.7	84.1	5	A191649	129-4			
9	185	29	62.9	261.2	62.8	260.4	6801.3	84.3	7.7	87.3	5	A227629	113-2			
10	186	29	67.5	111.9	59.4	64.5	6785.7	88.7	7.1	84.6	5	A263670	164-1			
11	187	29	67.8	206.5	56.3	231.9	6764.4	87.8	7.2	84.5	5	A299589	114-2			
12	188	25	69.1	69.2	50.4	31.2	6344.5	75.2	9.0	85.8	5	A355359	114-4			
13	188	27	69.2	78.9	61.8	52.4	6474.6	84.9	7.8	82.3	5	A35429	114-5			
14	188	29	66.6	106.8	62.9	70.4	6862.7	93.5	6.3	82.5	5	A356119	115-1			
15	189	29	67.0	289.2	58.3	229.0	6826.1	90.2	6.8	83.4	5	A371619	115-2			
16	190	3	-5.9	33.8	-8.1	55.9	5451.5	70.4	7.3	78.6	5	A438119	137-2			
17	191	25	58.9	210.0	55.7	205.0	6354.7	71.2	9.3	87.0	5	A443369	137-3			
18	191	27	70.6	258.1	52.7	202.7	6483.6	80.9	8.2	83.5	5	A443479	137-4			
19	192	25	58.9	74.4	53.9	17.1	6307.1	69.7	9.4	86.9	5	A470349	138-1			
20	192	27	70.8	69.0	52.2	16.8	6436.2	79.7	9.4	83.3	5	A479419	138-2			
21	192	29	67.0	92.1	56.0	30.2	6824.6	87.7	7.1	83.7	5	A479629	138-4			
22	194	27	66.6	103.9	55.2	20.3	6860.5	86.9	7.2	84.0	5	A551659	138-5			
23	195	23	69.9	219.0	49.9	178.8	6300.3	75.2	8.9	83.0	5	A587359	139-1			
24	196	25	68.8	28.0	48.7	352.5	6262.8	73.2	9.1	83.3	5	A623339	139-2			
25	199	23	73.7	246.3	59.7	174.7	6318.4	88.5	7.2	74.8	5	A731349	139-4			
26	200	25	67.6	8.5	47.8	334.1	6312.6	72.3	9.0	83.1	5	A767329	140-5			
27	201	11	-4.5	124.5	-19.4	120.0	4062.2	13.8	11.2	76.9	5	A811009	141-1			
28	203	1	-57.9	339.6	-51.4	18.7	5373.7	87.0	14.1	70.0	5	A871759	141-2			
29	204	25	64.3	338.6	44.9	312.1	6250.3	67.7	9.3	83.4	5	A911179	135-1			
30	206	24	58.7	334.1	55.9	326.9	6853.8	75.8	8.3	85.5	5	A983419	164-3			
31	209	1	-56.4	302.3	-54.9	352.7	6096.3	87.6	18.1	83.4	5	A987089	44-2			

Table XI-4l. Limb traces for wide-angle frames: 70°N to 70°S (see Fig. XI-20l)

Index number	Rev	Frame number	Limb profile								Filter	DAS time	Microfiche ID			
			Left margin		Right margin		Center of limb									
			Latitude, deg	Longitude, deg	Latitude, deg	Longitude, deg	Range, km	Lighting angle, deg	Hour angle, h	Phase angle, deg						
1	218	20	54.8	255.5	37.0	238.4	6180.8	57.1	0.7	83.0	5	0414400	135-3			
2	219	17	57.0	113.2	54.3	98.9	7036.6	83.6	7.0	85.8	5	0451150	126-3			
3	220	16	22.2	116.6	35.2	122.5	4106.4	80.1	17.1	16.3	5	0445039	154-2			
4	222	18	55.5	331.2	55.4	272.2	7703.3	99.9	5.0	78.4	5	0559030	155-3			
5	229	8	3.5	291.2	9.0	301.6	3795.5	32.9	14.1	69.0	5	0708010	136-1			
6	230	10	38.3	137.0	35.8	144.7	3843.6	39.0	12.4	57.3	5	0844630	166-3			
7	234	2	-57.1	12.8	-57.1	31.9	5918.4	91.6	18.3	85.4	5	0806110	136-2			
8	235	11	50.2	351.3	32.9	337.6	6010.4	52.6	9.7	78.2	5	10026130	136-3			
9	239	11	56.1	31.0	52.7	7.7	7657.1	86.8	6.4	81.2	5	10171110	136-4			
10	245	6	53.5	340.6	53.1	338.7	7749.1	80.6	7.1	81.1	5	10386810	24-2			
11	245	10	54.1	349.9	53.1	342.2	7875.6	84.2	6.7	80.8	5	10386010	24-3			
12	245	12	54.0	34.8	52.9	345.4	8000.0	88.1	6.2	80.3	5	10386030	24-4			
13	259	4	54.0	273.9	53.6	272.2	7667.2	81.9	6.8	75.6	5	10616554	21-5			
14	259	6	55.1	283.4	53.7	276.1	7793.9	85.7	6.4	75.2	5	10616634	25-1			
15	259	8	55.6	294.9	53.6	270.9	7920.2	89.0	5.9	74.7	5	10616704	25-2			
16	261	6	23.7	107.4	35.6	112.8	4131.0	67.7	16.3	24.3	5	10686424	164-4			
17	262	2	-57.4	175.4	-61.3	207.4	4949.0	117.5	22.0	53.7	5	10720514	131-5			
18	262	4	-61.0	183.3	-61.9	191.4	4835.8	117.1	22.2	49.7	5	10720584	132-1			

Table XI-4m. Limb traces for wide-angle frames: 70°N to 70°S (see Fig. XI-20m)

Index number	Rev	Frame number	Limb profile								Filter	DAS time	Microfiche ID			
			Left margin		Right margin		Center of limb									
			Latitude, deg	Longitude, deg	Latitude, deg	Longitude, deg	Range, km	Lighting angle, deg	Hour angle, h	Phase angle, deg						
1	416	13	54.7	176.8	59.4	154.8	7495.3	104.6	22.5	14.6	5	11445049	132-2			
2	417	13	55.5	348.7	59.2	330.5	7510.6	104.7	22.6	14.7	5	11481069	132-3			
3	422	13	59.5	130.4	60.3	124.1	7451.3	103.3	23.2	13.4	5	11622765	132-4			
4	423	13	60.5	301.0	60.7	299.0	7419.5	102.8	23.3	13.0	5	11654745	132-5			
5	459	1	-80.6	258.6	-65.1	267.0	3890.1	92.1	13.0	84.1	5	12535030	133-2			
6	459	3	-77.8	272.4	-59.7	272.5	3843.5	87.6	12.6	83.0	5	12525110	133-3			
7	459	5	-58.5	278.4	-54.9	278.1	3778.1	75.4	12.1	86.5	5	12535240	133-4			
8	478	9	5.9	37.4	-26.2	334.8	16235.5	56.3	15.0	84.3	5	12874645	134-1			
9	478	10	51.0	171.8	28.9	66.5	16297.8	40.9	9.3	86.8	5	12874568	134-2			
10	479	12	-21.0	164.4	-24.9	145.6	15810.3	81.9	16.8	77.0	5	12909088	134-3			
10	479	12	2.6	207.8	-8.8	191.2	15810.3	35.1	13.8	85.4	5	12909049	134-3			
11	479	13	39.7	262.9	7.4	214.2	15675.7	9.0	11.4	87.7	5	12910558	134-4			
12	528	12	47.5	215.7	36.9	206.0	16160.9	66.0	6.7	70.2	5	12909242	146-5			
13	528	13	41.1	218.5	9.7	170.9	16223.2	23.7	10.3	77.0	5	12909112	146-4			
14	528	14	-1.6	156.7	-27.2	89.5	16284.5	57.4	14.7	72.5	5	12909382	145-5			
15	529	9	44.9	95.3	40.6	51.6	14049.5	82.4	5.2	58.3	5	13028122	145-1			
16	667	12	42.4	109.3	41.8	174.8	11821.4	112.8	23.9	23.1	5	13317545	146-1			
17	667	13	-29.5	64.5	-22.0	300.4	19860.3	91.0	15.9	48.0	5	13328745	146-2			
18	668	10	42.7	6.8	41.7	350.8	11506.9	113.0	*0	23.5	5	13353315	146-5			
19	668	12	1.5	241.4	-9.2	205.1	11906.6	51.5	9.1	50.7	5	13353505	146-4			
20	668	14	-n.0	141.1	14.0	92.6	12855.3	68.7	16.5	43.4	5	13345205	147-1			
21	668	17	-21.8	117.3	19.8	74.4	18365.3	116.9	19.9	31.6	5	13360385	147-2			
22	675	10	-29.0	358.4	-19.6	260.9	18632.7	81.0	15.6	41.5	5	13471128	147-3			
23	676	11	-15.3	135.1	2.6	77.5	12842.9	50.0	14.6	49.3	5	13500528	147-4			
24	676	13	-21.9	148.7	-11.9	80.0	15606.7	62.9	14.9	42.8	5	13502978	147-5			
25	676	15	-29.6	155.9	-12.0	70.2	17662.2	79.3	15.9	39.6	5	13505428	148-1			
26	676	17	-35.5	101.7	6.4	51.0	19001.5	112.3	19.1	33.7	5	13507048	148-2			

Note: Double entries correspond to two separate sectors of the limb appearing in a single picture.

Table XI-5. Limb traces for narrow-angle frames: 70°N to 70°S (see Fig. XI-21)

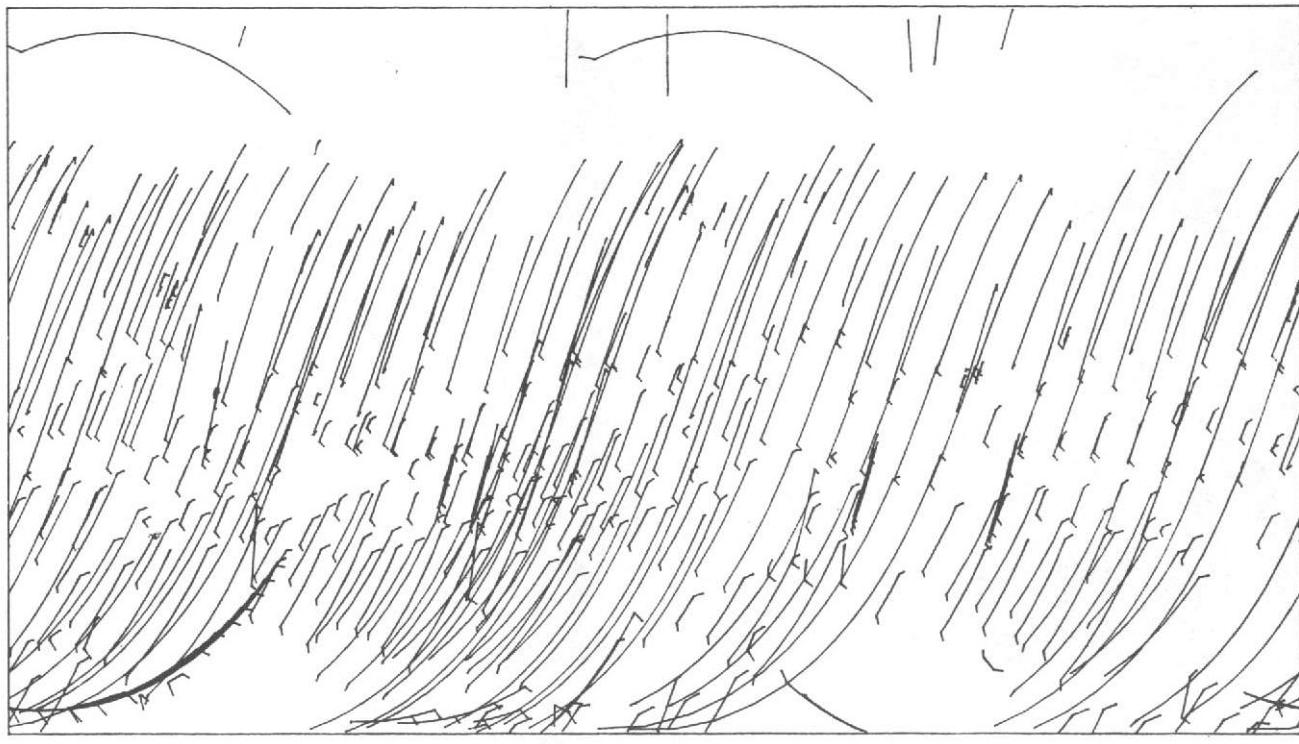
Index number	Rev	Frame number	Limb profile								Filter	DAS time	Microfiche ID			
			Left margin		Right margin		Center of limb									
			Latitude, deg	Longitude, deg	Latitude, deg	Longitude, deg	Range, km	Lighting angle, deg	Hour angle, h	Phase angle, deg						
1	6	1	-34.1	105.2	-32.8	107.7	5492.7	76.0	17.8	42.9	1A14820					
2	9	33	-60.7	225.3	-60.3	229.8	7123.8	86.8	20.5	35.9	1921780	77-3				
3	11	31	-32.8	230.7	-31.9	232.0	4226.3	100.9	20.0	19.6	1995140	78-5				
4	16	8	-19.0	96.0	-17.8	98.1	6230.9	39.7	14.8	64.1	2173570	79-5				
5	24	1	50.3	120.4	52.3	128.3	12796.3	83.8	8.8	66.6	2456720	11-2				
6	24	2	47.7	115.1	50.2	122.3	12701.2	79.5	9.2	67.5	2456790	94-1				
7	26	1	-11.7	59.2	-7.7	60.6	12916.3	12.7	12.4	81.4	2528400	1-1				
8	26	2	-11.2	59.5	-7.3	60.9	12823.2	13.1	12.4	81.2	2528470	1-2				
9	27	3	2.6	239.5	6.8	241.2	12892.5	25.8	12.0	80.6	2564310	162-2				
10	27	4	2.5	239.7	6.6	241.4	12798.4	25.7	12.0	80.3	2564380	162-3				
11	28	1	-11.7	49.3	-7.7	50.7	12872.9	12.3	12.3	82.1	2600220	60-1				
12	28	2	-11.8	49.4	-10.0	50.1	12778.8	11.4	12.4	81.9	2600290	60-2				
13	29	1	-30.0	218.5	-25.9	219.7	12954.5	11.5	12.7	82.7	2636060	7-3				
14	29	2	-30.1	218.5	-26.0	219.7	12860.5	11.8	12.7	82.4	2636130	7-4				
15	30	1	-12.9	39.1	-11.5	39.5	12855.5	9.9	12.3	82.9	2672040	130-5				
16	30	2	-15.5	76.3	-11.5	39.7	12761.2	9.1	12.4	82.7	2672110	131-1				
17	31	1	-17.2	212.7	-13.2	213.9	12950.4	7.6	12.4	83.6	2707950	130-1				
18	31	2	-16.0	213.2	-12.0	214.5	12856.3	8.4	12.3	83.3	2707950	13-1				
19	32	1	52.0	84.9	53.7	93.3	12866.7	87.9	8.3	68.9	2743850	13-5				
20	32	2	49.8	79.5	52.0	87.3	12771.5	83.8	8.7	69.7	2743930	14-1				
21	32	20	31.9	131.6	30.3	136.2	9999.1	101.2	6.0	51.1	2745820	130-2				
22	33	1	49.8	252.6	52.2	260.5	12881.1	83.3	8.8	70.6	2779770	2-2				
23	33	2	47.7	249.0	50.1	255.2	12877.6	79.6	9.1	71.3	2779840	2-3				
24	34	1	-73.0	352.0	-68.9	356.6	12906.0	53.0	13.9	78.6	2815690	4-1				
25	34	2	-74.7	348.3	-69.7	354.9	12811.9	54.5	14.1	78.0	2815750	162-4				
26	35	3	-71.4	148.5	-68.8	171.2	12838.7	52.3	13.0	79.0	2851660	15-4				
27	36	1	-70.1	345.5	-67.1	348.3	12874.9	50.7	13.7	79.8	2887570	60-3				
28	36	2	-65.3	319.0	-65.0	349.3	12780.8	47.3	13.6	80.2	2887640	60-4				
29	37	1	12.1	105.3	16.6	197.6	12818.1	35.8	11.4	82.7	2923550	62-2				
30	37	2	11.1	105.2	12.1	195.7	12722.9	32.8	11.5	82.0	2923620	74-2				
31	38	1	-74.1	321.8	-68.4	338.3	12955.6	53.2	13.8	80.2	2959390	130-3				
32	38	2	-69.4	326.5	-66.4	339.2	12861.5	50.0	13.6	80.6	2959460	152-2				
33	39	1	14.7	186.7	19.4	189.2	12897.7	38.8	11.3	83.2	2959375	63-1				
34	39	2	13.0	180.3	17.5	188.6	12803.6	36.8	11.3	83.2	2959445	63-2				
35	40	1	-73.7	321.6	-67.5	328.7	12849.1	52.8	13.8	80.7	3031355	18-2				
36	40	2	-70.5	324.6	-65.5	329.6	12753.9	50.3	13.7	80.9	3031425	18-1				
37	42	1	50.4	52.3	52.5	40.2	12838.7	85.8	8.4	73.2	3103445	152-4				
38	42	21	-7.0	352.6	-7.3	354.1	5546.6	15.5	12.6	75.7	3107515	8-5				
39	42	23	-7.2	350.6	-6.9	358.4	5410.3	14.1	12.4	76.3	3107595	8-1				
40	43	5	-73.0	128.7	-67.3	134.7	12876.6	52.3	13.6	82.0	3139155	72-4				
41	43	6	-71.4	129.7	-69.4	132.0	12781.6	52.8	13.7	81.6	3139225	72-5				
42	44	1	24.2	343.3	24.9	348.8	12907.0	47.5	10.9	83.4	3175655	73-1				
43	44	2	20.4	346.4	25.5	349.7	12812.9	45.7	10.9	83.5	3175135	73-2				
44	45	1	22.2	163.0	25.7	165.6	12745.6	47.0	10.8	83.4	3211115	152-5				
45	46	1	-71.5	206.0	-65.8	301.4	12857.4	50.8	13.5	83.4	3246955					
46	46	2	-68.4	208.4	-65.1	301.3	12762.2	49.0	13.4	83.4	3247025	150-2				
47	47	1	-72.4	110.1	-67.2	115.5	12870.8	52.0	13.5	83.5	3282865	140-3				
48	47	2	-70.7	111.3	-65.7	116.0	12776.7	50.5	13.5	83.6	3282935	140-4				
49	48	1	32.6	335.4	36.6	339.3	12872.9	59.9	10.2	82.2	3318775	94-5				
50	48	2	30.8	334.5	34.1	337.5	12778.6	57.3	10.3	82.5	3318845	46-1				
51	49	1	34.6	152.6	35.6	153.3	12870.8	60.8	10.2	82.4	3354695	25-1				
52	49	2	31.4	150.1	36.2	154.0	12776.7	59.1	10.2	82.4	3354755	153-5				
53	49	16	-57.7	337.0	-57.8	340.5	5598.1	102.0	23.2	10.5	3358055	80-3				
54	51	1	37.7	145.9	41.5	150.6	12842.9	66.8	9.8	81.6	3426505	80-5				
55	51	2	34.9	143.7	38.8	148.1	12747.7	63.3	9.9	82.1	3426575	41-1				
56	52	1	53.0	351.3	54.5	+1	12911.1	92.6	7.6	75.5	3462345	75-3				
57	52	2	51.0	345.5	52.9	353.6	12817.0	88.3	8.0	76.3	3462115	75-4				
58	53	1	53.1	167.3	54.4	176.2	12882.2	93.2	7.5	75.6	3498255	83-4				
59	53	2	51.0	161.1	52.9	169.2	12788.1	88.7	7.9	76.5	3498325	83-5				
60	53	12	20.5	131.3	20.6	131.4	11169.8	45.1	10.6	82.2	3499445	37-2				
61	53	13	20.7	132.1	24.5	136.0	11062.1	48.0	10.4	81.3	3499515	37-3				
62	53	14	19.6	131.8	22.8	135.0	10952.2	46.3	10.5	81.3	3499585	37-4				
63	53	15	18.0	130.9	21.3	134.1	10842.3	44.4	10.5	81.4	3499655	37-5				
64	54	1	53.5	345.4	54.5	354.4	12848.1	95.1	7.2	75.4	3534165					
65	54	2	51.8	340.0	53.3	348.4	12752.9	91.2	7.6	76.0	3534235	38-1				
66	55	1	53.7	159.5	54.8	168.6	12903.9	95.0	7.3	76.0	3570005	39-4				
67	55	2	52.0	154.2	53.6	162.6	12809.6	91.2	7.7	76.7	3570075	39-5				
68	55	4	31.7	123.8	32.7	124.8	12327.2	58.5	10.0	83.5	3570425					
69	55	5	28.0	121.0	32.7	125.6	12228.6	56.3	10.1	83.7	3570495	80-5				
70	55	6	27.3	121.1	29.1	122.7	12129.0	53.7	10.2	84.0	3570565	40-1				

Table XI-5. (contd)

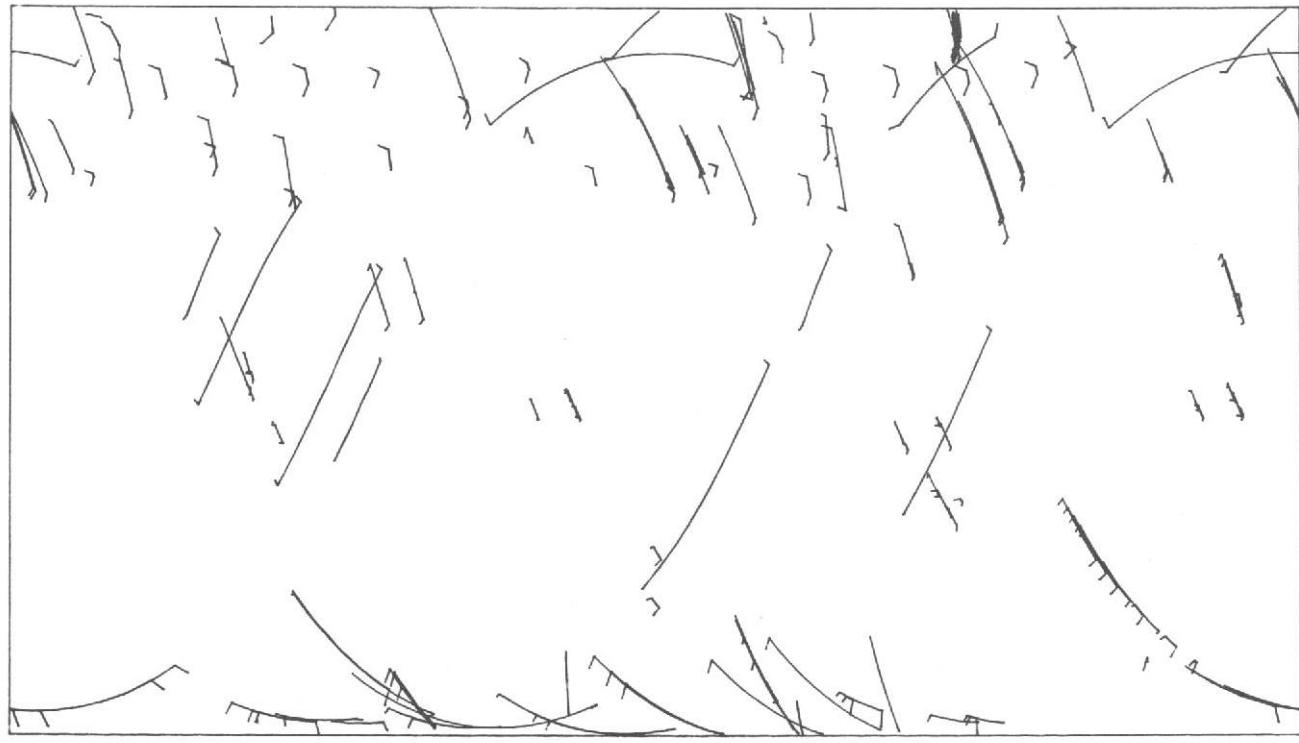
Index number	Rev	Frame number	Limb profile								Filter	DAS time	Microfiche ID			
			Left margin		Right margin		Center of limb									
			Latitude, deg	Longitude, deg	Latitude, deg	Longitude, deg	Range, km	Lighting angle, deg	Hour angle, h	Phase angle, deg						
71	56	1	54.5	342.9	54.9	352.3	12863.6	99.9	6.7	74.9		3605915				
72	56	2	53.1	336.0	54.1	348.8	12769.4	95.3	7.2	75.8		3605945	34-2			
73	57	1	54.6	163.9	54.6	168.8	12820.1	102.0	6.4	74.6		3641825				
74	57	2	53.8	158.3	54.0	161.7	12725.0	98.0	6.8	75.3		3641845				
75	57	12	32.2	126.4	32.8	127.4	10989.9	63.2	9.4	78.7		3643185	35-5			
76	57	13	29.2	123.1	32.4	128.0	10880.0	61.0	9.6	78.9		3643155	36-1			
77	57	14	27.4	121.6	28.3	122.9	10770.0	56.7	9.8	79.7		3643225	36-2			
78	58	1	42.1	205.7	45.4	301.0	12872.9	73.3	9.2	82.8		3677665	36-3			
79	58	2	39.0	292.7	43.0	298.0	12777.7	69.6	9.5	A3.5		3677735	36-4			
80	59	1	65.1	188.2	60.5	198.8	15681.4	126.0	3.0	A1.7		3711125	65-5			
81	59	2	43.8	112.6	47.3	118.7	12922.5	75.9	9.0	B2.7		3713505	65-1			
82	59	3	40.3	108.7	44.2	114.3	12828.4	71.3	9.3	B3.6		3713575	66-2			
83	60	1	52.1	307.1	53.9	315.6	12884.3	91.1	7.6	79.0		3749115	67-3			
84	60	2	49.9	302.0	52.2	309.8	12790.1	87.1	8.0	79.7		3749135	67-4			
85	61	10	-6.2	122.2	-6.4	123.2	5568.9	42.2	9.2	70.2		3789595	32-5			
86	61	18	-8.1	122.4	-8.6	124.6	5432.7	41.9	9.2	70.2		3789665	33-1			
87	61	20	-10.3	123.1	-10.4	123.7	5296.7	40.9	9.2	70.6		3789735	33-2			
88	62	1	52.3	207.0	54.0	305.5	12907.0	91.5	7.6	79.8		3821165	33-3			
89	62	2	49.9	291.3	52.2	299.0	12812.9	87.0	8.0	B0.6		3821135	33-5			
90	62	21	-7.6	253.8	-7.1	255.6	5658.8	11.2	12.1	79.0		3825435	55-1			
91	62	23	-7.6	254.7	-7.2	256.5	5522.0	11.1	12.0	79.1		3825575	55-2			
92	62	25	-7.6	255.7	-7.4	257.4	5385.5	11.0	12.0	79.2		3825575	55-3			
93	62	27	-10.8	254.6	-11.2	256.0	4356.2	8.3	12.2	A3.6		3826135	55-4			
94	63	6	51.7	110.5	53.6	118.8	12877.0	90.5	7.7	80.3		3857175	56-3			
95	63	9	49.4	105.4	51.8	113.0	12782.9	86.3	P.1	A1.1		3857145	56-4			
96	63	23	-7.0	120.0	-7.3	121.4	5614.5	50.2	P.6	66.8		3861345	50-3			
97	63	25	-9.2	120.3	-9.3	120.8	5477.4	49.2	P.7	67.1		3861415	50-4			
98	63	27	-11.6	120.9	-11.7	121.1	5341.7	48.6	P.7	67.2		3861495	50-5			
99	64	14	-58.4	198.4	-55.9	193.1	9048.9	51.3	15.0	77.9		3894335	141-4			
100	66	14	-58.3	190.0	-58.0	180.5	9135.3	51.7	15.0	78.8		3967195	97-4			
101	66	19	-6.0	240.5	-5.7	242.3	5676.3	14.2	11.5	79.3		3968005	97-5			
102	66	21	-7.1	236.9	-6.8	238.7	5539.6	11.7	11.8	79.6		3968075	98-1			
103	66	23	-8.0	233.5	-7.7	235.2	5403.4	10.3	12.0	79.8		3969145	98-2			
104	67	14	19.3	103.5	19.5	107.2	7963.2	71.7	7.8	67.1		4003725	141-5			
105	67	17	18.0	102.6	18.2	104.8	7851.6	69.5	P.0	67.5		4003795	142-1			
106	68	14	-53.8	177.6	-50.7	181.8	9135.3	43.8	14.3	B1.7		4039005	150-4			
107	68	16	-49.8	178.7	-49.5	179.1	8634.5	43.4	14.5	80.1		4039285	150-5			
108	68	17	-50.8	176.0	-48.0	179.9	8506.5	44.0	14.6	79.5		4039355	151-1			
109	68	18	-49.4	176.7	-49.1	177.1	8378.3	44.7	14.7	78.9		4039425	122-5			
110	69	16	19.6	104.6	19.4	108.1	8004.9	91.6	7.1	63.4		4075545	162-5			
111	69	17	19.5	102.1	18.3	105.7	7872.3	78.7	7.3	64.0		4075615	144-4			
112	70	19	-5.8	221.3	-5.7	221.8	5715.9	14.6	11.4	79.9		4112645	124-4			
113	70	21	-6.9	217.8	-6.6	219.6	5578.3	12.2	11.6	80.1		4112715	124-5			
114	70	23	-7.9	214.3	-7.6	216.0	5442.1	10.2	11.9	80.4		4112785	142-2			
115	71	16	-43.8	345.9	-42.3	347.9	7933.2	39.1	14.4	79.9		4147435	118-3			
116	71	17	-43.4	345.2	-41.8	347.4	7800.4	39.5	14.4	79.4		4147505	142-4			
117	74	19	-6.4	200.3	-6.0	202.1	5630.8	14.1	11.4	80.6		4256425	120-4			
118	74	21	-7.4	196.7	-7.1	198.5	5493.8	11.2	11.7	80.8		4256495	120-5			
119	74	23	-8.3	193.2	-8.0	194.9	5357.1	9.3	11.9	81.0		4256565	121-1			
120	77	16	-65.5	234.6	-65.6	242.7	7999.5	83.3	19.5	65.2		4363035	57-5			
121	77	17	-65.0	244.1	-64.7	252.0	7867.9	80.1	18.9	66.0		4363105	58-1			
122	79	16	-50.8	207.3	-48.7	300.9	7982.1	46.9	14.8	80.2		4434925	158-2			
123	79	17	-48.2	300.2	-45.8	303.9	7850.5	44.1	14.6	80.6		4434995	158-3			
124	81	17	17.2	52.3	16.7	55.6	7809.1	88.3	6.5	63.0		4506845	6-3			
125	83	16	15.1	60.4	14.1	63.2	7998.4	104.9	5.2	57.0		4578635	68-2			
126	83	17	14.9	56.3	13.9	59.6	7866.9	101.0	5.5	57.9		4578705	68-4			
127	85	17	14.8	47.8	14.3	49.2	7882.1	101.9	5.4	58.3		4650525	70-2			
128	87	15	-49.7	126.6	-52.2	131.0	7988.7	112.2	23.4	54.9		4722275				
129	87	16	-52.4	131.5	-54.6	136.2	7857.1	109.2	23.0	55.2		4722345	71-4			
130	91	16	19.3	357.0	19.1	.5	7965.6	87.0	6.6	68.2		486545	163-2			
131	91	17	18.1	354.8	18.0	358.2	7834.2	84.3	6.8	68.5		4865915	89-5			
132	91	18	-17.7	16.7	-18.8	18.9	5650.7	89.0	5.7	47.3		4867035	159-5			
133	91	20	-18.8	13.0	-19.9	15.2	5513.8	85.0	6.0	49.0		4867105	16-4			
134	91	22	-19.8	8.8	-20.8	11.0	5378.4	80.7	6.3	51.1		4867175	16-5			
135	100	30	61.7	7.5	61.2	11.1	4315.6	90.0	16.0	74.9		5168518	116-3			
136	101	32	68.4	187.8	67.6	192.3	4543.5	91.9	15.7	79.3		5204638	117-2			
137	102	7	-6.7	57.3	-6.4	59.2	5584.1	13.1	11.3	83.4		5238028	81-1			
138	102	9	-7.3	53.8	-7.0	55.6	5459.7	9.9	11.6	83.3		5238098	81-2			
139	103	6	-6.3	300.0	-7.1	302.5	6063.1	78.2	6.7	59.3		5273728	83-1			
140	103	9	-5.9	248.5	-6.0	250.5	5432.7	27.1	10.3	80.0		5274078	126-2			

Table XI-5. (contd)

Index number	Rev	Frame number	Limb profile								Filter	DAS time	Microfiche ID			
			Left margin		Right margin		Center of limb									
			Latitude, deg	Longitude, deg	Latitude, deg	Longitude, deg	Range, km	Lighting angle, deg	Hour angle, h	Phase angle, deg						
141	105	6	-9.8	299.3	-10.7	301.7	6031.0	86.2	6.1	54.2	5345648	1A-3				
142	105	9	-7.0	250.6	-7.3	252.7	5400.8	38.1	9.5	76.4	5346038	1B-4				
143	107	6	-2.1	271.0	-2.3	272.0	6162.6	70.0	7.3	66.1	541757A	161-1				
144	107	9	-23.6	298.1	-24.1	299.2	5526.7	89.0	5.6	46.4	5417928	92-5				
145	110	30	41.4	259.0	42.5	259.5	4363.8	122.4	20.1	43.4	5528318	161-2				
146	114	7	-12.9	67.4	-13.1	67.9	5632.0	75.9	6.8	50.1	5669858	95-3				
147	114	9	-15.0	66.5	-15.1	66.9	5506.8	74.3	6.9	58.8	5669028	95-4				
148	115	6	-1.9	195.5	-1.5	197.6	6187.7	35.3	9.8	83.7	5705558	96-4				
149	115	9	-23.5	263.2	-24.6	265.4	5550.2	93.1	5.4	45.2	5705908	127-1				
150	120	7	-19.7	54.8	-20.7	57.1	5595.6	90.6	5.6	49.2	5885878	157-3				
151	120	9	-21.9	53.5	-22.9	55.7	5470.3	88.6	5.7	49.0	5885048	157-4				
152	122	7	-20.4	48.1	-20.9	49.2	5614.5	92.9	5.5	48.2	5957838	162-1				
153	127	32	65.1	82.2	63.9	85.5	4528.5	91.2	14.3	75.9	6140258	103-5				
154	129	32	68.5	53.3	67.9	58.1	4509.7	88.5	15.5	68.8	6212148	104-6				
155	131	8	-56.8	321.8	-56.4	326.1	5661.2	96.2	20.1	48.9	6281448	105-5				
156	131	10	-55.8	329.6	-55.2	333.6	5536.1	93.1	19.6	49.2	6281518	106-1				
157	130	33	65.9	167.0	66.6	171.3	4474.7	97.8	17.5	56.4	6463728					
158	154	6	-5.4	119.7	-5.0	120.9	4217.3	35.4	14.4	74.3	7109688	112-2				
159	167	3	-54.5	174.2	-53.7	179.0	5581.8	84.5	18.1	65.8	7576588	128-4				
160	167	4	-53.9	175.0	-53.4	177.3	5456.2	84.7	18.1	63.6	7576658	128-5				
161	179	30	66.3	320.9	65.9	313.9	6879.4	96.8	5.9	83.9	A011848	43-1				
162	181	1	-57.3	87.0	-57.3	91.7	6050.5	93.2	19.1	71.6	A079608	43-3				
163	181	20	25.2	209.9	23.9	210.5	3991.7	71.3	11.8	75.3	A081098	44-1				
164	184	28	66.7	85.2	65.1	79.7	6482.5	84.9	7.9	83.6	A191474	112-5				
165	184	30	66.0	110.0	65.3	103.3	6870.5	93.8	6.3	83.7	A191694	113-1				
166	186	5	-54.4	259.7	-53.4	262.7	4912.6	87.1	18.2	55.7	A260114	113-3				
167	186	6	-53.4	262.4	-52.3	265.3	4800.4	85.8	18.1	53.9	A260214	113-4				
168	187	7	-12.2	119.3	-11.1	120.8	3985.1	52.7	15.5	61.0	A296824	113-5				
169	187	8	-9.7	118.6	-8.7	119.0	3923.2	53.9	15.6	58.4	A296894	114-1				
170	187	30	65.5	267.5	64.5	261.2	6829.2	90.3	6.8	84.0	A299624	114-3				
171	189	7	-1.9	180.6	-2.5	181.8	4019.2	18.1	10.8	79.7	A368794	126-4				
172	190	1	-5.6	50.3	-5.9	52.7	5639.0	77.6	6.8	77.2	A403714	165-2				
173	190	2	-6.8	48.5	-7.2	50.8	5513.8	75.3	6.9	76.6	A401794	165-3				
174	191	28	64.4	228.9	62.8	223.9	6549.0	82.1	8.0	83.7	A443474	137-5				
175	192	28	63.9	41.1	62.2	36.4	6501.7	80.7	8.2	83.5	A479454	138-3				
176	195	24	61.1	196.5	59.1	192.7	6364.9	75.0	8.9	83.9	A587394					
177	196	26	60.2	9.4	58.2	5.9	6327.5	73.5	9.0	83.9	A623374	139-3				
178	201	12	-8.9	123.2	-10.2	122.9	4099.9	12.4	11.2	77.7	A801944	126-5				
179	203	2	-55.1	1.9	-54.4	5.6	5312.1	85.2	17.9	70.0	A871804	134-5				
180	204	26	55.7	325.4	53.8	322.8	6315.0	67.9	9.3	84.1	A911214					
181	218	19	45.0	244.8	42.6	242.7	6116.9	54.5	9.9	83.5	9414374	135-4				
182	220	17	30.3	117.7	30.4	117.8	4146.5	81.5	17.2	15.2	9485074	135-5				
183	668	3	16.7	135.5	18.4	132.4	9370.7	36.3	14.6	64.1	13351950	146-3				
184	676	10	-7.5	103.3	-7.2	102.5	12797.4	51.0	14.7	49.1	13500493	147-3				

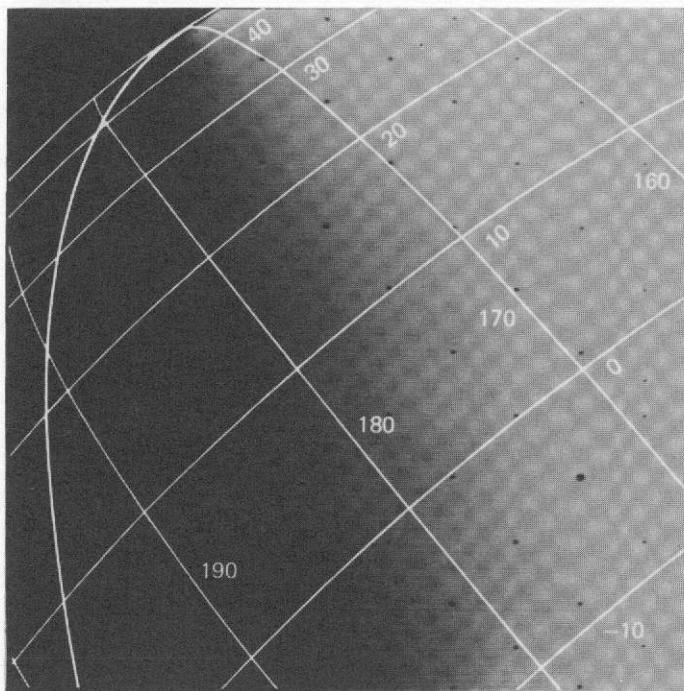


(a) MORNING TERMINATOR

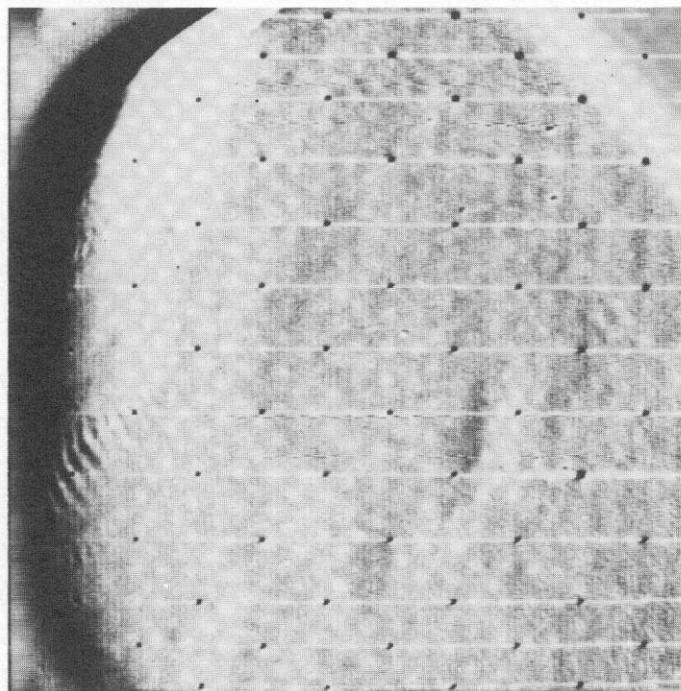


(b) EVENING TERMINATOR

Fig. XI-22. Traces of the terminator for wide-angle frames.



(a) SHADING-CORRECTED



(b) HPF

Fig. XI-23. Martian terminator during Rev 18. In Fig. XI-23b, north is at the top.

Note:

Names used in this section are informal and classical names consistent with those used in earlier publications on atmospheric phenomena visible in the Mariner 9 pictures.

References

- XI-1. Briggs, G. A., and Leovy, C. B., "Mariner 9 Observations of the Mars North Polar Hood," *Bull. Am. Meteorolog. Soc.*, Vol. 55, 1974.
- XI-2. Leovy, C. B., Briggs, G. A., Young, A. T., Smith, B. A., Pollack, J. B., Shipley, E. N., and Wildey, R. L., "The Martian Atmosphere: Mariner 9 Television Experiment Progress Report," *Icarus*, Vol. 17, p. 373, 1972.
- XI-3. Leovy, C. B., Briggs, G. A., and Smith, B. A., "Mars Atmosphere During the Mariner 9 Extended Mission: Television Results," *J. Geophys. Res.*, Vol. 78, p. 4252, 1973.

XII. Satellites

Pre-orbital and orbital pictures have yielded new information regarding the orbits, rotation periods, sizes, shapes, albedos, and surface characteristics of the Martian satellites, Phobos and Deimos (see Figs. XII-1 and XII-2). The most comprehensive data were acquired using the narrow-angle camera; the wide-angle camera was used to obtain additional color and polarimetric information. To photograph Phobos and Deimos at close range, it was necessary to obtain improved orbits for the satellites (Refs. XII-1 and XII-2). The first refinements of their orbits were based on 21 pictures, taken during the pre-orbital science (POS) sequences, that contain Phobos or Deimos together with stars (see Table 6-1 of Volume II). In most of these images, both Phobos and Deimos were 1 pixel or less in diameter, and the images had to be greatly overexposed to show adequately even bright stars. All pictures were taken at a phase angle of about 60° with an exposure of 6.144 s, except for frames 60 and 61, which were 6-ms exposures of Phobos transits. Frame 60 was successful (Fig. XII-3), but in frame 61 the satellite did not appear in the field of view.

Additional information on these pre-orbital pictures of the satellites is presented in Table XII-1; the diameters given in the table are computed assuming the satellites to be spherical

(with diameters of 23.5 km for Phobos and 13.5 km for Deimos). Actually, Phobos and Deimos are highly irregular objects; Phobos is estimated to range from a maximum dimension of 27 km to a minimum of 19 km, and Deimos from 15 km to 11 km (Ref. XII-3). Motion of the instrument platform during the long 6.144-s exposures caused smearing of the images of the satellites and stars. Estimates of the magnitude of the smearing are given in Table XII-1. These estimates would be useful in any reanalyses of the pictures for the purpose of detecting new satellites or stars.

After Mariner 9 was inserted into Mars orbit, other narrow-angle images were obtained at close encounters with the satellites. These pictures show considerable detail in the crater-pocked surfaces. To locate the satellites with sufficient accuracy for any closeup pictures was a significant technical feat. However, the orbit of Deimos was so well determined on the basis of POS pictures that none of the satellite pre-orbital frames "missed" the satellite because of navigation inaccuracies.

The orbit of Phobos was not known adequately because only two pictures of the satellite were obtained from pre-

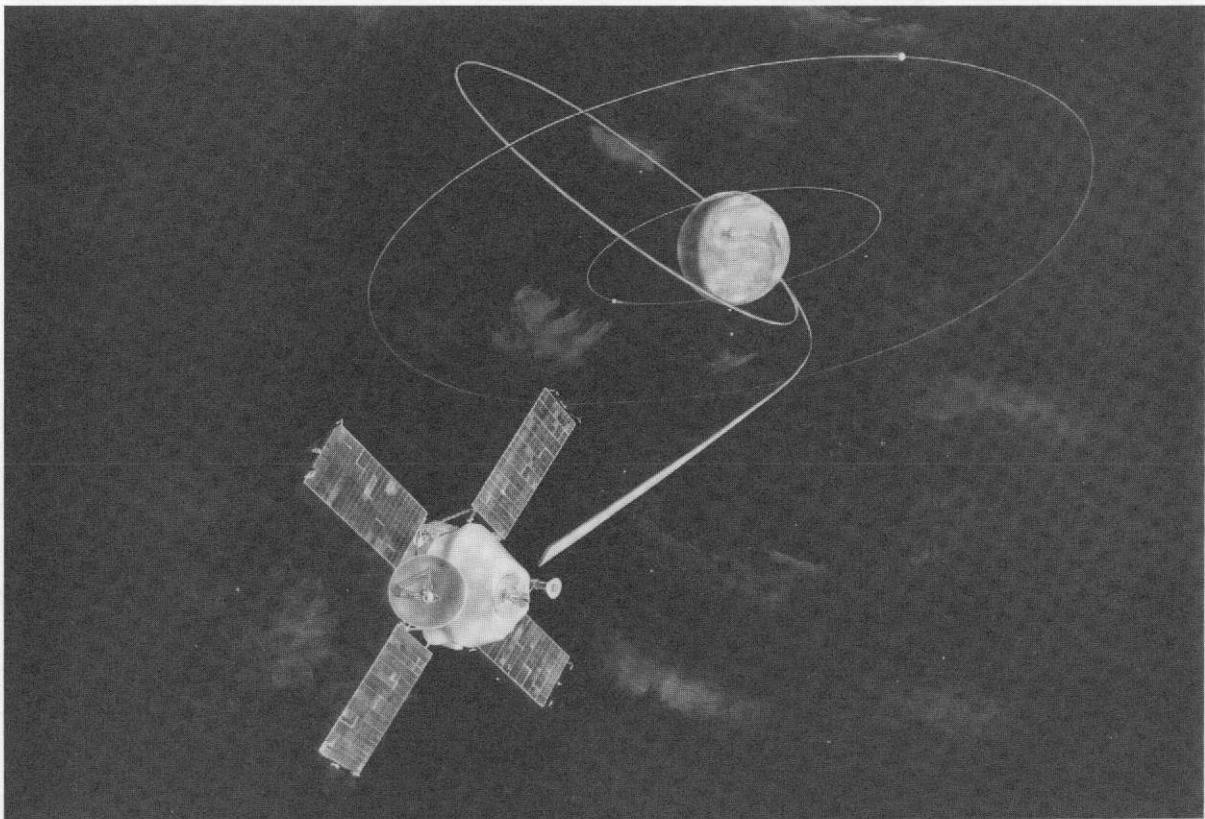


Fig. XII-1. Approach trajectory and orbit of Mariner 9 shown with the orbits of the two natural satellites, Phobos and Deimos.

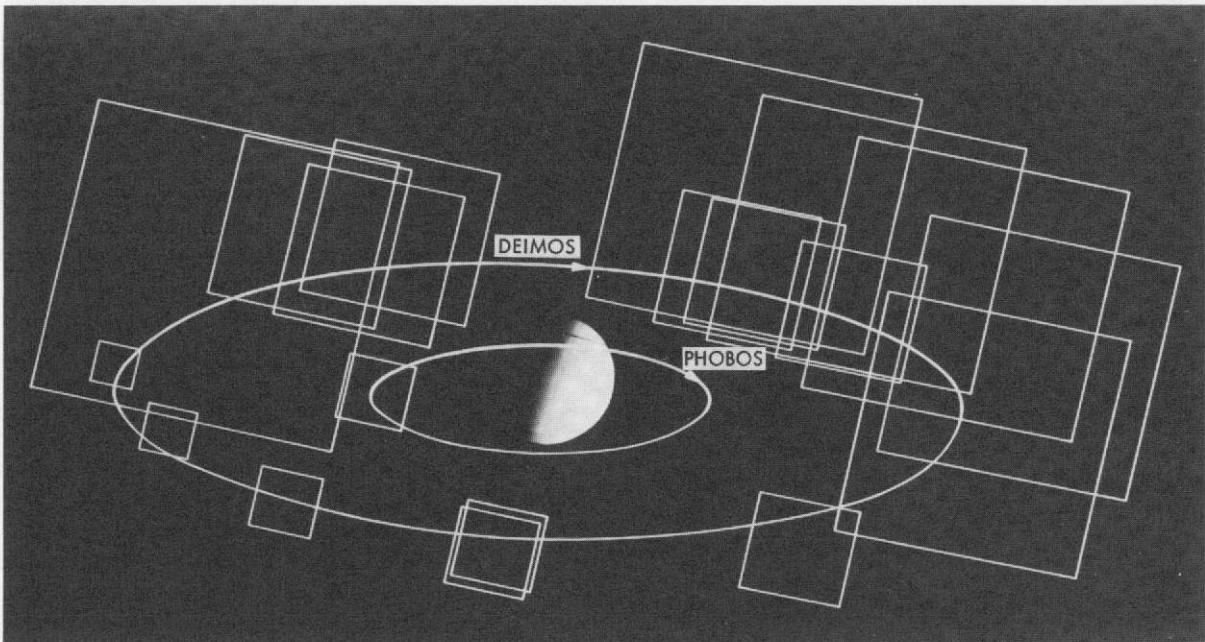


Fig. XII-2. Footprints of pre-orbital satellite pictures. The satellite orbits are within a few degrees of being coplanar with the equator of Mars; in this view, the north pole of the planet is directed toward the top of the page and at about 20° into the plane of the paper. Mars and the orbits of Phobos and Deimos are drawn as seen from the spacecraft. These pictures were searched for the presence of new satellites.

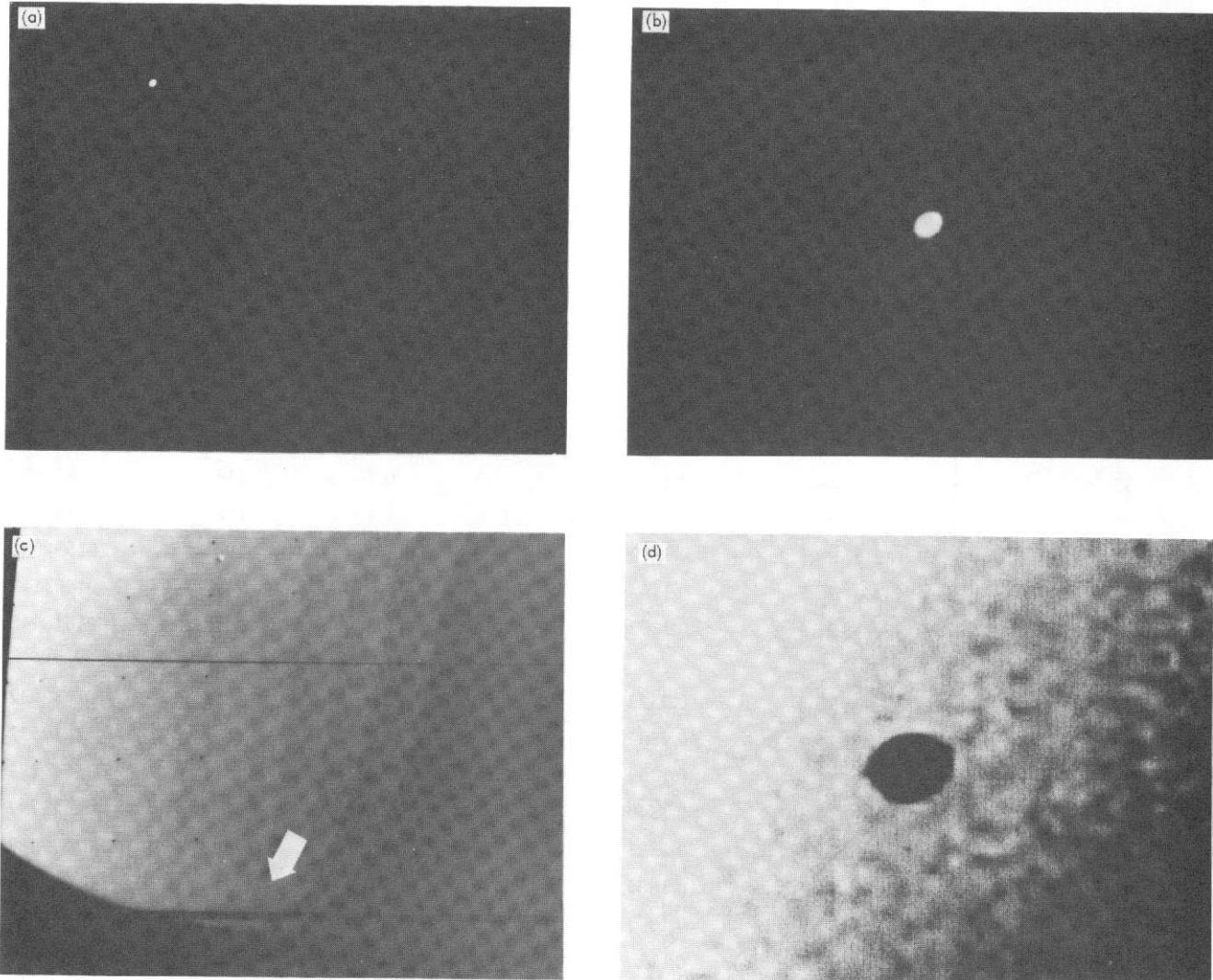


Fig. XII-3. POS-3 pictures of Phobos and Deimos. (a) Deimos: frame 72. Deimos was photographed when the spacecraft was at a distance of about 140,000 km. As the planet was not in the field of view, the picture was deliberately overexposed (6.144 s) to reveal the star background for an approach-navigation test (see Refs. XII-1 and XII-2). (b) Deimos: frame 72. This enlargement shows a saturated image that was smeared by the relative motion and rotation of the spacecraft and satellite. (c) Phobos transit: frame 60. Phobos was imaged some hours previously, when the spacecraft was about 150,000 km away. In this case, only a 6-ms exposure was used, and the satellite appears as a dark spot against the much brighter planet. (d) Phobos: frame 60. Computer-enhanced picture of Phobos.

Table XII-1. Pre-orbital satellite coverage

POS ^a	Frame number ^b	Satellite	Time before insertion, h	Range, km × 10 ⁶	Diameter, pixels	Image motion, ^c pixels	Mean anomaly, deg	DAS time
1	- 2	Deimos	66.0	0.7726	0.60	2.0	95	01483492
	6		59.5	0.6920	0.66	3.5	180	01504492
	9		57.5	0.6765	0.68	4.5	204	01510512
	12		55.5	0.6624	0.70	2.0	228	01516532
	14		54.3	0.6537	0.70	3.5	243	01520242
	16		53.2	0.6456	0.72	2.0	256	01523532
2	31	Deimos	36.5	0.4228	1.10	6.0	92	01573512
	33		35.5	0.4081	1.14	6.5	104	01576522
	35		34.5	0.3942	1.18	0.7	116	01579532
	41		29.5	0.3398	1.36	1.3	176	01594512
	43		28.3	0.3310	1.40	1.0	190	01598012
	46		26.5	0.3167	1.46	1.5	212	01603542
	52		21.5	0.2802	1.66	2.5	271	01618242
3	53	Deimos	15.5	0.2322	2.00	2.0	325	01632032
	54	Deimos	15.5	0.2302	2.02	2.5	327	01632522
	59	Phobos	14.3	0.1709	5.81	3.0	130	01640292
	60	Phobos	13.1	0.1540	6.52	3.0	186	01643792
	61	Phobos	12.9	0.1523	6.54	2.0	194	01644282
	65	Deimos	12.5	0.1684	2.74	3.0	18	01645542
	71	Deimos	10.3	0.1337	3.46	3.5	43	01652052
	72	Deimos	9.0	0.1120	4.14	5.0	59	01656042

^aPictures on 3 successive days were taken before Mariner 9 was inserted into Mars orbit. Each of the three pre-orbital science sequences (POS-1, POS-2, POS-3) included one tapeload of data.

^bFrame number under which the picture is listed in Volume II. Because of an error, the first 11 frames, including one satellite frame, were omitted from the listing of preinsertion frames. Therefore, the first entry here is given as a negative number.

^cData generated by W. G. Breckenridge by smoothing telemetered spacecraft limit-cycle position data.

Table XII-2. Narrow-angle satellite frames after orbit insertion

Index number	Rev	Frame number	Range, ^a km	Diameter, ^a pixels	Subspacecraft point		Phase angle, ^a deg	Exposure time, ms	Filter	DAS time	Comments
					Latitude ^a	Longitude ^a					
Phobos											
1	31	16	14,530	59	26°S	341°W	76	24	—	02711170	
2	34	05	5,730	150	69°S	157°W	58	24	—	02816240	Partly out of frame
3	34	06	5,720	150	70°S	161°W	59	24	—	02816310	
4	41 ^b	03	7,280	118	43°S	109°W	34	24	—	03067335	
5	43	01	7,390	116	18°S	152°W	66	24	—	03136565	
6	43	03	6,450	133	28°S	176°W	73	24	—	03137335	Partly out of frame
7	48	18	7,160	120	63°S	56°W	49	24	—	03320875	
8	48	19	7,180	120	63°S	53°W	50	24	—	03320945	
9	53	16	11,880	72	33°S	24°W	26	24	—	03501965	
10	57	—	5,990	144	61°S	131°W	52	24	—	03642245	
11	73	03	6,460	133	42°S	135°W	57	48	—	04215685	
12	77	29	8,140	106	30°S	344°W	80	48	—	04365205	
13	80	16	7,000	123	67°S	356°W	81	48	—	04470485 ^b	Partly out of frame
14	80	18	7,160	120	65°S	356°W	83	48	—	04470625	
15	87	05	7,110	121	58°S	77°W	42	24	—	04720805	
16	89	03	5,760	149	47°S	172°W	80	48	—	04790455	
17	117	01	10,170	84	28°S	86°W	55	48	—	05773388	
18	129	06	12,500	69	31°S	17°W	18	24	—	06209278	
19	129	09	12,650	68	28°S	13°W	19	24	—	06209628	
20	131	01	10,400	76	36°S	66°W	45	48	—	06278438	
21	133	01	6,220	128	84°S	41°W	73	48	—	06350468	
22	145	01	15,250	52	21°S	52°W	70	48	—	06781038	
23	150	32	14,500	55	24°N	344°W	64	48	—	06968708	
24	161	01	9,990	79	40°S	21°W	45	6	—	07360358	
25	171	32	13,590	58	43°N	333°W	71	48	—	07725968	
26	207	02	6,940	114	67°S	47°W	63	192	—	09013274	
27	221	01	9,800	90	41°S	23°W	41	48	—	09518254	
28	430	18	10,710	74	62°N	341°W	77	24	—	11801376	
29	444	16	13,040	60	79°N	249°W	65	24	—	12159222	
30	675	9	13,950	56	69°N	241°W	43	24	—	13469623	
31	676	19	17,320	46	33°N	94°W	73	6144	—	13511833	Deliberately overexposed
Deimos											
32	25	01	8,830	52	14°S	20°W	68	24	—	02490320	
33	63	02	7,780	59	12°S	7°W	73	48	—	03854625	
34	73	02	10,070	46	4°S	41°W	22	24	—	04212605	
35	111	01	7,210	64	0	27°W	31	48	—	05553378	
36	121	01	15,310	30	21°S	13°W	44	48	—	05918708	
37	149	01	5,470	85	28°N	355°W	65	48	—	06918168	
38	159 ^b	01	10,050	46	19°S	3°W	51	48	—	07283428	
39	197	01	7,360	63	1°S	335°W	73	192	—	08647664	
40	436	01	8,590	54	46°N	323°W	28	24	—	11994754 ^a	

^aData generated by T. Duxbury (see Ref. XII-4).^bAnother frame taken on Rev 41 (DAS 03067265) shows only a small part of the satellite (see Table XII-3).

Table XII-3. Narrow-angle frames that "missed" the satellite or included no useful detail

Rev	DAS time	Comments	Rev	DAS time	Comments
Phobos					
27	02562560	Contains residual from false shutter	59 ^a	03711125	
33	02782920		77 ^a	04365065	
34	02816100		77 ^a	04365135	
34	02816170		77 ^a	04365275	No MTVS
41	03066215		80 ^a	04470415	
41	03067265	Small part of satellite in view	80 ^a	04470555	
41	03069015		87 ^a	04720595	Noisy
47	03286715		87 ^a	04720665	Noisy
48	03320805		87	04720735	Lost in snowstorm. No MTVS, but residual visible in 04720805
48	03321015	Residual from previous frame (03320945)	89 ^a	04790385	
50	03390595		89 ^a	04790525	Lost in snowstorm. No MTVS
50	03390665		139	06569078	
57 ^a	03642175		161 ^b	07357768	In eclipse
57 ^a	03642315	Residual from previous frame (03642245)	207 ^b	09011734	In eclipse
57 ^a	03642385		221	09518464	
Deimos					
35	02849770	Contains residual from false shutter	63 ^a	03854695	Contains residual from previous frame (03854625)
63 ^a	03852665		63 ^a	03854765	

^aPictures lost because no camera slewing was allowed within fixed picture sequences.

^bPictures obtained with 6.144-s exposures as planned.

orbital sequences. Until Rev 50, many possible satellite frames were missed because only one picture in a picture block (triad or tetrad) could be targeted at the satellite due to onboard computer limitations. Any other narrow-angle pictures in the block inevitably did not include the satellite.

High-resolution frames of Phobos and Deimos, which include major portions of the satellite within the field of view, are listed in Table XII-2. Many enhancements of these satellite pictures were produced at the JPL Image Processing Laboratory (IPL) and at the Stanford University Artificial Intelligence Laboratory (AIL). The best enhancement available was used in Fig. XII-4, where the index numbers correspond directly to the index numbers of Table XII-2; Fig. XII-5

is an enlargement of one of these enhancements (index number 3). Three different versions of a single frame are shown in Fig. XII-6. Frames pointed at a satellite but which did not include it in the field of view, frames lost because of onboard computer limitations, and frames in which the quality of the data returned was poor are listed in Table XII-3. Also listed are two frames taken with 6.144-s exposures when Phobos was in the Penumbra of Mars and when the infrared radiometer was acquiring data for an eclipse cooling curve. Both images show bright stars, but in each frame the satellite can be recognized only as a faint splotch of light.

To characterize the shape and surface features of the satellites, it was desirable to photograph the irregular objects

from as many different "sides" as possible. The variety of achievable views of the satellites was constrained by the:

- (1) Fact that the satellites are in synchronous rotation about Mars (Ref. XII-5), and therefore always present the same face toward the planet.
- (2) Need to take pictures at close range so that the satellite images were at least tens of pixels across.
- (3) Fact that the spacecraft and mission designs were optimized to photograph Mars and not its satellites.

Cartesian plots of the "latitude" and "longitude" at the center of each satellite image (Fig. XII-7a) show the diversity of views achieved. For such irregular objects, these parameters may seem unfamiliar, but they are useful polar coordinate representations of the direction of the spacecraft from the satellite at the time a particular picture was taken. The \vec{X} vector is defined as intersecting the satellite's surface at the equator at 0° longitude; east-west and north-south conventions are the same as those for Mars (see Fig. XII-7b). Information on the size of each satellite image is indicated by the size of the circles denoting the subspacecraft location for each picture.

Coverage of Deimos was limited to a small zone near the central meridian because Deimos frames were acquired only from inside the orbit of Deimos, which is the outer satellite. As the same side of Deimos always faces Mars, observations from Mariner 9, which orbited much closer to Mars than does Deimos, included views of one side only (see Fig. 5-10 of Volume II). Coverage of Phobos was much less restricted, and many opportunities occurred from several orbital locations.

An important variable, listed in Table XII-2 but not shown in Fig. XII-3, is phase angle, which determines how large a part of the illuminated side of the satellite actually appears in the image. It also affects the brightness of the satellite. Thus, camera exposures were determined on the basis of the phase angle of the satellite.¹ Another important variable is the azimuth of the Sun-satellite-spacecraft plane (plane of vision). Because the axis of the Mariner 9 camera was aligned with the Sun direction, the azimuth of the plane of vision was

Table XII-4. Principal axes^a of Phobos and Deimos (from Ref. XII-5)

Satellite	Largest axis, km	Intermediate axis, km	Smallest axis, km	Volume, km ³	Mass, ^b g $\times 10^{18}$
Phobos	13.5 ± 1	10.7 ± 1	9.5 ± 1	5748	17.2
Deimos	7.5^{+3}_{-1}	6.1 ± 1	5.5 ± 1	1054	3.16

^aThe axes are radii, not diameters.

^bA density of 3 g/cm³ has been assumed.

the same in all satellite images, regardless of the location of the satellite with respect to the spacecraft. In all narrow-angle pictures, this plane is aligned with the television scan lines, and the satellite bright limbs appear to the left with the terminators on the right. The projection of the satellite rotation axis in the image plane varies for each of the 40 pictures (Fig. XII-3), but the angle that the axis makes with the television raster has not been computed here. This angle can be determined with data on the pointing geometry given in Volume II and information on the orbital elements of Phobos and Deimos. Determination of the principal axes of the two satellites from the orbital narrow-angle frames are given in Table XII-4.

The wide-angle camera also was used to photograph Phobos and Deimos during orbital operations. Very little detail is apparent in these images, which are all less than 15 pixels in diameter, but they do contain important photometric, polarimetric, and colorimetric information (Ref. XII-6). Pictures and the corresponding photometric data are not reproduced here, but other numerical information on the images appears in Table XII-5. Because the raster of the wide-angle camera is rotated with respect to the camera and the scan platform, the plane of vision in wide-angle images is rotated by 30° .

With the pictures of Phobos and Deimos acquired by Mariner 9, considerable improvements can be made in the ephemerides of the two satellites. A complete catalog of satellite pictures and their enhancements is in preparation (Ref. XII-4). Although a complete revision of the orbital elements based on Mariner 9 data has not yet been published, some of the improvements are reported in Ref. XII-4.

¹T. Thorpe, unpublished data.

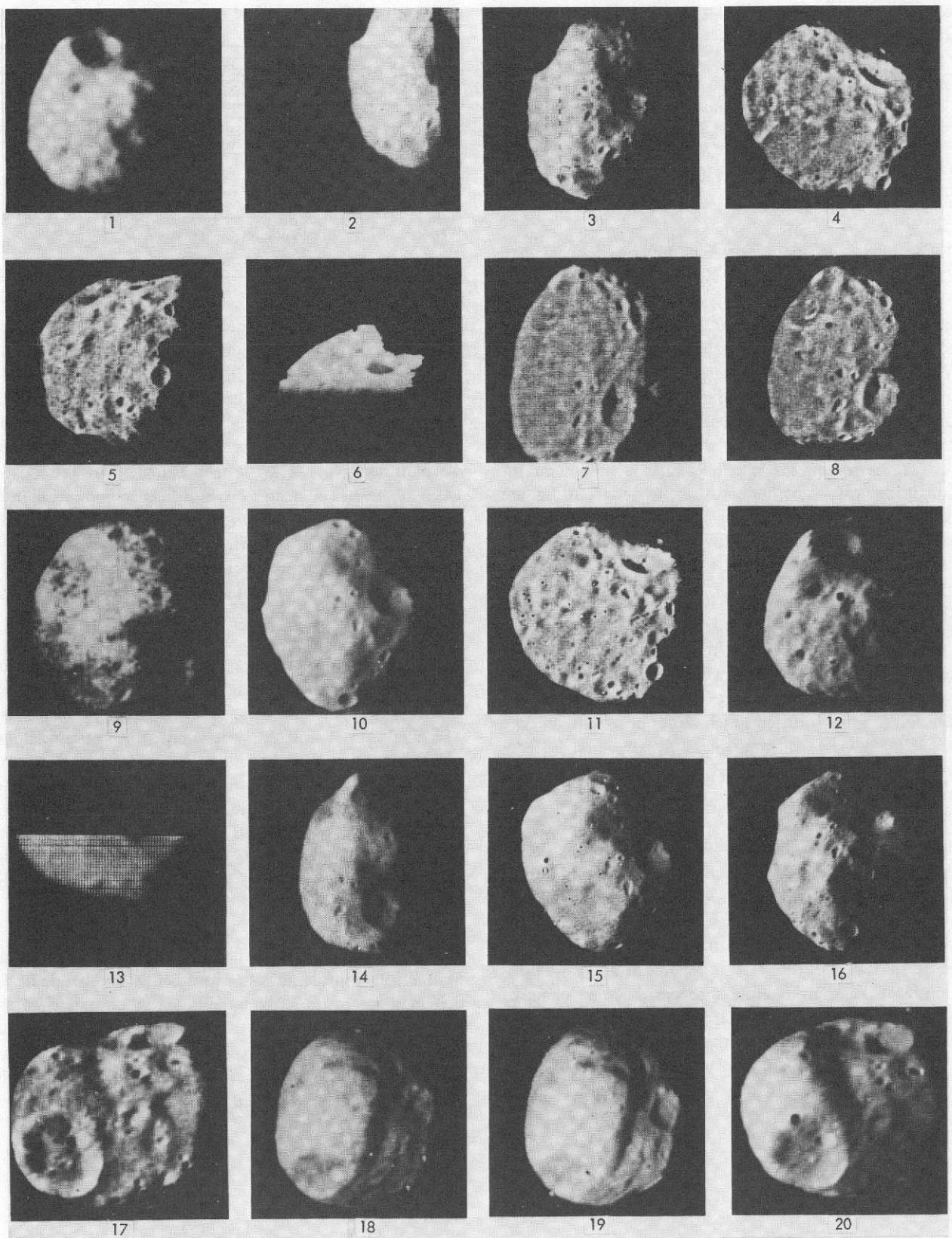


Fig. XII-4. Narrow-angle pictures of the satellites. Phobos: index numbers 1 — 31; Deimos: index numbers 32 — 40.

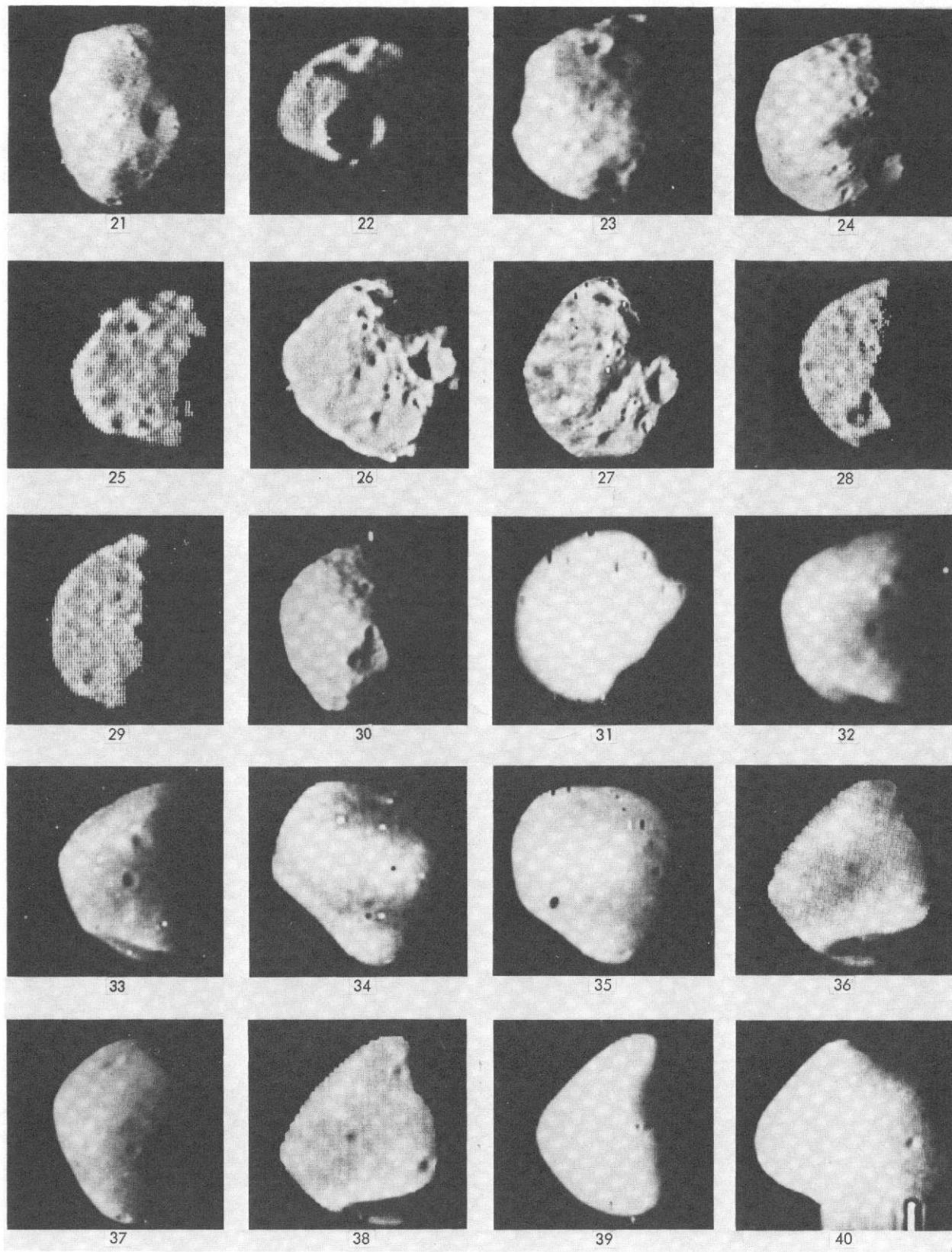


Fig. XII-4. (contd.).

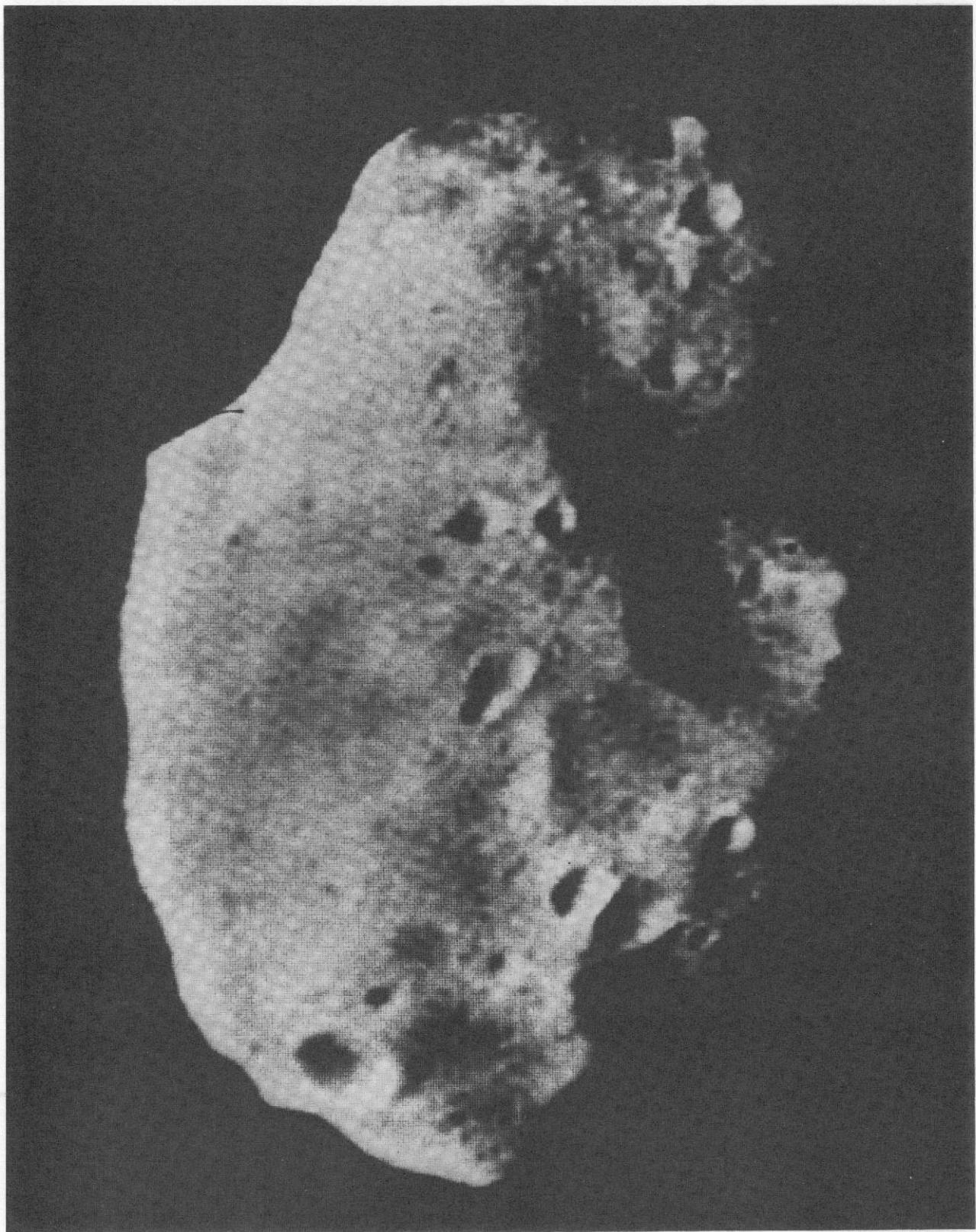


Fig. XII-5. Picture of Phobos obtained on Rev 34. This picture was computer-enhanced at the IPL and is probably the most detailed image of Phobos acquired.

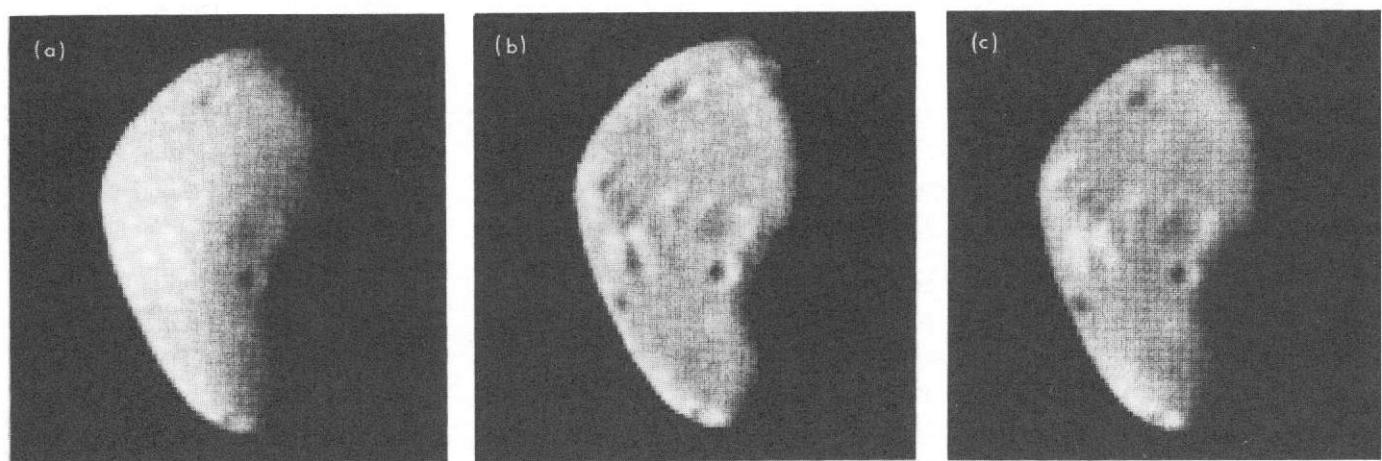


Fig. XII-6. Three versions of picture of Deimos taken during Rev 149 (index number 37 in Fig. XII-4). This picture was computer-enhanced at the AIL. (a) Contrast-stretched. (b) High-pass filtered (using an 11 by 11 pixel filter) to bring out topographic detail; contrast-stretched. (c) High-pass filtered (using a 21 by 21 pixel filter); contrast-stretched.

Table XII-5. Wide-angle satellite frames after orbit insertion

Rev	Frame number	Range, ^a km	Diameter, ^a pixels	Subspacecraft point		Phase angle, ^a deg	Exposure time, ms	Filter	DAS time	Comments
				Latitude ^a	Longitude ^a					
Phobos										
27	02	7,027	12.8	27.0°S	144.3°W	50.9	192	2	02562595	
31	_b	_b	_b	_b	_b	_b	24	_b	02711205	Invisible
33	17	16,027	5.6	23.5°S	358.0°W	50.5	192	2	02782955	Mars limb included
41	14	6,768	13.3	72.2°S	6.1°W	75.7	96	3	03069680	Polarizing filter, 0°
41	15	6,839	13.1	70.9°S	4.3°W	77.0	96	5	03069750	Polarizing filter, 60°
41	16	6,912	13.0	69.6°S	2.9°W	78.4	96	7	03069820	Polarizing filter, 120°
43	02	7,335	12.3	18.2°S	153.2°W	65.8	96	2	03136600	
43	04	6,420	14.0	28.9°S	176.6°W	73.5	192	8	03137370	
53	17	11,880	7.6	33.0°S	23.5°W	26.9	192	2	03502000	
77	24	8,771	10.3	30.7°S	344.3°W	82.3	384	3	04365030	Polarizing filter, 0°
77	26	8,520	10.7	30.4°S	344.3°W	81.4	384	5	04365100	Polarizing filter, 60°
77	28	8,265	10.9	30.1°S	344.3°W	80.5	384	7	04365170	Polarizing filter, 120°
77	30	8,009	11.4	29.6°S	344.3°W	79.6	384	8	04365240	Violet filter
89	02	5,778	15.6	46.5°S	170.7°W	79.6	384	3	04790420	Polarizing filter, 0°
89	04	_b	_b	_b	_b	_b	384	5	04790490	Lost in drop out
129	07	12,593	7.1	29.2°S	14.0°W	18.7	192	5	06209523	
129	08	12,632	7.1	28.7°S	13.1°W	19.2	192	5	06209593	
129	10	12,676	7.1	28.1°S	12.2°W	19.7	192	5	06209663	
139	02	12,532	6.6	28.1°S	346.9°W	86.4	384	5	06568973	
139	03	12,334	6.7	28.2°S	346.6°W	85.1	384	5	06567048	
150	31	14,492	5.7	23.1°N	344.3°W	63.2	384	5	06968673	
171	31	13,568	6.1	42.6°N	333.3°W	70.1	384	5	07725933	
221	02	9,800	8.5	41.0°S	23.0°W	41.0	384	5	09518289	
Deimos										
25	02	8,897	5.4	13.9°S	19.5°W	68.5	192	2	02490355	
35	02	12,393	3.9	13.0°S	25.8°W	36.4	192	2	02849805	Small, in center
63	03	7,823	6.2	12.5°S	7.1°W	73.4	384	3	03854660	Polarizing filter, 0°
63	05	7,909	6.1	12.9°S	6.7°W	73.9	384	5	03854730	Polarizing filter, 60°
63	07	7,997	6.1	13.3°S	6.4°W	74.4	384	7	03854800	Polarizing filter, 120°

^aPreviously unpublished data supplied by T. Duxbury.^bNot available.

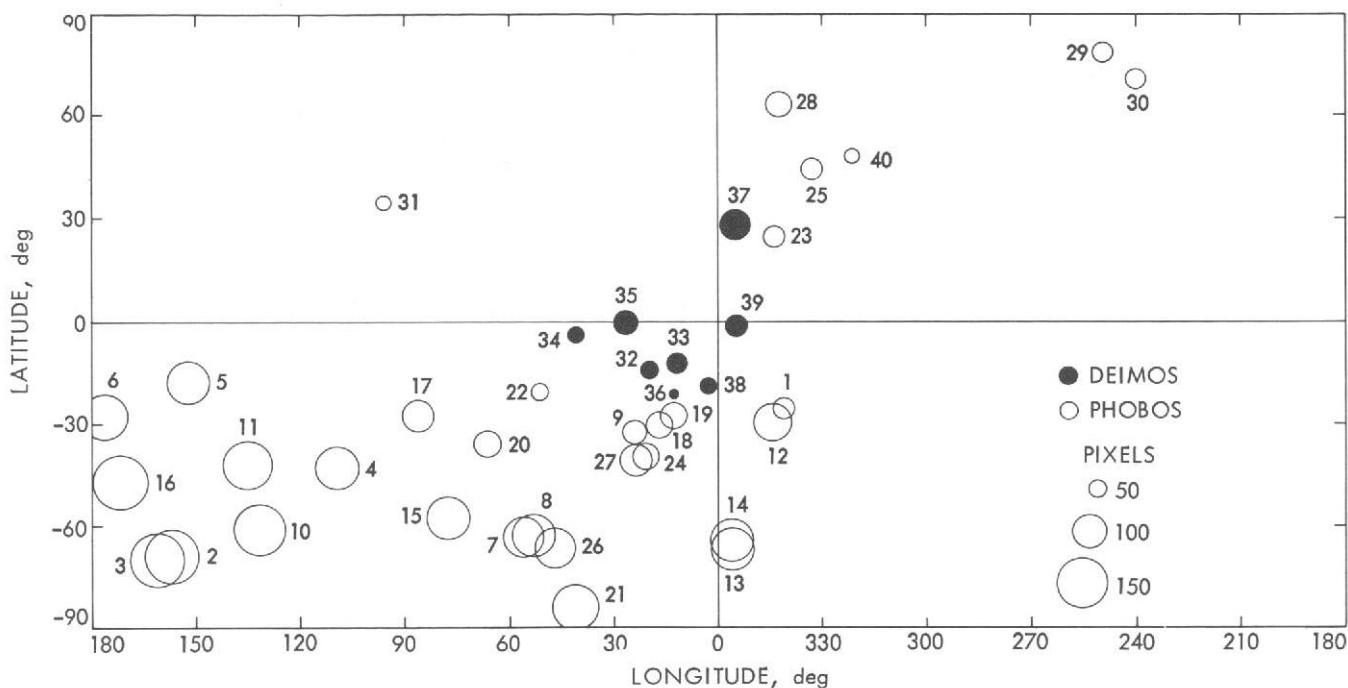
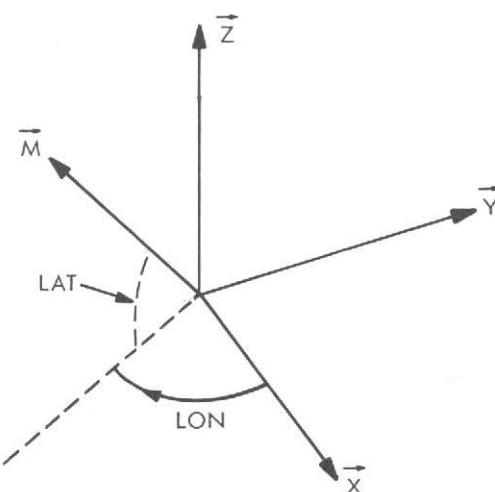


Fig. XII-7a. Cartesian plot of subsatellite locations. The size of the location circle is proportional to the image size in pixels. The index numbers correspond to those in Fig. XII-4 and in Table XII-2.



- \vec{X} VECTOR DIRECTED FROM CENTER OF SATELLITE TOWARD THE CENTER OF MARS
- \vec{Z} VECTOR PERPENDICULAR TO THE SATELLITE'S ORBIT
- \vec{Y} VECTOR IN THE PLANE OF THE SATELLITE'S ORBIT DIRECTED OPPOSITE TO MOTION OF THE SATELLITE
- \vec{M} VECTOR DIRECTED FROM CENTER OF SATELLITE TOWARD MARINER 9
- LAT, LON SOLAR COORDINATE REPRESENTATIONS OF THE DIRECTION OF THE SPACECRAFT FROM THE SATELLITE AT THE TIME A PARTICULAR PICTURE WAS TAKEN

Fig. XII-7b. Satellite geometry.

References

- XII-1. Duxbury, T.C., Born, G.H., and Jerath, N., *Viewing Phobos and Deimos for Navigating Mariner 9*, AIAA Paper No. 72-927, presented at AIAA/AAS Conference, Palo Alto, Calif., September 1972.
- XII-2. Duxbury, T.C., and Acton, C.H., *On-Board Optical Navigation Data from Mariner '71*, Institute of Navigation, National Space Meeting, March 1972.
- XII-3. Pollack, J.B., Veverka, J., Noland, M., Sagan, C., Duxbury, T.C., Acton, C.H., Born, G.H., Hartmann, W.K., and Smith, B.A., "Mariner 9 Television Observations of Phobos and Deimos, 2," *J. Geophys. Res.*, Vol. 78, p. 4313, 1973.
- XII-4. Veverka, J., Pollack, J.B., Noland, M., Green, W.B., Duxbury, T.C., Quam, L., Sugar, C., and Tucker, R., "Mariner 9 High-Resolution Photographs of Phobos and Deimos," *Icarus* (to be published).
- XII-5. Pollack, J.B., Veverka, J., Noland, M., Sagan, C., Hartmann, W.K., Duxbury, T.C., Born, G.H., Milton, D.J., and Smith, B.A., "Mariner 9 Television Observations of Phobos and Deimos," *Icarus*, Vol. 17, p. 394, 1972.
- XII-6. Noland, M., and Veverka, J., "Mariner 9 Polarimetry of Phobos and Deimos," *Icarus* (in press).

Appendix A

Martian Nomenclature

Figure A-1 is an albedo map in Mercator Projection, prepared from Earth-based observations, which shows the Martian planetary names in use during the planning stages of the Mariner Mars 1971 Project and during the Mariner 9 mission to Mars. The terminology shown on the map was derived from classical names first assigned to Schiaparelli (Ref. A-1); the nomenclature of the polar regions (see Fig. A-2) was derived from Antoniadi (Ref. A-2). This nomenclature was used in all previous Mariner 9 documents, including Volume II of this Technical Memorandum.

Five craters, named after the 1964 Mariner 4 flight to Mars, were approved in 1967 by the International Astronomical Union (IAU), the official body responsible for the nomenclature of all features on the Moon and planets. At the end of the Mariner 9 mission, the IAU Working Group on Martian Nomenclature submitted a list of proposed designations for craters and other Martian topographic features to other pertinent Committees of the IAU. All of the names proposed were accepted in August 1973; however, at this writing, some amendments to these accepted designations are being considered, and the decisions reached may result in minor changes in some of these new names.

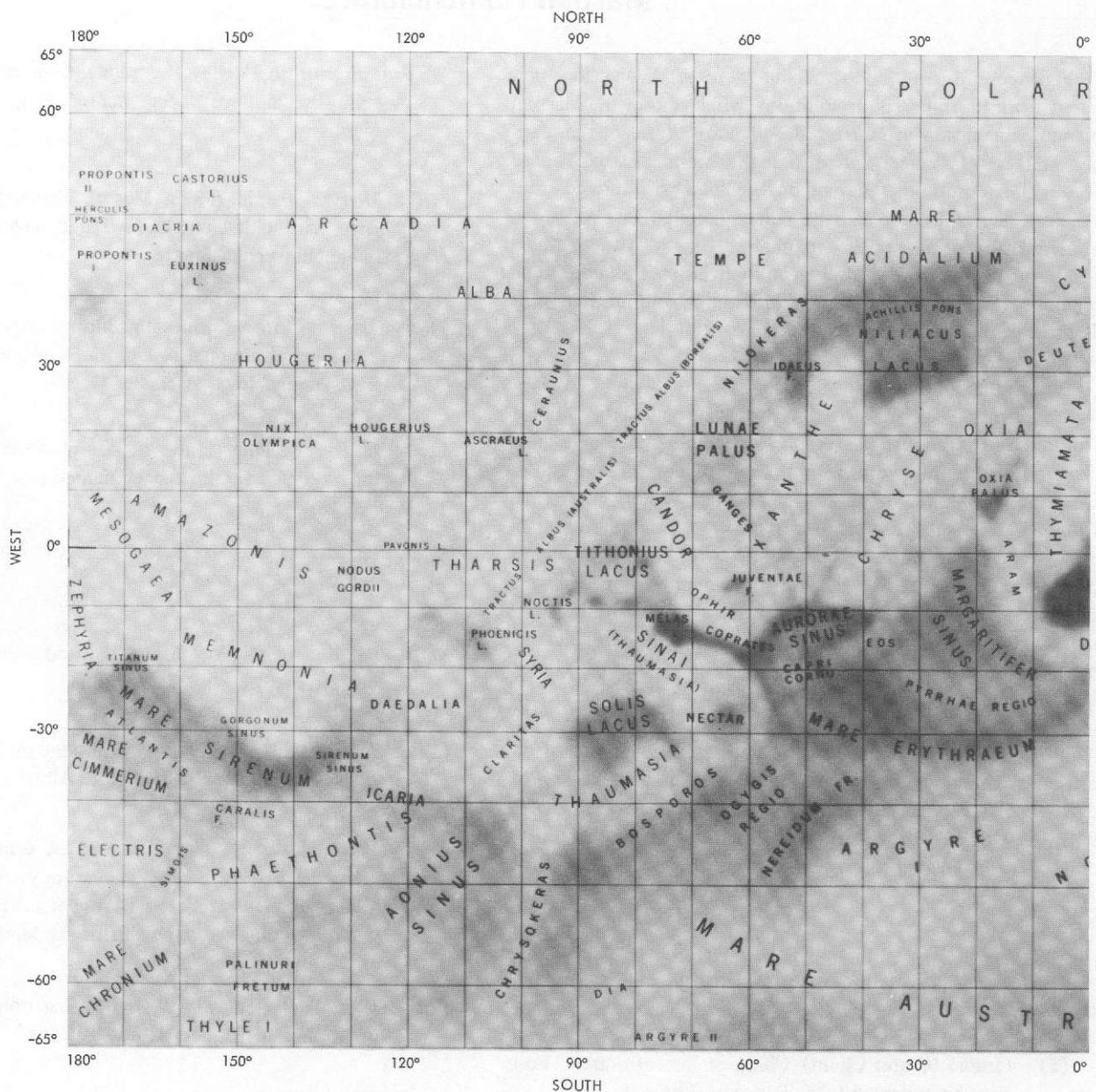
Most of the crater names submitted were in honor of deceased astronomers; some were after telescope builders, geologists, rocket pioneers, biologists, writers, and others associated with the study of the red planet. Some of the most prominent craters are listed in Table A-1 and are shown in Figs. A-3 and A-4.

Thirteen classes of non-craterform features have also been designated:

- (1) *Catena* (Crater Chain). Chain or line of craters. Four have been named (e.g., Tithonus Catena).
- (2) *Chasma* (Canyon). An elongated, steep-sided depression. Twelve have been named (e.g., Coprates Chasma).
- (3) *Dorsum, Dorsa* (Ridge, Ridges). Irregular, elongate prominence. One has been named (Argyre Dorsum).
- (4) *Fossa, Fossae* (Ditch, Ditches). Long, narrow, shallow depressions, generally occurring in groups, that are straight or curved. Thirteen have been named (e.g., Claritas Fossae).

- (5) *Labyrinthus* (Valley Complex). Complex intersecting valleys. One has been named (e.g., Labyrinthus Noctis).
- (6) *Mensa, Mensae* (Mesa, Mesas). Flat-topped prominence with cliff-like edges. Three have been named (e.g., Nilosyrtis Mensae).
- (7) *Mons, Montes* (Mountain, Mountains). Large topographic prominence or chain of elevations. Ten have been named (e.g., Ascraeus Mons).
- (8) *Patera*. Irregular crater or complex crater with scalloped edges. Ten have been named (e.g., Alba Patera).
- (9) *Planitia* (Plain). Smooth low area. Nine have been named (e.g., Hellas Planitia).
- (10) *Planum* (Plateau). Smooth elevated area. Three have been named (e.g., Solis Planum).
- (11) *Tholus* (Hill). Isolated domical small mountain or hill. Thirteen have been named (e.g., Albor Tholus).
- (12) *Vallis, Valles* (Valley, Valleys). A sinuous channel; many have tributaries. Valleys are named "Mars" in many languages. Eleven have been named (e.g., Al Quahira Vallis, the Arabic name for Mars).
- (13) *Vastitas* (Extensive plain). The vast northern circum-polar plain is named Vastitas Borealis.

The feature name generally consists of two parts. For features in 12 of the 13 classes, it is comprised of the name of a nearby classical feature, taken from Schiaparelli (see Ref. A-1) or Antoniadi (see Ref. A-2), followed by the feature class (e.g., Olympus Mons). For one class of feature, Vallis or Valles (Valley or Valleys), the name consists of the class designation following the word for Mars in various languages (e.g., Ares Vallis). One valley, Valles Marineris, was so termed in honor of the Mariner 9 mission. All of the feature names accepted to date are listed in Table A-2; a representative sampling of each is also presented in Figs. A-3 and A-4.



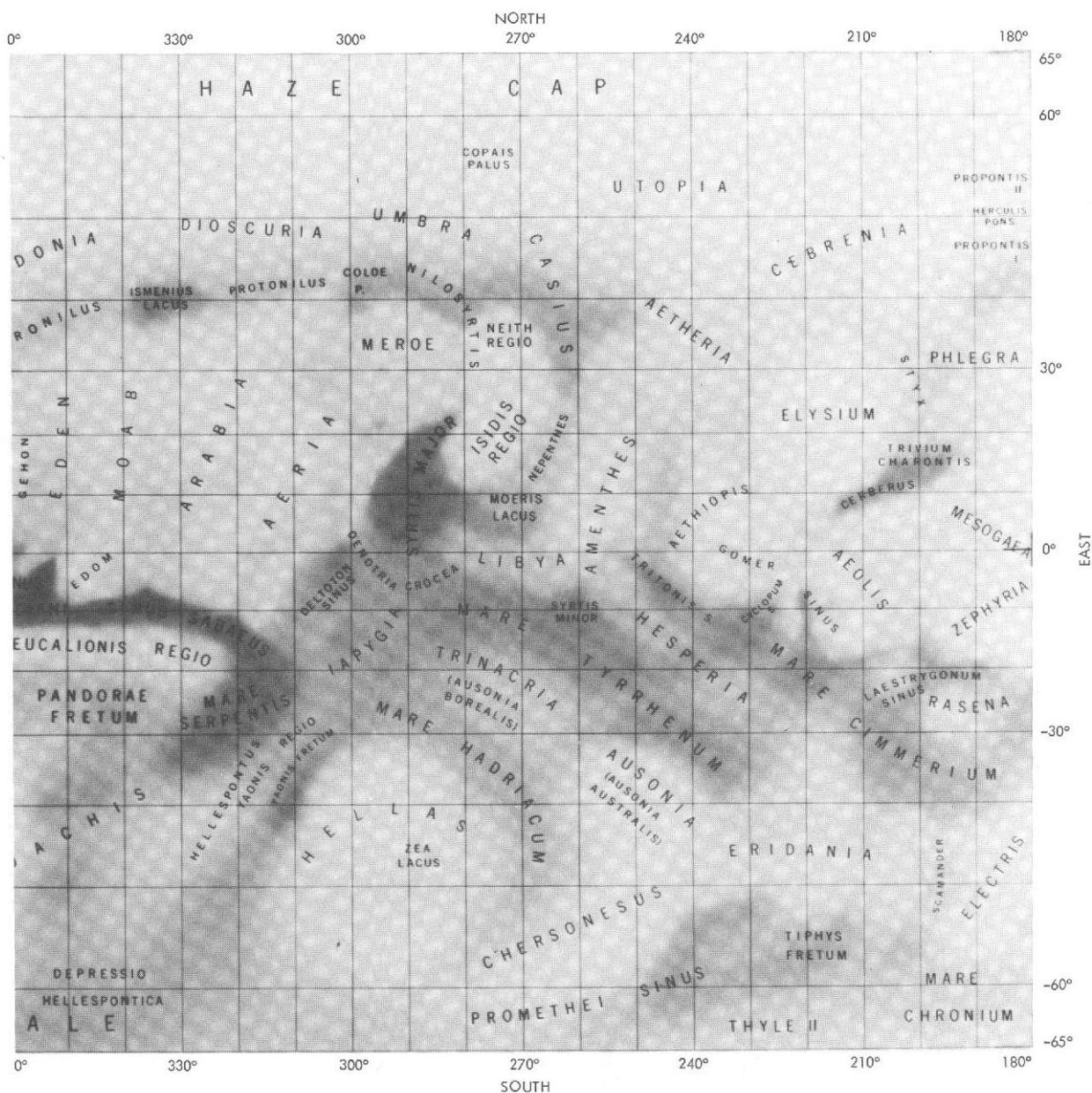


Fig. A-1. Albedo map of Mars from Earth-based observations showing the nomenclature used during the Mariner 9 mission. This map represents the large-scale albedo (bright and dark) patterns at the surface of Mars near its perihelic opposition in August 1971 and is based on visual and photographic observations using the 155-cm reflector at the Catalina Station of the Lunar and Planetary Laboratory of the University of Arizona (see Refs. A-3 through A-6). The map was prepared by J. Roth and K. Walker under the direction of Dr. G. de Vaucouleurs, Department of Astronomy, The University of Texas at Austin.

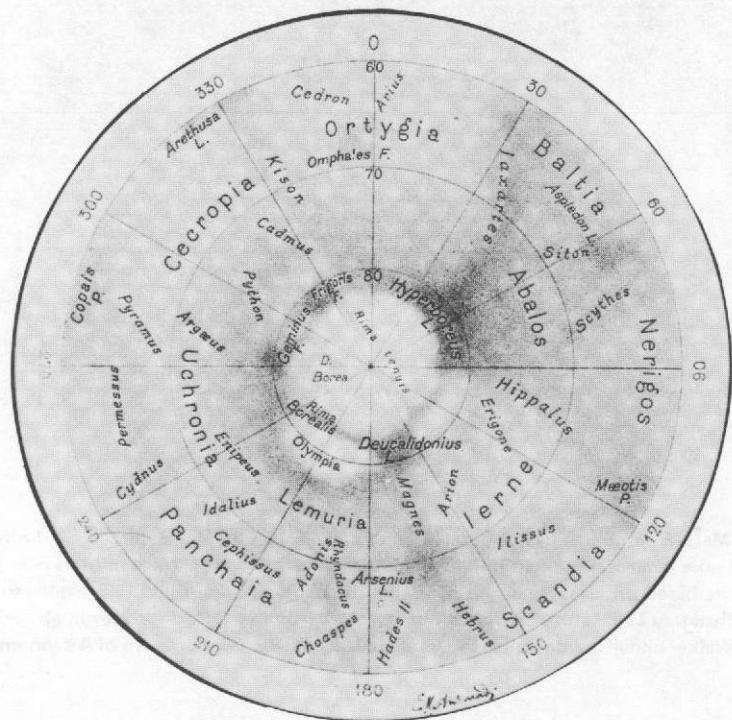
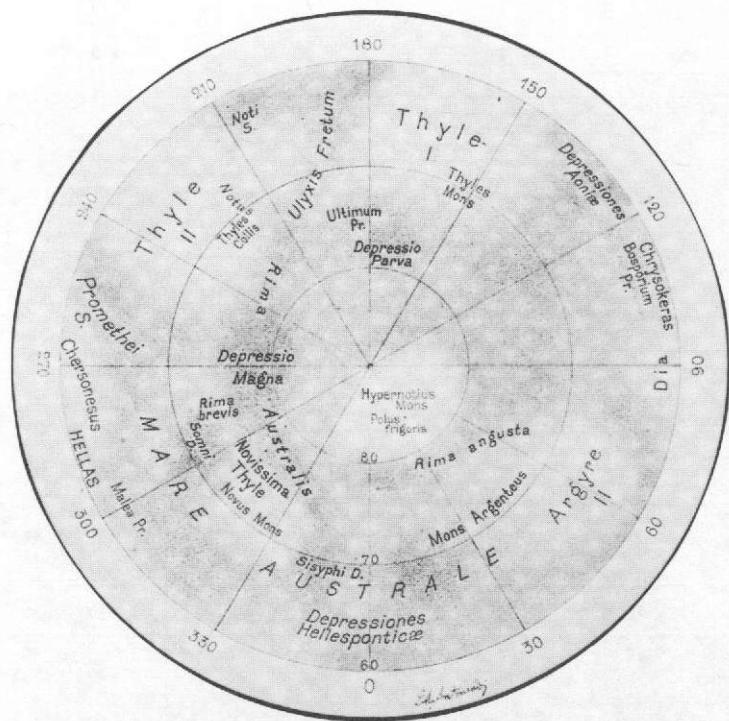


Fig. A-2. Nomenclature in the polar regions of Mars (from Antoniadi, Ref. A-2).

Table A-1. New names of craters shown in Figs. A-3 and A-4

Name	Latitude	Longitude	Name	Latitude	Longitude
Antoniadi	21°N	299°W	Lowell	52°S	81°W
Barnard	61°S	298°W	Lyot	50°N	331°W
Becquerel	22°N	8°W	Mie	48°N	221°W
Cassini	23°N	327°W	Milankovic	55°N	147°W
Copernicus	49°S	169°W	Mitchel	68°S	284°W
Darwin	57°S	20°W	Newton	40°S	158°W
Flaugergues	17°S	340°W	Proctor	48°S	331°W
Galle	51°S	31°W	Rutherford	19°N	11°W
Green	52°S	9°W	Schiaparelli	3°S	342°W
Holmes	76°S	294°W	Schmidt	72°S	79°W
Huygens	14°S	304°W	Secchi	58°S	259°W
Kaiser	46°S	340°W	South	77°S	339°W
Kepler	47°S	219°W	Stokes	56°N	188°W
Kunowskij	57°N	9°W	Stoney	69°S	140°W
Lomonosov	65°N	8°W	Trouvelot	16°N	13°W

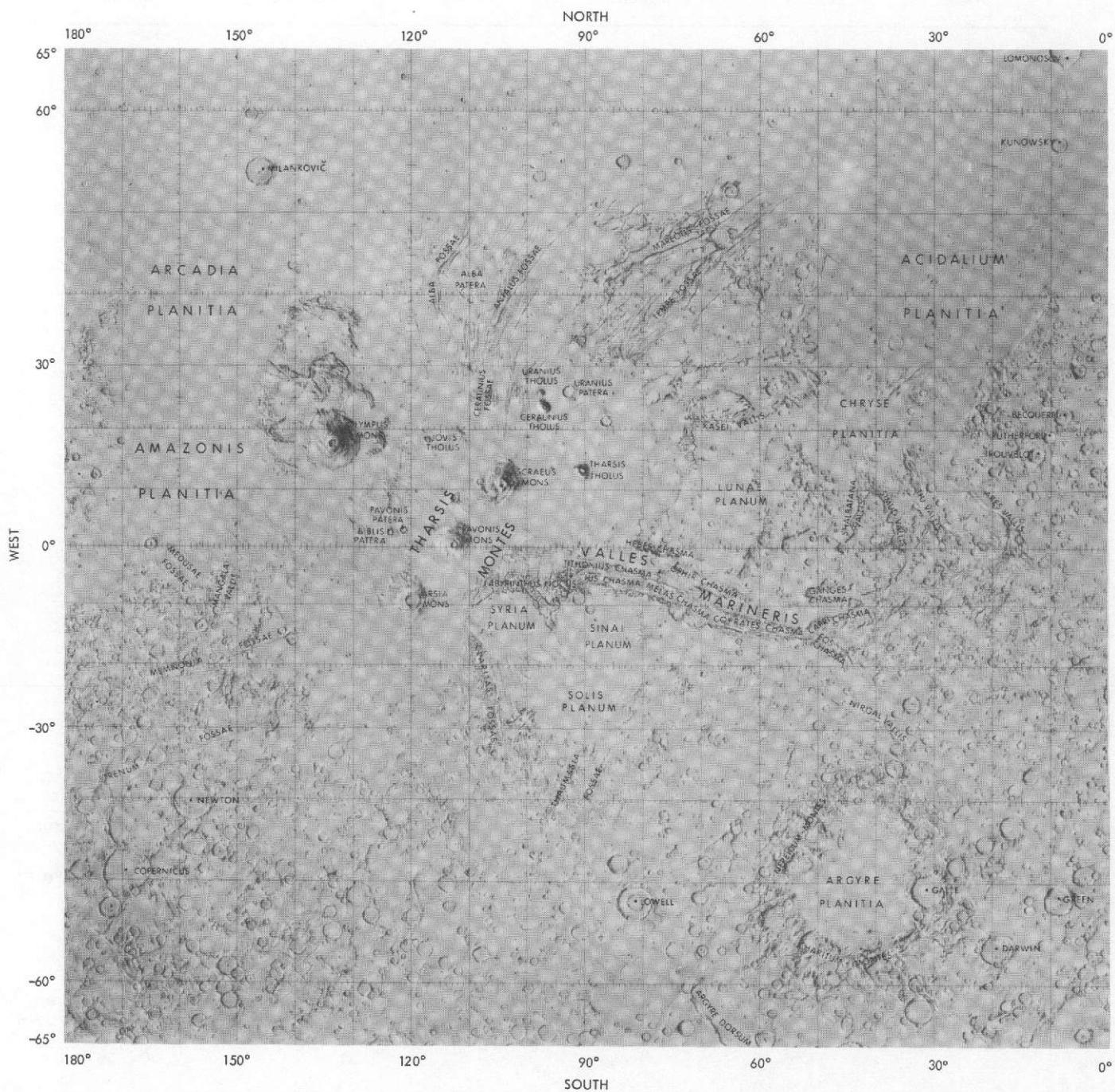
The names of four well known areas on the albedo map have been retained, as they contain no distinctive topographic features. These areas are:

Cerberus: 10°N, 208°W

Margaritifer Sinus: 10°N, 23°W

Sinus Meridiani: 5°S, 358°W

Sinus Sabaeus: 10°S, 330°W



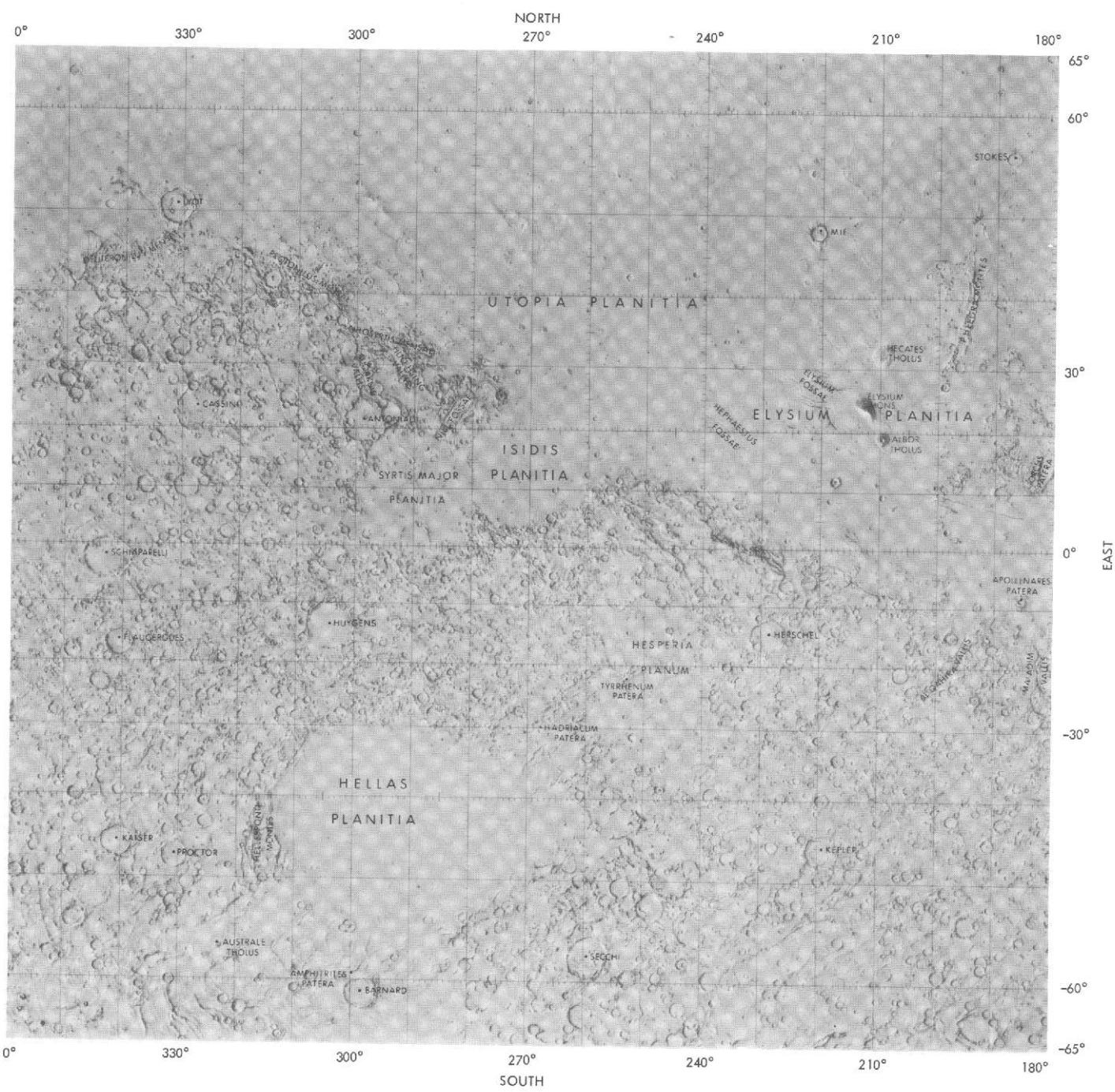
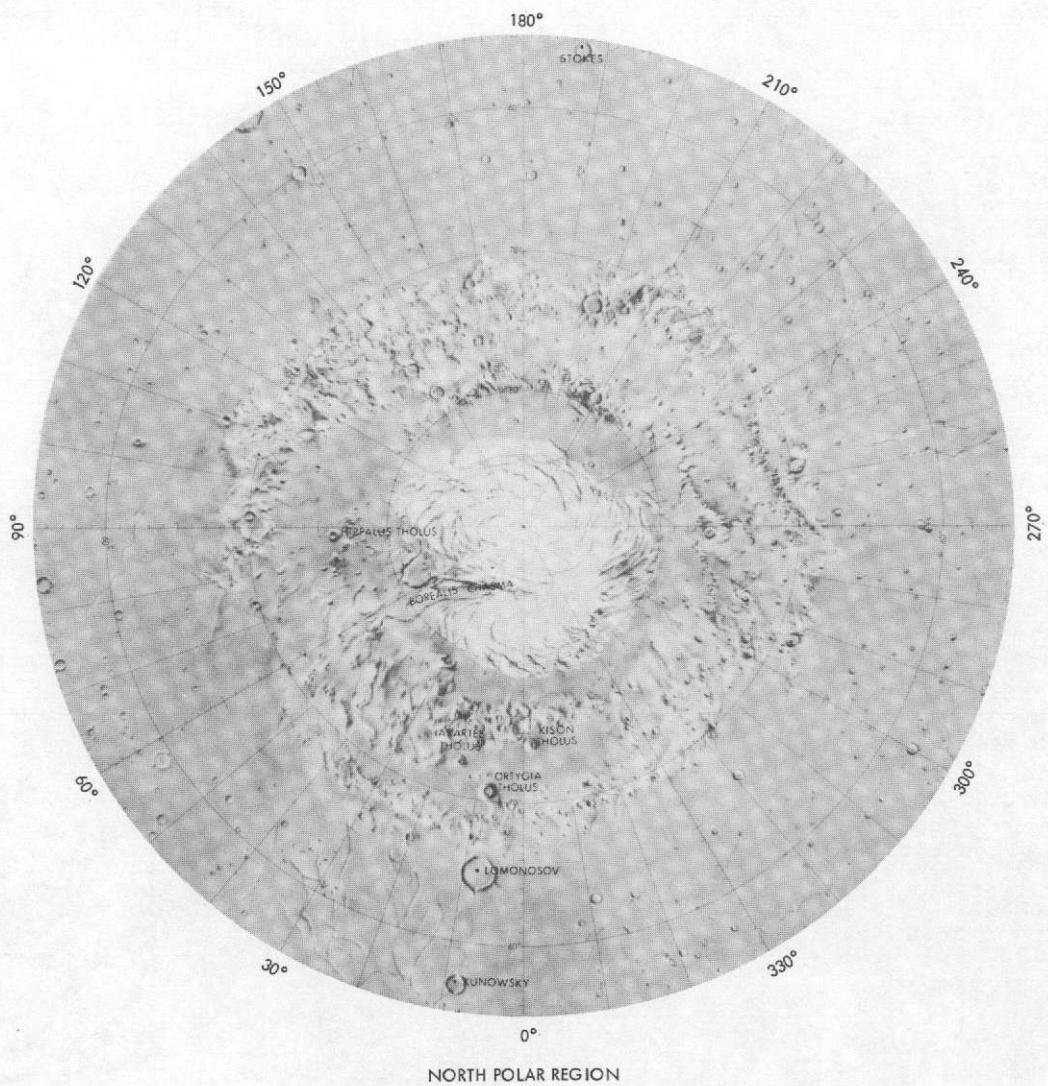


Fig. A-3. New nomenclature of prominent craters and some physiographic features shown in Mercator Projection on a shaded relief map of Mars. The basic map was prepared at the U. S. Geological Survey, Center of Astrogeology, Flagstaff, Arizona, under the direction of R. Batson. The names, derived from the most current IAU list, were added at the Jet Propulsion Laboratory, Pasadena, California.



Map showing the North Polar Region of Mars, centered on the pole. The map displays various geological features and labels several prominent tholi. The labels include: STOKES (at approximately 180°), TIPALUS THOLUS (near the top center), BOREALIS THOLUS (near the center), VENERIS THOLUS (near the bottom center), KISON THOLUS (near the bottom right), ORYCHA THOLUS (near the bottom center), LOMONOSOV (near the bottom center), and JUNOWSKY (near the bottom left). The map is gridded with latitude and longitude lines, ranging from 0° to 360°. The grid lines are labeled at 0°, 30°, 60°, 90°, 120°, 150°, 180°, 210°, 240°, 270°, and 300°.

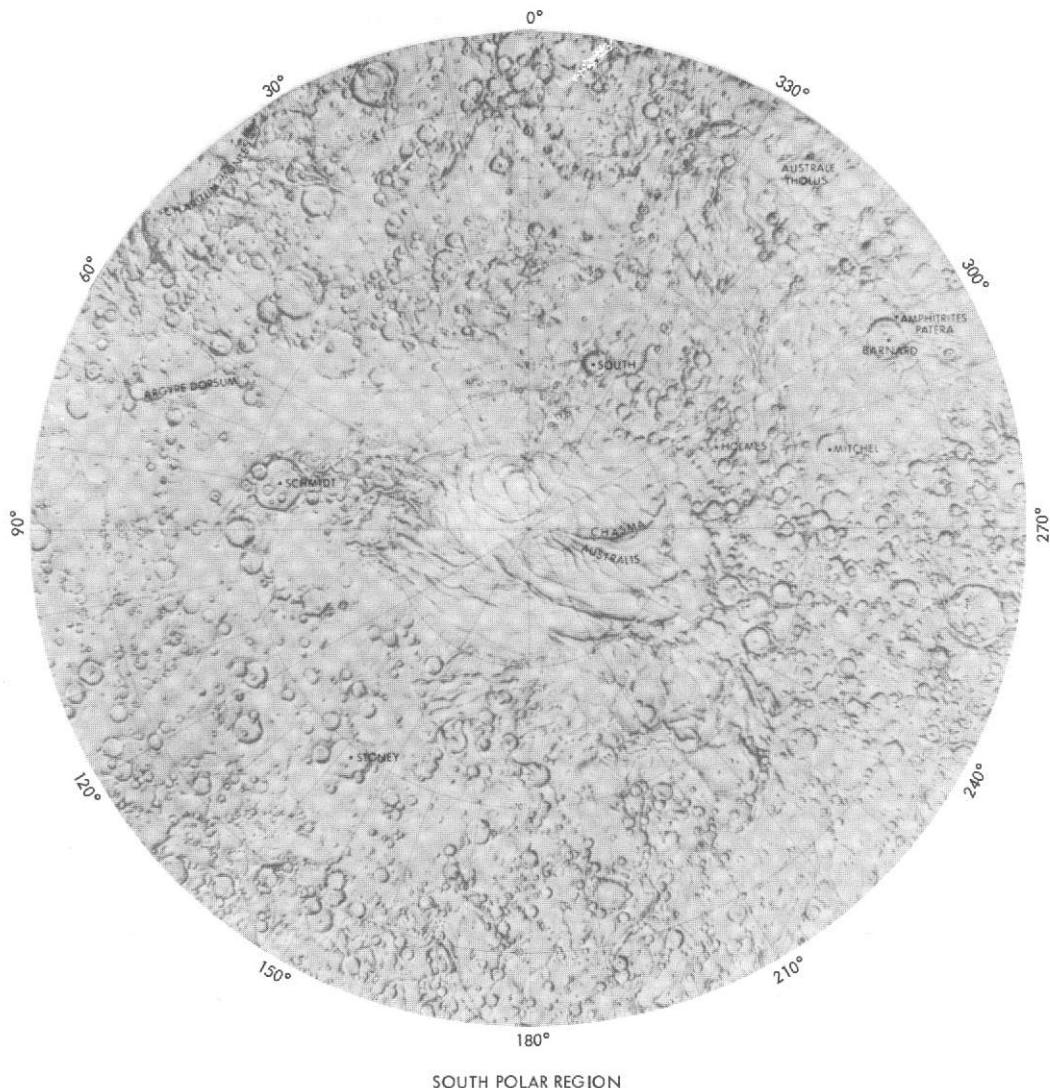


Fig. A-4. New nomenclature of prominent craters and some physiographic features in the Martian polar regions. The basic shaded relief maps were prepared at the U. S. Geological Survey, Center of Astrogeology, Flagstaff, Arizona, under the direction of R. Batson. The names, derived from the most current IAU list, were added at the Jet Propulsion Laboratory, Pasadena, California.

Table A-2. New names of non-craterform features

Name	Latitude	Longitude	Name	Latitude	Longitude
CATENA					
Coprates	15°S	56° to 66°W	Noctis	5° to 8°S	92° to 110°W
Ganges	2° to 3°S	67° to 71°W	MENSAE		
Tithonius	6°S	80° to 98°W	Deuteronilus	42° to 45°N	340° to 346°W
CHASMA					
Australis	80° to 88°S	270°W	Nilosyrtis	32°N	290°W
Borealis	85°N	30° to 65°W	Protonilus	38°N	315°W
Candor	4° to 6°S	73° to 78°W	MONS		
Capri	3° to 14°S	32° to 50°W	Arsia	11°S	119°W
Coprates	11° to 14°S	54° to 68°W	Ascreaus	11°N	104°W
Eos	16° to 17°N	32° to 51°W	Elysium	24°N	212°W
Ganges	8°S	48° to 51°W	Olympus	17°N	133°W
Hebes	1°N to 1°S	73° to 81°W	Pavonis	1°N	113°W
Ius	7°S	80° to 98°W	MONTES		
Juventae	4°S	61°W	Charitum	57°S	32° to 50°W
Melas	8° to 12°S	70°W to 78°W	Hellesponti	45° to 48°S	315°W
Ophir	3° to 9°S	64° to 77°W	Nereidum	38° to 48°S	43° to 57°W
Tithonius	4°S	80° to 90°W	Phlegra	31° to 46°S	195°W
DORSUM					
Argyre	61° to 65°S	70°W	Tharsis	12°S to 16°N	101° to 125°W
FOSSA, FOSSAE					
Alba	38° to 49°N	107° to 117°W	PATERA		
Ceraunius	25°N	107°W	Alba	40°N	110°W
Claritas	19° to 32°S	105° to 108°W	Aphetrides	59°S	299°W
Elysium	26° to 28°N	219° to 225°W	Apollinares	8°S	185°W
Hephaestus	18° to 22°N	233° to 240°W	Biblis	3°N	124°W
Mareotis	41° to 48°N	69° to 85°W	Hadriacum	31°S	267°W
Medusae	8°S	162°W	Orcus	14°N	181°W
Memnonia	15° to 22°S	140° to 158°W	Pavonis	3°N	121°W
Nili	20° to 26°N	279° to 284°W	Tyrrhenum	23°S	253°W
Sirenum	27° to 36°S	138° to 163°W	Uranius	26°N	93°W
Tantalus	34° to 47°N	99° to 105°W	PLANITIA		
Tempe	35° to 46°N	62° to 80°W	Acidalium	48°N	30°W
Thaumasia	36° to 40°S	80° to 100°W	Arcadia	48°N	155°W
			Amazonis	13°N	160°W
			Argyre	49°S	43°W
			Chryse	17°N	45°W
			Elysium	15°N	210°W

Table A-2. (contd)

Name	Latitude	Longitude	Name	Latitude	Longitude
Hellas	45°S	290°W	Kison	74°N	358°W
Isidis	15°N	270°W	Ortygia	71°N	8°W
Syrtis	15°N	290°W	Tharsis	13°N	91°W
Utopia	35°N	235°W	Uranius	27°N	98°W
PLANUM			VALLIS		
Aurorae	10° to 11°S	48° to 52°W	Al Qahira	15° to 23°S	194° to 202°W
Hesperia	10° to 30°S	240° to 260°W	Area	2° to 10°N	15° to 23°W
Lunae	5° to 20°N	60° to 70°W	Auquahu	28°N	298°W
Ophir	9° to 12°S	55° to 61°S	Huo Hsing	28° to 32°N	292° to 295°W
Solis	20° to 30°S	88° to 98°W	Maadim	20° to 27°S	183°W
Syria	10° to 18°S	105° to 110°W	Mangala	4° to 10°S	151°W
Sinai	10° to 20°S	70° to 90°W	Nirgal	27° to 32°S	36° to 44°W
Tithonus	13°S	84°W	Kasei	21°S	56° to 70°W
THOLUS			Shalbatana	1° to 15°N	45°W
Albor	19°N	210°W	Simud	0° to 14°N	37° to 40°W
Ceraunius	24°N	97°W	Tiu	10° to 18°N	32°W
Hecates	32°N	210°W	Valles Marineris (Mariner Valley)	5° to 15°S	45° to 95°W
Australe	57°S	323°W	VASTITAS		
Hippalus	76°N	89°W	Borealis	55° to 67°N	Continuous
Iaxartes	72°N	15°W			
Jovis	18°N	117°W			

References

- A-1. Schiaparelli, G. V., *II Planeta Marte*, Milano, 1893.
- A-2. Antoniadi, E. M., *La Planete Mars*, Paris, Hermann, 1930.
- A-3. de Vaucouleurs, G., "Telescopic Observations of Mars in 1971," *Sky and Telescope*, Vol. 42, p. 134, 1971.
- A-4. Larson, S. M., and Minton, R. B., "Some High Resolution Photographs of Mars," *Sky and Telescope*, Vol. 42, p. 260, 1971.
- A-5. de Vaucouleurs, G., "Telescopic Observations of Mars in 1971-II," *Sky and Telescope*, Vol. 42, p. 263, 1971.
- A-6. de Vaucouleurs, G., "Telescopic Observations of Mars in 1971-III," *Sky and Telescope*, Vol. 43, p. 20, 1972.

Appendix B

Mars Data

The equatorial diameter of Mars is about 6787 km (4218 mi) as opposed to 12,756 km (7926 mi) for Earth. The Martian polar diameter is 35 km (21.70 mi) less than its average equatorial diameter.

Other pertinent Mars data are:

Mars distance from the Sun

Maximum (aphelion): 249,226,000 km
(154,862,000 mi)

Minimum (perihelion): 206,656,800 km
(128,410,000 mi)

Mars distance from Earth

Maximum: 398,900,000 km
(247,900,000 mi)

Minimum: 55,810,000 km
(34,680,000 mi)

Martian day (mean solar day): 24^h39^m35^s

(Earth mean solar day): 24^h

Martian year: 670 days
(687 Earth days)

Inclination of equator to Mars orbit (spin-axis tilt): 25.2°

Inclination of Mars orbit to ecliptic: 1.85°

Martian surface atmospheric pressure

Maximum: 10 mb

Minimum (top of Pavonis Mons volcano): 1 mb

Average (approximate): 5 mb

(Earth mean surface pressure): 1013 mb

Martian mean surface gravity: 38% that of Earth

Appendix C

Technical Terms and Acronyms

ADAPTIVE MODE Design feature of the Mariner 9 mission that permitted significant and timely changes in overall mission strategy and in the structure of data-acquisition sequences in response to changing scientific and engineering needs.

AEC Automatic exposure control. Optional method of controlling camera exposure. Method utilized the response to a given exposure of the wide-angle camera to control the shutter speed for subsequent exposures of both the narrow- and wide-angle cameras.

AIL Artificial Intelligence Laboratory of Stanford University, California. Computer facility used for image differencing and special enhancements of picture data.

ALBEDO As most commonly used, the term refers to the ratio of the light reflected from a planetary feature to the total amount of light incident upon it. Low albedo features appear darker than higher albedo features.

APHELION Point of a heliocentric elliptical orbit where the comet, planet, or spacecraft is farthest from the Sun.

APOAPSIS Point of an orbit where the spacecraft is farthest from the central body.

AREOCENTRIC Relative to the center of Mars.

AUTO-CS Automatic center scan. Type of contrast enhancement applied in vertical automatic-gain control and high-pass filtered versions of real-time pictures. Implemented by scanning a histogram of the imaging data outward from the center or peak of the histogram.

AUTO-ES Automatic external scan. Type of contrast enhancement implemented by scanning a histogram of shading-corrected versions of real-time pictures from two points external to the peak of the histogram.

BER Bit-error rate. Fraction of the bits of data containing erroneous scientific and engineering information (see BIT).

BIT Contraction of "binary digit," the smallest unit of information in a binary number system. A bit can have only two values, usually denoted as 0 and 1.

BIT RATE Speed at which bits are transmitted. Those used for transmitting science data from Mariner 9 ranged from 1012 to 16,200 bps. During zenith passes early in the mission, data could be successfully received at rates as high as 16,200 bps at the Goldstone tracking station. Instructions for the spacecraft's central computer and sequencer were transmitted from Earth at 1 bps.

BLOCK A simple set of spacecraft commands yielding a simple predetermined amount of data.

CC&S Central computer and sequencer. Electronic subsystem on the spacecraft which stored and sequenced the commands used for control of various spacecraft functions.

CONE ANGLE Angle between the pointing direction of the boresighted instruments on the scan platform and the direction of the Sun. Limited range available because of mechanical constraints (see Fig. II-13 of this volume and Fig. 5-3 of Volume II).

CONTOURED PICTURE VERSION Real-time picture version in which brightness levels were contoured. Produced only during pre-orbital science operations.

CLOCK ANGLE Angle measured about an axis aligned with the spacecraft and the Sun between the pointing direction of the boresighted scan-platform instruments and the direction of the star Canopus. Limited range available because of mechanical constraints, but this restriction was alleviated by using stars other than Canopus for stabilization (see Fig. II-13 of this volume and Fig. 5-3 of Volume II).

CYCLE Period of 39 spacecraft revolutions of Mars or 19½ days required for Mariner 9 to retrace the same ground track.

DAS Data automation subsystem. Electronic subsystem that performed the timing and sequencing functions related to the acquisition and formatting of data from the television cameras and other science instruments.

DAS TIME Counter, incrementing in units of 1.2 s, which served as a fundamental time reference for science data acquired by Mariner 9 (see Section III).

DECALIBRATION Process of removing photometric and geometric distortions from television data using camera calibration information and creating a matrix of pixels called the Reduced Data Record.

DN Data number. Numerical value of the science or engineering sensor formatted by the data automation subsystem. Specifically, the numerical value of a pixel in either the Reduced Data Record or the Experiment Data Record.

DROPOUT Missing line in a television picture attributed to the loss of line synchronization because of errors in the synchronization code.

DYAD Pair of television pictures deliberately taken as a group close together in time and generally providing overlapping, nesting, or contiguous coverage.

EAS Experimenter analysis support. Data prepared at the Image Processing Laboratory for the Mariner 9 television experimenters on special request.

EDR Experiment Data Record. Magnetic tape record containing the numerical values of pixels (DN) on a 9-bit (0 to 511) scale for the 832-sample by 700-line matrix transmitted from the Mariner 9 cameras. Preliminary EDR or PTV tapes contain a preliminary version of these data which has not benefited from data error corrections.

EXTENDED MISSION Portion of the Mariner 9 mission that began on Rev 218 and ended with the termination of operations on Rev 676 (see STANDARD MISSION).

FIXED-FEATURE INVESTIGATION Mariner 9 study in orbit in which the topographic features were viewed with greater resolution than from Earth telescopes and more completely than from earlier spacecraft (see VARIABLE-FEATURE INVESTIGATION).

FLAT FIELD Scene of uniform spatial intensity used in calibration of sensitivity variations across the fields of view of the television cameras.

GEOMETRIC DISTORTION Functional relationship between the geometry of an image and an object.

HGA High-gain antenna. A two-position parabolic antenna used to transmit science data to the tracking stations on Earth.

HGAM High-gain antenna maneuver. Non-propulsive (usually roll only) maneuver designed to aim the high-gain antenna directly at Earth. Maneuver involved temporarily using gyros for inertial stabilization rather than the celestial references.

HISTOGRAM When used on a processed Mariner 9 picture, the histogram is the graphical representation of the frequency of occurrence of different data number values in an image.

HPF(H) High-pass filter (horizontal). One of the routinely produced real-time picture versions for which a process of horizontal digital filtering was used in the enhancement of fine picture detail.

HPF(V) High-pass filter (vertical). One of two routinely produced enhancements of the Reduced Data Record for which a process of vertical digital filtering was used in the enhancement of fine picture detail.

INCLINATION Dihedral angle between the orbital plane and the equatorial plane of Mars.

IPL Image Processing Laboratory of the Jet Propulsion Laboratory. Computer facility for off-line processing of imaging data which produced the Reduced Data Record, rectified and scaled pictures, and special enhancements of Mariner 9 television data.

IRIS Infrared interferometer spectrometer. An instrument boresighted with the television cameras which acquired spectra for a relatively wide field of view in the thermal region of from 200 to 2000 cm^{-1} .

IRR Infrared radiometer. An instrument boresighted with the television cameras which measured heat radiation from planetary features in the thermal infrared region of from 8 to 12 μm and from 18 to 24 μm .

LIGHT-TRANSFER FUNCTION Relationship between light exposure and camera response.

LIMB Horizon of a planet viewed from outside its atmosphere. Many pictures of the illuminated limb of Mars were obtained by Mariner 9, and instrument scans were also made across the dark unilluminated limb.

LINK Observational units requiring the execution of several spacecraft blocks in one continuous sequence (example: sextad).

MANEUVER Any operation of the three-axis stabilized spacecraft that was designed to change its velocity (propulsive maneuver) or alter its orientation in space (non-propulsive maneuver).

MAPPING Process of acquiring systematic, contiguous wide-angle coverage with nested narrow-angle coverage of the surface of Mars.

MTC Mission test computer. Computer facility that provided real-time television data and the Experiment Data Record.

MTF Modulation-transfer function. A measure of resolution defined as the function relating the contrast in the image of a target with sinusoidally varying intensity to the amplitude of these variations in the target.

NADIR Point on the celestial sphere directly below a given position or observer and diametrically opposite to the zenith.

NADIR PASS Odd-numbered revolution during which Mars and Mariner 9 were below the horizon as viewed from the Goldstone tracking station, prohibiting the reception of high-rate data from the spacecraft.

NSSDC National Space Science Data Center, Code 601, Goddard Space Flight Center, Greenbelt, Maryland 20771.

OCCULTATION OF THE SPACECRAFT Interruption of electromagnetic radiation to or from the spacecraft by the intervention of Mars as viewed from another celestial body (e.g., Earth, Sun, or Canopus).

PENTAD Five television pictures deliberately taken as a group close together in time and generally providing overlapping, nesting, or contiguous coverage.

PERIAPSIS Point in an eccentric orbit that is closest to the center of attraction.

PERIHELION Point of a heliocentric elliptical orbit where the comet, planet, or spacecraft is closest to the Sun.

PHOTOMETRIC DISTORTION Functional relationship between light exposure and camera signal at all points in the field of an imaging device.

PIXEL Contraction of "picture element." Television data in the format scanned by the cameras and ultimately recorded as an Experiment Data Record consist of a matrix of 832 by 700 pixels, each with possible numerical values between 0 and 511.

PN CODE Pseudonoise code. Code used to identify the beginning of a data format (e.g., picture lines) in a telemetry stream.

POGASIS Planetary orbital geometry and science instrument scan. Computer program used to plan Mariner 9 data-acquisition sequences.

POS Pre-orbital science. Data acquired by the science instruments before insertion into orbit and intended for a broader scientific objective than calibration of the cameras.

RAW PICTURE VERSION One of the routinely produced real-time picture versions for which minimal processing was applied to the digital image.

RDR Reduced Data Record. Form of data produced by processing the Experiment Data Record at the Image Processing Laboratory to correct photometric and geometric distortions. Each pixel in this record has a value between 0 and 511 in a matrix of 950 samples on 800 lines. The Reduced Data Record is derived from the Experiment Data Record or preliminary EDR data with a matrix of 832 samples and 700 lines. Reseau marks or image detail have different line and sample locations in the Reduced Data Record and in the Experiment Data Record.

REAL TIME In the context of the Mariner 9 television experiment, pictures or data displayed almost immediately after being received from the spacecraft.

RESEAU MARKS Network of small metallic deposits on the faceplates of the television cameras used as geometric reference points.

RESIDUAL IMAGE That part of an image which is attributable to previous exposures of a camera rather than to the current exposure. High-contrast features such as the limb and polar-cap edge persist as ghosts for several frames after the one in which they were imaged.

R&S Rectified and scaled. This term was originally intended to designate orthographic projections of Mariner 9 television data. It was also used to describe mapping projections (Mercator, Lambert, Polar Stereographic) produced by digital processing at the Image Processing Laboratory.

SEDR Supplementary Experiment Data Record. Numerical information on latitude, longitude, solar illumination angle, etc., for the entire set of Mariner 9 pictures.

SEXTAD Six television pictures deliberately taken as a group close together in time and generally providing overlapping, nesting, or contiguous coverage.

SHADING-CORRECTED PICTURE VERSION One of the routinely produced real-time picture versions for which a shading correction was applied to reduce the effects of sensitivity variations across the fields of view of the television cameras on the quality of the image.

SLEW Change in pointing of the science instruments, achieved by driving the spacecraft's scan platform.

SMD Standard mission day. Concept whereby data-acquisition operations could be made almost identical in structure from day to day, yet still permit considerable flexibility in terms of science objectives.

SPIKES Pixels that are anomalously higher in value (lighter) or lower in value (darker) than the surrounding pixels because of bit errors in the higher-order bits of the 9-bit code that represents the numerical value of that pixel.

STANDARD MISSION Portion of the mission that ended on Rev 217 when three successive 18½-day cycles of mapping photography had been executed and more than 75 percent of Mars had been photographed at medium resolution (see EXTENDED MISSION).

STRETCH Contrast enhancement.

TERMINATOR Dividing line between light and dark parts of the planet's surface.

TETRAD Four television pictures deliberately taken as a group close together in time and generally providing overlapping, nesting, or contiguous coverage.

TRIAD Three television pictures deliberately taken as a group close together in time and generally providing overlapping, nesting, or contiguous coverage.

TVS Television subsystem. Two cameras and associated electronics in the main portion of the spacecraft which provided most of the functional elements necessary to obtain pictures.

UVS Ultraviolet spectrometer. Science instrument boresighted with the television cameras which acquired spectra in the wavelength range of 1100 to 3400 Å.

VARIABLE-FEATURE INVESTIGATION Mariner 9 television study in orbit in which time-variable phenomena on the surface and in the Martian atmosphere were investigated (see FIXED-FEATURE INVESTIGATION).

VAGC Vertical automatic-gain control. One of the routinely produced real-time picture versions for which a process of vertical averaging was used in the enhancement of fine picture detail.

ZENITH Point on the celestial sphere directly above a given position or observer and diametrically opposite to the nadir.

ZENITH PASS Even-numbered revolution during which Mars and Mariner 9 were above the horizon as viewed from the Goldstone tracking station, permitting the reception of high-rate data from the spacecraft.